

Design and Synthesis of Step-Growth Monomers Starting from Bio-Based Chemicals and Polymers Therefrom

Thesis Submitted to AcSIR For the Award of
the Degree of

DOCTOR OF PHILOSOPHY

In
Chemical Sciences



By

Sachin S. Kuhire

(AcSIR Reg. No.:10CC12A26003)

Under the guidance of

Dr. Prakash P. Wadgaonkar

CSIR-National Chemical Laboratory,

Pune-411008, INDIA

2017



*To My Mentor
Dr. Prakash P. Wadgaonkar*

सीएसआईआर - राष्ट्रीय रासायनिक प्रयोगशाला

(वैज्ञानिक तथा औद्योगिक अनुसंधान परिषद)

डॉ. होमी भाभा मार्ग, पुणे - 411 008, भारत



CSIR - NATIONAL CHEMICAL LABORATORY

(Council of Scientific & Industrial Research)

Dr. Homi Bhabha Road, Pune - 411 008, India

Certificate

This is to certify that the work incorporated in this Ph.D. thesis entitled “**Design and Synthesis of Step-Growth Monomers Starting from Bio-Based Chemicals and Polymers Therefrom**” submitted by **Mr. Sachin S. Kuhire** to Academy of Scientific and Innovative Research (AcSIR) in fulfillment of the requirements for the award of the Degree of **Doctor of Philosophy in Chemical Sciences**, embodies original research work under my supervision. I further certify that this work has not been submitted to any other University or Institution in part or full for the award of any degree or diploma. Research material obtained from other sources has been duly acknowledged in the thesis. Any text, illustration, table etc., used in the thesis from other sources, have been duly cited and acknowledged.

Sachin S. Kuhire

(Student)

Prakash P. Wadgaonkar

(Supervisor)

Communication Channels

NCL Level DID : 2590
NCL Board No. : +91-20-25902000
EPABX : +91-20-25893300
: +91-20-25893400



FAX

Director's Office : +91-20-25902601
COA's Office : +91-20-25902660
SPO's Office : +91-20-25902664

WEBSITE

www.ncl-india.org

Declaration by the Candidate

I hereby declare that the original research work embodied in this thesis entitled, **“Design and Synthesis of Step-Growth Monomers Starting from Bio-Based Chemicals and Polymers Therefrom”** submitted to the Academy of Scientific and Innovative Research (AcSIR) for the award of the Degree of the Doctor of Philosophy (Ph.D.) is the outcome of experimental investigations carried out by me under the supervision of Dr. Prakash P. Wadgaonkar, Chief Scientist, CSIR-National Chemical Laboratory, Pune. I affirm that the work incorporated is original, and has not been submitted to any other Academy, University or Institute for the award of any Degree or Diploma.

November 2017
CSIR-National Chemical Laboratory
Pune-411008



Sachin S. Kuhire
(Research Student)

Acknowledgement

The journey of my PhD work has been a very memorable and fruitful part of my life which could not have been possible without support and encouragement of some very special people. I would like to express my gratitude towards them for their invaluable help.

*The first and foremost, I would like to thank my research supervisor **Dr. Prakash P. Wadgaonkar** for his continuous and fruitful guidance, encouragement and patience during the completion of research work and achieving the endeavour. He has been open to share and discuss his scientific knowledge and experience at all times. His technical and personal guidance has been invaluable in making me become a better professional and a person. This work would not have been possible without his inspiration.*

I express my thanks to the University Grants Commission (UGC) for the research fellowship and financial support. I would also like to express my gratitude to Prof. Ashwinikumar Nangia (Director, CSIR-NCL), Dr. Vijayamohanan Pillai and Dr. Sourav Pal (former Directors of CSIR-NCL) for giving me the opportunity to work at CSIR-NCL. It is my pleasure to thank Dr. U. K. Kharul (Chair, PSE Division), Dr. Ashish Lele (former Chair, PSE Division) and Dr. A. J. Varma (former Chair, PSE Division) for allowing me to work in Polymer Science and Engineering Division and providing the instrumental facilities and infrastructure to perform the research work.

I am thankful to my Doctoral Advisory Committee (DAC) members Dr. M. V. Badiger, Dr. S. K. Asha, and Dr. Ravi Kumar for the regular assessment of my research work, suggestions, valuable advices and fruitful discussions during the DAC meetings which helped me to build and to improve upon my research skills.

I owe my gratitude to Dr. C. V. Avadhani, Dr. Ashootosh V. Ambade, Dr. K. Guruswamy, Dr. Ajith Kumar, Dr. Rajesh Gonnade, Dr. Satish Ogale, Dr. Samir Chikkali, Dr. S. P. Chavan, Dr. J. Nithyanandhan, Dr. Sayam Sen Gupta, Dr. C. Ramesh, Dr. B. B. Idage, Dr. (Mrs.). S. B. Idage, Dr. D. S. Reddy, Dr. A. T Biju, Dr. Kadhiravan Shanmuganathan, Dr. K. Krishnamoorthy and Dr. Suman Chakrabarty for their kind support and help throughout the PhD tenure.

I would like to express my special thanks to Professor M. Jayakannan (IISER, Pune), Dr. C. P. R. Nair (VSSC, Thiruvananthapuram), Professor Henri Cramail (LCPO, University of Bordeaux, France), Dr. U. P. Mulik (CMET, Pune), Professor Vaishali. S. Shinde (Savitribai Phule Pune University, Pune), Professor S. V. Lonikar (Solapur University, Solapur), Professor N. N. Maldar (Solapur University, Solapur) and Dr. Bimlesh Lochab (Shiv Nadar University, Noida) for the suggestions.

I would like to express my sincere thanks to Dr. Suresh Bhat, Mrs. Deepa Dhoble, Dr. Neelima Bulakh, Mrs. Sangeeta Hambir, Mrs. Poorvi Purohit, Dr. B. Santhakumari and Mr. R. Gholap for allowing me to use the instruments and providing the analytical facilities.

I extend my gratitude towards Mr. Shamal K. Menon, Mr. Anandrao S. Patil and Dr. Nilakshi Sadavarte for their guidance and continuous support.

I would like to acknowledge entire NMR facility especially Dr. P. R. Rajamohanan and electron microscopic technique group from CMC. I extend my sincere thanks to the members of Glass Blowing, Workshop, Stores, Purchase, Accounts and Bill Section and other office staff for their timely help.

I appreciate Student Academic Office (SAO) Chairman Dr. M. S. Shashidhar and Dr. C. G. Suresh and staff members including Mrs. Kolhe Madam and Shri. S. Iyer Sir for their kind help and co-operation throughout the PhD tenure.

I would like to express my sincere thanks to Dr. Ankush Mane, Dr. Pandurang Honkhambe, Dr. Arvind More, Dr. Arun Kulkarni, Dr. Anjana Sarkar, Dr. Snehalata Bapat, Dr. Dnyaneshwar Palaskar, Dr. Prakash Sane, Dr. Sharad Pasale, Dr. Savita Kumari, Dr. Bhausheeb Tawade, Dr. Dilip Raut, Dr. Shyambo, Dr. Murugesan, Dr. Aarti Shedde, Dr. Prakash Babu and Dr. Ravindra Patil for valuable suggestions during my Ph D. tenure.

I am thankful to all lab members and friends Dr. Nagendra Kalva, Dr. Naganath Patil, Nitin Basutkar, Indravadan Parmar, Samadhan, Deepak, Geethika, Namdev, Shakeeb, Deepshikha, Kavita, Vikas, Sachin Basutkar, Ashwini, Uday, Sagar, Dr. Shraddha, Dr. Sayali, Rupali, Bharat, Nitin Valsange, Jagdish, Amol, Dr. Satyawan, Abhijeet, Dr. Ikhlas Gadwal, Yogesh Nevare, Durgaprasad, Ketan and Clement Ravet for their kind help and maintaining friendly environment in the lab.

I wish to thank my friends Mr. Arun Torris, Mr. Suresha, Dr. Manoj Mane, Vijay, Shrikant, Shahaji, Nilesh, Rahul, Satej, Dr. Nagesh, Dr. Swapnil, Dr. Shekher, Shrikant, Navnath, Mukta, Dr. Prakash Chavan, Dr. Sachin Bhojgude, Balasaheb Jawale, Megha, Manoj Sharma, Kartika, Ram, Smita and Nagesh Gattuvar for their help.

No words would suffice to express my gratitude and love to my mother, father, brother (Shivaji) and sisters (Vandana and Ganga) for their enormous support throughout. No words would suffice to express my gratitude for their continuous affection, love and sacrifices. They are the ones who are my strength and motivation in all kinds of situations.

Sachin S. Kuhire

Table of Contents

	Description	Page No.
	● Abstract	i
	● Glossary	vi
	● List of Tables	viii
	● List of Schemes	x
	● List of Figures	xi
Chapter 1	Introduction and Literature Survey	
1.1	Introduction	1
1.2	Aromatic step growth monomers starting from renewable resources	4
1.2.1	CNSL-based step-growth monomers	4
1.2.2	Lignocellulose	8
1.2.2 .1	Step growth monomers based on furan derivatives	9
1.2.2.2	Aromatic difunctional monomers based on lignin	11
1.2.2 .2.1	Chemical structure and physical properties	12
1.2.2 .2.2	Chemical modification of lignin	13
1.3	Summary	19
	References	20
Chapter 2	Scope and Objectives	33
Chapter 3	Step Growth Monomers from Lignin-Derived Aromatics	
3.1	Introduction	37
3.2	Experimental	39
3.2.1	Materials	39
3.2.2	Characterization	39
3.3	Synthesis	40
3.3.1	Synthesis of diisocyanates containing oxyalkylene linkage	40
3.3.1.1	General procedure for synthesis of α,ω -dicarboxylic acids containing oxyalkylene linkage	40
3.3.1.1.1	Synthesis of 4,4'-(propane-1,3-diylbis(oxy))bis(3-methoxybenzoic acid)	40
3.3.1.1.2	Synthesis of 4,4'-(butane-1,4-diylbis(oxy))bis(3-methoxybenzoic acid)	40
3.3.1.1.3	Synthesis of 4,4'-(pentane-1,5-diylbis(oxy))bis(3-methoxybenzoic acid)	40

3.3.1.1.4	Synthesis of 4,4'-(propane-1,3-diylbis(oxy))bis(3,5-dimethoxybenzoic acid)	40
3.3.1.1.5	Synthesis of 4,4'-(butane-1,4-diylbis(oxy))bis(3,5-dimethoxybenzoic acid)	41
3.3.1.1.6	Synthesis of 4,4'-(pentane-1,5-diylbis(oxy))bis(3,5-dimethoxybenzoic acid)	41
3.3.1.2	General procedure for synthesis of α,ω -dicarboxylic acyl azides containing oxyalkylene linkage	41
3.3.1.2.1	Synthesis of 4,4'-(propane-1,3-diylbis(oxy))bis(3-methoxybenzoyl azide)	41
3.3.1.2.2	Synthesis of 4,4'-(butane-1,4-diylbis(oxy))bis(3-methoxybenzoyl azide)	42
3.3.1.2.3	Synthesis of 4,4'-(pentane-1,5-diylbis(oxy))bis(3-methoxybenzoyl azide)	42
3.3.1.2.4	Synthesis of 4,4'-(propane-1,3-diylbis(oxy))bis(3,5-dimethoxybenzoyl azide)	42
3.3.1.2.5	Synthesis of 4,4'-(butane-1,4-diylbis(oxy))bis(3,5-dimethoxybenzoyl azide)	42
3.3.1.2.6	Synthesis of 4,4'-(pentane-1,5-diylbis(oxy))bis(3,5-dimethoxybenzoyl azide)	42
3.3.1.3	General procedure for synthesis of α,ω -diisocyanates containing oxyalkylene linkage	42
3.3.1.3.1	Synthesis of 1,3-bis(4-isocyanato-2-methoxyphenoxy)propane	43
3.3.1.3.2	Synthesis of 1,4-bis(4-isocyanato-2-methoxyphenoxy)butane	43
3.3.1.3.3	Synthesis of 1,5-bis(4-isocyanato-2-methoxyphenoxy)pentane	43
3.3.1.3.4	Synthesis of 1,3-bis(4-isocyanato-2,6-dimethoxyphenoxy)propane	43
3.3.1.3.5	Synthesis of 1,4-bis(4-isocyanato-2,6-dimethoxyphenoxy)butane	43
3.3.1.3.6	Synthesis of 1,5-bis(4-isocyanato-2,6-dimethoxyphenoxy)pentane	44
3.3.2	Synthesis of 3,3'-diisocyanates containing biphenylene linkage	44
3.3.2.1	Synthesis of dimethyl 6,6'-dihydroxy-5,5'-dimethoxy-[1,1'-biphenyl]-3,3'-dicarboxylate	44
3.3.2.2	General procedure for synthesis of dimethyl 6,6'-alkoxy-5,5'-dimethoxy-[1,1'-biphenyl]-3,3'-dicarboxylate	44
3.3.2.2.1	Synthesis of dimethyl 5,5',6,6'-tetramethoxy-[1,1'-biphenyl]-3,3'-dicarboxylate	45

3.3.2.2.2	Synthesis of dimethyl 5,5'-dimethoxy-6,6'-bis(pentyloxy)-[1,1'-biphenyl]-3,3'-dicarboxylate	45
3.3.2.3	General procedure for synthesis of 6,6'-dialkoxy-5,5'-dimethoxy-[1,1'-biphenyl]-3,3'-dicarboxylic acid	45
3.3.2.3.1	Synthesis of 5,5',6,6'-tetramethoxy-[1,1'-biphenyl]-3,3'-dicarboxylic acid	45
3.3.2.3.2	Synthesis of 5,5'-dimethoxy-6,6'-bis(pentyloxy)-[1,1'-biphenyl]-3,3'-dicarboxylic acid	45
3.3.2.4	General procedure for synthesis of 6,6'-dialkoxy-5,5'-dimethoxy-[1,1'-biphenyl]-3,3'-dicarbonyl diazide	46
3.3.2.4.1	Synthesis of 5,5',6,6'-tetramethoxy-[1,1'-biphenyl]-3,3'-dicarbonyl diazide	46
3.3.2.4.2	Synthesis of 5,5'-dimethoxy-6,6'-bis(pentyloxy)-[1,1'-biphenyl]-3,3'-dicarbonyl diazide	46
3.3.2.5	General procedure for synthesis of 5,5'-diisocyanato-3,3'-dimethoxy-2,2'-bis(alkoxy)-1,1'-biphenyl	47
3.3.2.5.1	Synthesis of 5,5'-diisocyanato-2,2',3,3'-tetramethoxy-1,1'-biphenyl	47
3.3.2.5.2	Synthesis of 5,5'-diisocyanato-3,3'-dimethoxy-2,2'-bis(pentyloxy)-1,1'-biphenyl	47
3.3.3	Synthesis of A-B type monomers	47
3.3.3.1	General procedure for synthesis of methyl vanillate and methyl syringate	47
3.3.3.1.1	Synthesis of methyl 4-hydroxy-3-methoxybenzoate	47
3.3.3.1.2	Synthesis of methyl 4-hydroxy-3,5-dimethoxybenzoate	48
3.3.3.2	General procedure for synthesis of ω -hydroxyalkyleneoxy benzoic acid methyl esters	48
3.3.3.2.1	Synthesis of methyl 4-((6-hydroxyhexyl)oxy)-3-methoxybenzoate	48
3.3.3.2.2	Synthesis of methyl 4-((11-hydroxyundecyl)oxy)-3-methoxybenzoate	48
3.3.3.2.3	Synthesis of methyl 4-((6-hydroxyhexyl)oxy)-3,5-dimethoxybenzoate	49
3.3.3.2.4	Synthesis of methyl 4-((11-hydroxyundecyl)oxy)-3,5-dimethoxybenzoate	49
3.3.3.3	General procedure for synthesis of ω -hydroxyalkyleneoxy benzoic acids	49

3.3.3.3.1	Synthesis of 4-((6-hydroxyhexyl)oxy)-3-methoxybenzoic acid	49
3.3.3.3.2	Synthesis of 4-((11-hydroxyundecyl)oxy)-3-methoxybenzoic acid	50
3.3.3.3.3	Synthesis of 4-((6-hydroxyhexyl)oxy)-3,5-dimethoxybenzoic acid	50
3.3.3.3.4	Synthesis of 4-((11-hydroxyundecyl)oxy)-3,5-dimethoxybenzoic acid	50
3.3.3.4	General procedure for synthesis of ω -hydroxyalkyleneoxy benzoyl azides	50
3.3.3.4.1	Synthesis of 4-((6-hydroxyhexyl)oxy)-3-methoxybenzoyl azide	51
3.3.3.4.2	Synthesis of 4-((11-hydroxyundecyl)oxy)-3-methoxybenzoyl azide	51
3.3.3.4.3	Synthesis of 4-((6-hydroxyhexyl)oxy)-3,5-dimethoxybenzoyl azide	51
3.3.3.4.4	Synthesis of 4-((11-hydroxyundecyl)oxy)-3,5-dimethoxybenzoyl azide	51
3.3.4	Synthesis of furyl containing bisphenols	51
3.3.4.1	General procedure for synthesis of furyl containing bisphenols	51
3.3.4.1.1	Synthesis of 4, 4'-(furan-2-ylmethylene)bis(2,6-dimethoxyphenol)	52
3.3.4.1.2	Synthesis of 4,4'-(furan-2-ylmethylene)bis(2-methoxyphenol)	52
3.3.4.1.3	Synthesis of 4,4'-((5-methylfuran-2-yl)methylene)bis(2,6-dimethoxyphenol)	52
3.3.5	Synthesis of oxadiazole containing bisphenol	52
3.3.5.1	Synthesis of 4-acetoxy-3-methoxybenzoic acid	52
3.3.5.2	Synthesis of (hydrazine-1,2-dicarbonyl)bis(2-methoxy-4,1-phenylene) diacetate	53
3.3.5.3	Synthesis of (1,3,4-oxadiazole-2,5-diyl)bis(2-methoxy-4,1-phenylene) diacetate	53
3.3.5.4	Synthesis of 4,4'-(1,3,4-oxadiazole-2,5-diyl)bis(2-methoxyphenol)	54
3.3.6	Synthesis of α , ω -diacyl hydrazide containing oxyalkylene linkage	54
3.3.6.1	General procedure for synthesis of α , ω -diester containing oxyalkylene linkages	54
3.3.6.1.1	Synthesis of dimethyl 4,4'-(propane-1,3-diylbis(oxy))bis(3-methoxybenzoate)	54
3.3.6.1.2	Synthesis of dimethyl 4,4'-(propane-1,3-diylbis(oxy))bis(3,5-dimethoxybenzoate)	55

3.3.6.2	General procedure for synthesis of α , ω -diacyl hydrazide containing oxyalkylene linkages	55
3.3.6.2.1	Synthesis of 4,4'-(propane-1,3-diylbis(oxy)) bis(3-methoxybenzohydrazide)	55
3.3.6.2.2	Synthesis of 4,4'-(propane-1,3-diylbis(oxy)) bis(3,5-dimethoxybenzohydrazide)	55
3.3.7	Synthesis of 5,5'-dimethoxy-6,6'-bis(pentyloxy)-[1,1'-biphenyl]-3,3'-dicarbohydrazide	55
3.3.8	Synthesis of bis(4-formyl-2-methoxyphenyl) succinate	56
3.3.9	Synthesis of bis(4-(hydroxymethyl)-3-methoxyphenyl) succinate	56
3.3.10	General procedure for synthesis of diacid containing ester linkage	57
3.3.10.1	Synthesis of 4,4'-((furan-2,5-dicarbonyl)bis(oxy)) bis(3-methoxybenzoic acid)	57
3.3.10.2	Synthesis of 4,4'-((furan-2,5-dicarbonyl)bis(oxy)) bis(3,5-dimethoxybenzoic acid)	57
3.4	Results and discussion	58
3.4.1	Synthesis and characterization of diisocyanate monomers	58
3.4.1.1	Synthesis and characterization of new diisocyanate monomers containing oxyalkylene linkage	58
3.4.1.2	Bisphenols from guaiacol and syringol	67
3.4.2	Synthesis and characterization of ω -hydroxyalkyleneoxy benzoyl azides	77
3.4.3	Synthesis of bisphenols from guaiacol and syringol	84
3.4.3.1	Synthesis of furyl containing bisphenols	85
3.4.3.2	Synthesis and characterization of oxadiazole containing bisphenol	87
3.4.4	Synthesis of diacyl hydrazides containing oxypropylene linkage	94
3.4.4.1	Synthesis of α , ω -diacyl hydrazides containing oxyalkylene linkage	94
3.4.4.2	Synthesis of diacyl hydrazide containing biphenylene linkages	101
3.4.5	Synthesis of dialdehyde containing ester linkages	103
3.4.6	Synthesis of diol containing ester linkages	105
3.4.7	Synthesis of aromatic diacids containing ester linkage	107
3.5	Conclusions	110
	References	111

Chapter 4 Bio-Based Poly(ether urethane)s

Chapter 4a Poly(ether urethane)s from Aromatic Diisocyanates Based on Lignin-

Derived Phenolic Acids

4a.1	Introduction	115
4a.2	Experimental	117
	4a.2.1 Materials	117
	4a.2.2 Measurements	117
	4a.2.3 General procedure for synthesis of poly(ether urethane)s	118
4a.3	Results and discussion	119
	4a.3.1 Poly(ether urethane) synthesis	119
	4a.3.2 Structural characterization	120
	4a.3.3 Solubility	122
	4a.3.4 Thermal properties	122
4a.4	Conclusions	123
	References	124
Chapter 4b New Poly(ether urethane)s Based on Lignin-Derived Aromatic Chemicals <i>via</i> A-B Monomer Approach: Synthesis and Characterization		
4b.1	Introduction	127
4b.2	Experimental	128
	4b.2.1 Materials	128
	4b.2.2 Measurements	128
	4b.2.3 General procedure for synthesis of poly(ether urethane)s	129
4b.3	Results and discussion	130
	4b.3.1 Synthesis of poly(ether urethane)s	130
	4b.3.2 Structural characterization	131
	4b.3.3 Solubility	133
	4b.3.4 Thermal properties	133
4b.4	Conclusions	135
	References	136
Chapter 4c Polyurethane-Based Organogels: Preparation, Characterization and Application as Electrolyte in Dye-Sensitized Solar Cell		
4c.1	Introduction	139
4c.2	Experimental	140
	4c.2.1 Materials	140
	4c.2.2 Preparations and characterization	140
4c.3	Results and discussion	142
	4c.3.1 Microstructural study	143

4c.3.2	LiCl addition experiment	144
4c.3.3	Thermoreversibility of polyurethane organogel	144
4c.3.4	Rheological studies of polyurethane gel	145
4c.3.4.1	Viscoelastic property	145
4c.3.4.2	Effect of concentration	146
4c.3.4.3	Thermo-reversibility of gels	147
4c.3.5	Dye-sensitized solar cells (DSSC)	148
4c.4	Conclusions	152
	References	153
Chapter 5 Aromatic Polyesters and Polycarbonates Containing Pendant Furyl Groups		
Chapter 5a Synthesis and Characterization of Aromatic Polyesters Containing Pendant Furyl Groups		
5a.1	Introduction	157
5a.2	Experimental	158
5a.2.1	Materials	158
5a.2.2	Measurements	158
5a.2.3	General procedure for the synthesis of polyesters	159
5a.3	Results and discussion	161
5a.3.1	Polyester synthesis	161
5a.3.2	Structural characterization	162
5a.3.3	X-Ray diffraction studies	164
5a.3.4	Thermal properties	165
5a.3.5	Mechanical properties of polyesters	169
5a.4	Conclusions	170
	References	171
Chapter 5b Synthesis and Characterization of (Co)polycarbonates Containing Pendant Furyl Groups		
5b.1	Introduction	175
5b.2	Experimental	176
5b.2.1	Materials	176
5b.2.2	Measurements	176
5b.2.3	General procedure for the synthesis of (co)polycarbonates	177
5b.3	Results and discussion	178
5b.3.1	Synthesis of (co)polycarbonates	178

5b.3.2	Structural characterization	180
5b.3.3	X-ray diffraction studies	187
5b.3.4	Thermal properties	187
5b.3.5	Mechanical properties of (co)polycarbonates	191
5b.4	Conclusions	193
	References	194

Chapter 5c Thermally Reversible Crosslinked Polymers via Diels-Alder Click Chemistry

5c.1	Introduction	197
5c.2	Experimental	201
5c.2.1	Materials	201
5c.2.2	Measurements	201
5c.2.3	Preparations	201
5c.3	Results and discussion	202
5c.3.1	Preparation of crosslinked polymers	202
5c.3.2	Thermal studies of crosslinked polymers	203
5c.3.3	Solubility test of crosslinked and de-crosslinked polymers	204
5c.3.4	Mechanical properties of crosslinked polymers	205
5c.3.5	Mechanical properties of recycled polymers	206
5c.3.6	Thermoreversible gels via Diels-Alder reaction	208
5c.3.7	Rheological behavior of polyester gel	208
5c.4	Conclusions	211
	References	212

Chapter 6 Synthesis and Characterization of Poly(amide imide)s and Polyimides

Chapter 6a Synthesis and Characterization of Poly(amide imide)s Containing Oxyalkylene Linkages

6a.1	Introduction	215
6a.2	Experimental	215
6a.2.1	Materials	215
6a.2.2	Measurements	216
6a.2.3	Synthesis of poly(amide imide)s containing oxypropylene linkage	217
6a.3	Results and discussion	219
6a.3.1	Synthesis of poly(amide imide)s	219
6a.3.2	Structural characterization	221

6a.3.3	Solubility of poly(amide imide)s	223
6a.3.4	X-Ray diffraction studies	224
6a.3.5	Thermal properties of poly(amideimide)s	224
6a.3.6	Dynamic mechanical analysis	226
6a.3.7	Molecular dynamics simulation studies of representative poly(amide imide)s (PAI-1 and PAI-4)	228
6a.4	Conclusions	232
	References	233
Chapter 6b	Synthesis and Characterization of Aromatic Polyimides Containing Biphenylene Linkages	
6b.1	Introduction	235
6b.2	Experimental	236
6b.2.1	Materials	236
6b.2.2	Measurements	236
6b.2.3	Synthesis of polyimides	237
6b.3	Results and discussion	238
6b.3.1	Polymer synthesis	238
6b.3.2	Structural characterization	240
6b.3.3	Solubility of polyimides	242
6b.3.4	X-Ray diffraction studies	243
6b.3.5	Thermal properties of polyimides	244
6b.4	Conclusions	246
	References	246
Chapter 7	Summary and Conclusions	249
	Future Perspectives	253
	List of Publications	255

Abstract

Renewable resources have been used to produce polymers since the advent of polymer science, and in fact were the primary focus of research until the 1940's. Around the period of Second World War, the developments in the field of 'petro refinery' gave great boost to the industrial production of synthetic polymers. Beginning in the 1990's, however, there was general acceptance that petroleum was finite, and development of a 'bio refinery' concept as a source for energy, chemicals, and organic materials came into prominence.

It has been recognized that lignin- one of the three main components of non-edible lignocellulose biomass-is a renewable feedstock with great potential. As a matter of fact, lignin is considered as a "sleeping giant" capable of serving as a potential source of sustainable raw material for fuels and chemicals. The most attractive feature of lignin is that it is the most abundant renewable resource of aromatics on the earth.

Around 70 million tonnes of lignin is produced annually as a by-product of paper and pulp industries in the world. The depolymerisation of lignin yields various phenol derivatives such as vanillin, syringaldehyde, vanillic acid, syringic acid, syringol, guaiacol, ferulic acid, eugenol, etc. There are limited numbers of reports which describe the use of lignin-derived aromatics as starting materials for the synthesis of aromatic step-growth polymers. Therefore, design and synthesis of difunctional monomers and polymers from lignin-derived aromatics is an attractive proposition.

The overall objective of the present thesis was to design and synthesize difunctional monomers using bio-based chemicals as starting materials and utilize these difunctional monomers for the synthesis of step growth polymers. To achieve these goals, 23 new difunctional monomers *viz.* bisphenols, diacids, diisocyanates, diacylhydrazides, dialdehydes, diols and hydroxyl acyl azides were synthesized starting from lignin-derived aromatics. Aromatic polyesters, aromatic polycarbonates, poly(ether urethane)s, aromatic poly(amide imide)s and aromatic polyimides were synthesized from appropriate difunctional monomers. The thesis work has been presented in the following chapters:

Chapter 1 gives a brief literature survey concerning synthesis of monomers and polymers from renewable resources with particular focus on cashew nut shell liquid (CNSL), furan derivatives, and lignin. The literature references concerning step growth polymers based on bio-derived monomers are also indicated.

Chapter 2 describes scope and objectives of the thesis.

Chapter 3 deals with the design and synthesis of a library of difunctional monomers *viz.* diisocyanates containing oxyalkylene linkage, diisocyanates containing biphenylene linkage, ω -hydroxyalkyleneoxy benzoyl azides, bisphenols containing pendant furyl group, bisphenol containing oxadiazole ring, α , ω -diacyl hydrazides containing oxyalkylene linkage, 3,3'-diacyl hydrazide containing biphenylene linkage, dialdehyde containing ester linkage and diols containing ester linkage. The difunctional monomers and intermediates involved in their synthesis were characterized by FT-IR, ^1H NMR and ^{13}C NMR spectroscopy. Some of the monomers and intermediates were characterized by HRMS and single crystal X-ray diffraction analysis.

Chapter 4 is divided into three sections.

Chapter 4a describes synthesis of poly(ether urethane)s by the polymerization of new bio-based aromatic diisocyanates *viz.* 1,3-bis(4-isocyanato-2-methoxyphenoxy)propane and 1,3-bis(4-isocyanato-2,6-dimethoxyphenoxy)propane with potentially bio-based aliphatic diols *viz.* 1, 10-decanediol and 1, 12-dodecanediol. The chemical structures of poly(ether urethane)s were confirmed by FT-IR, ^1H NMR and ^{13}C NMR spectroscopy. Inherent viscosities and number average molecular weights (\overline{M}_n) of poly(ether urethane)s were in the range 0.58-0.68 dLg $^{-1}$ and 32,100-58,500 g mol $^{-1}$, respectively indicating formation of reasonably high molecular weight polymers. Poly(ether urethane)s exhibited 10 % weight loss in the temperature range 304-308 °C. The glass transition temperatures (T_g) of poly(ether urethane)s were in the range 49-74 °C and were dependent both on the number of methylene units in the diols and the number of methoxy substituents on the aromatic rings of diisocyanate component.

Chapter 4b deals with poly(ether urethane)s based on bio-derived A-B monomers *viz.* ω -hydroxyalkyleneoxy benzoyl azides which were self-polycondensed to afford polymers. Poly(ether urethane)s exhibited reasonably high molecular weights ($\eta_{\text{inh}} = 0.41\text{--}0.69$ dL g $^{-1}$ and $\overline{M}_n, (\text{GPC}) = 20,000\text{--}40,400$ g mol $^{-1}$) and film forming characteristics. The chemical structures of poly(ether urethane)s were confirmed by FT-IR, ^1H NMR and ^{13}C NMR spectroscopy. Poly(ether urethane) films exhibited 80.2–87.6% transmittance at 800 nm. Poly(ether urethane)s showed 10 % weight loss temperature and T_g values in the range 320–340 °C and 40–70 °C, respectively. T_g values of poly(ether urethane)s were dependent both on length of oxyalkylene spacer and number of methoxy substituents on aromatic ring.

Chapter 4c describes polyurethane-based organogel. The polyurethane based on A-B monomer *viz.* 4-((11-hydroxyundecyl)oxy)-3-methoxybenzoyl azide exhibited thermoreversible gelation at ambient temperature in polar organic solvents such as tetrahydrofuran (THF), *N,N*-dimethylformamide (DMF), *N,N*-dimethylacetamide (DMAc), *N*-methyl-2-pyrrolidone (NMP) and dimethyl sulfoxide (DMSO). DMF was selected as a solvent for detailed study of the phenomenon of organogelation. The gelation behaviour of polyurethane in this solvent was attributed to the combined effect of hydrophobic interactions and N-H...O hydrogen bonding. Gel-sol-gel phase transitions were studied by inverted vial method, DSC and rheology. The results of these studies indicated that the network formed in gel sample was reversible. DSC and rheology studies showed gel-sol transition at 56 °C and 57 °C, respectively for polyurethane gel in DMF (3 wt. % concentration). The utility of polyurethane-based organogel was demonstrated as a gel electrolyte for quasi-solid state dye-sensitized solar cells. Results showed better incident photon conversion efficiency (6.2%) for polyurethane gel electrolyte compared to the corresponding liquid electrolyte (DMF, 4.5%) and the stability was retained for 12 days.

Chapter 5 is divided into three sections.

Chapter 5a deals with synthesis of a series of new aromatic polyesters based on bio-based bisphenols containing pendant furyl group *viz.* 4, 4'-(furan-2-ylmethylene)bis(2,6-dimethoxyphenol) (BPF-1) and 4,4'-(furan-2-ylmethylene)bis(2-methoxyphenol) (BPF-2) and aromatic dicarboxylic acid chlorides *viz.* isophthaloyl chloride, terephthaloyl chloride and 2,5-furan dicarboxylic acid chloride. Aromatic polyesters were obtained by interfacial polycondensation using benzyltriethylammonium chloride (BTEAC) as a phase transfer catalyst. The chemical structures of polyesters were confirmed by FT-IR, ¹H NMR and ¹³C NMR spectroscopy which confirmed that the furyl groups were unaffected under the applied reaction conditions. Polyesters showed \overline{M}_n in the range 28,000-45,000 g mol⁻¹. T_g of polyesters were in the range 160-214 °C. Mechanical properties of polyesters were analyzed by tensile testing. Young's modulus and elongation at break were in the range 1.66-2.38 GPa and 15.5-56.2 %, respectively which qualify them to be useful as structural materials in several applications.

Chapter 5b describes new aromatic (co)polycarbonates prepared by polycondensation of bisphenol containing pendant furyl group *viz.* 4,4'-(furan-2-ylmethylene)bis(2-methoxyphenol) (BPF-2) or varying composition of BPF-2 and bisphenol-A with triphosgene. (Co) polycarbonates showed inherent viscosity in the range

0.50-0.72 dLg⁻¹ and \overline{M}_n obtained from GPC, were in the range 29,800-44,800 g mol⁻¹. (Co)polycarbonates could be cast into tough, transparent and flexible films from chloroform solution. By analysing triad sequence distribution using expanded ¹³C NMR spectra, it was found that the microstructure for all the copolycarbonates were random. X-Ray diffraction studies indicated amorphous nature of (co)polycarbonates. (Co)polycarbonate showed T_g values in the range 136-147 °C. Mechanical properties of (co)polycarbonates were studied by tensile testing. (Co)polycarbonates showed high Young's modulus (1.49 to 1.54 GPa) and yield strength (56 to 57.7 MPa), indicating good mechanical behaviour of bio-based (co)polycarbonates. A significant drop in % elongation at break was observed upon incorporation of bisphenol containing furyl group in (co)polycarbonates, indicating compromise on the ductility characteristics.

Chapter 5c describes preliminary studies on recyclable crosslinked aromatic polyesters and polycarbonates. Thermally reversible crosslinked polymers were prepared by reaction of furan functionalized polycarbonates/polyesters with bismaleimides *viz.* 1,1'-(methylenedi-1,4-phenylene)bismaleimide (BMI) and 1,8-bis(maleimido)-triethylene glycol (TEG). The resulting crosslinked polymers were characterized by solubility tests, and tensile testing. The crosslinked polymers were recycled twice without observing any significant deterioration of their mechanical properties.

Chapter 6 is divided into two sections.

Chapter 6a deals with synthesis of a series of new poly(amide imide)s by polycondensation of bio-based diacylhydrazide monomers *viz.* 4,4'-(propane-1,3-diylbis(oxy))bis(3-methoxybenzohydrazide) (DVHzC-3) and 4,4'-(propane-1,3-diylbis(oxy))bis(3,5-dimethoxybenzohydrazide) (DSHzC-3) with three commercially available aromatic dianhydrides *viz.* 3,3',4,4'-oxydiphthalic anhydride (ODPA), pyromellitic dianhydride (PMDA) and 3,3',4,4'-biphenyltetracarboxylic dianhydride (BPDA) *via* two-step thermal imidization method. Poly(amide imide)s showed inherent viscosity in the range 0.44-0.56 dLg⁻¹ and exhibited good solubility in organic solvents such as NMP, DMAc, DMSO, pyridine, *m*-cresol, *etc.* Poly(amide imide)s could be cast into transparent, flexible and tough films from their DMAc solution. Poly(amide imide)s showed 10 % weight loss in the temperature range 340- 364 °C indicating their satisfactory thermal stability. T_g values of poly(amide imides)s were measured by DSC and DMA which were in the range 201-223 °C and 214-248 °C, respectively. Higher T_g values were observed for DSHzC-3 -based poly(amide imide)s compared to DVHzC-3 based ones. To understand the molecular mechanism responsible for higher T_g of DSHzC-

3-based poly(amide imide), molecular dynamics simulation technique was used. The chain rigidity emerged out to be the dominant factor for observed higher T_g .

Chapter 6b illustrates the synthesis of partially bio-based polyimides based on 5,5'-diisocyanato-2,2',3,3'-tetramethoxy-1,1'-biphenyl and aromatic dianhydrides *viz* 4,4'-biphenyltetracarboxylic dianhydride (BPDA), 3,3',4,4'-benzophenonetetracarboxylic dianhydride (BTDA), 4,4'-oxydiphthalic anhydride (ODPA) and 4,4'-(hexafluoroisopropylidene) diphthalic anhydride (6-FDA). The structures of polyimides were characterized by FT-IR, ^1H NMR and ^{13}C NMR spectroscopy. Inherent viscosities and \overline{M}_n of polyimides were in the range 0.30-0.40 dLg $^{-1}$ and 25,100-32,200 g mol $^{-1}$, respectively. T_g values of biphenylene containing polyimides were in the range 262-329 °C and the values were dictated by the rigidity of the dianhydride used in the synthesis. T_{10} values of polyimides were in the range 459-473 °C indicating their good thermal stability.

Chapter 7 summarizes the results, salient conclusions and future prospect of the work reported in this thesis.

Glossary

CNSL	Cashew nut shell liquid
PET	Polyethylene terephthalate
T _g	Glass transition temperature
T ₁₀	10% Decomposition temperature
T _m	Melting transition
NaHCO ₃	Sodium bicarbonate
TLC	Thin layer chromatography
KOH	Potassium hydroxide
NaOH	Sodium hydroxide
PU	Polyurethane
PEU	Poly(ether urethane)s
DBTDL	Dibutyl tin dilurate
LMWOG	Low molecular weight organogelators
DSSC	Dye sensitized solar cells
SEM	Scanning electron microscopy
LiCl	Lithium chloride
J-V	Current-voltage
V _{oc}	Open circuit voltage
J _{sc}	Short circuit current
PTC	Phase transfer catalyst
TPC	Terephthalic acid chloride
IPC	Isophthalic acid chloride
FDCA	2,5-Furan dicarboxylic acid
FDAC	2,5-Furan dicarboxylic acid chloride
BPA	2,2-Bis(4-hydroxyphenyl)propane or bisphenol-A
BPF-1	4, 4'-(Furan-2-ylmethylene)bis(2,6-dimethoxyphenol)
BPF-2	4,4'-(Furan-2-ylmethylene)bis(2-methoxyphenol)
PE	Polyester
PC	Polycarbonate
BMI	1,1'-(Methylenedi-1,4-phenylene)bismaleimide
TEG	1,8-Bis(maleimido)-triethylene glycol
BTEAC	Benzyltriethylammonium chloride

ODA	4,4'-Oxydianiline
BPDA	3,3',4,4'-Biphenyl tetracarboxylic dianhydride
ODPA	4,4'-Oxydiphthalic anhydride
6-FDA	4,4'-(Hexafluoro isopropylidene)diphthalic anhydride
PAI	Poly(amide imide)
MD	Molecular dynamics
DSHC-3	4,4'-(Propane-1,3-diylbis(oxy))bis(3,5-dimethoxybenzohydrazide)
DVHC-3	4,4'-(Propane-1,3-diylbis(oxy))bis(3-methoxybenzohydrazide)
BDI	5,5'-Diisocyanato-2,2',3,3'-tetramethoxy-1,1'-biphenyl
PI	Polyimide
NMP	<i>N</i> -Methyl-2-pyrrolidone
DMAc	<i>N,N</i> -Dimethylacetamide
DMF	<i>N,N</i> -Dimethylformamide
THF	Tetrahydrofuran
CHCl ₃	Chloroform
η_{inh}	Inherent viscosity
GPC	Gel permeation chromatography
M _n	Number average molecular weight
M _w	Weight average molecular weight
WAXD	Wide angle X-ray diffraction
TGA	Thermogravimetric analysis
DSC	Differential scanning calorimetry

List of Tables

Table No.	Description	Page No.
1.1	List of selected commercialized bio-based polymers	3
1.2	CNSL-based difunctional condensation monomers	6
1.3	List of selected hemi-cellulose-based monomers	10
1.4	List of selected lignin-based monomers	15
3.1	Crystal data and structure refinement parameters for 1,3-bis(4-isocyanato-2-methoxyphenoxy)propane	66
3.2	X-Ray crystal data for 4,4'-(propane-1,3-diylbis(oxy))bis(3-methoxybenzohydrazide)	100
4a.1	Data on inherent viscosity, and molecular weight of poly(ether urethane)s	120
4a.2	Thermal properties of poly(ether urethane)s	122
4b.1	Inherent viscosity, molecular weight and % transmittance of poly(ether urethane)s	131
4b.2	Thermal properties of poly(ether urethane)s	134
4c.1	Gelation properties of 3% (w/v) solutions of PU-1, PU-2, PU-3 and PU-4 in various solvents	142
4c.2	Photovoltaic performance parameters of DSSC based on liquid electrolyte and polyurethane-based gel electrolyte with variable gelator concentration	151
4c.3	Photovoltaic performance parameters of DSSC using 3 wt. % polyurethane-based gel electrolyte	152
5a.1	Synthesis of aromatic polyesters from 4, 4'-(furan-2-ylmethylene)bis(2,6-dimethoxyphenol) and 4,4'-(furan-2-ylmethylene)bis(2-methoxyphenol) and aromatic diacid chlorides	162
5a.2	Thermal properties of polyesters derived from 4, 4'-(furan-2-ylmethylene)bis(2,6-dimethoxyphenol) and 4,4'-(furan-2-ylmethylene)bis(2-methoxyphenol) with aromatic diacid chlorides	166
5a.3	Mechanical properties of polyesters containing pendant furyl groups	169
5b.1	Synthesis of (co)polycarbonates from 4,4'-(furan-2-ylmethylene)bis(2-methoxyphenol) and/or bisphenol A with triphosgene	179
5b.2	Composition of copolycarbonate determined from ^1H NMR spectra	182
5b.3	Thermal properties of (co)polycarbonates	188
5b.4	Mechanical properties of (co)polycarbonates	192

5c.1	List of the selected crosslinkable polymers containing furyl as a pendant clickable group	198
5c.2	De-crosslinking temperature and absorbed energy for retro Diels-Alder reactions	204
5c.3	Mechanical properties of polyester and the corresponding crosslinked materials	205
5c.4	Mechanical properties of polycarbonate and the corresponding crosslinked materials	205
5c.5	Mechanical properties of recycled polyester	207
5c.6	Mechanical properties of recycled Polycarbonate	207
6a.1	Inherent viscosity and molecular weight data of poly(amideimide)s	221
6a.2	Solubility data of poly(amide imide)s	223
6a.3	Thermo-mechanical properties of poly(amide imide)s	225
6a.4	System details and calculated properties for poly(amideimide)s PAI-4 and PAI-1	229
6b.1	Synthesis of aromatic polyimides derived from 5,5'-diisocyanato-2,2',3,3'-tetramethoxy-1,1'-biphenyl and aromatic dianhydrides	240
6b.2	Solubility data of polyimides derived from 5,5'-diisocyanato-2,2',3,3'-tetramethoxy-1,1'-biphenyl and aromatic dianhydrides	242
6b.3	Thermal properties of polyimides derived from 5,5'-diisocyanato-2,2',3,3'-tetramethoxy-1,1'-biphenyl and aromatic dianhydrides	245

List of Schemes

Scheme No.	Description	Page No.
3.1	Synthesis of diisocyanates containing oxyalkylene linkage	59
3.2	Synthesis of diisocyanates containing biphenylene linkage starting from methyl vanillate	67
3.3	Synthesis of ω -hydroxyalkyleneoxy benzoyl azides starting from vanillic acid /syringic acid	77
3.4	Synthesis of bisphenols containing pendant furyl group	85
3.5	Synthesis of 4,4'-(1,3,4-oxadiazole-2,5-diyl)bis(2-methoxyphenol)	87
3.6	Synthesis of diacylhydrazide monomers starting from methyl vanillate/methyl syringate	94
3.7	Synthesis of diacyl hydrazide containing biphenyl linkage	101
3.8	Synthesis of dialdehyde/diol containing ester linkages starting from vanillin	103
3.9	Synthesis of diacids containing ester linkages starting from vanillic/syringic acid	107
4a.1	Synthesis of poly(ether urethane)s based on 1,3-bis(4-isocyanato-2-methoxyphenoxy)propane/1,3-bis(4-isocyanato-2,6-dimethoxyphenoxy)propane and aliphatic diols	119
4b.1	Synthesis of poly(ether urethane)s starting from ω -hydroxyalkyleneoxy benzoyl azides	130
5a.1	Synthesis of aromatic polyesters from 4, 4'-(furan-2-ylmethylene)bis(2,6-dimethoxyphenol)/4,4'-(furan-2-ylmethylene)bis(2-methoxyphenol) and aromatic diacid chlorides	161
5b.1	Synthesis of (co)polycarbonates from 4,4'-(furan-2-ylmethylene)bis(2-methoxyphenol) and/or bisphenol A and triphosgene	178
5c.1	Furan-maleimide Diels-Alder/retro Diels-Alder reaction	198
5c.2	Preparation of thermally reversible crosslinked polyester and polycarbonate from polymers containing pendant furyl groups and bismaleimide	203
6a.1	Synthesis of poly(amideimide)s from 4,4'-(propane-1,3-diylbis(oxy))bis(3-methoxybenzohydrazide)/4,4'-(propane-1,3-diylbis(oxy))bis(3,5-dimethoxybenzo hydrazide) and aromatic dianhydrides	220
6b.1	Synthesis of polyimides based on biphenylene containing diisocyanate and dianhydrides	239

List of Figures

Figure No.	Description	Page No.
1.1	Number of publications in each year on keyword 'bio-based polymers'	2
1.2	Chemical composition of industrial grade CNSL	5
1.3	Reactive sites of cardanol	6
1.4	Composition of lignocellulose	8
1.5	Synthesis and transformation of furans	9
1.6	A hypothetical native structure of lignin	12
1.7	Structure of monolignols of lignin	13
1.8	Building-blocks obtained from depolymerization of lignin	14
2.1	The theme of the thesis	35
3.1	New difunctional monomers synthesized in the present work starting from lignin-derived aromatics	38
3.2	¹ H NMR spectrum of 4,4'-(propane-1,3-diylbis(oxy))bis(3,5-dimethoxybenzoic acid) in DMSO-d ₆	59
3.3	¹³ C NMR spectrum of 4,4'-(propane-1,3-diylbis(oxy))bis(3,5-dimethoxybenzoic acid) in DMSO-d ₆	60
3.4	FT-IR spectrum of 4,4'-(propane-1,3-diylbis(oxy))bis(3,5-dimethoxybenzoyl azide)	61
3.5	¹ H NMR spectrum of 4,4'-(propane-1,3-diylbis(oxy))bis(3,5-dimethoxybenzoyl azide) in CDCl ₃	62
3.6	¹³ C NMR spectrum of 4,4'-(propane-1,3-diylbis(oxy))bis(3,5-dimethoxybenzoyl azide) in CDCl ₃	62
3.7	FT-IR spectrum of 1,3-bis(4-isocyanato-2,6 dimethoxyphenoxy) propane	63
3.8	¹ H NMR spectrum of 1,3-bis(4-isocyanato-2,6-dimethoxyphenoxy)propane in CDCl ₃	64
3.9	¹³ C NMR spectrum of 1,3-bis(4-isocyanato-2,6-dimethoxyphenoxy)propane in CDCl ₃	64
3.10	ORTEP diagram of 1,3-bis(4-isocyanato-2-methoxyphenoxy) propane	65
3.11	Molecular packing viewed the down <i>b</i> -axis showing layered arrangement on the <i>ac</i> plane	65
3.12	¹ H NMR spectrum of dimethyl 6,6'-dihydroxy-5,5'-dimethoxy-[1,1'-biphenyl]-3,3'-dicarboxylate in DMSO-d ₆	68
3.13	¹³ C NMR spectrum of dimethyl 6,6'-dihydroxy-5,5'-dimethoxy-[1,1'-biphenyl]-3,3'-dicarboxylate in DMSO-d ₆	68

3.14	FT-IR spectrum of dimethyl 5,5',6,6'-tetramethoxy-[1,1'-biphenyl]-3,3'-dicarboxylate	69
3.15	¹ H NMR spectrum of dimethyl 5,5',6,6'-tetramethoxy-[1,1'-biphenyl]-3,3'-dicarboxylate in CDCl ₃	70
3.16	¹³ C NMR spectrum of dimethyl 5,5'-dimethoxy-6,6'-bis(pentyloxy)-[1,1'-biphenyl]-3,3'-dicarboxylate in CDCl ₃	70
3.17	FT-IR spectrum of 5,5',6,6'-tetramethoxy-[1,1'-biphenyl]-3,3'-dicarboxylic acid	71
3.18	¹ H NMR spectrum of 5,5',6,6'-tetramethoxy-[1,1'-biphenyl]-3,3'-dicarboxylic acid in DMSO-d ₆	72
3.19	¹³ C NMR spectrum of 5,5',6,6'-tetramethoxy-[1,1'-biphenyl]-3,3'-dicarboxylic acid in DMSO-d ₆	72
3.20	FT-IR spectrum of 5,5',6,6'-tetramethoxy-[1,1'-biphenyl]-3,3'-dicarbonyl diazide	73
3.21	¹ H NMR spectrum of 5,5',6,6'-tetramethoxy-[1,1'-biphenyl]-3,3'-dicarbonyl diazide in CDCl ₃	74
3.22	¹³ C NMR spectrum of 5,5',6,6'-tetramethoxy-[1,1'-biphenyl]-3,3'-dicarbonyl diazide in CDCl ₃	74
3.23	FT-IR spectrum of 5,5'-diisocyanato-2,2',3,3'-tetramethoxy-1,1'-biphenyl	75
3.24	¹ H NMR spectrum of 5,5'-diisocyanato-3,3'-dimethoxy-2,2'-bis(pentyloxy)-1,1'-biphenyl	76
3.25	¹³ C NMR spectrum of 5,5'-diisocyanato-3,3'-dimethoxy-2,2'-bis(pentyloxy)-1,1'-biphenyl	76
3.26	FT-IR spectrum of methyl 4-((11-hydroxyundecyl)oxy)-3,5-dimethoxybenzoate	78
3.27	¹ H NMR spectrum of methyl 4-((11-hydroxyundecyl)oxy)-3,5-dimethoxybenzoate in CDCl ₃	78
3.28	¹³ C NMR spectrum of methyl 4-((11-hydroxyundecyl)oxy)-3,5-dimethoxybenzoate in CDCl ₃	79
3.29	FT-IR spectrum of 4-((11-hydroxyundecyl)oxy)-3,5-dimethoxybenzoic acid	80
3.30	¹ H NMR spectrum of 4-((11-hydroxyundecyl)oxy)-3,5-dimethoxybenzoic acid in DMSO-d ₆	80
3.31	¹³ C NMR spectrum of 4-((11-hydroxyundecyl)oxy)-3,5-dimethoxybenzoic acid in DMSO-d ₆	81
3.32	FT-IR spectrum of 4-((11-hydroxyundecyl)oxy)-3,5-dimethoxybenzoyl azide	82
3.33	¹ H NMR spectrum of 4-((11-hydroxyundecyl)oxy)-3,5-dimethoxybenzoyl azide in CDCl ₃	83
3.34	¹³ C NMR spectrum of 4-((11-hydroxyundecyl)oxy)-3,5-	83

	dimethoxybenzoyl azide in CDCl_3	
3.35	FT-IR spectrum of 4, 4'-(furan-2-ylmethylene)bis(2,6-dimethoxyphenol).	86
3.36	^1H NMR spectrum of 4, 4'-(furan-2-ylmethylene)bis(2,6-dimethoxyphenol) in CDCl_3	86
3.37	^{13}C NMR spectrum of 4, 4'-(furan-2-ylmethylene)bis(2,6-dimethoxyphenol) in CDCl_3	87
3.38	^1H NMR spectrum of (hydrazine-1,2-dicarbonyl)bis(2-methoxy-4,1-phenylene) diacetate in DMSO-d_6 .	88
3.39	^{13}C NMR spectrum of (hydrazine-1,2-dicarbonyl)bis(2-methoxy-4,1 phenylene) diacetate in DMSO-d_6	89
3.40	FT-IR spectrum of (1,3,4-oxadiazole-2,5-diyl)bis(2-methoxy-4,1-phenylene) diacetate.	90
3.41	^1H NMR spectrum of (1,3,4-oxadiazole-2,5-diyl)bis(2-methoxy-4,1-phenylene) diacetate in DMSO-d_6	91
3.42	^{13}C NMR spectrum of (1,3,4-oxadiazole-2,5-diyl)bis(2-methoxy-4,1-phenylene) diacetate in DMSO-d_6	91
3.43	FT-IR spectrum of 4,4'-(1,3,4-oxadiazole-2,5-diyl)bis(2-methoxyphenol)	92
3.44	^1H NMR spectrum of 4,4'-(1,3,4-oxadiazole-2,5-diyl)bis(2-methoxyphenol) in DMSO-d_6	93
3.45	^{13}C NMR spectrum of 4,4'-(1,3,4-oxadiazole-2,5-diyl)bis(2-methoxyphenol) in DMSO-d_6	93
3.46	HRMS spectrum of 4,4'-(1,3,4-oxadiazole-2,5-diyl)bis(2-methoxyphenol)	94
3.47	FT-IR spectrum of dimethyl 4,4'-(propane-1,3-diylbis(oxy))bis(3,5-dimethoxybenzoate)	95
3.48	^1H NMR spectrum of dimethyl 4,4'-(propane-1,3-diylbis(oxy))bis(3,5-dimethoxybenzoate) in CDCl_3	96
3.49	^{13}C NMR spectrum of dimethyl 4,4'-(propane-1,3-diylbis(oxy))bis(3,5-dimethoxybenzoate) in CDCl_3	96
3.50	FT-IR spectrum of 4,4'-(propane-1,3-diylbis(oxy))bis(3-methoxybenzohydrazide)	97
3.51	^1H NMR spectrum of 4,4'-(propane-1,3-diylbis(oxy))bis(3,5-dimethoxybenzohydrazide) in DMSO-d_6	98
3.52	^{13}C NMR spectrum of 4,4'-(propane-1,3-diylbis(oxy))bis(3,5-dimethoxybenzohydrazide) in DMSO-d_6	98
3.53	ORTEP diagram for DVHzC-3	99
3.54	Molecular packing viewed down b-axis showing association of adjoining molecules through N-H \cdots O, N-H \cdots π and C-H \cdots O interactions	101

3.55	FT-IR spectrum of 5,5'-dimethoxy-6,6'-bis(pentyloxy)-[1,1'-biphenyl]-3,3'-dicarbohydrazide	102
3.56	¹ H NMR spectrum of 5,5'-dimethoxy-6,6'-bis(pentyloxy)-[1,1'-biphenyl]-3,3'-dicarbohydrazide in DMSO-d ₆	102
3.57	FT-IR spectrum of bis(4-formyl-2-methoxyphenyl) succinate	104
3.58	¹ H NMR spectrum of bis(4-formyl-2-methoxyphenyl) succinate in CDCl ₃	104
3.59	¹³ C NMR spectrum of bis(4-formyl-2-methoxyphenyl) succinate in CHCl ₃	105
3.60	FT-IR spectrum of (4-(hydroxymethyl)-3-methoxyphenyl) succinate	106
3.61	¹ H NMR spectrum of (4-(hydroxymethyl)-3-methoxyphenyl) succinate in CDCl ₃	106
3.62	FT-IR spectrum of 4,4'-((furan-2,5-dicarbonyl)bis(oxy))bis(3-methoxybenzoic acid)	108
3.63	¹ H NMR spectrum of 4,4'-((furan-2,5-dicarbonyl)bis(oxy))bis(3-methoxybenzoic acid) in DMSO-d ₆	109
3.64	¹³ C NMR spectrum of 4,4'-((furan-2,5-dicarbonyl)bis(oxy))bis(3-methoxybenzoic acid) in DMSO-d ₆	109
4a.1	Applications of polyurethanes	115
4a.2	Reported synthetic strategies to polyurethanes <i>via</i> non-isocyanate routes	116
4a.3	FT-IR spectrum of poly(ether urethane) (PU-4) derived from 1,3-bis(4-isocyanato-2,6-dimethoxyphenoxy)propane and 1,12-dodecanediol	120
4a.4	¹ H NMR spectrum (in DMSO-d ₆) of poly(ether urethane) (PU-4) derived from 1,3-bis(4-isocyanato-2,6-dimethoxyphenoxy)propane and 1,12-dodecanediol	121
4a.5	¹³ C NMR spectrum (in DMSO-d ₆) of poly(ether urethane) (PU-4) derived from 1,3-bis(4-isocyanato-2,6-dimethoxyphenoxy)propane and 1,12-dodecanediol	121
4a.6	TG curves of poly(ether urethane)s	122
4a.7	DSC curves of poly(ether urethane)s	123
4b.1	FT-IR spectrum of poly(ether urethane) (PEU 3)	131
4b.2	¹ H NMR spectrum of PEU-3 in DMSO-d ₆	132
4b.3	¹³ C NMR spectrum of PEU-3 in DMSO-d ₆	133
4b.4	TG curves of poly(ether urethane)s	134
4b.5	DSC curves of poly(ether urethane)s	135
4c.1	Structures of poly urethanes for gel study	142

4c.2	Photograph of polyurethane gel	143
4c.3	SEM image of polyurethane-based xerogel gel	144
4c.4	LiCl mediated gel-sol transformation of polyurethane-based organogel in DMF	144
4c.5	DSC curves of polyurethane (PU-1) organogel	145
4c.6	(a) Amplitude and (b) frequency sweep measurements of polyurethane gel in DMF (3 wt. %)	146
4c.7	Plot of the storage modulus (G') versus concentration of polyurethane gels prepared in DMF	146
4c.8	Histogram of the <i>gel-to-sol</i> and <i>sol-to-gel</i> transition of polyurethane organogel in DMF (3 wt %). Storage and loss modulus is plotted as a function of temperature and time	147
4c.9	Schematic representation of the components of DSSC	148
4c.10	Current-voltage characteristics of the DSSCs using liquid and polyurethane-based gel electrolytes	150
4c.11	Current-voltage characteristics of DSSCs using 3 wt. % polyurethane-based gel electrolytes	151
5a.1	FT-IR spectrum of polyester (PE-3) derived from 4,4'-(furan-2-ylmethylene)bis(2,6-dimethoxyphenol) and 2,5-furan dicarboxylic acid chloride	163
5a.2	^1H NMR spectrum of polyester (PE-3) derived from 4,4'-(furan-2-ylmethylene)bis(2,6-dimethoxyphenol) and 2,5-furan dicarboxylic acid chloride in CDCl_3	163
5a.3	^{13}C NMR spectrum of polyester (PE-3) derived from 4,4'-(furan-2-ylmethylene)bis(2,6-dimethoxyphenol) and 2,5-furan dicarboxylic acid chloride in CDCl_3	164
5a.4	X-Ray diffractograms of aromatic polyesters containing pendant furyl groups	165
5a.5	TG curves of aromatic polyesters containing pendant furyl group	167
5a.6	DTG curves of aromatic polyesters derived from BPF-1 and 2, 5-furan dicarboxylic acid chloride	167
5a.7	DSC curves of aromatic polyesters containing pendant furyl groups	168
5a.8	Stress-Strain curves of aromatic polyesters containing pendant furyl groups	170
5b.1	GPC trace of polycarbonate (PC-2) derived from 4,4'-(furan-2-ylmethylene)bis(2-methoxyphenol): bisphenol A (50:50 mol. %) and triphosgene 1	180
5b.2	FT-IR spectrum of polycarbonate (PC-1) derived from 4,4'-(furan-2-ylmethylene)bis(2-methoxyphenol) and triphosgene	181
5b.3	^1H NMR spectrum of polycarbonate (PC-1) derived from 4,4'-(furan-2-ylmethylene)bis(2-methoxyphenol) and triphosgene in	181

	CDCl ₃	
5b.4	¹³ C NMR spectrum of polycarbonate (PC-1) derived from 4,4'-(furan-2-ylmethylene)bis(2-methoxyphenol) and triphosgene in CDCl ₃	182
5b.5	¹ H-NMR spectrum of polycarbonate (PC-2) derived from 4,4'-(furan-2-ylmethylene)bis(2-methoxyphenol): bisphenol A (50:50 mol %) and triphosgene in CDCl ₃	183
5b.6	Possible arrangement of monomers in copolycarbonate	184
5b.7	HMBC spectra of PC-2 in CDCl ₃	185
5b.8	¹³ C NMR spectra of (co)polycarbonates (PC-1, PC-2 and PC-5) in CDCl ₃	186
5b.9	X-Ray diffractograms of (co)polycarbonates	187
5b.10	TG curves of (co)polycarbonates	189
5b.11	DTG curve of PC-2 derived from 4,4'-(furan-2-ylmethylene)bis(2-methoxyphenol): bisphenol A (50:50 mol %) and triphosgene	189
5b.12	DSC curves of (co)polycarbonates	190
5b.13	T _g as a function of composition BPF-2 in copolycarbonates derived from mixture of BPF-1 and BPA with triphosgene	191
5b.14	Stress-strain curves of (co)polycarbonates	193
5c.1	DSC curves of first and second heating cycle of crosslinked polyester (PE6-BMI) (A) and polycarbonate (PC50-BMI) (B)	203
5c.2	Solubility test of crosslinked and de-crosslinked polymers	204
5c.3	Stress-strain curves of polyester/polycarbonate and the corresponding crosslinked materials	205
5c.4	Thermoreversibility of crosslinked polymers	206
5c.5	Stress-strain curves of recycled crosslinked polyester/polycarbonate	207
5c.6	Sol-gel transition of polymeric organogel	208
5c.7	Log-log plot of strain dependence versus storage and loss modulus of PE6-BMI-based gel.	209
5c.8	The angular frequency dependence of storage and loss modulus of PE6-BMI-based gel	210
5c.9	Thermo-reversibility of gel with repeated heating and cooling cycles from 40-120 °C and 120-40 °C	211
6a.1	FT-IR spectrum of PAI-1	221
6a.2	¹ H NMR spectrum of PAI-1 in DMSO-d ₆	222
6a.3	¹³ C NMR spectrum of PAI-1 in DMSO-d ₆	223
6a.4	X-Ray diffractograms of poly(amideimide)s	224
6a.5	TG curves of poly(amide imide)s	224

6a.6	DSC curves of poly(amideimide)s	226
6a.7	Dynamic mechanical curves of poly(amide imide)s	226
6a.8	Optimized geometries of (A) PAI-4 (B) PAI-1. The dihedral angle (α) between phenyl ring and oxyalkylene linkage is marked	228
6a.9	T_g of poly(amideimide)s measured by MD simulation. A. Poly(amideimide) based on DVHzC-3 (PAI-4) B. Poly(amide imide) based on DSHzC-3 (PAI-1)	229
6a.10	(A) RDF between the centres of mass of chains (B) RDF between the centres of mass of phenyl rings with other atoms in single chains	230
6a.11	Snapshots depicting distance between centre of mass of two chains: green and purple-carbon; blue-nitrogen; white-hydrogen; pink spheres: centre of mass of chains	230
6a.12	(A) Torsional angle distributions of PAI-4 and PAI-1 (B) Rotational energy barrier from PMF for PAI-4 and PAI-1	231
6a.13	Comparison of the decay of dihedral autocorrelation function ($C(t)$) for PAI-4 and PAI-1	232
6b.1	FT-IR spectrum of polyimide (PI-5) derived from BDI and aromatic dianhydrides	240
6b.2	^1H NMR spectrum of polyimide derived from BDI and PMDA in DMSO-d_6	241
6b.3	^{13}C NMR spectrum of polyimide derived from BDI and PMDA in DMSO-d_6	242
6b.4	X-Ray diffractograms of polyimides from BDI	243
6b.5	TG curves of polyimides and DTG curve of PI-2	244
6b.6	DSC curves of polyimides	246

Chapter - 1

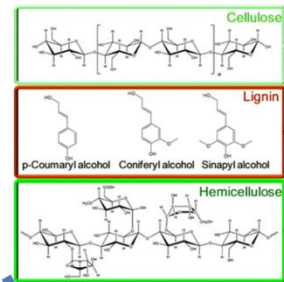
Introduction and Literature Survey



Biomass



Biorefinery



**Cellulose,
Hemi-Cellulose
and Lignin**



Bio-Based Product Development



Products

1.1 Introduction

It is difficult to imagine modern human life without the use of polymers. Polymers/plastics are one of the most commonly used materials for modernization of the world as well as to fulfil basic human needs such as food, clothing, health, shelter, transportation, etc. It is estimated that worldwide production of polymers has exceeded 311 million tonnes in 2014¹ and demand of polymers is increasing continuously along with increasing population and modernization of the world.

Generally, polymers are prepared by two common methods: chain-growth polymerization and step-growth polymerization. Step growth polymers are found as thermoplastics as well as thermosets. The prominent examples of thermoplastic polymers are linear polyesters, polycarbonates, poly(arylene ether)s, polyamides, polyimides and polyurethanes and examples of thermosets are epoxy resins, cyanate esters, polybenzoxazines, and crosslinked polyurethanes. Step-growth polymers have received tremendous demand for diverse applications, depending on their properties²⁻⁵.

Polyesters, for example, have been extensively used in various fields such as clothing, packaging, and coating applications. Furthermore, fully aromatic polyesters are known as engineering plastics because of their excellent mechanical, thermal and electrical properties and find applications in the automotive, aviation and electrical industries^{6,7}. Polycarbonates are tough and transparent materials and are mostly used in windshields, safety helmets, bulletproof glass, etc⁸. In addition, aliphatic polycarbonates are used for bio-medical applications due to their biodegradability, low-toxicity and good bio-comparability⁹⁻¹¹. Aliphatic polyamides are widely used in clothing, fibers, packaging, membranes, carpets and so on^{12,13} and the well-known class of aliphatic polyamide is Nylon^{14,15}. Aromatic polyamides and polyimides have outstanding properties such as thermo-oxidative stability, excellent mechanical and electrical properties and they find applications in gas separation membranes, polyelectrolytes, fuel cells, photoresists, liquid crystal alignments, electroluminescent devices, electrochromic materials, nanomaterial composites, blending applications, vapour phase depositions, and polymer memory materials¹⁶⁻²⁰. Polyurethane is the only class of versatile polymers which is found in thermoplastic, thermoset and elastomer materials. Polyurethanes are widely used in flexible foams, elastomeric materials, coatings, and adhesives²¹⁻²⁵.

The starting materials used for the synthesis of step-growth polymers such as polyesters, polycarbonates, polyamides, polyimides and polyurethanes are predominantly prepared from fossil resources, which are non-renewable²⁶⁻²⁸. Fossil resources are the

major source of fuels and industrial chemicals. Polymer industry consumes fossil resources to the tune of 7 %²⁹. However, complete dependence on petroleum resources is at risk because of its inexplicable limitations such as increasing pollution level and health hazards, continuous depletion of crude oil, gas emission, disposal, and non-recyclability^{27,30–34}.

Over the last several years, number of researchers have investigated new difunctional monomers from alternative sources *viz.* renewable resources. A variety of bio-based difunctional monomers and polymers have been reported based on agricultural products such as monosaccharides, starch, cellulose, fatty acids, lactic acid, natural amino acids and so on^{35–42}. Research programs are being ubiquitously administered for escalating need in the form of the increased funds for production of biomass-derived chemicals and polymers by the concerned Organizations and Institutions (e.g. EU, UNIDO, INCU, etc.) and the private industries⁴³. These efforts have been reflected in the form of rising number of scientific journals, papers, reviews, patents, books and conferences (**Figure 1.1**) as well as in the form of commercial products with maximum renewable carbon content. The selected examples of commercial renewable polymers are listed in **Table 1.1**.

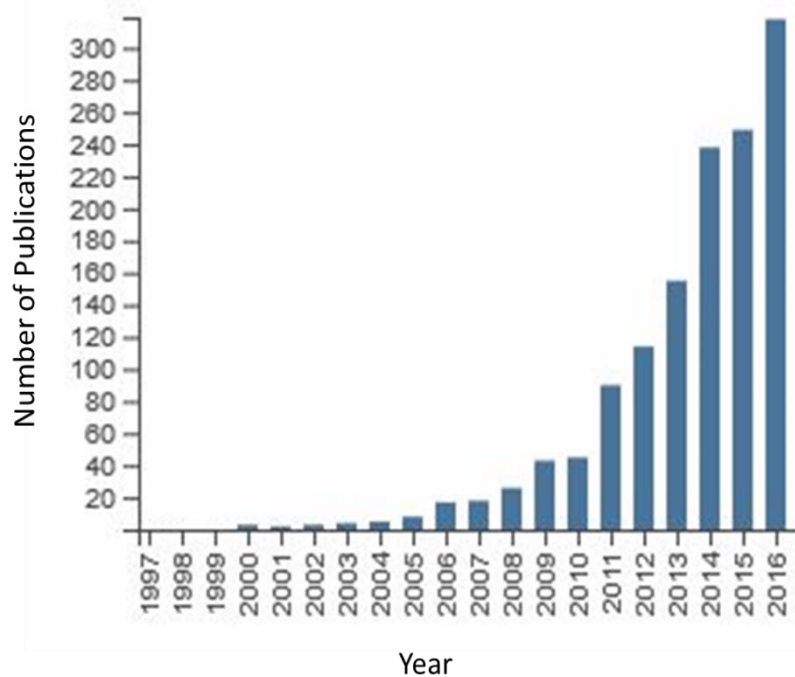


Figure 1.1 Number of publications in each year on keyword ‘bio-based polymers’ (Source: Web of Science)

Table 1.1 List of selected commercialized bio-based polymers⁴⁴⁻⁵⁰

Sr. No.	Renewable Resource	Polymer Class	Brand Name
1	Castor oil	Polyamide	Rilsan®
2	Castor oil	Thermoplastic polyurethane	Pearlthane®
3	Starch	Poly(trimethylene terephthalate)	Sorona®
4	Starch	Polyester	Hytrel®
5	Starch	Polyethylene	I'm green™
6	Starch	Poly(lactic acid)	Biomax®
7	Starch	Copolyamide	Ultramid®
8	Hemi-cellulose	Poly(ethylene furanoate)	

One of the main concerns in the large scale production of bio-based polymers is the utilization of edible feedstocks *viz.* sugars, starches, and vegetable oils. Firstly, they compete with food for their feedstock and/or fertile land and directly affect on food prices. Secondly, their potential availability is limited by the amount of fertile soil and the yield per hectare. These issues have motivated academic and industrial researchers to develop new bio-based monomers and polymers from non-edible resources such as lignocellulose, CNSL and so on⁵¹⁻⁵⁶. Sustainable production of bio-based polymers can be achieved from such resources without affecting food supply chain.

The current research efforts in the field of preparation of renewable polymers are focused on two strategies: a) synthesis of bio-based polymers containing 100 % renewable carbon content and ii) synthesis of bio-based polymers containing partial renewable carbon content. The industrial transition from fossil-based chemicals towards renewable resource-based chemicals is quite challenging and would not be possible without interdisciplinary approach^{26,57}.

The production of commodity chemicals from biomass is not necessarily atom efficient and does not take advantage of the range of functionalities Nature has to offer. Introducing these functionalities starting from conventional petrochemicals is not trivial and requires a number of synthetic steps, resulting in lower atom efficiency and lower yields compared to renewable monomers. Therefore, natural compounds should be used with minimal alteration to provide monomers which give rise to novel polymers with differentiated properties.

Most of the bio-based polymers are aliphatic and/or cyclo-aliphatic in nature^{58,59}. An extensive work has been carried out on the use of isosorbide and its derivatives as monomers for the synthesis of a range of polymers such as polyesters, polyamides, polyurethanes, etc⁶⁰. It is to be noted that polymers based on aliphatic monomers have limited applications due to their poor mechanical properties, lower thermal stability and low glass transition temperature^{61–63}. On the other hand, aromatic/semi-aromatic polymers exhibit good thermo-mechanical properties with additional superior properties such as rigidity, hydrophobicity, and fire resistance^{20,64}. Semi-aromatic polyesters such as poly(ethylene terephthalate) (PET) exhibit excellent thermomechanical and barrier properties and around 24 million tonnes of PET was produced worldwide in 2015⁵². Aromatic polyimides like Kapton® have superior thermo-mechanical properties and chemical resistance and are used for high performance applications⁶⁴. Bisphenol-A is one of the notable aromatic monomers used for the synthesis of diverse classes of polymers such as polycarbonates, polyesters, polyetherketones, polyethersulfones, cyanate esters and epoxy resins. The global annual production of BPA has reached up to 5.4 million tonnes in 2015⁵². All these aromatic/semi-aromatic polymers and monomers are currently industrially prepared from petroleum resources. Therefore, it is of interest to design aromatic/semi-aromatic monomers and polymers from renewable resources.

The thesis focuses on the study of the utilization of non-edible renewable resources as starting materials for synthesis of difunctional monomers and polymers therefrom. The aliphatic bio-based monomers and polymers have already been reviewed in the literature^{65,66}. The present chapter deals with the general introduction to renewable resources useful as starting materials for synthesis of aromatic difunctional monomers and step growth polymers. Specifically, the chapter gives a brief survey on the monomers and polymers derived from aromatic renewable resources *viz.* hemi-cellulose, lignin and cashew nut shell liquid (CNSL)^{26,51–53,67–69}.

1.2 Aromatic step growth monomers starting from renewable resources

The major sources of aromatic chemicals from renewable resources are cashew nut shell liquid (CNSL) obtained as a by-product of cashew industry, and lignocellulose-obtained from wood^{51,54–56,67,70–75}.

1.2.1 CNSL-based step-growth monomers

Cashew nut shell liquid (CNSL) is a greenish-yellow viscous liquid in the soft honeycomb of the shell of the cashew nut. CNSL is a by-product of cashew processing

industry and is abundantly available (In 2013, 44,50,000 metric tons per year), in many parts of the world especially Brazil, India, Bangladesh, Kenya, Tanzania, Mozambique, South-East and Far-East Asia, and tropical regions of Africa⁷⁶⁻⁸². A number of methods are applied for the extraction of oil from cashew nut shell, among them two popular methods are 1) cold processed CNSL- oil extracted by using solvents such as benzene, toluene, petroleum hydrocarbon solvents or alcohols^{78,83} or supercritical extraction of the oil using a mixture of CO₂ and isopropyl alcohol^{84,85}. The major components of cold-processed CNSL are anacardic acid (60–70%) and cardol (20–25%) 2) Hot processed CNSL- this method produces cardanol (60–70%) and cardol (20–25%) as major products^{55,56,86,87} Chemical composition of industrial grade CNSL is shown in **Figure 1.2**.

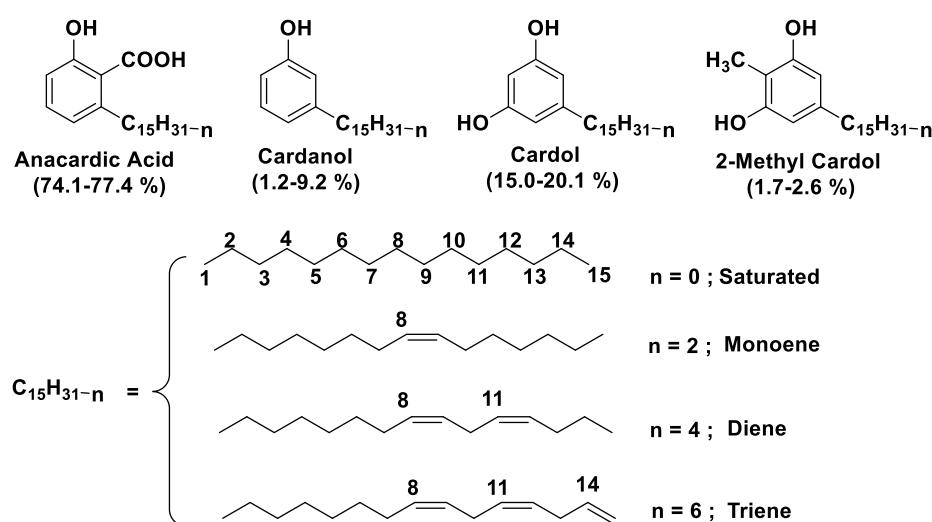


Figure 1.2 Chemical composition of industrial grade CNSL

Amongst the component of CNSL oil, anacardic acid is highly toxic in nature and exhibits medicinal properties such as antimicrobial and antitumour activities, enzyme inhibitor for tyrosinase and acetyltransferase. Industrial CNSL rarely contains anacardic acid because the anacardic acid gets converted into cardanol by decarboxylation while roasting at high temperature^{56,88,89}.

CNSL has been found to be interesting renewable resource for polymer synthesis due to the presence of unsaturated 15- carbon chain and phenolic moiety. As one can imagine, this entails that all organic chemistry around phenol and unsaturation could be used for modification of CNSL (**Figure 1.3**). The long aliphatic chain (15-carbon) provides hydrophobicity as well as processability for polymers synthesized from CNSL-based chemicals⁵⁶.

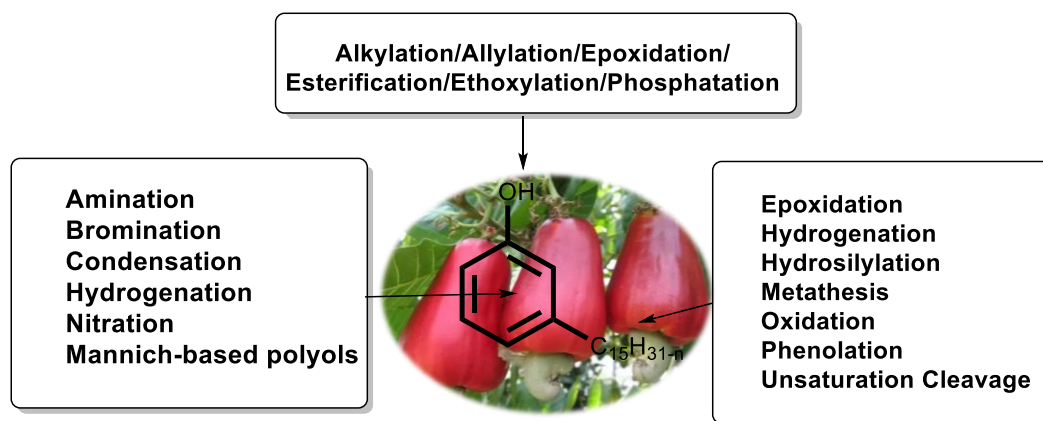
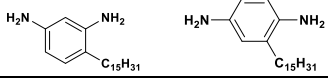
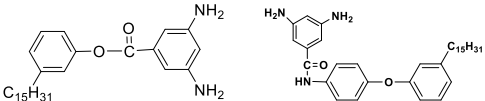
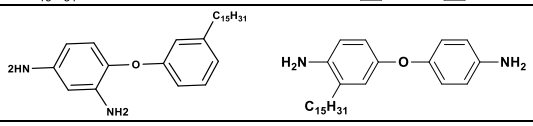
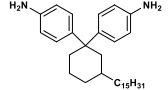
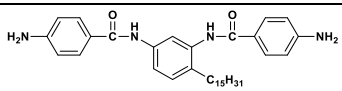
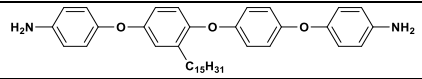
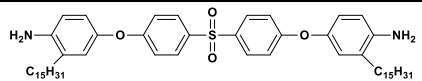
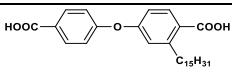
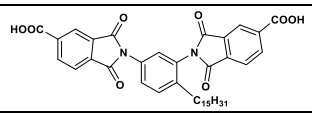
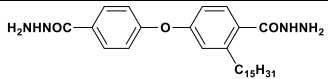
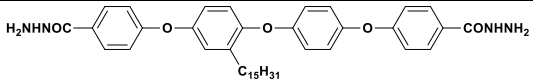
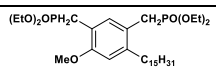
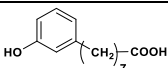


Figure 1.3 Reactive sites of cardanol

A number of difunctional monomers such as diamines, diacids, diols, diacylhydrazides, dialdehydes, etc have been reported from cardanol^{55,56,70}. A series of step growth polymers such as polyimides, polyamides, poly(azomethine)s, poly(amide imide)s, poly(ester imide)s, polyesters, polyhydrazides, poly(1,3,4-oxadiazole)s, etc. have been synthesized from cardanol-based difunctional monomers. The list of selected monomers derived from CNSL is presented in **Table 1.2**.

Table 1.2 CNSL-based difunctional condensation monomers

Sr.N	Monomers	Polymers	Ref.
1		Polycarbonates, (Co)polyesters	90 91
2		Poly(arylene ether)s, Polyurethanes	92 93,94
3		(Co)polyesters, Poly(arylene ether)s, Poly(ether ether ketone)s	95–98
		Polycarbonate	99
4		-	100
5		Epoxy resins	101

6		Polyimides, Polyamides and Polyazomethines	102–104
7		Polyimides and Polyamides	105
8		Polyimides, Polyamides Polyazomethines	105 106
9		(Co)polyimides	95,107
10		Poly(amide imide)s	108
11		Polyimides	109
12		Polyamides and Polyimides	110
13		Polyamides	111
14		Poly(ester imide)s	112
15		Poly(amide imide)s, Polyhydrazides and Poly(1,3,4-oxadiazole)s	113–115
16		Polyhydrazides and Poly(1,3,4-oxadiazole)s	92
17		Poly(<i>m</i> -phenylenevinylene)s	116
18		Polyesters	117–119

Cardanol, which is a major constituent of CNSL, has been amply demonstrated to be an attractive bio-based starting material for the synthesis of various types of difunctional monomers. These difunctional monomers are a welcome addition to the existing portfolio of difunctional condensation monomers and represent useful (co)monomers for the synthesis of step-growth polymers with attractive processability characteristics. The cardanol-based polymers bear pendent C-15 chains, which disturbs the interchain packing of the polymers and enhances chain mobility. The incorporation of pendent C-15 chain in aromatic step growth polymers resulted in significant improvements in the solubility characteristics of polymers and processability of various polymer classes, *viz.* aromatic polyimides, aromatic polyamides, aromatic polyesters and so on^{55,56,91,92,111–114,120}.

1.2.2 Lignocellulose

Lignocellulose biomass is extremely attractive due to its abundant availability and economic viability compared to food crops. Lignocellulose is a mixture of three components *viz.* cellulose, hemicellulose, and lignin and their proportion is dependant on the source^{73,121–125} (**Figure 1.4**).

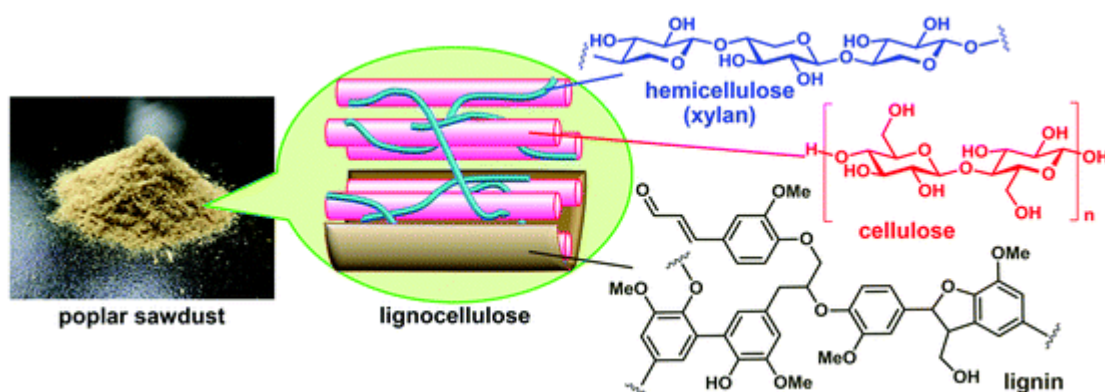


Figure 1.4 Composition of lignocellulose (Figure reproduced from H. Kobayashi and A. Fukuoka, *Green Chem.*, 2013, **15**, 1740. © 2014 Royal Society of Chemistry)⁷¹

Cellulose is a fibrous polysaccharide material containing linear chains of several hundreds to thousands β (1 \rightarrow 4) D-glucose ($C_6H_{10}O_5$)_n units. It is tough, water-insoluble and important substrate of primary cell wall of plant. Cellulose is mainly used for paper and textile products. It comprises approximately 40-50 % of the dry weight of plant material. Major source of renewable carbon present in the biosphere is in the form of cellulose and therefore production of fuels and value added chemicals from cellulose is of paramount importance¹²⁶.

Hemi-cellulose is a random and amorphous structure with approximate composition 23-32 % of the total dry weight of plant. Hemi-cellulose is the second most abundant polymer present in the biosphere which is made up of several heteropolymers including xylan, glucuronoxylan, arabinoxylan, galactomannan, glucomannan, and xyloglucan. The heteropolymers of hemicelluloses are composed of pentoses *viz.* xylose and arabinose and hexoses *viz.* mannose, glucose, and galactose. The pentoses and hexoses are potential starting materials for the synthesis of various furan derivatives^{126–129}.

Lignin is an aromatic crosslinked polymeric material, present in the internal part of plant cell wall. Lignin is an amorphous polymer containing three major components *viz.* coniferyl alcohol, sinapyl alcohol, and coumaryl alcohol^{74,130–132}.

1.2.2.1 Step growth monomers based on furan derivatives

Furan is a heterocyclic aromatic compound containing five membered ring. Furfural and 5-hydroxymethylfurfural (HMF) are well known starting materials for the synthesis of various renewable monomers and polymers. Furfural can be prepared from hemi-cellulose based pentose sugars by using strong acid catalyst such as sulphuric acid and hydrochloric acid (**Figure 1.5**). Further, HMF is also produced from hexose sugars and polysaccharides using similar process for furfural synthesis.

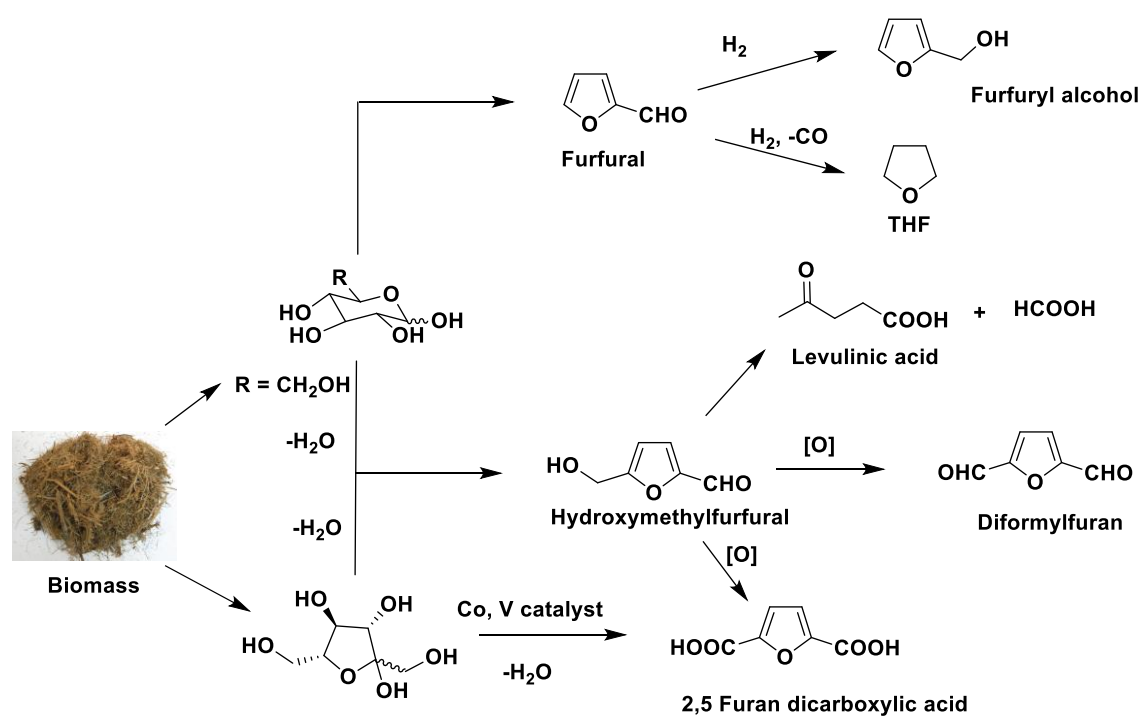


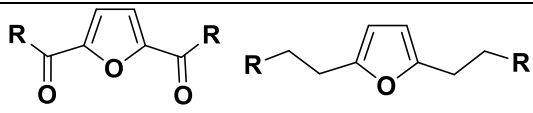
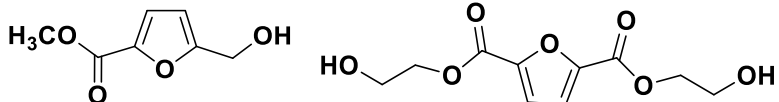
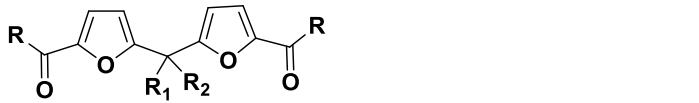
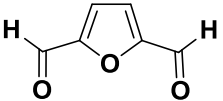
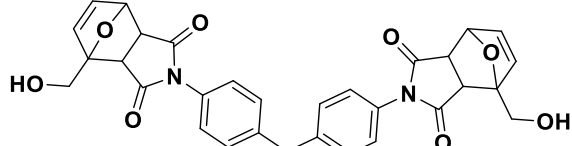
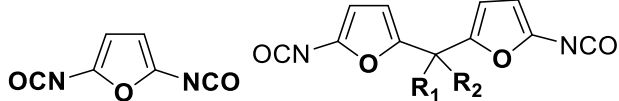
Figure 1.5 Synthesis and transformation of furans

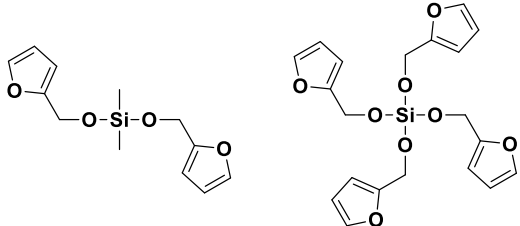
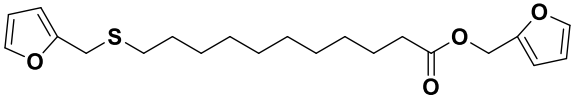
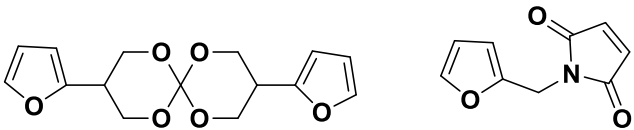
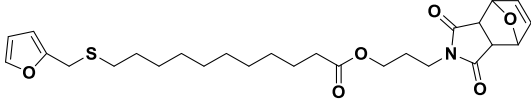
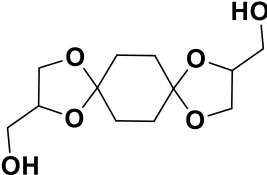
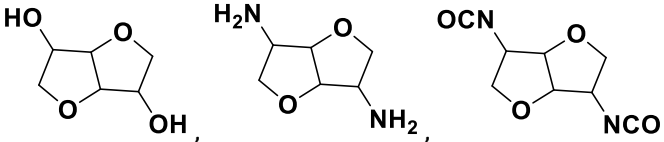
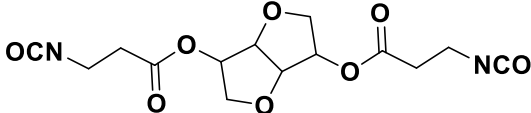
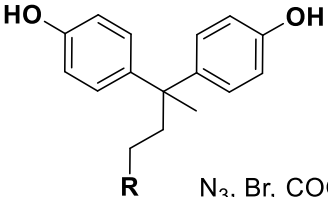
HMF is used for the synthesis of 2,5-furan dicarboxylic acid (FDCA), which is structurally mimic of the world's largest output dicarboxylic acid *i.e.* terephthalic acid. According to the ranking published by U.S. Department of Energy of the top twelve chemicals that can be produced from sugars, FDCA is second on the list. Terephthalic acid can be potentially replaced by FDCA for the synthesis of aliphatic-aromatic polyesters^{133–140}.

In addition to the furan-derived polyester, other polymers like furan derived polyamides have properties comparable to that of Kevlar¹⁴¹. Polyurethanes derived from furan-based monomers have thermoplastic elastomeric properties that enable formation of high graphenic residue on pyrolysis^{142,143}. Conjugated polymers and oligomers starting from furan-based monomers have good electronic conductivity on doping, photo- and electroluminescence and photo-cross-linking ability. Another advantage of furan containing polymers is to make smart polymer such as self-healing, and thermo-reversible polymers by click chemistry. Furan and some of its derivatives undergo Diels-Alder reaction which is a well known click reaction where furans act as diene¹⁴⁴⁻¹⁵³.

Diphenolic acid and bisphenols were prepared from levulinic acid, which is one of the top-ten platform chemicals, obtained from hemi-cellulosic waste^{154,155}. The list of selected monomers derived from hemi-cellulosic biomass is presented in **Table 1.3**

Table 1.3 List of selected hemi-cellulose-based monomers

Difunctional monomers	Polymers	Ref.
 $R = \text{OH}, \text{OCH}_3, \text{Cl},$ $R = \text{OH}, \text{NH}_2$	Polyesters, Polyamides, Polyurethanes	141,142, 156-158
	Polyesters	159
 $R = \text{OH}, \text{OCH}_3, \text{Cl}, \text{OC}_2\text{H}_5, \text{NHNH}_2$ $R_1 = \text{H}, \text{CH}_3, \text{C}_2\text{H}_5, \text{C}_6\text{H}_5$ $R_2 = \text{H}, \text{CH}_3, \text{C}_2\text{H}_5, \text{C}_6\text{H}_5$ 	Polyamides, Polyesters, Polyhydrazides, Poly(1,3,4-oxadiazole)s, Polyazomethines	160-164
	Polyurethanes, Polyesters	165
 $R_1 = \text{H}, \text{CH}_3$ $R_2 = \text{H}, \text{CH}_3$	NR	166,167

	Poly(furyl alcohol)	168
	AA monomer for DA polymerization by combination of furan and vegetable oil	169
	Diels-Alder polycondensation to form polyadducts	170
	AB monomer for DA polymerization	169
	Polyesters, Polycarbonates, Polyurethanes	171
	Polyesters, Polycarbonates, Polyurethanes, Polyamides, Polyacetals	172
	Polyurethanes	173
 <p style="text-align: center;">R N₃, Br, COOH, COOCH₃</p>	Polyesters, Polycarbonates	154,174–176

NR; not reported

1.2.2.2 Aromatic difunctional monomers based on lignin

'Lignin' is the term derived from Latin word '*lignum*' which means 'wood'. Anselme Payen first reported the reaction of wood with nitric acid and caustic soda and found two compounds, one is cellulose and other is called as incrusting material later which was named as lignin¹⁷⁷ (**Figure 1.6**). It is the second largest abundant natural

polymer after cellulose and contributing around 30% of all non-fossil renewable carbon content on the earth^{73,178–183}. Approximately 70 million tonnes of lignin is produced annually in the world as a by-product of paper and pulp industries and most of the lignin is utilized to generate energy in the plant. This material, which has been ignored in the past, is now being considered as a valuable resource^{54,132,184}. Additionally, based on interesting functionalities and properties, lignin offers perspective for higher value-added application such as polymer, carbon fiber, additive, food packaging, energy storage, biomedical applications and so on^{185–193}.

1.2.2.1 Chemical structure and physical properties of lignin

Lignin is a highly cross-linked amorphous aromatic polymer and is present around the hemicelluloses and cellulose in annual crops and trees. Lignin provides hydrophobicity, good strength, and structural support to woody plant. It also acts as a physical barrier to protect plant from pathogens and insect pest^{73,194}. Lignin is complex polyphenols compound and exact structure of lignin is not clear till now. Many authors predicted probable structure of lignin. A representative structure of lignin reported by Brunow et al.¹⁹⁵ is shown in **Figure 1.6**.

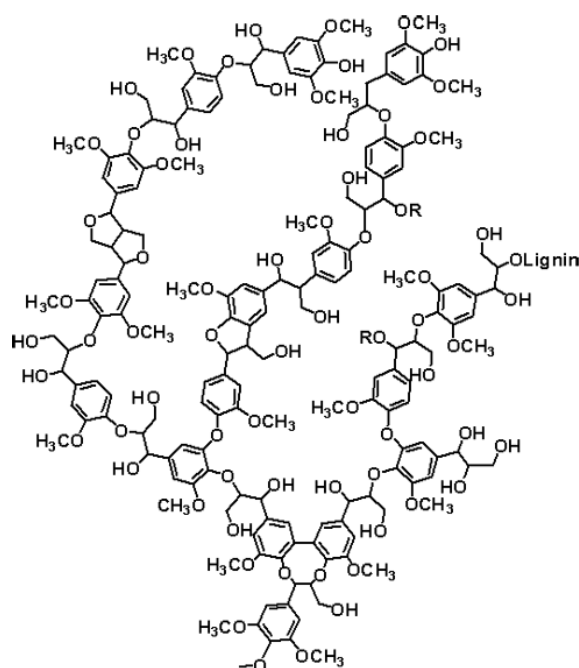


Figure 1.6 A hypothetical native structure of lignin

Lignin contains three phenylpropanes *viz.* syringyl, guaiacyl, and p-hydroxyphenyl units, originating from their respective monolignols *viz.* sinapyl alcohol, coniferyl alcohol, and coumaryl alcohol^{54,178,180,196–198} (**Figure 1.7**).

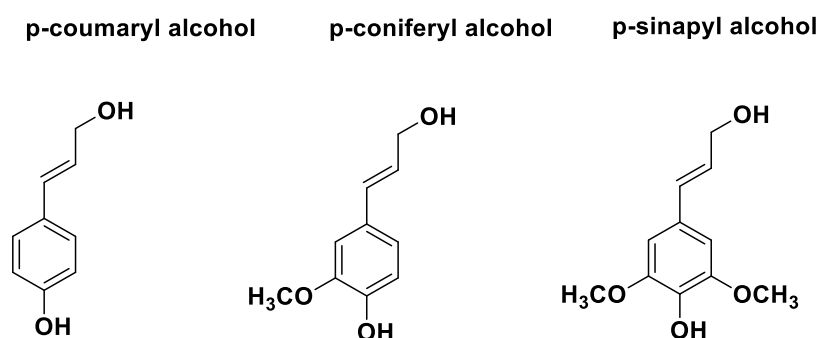


Figure 1.7 Structure of monolignols of lignin

Lignin is amorphous polymer and shows two local mode relaxation *viz.* glass transition temperature (T_g) and decomposition temperature (T_{10}). T_g values of lignin vary widely depending on the molecular weight, method of isolation, water content and thermal history. Goring¹⁹⁹ firstly reported T_g of different lignins, which is in the range of 127-277 °C. Irvine²⁰⁰ examined T_g of lignin isolated from different plant species as well as by different isolation methods and values were found in the range 90-150 °C. Thermal degradation of lignin is complex process due the presence of various oxygen-based functionalities. Lignin decomposes over broad range of temperature, first degradation starts due to the dehydration of hydroxyl moiety of benzylic group. Thereafter, second degradation takes place between 150-300 °C because of α -, β - aryl-alkyl-ether linkages. Finally, remaining part of lignin degrades at high temperature (500-700 °C) and 30-50 % char yield remained^{54,201,202}.

The isolation of various important components from the plant biomass is of great interest. A variety of processes have been reported to isolate lignin. However, the ideal standard procedure for the isolation of lignin does not exist yet. Each method produces different grades of lignin in terms of their physio-chemical properties and purity. Various methods have been used for the isolation of lignin such as kraft pulping process, sulfite pulping process, alkaline pulping process, organosolv pulping process and so on^{130,203-209}.

1.2.2.2.2 Chemical modification of lignin

Lignin is found in variety of structures based on the source and isolation process. In spite of these differences, two common functionalities are present in all the structures of lignin i.e. phenolic and phenylpropane hydroxyl groups. These functionalities of lignin provide an opportunity for further chemical modifications. The modification of lignin is carried out either by reaction on hydroxyl/phenol group or fragmentation of lignin into small aromatic molecules. Due to the presence of hydroxyl/phenol functionality, lignin can be directly used as a macromonomer for the synthesis of polyesters, polyurethanes,

epoxy resins, etc. Several research groups across the world have investigated and reviewed the possibility of conversion of lignin into useful aromatic compounds^{131,179,210–222}. Pyrolysis (thermolysis), hydrogenolysis, gasification, hydrolysis under supercritical conditions, and chemical oxidation are the common thermochemical methods studied for the depolymerization of lignin. These depolymerisation methods convert lignin to gaseous hydrocarbons, volatile liquids and substituted aromatics such as phenols, guaiacol, catechol, vanillic acid, syringic acid, vanillin, syringol, eugenol, ferulic acid, etc^{210,223–229} (Figure 1.8).

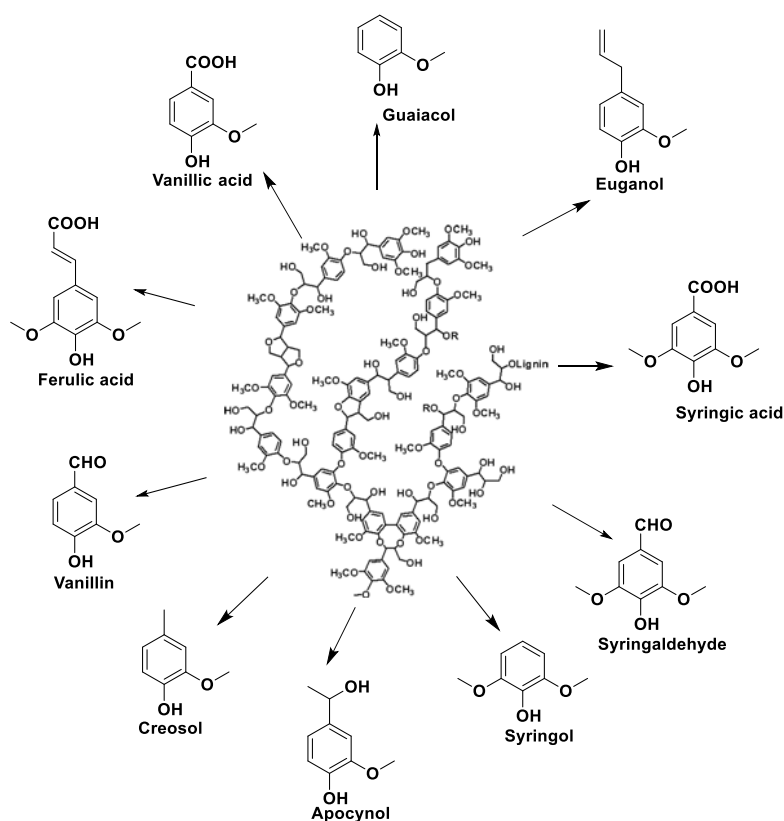


Figure 1.8 Building-blocks obtained from depolymerization of lignin

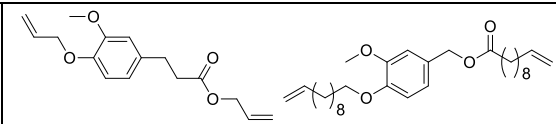
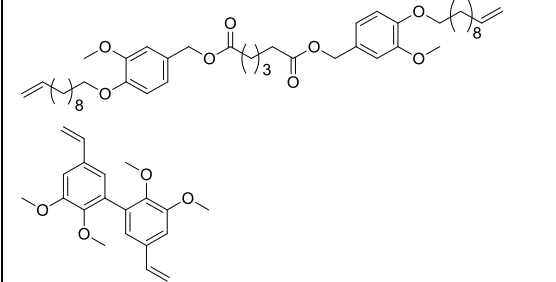
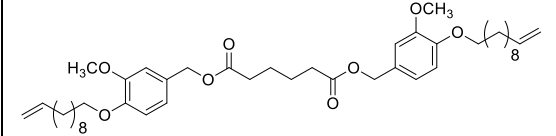
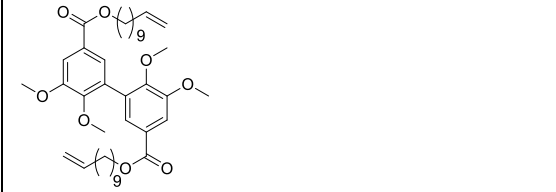
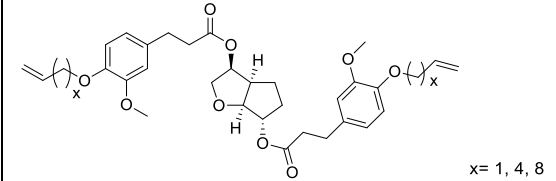
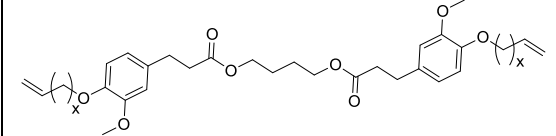
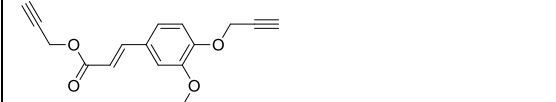
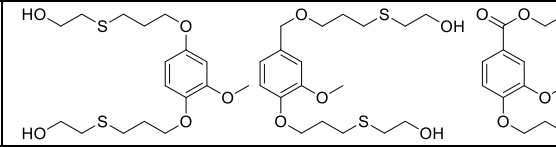
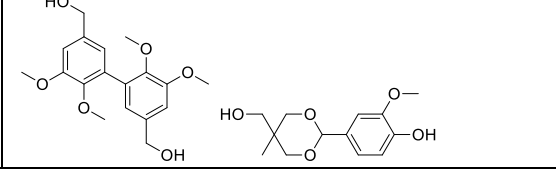

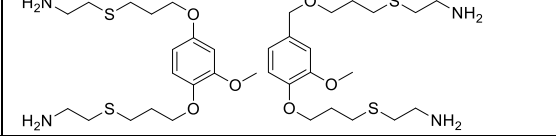
The proportion of aromatics depends on the depolymerisation method and source of lignin. In recent years, some approaches demonstrated selective depolymerisation of lignin for synthesis of phenol derivatives. For example, organosolv lignin was depolymerised using CO₂/acetone/water supercritical fluid system at temperatures of 300–370 °C under 10 MPa pressure to produce syringol and guaiacol as major products along with other aromatic products^{230–232}. Considerable attention from polymer scientists throughout the world is devoted to utilize lignin-derived aromatics to the replacement for petrochemical derivatives and has found use in many areas. Recently, lignin-derived aromatics have been used in the preparation of various polymers such as

polyesters, polycarbonates, polyurethanes, polyamides, epoxy resins, cyanate esters, etc.^{52,233}. The list of selected monomers based on lignin-derived aromatics is presented in

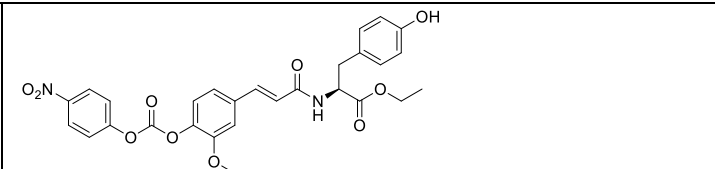

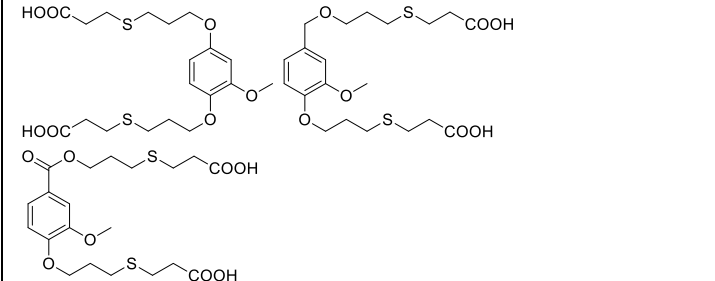
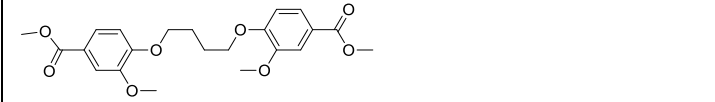

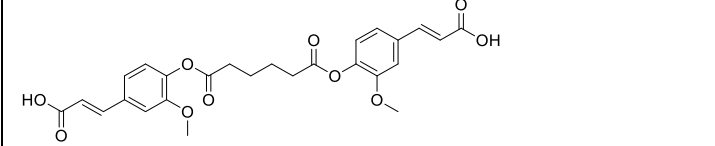
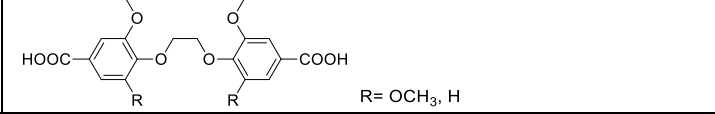
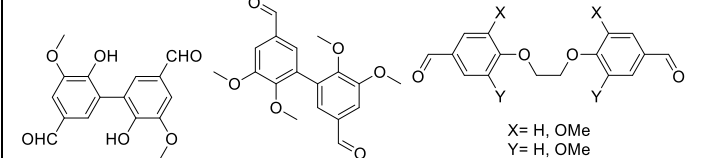
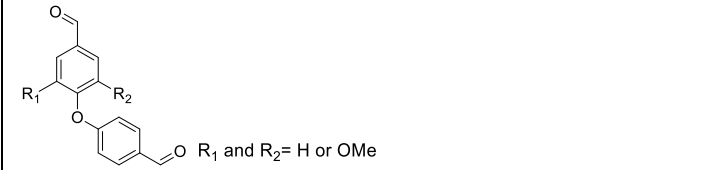

Table 1.4.

Table 1.4 List of selected lignin-based monomers

Sr. No	Monomer	Polymer	Ref
1		Epoxy resins	51
2		Epoxy resins	234
3		Epoxy resins	75,235
4		Epoxy resins	75
5		NR	69
6		NR	69
7		NR	69

8		ADMET Polymerization	38,236
9		ADMET Polymerization	38,236,2 37
10		ADMET Polymerization	
11		ADMET Polymerization	237,238
12		ADMET Polymerization	239
13		ADMET Polymerization	239
14		Oxidative Coupling	240
15		NR	69
16		Polyesters, Poly(vanillin oxalate)	241
17		NR	69
18		NR	69

19		NR	234
20		Cyanate esters	242,243
21		Cyanate esters Polycarbonate	244
22		Polyesters	245
23		Poly(carbonate amide)s	246
24		Poly(carbonate amide)s	246
25		Poly(vanillic acid)s	247
26		Polyesters	248
27		Poly(vanillic acid) Polyesters	247,248
28		Polyesters	249,250

29		Poly(carbonate amide)s	246
30		NR	69
31		NR	69
32		Polyesters	38
33		Polyesters	241
34		Poly(anhydride ester)	251
35		Polyesters	252
36		Poly(azomethine), Electrochemical polymerization, Polyacetals	237,253
37		Phenolic resins	254
38		Benzoxazines	255

39		Benzoxazines	255,256
40		Benzoxazines	257
41		Cyanate esters	242
42		Conjugated Polymer	258

NR-Polymers not reported

Lignin-derived aromatics offer many functionalities such as phenolic, carboxylic, formyl, hydroxyl, amine, cyclic carbonates, allyl, propargyl, thiol, epoxy, etc by chemical transformation. Lignin-derived aromatic monomers could, in principle, replace petroleum-based monomers such as bisphenol-A, styrene, terephthalic acid, etc. Lignin-derived polymers have wide range of applications such as high performance materials, sensing, bio-medical applications, etc. The in-built methoxy groups in the lignin-derived aromatics significantly affect on mechanical properties of the polymers by decreasing the crystallinity.

1.3 Summary

- Step-growth polymerization continues to receive intense academic and industrial attention for the preparation of polymeric materials used in a vast array of applications.
- In recent years, the utilization of renewable, non-edible, inexpensive, and abundantly available materials for the synthesis of value added chemicals and monomers have received significant attention.

- Lignocellulose and CNSL are the major sources of renewable aromatic monomers useful for the synthesis of aromatic/semi-aromatic step-growth polymers.
- Lignin is the most abundant aromatic polymer, which is made up of three repeating units namely, sinapyl alcohol, coniferyl alcohol, and coumaryl alcohol. Depolymerisation of lignin yields various aromatics such as phenols, guaiacol, catechol, vanillic acid, syringic acid, vanillin, syringol, eugenol, ferulic acid, etc. A wide range of step-growth polymers have been synthesized starting from lignin-derived aromatics. Still, there is a scope to explore potential use of lignin-derived aromatics for the synthesis of difunctional monomers and step-growth polymers therefrom.

References

- 1 M. Hong and E. Y. . Chen, *Green Chem.*, 2017, **19**, 3692–3706.
- 2 G. Odian, *Principles of Polymerization*, John Wiley & Sons, Inc., Hoboken, NJ, USA, 4th edn., 2004.
- 3 M. Zhang, S. M. June and T. E. Long, in *Polymer Science: A Comprehensive Reference*, Elsevier, 2012, vol. 5, pp. 7–47.
- 4 C. K. Ober and K. Müllen, *Ref. Modul. Mater. Sci. Mater. Eng.* 2012, **8**, 1–8.
- 5 V. Hasirci, P. Huri, T. Yilgor, G. Endogan Tanir and N. Eke, *Ref. Modul. Mater. Sci. Mater. Eng. Compr. Biomater. II*, 2017, **1**, 478–506.
- 6 M. Arroyo, *Handbook of Thermoplastics*, M. Dekker, New York, 1997.
- 7 P. E. Cassidy, *Thermally Stable Polymers :syntheses and properties*, M. Dekker ,New York, 1980.
- 8 K. Takeuchi, in *Polymer Science: A Comprehensive Reference*, ed. M. Schmidt, H. W.; Ueda, Elsevier B.V., Amstradam, 2012, vol. 5, pp. 363–376.
- 9 S. Cho, G. S. Heo, S. Khan, A. M. Gonzalez, M. Elsabahy and K. L. Wooley, *Macromolecules*, 2015, **48**, 8797–8805.
- 10 A. Pascual, J. P. K. Tan, A. Yuen, J. M. W. Chan, D. J. Coady, D. Mecerreyes, J. L. Hedrick, Y. Y. Yang and H. Sardon, *Biomacromolecules*, 2015, **16**, 1169–1178.
- 11 R. P. Brannigan, A. P. Dove, *Biomater. Sci.*, 2017, **5**, 9–21.
- 12 G. Rusu and E. Rusu, *Int. J. Polym. Anal. Charact.*, 2010, **15**, 509–523.
- 13 G. Rusu and E. Rusu, *Mater. Des.*, 2010, **31**, 4601–4610.
- 14 J. Xu, E. Feng and J. Song, *J. Appl. Polym. Sci.*, 2014, **131**, 39822.

- 15 J. Sun and D. Kuckling, *Polym. Chem.*, 2016, **7**, 1642–1649.
- 16 K. S. Y. Lau, *High-Performance Polyimides and High Temperature Resistant Polymers*, Elsevier Inc., 3rd edn., 2013.
- 17 I. Sava, S. Chisca, A. Wolinska-Grabczyk, A. Jankowski, M. Sava, E. Grabiec and M. Bruma, *Polym. Int.*, 2015, **64**, 154–164.
- 18 M. Ghosh, *Polyimides: Fundamentals and Applications*, M. Dekker, CRC Press, 1996.
- 19 H. R. Kricheldorf, *Progress in Polyimide Chemistry I*, 1999.
- 20 D. J. Liaw, K. L. Wang, Y. C. Huang, K. R. Lee, J. Y. Lai and C. S. Ha, *Prog. Polym. Sci.*, 2012, **37**, 907–974.
- 21 H. W. Engels, H. G. Pirkl, R. Albers, R. W. Albach, J. Krause, A. Hoffmann, H. Casselmann and J. Dormish, *Angew. Chem. Int. Ed.*, 2013, **52**, 9422–9441.
- 22 C. Varganici, O. Ursache, C. Gaina, V. Gaina, D. Rosu and B. C. Simionescu, *Ind. Eng. Chem. Res.*, 2013, **52**, 5287–5295.
- 23 A. S. More, B. Gadenne, C. Alfos and H. Cramail, *Polym. Chem.*, 2012, **3**, 1594–1605.
- 24 C. Zhang and M. R. Kessler, *ACS Sustain. Chem. Eng.*, 2015, **3**, 743–749.
- 25 H. Zhang, Y. Chen, Y. Zhang, X. Sun, H. Ye and W. Li, *J. Elastomers Plast.*, 2008, **40**, 161–177.
- 26 S. A. Miller, *ACS Macro Lett.*, 2013, **2**, 550–554.
- 27 S. A. Miller, *Polym. Chem.*, 2014, **5**, 3117.
- 28 Y. Zhu, C. Romain and C. K. Williams, *Nature*, 2016, **540**, 354–362.
- 29 R. Mülhaupt, *Macromol. Chem. Phys.*, 2013, **214**, 159–174.
- 30 C. Williams and M. Hillmyer, *Polym. Rev.*, 2008, **48**, 1–10.
- 31 J. C. Serrano-Ruiz, R. Luque and A. Sepúlveda-Escribano, *Chem. Soc. Rev.*, 2011, **40**, 5266–5281.
- 32 P. F. H. Harmsen, M. M. Hackmann and H. L. Bos, *Biofuels, Bioprod. Biorefining*, 2014, **8**, 306–324.
- 33 A. J. Ragauskas, *Science*, 2006, **311**, 484–489.
- 34 L. Shen, E. Worrell and M. Patel, *Biofuels, Bioprod. Biorefining*, 2010, **4**, 25–40.
- 35 D. V. Palaskar, A. Boyer, E. Cloutet, C. Alfos and H. Cramail, *Biomacromolecules*, 2010, **11**, 1202–1211.
- 36 A. S. More, T. Lebarbé, L. Maisonneuve, B. Gadenne, C. Alfos and H. Cramail, *Eur. Polym. J.*, 2013, **49**, 823–833.

- 37 L. Hojabri, X. Kong and S. S. Narine, *Biomacromolecules*, 2010, **11**, 911–918.
- 38 C. Pang, J. Zhang, G. Wu, Y. Wang, H. Gao, J. Ma, *Polym. Chem.*, 2014, **5**, 2843–2853.
- 39 A. Gandini and T. M. Lacerda, *Prog. Polym. Sci.*, 2015, **48**, 1–39.
- 40 S. Inkinen, M. Hakkarainen, A. C. Albertsson and A. Sodergard, *Biomacromolecules*, 2011, **12**, 523–32.
- 41 F. Bachmann, J. Reimer, M. Ruppenstein and J. Thiem, *Macromol. Rapid Commun.*, 1998, **19**, 21–26.
- 42 T. Calvo-Correas, A. Santamaria-Echart, A. Saralegi, L. Martin, Á. Valea, M. A. Corcuera and A. Eceiza, *Eur. Polym. J.*, 2015, **70**, 173–185.
- 43 <https://www.iucn.org/>
- 44 <https://www.arkema.com/en/products/product-finder/range-viewer/Rilsan-Polyamide-Family/>, .
- 45 https://www.lubrizol.com/Engineered-Polymers/Products/Pearlthane-ECO-TPU, .
- 46 <http://sorona.com/>, .
- 47 <http://www.braskem.com/site.aspx/Im-green>, .
- 48 <http://www.dupont.com/products-and-services/plastics-polymers-resins/ethylene-copolymers/brands/biomax-resin-modifiers.html>, .
- 49 <http://product-finder.basf.com/group/corporate/product-finder/en/brand/ULTRAMID>, .
- 50 <http://www.dupont.co.in/products-and-services/plastics-polymers-resins/thermoplastics/brands/hytrel-thermoplastic-elastomer.html>, .
- 51 M. Fache, B. Boutevin and S. Caillol, *Eur. Polym. J.*, 2015, **68**, 488–502.
- 52 A. Llevot, E. Grau, S. Carlotti, S. Grelier and H. Cramail, *Macromol. Rapid Commun.*, 2016, **37**, 9–28.
- 53 A. Gandini, D. Coelho, M. Gomes, B. Reis and A. Silvestre, *J. Mater. Chem.*, 2009, **19**, 8656.
- 54 S. Laurichesse and L. Avérous, *Prog. Polym. Sci.*, 2014, **39**, 1266–1290.
- 55 D. Chatterjee, N. V. Sadavarte, R. D. Shingte, A. S. More, B. V. Tawade, A. D. Kulkarni, A. B. Ichake, C. V. Avadhani and P. P. Wadgaonkar, in *Cashew Nut Shell Liquid*, ed. Parambath Anilkumar, Springer International Publishing, Cham, 1st edn., 2017, pp. 163–214.
- 56 C. Voirin, S. Caillol, N. V. Sadavarte, B. V. Tawade, B. Boutevin and P. P. Wadgaonkar, *Polym. Chem.*, 2014, **5**, 3142–3162.

- 57 A. Llevot and M. A. R. Meier, *Green Chem.*, 2016, **18**, 4800–4803.
- 58 D. K. Schneiderman and M. A. Hillmyer, *Macromolecules*, 2017, **50**, 3733–3749.
- 59 M. Bocqué, C. Voirin, V. Lapinte, S. Caillol and J. J. Robin, *J. Polym. Sci. Part A Polym. Chem.*, 2016, **54**, 11–33.
- 60 F. Fenouillot, A. Rousseau, G. Colomines, R. Saint Loup and J. P. Pascault, *Prog. Polym. Sci.*, 2010, **35**, 578–622.
- 61 G. Lligadas, J. C. Ronda, M. Galià and V. Cádiz, *J. Polym. Sci. Part A Polym. Chem.*, 2013, **51**, 2111–2124.
- 62 L. Montero De Espinosa and M. A. R. Meier, *Eur. Polym. J.*, 2011, **47**, 837–852.
- 63 F. Seniha Güner, Y. Yağcı and A. Tuncer Erciyes, *Prog. Polym. Sci.*, 2006, **31**, 633–670.
- 64 J. M. García, F. C. García, F. Serna and J. L. de la Peña, *Prog. Polym. Sci.*, 2010, **35**, 623–686.
- 65 S. A. Madbouly, Z. Chaoqum and K. R. Michael, *Bio-Based Plant Oil Polymers and Composites*, Amstradam, 2016.
- 66 M. A. R. Meier, J. O. Metzger and U. S. Schubert, *Chem. Soc. Rev.*, 2007, **36**, 1788–1802.
- 67 A. Gandini, *Macromolecules*, 2008, **41**, 9491–9504.
- 68 L. Mialon, A. G. Pemba and S. A. Miller, *Green Chem.*, 2010, **12**, 1704–1706.
- 69 M. Fache, E. Darroman, V. Besse, R. Auvergne, S. Caillol and B. Boutevin, *Green Chem.*, 2014, **16**, 1987–1998.
- 70 B. Lochab, S. Shukla and I. K. Varma, *RSC Adv.*, 2014, **4**, 21712–21722.
- 71 H. Kobayashi and A. Fukuoka, *Green Chem.*, 2013, **15**, 1740–1763.
- 72 I. Delidovich, P. J. C. Hausoul, L. Deng, R. Pfützenreuter, M. Rose and R. Palkovits, *Chem. Rev.*, 2016, **116**, 1540–1599.
- 73 F. H. Isikgor and C. R. Becer, *Polym. Chem.*, 2015, **6**, 4497–4559.
- 74 M. Graglia, N. Kanna and D. Esposito, *Chem. Bio. Eng. Rev.*, 2015, **2**, 377–392.
- 75 S. Zhao and M. M. Abu-Omar, *Macromolecules*, 2017, **50**, 3573–3581.
- 76 J. H. P. Tyman, *Synthetic and natural phenols*, Elsevier, 1996.
- 77 M. T. Harvey and S. Caplan, *Ind. Eng. Chem.*, 1940, **32**, 1306–1310.
- 78 R. Paramashivappa, P. Phani Kumar, P. J. Vithayathil and A. Srinivasa Rao, *J. Agric. Food Chem.*, 2001, **49**, 2548–2551.
- 79 G. Mele, D. Lomonaco and S. E. Mazzetto, in *Cashew Nut Shell Liquid*, ed. Parambath Anilkumar, Springer International Publishing, Cham, 1st edn., 2017, pp.

- 39–56.
- 80 D. Lomonaco, G. Mele and S. E. Mazzetto, in *Cashew Nut Shell Liquid*, ed. Parambath Anilkumar, Springer International Publishing, Cham, 1st edn., 2017, pp. 19–38.
- 81 G. Mele and G. Vasapollo, *Mini. Rev. Org. Chem.*, 2008, **5**, 243–253.
- 82 P. H. Gedam and P. S. Sampathkumaran, *Prog. Org. Coatings*, 1986, **14**, 115–157.
- 83 J. H. P. Tyman, R. A. Johnson, M. Muir and R. Rokhgar, *J. Am. Oil Chem. Soc.*, 1989, **66**, 553–557.
- 84 R. K. Jain and S. Kumar, *J. Food Eng.*, 1997, **32**, 339–345.
- 85 R. N. Patel, S. Bandyopadhyay and A. Ganesh, *Energy*, 2011, **36**, 1535–1542.
- 86 S. Manjula, C. K. S. Pillai and V. G. Kumar, *Thermochim. Acta*, 1990, **159**, 255–266.
- 87 M. C. Lubi and E. T. Thachil, *Des. Monomers Polym.*, 2000, **3**, 123–153.
- 88 P. Anilkumar, *Cashew nut shell liquid*: Springer International Publishing, Cham, 2017.
- 89 M. T. S. Trevisan, B. Pfundstein, R. Haubner, G. Würtele, B. Spiegelhalder, H. Bartsch and R. W. Owen, *Food Chem. Toxicol.*, 2006, **44**, 188–197.
- 90 A. J. Varma and S. Sivaram, (Hydroxyalkyl)phenols, method for their preparation, and uses thereof US6451957 B1, 2000.
- 91 B. V. Tawade, J. K. Salunke, P. S. Sane and P. P. Wadgaonkar, *J. Polym. Res.*, 2014, **21**, 617.
- 92 B. V. Tawade, S. V. Shaligram, N. G. Valsange, U. K. Kharul and P. P. Wadgaonkar, *Polym. Int.*, 2016, **65**, 567–576.
- 93 H. P. Bhunia, R. N. Jana, A. Basak, S. Lenka and G. B. Nando, *J. Polym. Sci. Part A Polym. Chem.*, 1998, **36**, 391–400.
- 94 H. P. Bhunia, G. B. Nando, T. K. Chaki, A. Basak, S. Lenka and P. L. Nayak, *Eur. Polym. J.*, 1999, **35**, 1381–1391.
- 95 R. D. Shingate and P. P. Wadgaonkar, 1,1-Bis(4-aminophenyl)-3-alkylcyclohexanes and method of preparation thereof, US6790993B1, 2004.
- 96 A. S. More, S. K. Pasale, P. N. Honkhambe and P. P. Wadgaonkar, *J. Appl. Polym. Sci.*, 2011, **121**, 3689–3695.
- 97 A. S. More, P. V. Naik, K. P. Kumbhar and P. P. Wadgaonkar, *Polym. Int.*, 2010, **59**, 1408–1414.
- 98 A. S. More and P. P. Wadgaonkar, Bisphenol compound and process for

- preparation thereof , US7446234 B2, 2006.
- 99 A. S. Trita, L. C. Over, J. Pollini, S. Baader, S. Riegsinger, M. A. R. Meier and L. J. Gooßen, *Green Chem.*, 2017, **19**, 3051–3060.
- 100 G. A. Bhavsar and S. K. Asha, *Chem. A Eur. J.*, 2011, **17**, 12646–12658.
- 101 S. M. Ramasri M, Srinivasa Rao GS, Sampatkumaran PS, *Indian J. Chem.*, 1987, **26B**, 683.
- 102 N. V. Sadavarte, M. R. Halhalli, C. V. Avadhani and P. P. Wadgaonkar, *Eur. Polym. J.*, 2009, **45**, 582–589.
- 103 N. V. Sadavarte, C. V. Avadhani and P. P. Wadgaonkar, *High Perform. Polym.*, 2011, **23**, 494–505.
- 104 N. D. Ghatge and N. N. Maldar, *Polymer*, 1984, **25**, 1353–1356.
- 105 S. M. Mathew, S. P. Vernekar, R. Mercier, R. Kerboua, Polyimides, process for the preparation thereof and use thereof as alignment films for liquid crystal devices, US20020142110, 2001.
- 106 A. S. More, P. S. Sane, A. S. Patil and P. P. Wadgaonkar, *Polym. Degrad. Stab.*, 2010, **95**, 1727–1735.
- 107 R. D. Shingte, B. V. Tawade and P. P. Wadgaonkar, *Green Mater.*, 2017, **5**, 1–11.
- 108 N. V. Sadavarte, C. V. Avadhani, P. V. Naik and P. P. Wadgaonkar, *Eur. Polym. J.*, 2010, **46**, 1307–1315.
- 109 B. V. Tawade, A. D. Kulkarni and P. P. Wadgaonkar, *Polym. Int.*, 2015, **64**, 1770–1778.
- 110 A. S. Jadhav, S. P. Vernekar and N. N. Maldar, *Polym. Int.*, 1993, **32**, 5–11.
- 111 A. S. More, S. K. Pasale and P. P. Wadgaonkar, *Eur. Polym. J.*, 2010, **46**, 557–567.
- 112 N. V. Sadavarte, S. S. Patil, C. V. Avadhani and P. P. Wadgaonkar, *High Perform. Polym.*, 2013, **25**, 735–743.
- 113 A. S. More, A. S. Patil and P. P. Wadgaonkar, *Polym. Degrad. Stab.*, 2010, **95**, 837–844.
- 114 A. S. More, S. K. Menon and P. P. Wadgaonkar, *J. Appl. Polym. Sci.*, 2012, **124**, 1281–1289.
- 115 S. Seo, Y. Kim, J. You, B. D. Sarwade, P. P. Wadgaonkar, S. K. Menon, A. S. More and E. Kim, *Macromol. Rapid Commun.*, 2011, **32**, 637–643.
- 116 A. Cyriac, S. R. Amrutha and M. Jayakannan, *J. Polym. Sci. Part A Polym. Chem.*, 2008, **46**, 3241–3256.
- 117 C. K. S. Pillai, D. C. Sherrington and A. Sneddon, *Polymer*, 1992, **33**, 3968–3970.

- 118 S. Abraham, V. Prasad, C. Pillai and M. Ravindranathan, *Polym. Int.*, 2002, **51**, 475–480.
- 119 D. G. Lee and V. S. Chang, *J. Org. Chem.*, 1978, **43**, 1532–1536.
- 120 N. V. Sadavarte, C. V. Avadhani and P. P. Wadgaonkar, *High Perform. Polym.*, 2011, **23**, 494–505.
- 121 C. Somerville, H. Youngs, C. Taylor, S. C. Davis and S. P. Long, *Science* 2010, **329**, 790–792.
- 122 E. Taarning, C. M. Osmundsen, X. Yang, B. Voss, S. I. Andersen, C. H. Christensen, L. Palumbo, S. Bordiga and U. Olsbye, *Energy Environ. Sci.*, 2011, **4**, 793–804.
- 123 A. Barakat, H. de Vries and X. Rouau, *Bioresour. Technol.*, 2013, **134**, 362–373.
- 124 F. Cherubini, *Energy Convers. Manag.*, 2010, **51**, 1412–1421.
- 125 V. Menon and M. Rao, *Prog. Energy Combust. Sci.*, 2012, **38**, 522–550.
- 126 T. Heinze and K. Petzold, in *Monomers, Polymers and Composites from Renewable Resources*, eds. M. Belgacem and A. Gandini, Amstradam, Elsevier, 2008, pp. 343–368.
- 127 D. M. Alonso, J. Q. Bond and J. A. Dumesic, *Green Chem.*, 2010, **12**, 1493.
- 128 I. Spiridon and V. I. Popa, in *Monomers, Polymers and Composites from Renewable Resources*, eds. M. Belgacem and A. Gandini, Amstradam, Elsevier, 2008, pp. 289–304.
- 129 F. Hu and A. Ragauskas, *BioEnergy Res.*, 2012, **5**, 1043–1066.
- 130 X. Huang, T. I. Korányi, M. D. Boot and E. J. M. Hensen, *ChemSusChem*, 2014, **7**, 2276–2288.
- 131 J. M. Harkin, in *Naturstoffe*, Springer Berlin Heidelberg, 1996, pp. 101–158.
- 132 D. Kai, M. J. Tan, P. L. Chee, Y. K. Chua, Y. L. Yap, X. J. Loh, *Green Chem.*, 2016, **18**, 1175–1200.
- 133 J. P. Lange, E. van der Heide, J. van Buijtenen and R. Price, *ChemSusChem*, 2012, **5**, 150–166.
- 134 G. Li, N. Li, Z. Wang, C. Li, A. Wang, X. Wang, Y. Cong and T. Zhang, *ChemSusChem*, 2012, **5**, 1958–1966.
- 135 W. Yang and A. Sen, *ChemSusChem*, 2010, **3**, 597–603.
- 136 B. Saha and M. M. Abu-Omar, *ChemSusChem*, 2015, **8**, 1133–1142.
- 137 E. De Jong, M. A. Dam, L. Sipos and G. M. Gruter, in *Biobased Monomers, Polymers, and Materials* ed. Smith and Gross, American Chemical Society:

- Washington, DC, 2012. 1–13.
- 138 A. F. Sousa, A. C. Fonseca, A. C. Serra, C. S. R. Freire, A. J. D. Silvestre and J. F. J. Coelho, *Polym. Chem.*, 2016, **7**, 1049–1058.
- 139 Y. S. Jang, B. Kim, J. H. Shin, Y. J. Choi, S. Choi, C. W. Song, J. Lee, H. G. Park and S. Y. Lee, *Biotechnol. Bioeng.*, 2012, **109**, 2437–2459.
- 140 A. M. Hanlon, I. Martin, E. R. Bright, J. Chouinard, K. J. Rodriguez, G. E. Patenotte, E. B. Berda, *Polym. Chem.*, 2017, **124**, 8653–8660.
- 141 A. Mitiakoudis and A. Gandini, *Macromolecules*, 1991, **24**, 830–835.
- 142 S. Boufi, A. Gandini and M. N. Belgacem, *Polymer*, 1995, **36**, 1689–1696.
- 143 C. Moreau, M. N. Belgacem and A. Gandini, *Top. Catal.*, 2004, **27**, 11–30.
- 144 A. Gandini, *Polymers*, 2005, **15**, 95–101.
- 145 Y.-L. Liu and C.-Y. Hsieh, *J. Polym. Sci. Part A Polym. Chem.*, 2006, **44**, 905–913.
- 146 A. Gandini, *Prog. Polym. Sci.*, 2013, **38**, 1–29.
- 147 Y. Zhang, A. A. Broekhuis and F. Picchioni, *Macromolecules*, 2009, **42**, 1906–1912.
- 148 T. E. Long, *Science* 2014, **344**, 706–707.
- 149 C. Zeng, H. Seino, J. Ren, K. Hatanaka and N. Yoshie, *Polymer* 2013, **54**, 5351–5357.
- 150 C. Zeng, H. Seino, J. Ren, K. Hatanaka and N. Yoshie, *Macromolecules*, 2013, **46**, 1794–1802.
- 151 C. Fan, C. Pang, X. Liu, J. Ma and H. Gao, *Green Chem.*, 2016, **18**, 6320–6328.
- 152 T. Ikezaki, R. Matsuoka, K. Hatanaka and N. Yoshie, *Polym. Chem.*, 2013, **52**, 216–222.
- 153 Y. N. Yuksekdog, T. N. Gevrek and A. Sanyal, *ACS Macro Lett.*, 2017, **6**, 415–420.
- 154 S. S. Nagane, P. S. Sane, B. V. Tawade and P. P. Wadgaonkar, 2, 2'-Bis (4-hydroxyphenyl) alkyl azides and process for the preparation thereof, US US 9562004 B2.
- 155 A. Maiorana, S. Spinella and R. A. Gross, *Biomacromolecules*, 2015, **16**, 1021–1031.
- 156 J. A. Moore and J. E. Kelly, *Macromolecules*, 1978, **11**, 568–573.
- 157 J. A. Moore and E. M. Partain, *Macromolecules*, 1983, **16**, 338–339.
- 158 S. Boufi, M. N. Belgacem, J. Quillerou and A. Gandini, *Macromolecules*, 1993,

- 26, 6706–6717.
- 159 J. A. Moore and J. E. Kelly, *J. Polym. Sci. Polym. Chem. Ed.*, 1984, **22**, 863–864.
- 160 S. Gharbi and A. Gandini, *Acta Polym.*, 1999, **50**, 293–297.
- 161 C. Méalares and A. Gandini, *Polym. Int.*, 1996, **40**, 33–39.
- 162 S. Gharbi, A. Afli, R. El Gharbi and A. Gandini, *Polym. Int.*, 2001, **50**, 509–514.
- 163 A. Afli, S. Gharbi, R. El Gharbi, Y. Le Bigot and A. Gandini, *Eur. Polym. J.*, 2002, **38**, 667–673.
- 164 Z. Hui and A. Gandini, *Eur. Polym. J.*, 1992, **28**, 1461–1469.
- 165 A. Gandini, T. M. Lacerda, A. J. F. Carvalho and E. Trovatti, *Chem. Rev.*, 2016, **116**, 1637–1669.
- 166 N. Jerzy, *Polish J. Appl. Chem.*, 1993, **36**, 317–323.
- 167 J. L. Cawse, J. L. Stanford and R. H. Still, *Die Makromol. Chemie*, 1984, **185**, 697–707.
- 168 S. Grund, P. Kempe, G. Baumann, A. Seifert and S. Spange, *Angew. Chemie Int. Ed.*, 2007, **46**, 628–632.
- 169 C. Vilela, L. Cruciani, A. J. D. Silvestre and A. Gandini, *Macromol. Rapid Commun.*, 2011, **32**, 1319–1323.
- 170 C. Goussé and A. Gandini, *Polym. Int.*, 1999, **48**, 723–731.
- 171 S. Lingier, Y. Spiesschaert, B. Dhanis, S. De Wildeman and F. E. Du Prez, *Macromolecules*, 2017, **50**, 5346–5352.
- 172 J. A. Galbis and M. G. García-Martín, in *Monomers, Polymers and Composites from Renewable Resources*, eds. M. Belgacem and A. Gandini, Amstradam, Elsevier, 2008, pp. 89–114.
- 173 M. D. Zenner, Y. Xia, J. S. Chen and M. R. Kessler, *ChemSusChem*, 2013, **6**, 1182–1185.
- 174 R. Zhang and J. A. Moore, *Macromol. Symp.*, 2003, **199**, 375–390.
- 175 Z. Ping, W. Linbo and L. Bo-Geng, *Polym. Degrad. Stab.*, 2009, **94**, 1261–1266.
- 176 C. Wang and S. Nakamura, *J. Polym. Sci. Part A Polym. Chem.*, 1995, **33**, 2157–2163.
- 177 L. Joseph, McCarthy and I. Aminul, in *Lignin: Historical, Biological, and Materials Perspectives*, eds. Wolfgang G., R. A. Glasser, T. P. Northey and Schultz, American Chemical Society, Washington, 1st edn., 1999, pp. 2–99.
- 178 B. M. Upton and A. M. Kasko, *Chem. Rev.*, 2016, **116**, 2275–2306.
- 179 J. Zakzeski, P. C. A. Bruijninx, A. L. Jongerius and B. M. Weckhuysen, *Chem.*

- Rev.*, 2010, **110**, 3552–3599.
- 180 H. Chung and N. R. Washburn, *Green Mater.*, 2013, **1**, 137–160.
- 181 J. S. Luterbacher, D. Martin Alonso, J. A. Dumesic, *Green Chem.*, 2014, **16**, 4816–4838.
- 182 E. Ten and W. Vermerris, *J. Appl. Polym. Sci.*, 2015, **132**.
- 183 H. Lange, S. Decina and C. Crestini, *Eur. Polym. J.*, 2013, **49**, 1151–1173.
- 184 <http://www.reuters.com/brandfeatures/venture-capital/article?id=4789>, .
- 185 H. M. Caicedo, L. A. Dempere and W. Vermerris, *Nanotechnology*, 2012, **23**, 105605.
- 186 S. Domenek, A. Louaifi, A. Guinault and S. Baumberger, *J. Polym. Environ.*, 2013, **21**, 692–701.
- 187 S. Xiao, J. Feng, J. Zhu, X. Wang, C. Yi and S. Su, *J. Appl. Polym. Sci.*, 2013, **130**, 1308–1312.
- 188 A. Arshanitsa, J. Ponomarenko, T. Dizhbite, A. Andersone, R. J. A. Gosselink, J. van der Putten, M. Lauberts and G. Telysheva, *J. Anal. Appl. Pyrolysis*, 2013, **103**, 78–85.
- 189 K. Johansson, S. Winstrand, C. Johansson, L. Järnström and L. J. Jönsson, *J. Biotechnol.*, 2012, **161**, 14–18.
- 190 J. R. Dahn, T. Zheng, Y. Liu and J. S. Xue, *Science*, 1995, **270**, 590–593.
- 191 A. S. Hoffman, *Adv. Drug Deliv. Rev.*, 2002, **54**, 3–12.
- 192 D. Yiamsawas, G. Baier, E. Thines, K. Landfester, F. R. Wurm, M. J. Pecyna, P. Nousiainen, J. Sipilä, M. H. le, M. Hofrichter and C. Liers, *RSC Adv.*, 2014, **4**, 11661–11663.
- 193 Y. Nordström, R. Joffe and E. Sjöholm, *J. Appl. Polym. Sci.*, 2013, **130**, 3689–3697.
- 194 E. M. Rubin, *Nature*, 2008, **454**, 841–845.
- 195 G. Brunow, Brunow and Gösta, in *Biopolymers Online*, eds. A. Steinbüchel and M. Hofrichter, Wiley-VCH Verlag GmbH & Co. KGaA, Weinheim, Germany, 2005.
- 196 A. M. Abdel-Hamid, J. O. Solbiati and I. K. O. Cann, *Adv. Appl. Microbiol.* 2013, pp. 1–28.
- 197 Y. Y. Wang, L. L. Ling and H. Jiang, *Green Chem.*, 2016, **18**, 4032–4041.
- 198 A. Rahimi, A. Ulbrich, J. J. Coon and S. S. Stahl, *Nature*, 2014, **515**, 249–52.
- 199 D. A. I. Goring, *Pulp Pap. Mag. Canada*, 1963, **62**, 517–527.
- 200 G. M. Irvine, *Tappi*, 1984, **67**, 118–121.

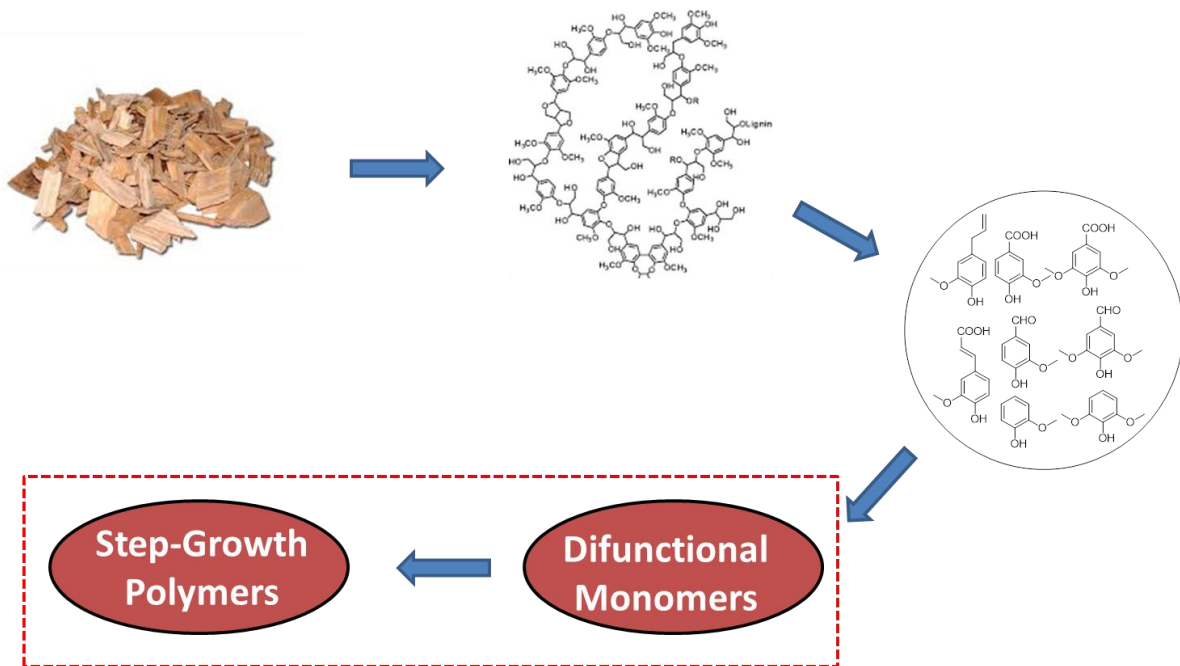
- 201 T. Hatakeyama and H. Hatakeyama, in *Thermal Properties of Green Polymers and Biocomposites*, Kluwer Academic Publishers, Dordrecht, 2004, pp. 171–215.
- 202 S. Y. Lin and C. W. Dence, *Methods in Lignin Chemistry*, Springer Berlin Heidelberg, 1992.
- 203 J. Li, G. Henriksson and G. Gellerstedt, *Bioresour. Technol.*, 2007, **98**, 3061–3068.
- 204 G. GUO, W. CHEN, W. CHEN, L. MEN and W. HWANG, *Bioresour. Technol.*, 2008, **99**, 6046–6053.
- 205 M. Zhang, Y. Xu and K. Li, *J. Appl. Polym. Sci.*, 2007, **106**, 630–636.
- 206 J. Gierer, *Wood Sci. Technol.*, 1980, **14**, 241–266.
- 207 W. O. S. Doherty, P. Mousavioun and C. M. Fellows, *Ind. Crops Prod.*, 2011, **33**, 259–276.
- 208 S. Y. Lin, I. S. Lin, S. Y. Lin and I. S. Lin, in *Ullmann's Encyclopedia of Industrial Chemistry*, Wiley-VCH Verlag GmbH & Co. KGaA, Weinheim, Germany, 2000.
- 209 X. Pan, D. Xie, K. Y. Kang, S. L. Yoon and J. N. Saddler, *Appl. Biochem. Biotechnol.*, 2007, **137–140**, 367–377.
- 210 C. Amen-Chen, H. Pakdel and C. Roy, *Bioresour. Technol.*, 2001, **79**, 277–299.
- 211 G. W. Huber, S. Iborra and A. Corma, *Chem. Rev.*, 2006, **106**, 4044–4098.
- 212 E. Dorrestijn, L. J. J. Laarhoven, I. W. C. E. Arends and P. Mulder, *J. Anal. Appl. Pyrolysis*, 2000, **54**, 153–192.
- 213 A. J. Ragauskas, G. T. Beckham, M. J. Bidy, R. Chandra, F. Chen, M. F. Davis, B. H. Davison, R. A. Dixon, P. Gilna, M. Keller, P. Langan, A. K. Naskar, J. N. Saddler, T. J. Tschaplinski, G. A. Tuskan and C. E. Wyman, *Science*, 2014, **344**, 1246843-1246843.
- 214 A. Gandini, M. N. Belgacem, Z.X. Guo and S. Montanari, in *Chemical Modification, Properties, and Usage of Lignin*, Springer US, Boston, 2002, pp. 57–80.
- 215 Z. X. Guo and A. Gandini, *Eur. Polym. J.*, 1991, **27**, 1177–1180.
- 216 Z. X. Guo, A. Gandini and F. Pla, *Polym. Int.*, 1992, **27**, 17–22.
- 217 R. R. N. Sailaja and M. V. Deepthi, *Mater. Des.*, 2010, **31**, 4369–4379.
- 218 W. Thielemans and R. P. Wool, *Biomacromolecules*, 2005, **6**, 1895–1905.
- 219 A. Effendi, H. Gerhauser and A. V. Bridgwater, *Renew. Sustain. Energy Rev.*, 2008, **12**, 2092–2116.
- 220 Y. Li and A. J. Ragauskas, *J. Wood Chem. Technol.*, 2012, **32**, 210–224.

- 221 Y. Li, A. J. Ragauskas, R. W. Yu, D. Lam, J. N. Saddler, G. Xu and V. E. Musteata, *RSC Adv.*, 2012, **2**, 3347–3351.
- 222 M. N. Vanderlaan and R. W. Thring, *Biomass and Bioenergy*, 1998, **14**, 525–531.
- 223 D. Mohan, C. U. Pittman, and P. H. Steele, *Energy & Fuels*, 2006, **20**, 848–889.
- 224 A. Leonowicz, A. Matuszewska, J. Luterek, D. Ziegenhagen, M. Wojtaś-Wasilewska, N.-S. Cho, M. Hofrichter and J. Rogalski, *Fungal Genet. Biol.*, 1999, **27**, 175–185.
- 225 M. Brebu and I. Spiridon, *Polym. Degrad. Stab.*, 2012, **97**, 2104–2109.
- 226 J. D. P. Araújo, C. A. Grande and A. E. Rodrigues, *Chem. Eng. Res. Des.*, 2010, **88**, 1024–1032.
- 227 E. A. B. da Silva, M. Zabkova, J. D. Araújo, C. A. Cateto, M. F. Barreiro, M. N. Belgacem and A. E. Rodrigues, *Chem. Eng. Res. Des.*, 2009, **87**, 1276–1292.
- 228 V. E. Tarabanko, N. V. Koropatchinskaya, A. V. Kudryashev and B. N. Kuznetsov, *Russ. Chem. Bull.*, 1995, **44**, 367–371.
- 229 A. R. Gonçalves and P. Benar, *Bioresour. Technol.*, 2001, **79**, 103–111.
- 230 N. Yan, C. Zhao, P. J. Dyson, C. Wang, L. Liu and Y. Kou, *ChemSusChem*, 2008, **1**, 626–629.
- 231 T. Wahyudiono, M. Sasaki and M. Goto, *Fuel*, 2009, **88**, 1656–1664.
- 232 T. Wahyudiono, T. Kanetake, M. Sasaki and M. Goto, *Chem. Eng. Technol.*, 2007, **30**, 1113–1122.
- 233 M. Fache, R. Auvergne, B. Boutevin and S. Caillol, *Eur. Polym. J.*, 2015, **67**, 527–538.
- 234 T. Koike, *Polym. Eng. Sci.*, 2012, **52**, 701–717.
- 235 M. Shibata and T. Ohkita, *Eur. Polym. J.*, 2017, **92**, 165–173.
- 236 M. Firdaus and M. A. R. Meier, *Eur. Polym. J.*, 2013, **49**, 156–166.
- 237 A. Llevot, E. Grau, S. Carlotti, S. Grelier, H. Cramail, W. DeBoer and T. Masuda, *Polym. Chem.*, 2015, **6**, 7693–7700.
- 238 O. Kreye, T. Tóth and M. A. R. Meier, *Eur. Polym. J.*, 2011, **47**, 1804–1816.
- 239 I. Barbara, A. L. Flourat and F. Allais, *Eur. Polym. J.*, 2015, **62**, 236–243.
- 240 M. F. Beristain, M. Nakamura, K. Nagai and T. Ogaw, *Des. Monomers Polym.*, 2009, **12**, 257–263.
- 241 A. Llevot, E. Grau, S. Carlotti, S. Grelier, H. Cramail, *Polym. Chem.*, 2015, **6**, 6058–6066.
- 242 H. A. Meylemans, T. J. Groshens and B. G. Harvey, *ChemSusChem*, 2012, **5**, 206–

- 210.
- 243 H. A. Meylemans, B. G. Harvey, J. T. Reams, A. J. Guenther, L. R. Cambrea, T. J. Groshens, L. C. Baldwin, M. D. Garrison and J. M. Mabry, *Biomacromolecules*, 2013, **14**, 771–780.
- 244 B. G. Harvey, A. J. Guenther, H. A. Meylemans, S. R. L. Haines, K. R. Lamison, T. J. Groshens, L. R. Cambrea, M. C. Davis and W. W. Lai, *Green Chem.*, 2015, **17**, 1249–1258.
- 245 F. Pion, P.-H. Ducrot and F. Allais, *Macromol. Chem. Phys.*, 2014, **215**, 431–439.
- 246 A. Noel, Y. P. Borguet, J. E. Raymond and K. L. Wooley, *Macromolecules*, 2014, **47**, 2974–2983.
- 247 H. R. Kricheldorf and G. Löhden, *Polymer*, 1995, **36**, 1697–1705.
- 248 W. Lange and O. Kordsachia, *Holz als Roh- und Werkst.*, 1981, **39**, 107–112.
- 249 O. Kreye, S. Oelmann and M. A. R. Meier, *Macromol. Chem. Phys.*, 2013, **214**, 1452–1464.
- 250 L. Mialon, R. Vanderhenst, A. G. Pemba and S. A. Miller, *Macromol. Rapid Commun.*, 2011, **32**, 1386–1392.
- 251 M. A. Ouimet, J. Griffin, A. L. Carbone-Howell, W.-H. Wu, N. D. Stebbins, R. Di and K. E. Uhrich, *Biomacromolecules*, 2013, **14**, 854–861.
- 252 L. H. Bock and J. K. Anderson, *J. Polym. Sci.*, 1955, **17**, 553–558.
- 253 A. S. Amarasekara and A. Razzaq, *Polym. Sci.*, 2012, **2012**, 1–5.
- 254 G. Foyer, B.-H. Chanfi, D. Virieux, G. David and S. Caillol, *Eur. Polym. J.*, 2016, **77**, 65–74.
- 255 N. K. Sini, J. Bijwe and I. K. Varma, *J. Polym. Sci. Part A Polym. Chem.*, 2014, **52**, 7–11.
- 256 C. Wang, J. Sun, X. Liu, A. Sudo, T. Endo, *Green Chem.*, 2012, **14**, 2799–2806.
- 257 A. Van, K. Chiou and H. Ishida, *Polymer.*, 2014, **55**, 1443–1451.
- 258 J. Wang, B. Wu, S. Li, G. Sinawang, X. Wang and Y. He, *ACS Sustain. Chem. Eng.*, 2016, **4**, 4036–4042.

Chapter - 2

Scope and Objectives



Since Carother's classical discovery of synthesis of polyester and polyamide^{1,2}, the chemistry of step-growth polymerization has been dominated by synthetic organic chemists in terms of synthesis of new difunctional monomers and polymer forming reactions. Step-growth polymerization processes have been enjoying strong academic and industrial interest for the synthesis of polymeric materials with tunable properties³. Step-growth polymers have played important role in industries for the preparation of materials of daily use as well as advanced materials. The prominent examples of industrially important step-growth polymers are polyesters, polycarbonates, polyamides, polyurethanes, polyimides, polysulfones, polyetherketones, epoxy resins, cyanate esters, etc³⁻⁵. The monomers used for the preparation of step-growth polymers are generally synthesized starting from organic chemicals which are mostly derived from fossil resources *viz.* natural gas, petroleum and coal. Almost all organic chemicals can be derived from seven basic building blocks, namely, syngas, ethylene, propylene, butanes, butylenes, butadiene and BTX (mixture of benzene, toluene and xylene) which are mostly obtained from fossil resources. Due to the rapid depletion of fossil fuels, the search for alternate resources for organic chemicals and monomers has come to forefront^{6,7}.

From the history to the present, human beings have always relied on the application of various bio-polymers such as cellulose, plant fiber, jute, flax, ramie, silk, cotton, natural rubber, animal skin, etc⁸. However, most of these polymers have limitations in terms of inferior property profile compared to polymers based on fossil resources⁹⁻¹². Therefore, there is an urgent need to develop low cost and scalable bio-based polymers with potential to replace present petroleum-derived polymers. In recent years, significant efforts have been made concerning the synthesis of polymers using various bio-based starting materials such as cellulose, starch, monosaccharides, fatty acids, lactic acid, natural amino acids, and so on¹³⁻¹⁵. These efforts have been reflected in the form of increased number of patents, publications, books as well as commercial products such as polylactic acid from starch, polyamide from castor oil (Rilsan®), thermoplastic polyurethane (Pearlthane®), Sorona®, and polyester derived from sugar (Hytrel®). The major concern with some of these polymers is the utilization of edible resources such as starch, vegetable oils or sugars as starting materials which strongly affect the food supply chain and create ethical issues. Additionally, most of these polymers are aliphatic in nature. In general, aliphatic polymers possess poor

thermomechanical properties and are not suitable for high performance or engineering applications^{10,16,17}.

The prominent non-edible resources of aromatic chemicals are lignin and cashew nut shell liquid (CNSL)¹⁸. Lignin is the second most abundant material containing renewable carbon after cellulose on the earth. Lignin consists of three monolignols including coumaryl alcohol, syringyl alcohol, and coniferyl alcohol. Lignin can be isolated from lignocellulose material by various methods such as kraft pulping, lignosulfate pulping, organosol pulping, soda pulping, etc⁷. Kraft pulping is the most common method for lignin isolation. Around 70 million tonnes of lignin is produced worldwide as a by-product of pulp and paper industries and most of the lignin is utilized to generate energy. Only ~ 2% of lignin is currently being utilized for the synthesis of chemicals, polymers, etc^{19,20}. A range of polymers such as polyurethanes, epoxy resins, phenolic resins, etc have been synthesized using modified or unmodified lignin as a macromonomer^{7,20-22}.

The attractiveness of lignin originates from the presence of substituted aromatics in the polymeric form that yield valuable aromatic chemicals on selective depolymerisation. Different strategies that have been applied for depolymerisation of lignin include pyrolysis, hydrogenolysis, hydrolysis and enzymatic reactions. The lignin-based aromatics include phenol, guaiacol, catechol, vanillic acid, syringic acid, vanillin, syringol, eugenol, ferulic acid, etc⁷. The proportion of these aromatics depends on the depolymerisation method and the source of lignin. These lignin-derived aromatics have been utilized in the past as valuable starting materials for synthesis of monomers useful in the preparation of polycarbonates, polyesters, poly(ether ester)s, polyacetals, polyurethanes, (meth)acrylic polymers, epoxies, polybenzoxazines, cyanate ester resins, etc²³⁻²⁵.

Although there is voluminous literature available on the applications of lignin, many areas remain uncovered. Notably, the utilization of lignin in the field of step-growth polymers has not been fully exploited. Thus, design and synthesis of difunctional condensation monomers for step-growth polymers based on lignin-derived aromatics could be an attractive proposition.

The overall objective of the present thesis was to synthesize difunctional monomers based on lignin-derived phenolic derivatives *viz.* vanillic acid, syringic acid, vanillin, guaiacol and syringol and their utilization for the synthesis of step growth polymers. The following graphic (**Figure 2.1**) suitably illustrates the theme of the thesis.

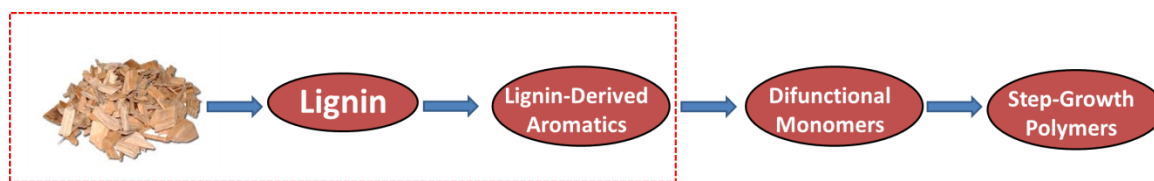


Figure 2.1 The theme of the thesis

The difunctional monomers were designed in such a way that they possess one or more of the structural features such as: i) the presence of flexible oxyalkylene linkage, ii) kinked structure, iii) the presence of pendant furyl group and iv) the presence of naturally gifted methoxy substituents. Thus, the specific objectives of the present thesis are:

1. Design and synthesis of aromatic diisocyanates and diacylhydrazides containing oxyalkylene linkage.
2. Design and synthesis of aromatic diisocyanates and diacylhydrazides containing biphenylene linkage.
3. Design and synthesis of A-B type monomers viz. ω -hydroxyalkyleneoxy benzoyl azides
4. Design and synthesis of bisphenols containing pendant furyl group
5. Design and synthesis of bisphenol containing oxadiazole group
6. Design and synthesis of diacids, diol and dialdehyde containing ester linkage
7. Synthesis of step-growth polymers viz. poly(ether urethane)s, aromatic polyesters, aromatic polycarbonates, aromatic poly(amide imide)s and aromatic polyimides
8. To investigate the effect of methoxy substituents on the polymer properties such as solubility characteristics, thermal, and mechanical properties
9. Synthesis of recyclable crosslinked aromatic polycarbonates and aromatic polyesters using furan-maleimide Diels-Alder chemistry

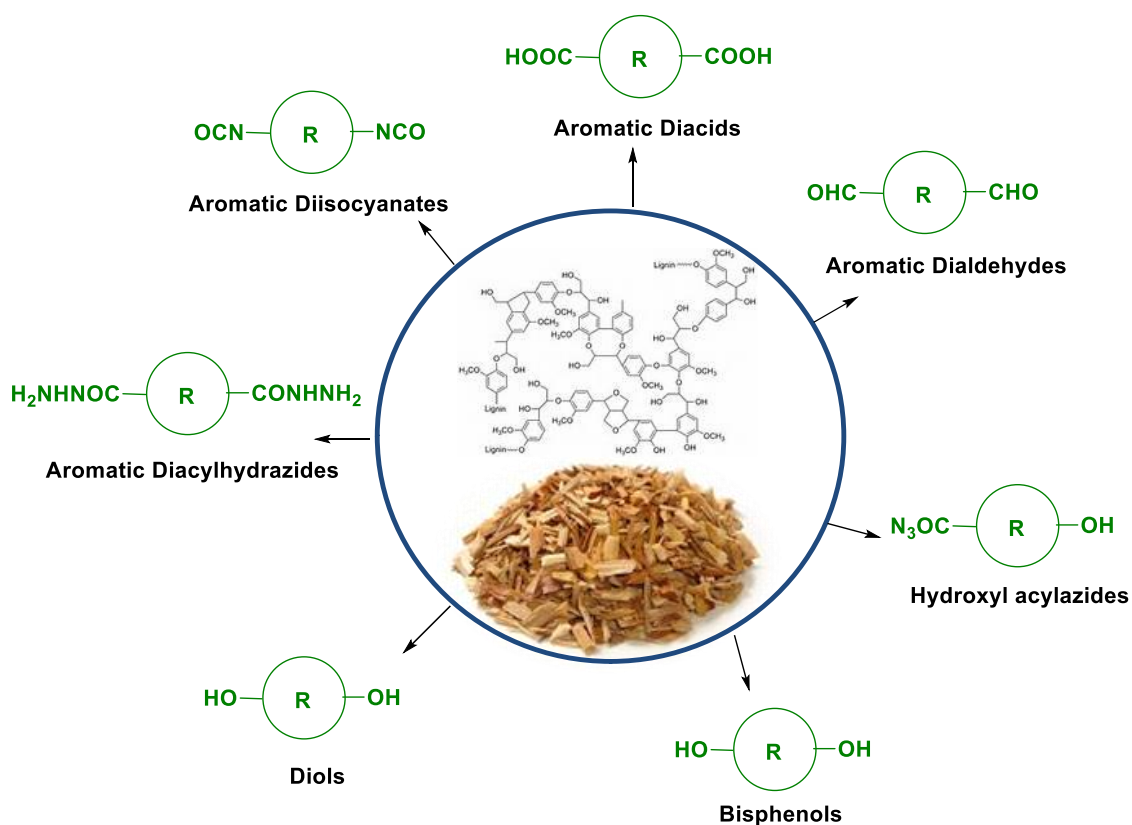
References

- 1 K. Steen, *Isis*, 1999, **90**, 841–842.
- 2 R. Bud and W. J. Reader, *Isis*, 1989, **80**, 732–734.
- 3 M. Zhang, S. M. June and T. E. Long, in *Polymer Science: A Comprehensive Reference*, Elsevier, 2012, vol. 5, pp. 7–47.
- 4 T. Yokozawa, *Chain-Growth Condensation Polymerization*, Elsevier B.V. Amstradam, 2012
- 5 Y. Imai, *React. Funct. Polym.*, 1996, **30**, 3–15.

- 6 A. J. Ragauskas, *Science*, 2006, **311**, 484–489.
- 7 F. H. Isikgor and C. R. Becer, *Polym. Chem.*, 2015, **6**, 4497–4559.
- 8 X. S. Wool, Richard P., Sun, *Bio-Based Polymers and Composites*, Elsevier Inc., Amstradam, 2005.
- 9 M. Desroches, M. Escouvois, R. Auvergne, S. Caillol and B. Boutevin, *Polym. Rev.*, 2012, **52**, 38–79.
- 10 L. Montero de Espinosa and M. A. R. Meier, *Eur. Polym. J.*, 2011, **47**, 837–852.
- 11 M. A. R. Meier, J. O. Metzger, U. S. Schubert, *Chem. Soc. Rev.*, 2007, **36**, 1788.
- 12 A. Gandini and T. M. Lacerda, *Prog. Polym. Sci.*, 2015, **48**, 1–39.
- 13 A. Gandini, *Macromolecules*, 2008, **41**, 9491–9504.
- 14 F. Bachmann, J. Reimer, M. Ruppenstein and J. Thiem, *Macromol. Rapid Commun.*, 1998, **19**, 21–26.
- 15 J. A. Galbis and M. G. García-Martín, in *Monomers, Polymers and Composites from Renewable Resources*, eds M. Belgacem A. Gandini, Elsevier, Amstradam, 1st edn 2008, pp. 89–114.
- 16 M. N. Belgacem and A. Gandini, in *Monomers, Polymers and Composites from Renewable Resources*, eds M. Belgacem A. Gandini, Elsevier, Amstradam, 1st edn 2008, pp. 39–66.
- 17 L. Maisonneuve, O. Lamarzelle, E. Rix, E. Grau and H. Cramail, *Chem. Rev.*, 2015, **115**, 12407–12439.
- 18 B. Lochab, S. Shukla and I. K. Varma, *RSC Adv.*, 2014, **4**, 21712.
- 19 <http://www.reuters.com/brandfeatures/venture-capital/article?id=4789>, .
- 20 S. Laurichesse and L. Avérous, *Prog. Polym. Sci.*, 2014, **39**, 1266–1290.
- 21 B. M. Upton and A. M. Kasko, *Chem. Rev.*, 2016, **116**, 2275–2306.
- 22 E. Ten and W. Vermerris, *J. Appl. Polym. Sci.*, 2015, **132**.
- 23 M. Fache, B. Boutevin and S. Caillol, *Eur. Polym. J.*, 2015, **68**, 488–502.
- 24 A. Llevot, E. Grau, S. Carlotti, S. Grelier and H. Cramail, *Macromol. Rapid Commun.*, 2016, **37**, 9–28.
- 25 M. Fache, E. Darroman, V. Besse, R. Auvergne, S. Caillol and B. Boutevin, *Green Chem.*, 2014, **16**, 1987–1998.

Chapter - 3

Step Growth Monomers from Lignin-Derived Aromatics



3.1 Introduction

The structure of a monomer is the most important parameter which decides the final properties of a polymer. With the judicious selection of appropriate combination of monomers, the properties such as thermo-mechanical and processing characteristics of step-growth polymers could be tailored¹⁻³. In this context, a variety of difunctional monomers such as diacids, bisphenols, dialdehydes, diisocyanates, diamines, diols, etc have been designed and synthesized with an objective to modify the properties of step growth polymers⁴. The cost, availability, renewability, carbon footprint, etc. are the important factors which should be considered in the design of new monomers. Currently, most of the starting materials used for the synthesis of difunctional monomers are derived from fossil resources^{5,6}. However, the use of fossil resources for the synthesis of monomers and polymers is insecure because of their finite stocks, non-renewability and environmental issues⁷⁻⁹.

As a result of these issues, a paradigm shift in the chemical infrastructure towards a sustainable production and use of chemical intermediates needs to be established. The possible solutions have been presented in the concepts of Anastas and Warner, who also postulated the 12 principles of green chemistry. An important aspect of these principles is the use of renewable feedstocks to provide chemical building blocks, intermediates and reagents¹⁰. A great deal of attention has been paid recently both in industrial and academic laboratories to exploit biomass as a raw material for energy and chemical production which bears several advantages such as an ecologically benign production and the “renewability” of the resources in contrast to the continual depletion of coal and petroleum^{7,8,11}.

Over the last few years, a large numbers of monomers and polymers have been reported from renewable resources such as cellulose, monosaccharides, fatty acids, starch, natural amino acids, etc. Some bio-based monomers and polymers have been commercialized^{8,12-14}. However, applications of these bio-based polymers are limited due to their aliphatic nature which makes them weak in their thermomechanical properties^{15,16}.

A limited number of examples of aromatic/semi-aromatic monomers and polymers have been commercialized from bio-based chemicals¹⁷⁻¹⁹. The significant

sources of bio-based aromatic monomers are lignin, furan derivatives, pentadecylphenol, terpene, eugenol, 4-aminophenylalanine, etc²⁰⁻²⁶.

Lignin is the non-edible abundant source of aromatics and is a by-product of paper and pulp industries. Phenolic moiety of lignin-derived aromatics offers a variety of possibilities for the synthetic chemist. A numbers of monomers and polymers based on lignin-derived aromatics have been documented in various patents and papers^{21,22,27}.

In the present work, new bio-based aromatic monomers of AA type *viz.* bisphenols, diisocyanates, diacids, diols, dialdehydes, diacylhydrazides and of AB type *viz.* hydroxyl acylazides were designed and synthesized starting from lignin-derived aromatics (**Figure 3.1**).

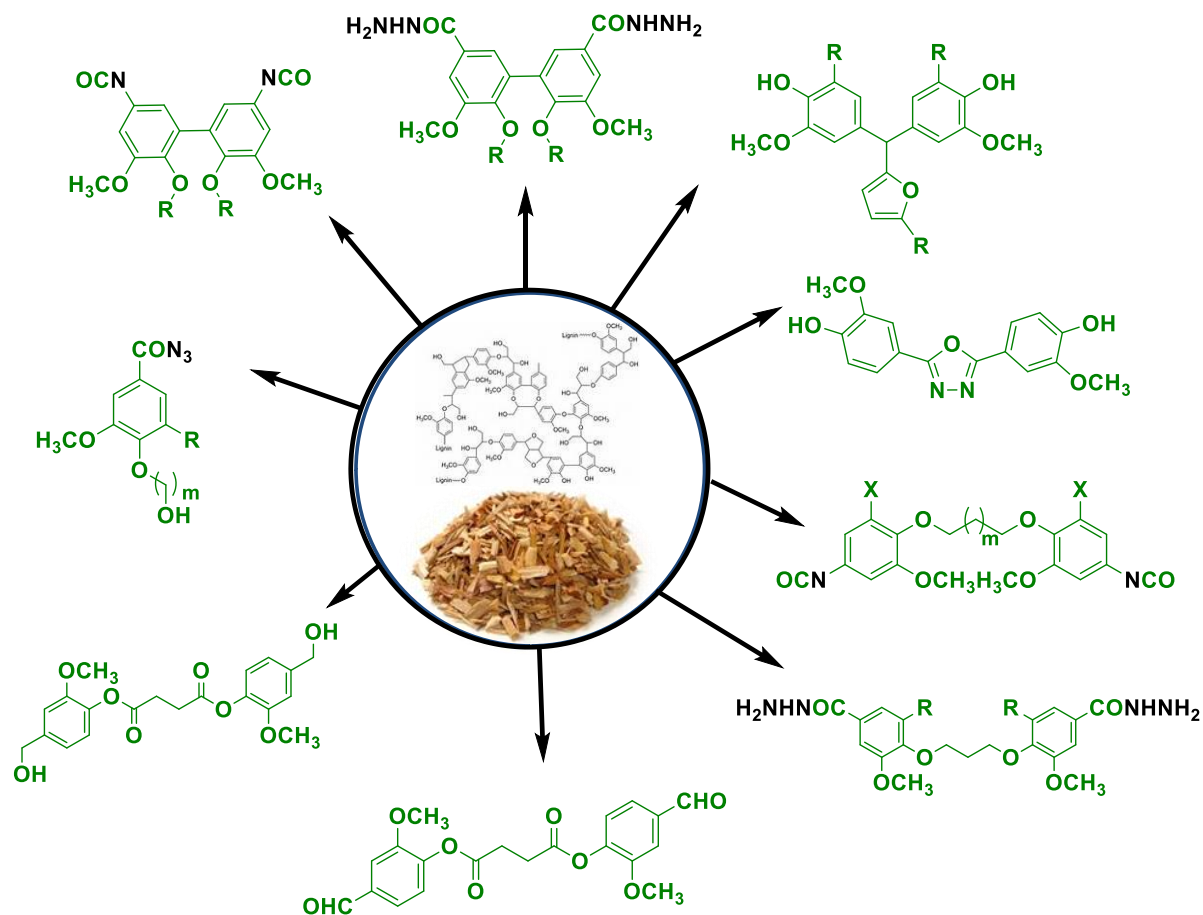


Figure 3.1 New difunctional monomers synthesized in the present work starting from lignin-derived aromatics

3.2 Experimental

3.2.1 Materials

Vanillic acid (97 %), syringic acid (95 %), guaiacol (98 %), syringol (99 %), vanillin (99 %), 1,3-dibromopropane (99 %), 1,4-dibromobutane (99 %), 1,5-dibromopentane (98 %), iodomethane, 1-bromopentane (80 %), 6-chlorohexanol (96 %), furfural (99 %), methyl furfural (99 %). Laccase from *Trametes versicolor* (0.5 U/mg), 2,5-furandicarboxylic acid (95 %), succinyl chloride (95 %) and dibutyltin dilaurate (DBTDL) (95 %) were purchased from Sigma-Aldrich. 11-Bromoundecanol was purchased from Across Organics. Sodium borohydride, sodium acetate (NaOAc), pyridine, thionyl chloride, sodium azide, hydrazine hydrate, acetic anhydride, sodium sulphate, potassium carbonate, sodium hydroxide, hydrochloric acid, dichloromethane sulphuric acid, sodium hydroxide, potassium carbonate, hydrochloric acid, sulphuric acid, ethyl chloroformate, triethyl amine and solvents were purchased from Thomas Baker, Mumbai and were used as received. Toluene, *N*-methyl-2-pyrrolidone (NMP) and *N,N*-dimethylformamide (DMF) were dried over calcium hydride and distilled prior to use.

3.2.2 Characterization

Melting points were recorded on Electrothermal MEL-TEMP apparatus.

FT-IR spectra were recorded on a Perkin-Elmer Spectrum GX spectrometer.

¹H and ¹³C NMR spectra were recorded on a Bruker-AV 200, 400, 500 MHz spectrometer using DMSO-*d*₆ or CDCl₃ (TMS as an internal standard) as solvents.

High resolution mass spectroscopy (HRMS) was used to determine exact mass of monomers/intermediates and spectra were recorded on a Thermo Scientific Q-Exactive, Accela 1250 pump.

X-Ray intensity data measurements were carried out on a Bruker SMART APEX II CCD diffractometer with graphite-monochromatized (MoK_α = 0.71073 Å) radiation. The X-ray generator was operated at 50 kV and 30 mA. A preliminary set of cell constants and an orientation matrix were calculated from three sets of 36 frames. Data were collected with ω scan width of 0.5° at different settings of φ and 2θ with a frame time of 10 secs keeping the sample-to-detector distance fixed at 5.0 cm. The X-ray data collection was monitored by APEX2 program (Bruker, 2006). All the data were corrected for Lorentzian, polarization and absorption effects using SAINT and

SADABS programs (Bruker, 2006). SHELX-97 was used for structure solution and full matrix least-squares refinement on F^2 .

3.3 Synthesis

3.3.1 Synthesis of diisocyanates containing oxyalkylene linkage.

3.3.1.1 General procedure for synthesis of α,ω -dicarboxylic acids containing oxyalkylene linkage.

Into a 250 mL two-necked round bottom flask equipped with a reflux condenser, a nitrogen inlet and an addition funnel were charged, vanillic/syringic acid (20 mmol), sodium hydroxide (50 mmol) and water (100 mL). The reaction mixture was refluxed for 1 h and then α,ω -dibromoalkane (24 mmol) was added drop wise over a period of 30 min and the heating was continued for 24 h. The reaction mixture was washed with ethyl acetate and aqueous layer was acidified with aqueous hydrochloric acid (3 M). The precipitate was filtered and dried under vacuum at 60 °C for 24 h. The product was recrystallized from aqueous ethanol.

3.3.1.1.1 Synthesis of 4,4'-(propane-1,3-diylbis(oxy))bis(3-methoxybenzoic acid)

Yield 72 %; Melting point- 259 °C; ^1H NMR (200 MHz, DMSO- d_6 , δ /ppm): 2.19-2.25 (m, 2H), 3.79 (s, 6H), 4.19 (t, 4H), 7.08 (d, 2H), 7.44 (d, 2H), 7.54 (dd, 2H); ^{13}C NMR (50 MHz, DMSO- d_6 , δ /ppm) 28.5, 55.5, 65.0, 112.0, 112.1, 123.1, 123.2, 148.4, 151.8, 167.1,

3.3.1.1.2 Synthesis of 4,4'-(butane-1,4-diylbis(oxy))bis(3-methoxybenzoic acid)

Yield 69 %; Melting point- 220 °C; ^1H NMR (200 MHz, DMSO- d_6 , δ /ppm) 1.88-1.92 (m, 4H), 3.79 (s, 6H), 4.11 (t, 4H), 7.04 (d, 2H), 7.44 (d, 2H), 7.55 (dd, 2H), 12.61 (br.s, 2H); ^{13}C NMR (50 MHz, DMSO- d_6 , δ /ppm) 25.4, 55.5, 68.0, 111.8, 112.1, 122.9, 123.1, 148.4, 152.0, 167.1

3.3.1.1.3 Synthesis of 4,4'-(pentane-1,5-diylbis(oxy))bis(3-methoxybenzoic acid)

Yield 70 %; Melting point- 244 °C; ^1H NMR (200 MHz, DMSO- d_6 , δ /ppm): 1.56-1.75 (m, 2H), 1.75-1.88 (m, 4H), 3.79 (s, 6H), 4.05 (t, 4H), 7.04 (d, 2H), 7.44 (d, 2H), 7.54 (dd, 2H), 12.66 (br.s, 2H); ^{13}C NMR (50 MHz, DMSO- d_6 , δ /ppm): 22.2, 28.3, 55.5, 68.2, 111.9, 112.1, 122.8, 123.2, 148.4, 152.0, 167.1

3.3.1.1.4 Synthesis of 4,4'-(propane-1,3-diylbis(oxy))bis(3,5-dimethoxybenzoic acid)

Yield 70 %; Melting point- 266 °C; ¹H NMR (200 MHz, DMSO-*d*₆, δ/ppm): 1.92-2.01 (m, 2H), 3.79 (s, 12H), 4.13 (t, 4H), 7.21 (s, 4H), 12.93 (br.s, 2H); ¹³C NMR (50 MHz, DMSO-*d*₆, δ/ppm): 30.6, 55.9, 69.8, 106.4, 125.7, 140.5, 152.7, 167.0

3.3.1.1.5 Synthesis of 4,4'-(butane-1,4-diylbis(oxy))bis(3,5-dimethoxybenzoic acid)

Yield 67 %; Melting point- 263 °C; ¹H NMR (200 MHz, DMSO-*d*₆, δ/ppm): 1.62-1.71 (m, 4H), 3.81 (s, 12H), 3.92 (t, 4H), 7.22 (s, 4H), 12.93 (br.s, 2H); ¹³C NMR (50 MHz, DMSO-*d*₆, δ/ppm): 26.2, 55.9, 72.2, 106.6, 125.8, 140.6, 152.9, 167.0

3.3.1.1.6 Synthesis of 4,4'-(pentane-1,5-diylbis(oxy))bis(3,5-dimethoxybenzoic acid)

Yield 73 %; Melting point- 211 °C; ¹H NMR (200 MHz, DMSO-*d*₆, δ/ppm): 1.56-1.73 (m, 6H), 2.92 (br.s, 2H), 3.81(s, 12H), 3.92 (t, 4H), 7.22 (s, 4H); ¹³C NMR (50 MHz, DMSO-*d*₆, δ/ppm): 21.7, 29.3, 55.9, 72.4, 106.5, 125.7, 140.6, 152.8, 167.0

3.3.1.2 General procedure for synthesis of α,ω-dicarboxylic acyl azides containing oxyalkylene linkage.

Into a 250 mL two-necked round bottom flask equipped with a reflux condenser, an argon inlet and an addition funnel were charged, α,ω-dicarboxylic acid (20 mmol) and a mixture of tetrahydrofuran : water (3:1, v/v) (100 mL). The reaction mixture was cooled to 0 °C and the solution of triethyl amine (12 g, 120 mmol) in tetrahydrofuran (20 mL) was added drop wise over a period of 15 min. To the reaction mixture, ethylchloroformate (12.8 g, 120 mmol) was added dropwise over a period of 10 min and stirred for 2 h. The solution of sodium azide (7.8 g, 160 mmol) in water (30 mL) was added dropwise over a period of 10 min and mixture was stirred at 0 °C for 2 h and then at room temperature for 4 h. Ice cold water (250 mL) was added gradually to the reaction mixture and solid was precipitated out. The precipitate was filtered and washed with water. Then the product was dissolved in dichloromethane and washed with water (150 mL), dried over anhydrous sodium sulfate, filtered, and concentrated under reduced pressure at 25 °C to afford a white solid.

3.3.1.2.1 Synthesis of 4,4'-(propane-1,3-diylbis(oxy))bis(3-methoxybenzoyl azide)

Yield 78 %; IR (KBr): 2140, 1680 cm⁻¹; ¹H NMR (200 MHz, CDCl₃, δ/ppm): 2.36-2.48 (m, 2H), 3.90 (s, 6H), 4.31 (t, 2H), 6.93 (d, 2H), 7.51 (d, 2H), 7.66 (dd, 2H); ¹³C NMR (50 MHz, CDCl₃, δ/ppm): 28.8, 56.0, 65.3, 111.7, 111.8, 123.4, 123.9, 149.2,

153.6, 171.6; HRMS (ESI): m/z calculated for $C_{19}H_{18}N_6O_6$ (M+Na), 449.1180; found, 449.1162.

3.3.1.2.2 Synthesis of 4,4'-(butane-1,4-diylbis(oxy))bis(3-methoxybenzoyl azide)

Yield 80 %; IR (KBr): 2143, 1686 cm^{-1} ; 1H NMR (200 MHz, $CDCl_3$, δ/ppm): 1.95-2.15 (m, 4H), 3.89 (s, 6H), 4.20 (t, 2H), 6.89 (d, 2H), 7.51 (d, 2H), 7.66 (dd, 2H); ^{13}C NMR (50 MHz, $CDCl_3$, δ/ppm): 25.7, 55.9, 68.5, 111.3, 111.6, 123.1, 123.9, 149.0, 154.0, 171.7; HRMS (ESI): m/z calculated for $C_{20}H_{20}N_6O_6$ (M+Na), 463.1342; found, 463.1360

3.3.1.2.3 Synthesis of 4,4'-(pentane-1,5-diylbis(oxy))bis(3-methoxybenzoyl azide)

Yield 75 %; IR (KBr): 2143, 1677 cm^{-1} ; 1H NMR (200 MHz, $CDCl_3$, δ/ppm): 1.64-1.74 (m, 2H), 1.91-2.01 (m, 4H), 3.91 (s, 6H), 4.12 (t, 2H), 6.87 (d, 2H), 7.53 (d, 2H), 7.65 (dd, 2H); ^{13}C NMR (50 MHz, $CDCl_3$, δ/ppm): 22.5, 28.6, 56.0, 68.7, 111.4, 111.8, 123.1, 124.0, 149.1, 153.8, 171.7; HRMS (ESI): m/z calculated for $C_{21}H_{22}N_6O_6$ (M+Na), 477.1493 ; found, 477.1474

3.3.1.2.4 Synthesis of 4,4'-(propane-1,3-diylbis(oxy))bis(3,5-dimethoxybenzoyl azide)

Yield 81 %; IR (KBr): 2146, 1684 cm^{-1} ; 1H NMR (200 MHz, $CDCl_3$, δ/ppm): 2.11-2.24 (m, 2H), 3.83 (s, 12H), 4.32 (t, 4H), 7.25 (s, 4H); ^{13}C NMR (50 MHz, $CDCl_3$, δ/ppm): 31.1, 56.1, 70.7, 106.6, 125.3, 143.0, 153.1, 171.8; HRMS (ESI): m/z calculated for $C_{21}H_{22}N_6O_8$ (M+Na), 509.1391 ; found, 509.1393

3.3.1.2.5 Synthesis of 4,4'-(butane-1,4-diylbis(oxy))bis(3,5-dimethoxybenzoyl azide)

Yield 78 %; IR (KBr): 2145, 1684 cm^{-1} ; 1H NMR (200 MHz, $CDCl_3$, δ/ppm): 1.93-1.99 (m, 4H), 3.87 (s, 12H), 4.13 (t, 4H), 7.28 (s, 4H); ^{13}C NMR (50 MHz, $CDCl_3$, δ/ppm): 25.8, 55.5, 71.8, 106.1, 125.3, 140.1, 152.4, 166.6; HRMS (ESI): m/z calculated for $C_{22}H_{24}N_6O_8$ (M+H), 501.1728; found, 501.1620

3.3.1.2.6 Synthesis of 4,4'-(pentane-1,5-diylbis(oxy))bis(3,5-dimethoxybenzoyl azide)

Yield 83 %; IR (KBr): 2143, 1684 cm^{-1} ; 1H NMR (200 MHz, $CDCl_3$, δ/ppm): 1.60-1.86 (m, 6H), 3.88 (s, 12H), 4.08 (t, 4H), 7.28 (s, 4H); ^{13}C NMR (50 MHz, $CDCl_3$, δ/ppm): 21.9, 29.7, 56.1, 73.3, 106.6, 125.2, 142.8, 153.2, 171.7; HRMS (ESI): m/z calculated for $C_{23}H_{26}N_6O_8$ (M+H), 515.1885; found, 515.1779

3.3.1.3 General procedure for synthesis of α,ω -diisocyanates containing oxyalkylene linkage.

Into a 100 mL two-necked round bottom flask equipped with a reflux condenser and a nitrogen inlet were charged, α,ω -diacyl azide (4.69 mmol) and dry toluene (25 mL). The reaction mixture was heated at 80 °C for 8 h. The toluene was removed under reduced pressure at 60 °C and white solid compound was obtained.

3.3.1.3.1 Synthesis of 1,3-bis(4-isocyanato-2-methoxyphenoxy)propane

Yield 83 %; Melting point- 136 °C; IR (KBr): 2292 cm^{-1} ; ^1H NMR (400 MHz, CDCl_3 , δ/ppm): 2.27-2.39 (m, 2H), 3.83 (s, 6H), 4.21 (t, 4H), 6.63 (dd, 4H), 6.84 (d, 2H); ^{13}C NMR (50 MHz, CDCl_3 , δ/ppm): 29.2, 56.0, 66.0, 108.8, 113.9, 116.6, 124.2, 126.5, 146.4, 150.0; HRMS (ESI): m/z calculated for $\text{C}_{19}\text{H}_{18}\text{N}_2\text{O}_6$ (M+H), 371.1238; found, 371.1249.

3.3.1.3.2 Synthesis of 1,4-bis(4-isocyanato-2-methoxyphenoxy)butane

Yield 78 %; Melting point- 90 °C; IR (KBr): 2290 cm^{-1} ; ^1H NMR (400 MHz, CDCl_3 , δ/ppm): 2.0-2.06 (m, 4H), 3.83 (s, 6H), 4.04 (t, 4H), 6.61 (d, 2H), 6.65 (dd, 2H), 6.80 (d, 2H); ^{13}C NMR (100 MHz, CDCl_3 , δ/ppm): 25.8, 55.9, 68.8, 108.7, 113.3, 116.5, 124.1, 126.1, 146.4, 149.8; HRMS (ESI): m/z calculated for $\text{C}_{20}\text{H}_{20}\text{N}_2\text{O}_6$ (M+Na), 407.1219; found, 407.1228

3.3.1.3.3 Synthesis of 1,5-bis(4-isocyanato-2-methoxyphenoxy)pentane

Yield 81 %; Melting point- 93 °C; IR (KBr) : 2284 cm^{-1} ; ^1H NMR (200 MHz, CDCl_3 , δ/ppm): 1.60-1.69 (m, 2H), 1.84-1.98 (m, 4H), 3.84 (s, 6H), 4.01 (t, 4H), 6.61 (d, 2H), 6.65 (dd, 2H), 6.78 (d, 2H); ^{13}C NMR (100 MHz, CDCl_3 , δ/ppm): 22.5, 28.9, 56.0, 69.1, 108.7, 113.4, 116.5, 124.1, 126.2, 146.5, 149.9; HRMS (ESI): m/z calculated for $\text{C}_{21}\text{H}_{22}\text{N}_2\text{O}_6$ (M+Na), 421.1370; found, 421.1369

3.3.1.3.4 Synthesis of 1,3-bis(4-isocyanato-2,6-dimethoxyphenoxy)propane

Yield 87 %; Melting point- 105 °C; IR (KBr): 2268 cm^{-1} ; ^1H NMR (400 MHz, CDCl_3 , δ/ppm): 2.12-2.19 (m, 2H), 3.79 (s, 12H), 4.16 (t, 4H), 6.31 (s, 4H); ^{13}C NMR (50 MHz, CDCl_3 , δ/ppm): 30.8, 56.1, 70.9, 102.2, 128.8, 153.4, 153.8; HRMS (ESI): m/z calculated for $\text{C}_{21}\text{H}_{22}\text{N}_2\text{O}_8$ (M+Na), 453.1268; found, 453.1272

3.3.1.3.5 Synthesis of 1,4-bis(4-isocyanato-2,6-dimethoxyphenoxy)butane

Yield 88 %; Melting point- 60 °C; IR (KBr): 2280 cm^{-1} ^1H NMR (400 MHz, CDCl_3 , δ/ppm): 2.87-2.9 (m, 4H), 4.76 (s, 12H), 4.96 (t, 4H), 7.27 (s, 4H); ^{13}C NMR (50 MHz,

CDCl₃, δ/ppm): 26.4, 56.1, 73.1, 102.3, 124.4, 128.7, 135.3, 153.8; HRMS (ESI): m/z calculated for C₂₂H₂₄N₂O₈ (M+Na), 467.1425; found, 467.1424.

3.3.1.3.6 Synthesis of 1,5-bis(4-isocyanato-2,6-dimethoxyphenoxy)pentane

Yield 85 %; Melting point- 62 °C; IR (KBr): 2288 cm⁻¹; ¹H NMR (200 MHz, CDCl₃, δ/ppm): 1.60-1.67 (m, 2H), 1.74-1.84 (m, 4H), 3.81 (s, 12H), 3.94 (t, 4H), 6.31 (s, 4H); ¹³C NMR (50 MHz, CDCl₃, δ/ppm): 22.0, 29.7, 56.1, 73.4, 102.2, 124.4, 128.7, 135.4, 152.8; HRMS (ESI): m/z calculated for C₂₃H₂₆N₂O₈ (M+H), 459.1762; found, 459.1704.

3.3.2 Synthesis of 3,3'-diisocyanates containing biphenylene linkage

3.3.2.1 Synthesis of dimethyl 6,6'-dihydroxy-5,5'-dimethoxy-[1,1'-biphenyl]-3,3'-dicarboxylate

Into a 2 L two-necked round bottom flask were charged methyl vanillate (15 g, 82.3 mmol), NaOAc buffer (1800 mL, 0.1 M, pH 5.0) and acetone (200 mL). The solution was saturated with O₂ for 5 min. Laccase from *Trametes versicolor* (124 mg) was added and the reaction mixture was stirred at room temperature for 24 h. The precipitate was filtered off and the product was dried overnight at 90 °C.

Yield 89 %; IR (KBr): 1716, 3432 cm⁻¹; ¹H NMR (200 MHz, CDCl₃, δ/ppm): 3.80 (s, 6H), 3.89 (s, 6H), 7.45 (s, 4H), 9.68 (br. s, 2H); ¹³C NMR (50 MHz, CDCl₃, δ/ppm): 51.7, 56.0, 110.9, 119.2, 124.5, 125.4, 147.6, 149.3, 166.1; HRMS ESI⁺: (M+H)⁺ m/z calculated for C₁₈H₁₉O₈: 363.1074, found: 363.1071.

3.3.2.2 General procedure for synthesis of dimethyl 6,6'-alkoxy-5,5'-dimethoxy-[1,1'-biphenyl]-3,3'-dicarboxylate

Into a 500 mL two-necked round bottom flask equipped with a reflux condenser and an argon inlet were charged, dimethyl 6,6'-dihydroxy-5,5'-dimethoxy-[1,1'-biphenyl]-3,3'-dicarboxylate (8 g, 22.0 mmol), potassium carbonate (12.2 g, 88.3 mmol) and N,N-dimethylformamide (100 mL). The reaction mixture was heated at 100 °C for 1 h and then alkyl iodide/bromide (55.2 mmol) was added and heating was continued for 12 h. The reaction mixture was poured into ice cold water (1000 mL). The precipitate was filtered, dried and dissolved in dichloromethane (100 mL). The dichloromethane solution was washed with water (2 x 500 mL), dried over anhydrous sodium sulfate, filtered, and concentrated under reduced pressure. The crude product

was purified by column chromatography using pet ether: ethyl acetate (70:30 v/v) as an eluent to afford a white solid.

3.3.2.2.1 Synthesis of dimethyl 5,5',6,6'-tetramethoxy-[1,1'-biphenyl]-3,3'-dicarboxylate

Yield 95 %; IR (KBr): 1725 cm^{-1} ; ^1H NMR (200 MHz, CDCl_3 , δ/ppm): 3.72 (s, 6H), 3.89 (s, 6H), 3.96 (s, 6H), 7.58 (d, 2H), 7.63 (d, 2H); ^{13}C NMR (50 MHz, CDCl_3 , δ/ppm): 52.1, 56.0, 60.8, 113.0, 125.0, 125.1, 131.7, 150.9, 152.4, 166.6; HRMS ESI⁺: (M+H)⁺ m/z calculated for $\text{C}_{20}\text{H}_{23}\text{O}_8$: 391.1387, found: 391.1383.

3.3.2.2.2 Synthesis of dimethyl 5,5'-dimethoxy-6,6'-bis(pentyloxy)-[1,1'-biphenyl]-3,3'-dicarboxylate

Yield 91 %; Melting point- 44 °C; IR (KBr): 1728 cm^{-1} ; ^1H NMR (200 MHz, CDCl_3 , δ/ppm): 0.76 (t, 6H), 1.03-1.11 (m, 8H), 1.39-1.53 (m, 4H), 3.85 (t, 4H), 3.88 (s, 6H), 3.93 (s, 6H), 7.60 (d, 2H), 7.62 (d, 2H); ^{13}C NMR (50 MHz, CDCl_3 , δ/ppm): 13.9, 22.3, 27.8, 29.7, 52.0, 56.0, 73.3, 112.7, 125.3; HRMS ESI⁺: (M+H)⁺ m/z calculated for $\text{C}_{28}\text{H}_{39}\text{O}_8$: 503.2639, found: 503.2619.

3.3.2.3 General procedure for synthesis of 6,6'-dialkoxy-5,5'-dimethoxy-[1,1'-biphenyl]-3,3'-dicarboxylic acid

Into a 500 mL two-necked round bottom flask equipped with a reflux condenser were charged dimethyl 6,6'-alkoxy-5,5'-dimethoxy-[1,1'-biphenyl]-3,3'-dicarboxylate (30 mmol), sodium hydroxide (6 g, 150 mmol), methanol (100 mL) and water (100 mL). The reaction mixture was refluxed for 12 h and then excess methanol was removed under reduced pressure. The solution was diluted with water and acidified with aqueous hydrochloric acid (3M). The precipitate was filtered and dried in vacuum oven at 60 °C for 4 h and then recrystallized from aqueous ethanol.

3.3.2.3.1 Synthesis of 5,5',6,6'-tetramethoxy-[1,1'-biphenyl]-3,3'-dicarboxylic acid

Yield 95 %; IR (KBr): 1671 cm^{-1} ; ^1H NMR (200 MHz, CDCl_3 , δ/ppm): 3.61 (s, 6H), 3.91 (s, 6H), 7.38 (d, 2H), 7.57 (d, 2H), 12.95 (s, 2H); ^{13}C NMR (50 MHz, CDCl_3 , δ/ppm): 55.8, 60.2, 112.9, 124.1, 125.9, 131.3, 150.0, 152.1, 166.8; HRMS ESI⁺: (M+Na)⁺ m/z calculated for $\text{C}_{18}\text{H}_{18}\text{O}_8$ Na: 385.0894, found: 385.0892.

3.3.2.3.2 Synthesis of 5,5'-dimethoxy-6,6'-bis(pentyloxy)-[1,1'-biphenyl]-3,3'-dicarboxylic acid

Yield 94 %; Melting point- 222 °C; IR (KBr): 1672 cm⁻¹; ¹H NMR (200 MHz, CDCl₃, δ/ppm): 0.69 (t, 6H), 0.90-1.09 (m, 8H), 1.32-1.42 (m, 4H), 3.80 (t, 4H), 3.88 (s, 6H), 7.41 (d, 4H), 7.55 (d, 2H), 12.88 (s, 2H); ¹³C NMR (50 MHz, CDCl₃, δ/ppm): 13.8, 21.7, 27.3, 29.1, 55.8, 72.4, 112.7, 124.4, 125.5, 131.6, 149.5, 152.3, 166.8

3.3.2.4 General procedure for synthesis of 6,6'-dialkoxy-5,5'-dimethoxy-[1,1'-biphenyl]-3,3'-dicarbonyl diazide

Into a 250 mL two-necked round bottom flask equipped with a reflux condenser, an argon inlet and an addition funnel were charged, 6,6'-dialkoxy-5,5'-dimethoxy-[1,1'-biphenyl]-3,3'-dicarboxylic acid (20 mmol) and a mixture of tetrahydrofuran: water (3:1 v/v) (100 mL). The reaction mixture was cooled to 0 °C and the solution of triethyl amine (12 g, 120 mmol) in tetrahydrofuran (20 mL) was added drop wise over a period of 15 min. To the reaction mixture, ethylchloroformate (12.8 g, 120 mmol) was added dropwise over a period of 10 min and stirred for 2 h. The solution of sodium azide (7.8 g, 160 mmol) in water (30 mL) was added dropwise over a period of 10 min and the reaction mixture was stirred at 0 °C for 2 h and then at 25 °C for 4 h. Ice cold water (250 mL) was added gradually to the reaction mixture and solid was precipitated out. The precipitate was filtered and washed with water. The product was dissolved in dichloromethane (200 mL) and washed with water (150 mL), dried over anhydrous sodium sulfate, filtered, and concentrated under reduced pressure at 25 °C to afford a white solid.

3.3.2.4.1 Synthesis of 5,5',6,6'-tetramethoxy-[1,1'-biphenyl]-3,3'-dicarbonyl diazide

Yield 80 %; IR (KBr): 2143, 1680 cm⁻¹; ¹H NMR (200 MHz, CDCl₃, δ/ppm): 3.75 (d, 6H), 3.96 (d, 6H), 7.55 (s, 2H), 7.61 (s, 2H); ¹³C NMR (50 MHz, CDCl₃, δ/ppm): 55.9, 60.8, 112.5, 124.9, 125.5, 131.4, 152.1, 152.5, 171.5; HRMS ESI⁺: (M+H)⁺ m/z calculated for C₁₈H₁₇N₆O₈: 413.1204, found: 413.2663.

3.3.2.4.2 Synthesis of 5,5'-dimethoxy-6,6'-bis(pentyloxy)-[1,1'-biphenyl]-3,3'-dicarbonyl diazide

Yield 84 %; IR (KBr): 2145, 1678 cm⁻¹; ¹H NMR (200 MHz, CDCl₃, δ/ppm): 0.77 (t, 6H), 1.03-1.13 (m, 8H), 1.43-1.50 (m, 4H), 3.89 (t, 4H), 3.94 (s, 6H), 7.60 (s, 4H); ¹³C NMR (50 MHz, CDCl₃, δ/ppm): 13.9, 22.2, 27.8, 29.7, 56.0, 73.5, 112.3, 125.2, 125.4, 131.9, 151.9, 152.8, 171.7; HRMS ESI⁺: (M+H)⁺ m/z calculated for C₂₆H₃₃O₆N₆: 525.2456, found: 525.2436.

3.3.2.5 General procedure for synthesis of 5,5'-diisocyanato-3,3'-dimethoxy-2,2'-bis(alkoxy)-1,1'-biphenyl

Into a 100 mL two-necked round bottom flask equipped with a reflux condenser and a nitrogen inlet were charged, 5,5',6,6'-tetramethoxy-[1,1'-biphenyl]-3,3'-dicarbonyl diazide (1.9 g, 4.69 mmol) and dry toluene (25 mL). The reaction mixture was heated at 80 °C for 8 h. The toluene was removed under reduced pressure at 60 °C and white solid compound was obtained.

3.3.2.5.1 Synthesis of 5,5'-diisocyanato-2,2',3,3'-tetramethoxy-1,1'-biphenyl

Yield 85 %; Melting point- 95 °C; IR (KBr): 2268 cm^{-1} ; ^1H NMR (200 MHz, CDCl_3 , δ/ppm): 3.54 (d, 6H), 3.78 (d, 6H), 6.47 (s, 2H), 7.61 (s, 2H); ^{13}C NMR (50 MHz, CDCl_3 , δ/ppm): 56.0, 60.8, 108.7, 118.7, 124.5, 128.6, 132.3, 144.6, 153.2; HRMS ESI⁺: (M+H)⁺ m/z calculated for $\text{C}_{18}\text{H}_{17}\text{N}_2\text{O}_6$: 357.1081, found: 357.1079.

3.3.2.5.2 Synthesis of 5,5'-diisocyanato-3,3'-dimethoxy-2,2'-bis(pentyloxy)-1,1'-biphenyl

Yield 88 %; IR (KBr): 2260 cm^{-1} ; ^1H NMR (200 MHz, CDCl_3 , δ/ppm): 0.69 (t, 6H), 0.92-1.09 (m, 8H), 1.29-1.42 (m, 4H), 3.80 (t, 4H), 3.88 (s, 6H), 7.41 (d, 2H), 7.55 (d, 2H), 12.88 (br.s, 2H); ^{13}C NMR (50 MHz, CDCl_3 , δ/ppm): 13.9, 22.2, 27.8, 29.7, 56.0, 73.5, 109.0, 118.9, 125.0, 128.3, 131.0, 146.2, 153.6; HRMS ESI⁺: (M+H)⁺ m/z calculated for $\text{C}_{26}\text{H}_{33}\text{N}_2\text{O}_6$: 468.2260, found: 468.2230.

3.3.3 Synthesis of A-B type monomers

3.3.3.1 Procedure for synthesis of methyl vanillate and methyl syringate

Into a 250 mL two-necked round bottom flask equipped with a reflux condenser and an argon inlet were charged vanillic acid or syringic acid (50 mmol), sulphuric acid (1 mL) and methanol (100 mL). The reaction mixture was refluxed for 10 h. After completion of reaction, excess methanol was removed under reduced pressure. The reaction mixture was dissolved in dichloromethane (100 mL). The dichloromethane solution was washed with water (2 × 100 mL), dried over anhydrous sodium sulfate, filtered, and concentrated under reduced pressure. The crude product was filtered through short bed of silica column using pet ether: dichloromethane as an eluent to afford white solid.

3.3.3.1.1 Synthesis of methyl 4-hydroxy-3-methoxybenzoate

Yield 95 %; Melting point- 64 °C (lit 63-64)²⁸; IR (KBr): 1692 cm⁻¹; ¹H NMR (200 MHz, CDCl₃, δ/ppm): 3.90 (s, 3H), 3.95 (s, 3H), 6.05 (s, 1H), 6.94 (d, 1H), 7.56 (d, 1H), 7.66 (dd, 1H); ¹³C NMR (50 MHz, CDCl₃, δ/ppm): 51.88, 56.01, 111.76, 114.08, 122.18, 124.14, 146.18, 150.05, 166.87; HRMS (ESI) calculated for C₉H₁₀O₄ (M +H), 183.0657; found, 183.0652.

3.3.3.1.2 Synthesis of methyl 4-hydroxy-3,5-dimethoxybenzoate

Yield 94 %; Melting point- 107 °C (lit. 105-107 °C)²⁹; IR (KBr): 1685 cm⁻¹; ¹H NMR (200 MHz, CDCl₃, δ/ppm): 3.89 (s, 3H), 3.93 (s, 6H), 5.99 (s, 1H), 7.32 (s, 2H); ¹³C NMR (100 MHz, CDCl₃, δ/ppm): 52.06, 56.37, 106.59, 121.01, 139.15, 146.58, 166.83; HRMS (ESI) calculated for C₁₀H₁₂O₅ (M+Na), 235.0582; found, 235.0577.

3.3.3.2 General procedure for synthesis of ω-hydroxyalkyleneoxy benzoic acid methyl esters

Into a 250 mL two-necked round bottom flask equipped with a reflux condenser and an argon inlet were charged, methyl vanillate/ methyl syringate (40 mmol), potassium carbonate (22.1 g, 160 mmol) and *N,N*-dimethylformamide (100 mL). The reaction mixture was heated at 100 °C for 1 h and then 11-bromoundecanol or 6-chlorohexanol (48 mmol) was added and heating was continued for 12 h. The reaction mixture was poured into ice cold water (250 mL). The precipitate was filtered and dissolved in dichloromethane (100 mL). The dichloromethane solution was washed with water (2 x 100 mL), dried over anhydrous sodium sulfate, filtered, and concentrated under reduced pressure. The crude product was purified by column chromatography using pet ether: ethyl acetate as an eluent to afford white solid.

3.3.3.2.1 Synthesis of methyl 4-((6-hydroxyhexyl)oxy)-3-methoxybenzoate

Yield 87 %; Melting point- 62 °C; IR (KBr): 3367, 1714 cm⁻¹; ¹H NMR (400 MHz, CDCl₃, δ/ppm): 1.41-1.53 (m, 4H), 1.57-1.64 (m, 2H), 1.84-1.91 (m, 2H), 3.65 (t, 2H), 3.89 (s, 3H), 3.91 (s, 3H), 4.07 (t, 2H), 6.87 (d, 1H), 7.53 (d, 1H), 7.64 (dd, 1H); ¹³C NMR (100 MHz, CDCl₃, δ/ppm): 25.45, 25.72, 28.88, 32.55, 51.91, 56.0, 62.75, 68.80, 111.35, 112.27, 122.37, 123.49, 148.78, 152.52, 166.90; HRMS (ESI) calculated for C₁₅H₂₂O₅ (M+Na), 305.1359; found 305.1348.

3.3.3.2.2 Synthesis of methyl 4-((11-hydroxyundecyl)oxy)-3-methoxybenzoate

Yield 80 %; Melting point- 45 °C; IR (KBr): 3382, 1717 cm⁻¹; ¹H NMR (200 MHz, CDCl₃, δ/ppm): 1.27-1.99 (m, 18H), 3.64 (t, 2H), 3.89 (s, 3H), 3.92 (s, 3H), 4.07 (t,

2H), 6.88 (d, 1H), 7.54 (d, 1H), 7.66 (dd, 1H); ^{13}C NMR (100 MHz, CDCl_3 , δ/ppm): 25.7, 25.8, 29.3, 29.4, 29.5, 32.7, 51.9, 56.0, 62.9, 68.9, 111.3, 112.2, 122.2, 123.5, 148.7, 152.5, 166.9; HRMS (ESI) calculated for $\text{C}_{20}\text{H}_{32}\text{O}_5$ (M+Na), 375.2147; found 375.2142.

3.3.3.2.3 Synthesis of methyl 4-((6-hydroxyhexyl)oxy)-3,5-dimethoxybenzoate

Yield 92 %; Melting point- 42 °C; IR (KBr): 3382, 1714 cm^{-1} ; ^1H NMR (400 MHz, CDCl_3 , δ/ppm): 1.37-1.59 (m, 6H), 1.71-1.76 (m, 2H), 3.63 (t, 2H), 3.86 (s, 6H), 3.88 (s, 3H), 4.01 (t, 2H), 7.27 (s, 2H); ^{13}C NMR (100 MHz, CDCl_3 , δ/ppm): 25.4, 25.5, 29.9, 32.6, 52.1, 56.1, 62.8, 73.3, 106.8, 124.8, 141.4, 153.1, 166.7; HRMS (ESI) calculated for $\text{C}_{16}\text{H}_{24}\text{O}_6$ (M+Na), 335.1465; found, 335.1452.

3.3.3.2.4 Synthesis of methyl 4-((11-hydroxyundecyl)oxy)-3,5-dimethoxybenzoate

Yield 78 %; Melting point- 81 °C; IR (KBr): 3412, 1708 cm^{-1} ; ^1H NMR (200 MHz, CDCl_3 , δ/ppm): 1.26-1.75 (m, 18H), 3.64 (t, 2H), 3.89 (s, 6H), 3.91 (s, 3H), 4.03 (t, 2H), 7.29 (s, 2H); ^{13}C NMR (50 MHz, CDCl_3 , δ/ppm): 25.6, 29.2, 29.3, 29.4, 29.4, 32.7, 52.0, 56.1, 62.8, 73.4, 106.8, 124.7, 141.5, 153.1, 166.7; HRMS (ESI) calculated for $\text{C}_{21}\text{H}_{34}\text{O}_6$ (M+Na), 405.2253; found, 405.2248.

3.3.3.3 General procedure for synthesis of ω -hydroxyalkyleneoxy benzoic acids

Into a 250 mL two-necked round bottom flask equipped with a reflux condenser were charged, ω -hydroxyalkyleneoxy benzoic acid methyl ester (30 mmol), sodium hydroxide (6 g, 150 mmol), methanol (100 mL) and water (100 mL). The reaction mixture was refluxed for 12 h, and excess methanol was removed under reduced pressure. The solution was diluted with water and acidified with aqueous hydrochloric acid (3M). The precipitate was filtered and dried in vacuum oven at 60 °C for 4 h and then recrystallized from aqueous ethanol.

3.3.3.3.1 Synthesis of 4-((6-hydroxyhexyl)oxy)-3-methoxybenzoic acid

Yield 78 %; Melting point-131 °C (129-130 °C)³⁰; IR (KBr): 3354, 1685 cm^{-1} ; ^1H NMR (200 MHz, $\text{DMSO}-d_6$, δ/ppm): 1.37-1.43 (m, 6H), 1.70-1.75 (m, 2H), 3.37 (t, 2H), 3.80 (s, 3H), 4.01 (t, 2H), 4.35 (t, 1H), 7.03 (d, 1H), 7.44 (d, 1H), 7.53 (dd, 1H), 12.64 (br. s, 1H); ^{13}C NMR (50 MHz, $\text{DMSO}-d_6$, δ/ppm): 25.3, 25.4, 28.7, 32.5, 55.5, 60.7, 68.3, 111.9, 112.2, 122.8, 123.3, 148.5, 152.1, 167.2; HRMS (ESI): m/z calculated for $\text{C}_{14}\text{H}_{20}\text{O}_5$ (M+Na)⁺, 291.1111 ; found, 291.1203.

3.3.3.3.2 Synthesis of 4-((11-hydroxyundecyl)oxy)-3-methoxybenzoic acid

Yield 94 %; Melting point- 110 °C; IR (KBr): 3326, 1683 cm⁻¹; ¹H NMR (200 MHz, DMSO-*d*₆, δ/ppm): 1.25-1.39 (m, 16H), 1.70-1.76 (m, 2H), 3.36 (t, 2H), 4.01 (t, 2H), 4.32 (br. s, 1H), 7.03 (d, 1H), 7.42 (d, 1H), 7.53 (dd, 1H), 12.62 (br. s, 1H); ¹³C NMR (100 MHz, DMSO-*d*₆, δ/ppm): 25.5, 25.5, 28.6, 28.8, 29.0, 29.1, 32.6, 55.5, 60.7, 68.2, 111.8, 112.1, 122.9, 123.2, 148.4, 152.0, 167.2; HRMS (ESI) calculated for C₁₉H₃₀O₅ (M+Na), 361.1993; found 361.1985.

3.3.3.3.3 Synthesis of 4-((6-hydroxyhexyl)oxy)-3,5-dimethoxybenzoic acid

Yield 75 %; Melting point- 82 °C; IR (KBr): 3306, 1683 cm⁻¹; ¹H NMR (400 MHz, DMSO-*d*₆, δ/ppm): 1.24-1.44 (m, 2H), 1.54-1.69 (m, 4H), 3.39 (t, 2H), 3.81 (s, 6H), 3.91 (t, 2H), 4.33 (t, 1H), 7.22 (s, 2H), 12.90 (br. s, 1H); ¹³C NMR (100 MHz, DMSO-*d*₆, δ/ppm): 25.3, 29.7, 32.6, 55.9, 60.7, 72.5, 106.6, 125.7, 140.7, 152.8, 167.0; HRMS (ESI) calculated for C₁₅H₂₂O₆ (M+Na), 321.1316; found, 321.1309.

3.3.3.3.4 Synthesis of 4-((11-hydroxyundecyl)oxy)-3,5-dimethoxybenzoic acid

Yield 96 %; Melting point- 81 °C; IR (KBr): 3317, 1688 cm⁻¹; ¹H NMR (400 MHz, DMSO-*d*₆, δ/ppm): 1.13-1.44 (m, 16H), 1.55-1.71 (m, 2H), 3.36 (t, 2H), 3.80 (s, 6H), 3.90 (t, 2H), 4.31 (br. s, 1H), 7.22 (s, 2H); ¹³C NMR (50 MHz, DMSO-*d*₆, δ/ppm): 25.3, 25.5, 28.7, 29.0, 29.0, 29.1, 29.6, 32.5, 55.9, 60.7, 72.4, 106.6, 125.6, 140.6, 152.8, 166.9; HRMS (ESI) calculated for C₂₀H₃₂O₆ (M+Na), 391.2099; found 391.2091.

3.3.3.4 General procedure for synthesis of ω-hydroxyalkyleneoxy benzoyl azides

Into a 250 mL two-necked round bottom flask equipped with a reflux condenser, an argon inlet and an addition funnel were charged ω-hydroxyalkyleneoxy benzoic acid (20 mmol) and a mixture of tetrahydrofuran : water (3:1, v/v) (50 mL). The reaction mixture was cooled to 0 °C and the solution of triethyl amine (6 g, 60 mmol) in tetrahydrofuran (15 mL) was added dropwise over a period of 15 min. To the reaction mixture, ethylchloroformate (6.4 g, 60 mmol) was added dropwise over a period of 10 min. and stirred for 2 h. The solution of sodium azide (3.9 g, 80 mmol) in water (25 mL) was added dropwise over a period of 10 min. and the mixture was stirred at 0 °C for 2 h and then stirring was continued at room temperature for 4 h. Ice cold water (200 mL) was added gradually to the reaction mixture to obtain white solid. The crude product was dissolved in dichloromethane and washed with water (2 × 100

mL). The dichloromethane solution was dried over anhydrous sodium sulfate, filtered and concentrated under reduced pressure at 25 °C to afford a white solid.

3.3.3.4.1 Synthesis of 4-((6-hydroxyhexyl)oxy)-3-methoxybenzoyl azide

Yield 80 %; Melting point- 74 °C; IR (KBr): 3286, 2152, 1681 cm^{-1} ; ^1H NMR (200 MHz, CDCl_3 , δ/ppm): 1.50-1.64 (m, 6H), 1.83-1.96 (m, 2H), 3.67 (t, 2H), 3.92 (s, 3H), 4.1 (t, 2H), 6.88 (d, 1H), 7.53 (d, 1H), 7.66 (dd, 1H); ^{13}C NMR (100 MHz, CDCl_3 , δ/ppm): 25.5, 25.7, 28.8, 32.6, 56.1, 62.8, 68.9, 111.3, 111.8, 123.0, 124.0, 149.1, 153.9, 171.7; HRMS (ESI) calculated for $\text{C}_{14}\text{H}_{19}\text{N}_3\text{O}_4$ (M+Na), 316.1273; found, 316.1268.

3.3.3.4.2 Synthesis of 4-((11-hydroxyundecyl)oxy)-3-methoxybenzoyl azide

Yield 76 %; Melting point- 89 °C; IR (KBr): 3231, 2153, 1676 cm^{-1} ; ^1H NMR (400 MHz, CDCl_3 , δ/ppm): 1.29-1.58 (m, 18H), 1.83-1.90 (m, 2H), 3.64 (t, 2H), 3.92 (s, 3H), 4.08 (t, 2H), 6.87 (d, 1H), 7.51 (d, 1H), 7.66 (dd, 1H); ^{13}C NMR (100 MHz, CDCl_3 , δ/ppm): 25.7, 25.8, 28.8, 29.3, 29.4, 29.4, 29.5, 32.7, 56.0, 63.0, 69.1, 111.2, 111.7, 122.9, 124.0, 149.1, 154.0, 171.7; HRMS (ESI) calculated for $\text{C}_{19}\text{H}_{29}\text{N}_3\text{O}_4$ (M+Na), 386.2056; found, 386.2050.

3.3.3.4.3 Synthesis of 4-((6-hydroxyhexyl)oxy)-3,5-dimethoxybenzoyl azide

Yield 78 %; Melting point- 44 °C; IR (KBr): 3282, 2155, 1682 cm^{-1} ; ^1H NMR (200 MHz, CDCl_3 , δ/ppm): 1.43-1.83 (m, 8H), 3.68 (t, 2H), 3.91 (s, 6H), 4.07 (t, 2H), 7.37 (s, 2H); ^{13}C NMR (50 MHz, CDCl_3 , δ/ppm): 25.4, 25.5, 30.0, 32.7, 56.2, 62.9, 73.5, 106.8, 125.3, 143.0, 153.3, 171.8; HRMS (ESI) calculated for $\text{C}_{15}\text{H}_{21}\text{N}_3\text{O}_5$ (M+Na), 346.1379; found, 346.1373.

3.3.3.4.4 Synthesis of 4-((11-hydroxyundecyl)oxy)-3,5-dimethoxybenzoyl azide

Yield 75 %; Melting point- 57 °C; IR (KBr): 3440, 2155, 1688 cm^{-1} ; ^1H NMR (400 MHz, CDCl_3 , δ/ppm): 1.25-1.37 (m, 12H), 1.40-1.49 (m, 2H), 1.53-1.62 (m, 2H), 1.71-1.78 (m, 2H), 3.65 (t, 2H), 3.89 (s, 6H), 4.06 (t, 2H), 7.28 (s, 2H); ^{13}C NMR (100 MHz, CDCl_3 , δ/ppm): 25.7, 29.3, 29.4, 29.5, 29.5, 30.0, 32.7, 56.2, 63.0, 73.7, 106.7, 125.2, 143.0, 153.3, 171.8; HRMS (ESI) calculated for $\text{C}_{20}\text{H}_{31}\text{N}_3\text{O}_5$ (M+Na), 416.2161; found, 416.2156.

3.3.4 Synthesis of furyl containing bisphenols

3.3.4.1 General procedure for synthesis of furyl containing bisphenols

Into a 500 mL two necked round bottom flask equipped with a reflux condenser, an addition funnel and a magnetic stirring bar were charged guaiacol or syringol (64.93 mmol) and 20% aqueous NaOH (5% by weight based on guaiacol or syringol) at room temperature. Furfural/ methyl furfural (32.40 mmol) was added dropwise with stirring. The reaction mixture was stirred at room temperature for 4 h and then heated at 100 °C for 4 h. The reaction mixture was cooled to room temperature and diluted with cold water (500 mL) with stirring. The solution was neutralized with dilute hydrochloric acid. The precipitated product was separated out by filtration and washed with cold water. The product was dissolved in dichloromethane (200 mL) and the solution was dried over anhydrous sodium sulphate, filtered and dichloromethane was removed under reduced pressure at room temperature. The product was recrystallized from ethanol: water to afford solid product.

3.3.4.1.1 Synthesis of 4, 4'-(furan-2-ylmethylene)bis(2,6-dimethoxyphenol)

Yield 82%; Melting point- 125 °C; ¹H NMR (500 MHz, CDCl₃, δ/ppm): 3.81 (s, 12H) 5.31 (s, 1H) 5.45 (br. s, 2H) 5.94 (d, 1H) 6.31-6.33 (m, 1H) 6.39 (s, 4H) 7.39 (br.s, 1H); ¹³C NMR (125 MHz, CDCl₃ δ/ppm): 50.6, 56.2, 105.4, 108.1, 110.1, 132.8, 133.5, 141.8, 146.8, 156.9; HRMS ESI⁺: (M+Na)⁺ m/z calculated for C₂₁H₂₂O₇Na: 409.1264, found: 409.1258.

3.3.4.1.2 Synthesis of 4,4'-(furan-2-ylmethylene)bis(2-methoxyphenol)

Yield 58%; Melting point- 145 °C; ¹H NMR (500 MHz, CDCl₃, δ/ppm): 3.81 (s, 6H) 5.32 (s, 1H) 5.54 (br. s, 2H) 5.91(d, 1H) 6.30-6.32 (m 1H) 6.64 (dd, 2H) 6.68 (d, 2H) 6.85 (d, 2H) 7.38 (br.s, 1H); ¹³C NMR (50 MHz, CDCl₃ δ/ppm): 50.3, 55.9, 108.6, 110.2, 113.2, 119.9, 121.0, 122.5, 137.7, 140.7, 142.1, 146.5, 150.9, 155.6, 155.8; HRMS ESI⁺: (M+Na)⁺ m/z calculated for C₁₉H₁₈O₅Na: 349.1046, found: 349.1043.

3.3.4.1.3 Synthesis of 4,4'-((5-methylfuran-2-yl)methylene)bis(2,6-dimethoxyphenol)

Yield 85%; Melting point- 118 °C; ¹H NMR (200 MHz, CDCl₃, δ/ppm): 2.26(s, 3H), 3.80 (s, 12H), 5.25 (s, 1H), 5.50 (s, 1H), 5.76 (d, 1H), 5.88 (d, 1H), 6.40 (s, 4H); ¹³C NMR (50 MHz, CDCl₃ δ/ppm): 13.5, 50.7, 56.2, 105.5, 105.8, 108.9, 133.0, 133.4, 146.8, 151.3, 155.0; HRMS ESI⁺: (M+Na)⁺ m/z calculated for C₂₂H₂₄O₇Na: 423.1410, found: 423.1414.

3.3.5 Synthesis of oxadiazole containing bisphenols

3.3.5.1 Synthesis of 4-acetoxy-3-methoxybenzoic acid

Into a 250 mL two-necked round bottom flask equipped with a reflux condenser, an argon inlet and an addition funnel were charged, vanillic acid (5 g, 29 mmol), acetic anhydride (10 mL, 98 mmol) and sulphuric acid (1 mL). The reaction mixture was heated to 70 °C for 2 h. Ice cold water (250 mL) was added gradually to the reaction mixture and solid was precipitated out. The precipitate was filtered and washed with water. The crude product was recrystallized from water: ethanol mixture. Yield 96%; Melting point- 144 °C; ¹H NMR (400 MHz, DMSO-d₆, δ/ppm): 2.28 (s, 3H); 3.86 (s, 3H), 7.20 (dd, 1H), 7.58 (d, 1H), 7.60 (d, 1H), 13.08 (s, 1H); ¹³C NMR (50 MHz, DMSO-d₆, δ/ppm): 20.4, 55.9, 113.1, 122.2, 123.1, 129.5, 143.0, 150.8, 166.7, 168.2.

3.3.5.2 Synthesis of (hydrazine-1,2-dicarbonyl)bis(2-methoxy-4,1-phenylene) diacetate

Into a 250 mL two-necked round bottom flask equipped with a reflux condenser, an argon inlet and an addition funnel were charged, 4-acetoxy-3-methoxybenzoic acid (1.5 g, 3.6 mmol) and thionyl chloride (3 mL, 41 mmol). The reaction mixture was refluxed for 3 h, and then excess thionyl chloride was distilled out. To the reaction mixture, NMP (7 mL) was added and the reaction mixture was cooled to 0 °C. The solution of hydrazine hydrate (0.1 mL, 1.8 mmol) in NMP (3 mL) was added drop wise over a period of 15 min and stirring was continued for 1 h at 25 °C. Ice cold water (250 mL) was added gradually to the reaction mixture and solid was precipitated out. The precipitate was filtered and washed with water.

Yield 85%; Melting point- 176 °C; ¹H NMR (200 MHz, DMSO-d₆, δ/ppm): 2.29 (s, 6H), 3.86 (s, 6H), 7.25 (d, 2H), 7.54 (dd, 2H), 7.64 (d, 2H), 10.59 (s, 2H); ¹³C NMR (50 MHz, DMSO-d₆ δ/ppm): 20.4, 56.0, 111.8, 120.2, 123.0, 131.2, 142.1, 150.8, 165.1, 168.3

3.3.5.3 Synthesis of (1,3,4-oxadiazole-2,5-diyl)bis(2-methoxy-4,1-phenylene) diacetate

Into a 250 mL two-necked round bottom flask equipped with a reflux condenser, an argon inlet and an addition funnel were charged, (hydrazine-1,2-dicarbonyl)bis(2-methoxy-4,1-phenylene) diacetate (1 g, 24 mmol) and thionyl chloride (10 mL). The reaction mixture was refluxed for 2 h and excess thionyl chloride was removed under reduced pressure. The solid product was recrystallized from acetone.

Yield 90 %; Melting point- 189 °C; ¹H NMR (200 MHz, DMSO-d₆, δ/ppm): 2.31(s, 6H), 3.93 (s, 6H), 7.37 (d, 2H), 7.76 (dd, 2H), 7.80 (d, 2H); ¹³C NMR (50 MHz, DMSO-d₆, δ/ppm): 20.4, 56.2, 110.7, 119.7, 121.9, 124.1, 142.3, 151.5, 163.7, 168.2.

3.3.5.4 Synthesis of 4,4'-(1,3,4-oxadiazole-2,5-diyl)bis(2-methoxyphenol)

Into a 100 mL single-necked round bottom flask equipped with a magnetic stirring bar were charged, (1,3,4-oxadiazole-2,5-diyl)bis(2-methoxy-4,1-phenylene)diacetate (1 g, 2.5 mmol), sodium hydroxide (0.65 g, 16 mmol) and methanol (50 mL). The reaction mixture was stirred for 4 h at room temperature and excess methanol was removed under reduced pressure. The solution was diluted with water and acidified with aqueous hydrochloric acid (3M). The precipitate was filtered and dried in vacuum oven at 80 °C for 10 h and then recrystallized from aqueous ethanol.

Yield 93 %; Melting point- 210 °C; ¹H NMR (200 MHz, DMSO-d₆, δ/ppm): 3.89 (s, 6H), 6.96 (d, 2H), 7.56 (br. s, 4H), 9.95 (br. s, 2H); ¹³C NMR (100 MHz, DMSO-d₆, δ/ppm): 55.8, 110.0, 114.5, 116.0, 120.5, 148.1, 150.3, 163.7.; HRMS ESI⁺: (M+H)⁺ m/z calculated for C₁₆H₁₅N₂O₅: 315.0975, found: 315.0792.

3.3.6 Synthesis of α, ω-diacyl hydrazides containing oxyalkylene linkage.

3.3.6.1 General procedure for synthesis of α, ω-diester containing oxyalkylene linkages

Into a 250 mL two-necked round bottom flask equipped with a reflux condenser and an argon inlet were charged, methyl vanillate or methyl syringate (40 mmol), potassium carbonate (22.1 g, 160 mmol) and DMF (100 mL). The reaction mixture was heated at 100 °C for 1 h and then 1, 3-dibromopropane (20 mmol) was added and heating was continued for 12 h. The reaction mixture was poured into ice cold water (250 mL). The precipitate was filtered and dissolved in dichloromethane (100 mL). The dichloromethane solution was washed with water (2 x 100 mL), dried over anhydrous sodium sulfate, filtered, and concentrated under reduced pressure. The crude product was purified by column chromatography using pet ether: ethyl acetate as an eluent to afford white solid.

3.3.6.1.1 Synthesis of dimethyl 4,4'-(propane-1,3-diylbis(oxy))bis(3-methoxybenzoate)

Yield: 80 %; Melting point-158 °C; ¹H NMR (200 MHz, CDCl₃, δ/ppm): 2.35-2.48 (m, 2H), 3.90 (s, 6H), 4.30 (t, 2H), 6.94 (d, 2H), 7.54 (d, 2H), 7.64 (dd, 2H). ¹³C NMR (50

MHz, CDCl₃, δ/ppm): 28.9, 52.0, 56.0, 65.4, 111.5, 112.3, 122.8, 123.4, 148.9, 152.2, 166.8.

3.3.6.1.2 Synthesis of dimethyl 4,4'-(propane-1,3-diylbis(oxy))bis(3,5-dimethoxybenzoate)

Yield: 76 %; Melting point-120 °C; ¹H NMR (200 MHz, CDCl₃, δ/ppm): 2.12-2.24(m, 2H), 3.83 (s, 12H), 3.91 (s, 6H), 4.30 (t, 4H), 7.27 (s, 4H); ¹³C NMR (50 MHz, CDCl₃, δ/ppm): 31.4, 52.5, 56.4, 71.0, 107.1, 125.2, 141.9, 153.4, 167.1.

3.3.6.2 General procedure for synthesis of α, ω-acyl hydrazides containing oxyalkylene linkage

Into a 500 mL two necked round bottom flask equipped with a magnetic stirrer and a reflux condenser were placed α, ω-diester (28 mmol) and ethanol (100 mL). Hydrazine hydrate (98 %) (28 g, 56 mmol) was added dropwise over a period of 15 min and the reaction mixture was refluxed for 12 h. The reaction mixture was cooled to room temperature and the precipitate was filtered, dried and recrystallized from water: ethanol mixture.

3.3.6.2.1 Synthesis of 4,4'-(propane-1,3-diylbis(oxy))bis(3-methoxybenzohydrazide)

Yield: 90 %; Melting point 208 °C; ¹H NMR (200 MHz, DMSO-d₆, δ/ppm): 2.16-2.22 (m, 2H), 3.79 (s, 6H), 4.16 (t, 4H), 4.42 (s, 4H), 7.04 (d, 2H), 7.41 (d, 2H), 7.43 (dd, 2H), 9.63 (s, 2H); ¹³C NMR (50 MHz, DMSO-d₆, δ/ppm): 28.6, 55.6, 64.9, 110.5, 112.2, 120.1, 125.7, 148.4, 150.2, 165.6; HRMS ESI⁺: (M+H)⁺ m/z calculated for C₁₉H₂₅N₄O₆: 405.1769, found: 405.1768.

3.3.6.2.2 Synthesis of 4,4'-(propane-1,3-diylbis(oxy))bis(3,5-dimethoxybenzohydrazide)

Yield: 97 %; Melting point- 222 °C; ¹H NMR (200 MHz, DMSO-d₆, δ/ppm): 1.87-2.0 (m, 2H), 3.76 (s, 12H), 4.09 (t, 4H), 4.47 (s, 4H), 7.15 (s, 4H); ¹³C NMR (50 MHz, DMSO-d₆, δ/ppm): 30.6, 55.9, 69.8, 104.4, 128.2, 138.9, 152.7, 165.4; HRMS ESI⁺: (M+H)⁺ m/z calculated for C₂₁H₂₉N₄O₈: 465.1980, found: 465.1975.

3.3.7 Synthesis of 5,5'-dimethoxy-6,6'-bis(pentyloxy)-[1,1'-biphenyl]-3,3'-dicarbohydrazide

Into a 250 mL two-necked round bottom flask equipped with a magnetic stirring bar, a nitrogen inlet, an addition funnel and a reflux condenser were charged, dimethyl 6,6'-dimethyl 5,5'-dimethoxy-6,6'-bis(pentyloxy)-[1,1'-biphenyl]-3,3'-dicarboxylate (5 g, 10 mmol), and ethanol (10 mL). Hydrazine hydrate (1 g, 20 mmol) (80%) was added dropwise to the reaction mixture over a period of 15 min and refluxed for 12 h. The precipitate was filtered and dried in vacuum oven at 60 °C for 4 h and then recrystallized from aqueous ethanol.

Yield 84 %; Melting point- 98 °C; IR (KBr): 3300, 1630 cm^{-1} ; ^1H NMR (200 MHz, CDCl_3 , δ/ppm): 0.7 (t, 6H), 0.95-1.06 (m, 8H), 1.34-1.40 (m, 4H), 3.76 (t, 4H), 3.86 (s, 6H), 4.46 (s, 4H), 7.32 (d, 2H), 7.52 (d, 2H), 9.71 (s, 2H); ^{13}C NMR (50 MHz, CDCl_3 , δ/ppm): 13.9, 22.2, 27.8, 29.7, 55.9, 73.3, 111.1, 121.5, 131.9, 149.2, 152.9, 153.0, 167.9; HRMS ESI⁺: (M+H)⁺ m/z calculated for $\text{C}_{26}\text{H}_{39}\text{N}_4\text{O}_6$: 503.2864, found: 503.2845.

3.3.8 Synthesis of bis(4-formyl-2-methoxyphenyl) succinate

Into a 250 mL three-necked round bottom flask fitted with an addition funnel, a magnetic stirrer bar and a nitrogen inlet were charged vanillin (1.96 g, 12.9 mmol), pyridine (1.56 mL, 19.3 mmol) and chloroform (100 mL). After stirring at 0 °C for 2 h, succinyl chloride (0.99 g, 6.45 mmol) in chloroform (7 mL) was added dropwise over 30 min and the reaction mixture was stirred at room temperature for 12 h. The chloroform solution was washed with water (2 x 100 mL), dried over anhydrous sodium sulphate, filtered, and concentrated under reduced pressure. The crude product was purified by column chromatography using pet ether: ethyl acetate as an eluent to afford white solid.

Yield 81 %; Melting point- 137 °C; IR (KBr): 2942, 2830, 2723, 1558, 1704 cm^{-1} ; ^1H NMR (200 MHz, CDCl_3 , δ/ppm): 3.08 (t, 4H), 3.88 (s, 6H), 7.23 (d, 2H), 7.46 (dd, 2H), 7.50 (d, 2H), 9.94 (s, 2H); ^{13}C NMR (100 MHz, CDCl_3 , δ/ppm): 28.9, 56.1, 110.9, 123.3, 124.6, 135.3, 144.7, 151.9, 169.5, 190.9; HRMS ESI⁺: (M+H)⁺ m/z calculated for $\text{C}_{20}\text{H}_{18}\text{O}_8$: 387.1080, found: 387.1250.

3.3.9 Synthesis of bis(4-(hydroxymethyl)-3-methoxyphenyl) succinate

Into a 100 mL three-necked round bottom flask fitted with an addition funnel, a magnetic stirrer bar and a nitrogen inlet were charged bis(4-formyl-2-methoxyphenyl) succinate (1.9 g, 5 mmol) and tetrahydrofuran (100 mL). After stirring at 0 °C, sodium borohydride (586 mg, 15.5 mmol) in tetrahydrofuran (5 mL) was added dropwise over

15 min and stirring was continued at 0 °C for 3 h. After completion of reaction, tetrahydrofuran was evaporated under reduced pressure at 30 °C. The residue was dissolved in ethyl acetate, washed with water (2 x 100 mL), dried over anhydrous sodium sulphate, filtered, and concentrated under reduced pressure. The crude product was purified by column chromatography using pet ether: ethyl acetate as an eluent to afford white solid.

Yield 96 %; Melting point- 126 °C; IR (KBr): 3533, 1743 cm^{-1} ; ^1H NMR (200 MHz, CDCl_3 , δ/ppm): 3.05 (t, 4H), 3.82 (s, 6H), 4.66 (s, 4H), 6.89 (d, 2H), 7.0 (d, 2H), 7.04 (d, 2H); ^{13}C NMR (50 MHz, CDCl_3 , δ/ppm): 29.0, 55.9, 64.9, 113.3, 122.2, 123.8, 126.0, 139.5, 151.1, 170.0; HRMS ESI⁺: (M+Na)⁺ m/z calculated for $\text{C}_{20}\text{H}_{22}\text{O}_8\text{Na}$: 413.1198, found: 413.1207.

3.3.10 General procedure for synthesis of diacid containing ester linkage

Into a 250 mL three-necked round bottom flask fitted with an addition funnel, a magnetic stirrer bar and a nitrogen inlet were charged vanillic acid/ syringic acid (60 mmol), triethyl amine (13 mmol) and chloroform (100 mL). After stirring at 0 °C for 2 h, the solution of 2,5-furandicarboxylic acid chloride (30 mmol) in chloroform (5 mL) was added dropwise over 30 min and the reaction mixture was stirred at room temperature for 12 h. After completion of reaction, chloroform was removed under reduced pressure and the residue was dissolved in water (100 mL) and acidified with dilute hydrochloric acid (3M). The resulting diacid was filtered and dried at 70 °C for 10 h under reduced pressure.

3.3.10.1 Synthesis of 4,4'-((furan-2,5-dicarbonyl)bis(oxy))bis(3-methoxybenzoic acid)

Yield 84 %; IR (KBr): 2960, 1780, 1706 cm^{-1} ; ^1H NMR (200 MHz, DMSO-d_6 , δ/ppm): 3.86 (s, 12H), 7.44 (d, 2H), 7.65 (dd, 2H), 7.68 (d, 2H), 7.81 (s, 2H), 13.18 (s, 2H); ^{13}C NMR (50 MHz, DMSO-d_6 , δ/ppm): 56.1, 113.4, 121.2, 122.3, 123.1, 130.3, 141.8, 145.5, 150.6, 154.9, 166.6; HRMS ESI⁺: (M+Na)⁺ m/z calculated for $\text{C}_{22}\text{H}_{16}\text{O}_{11}\text{Na}$: 479.0584, found: 479.0583.

3.3.10.2 Synthesis of 4,4'-((furan-2,5-dicarbonyl)bis(oxy))bis(3,5-dimethoxybenzoic acid)

Yield 82 %; IR (KBr): 2964, 1783, 1700 cm^{-1} ; ^1H NMR (200 MHz, DMSO-d_6 , δ/ppm): 3.86 (s, 12H), 7.36 (s, 4H), 7.84 (s, 2H); ^{13}C NMR (50 MHz, DMSO-d_6 , δ/ppm): 55.9,

109.2, 128.3, 139.2, 150.9, 150.8, 155.3, 168.3; HRMS ESI⁺: (M+Na)⁺ m/z calculated for C₂₄H₂₀O₁₃Na: 539.0802, found: 539.1031.

3.4 Results and discussion

3.4.1 Synthesis and characterization of diisocyanate monomers

Aromatic diisocyanates are useful class of monomers in polymer industry, as they find applications in the synthesis of various step-growth polymers such as polyurethanes, polyureas, polyimides, polyamides and so on. More than 90% market of diisocyanates is captured by aromatic diisocyanates. The most commonly used aromatic diisocyanates *viz.* toluene diisocyanate and methylenediphenyl diisocyanate are obtained from petroleum-derived chemicals.

The reports on synthesis of aromatic diisocyanates based on bio-derived chemicals are scanty expect for furan derivatives *viz.* 2,5-diisocyanatofuran, bis(5-isocyanatofurfuryl)ether, diisocyanates containing difurylalkane moieties and CNSL-based diisocyanates^{20,26,31,32}

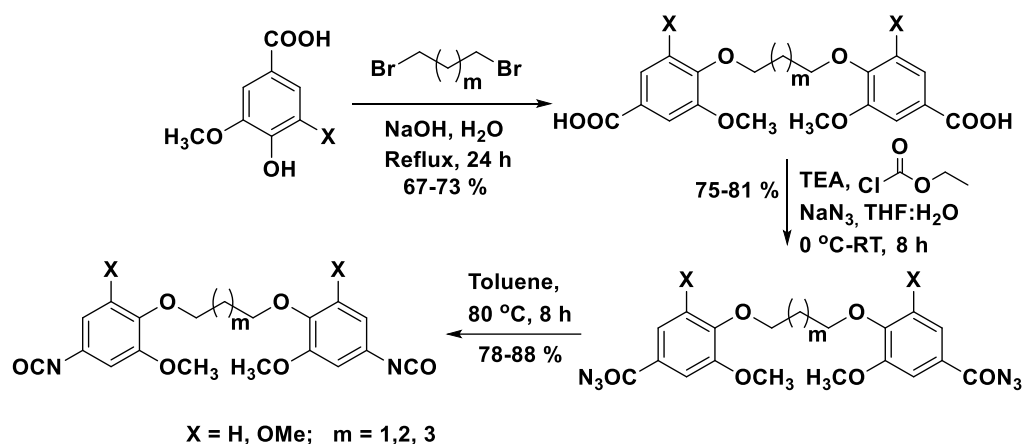
Diisocyanates are usually synthesized by reaction of phosgene with diamine or its salt. However, the high toxicity and gaseous nature of phosgene has generated interest to develop new phosgene-free routes for the synthesis of diisocyanates. In order to avoid use of phosgene, phosgene equivalents such as triphosgene or diphosgene have been used for the synthesis of diisocyanates³³⁻³⁵. Additionally, some lab-scale phosgene-free methods are known in the literature such as Curtius, Hofmann and Lossen rearrangement³⁶.

In the present work, new aromatic diisocyanate monomers containing oxyalkylene/biphenylene linkage were designed and synthesized starting from lignin-derived aromatics.

3.4.1.1 Synthesis and characterization of new diisocyanate monomers containing oxyalkylene linkage

Scheme 3.1 depicts the route for synthesis of diisocyanates containing oxyalkylene linkage. The synthesis of diisocyanates involved three steps. In the first step, diacids were prepared by o-alkylation of vanillic/syringic acids with α , ω -dibromoalkane *viz.* 1,3-dibromopropane, 1,4-dibromobutane, or 1,5-dibromopentane in the presence of sodium hydroxide. The product in each case was recrystallized from water-ethanol mixture and was characterized by ¹H NMR and ¹³C NMR spectroscopy.

^1H NMR spectrum of 4,4'-(propane-1,3-diylbis(oxy))bis(3,5-dimethoxybenzoic acid) is shown in **Figure 3.2**. A singlet appeared at 12.93 δ ppm corresponds to acid proton 'a'. The aromatic protons 'b' showed a singlet at 7.21 δ ppm and methylene protons 'c' attached to the ether linkage exhibited a triplet at 4.13 δ ppm. The methoxy protons 'd' attached to aromatic rings showed a singlet at 3.82 δ ppm and methylene protons 'e' appeared as a multiplet over the range 1.92-2.01 δ ppm. ^{13}C NMR spectrum of 4,4'-(propane-1,3-diylbis(oxy))bis(3,5-dimethoxybenzoic acid) along with assignments is shown in **Figure 3.3**



Scheme 3.1: Synthesis of diisocyanates containing oxyalkylene linkage

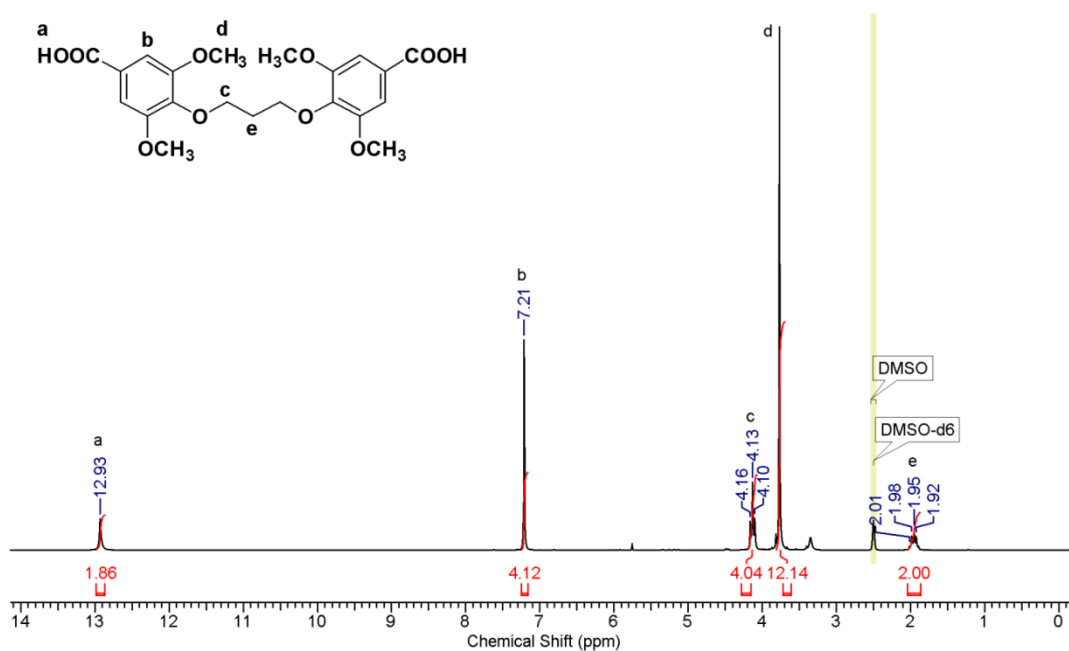


Figure 3.2 ^1H NMR spectrum of 4,4'-(propane-1,3-diylbis(oxy))bis(3,5-dimethoxybenzoic acid) in DMSO-d_6

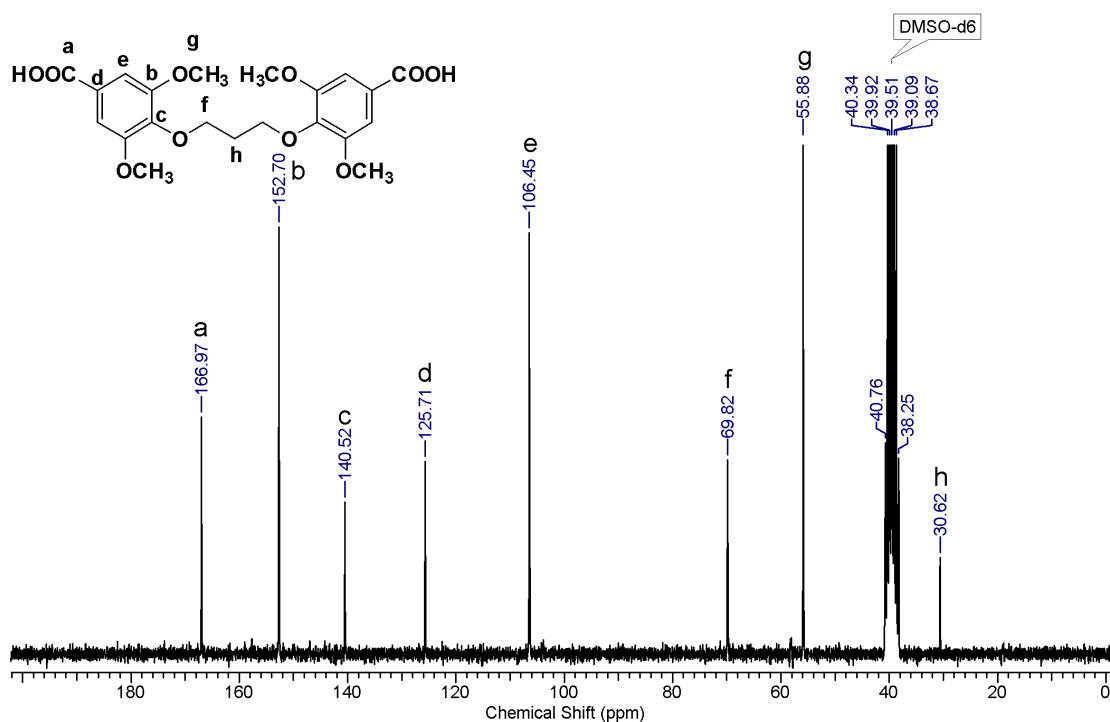


Figure 3.3 ^{13}C NMR spectrum of 4,4'-(propane-1,3-diylbis(oxy))bis(3,5-dimethoxybenzoic acid) in DMSO-d_6

The acyl azides can be prepared by two methods 1) from acid derivative *viz.* acid chloride or acid hydrazide^{37,38}, and 2) from acid using acid activator like ethyl chloroformate, phenyldichloroformate, SOCl_2 -DMF, NCS-triphenylphosphate, triphosgene, 3,4,5-trifluorobenzeneboronic acid or cyanuric chloride followed by reaction with sodium azide³⁹⁻⁴¹. In the present work, diacyl azides were synthesized from diacid *via* the elegant ‘one-pot’ Weinstock modification of the Curtius reaction. The diacid was treated with triethyl amine to afford salt. This salt was reacted with ethyl chloroformate to obtain mixed carboxylic-carbonic anhydride, which was treated with sodium azide to afford diacyl azide. Diacyl azide was characterized by FT-IR, ^1H NMR and ^{13}C NMR spectroscopy. FT-IR spectrum of 4,4'-(propane-1,3-diylbis(oxy))bis(3,5-dimethoxybenzoyl azide) is displayed in **Figure 3.4**. FT-IR spectrum showed absorption band at 2146 cm^{-1} which corresponds to $-\text{N}_3$ group. A band appeared at 1684 cm^{-1} due to carbonyl group.

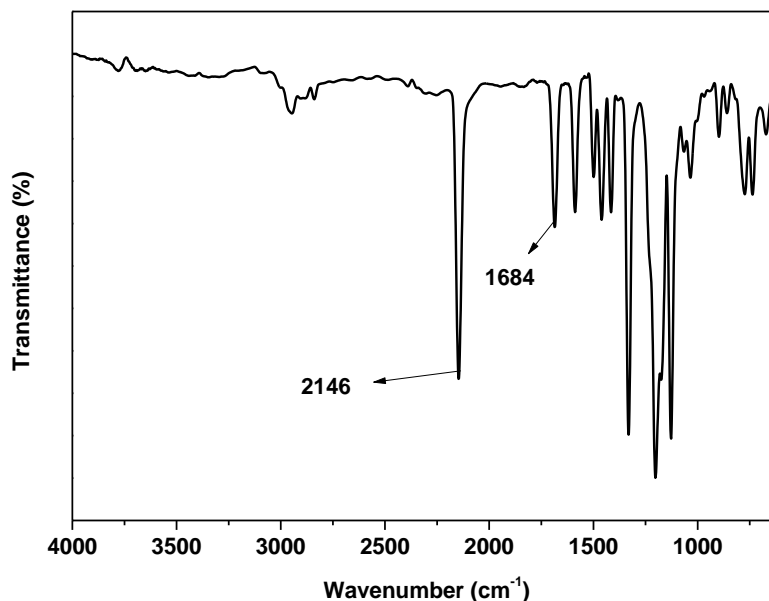


Figure 3.4 FT-IR spectrum of 4,4'-(propane-1,3-diylbis(oxy))bis(3,5-dimethoxybenzoyl azide)

^1H NMR spectrum of 4,4'-(propane-1,3-diylbis(oxy))bis(3,5-dimethoxybenzoyl azide) is reproduced in **Figure 3.5**, which shows disappearance of peak at 12.93 δ ppm corresponding to acid protons. The order as well as splitting of protons was similar as in the case of 4,4'-(propane-1,3-diylbis(oxy))bis(3,5-dimethoxybenzoic acid) (**Figure 3.2**). ^{13}C NMR spectrum of 4,4'-(propane-1,3-diylbis(oxy))bis(3,5-dimethoxybenzoyl azide) with assignments is presented in **Figure 3.6**.

Diacyl azides were found to be safe to handle in the laboratory. However, it is recommended to follow standard safety precautions while handling the diacyl azides.

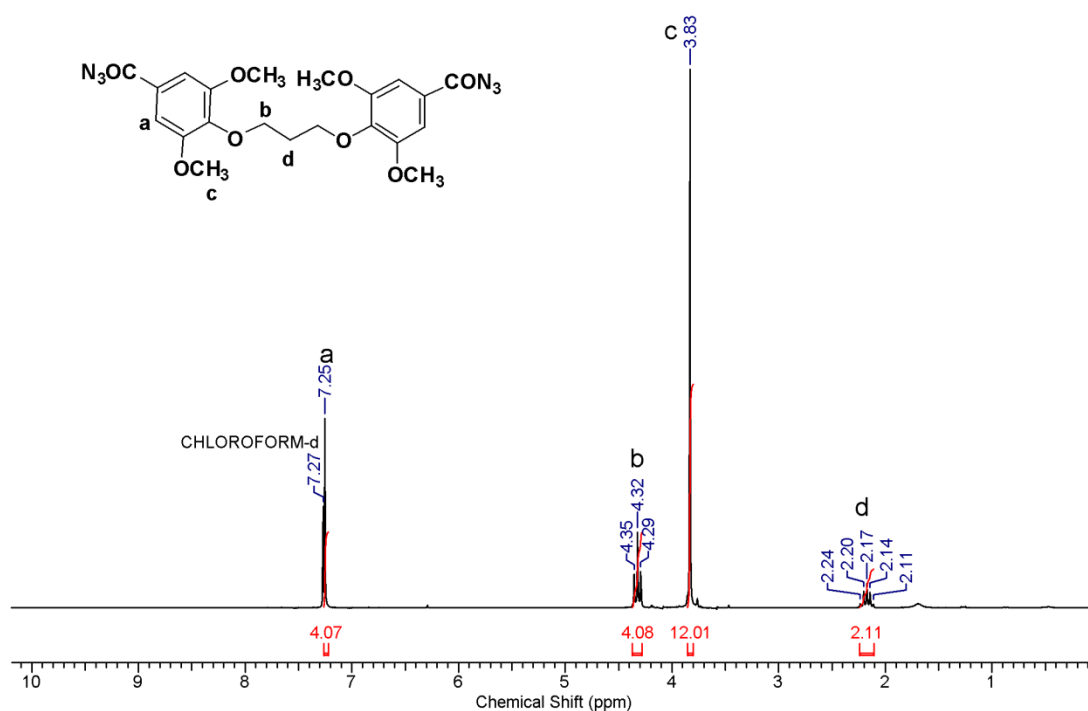


Figure 3.5 ¹H NMR spectrum of 4,4'-(propane-1,3-diylbis(oxy))bis(3,5-dimethoxybenzoyl azide) in CDCl₃

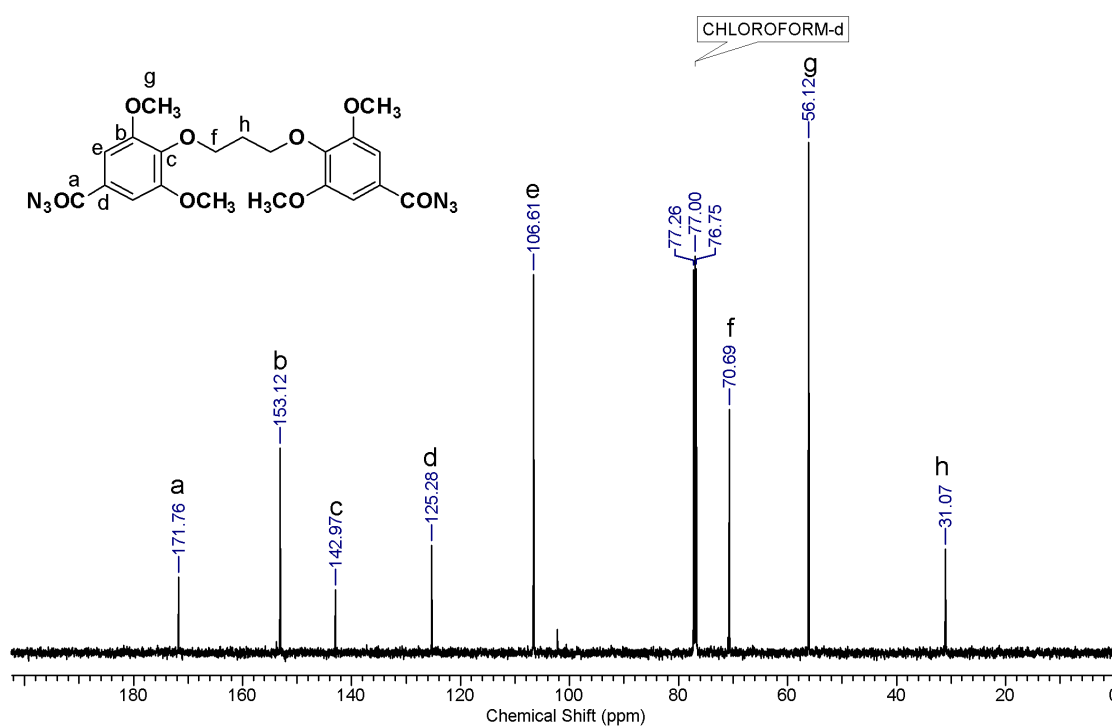


Figure 3.6 ¹³C NMR spectrum of 4,4'-(propane-1,3-diylbis(oxy))bis(3,5-dimethoxybenzoyl azide) in CDCl₃

Finally, diacyl azide was converted into diisocyanate by thermal decomposition of acyl azide group in toluene at 80 °C. The progress of reaction was monitored by FT-IR spectroscopy. After complete conversion of diacyl azide, toluene was evaporated under reduced pressure to afford diisocyanate monomer. All the synthesized diisocyanates are solids at room temperature with a melting point in the range 60-136 °C. Thus, these diisocyanates should present minimal inhalation hazards. Diisocyanates were characterized by FT-IR, ^1H NMR and ^{13}C NMR spectroscopy. A representative FT-IR spectrum of 1,3-bis(4-isocyanato-2,6-dimethoxyphenoxy)propane is reproduced in **Figure 3.7**. The disappearance of C=O and $-\text{N}_3$ stretching indicated complete conversion of acyl azide to isocyanato group. The characteristic band of the $-\text{NCO}$ asymmetric stretching appeared at 2268 cm^{-1} .

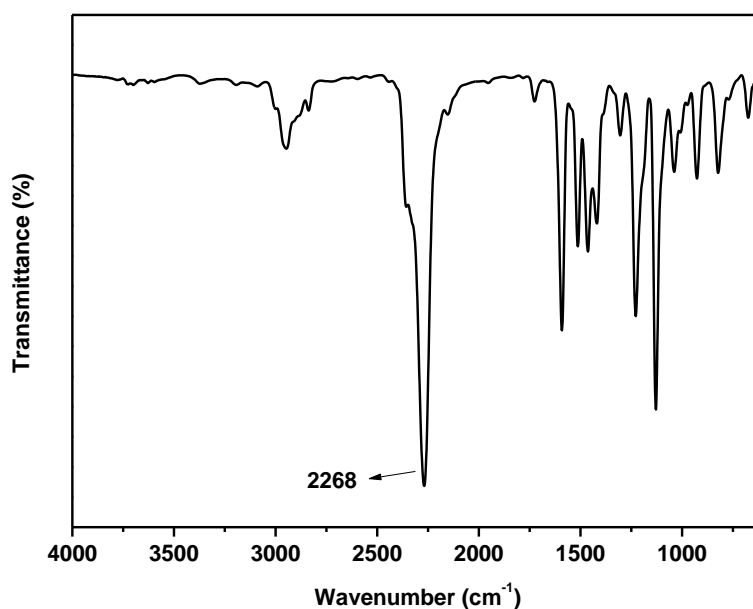


Figure 3.7 FT-IR spectrum of 1,3-bis(4-isocyanato-2,6-dimethoxyphenoxy)propane

^1H NMR spectrum of 1,3-bis(4-isocyanato-2,6-dimethoxyphenoxy)propane is displayed in **Figure 3.8**. The aromatic protons appeared in the upfield at $6.31\ \delta$ ppm as compared to the same protons which appeared at $7.25\ \delta$ ppm for its acyl azide precursor (**Figure 3.5**). This could be attributed due to electron donating effect of isocyanato group. A triplet was observed at $4.16\ \delta$ ppm which corresponds to methylene group attached to ether linkage while protons of methoxy group exhibited a singlet at $3.79\ \delta$ ppm. The signal of remaining aliphatic protons appeared as a multiplet in the range 2.12 - 2.19 ppm. ^{13}C NMR spectrum of 1,3-bis(4-isocyanato-2,6-

dimethoxyphenoxy)propane along with the assignments of carbon atoms is displayed in **Figure 3.9**. A signal at 153.8 δ ppm was observed corresponding to $-\text{NCO}$ group.

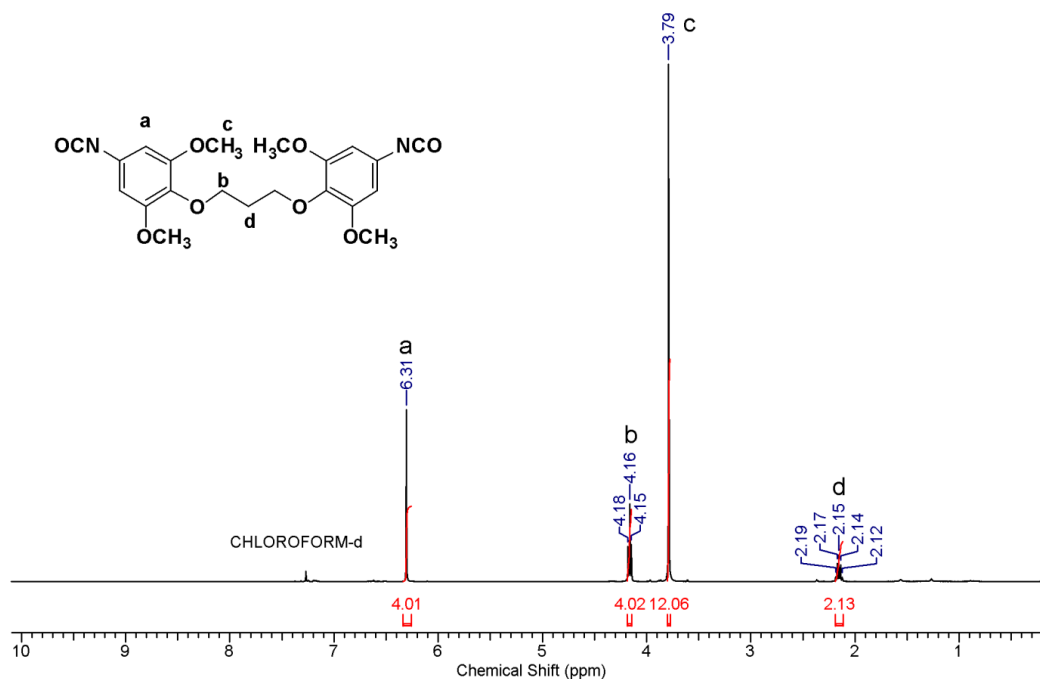


Figure 3.8 ^1H NMR spectrum of 1,3-bis(4-isocyanato-2,6-dimethoxyphenoxy)propane in CDCl_3

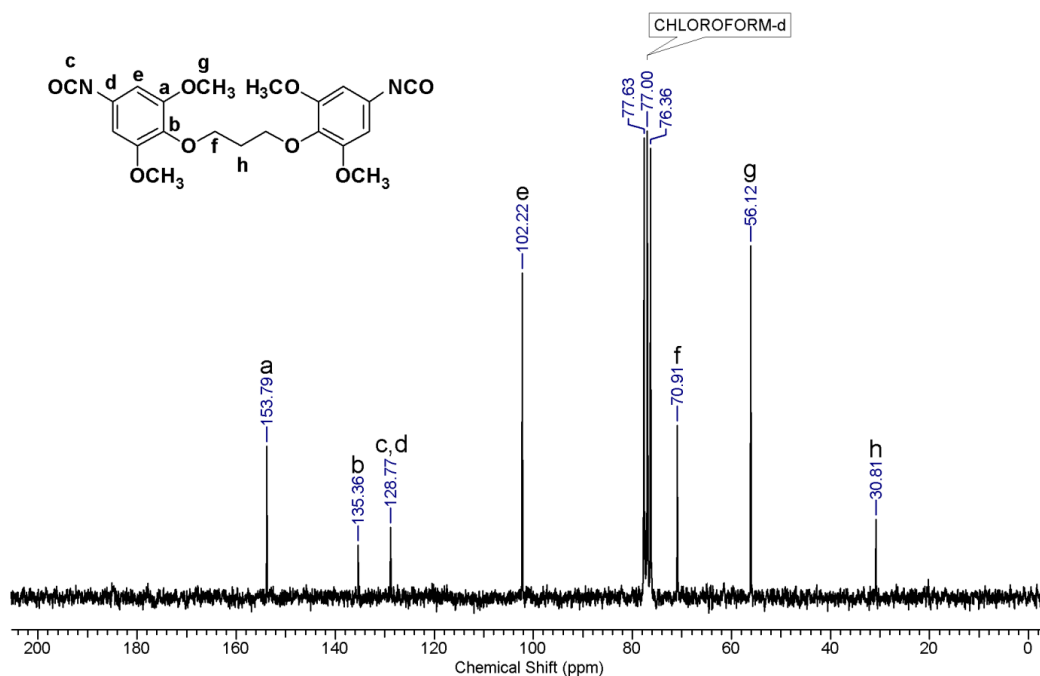


Figure 3.9 ^{13}C NMR spectrum of 1,3-bis(4-isocyanato-2,6-dimethoxyphenoxy)propane in CDCl_3

The structure of diisocyanate was further confirmed by single crystal X-ray diffraction analysis. Crystal structure data for representative aromatic diisocyanate viz. 1,3-bis(4-isocyanato-2-methoxyphenoxy)propane was determined using Bruker Single Crystal X-ray diffractometer. Good quality single crystals of 1,3-bis(4-isocyanato-2-methoxyphenoxy)propane were obtained by slow evaporation from toluene. The crystals were of the monoclinic type with $P2_1/c$ space group containing one molecule in the asymmetric unit. The ORTEP of 1,3-bis(4-isocyanato-2-methoxyphenoxy)propane drawn at the 50% ellipsoid probability level is shown in **Figure 3.10**. The H-atoms are drawn with an arbitrary radii. The crystallographic data is summarized in **Table 3.1**. View of molecular packing down the b -axis is shown in **Figure 3.11**. The adjacent molecules along the a -axis are associated centrosymmetrically through short dipolar $C=O\cdots C=O$ contact supported by dimeric $C-H\cdots O$ contact across the inversion center thereby generating an extended chain. The neighboring parallel waves along the c -axis are linked through weak $C-H\cdots O$ contact to yield 2D packing.

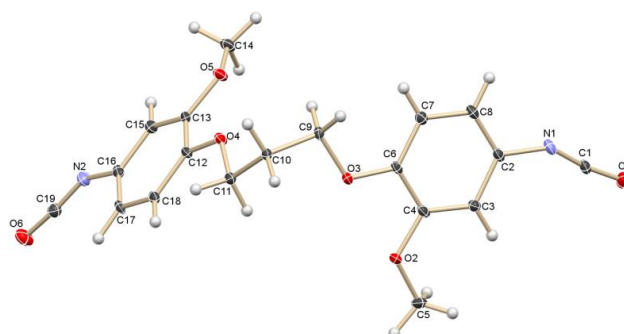


Figure 3.10 ORTEP diagram of 1,3-bis(4-isocyanato-2-methoxyphenoxy)propane

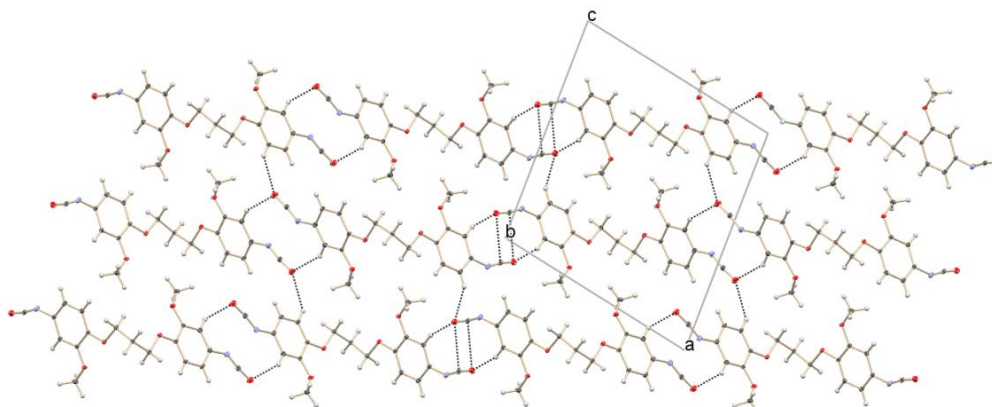


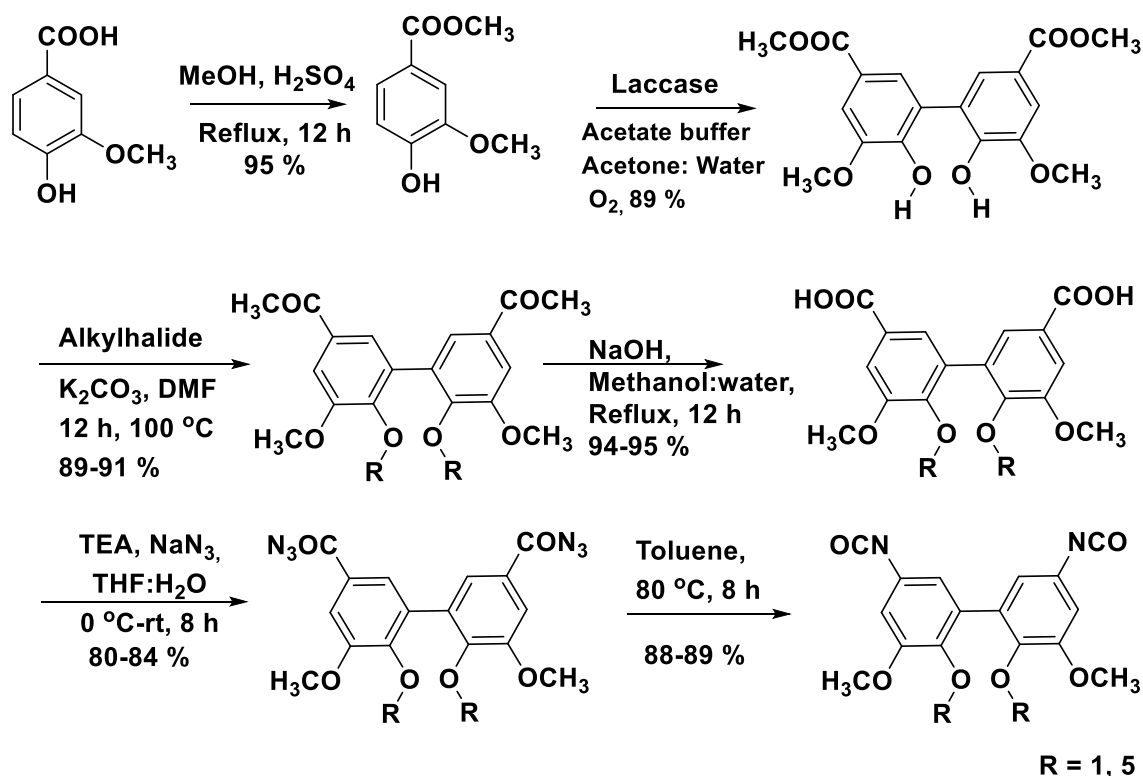
Figure 3.11 Molecular packing viewed the down b -axis showing layered arrangement on the ac plane

Table 3.1 Crystal data and structure refinement parameters for 1,3-bis(4-isocyanato-2-methoxyphenoxy)propane

Empirical formula	C ₁₉ H ₁₈ N ₂ O ₆
Formula weight	370.35
Temperature	150(2) K
Wavelength	0.71073 Å
Crystal system	Monoclinic
Space group	<i>P</i> 2 ₁ / <i>c</i>
Unit cell dimensions	<i>a</i> = 13.1016(7) Å $\alpha = 90^\circ$
	<i>b</i> = 9.4677(6) Å $\beta = 101.019(4)^\circ$
	<i>c</i> = 14.3180(8) Å $\gamma = 90^\circ$
Volume	1743.29(17) Å ³
Z	4
Density (calculated)	1.411 Mg/m ³
Absorption coefficient	0.106 mm ⁻¹
F(000)	776
Crystal size	0.47 x 0.31 x 0.27 mm ³
Theta range for data collection	1.58 to 24.99°.
Index ranges	-15 ≤ <i>h</i> ≤ 15, -11 ≤ <i>k</i> ≤ 11, -16 ≤ <i>l</i> ≤ 17
Reflections collected	14217
Independent reflections	3025 [R(int) = 0.1381]
Completeness to theta = 24.99°	98.4 %
Absorption correction	Semi-empirical from equivalents
Max. and min. transmission	0.9718 and 0.9517
Refinement method	Full-matrix least-squares on <i>F</i> ²
Data / restraints / parameters	3025 / 0 / 246
Goodness-of-fit on <i>F</i> ²	1.246
Final <i>R</i> indices [<i>I</i> > 2σ(<i>I</i>)]	<i>R</i> 1 = 0.0990, <i>wR</i> 2 = 0.3002
<i>R</i> indices (all data)	<i>R</i> 1 = 0.2170, <i>wR</i> 2 = 0.3893
Largest diff. peak and hole	0.647 and -0.741 e Å ⁻³

3.4.1.2 Synthesis of diisocyanates containing biphenylene linkage

Scheme 3.2 depicts synthesis of diisocyanates containing biphenylene linkage



Scheme 3.2 Synthesis of diisocyanates containing biphenylene linkage starting from methyl vanillate

Two new diisocyanates namely, 5,5'-diisocyanato-3,3'-dimethoxy-2,2'-bis(pentyloxy)-1,1'-biphenyl and 5,5'-diisocyanato-2,2',3,3'-tetramethoxy-1,1'-biphenyl were synthesized starting from vanillic acid.

The synthesis of diisocyanates involved six steps. In the first step, vanillic acid was reacted with methanol in the presence of sulphuric acid to afford methyl vanillate. In the second step, dimer of methyl vanillate was synthesized from methyl vanillate by enzyme catalyzed coupling reaction. The reaction was carried out in the presence of Laccase from *Trametes versicolor* and NaOAc buffer in acetone-water mixture at pH 5.0. The reaction mixture turned yellow, which might be due to radical formation. After completion of reaction, solid precipitated out. The precipitate was filtered and dried under reduced pressure at 90 °C. The filtrate can be reused for next batch. The product was characterized by ^1H NMR and ^{13}C NMR spectroscopy. ^1H NMR and ^{13}C NMR spectra of dimethyl 6,6'-dihydroxy-5,5'-dimethoxy-[1,1'-biphenyl]-3,3'-dicarboxylate (DVE) are displayed in **Figure 3.12** and **3.13**, respectively.

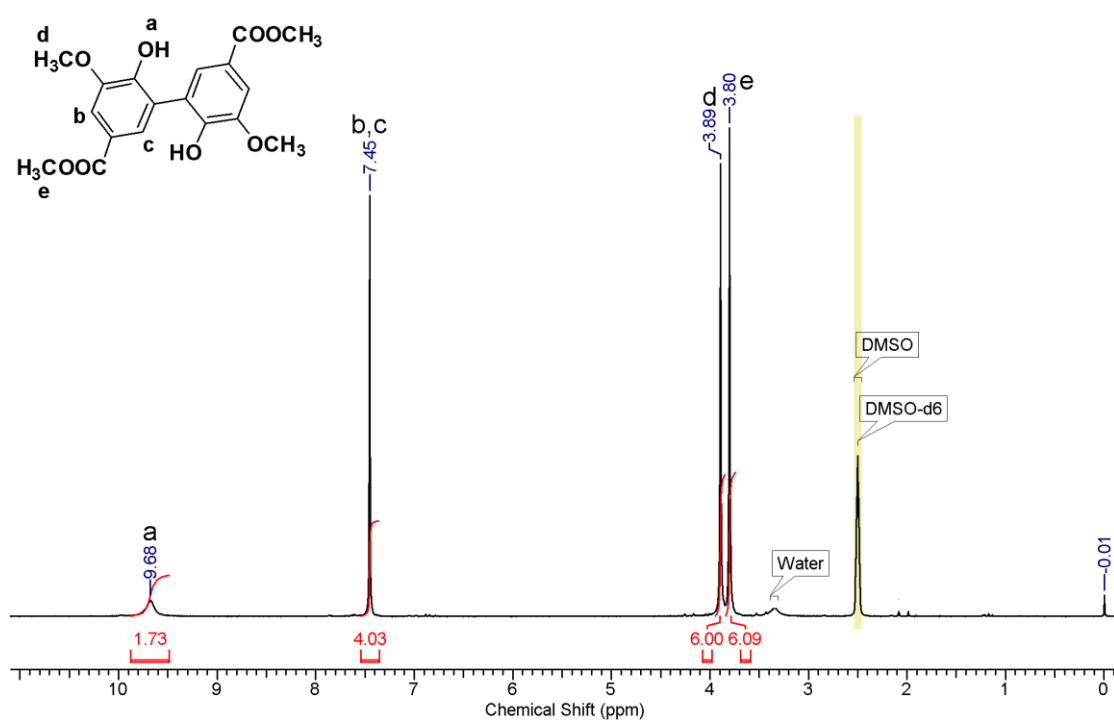


Figure 3.12 ¹H NMR spectrum of dimethyl 6,6'-dihydroxy-5,5'-dimethoxy-[1,1'-biphenyl]-3,3'-dicarboxylate in DMSO-d₆

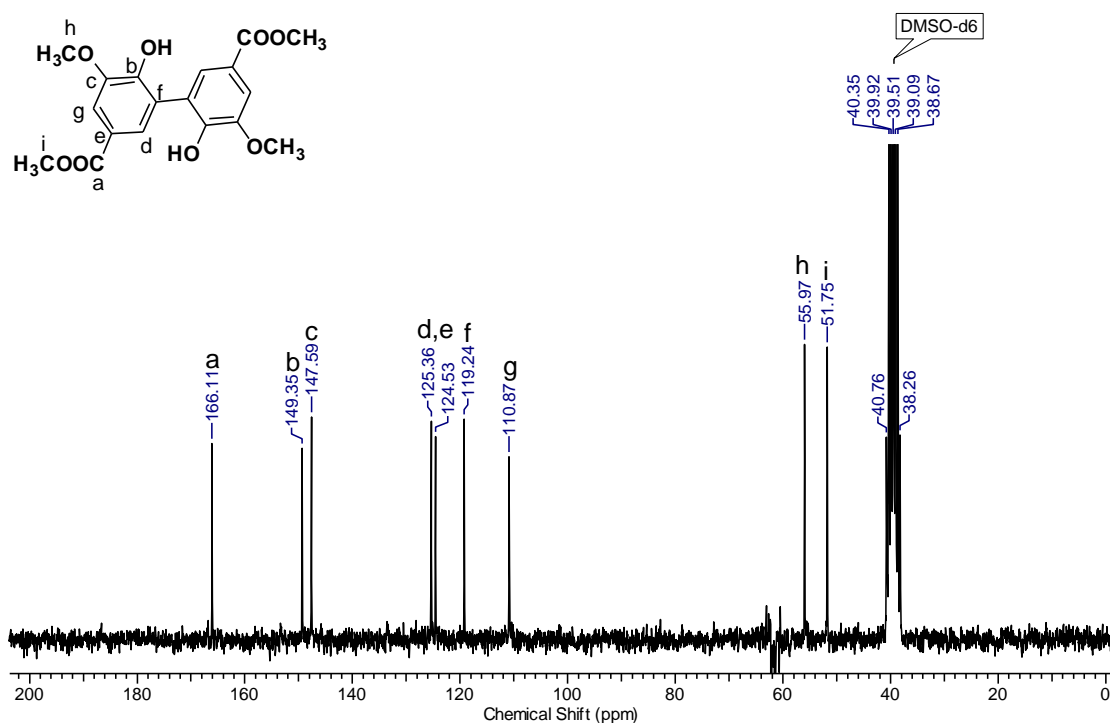


Figure 3.13 ¹³C NMR spectrum of dimethyl 6,6'-dihydroxy-5,5'-dimethoxy-[1,1'-biphenyl]-3,3'-dicarboxylate in DMSO-d₆

The hydroxyl proton appeared as a broad singlet at 9.68 δ ppm. Aromatic protons exhibited a singlet at 7.45 δ ppm. Methoxy protons appeared as a singlet at 3.89 δ ppm while methyl group protons of methyl ester exhibited a singlet at 3.8 δ ppm.

In the third step, alkylation of DVE was carried out using alkyl bromide/iodide in the presence of potassium carbonate in DMF to form dimethyl 6,6'-alkoxy-5,5'-dimethoxy-[1,1'-biphenyl]-3,3'-dicarboxylate (DVME). Iodomethane and 1-bromopentane were used as alkylating agents. The synthesized diester was purified by column chromatography and characterized by FT-IR, ^1H NMR and ^{13}C NMR spectroscopy. FT-IR spectrum of dimethyl 5,5'-dimethoxy-6,6'-bis(pentyloxy)-[1,1'-biphenyl]-3,3'-dicarboxylate is reproduced in **Figure 3.14**, which showed complete disappearance of hydroxyl peak in the range of 3100-3300 cm^{-1}

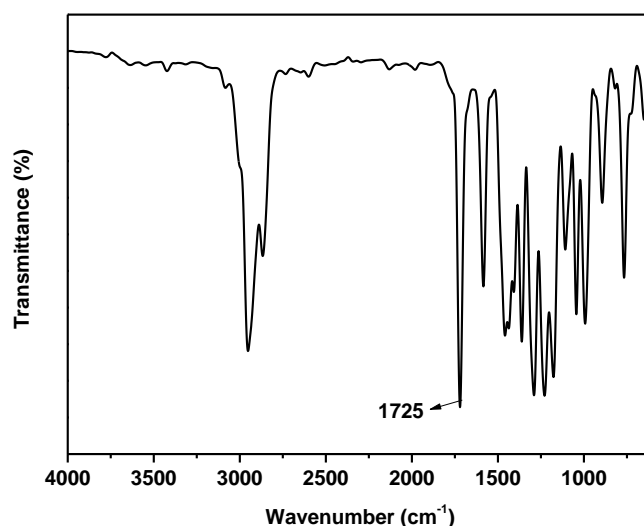


Figure 3.14 FT-IR spectrum of dimethyl 5,5',6,6'-tetramethoxy-[1,1'-biphenyl]-3,3'-dicarboxylate

^1H NMR spectrum of dimethyl 5,5',6,6'-tetramethoxy-[1,1'-biphenyl]-3,3'-dicarboxylate is displayed in **Figure 3.15**. The disappearance of $-\text{OH}$ peak at 9.63 δ ppm indicated the complete alkylation of phenolic group. Aromatic protons 'a' and 'b' exhibited doublets at 7.58 δ ppm and 7.63 δ ppm, respectively. The methoxy protons *para* and *meta* to the ester group appeared as singlets at 3.89 δ ppm and 3.72 ppm, respectively while methyl group protons of methyl ester exhibited a singlet at 3.96 δ ppm.

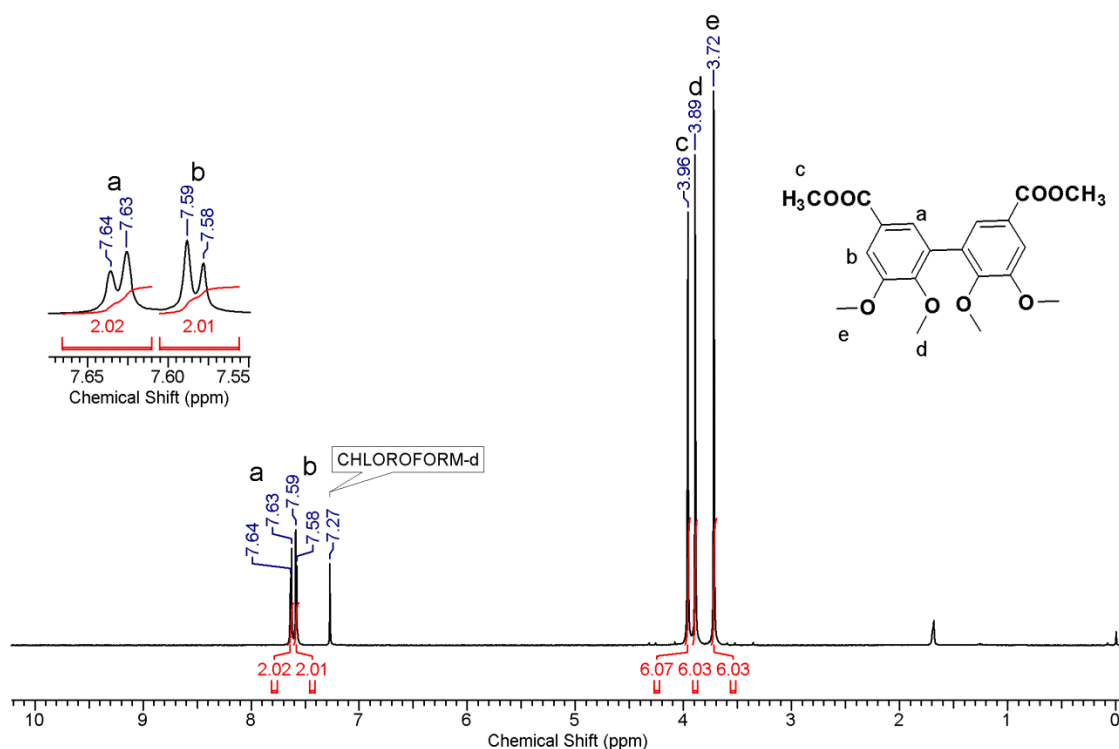


Figure 3.15 ^1H NMR spectrum of dimethyl 5,5',6,6'-tetramethoxy-[1,1'-biphenyl]-3,3'-dicarboxylate in CDCl_3

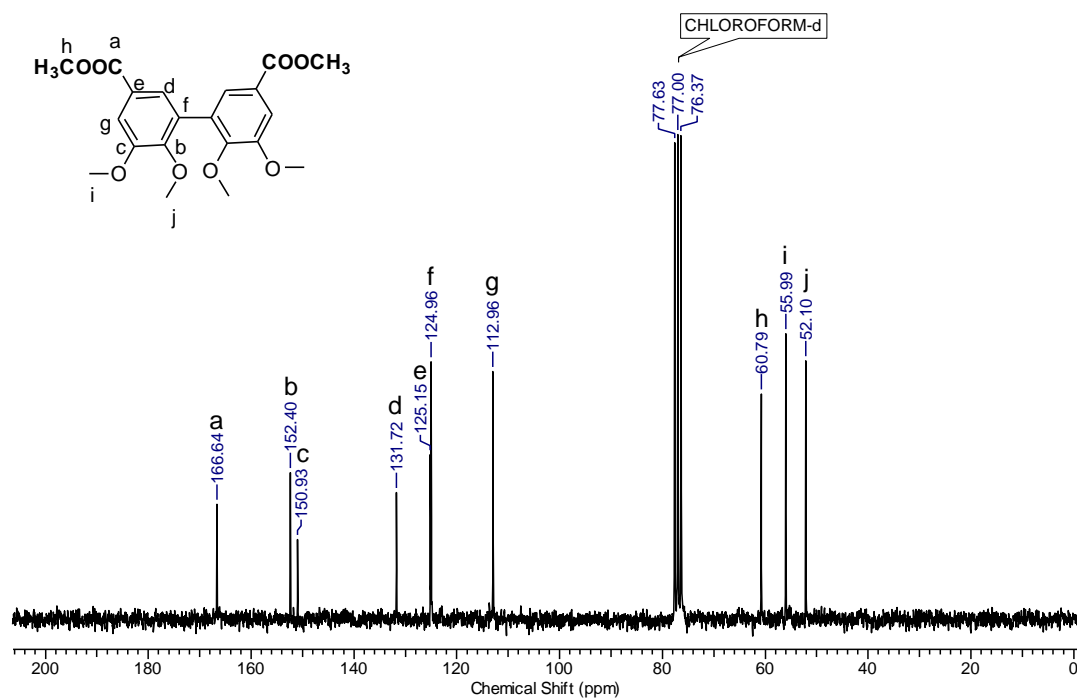


Figure 3.16 ^{13}C NMR spectrum of dimethyl 5,5'-dimethoxy-6,6'-bis(pentyloxy)-[1,1'-biphenyl]-3,3'-dicarboxylate in CDCl_3

^{13}C NMR spectrum of dimethyl 5,5',6,6'-tetramethoxy-[1,1'-biphenyl]-3,3'-dicarboxylate along with the assignments of carbon atoms is presented in **Figure 3.16**.

In the fourth step, diester was hydrolyzed into corresponding diacid using sodium hydroxide in methanol:water (50:50 v/v) mixture. The product was characterized by FT-IR, ^1H NMR and ^{13}C NMR spectroscopy. FT-IR spectrum of 5,5',6,6'-tetramethoxy-[1,1'-biphenyl]-3,3'-dicarboxylic acid is displayed in **Figure 3.17**. The broad absorption band was observed in the range $2300\text{--}3200\text{ cm}^{-1}$ due to acid group. The band at 1671 cm^{-1} was assigned to the carbonyl of acid group.

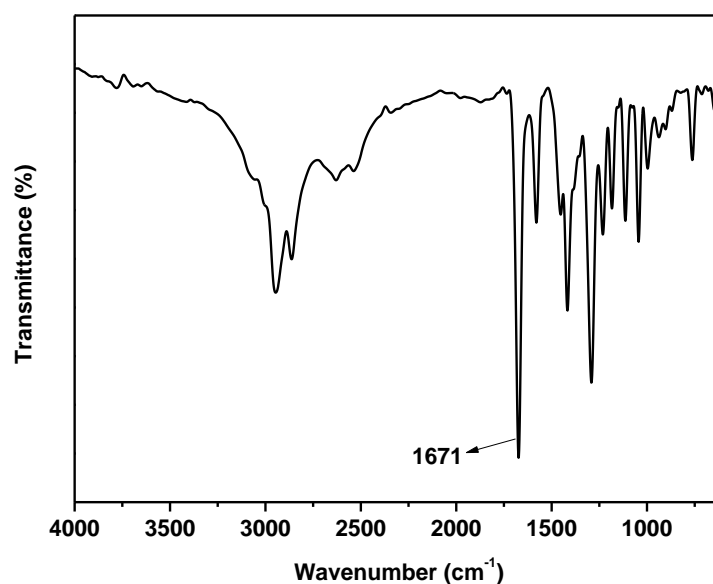


Figure 3.17 FT-IR spectrum of 5,5',6,6'-tetramethoxy-[1,1'-biphenyl]-3,3'-dicarboxylic acid

^1H NMR spectrum of 5,5',6,6'-tetramethoxy-[1,1'-biphenyl]-3,3'-dicarboxylic acid is reproduced in **Figure 3.18**. A new peak exhibited at $12.95\text{ }\delta$ ppm (labelled as 'a') corresponds to the acid protons. Aromatic protons showed two doublets at 7.57 ppm and $7.38\text{ }\delta$ ppm whereas two methoxy group protons appeared as two separate singlets at $3.91\text{ }\delta$ ppm and $3.61\text{ }\delta$ ppm. ^{13}C NMR spectrum of 5,5',6,6'-tetramethoxy-[1,1'-biphenyl]-3,3'-dicarboxylic acid along with the assignments is shown in **Figure 3.19**.

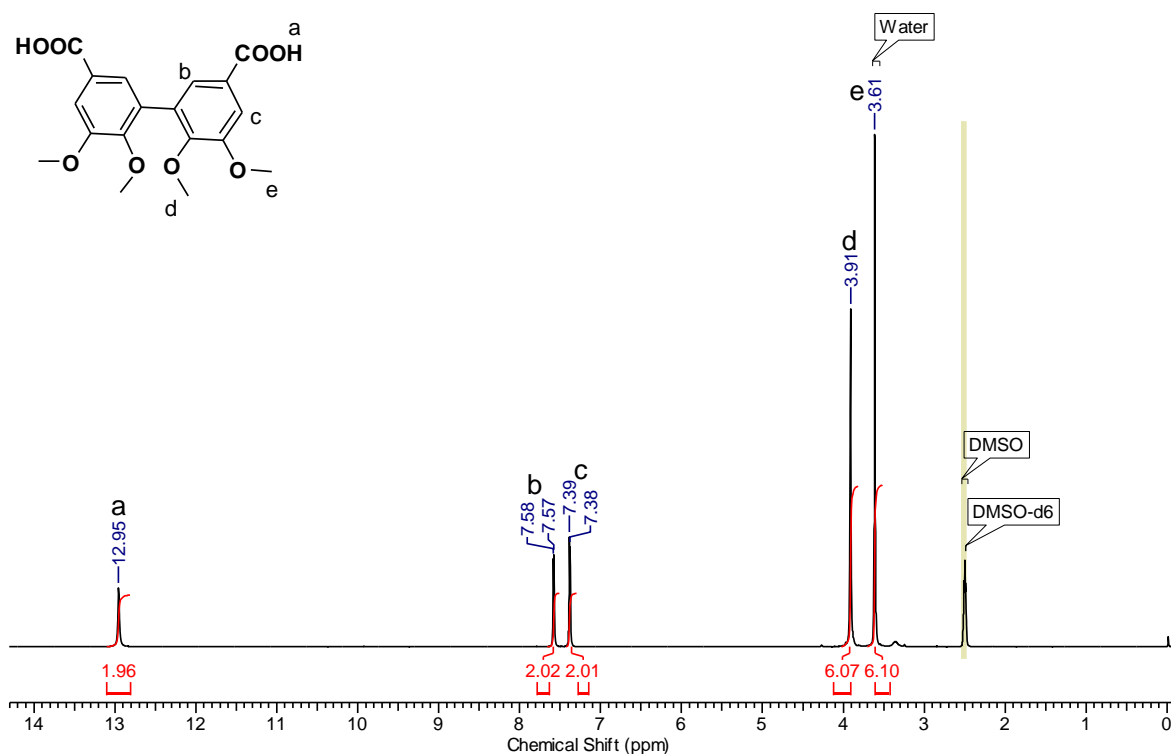


Figure 3.18 ^1H NMR spectrum of 5,5',6,6'-tetramethoxy-[1,1'-biphenyl]-3,3'-dicarboxylic acid in DMSO-d_6

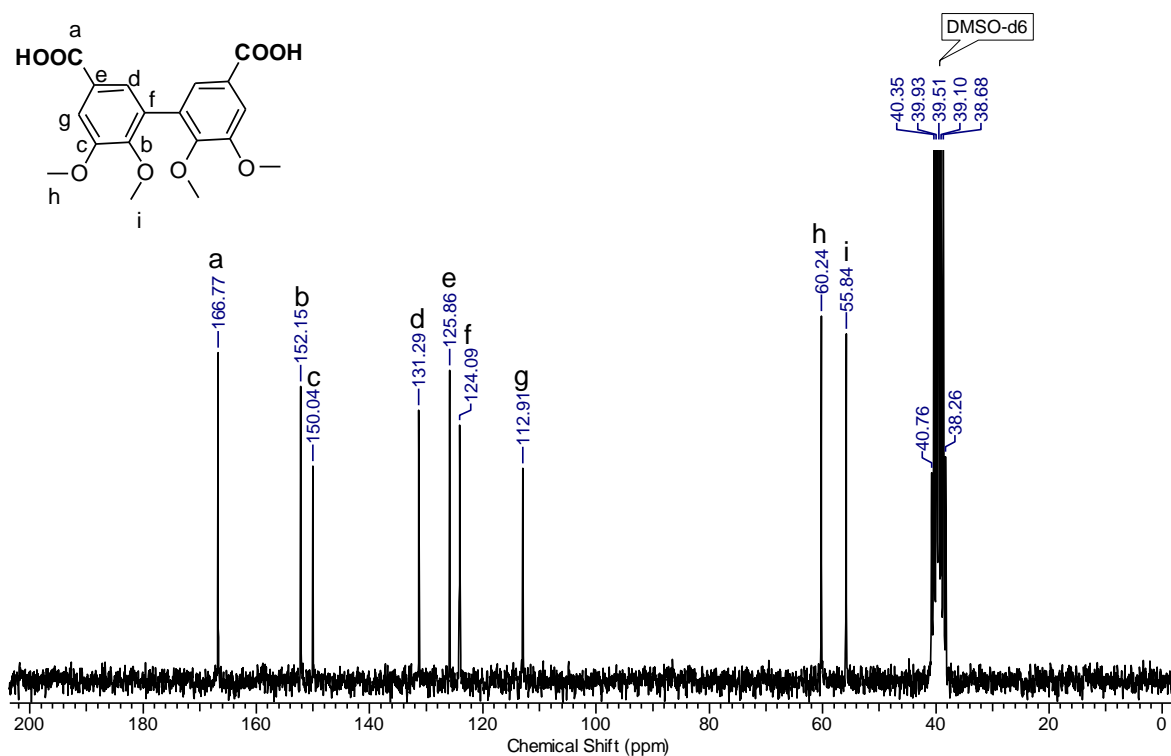


Figure 3.19 ^{13}C NMR spectrum of 5,5',6,6'-tetramethoxy-[1,1'-biphenyl]-3,3'-dicarboxylic acid in DMSO-d_6

In the fifth step, diacyl azide was obtained by the reaction of diacid with triethyl amine, ethyl chloroformate and sodium azide in that succession in tetrahydrofuran-water mixture. FT-IR spectrum (**Figure 3.20**) of 5,5',6,6'-tetramethoxy-[1,1'-biphenyl]-3,3'-dicarbonyl diazide showed the characteristic absorption bands at 2143 cm^{-1} and 1680 cm^{-1} corresponding to $-\text{N}_3$ group and carbonyl stretching, respectively.

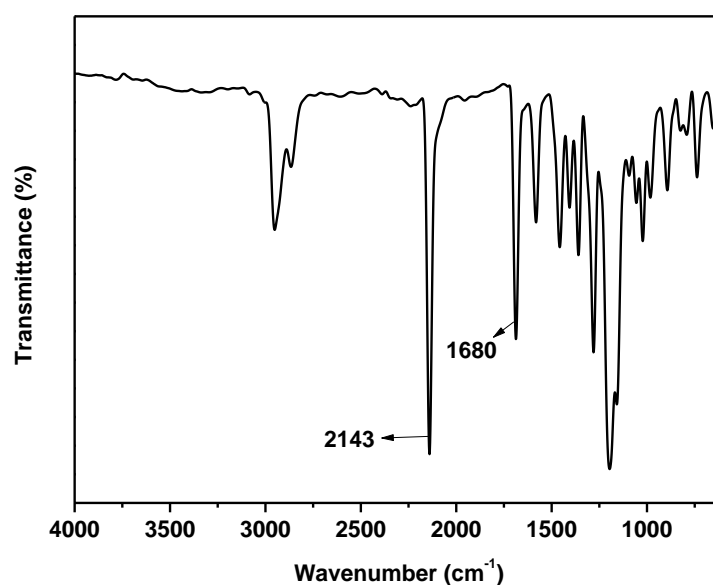


Figure 3.20 FT-IR spectrum of 5,5',6,6'-tetramethoxy-[1,1'-biphenyl]-3,3'-dicarbonyl diazide

^1H NMR spectrum of 5,5',6,6'-tetramethoxy-[1,1'-biphenyl]-3,3'-dicarbonyl diazide showed the absence of proton at $12.95\ \delta$ ppm corresponding to acid group (**Figure 3.21**). Two doublets at 7.61 and $7.56\ \delta$ ppm were observed corresponding to aromatic protons labelled as 'a' and 'b' respectively. Two singlets were observed at 3.90 and $3.66\ \delta$ ppm corresponding to methoxy group protons. ^{13}C NMR spectrum of 5,5',6,6'-tetramethoxy-[1,1'-biphenyl]-3,3'-dicarbonyl diazide along with the assignments is shown in **Figure 3.22**.

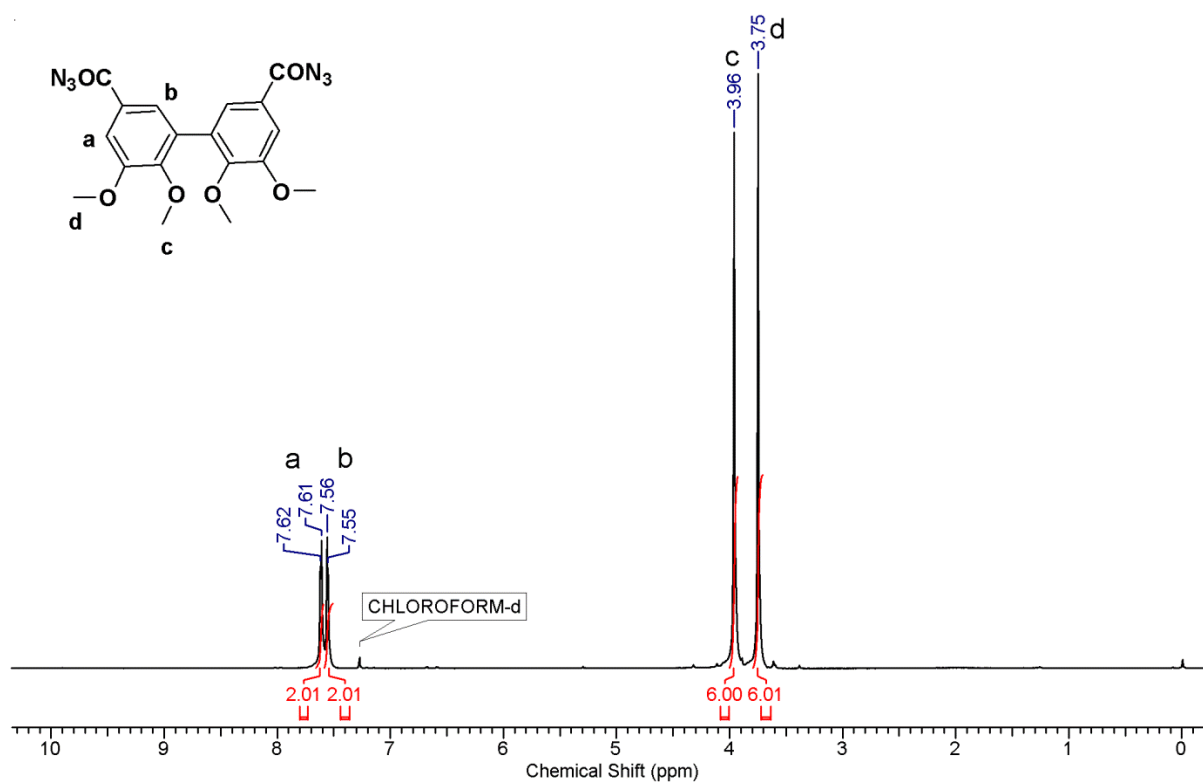


Figure 3.21 ^1H NMR spectrum of 5,5',6,6'-tetramethoxy-[1,1'-biphenyl]-3,3'-dicarbonyl diazide in CDCl_3

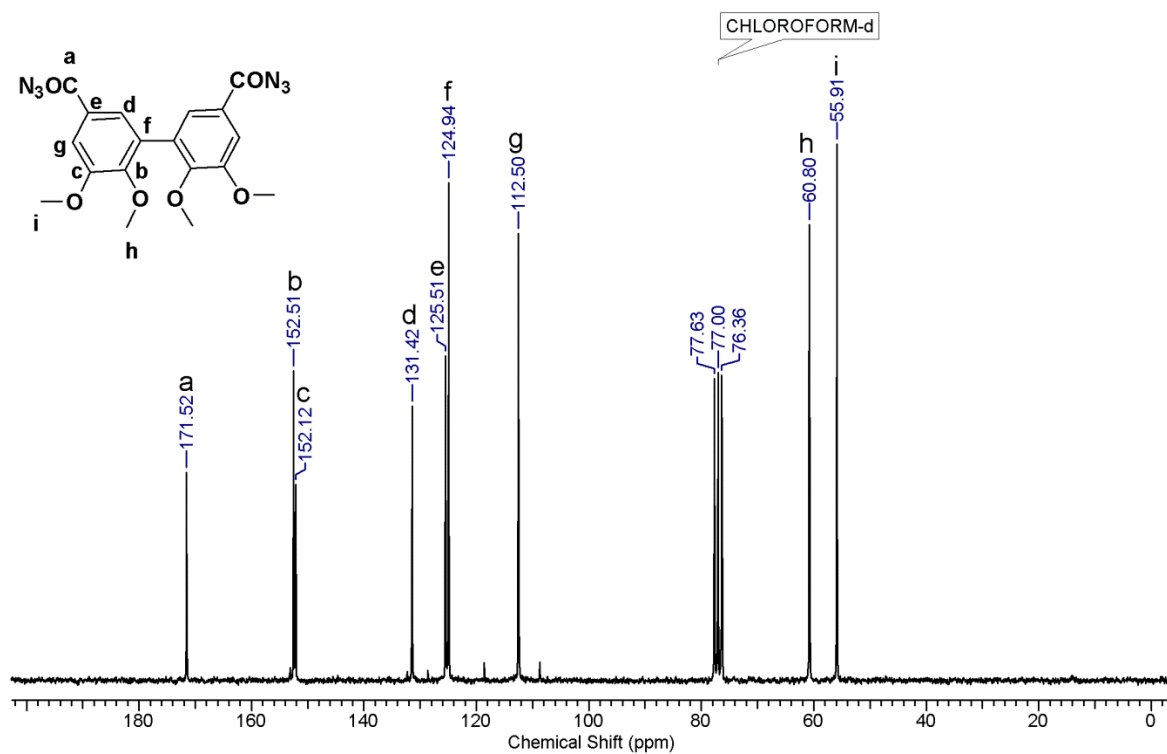


Figure 3.22 ^{13}C NMR spectrum of 5,5',6,6'-tetramethoxy-[1,1'-biphenyl]-3,3'-dicarbonyl diazide in CDCl_3

In the final step, diacyl azide was converted into diisocyanate by the thermal decomposition of acyl azide group in toluene. The reaction was monitored by FT-IR spectroscopy. The disappearance of band at 2143 cm^{-1} and 1680 cm^{-1} corresponding to azido and carbonyl group indicated the complete conversion of acyl azide into isocyanate (**Figure 3.23**). The strong absorption band was observed at 2268 cm^{-1} due to isocyanato group.

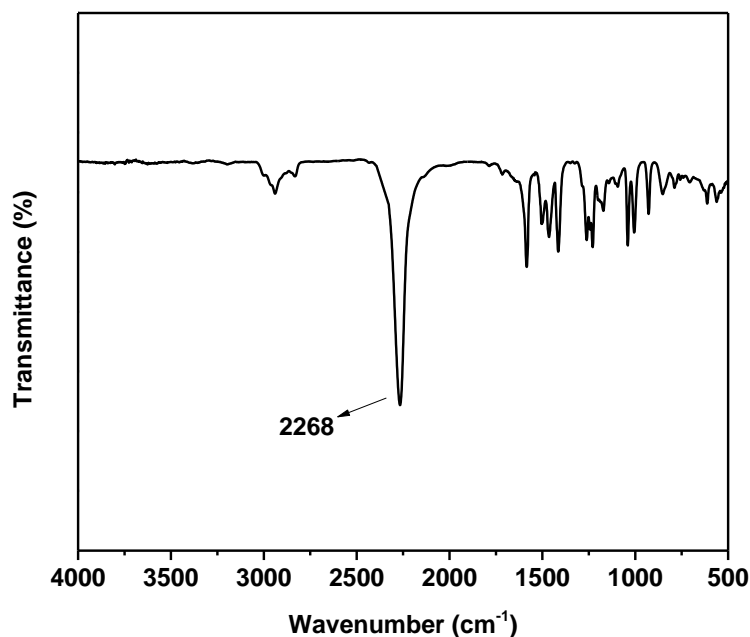


Figure 3.23 FT-IR spectrum of 5,5'-diisocyanato-2,2',3,3'-tetramethoxy-1,1'-biphenyl

^1H NMR spectrum of 5,5'-diisocyanato-2,2',3,3'-tetramethoxy-1,1'-biphenyl is displayed in **Figure 3.24**. The aromatic protons exhibited two doublets at $6.67\ \delta$ ppm and $6.60\ \delta$ ppm corresponding to proton 'a' and proton 'b', respectively. Methoxy group protons *para* to isocyanato group exhibited a singlet at $3.66\ \delta$ ppm while methoxy group protons *meta* to isocyanato group appeared as a singlet at $3.90\ \delta$ ppm. ^{13}C NMR spectrum of 5,5'-diisocyanato-2,2',3,3'-tetramethoxy-1,1'-biphenyl along with the assignments is shown in **Figure 3.25**

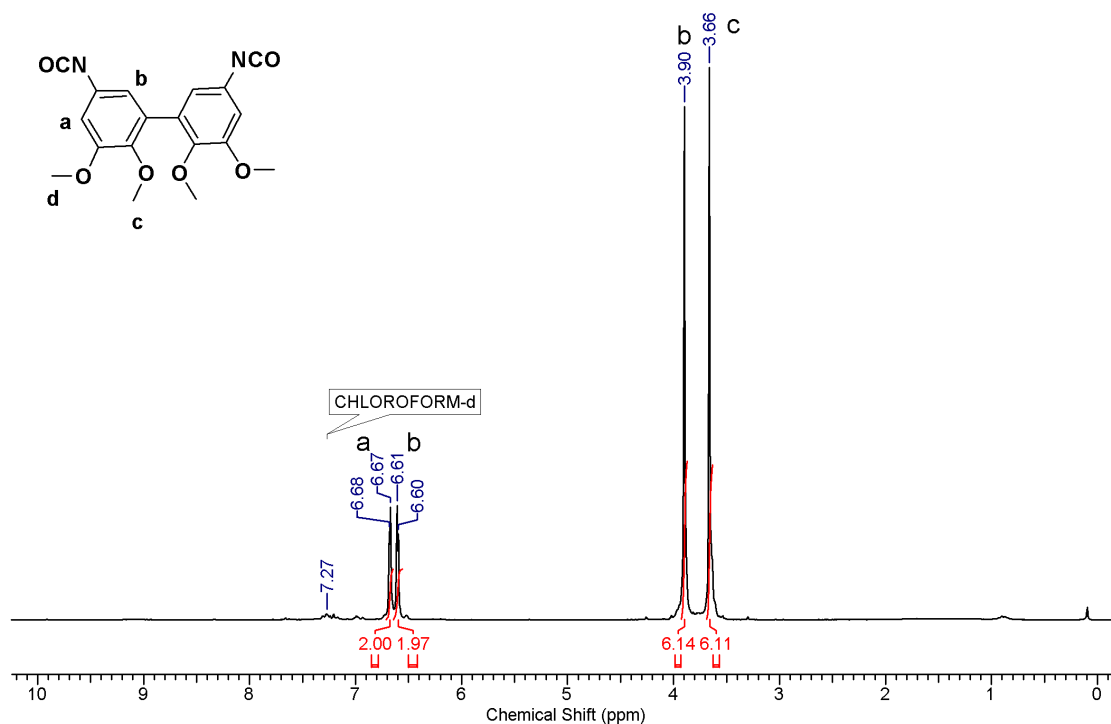


Figure 3.24 ^1H NMR spectrum of 5,5'-diisocyanato-3,3'-dimethoxy-2,2'-bis(pentyloxy)-1,1'-biphenyl

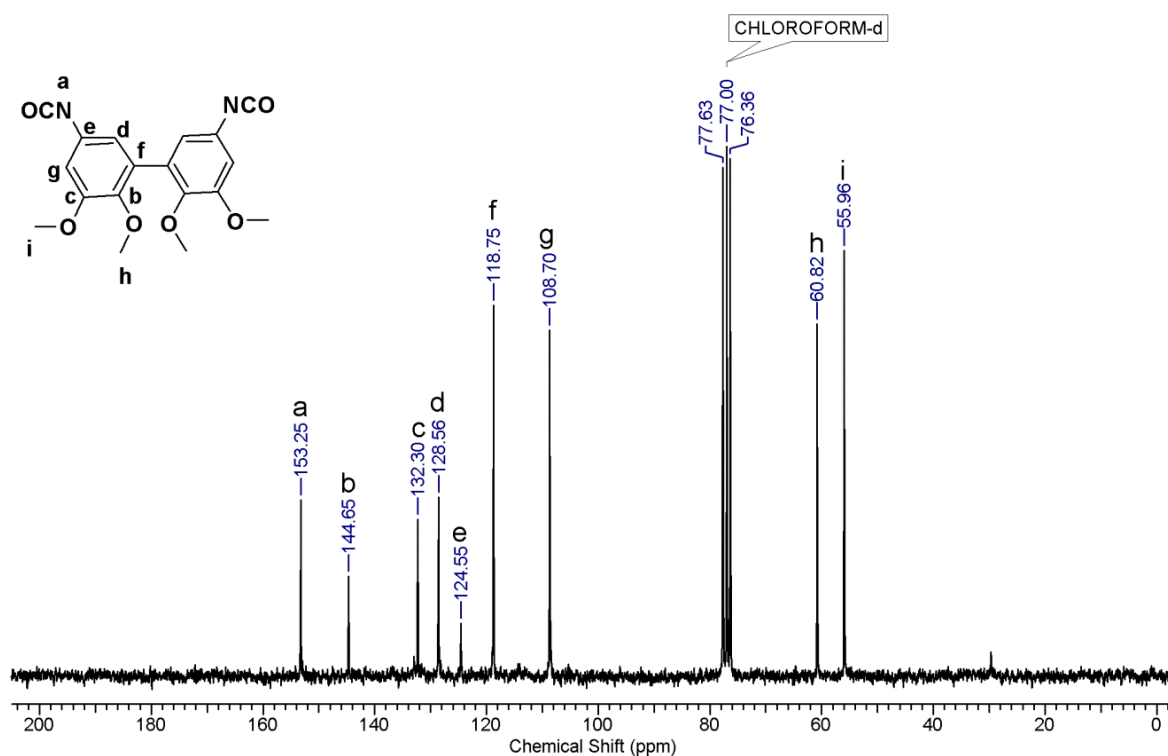
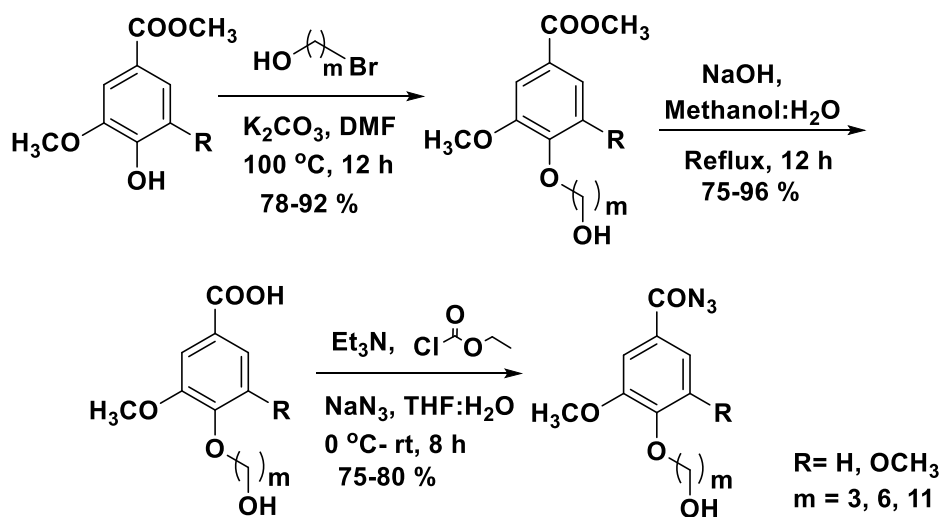


Figure 3.25 ^{13}C NMR spectrum of 5,5'-diisocyanato-3,3'-dimethoxy-2,2'-bis(pentyloxy)-1,1'-biphenyl

3.4.2 Synthesis and characterization of ω -hydroxyalkyleneoxy benzoyl azides.

The synthetic route to A-B type monomers *viz.* ω -hydroxyalkyleneoxy benzoyl azides is depicted in **Scheme 3.3**.



Scheme 3.3 Synthesis of ω -hydroxyalkyleneoxy benzoyl azides starting from vanillic acid /syringic acid.

In the first step, the solution of 6-chlorohexanol / 11-bromoundecanol in dry DMF was added slowly to a stirred mixture of methyl vanillate / methyl syringate and DMF in the presence of potassium carbonate under nitrogen atmosphere. The reaction mixture was stirred at 100 °C for 12 h and the progress of reaction was monitored by TLC. The resulting reaction mixture was added to the ice cold water and filtered. The product was purified by column chromatography. The hydroxyl ester was characterized by FT-IR, ¹H NMR and ¹³C NMR spectroscopy. FT-IR spectrum of methyl 4-((11-hydroxyundecyl)oxy)-3,5-dimethoxybenzoate (**Figure 3.26**) showed characteristic absorption band at 1708 cm⁻¹ corresponding to the ester linkage.

¹H NMR spectrum of methyl 4-((11-hydroxyundecyl)oxy)-3,5-dimethoxybenzoate is displayed in **Figure 3.27**.

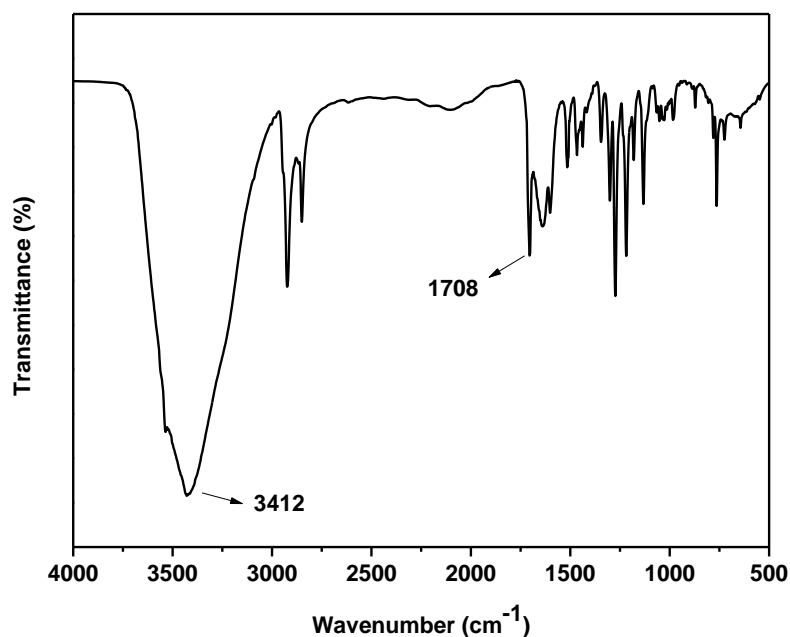


Figure 3.26 FT-IR spectrum of methyl 4-((11-hydroxyundecyl)oxy)-3,5-dimethoxybenzoate

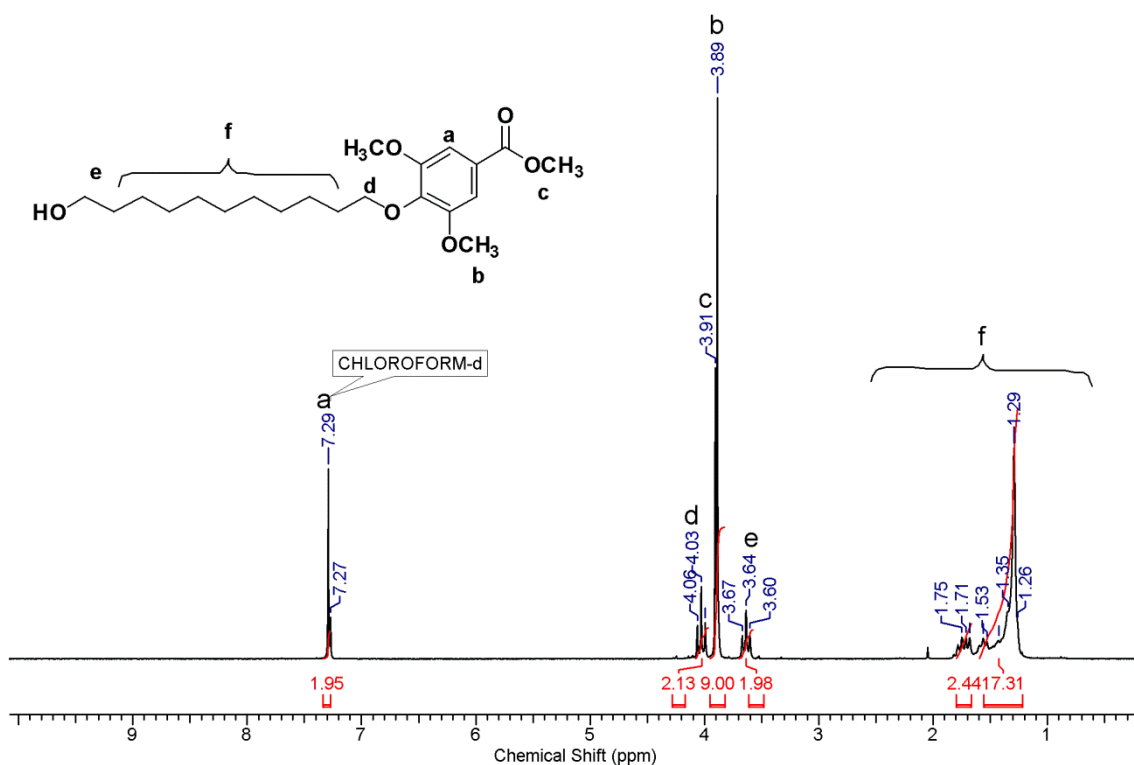


Figure 3.27 ^1H NMR spectrum of methyl 4-((11-hydroxyundecyl)oxy)-3,5-dimethoxybenzoate in CDCl_3

A singlet was observed at 7.29 δ ppm due to aromatic proton. The methylene protons attached to ether linkage appeared as a triplet at 4.03 δ ppm whereas methylene protons attached to hydroxyl group exhibited a triplet at 3.64 δ ppm. Methoxy protons and methyl protons of methyl ester group showed separate singlets at 3.89 and 3.91 δ ppm, respectively. The remaining alkylene protons appeared as a multiplet in the range 1.26-1.75 δ ppm.

^{13}C NMR spectrum of methyl 4-((11-hydroxyundecyl)oxy)-3,5-dimethoxybenzoate along with assignments is reproduced in **Figure 3.28**.

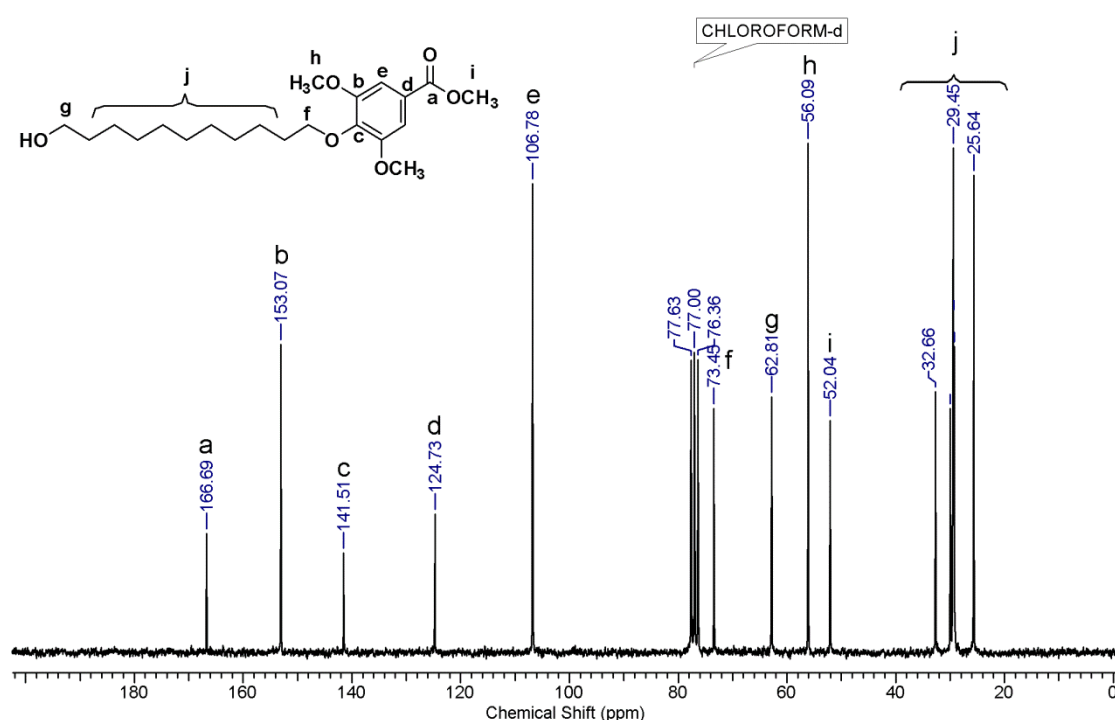


Figure 3.28 ^{13}C NMR spectrum of methyl 4-((11-hydroxyundecyl)oxy)-3,5-dimethoxybenzoate in CDCl_3

In the second step, hydroxyl-esters and sodium hydroxide in methanol-water mixture were refluxed for 12 h. The excess methanol was evaporated under reduced pressure and acidified with dilute HCl. The precipitate was collected by filtration and dried in vacuum oven. The chemical structure of 4-((11-hydroxyundecyl)oxy)-3,5-dimethoxybenzoic acid was confirmed by FT-IR, ^1H NMR and ^{13}C NMR spectroscopy. FT-IR spectrum of 4-((11-hydroxyundecyl)oxy)-3,5-dimethoxybenzoic acid is reproduced in **Figure 3.29**. The strong band appeared at 1691 cm^{-1} corresponds to the carbonyl stretching of acid group.

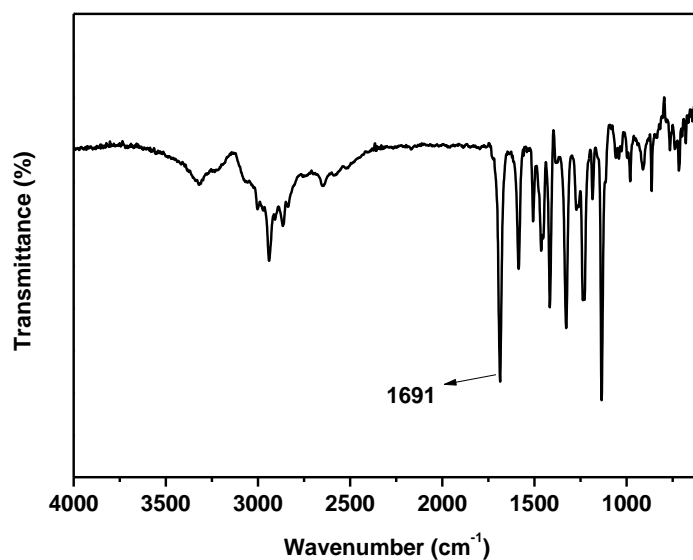


Figure 3.29 FT-IR spectrum of 4-((11-hydroxyundecyl)oxy)-3,5-dimethoxybenzoic acid

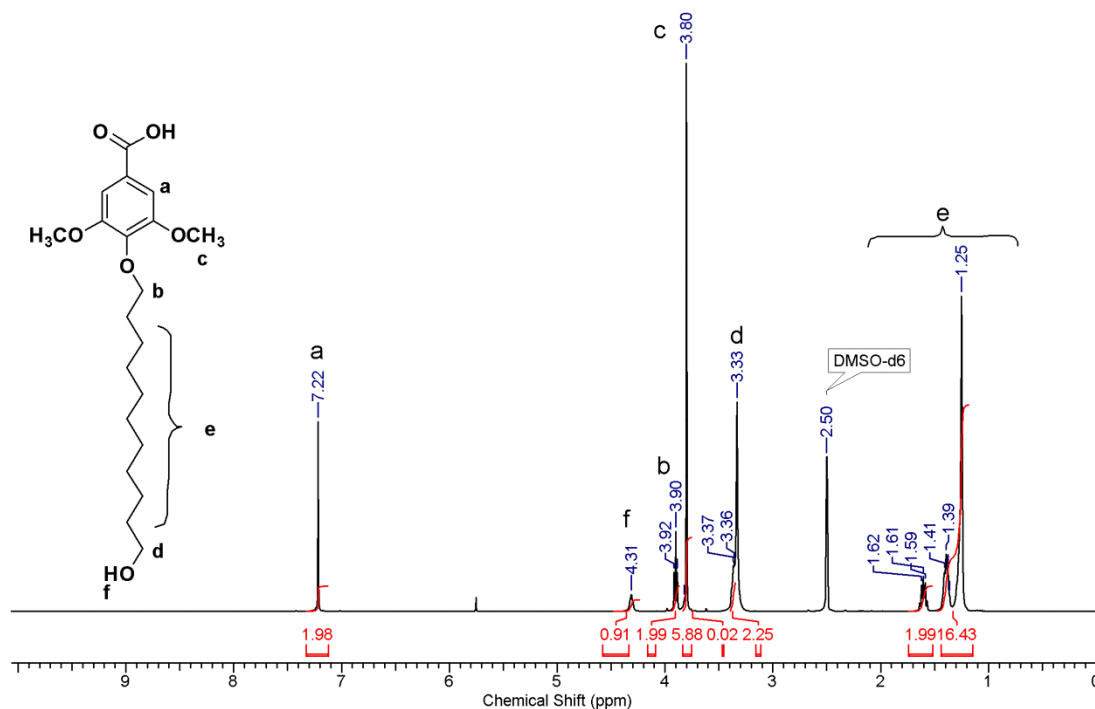


Figure 3.30 ^1H NMR spectrum of 4-((11-hydroxyundecyl)oxy)-3,5-dimethoxybenzoic acid in DMSO-d_6

^1H NMR spectrum of 4-((11-hydroxyundecyl)oxy)-3,5-dimethoxybenzoic acid (**Figure 3.30**) showed disappearance of peak at 3.91 δ ppm corresponding to methyl

proton of methyl ester (**Figure 3.27**). Aromatic proton (labelled as 'a') appeared at 7.22 δ ppm and methoxy group protons appeared at 3.80 δ ppm as singlet.

^{13}C NMR spectrum of 4-((11-hydroxyundecyl)oxy)-3,5-dimethoxybenzoic acid along with assignments is displayed in **Figure 3.31**.

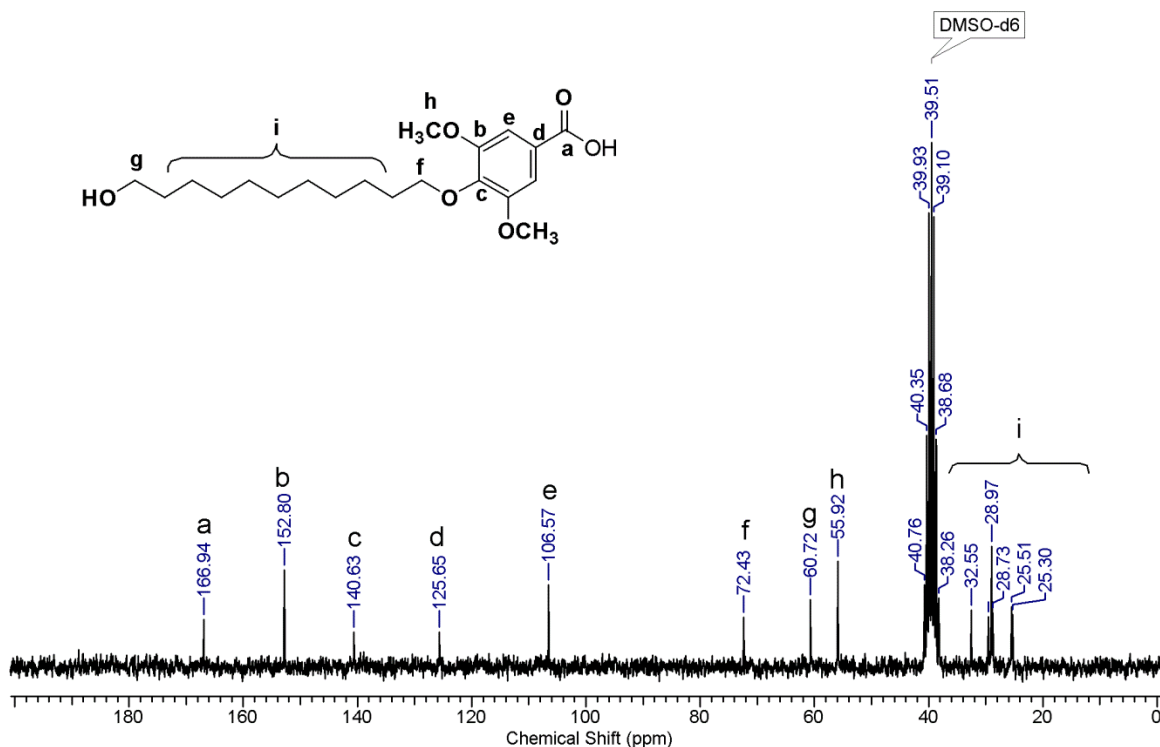


Figure 3.31 ^{13}C NMR spectrum of 4-((11-hydroxyundecyl)oxy)-3,5-dimethoxybenzoic acid in DMSO-d_6

In the last step, ω -hydroxyalkyleneoxy benzoyl azides were obtained from the synthesized hydroxyl-acids using triethyl amine, ethyl chloroformate and sodium azide *via* the elegant 'one-pot' Weinstock modification of the Curtius reaction.

All the obtained hydroxyl acyl azide monomers, namely, 4-(3-hydroxypropoxy)-3,5-dimethoxybenzoyl azide, 4-(3-hydroxypropoxy)-3-methoxybenzoyl azide, 4-((6-hydroxyhexyl)oxy)-3-methoxybenzoyl azide, 4-((6-hydroxyhexyl)oxy)-3,5-dimethoxybenzoyl azide, 4-((11-hydroxyundecyl)oxy)-3,5-dimethoxybenzoyl azide and 4-((11-hydroxyundecyl)oxy)-3-methoxybenzoyl azide were characterized by FT-IR, ^1H NMR, and ^{13}C NMR spectroscopy and HRMS.

A representative FT-IR spectrum of 4-((11-hydroxyundecyl)oxy)-3,5-dimethoxybenzoyl azide along with assignments is shown in **Figure 3.32**

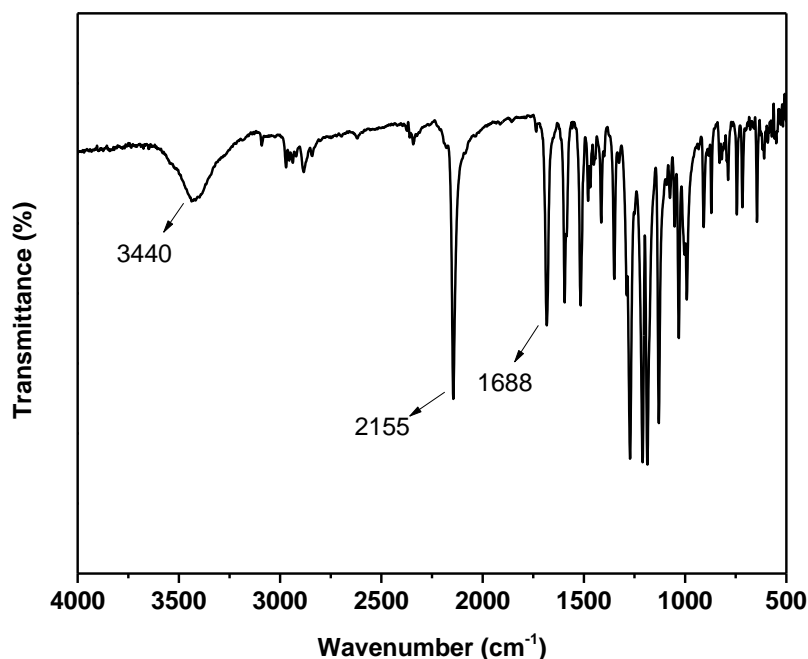


Figure 3.32 FT-IR spectrum of 4-((11-hydroxyundecyl)oxy)-3,5-dimethoxybenzoyl azide

FT-IR spectrum showed absorption band at 1688 cm^{-1} for carbonyl group stretching and at 2155 cm^{-1} for asymmetric stretching vibration of azido group. The representative ^1H and ^{13}C NMR spectra of 4-((11-hydroxyundecyl)oxy)-3,5-dimethoxybenzoyl azide monomer with assignments are shown in **Figure 3.33** and **3.34**, respectively. Aromatic protons of 4-((11-hydroxyundecyl)oxy)-3,5-dimethoxybenzoyl azide appeared as a singlet at $7.28\ \delta$ ppm. Two triplets were observed at $4.06\ \delta$ ppm and at $3.65\ \delta$ ppm corresponding to methylene protons attached to ether linkage and hydroxyl group, respectively. Methoxy protons showed a singlet at $3.89\ \delta$ ppm. ^{13}C NMR spectrum of 4-((6-hydroxyhexyl)oxy)-3,5-dimethoxybenzoyl azide showed a peak at $171.8\ \delta$ ppm corresponding to acyl-azide carbon.

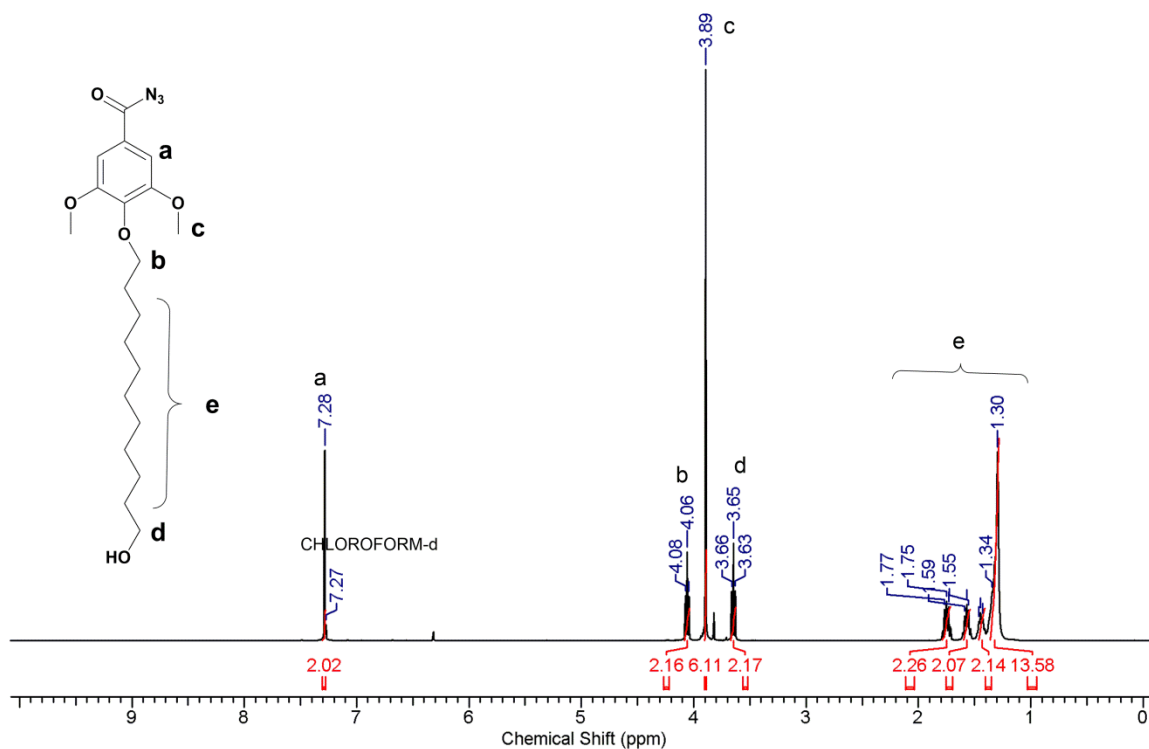


Figure 3.33 ^1H NMR spectrum of 4-((11-hydroxyundecyl)oxy)-3,5-dimethoxybenzoyl azide in CDCl_3

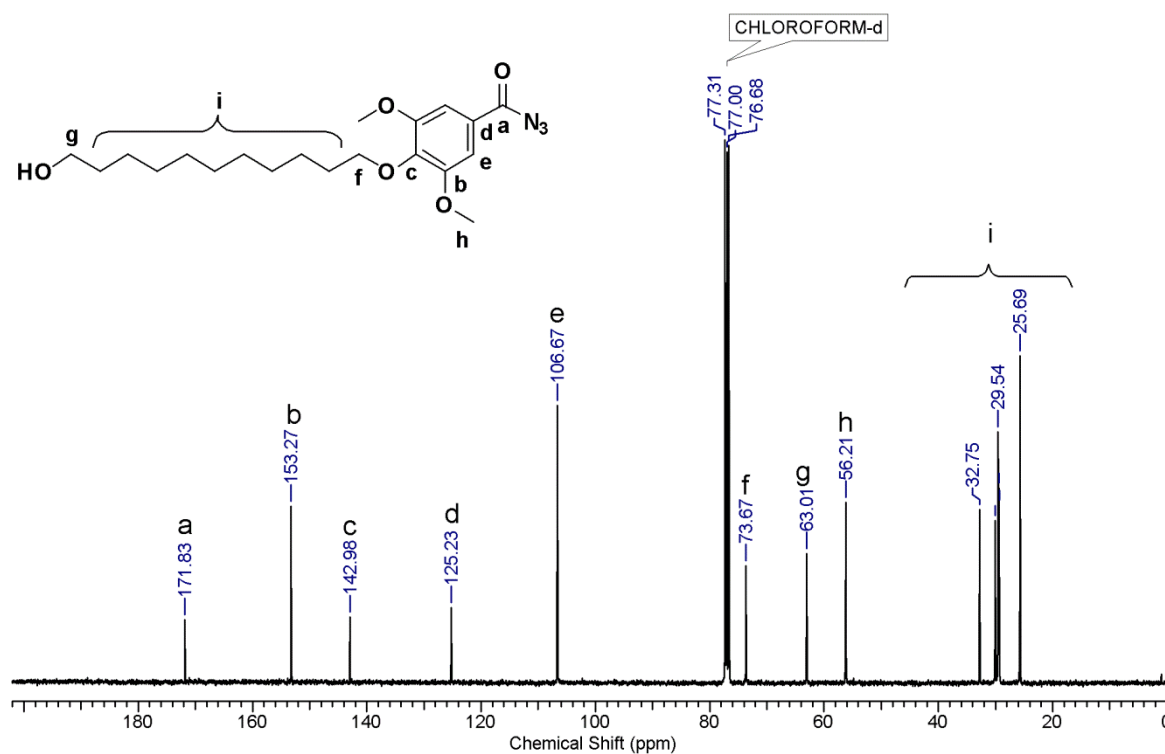


Figure 3.34 ^{13}C NMR spectrum of 4-((11-hydroxyundecyl)oxy)-3,5-dimethoxybenzoyl azide in CDCl_3

3.4.3 Bisphenols from guaiacol and syringol

Bisphenols are versatile monomers which are useful for synthesis of thermoplastics such as polycarbonates, polyesters, poly(ether ether ketone)s, poly(arylene ether sulfone)s, poly(ether imide)s, etc. Bisphenols are also used in the synthesis of thermosets such as epoxy resins, phenoxy resins, cyanate esters, etc^{42,43}. Bisphenols are usually synthesized by the acid-catalyzed condensation of an aldehyde or a ketone with a phenol. A variety of aldehydes/ketones and substituted phenols have been utilized for the synthesis of bisphenols.

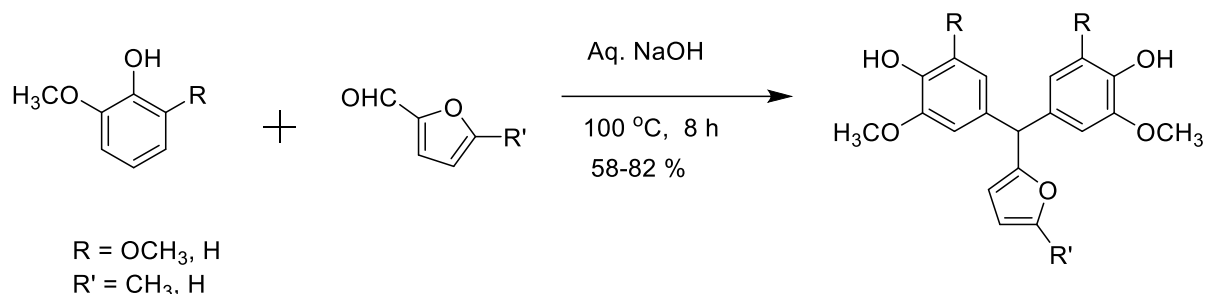
Bisphenol-A (BPA), obtained by condensation of acetone with phenol, is the most commonly used and the highest volume bisphenol. Approximately, 5.4 million tons of BPA is produced worldwide⁴⁴. However, BPA is currently under scrutiny due to its potential health hazards and it has been banned for food packaging applications^{45,46}. Additionally, BPA is produced from petroleum-derived chemicals which are non-renewable. Because of the limited stocks, non-renewability and environmental issues associated with petroleum-derived chemicals, it has been recognized that sustainable and renewable resources should be used for monomer and polymer synthesis in near future¹³.

Over the last several years, researchers from academia and industries have been searching for new sustainable bisphenols as a replacement for BPA. In this context, several renewable bisphenols were reported starting from levulinic acid, limonene, cashew nut shell liquid (CNSL) and creosol^{20,26,44,47-51}. However, it is unclear whether these bisphenols are endocrine disruptor or not. Amongst them Trita et al. reported that CNSL-based bisphenol showed estrogenic activity in the same range as that of BPA⁵¹. In contrast, renewable bisphenols derived from eugenol, ferulic acid and guaiacol were found to be non-estrogenic^{44,51,52}. The presence of *ortho* methoxy group in all these bisphenols may disrupt the hydrogen bonding interaction between the phenol and receptor site. Shetty et al. evaluated the effect of substituent of bisphenol on estrogenic activity and concluded that presence of *ortho* alkoxy substituents reduces estrogenic activity of bisphenol⁵².

In the present work, two classes of bio-based bisphenols *viz.* 1) bisphenols containing pendant furyl group, and 2) bisphenol containing oxadiazole group were synthesized starting from lignocellulose-based aromatics.

3.4.3.1 Synthesis of furyl containing bisphenols

Scheme 3.4 outlines route for the synthesis of bisphenols containing pendant furyl group from lingocellulose derived chemicals.



Scheme 3.4 Synthesis of bisphenols containing pendant furyl group.

Bisphenols containing pendant furyl group were readily synthesized in one-step reaction by condensation of methyl furfural/furfural with guaiacol/syringol in the presence of aqueous sodium hydroxide as a base at 100 °C. After completion of reaction, dark red solid was obtained, which was dissolved in excess water and acidified with 2 M HCl. The product was collected by filtration and was purified using column chromatography followed by recrystallization from water-ethanol system. Bisphenols containing pendant furyl group were characterized by FT-IR, ^1H NMR, ^{13}C NMR spectroscopy, and HRMS.

FT-IR spectrum of 4, 4'-(furan-2-ylmethylene)bis(2,6-dimethoxyphenol) is reproduced in **Figure 3.35**. The absorption band was observed at 3456 cm^{-1} corresponding to phenolic group. The furan ring (C=C) band was observed at 1507 cm^{-1} whereas furan breathing bands were observed at 1020 and 1070 cm^{-1} .

^1H NMR spectrum of 4, 4'-(furan-2-ylmethylene)bis(2,6-dimethoxyphenol) are shown in **Figure 3.36**. The proton adjacent to oxygen atom of furyl group appeared as a singlet at $7.39\text{ }\delta$ ppm. A singlet was observed at $6.39\text{ }\delta$ ppm for aromatic proton *meta* to phenolic group on both aromatic rings. The remaining furyl protons 'b' and 'c' appeared as a singlet at $6.33\text{ }\delta$ ppm and a doublet at $5.94\text{ }\delta$ ppm, respectively. Benzylic proton displayed a singlet at $5.31\text{ }\delta$ ppm. Methoxy proton attached to aromatic ring exhibited a singlet at $3.81\text{ }\delta$ ppm for 12 protons. The remaining protons were in good agreement with the proposed structure.

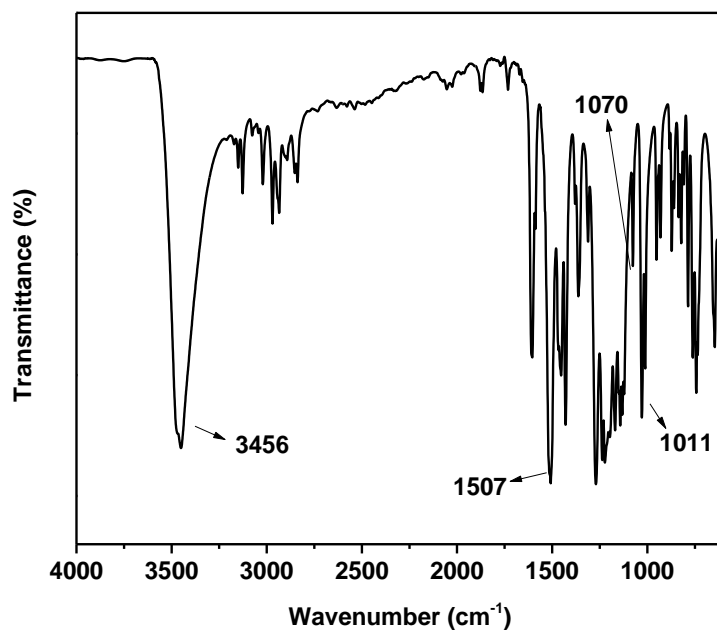


Figure 3.35 FT-IR spectrum of 4, 4'-(furan-2-ylmethylene)bis(2,6-dimethoxyphenol)

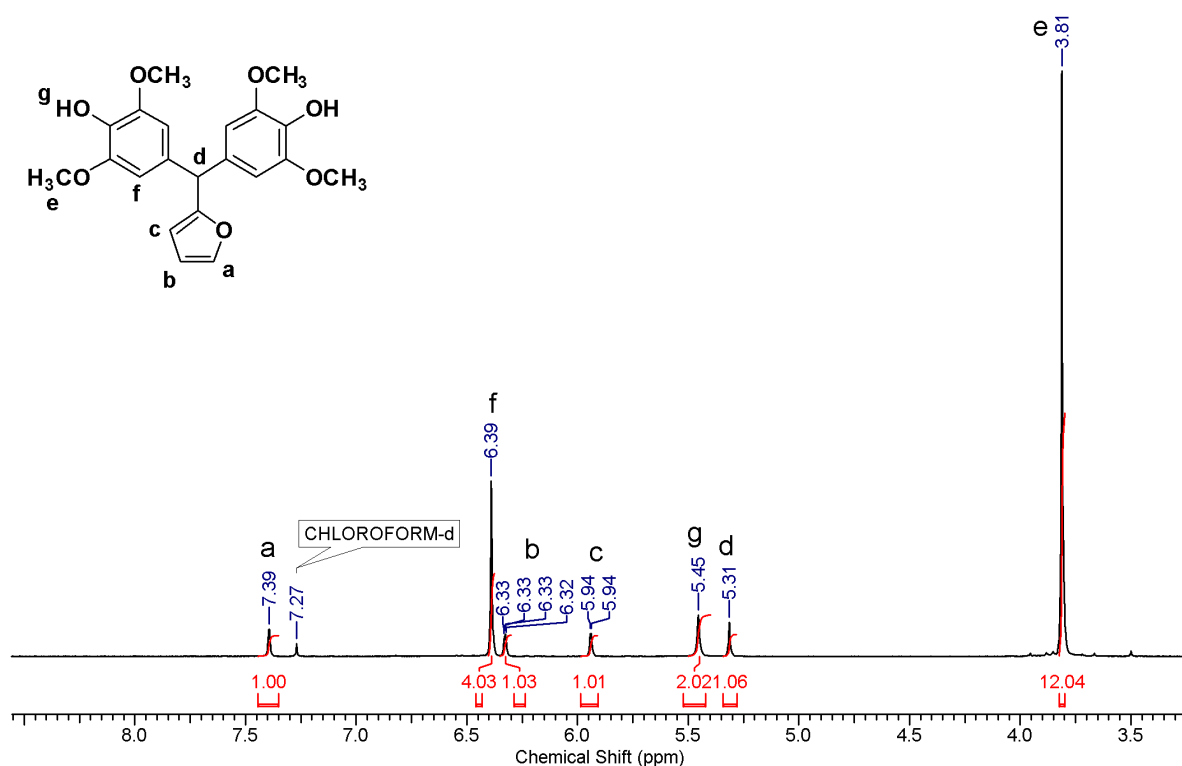


Figure 3.36 ^1H NMR spectrum of 4, 4'-(furan-2-ylmethylene)bis(2,6-dimethoxyphenol) in CDCl_3

^{13}C NMR spectrum of 4, 4'-(furan-2-ylmethylene)bis(2,6-dimethoxyphenol) (**Figure 3.37**) was in accordance with the structure.

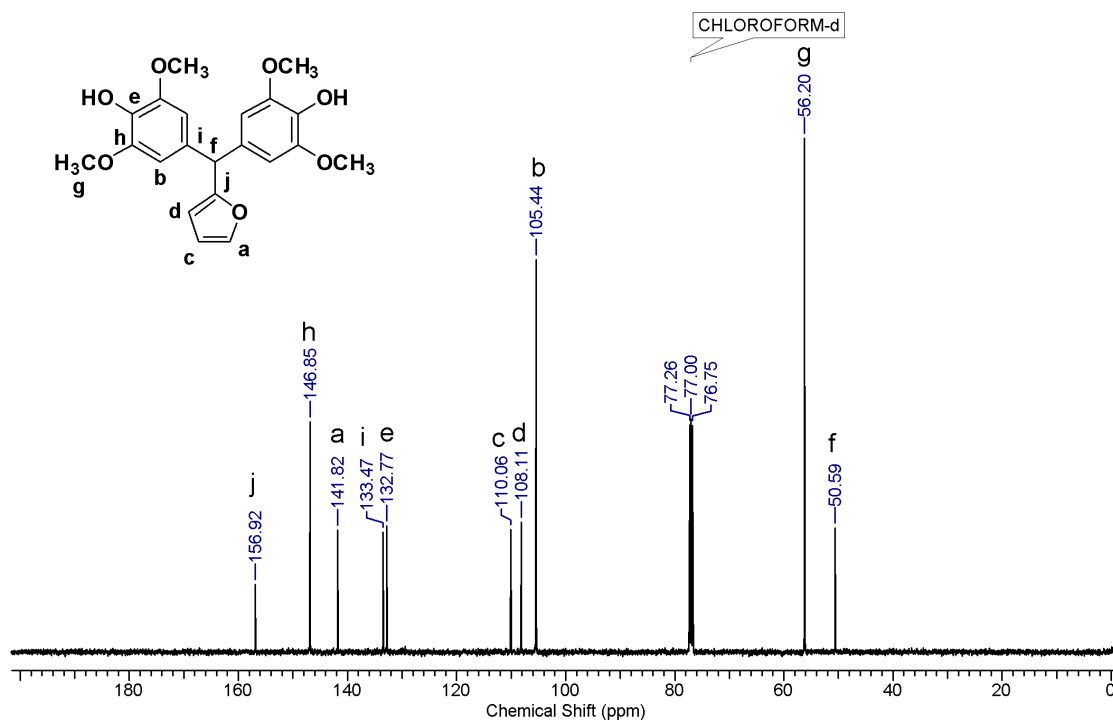
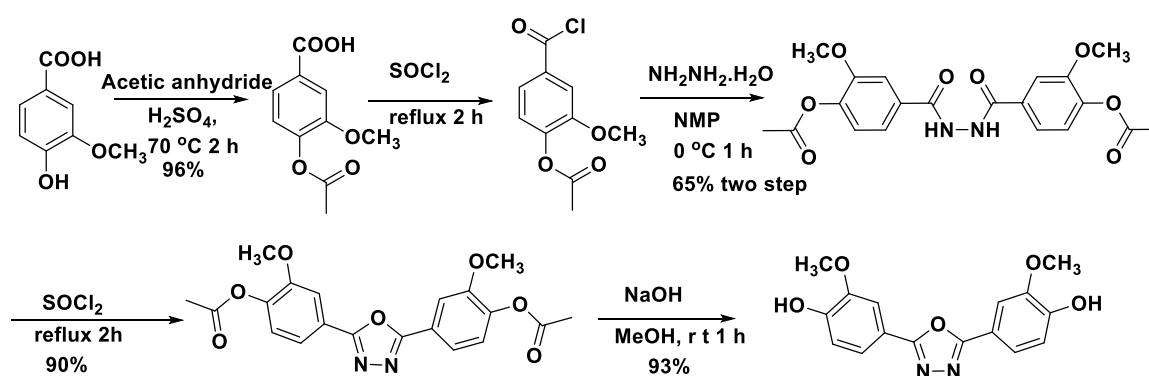


Figure 3.37 ^{13}C NMR spectrum of 4, 4'-(furan-2-ylmethylene)bis(2,6-dimethoxyphenol) in CDCl_3

3.4.3.2 Synthesis and characterization of oxadiazole containing bisphenol.

New fully bio-based oxadiazole containing bisphenol namely, 4,4'-(1,3,4-oxadiazole-2,5-diyl)bis(2-methoxyphenol) was synthesized starting from vanillic acid. **Scheme 3.5** outlines route for the synthesis of 4,4'-(1,3,4-oxadiazole-2,5-diyl)bis(2-methoxyphenol).



Scheme 3.5 Synthesis of 4,4'-(1,3,4-oxadiazole-2,5-diyl)bis(2-methoxyphenol)

In the first step, phenolic group of vanillic acid was protected using excess acetic anhydride as an acylating agent and sulphuric acid as the catalyst. The reaction mixture was poured into excess ice cold water and product was collected by filtration.

In the second step, acid chloride was formed by the reaction of protected acetyl vanillic acid with thionyl chloride. After completion of reaction, excess thionyl chloride was distilled out and the product was used for next step without any further purification. The synthesized acid chloride was treated with hydrazine hydrate in dry NMP at room temperature. The reaction mixture was poured into an excess ice cold water to afford solid precipitate. The precipitate was collected by filtration and dried under vacuum at 100 °C. The product was characterized by FT-IR and NMR spectroscopy.

^1H NMR spectrum of (hydrazine-1,2-dicarbonyl)bis(2-methoxy-4,1-phenylene) diacetate is reproduced in **Figure 3.38**. A signal at downfield shift was observed for -NH protons as a singlet at 10.59 δ ppm. The aromatic protons *ortho* to methoxy group appeared as a doublet at 7.64 δ ppm. Aromatic protons *para* to methoxy group exhibited doublet of doublet at 7.54 δ ppm while aromatic protons *meta* to methoxy group appeared as a doublet at 7.25 δ ppm. Methoxy protons showed a singlet at 3.86 δ ppm and acetyl group protons appeared as a singlet at 2.29 δ ppm. ^{13}C NMR spectrum of (hydrazine-1,2-dicarbonyl)bis(2-methoxy-4,1-phenylene) diacetate along with assignments of carbon atoms is displayed in **Figure 3.39**

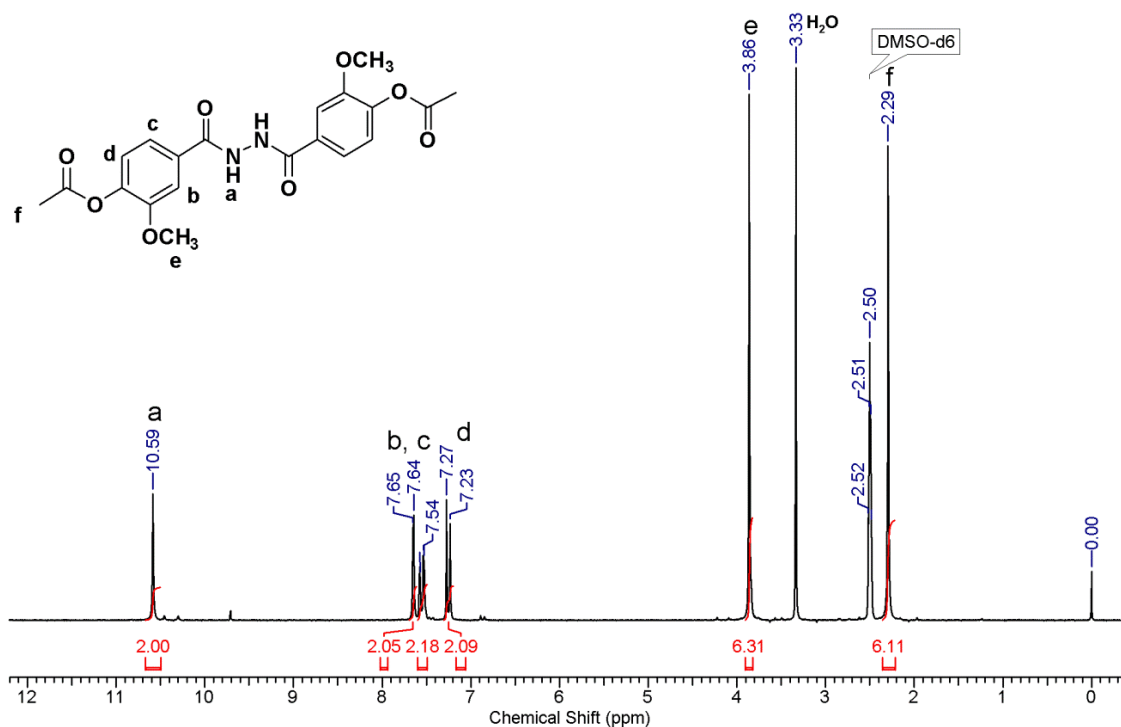


Figure 3.38 ^1H NMR spectrum of (hydrazine-1,2-dicarbonyl)bis(2-methoxy-4,1-phenylene) diacetate in DMSO-d_6

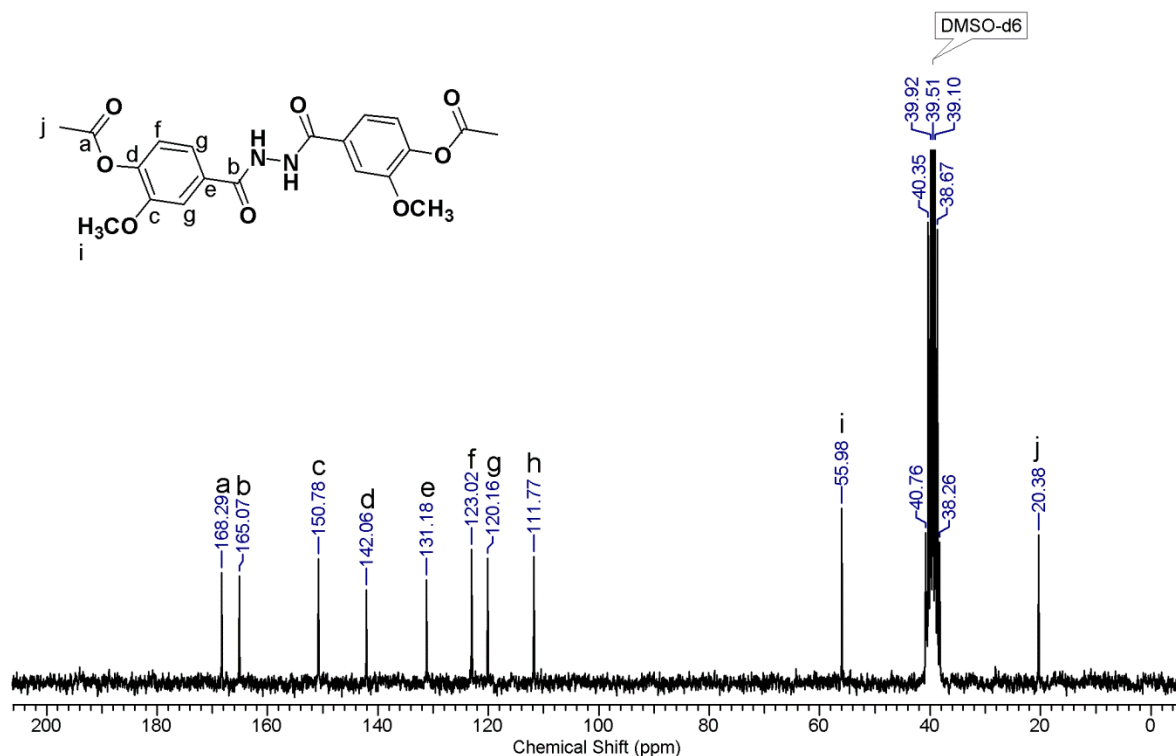


Figure 3.39 ^{13}C NMR spectrum of (hydrazine-1,2-dicarbonyl)bis(2-methoxy-4,1-phenylene) diacetate in DMSO-d_6

In the next step, (hydrazine-1,2-dicarbonyl)bis(2-methoxy-4,1-phenylene) diacetate was cyclized using thionyl chloride as a dehydrating agent. The reaction mixture was refluxed for 2 h. After completion of reaction excess thionyl chloride was removed by distillation and product was purified by column chromatography. The structure of (1,3,4-oxadiazole-2,5-diyl)bis(2-methoxy-4,1-phenylene) diacetate was confirmed by FT-IR and NMR spectroscopy.

FT-IR spectrum of (1,3,4-oxadiazole-2,5-diyl)bis(2-methoxy-4,1-phenylene) diacetate is reproduced in **Figure 3.40**. FT-IR spectrum showed absorption band at 1773 cm^{-1} corresponding to carbonyl stretching of acetyl group. The characteristic bands of oxadiazole ring were observed at 1028 cm^{-1} ($=\text{C}-\text{O}-\text{C}=\text{O}$) and 1605 cm^{-1} ($-\text{C}=\text{N}-$), confirming the formation of oxadiazole ring.

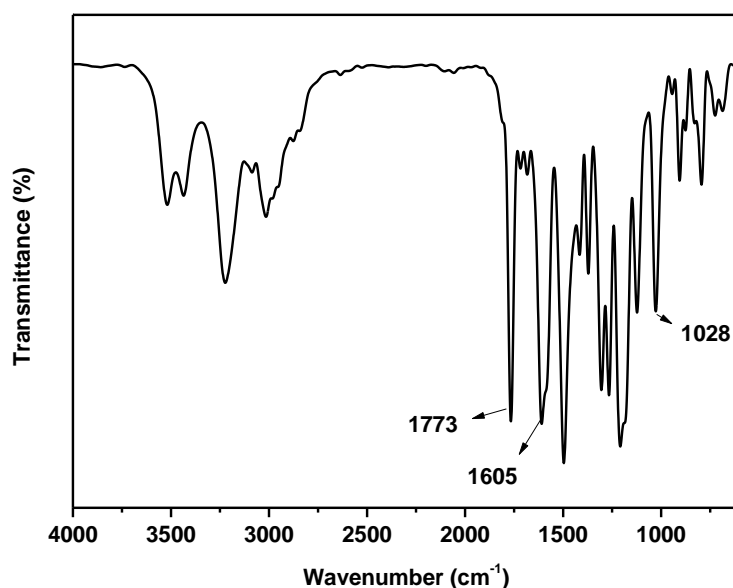


Figure 3.40 FT-IR spectrum of (1,3,4-oxadiazole-2,5-diyl)bis(2-methoxy-4,1-phenylene) diacetate

^1H NMR and ^{13}C NMR spectra of (1,3,4-oxadiazole-2,5-diyl)bis(2-methoxy-4,1-phenylene) diacetate are shown in **Figure 3.41** and **3.42**, respectively. ^1H NMR spectrum confirmed the complete cyclization of (hydrazine-1,2-dicarbonyl)bis(2-methoxy-4,1-phenylene) diacetate into (1,3,4-oxadiazole-2,5-diyl)bis(2-methoxy-4,1-phenylene) diacetate as the peak of hydrazide protons (-NH-, 10.59 ppm) which was present in ^1H NMR spectrum of (hydrazine-1,2-dicarbonyl)bis(2-methoxy-4,1-phenylene) (vide **Figure 3.38**) was absent in ^1H NMR spectrum of (1,3,4-oxadiazole-2,5-diyl)bis(2-methoxy-4,1-phenylene).

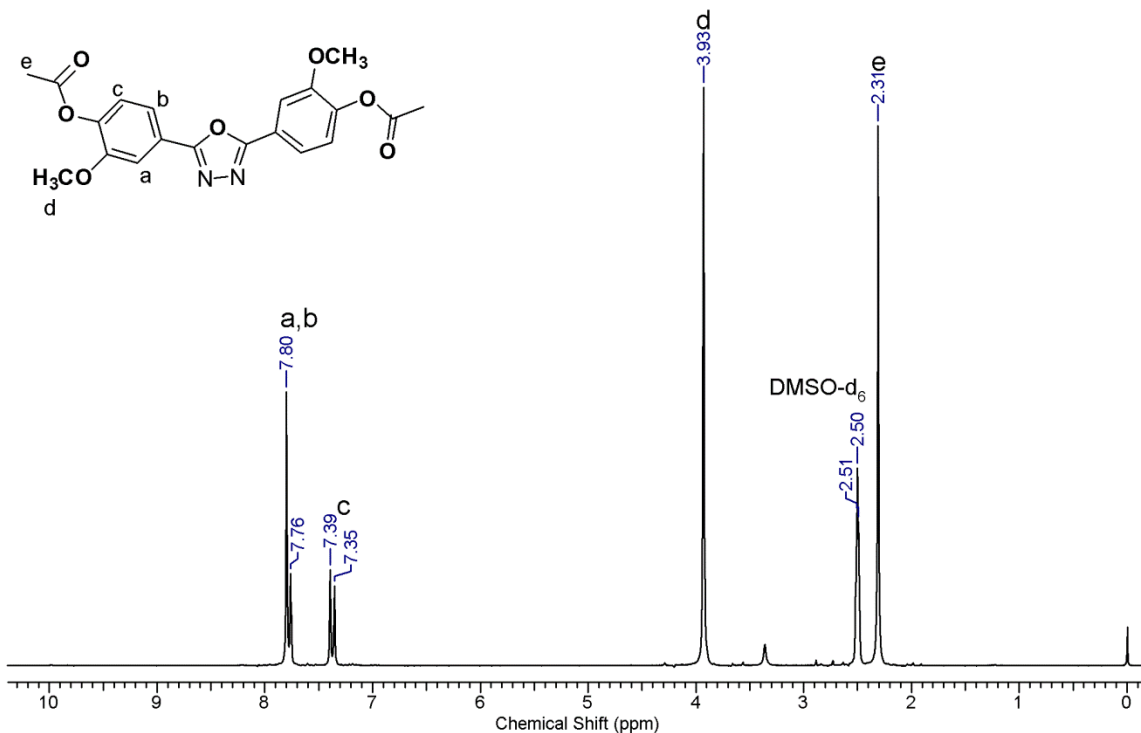


Figure 3.41 ¹H NMR spectrum of (1,3,4-oxadiazole-2,5-diyl)bis(2-methoxy-4,1-phenylene) diacetate in DMSO-d₆

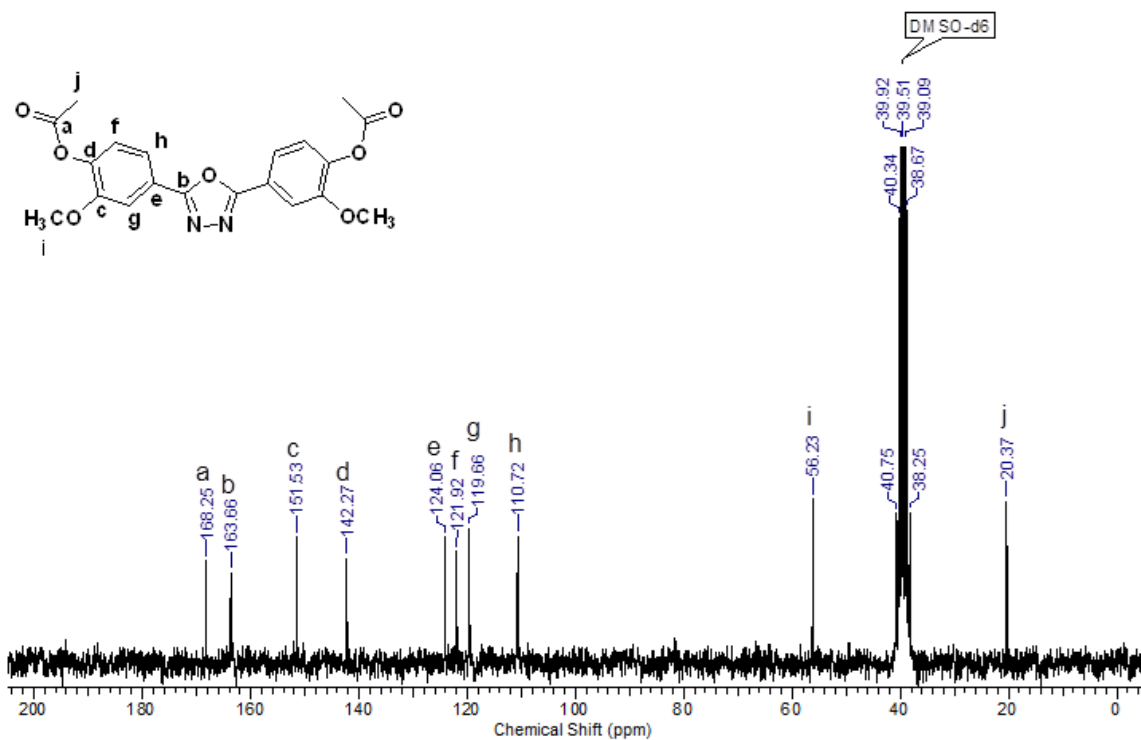


Figure 3.42 ¹³C NMR spectrum of (1,3,4-oxadiazole-2,5-diyl)bis(2-methoxy-4,1-phenylene) diacetate in DMSO-d₆

Finally, bisphenol containing oxadiazole group was obtained by deprotection of (1,3,4-oxadiazole-2,5-diyl)bis(2-methoxy-4,1-phenylene) diacetate using sodium hydroxide in a mixture of water-methanol (50:50 v/v). The obtained product was characterized by FT-IR, ^1H NMR, ^{13}C NMR spectroscopy and HRMS. FT-IR spectrum of 4,4'-(1,3,4-oxadiazole-2,5-diyl)bis(2-methoxyphenol) is reproduced in **Figure 3.43**, which showed complete disappearance of carbonyl band of acetyl group.

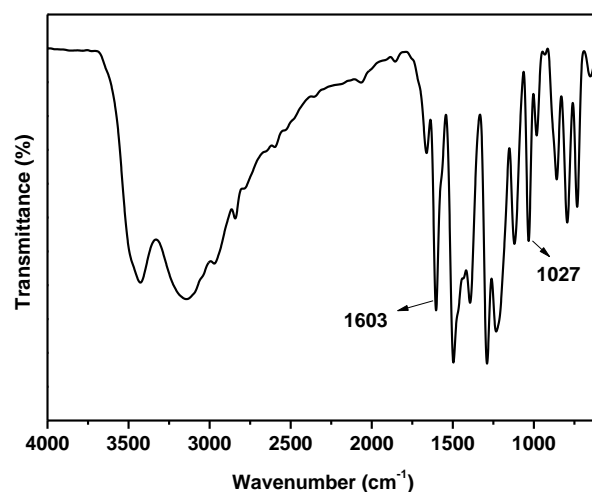


Figure 3.43 FT-IR spectrum of 4,4'-(1,3,4-oxadiazole-2,5-diyl)bis(2-methoxyphenol)

^1H NMR spectrum of 4,4'-(1,3,4-oxadiazole-2,5-diyl)bis(2-methoxyphenol) is presented in **Figure 3.44**. The phenolic hydroxyl proton showed a broad singlet at 9.95 δ ppm. The protons *ortho* to oxadiazole ring (labelled as 'b' and 'c') are merged together and exhibited singlet at 7.56 δ ppm. The proton *meta* to oxadiazole ring appeared as doublet at 9.97 δ ppm and methoxy proton showed a singlet at 3.89 δ ppm. ^{13}C NMR and HRMS spectrum of 4,4'-(1,3,4-oxadiazole-2,5-diyl)bis(2-methoxyphenol) are presented in **Figure 3.45** and **3.46**, respectively

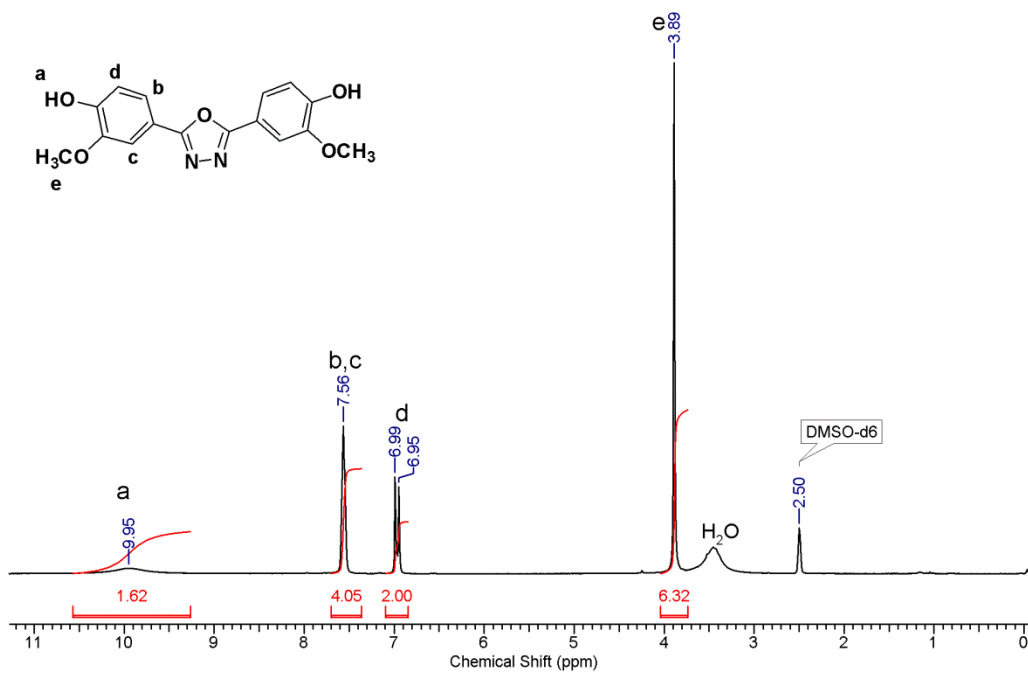


Figure 3.44 ^1H NMR spectrum of 4,4'-(1,3,4-oxadiazole-2,5-diyl)bis(2-methoxyphenol) in DMSO-d_6

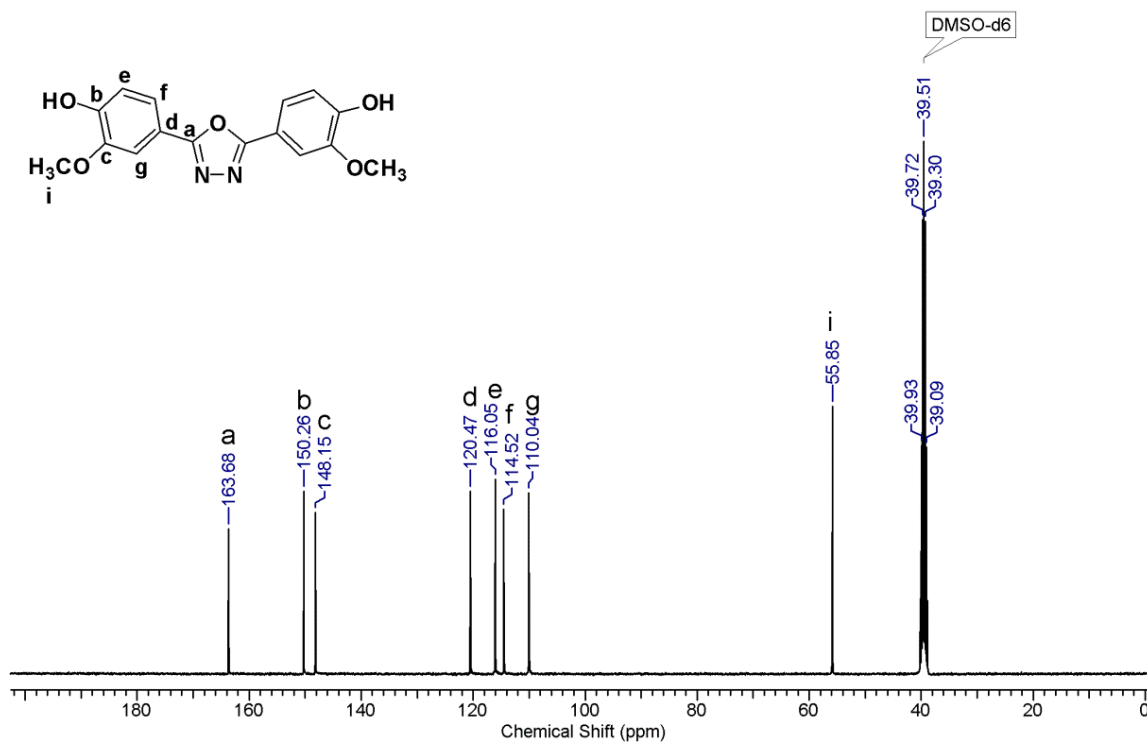


Figure 3.45 ^{13}C NMR spectrum of 4,4'-(1,3,4-oxadiazole-2,5-diyl)bis(2-methoxyphenol) in DMSO-d_6

OXA-BP #97 RT: 0.43 AV: 1 NL: 5.83E8
T: FTMS + p ESIFull.ms [100.00-1500.00]

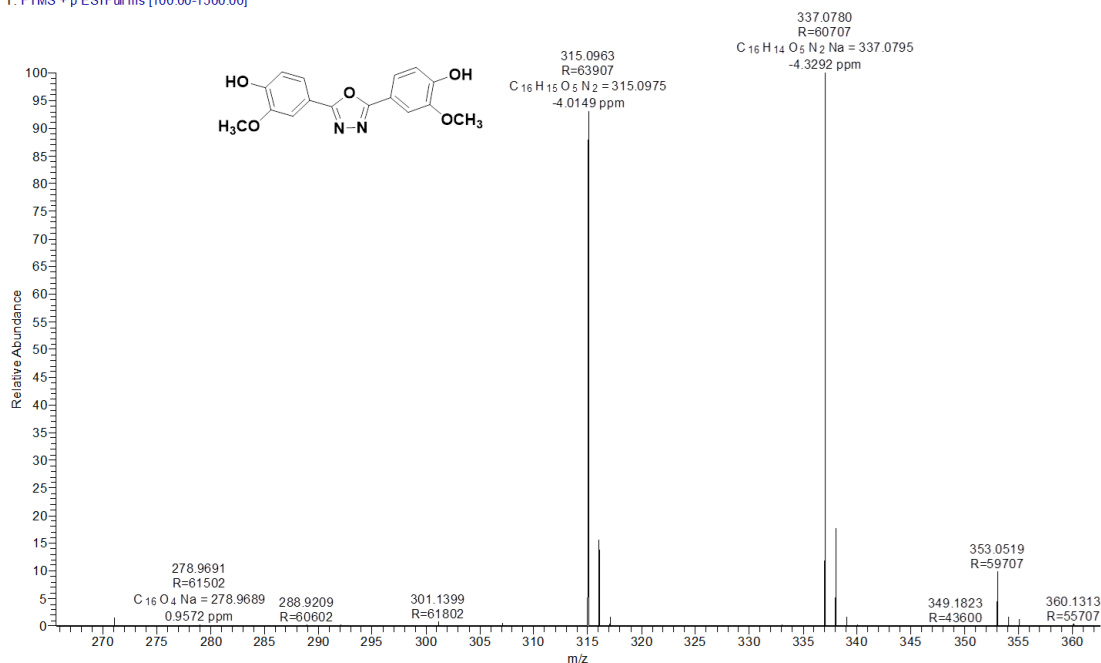
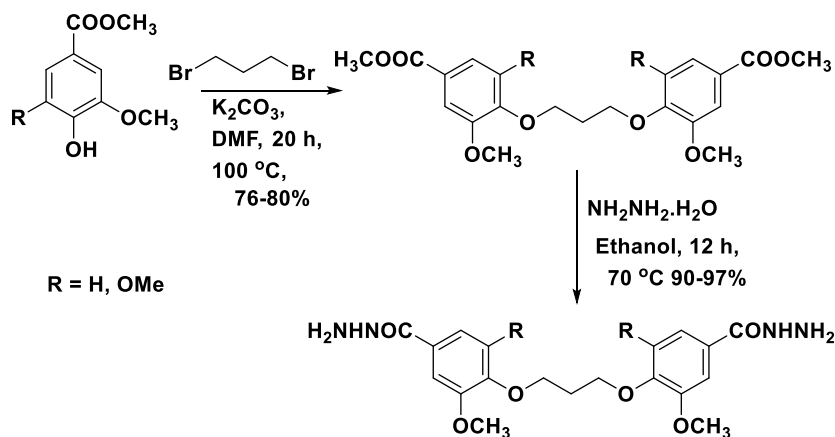


Figure 3.46 HRMS of 4,4'-(1,3,4-oxadiazole-2,5-diyl)bis(2-methoxyphenol)

3.4.4 Synthesis of diacyl hydrazides containing oxypropylene linkage.

3.4.4.1 Synthesis of α, ω -diacyl hydrazides containing oxypropylene linkage

Scheme 3.6 depicts route followed for synthesis of new fully bio-based diacylhydrazide monomers namely, 4,4'-(propane-1,3-diylbis(oxy))bis(3-methoxybenzohydrazide) (DVHzC-3) and 4,4'-(propane-1,3-diylbis(oxy))bis(3,5-dimethoxybenzohydrazide) (DSHzC-3).



Scheme 3.6 Synthesis of diacylhydrazide monomers starting from methyl vanillate/methyl syringate.

Diesters were synthesized by Williamson etherification reaction of methyl vanillate/methyl syringate with 1,3-dibromopropane in the presence of potassium

carbonate in DMF at 100 °C. The reaction mixture was cooled to room temperature and was precipitated in excess ice cold water. The precipitate was filtered and dried under reduced pressure at 100 °C for 12 h. The product was purified by column chromatography and characterized by FT-IR and NMR spectroscopy. FT-IR spectrum of dimethyl 4,4'-(propane-1,3-diylbis(oxy))bis(3,5-dimethoxybenzoate) is reproduced in **Figure 3.47** FT-IR spectrum showed absence of band at 3100-3400 cm^{-1} corresponding to hydroxyl group and appearance of characteristic band corresponding to carbonyl group at 1719 cm^{-1} .

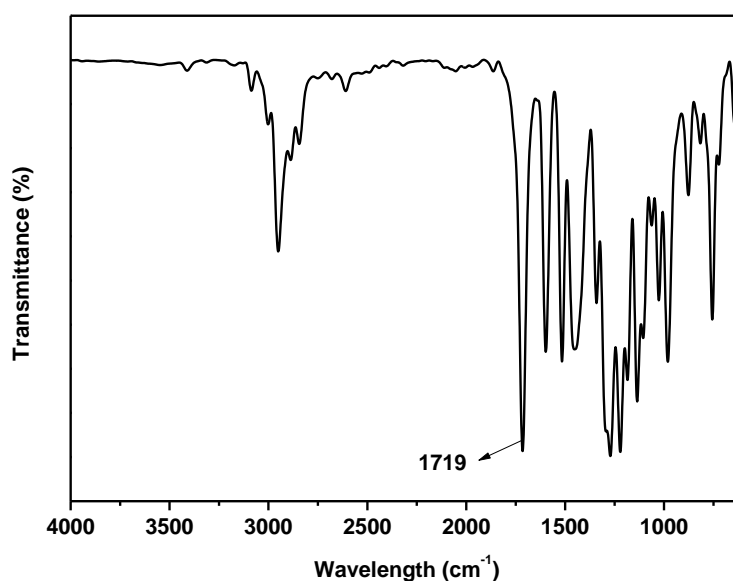


Figure 3.47 FT-IR spectrum of dimethyl 4,4'-(propane-1,3-diylbis(oxy))bis(3,5-dimethoxybenzoate)

^1H NMR spectrum of dimethyl 4,4'-(propane-1,3-diylbis(oxy))bis(3,5-dimethoxybenzoate) is shown in **Figure 3.48**. The four aromatic protons *ortho* to ester group exhibited a singlet at 7.27 δ ppm. A triplet was observed at 4.30 δ ppm which was assigned to methylene protons attached to ether linkage. Methoxy protons exhibited a singlet at 3.91 δ ppm while methyl protons of methyl ester appeared as a singlet 3.83 δ ppm. The remaining methylene protons exhibited a multiplet in the range 2.12-2.24 δ ppm.

^{13}C NMR spectrum of dimethyl 4,4'-(propane-1,3-diylbis(oxy))bis(3,5-dimethoxybenzoate) along with the assignments is reproduced in **Figure 3.49**

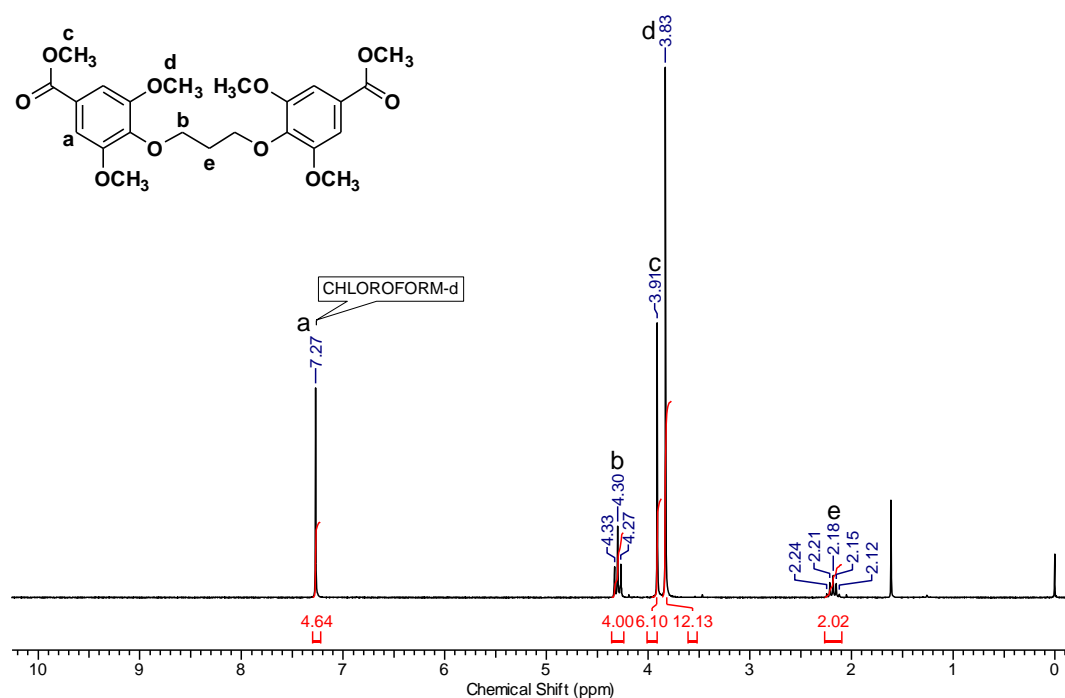


Figure 3.48 ^1H NMR spectrum of dimethyl 4,4'-(propane-1,3-diylbis(oxy))bis(3,5-dimethoxybenzoate) in CDCl_3

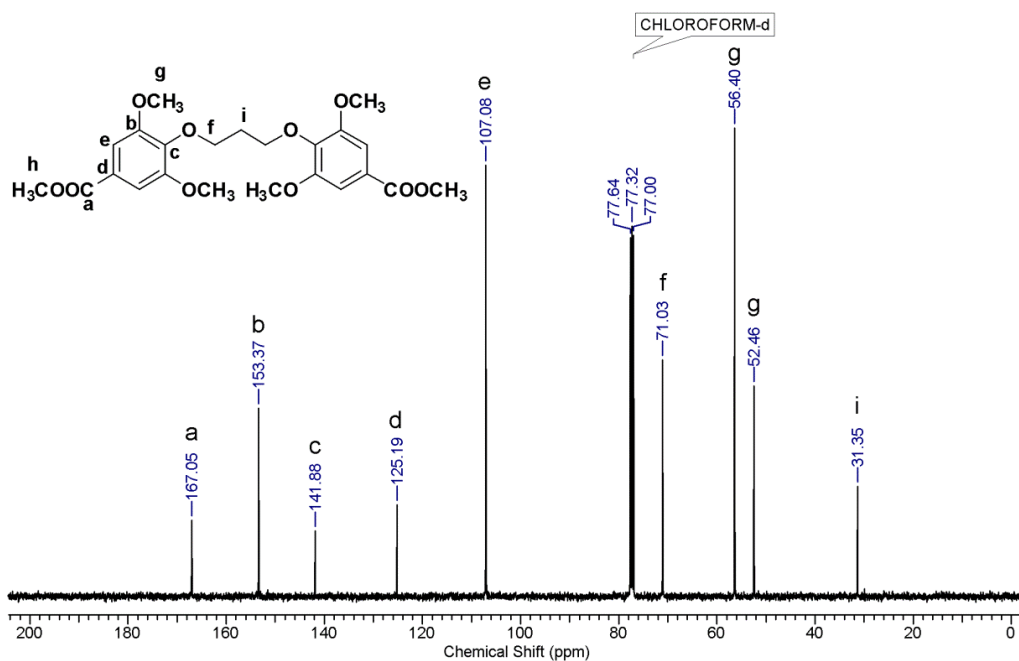


Figure 3.49 ^{13}C NMR spectrum of dimethyl 4,4'-(propane-1,3-diylbis(oxy))bis(3,5-dimethoxybenzoate) in CDCl_3

In the second step, the synthesized diesters were reacted with hydrazine hydrate in ethanol at $70\text{ }^\circ\text{C}$ to afford diacylhydrazide monomers. The formation of

diacylhydrazide monomer was confirmed by FT-IR, ^1H NMR, ^{13}C NMR, HRMS and single crystal X-ray diffraction. FT-IR spectrum of 4,4'-(propane-1,3-diylbis(oxy))bis(3-methoxybenzohydrazide) is shown in **Figure 3.50**.

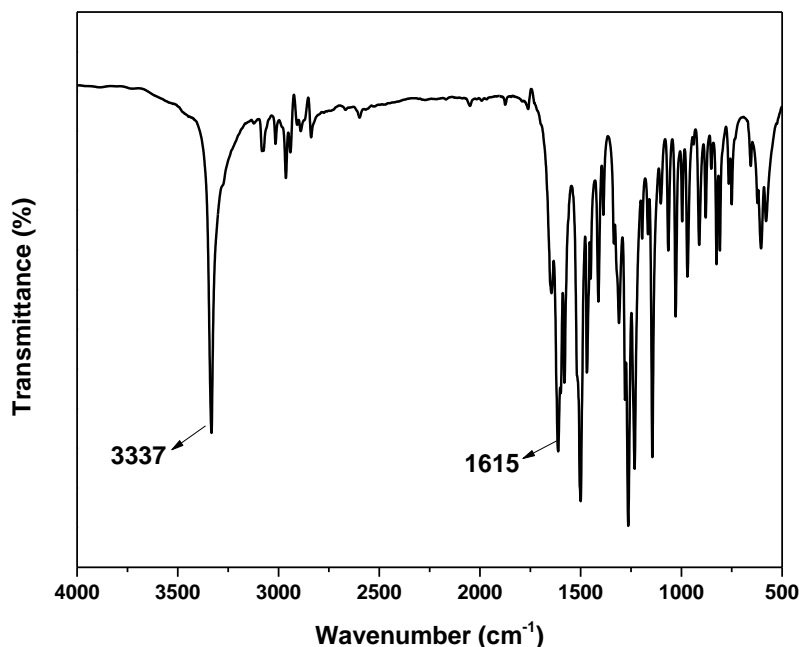


Figure 3.50 FT-IR spectrum of 4,4'-(propane-1,3-diylbis(oxy))bis(3-methoxybenzohydrazide)

FT-IR spectrum showed absorption band at 3337 cm^{-1} and 1615 cm^{-1} corresponding to the $-\text{NH}/-\text{NH}_2$ and $-\text{C}=\text{O}$ group, respectively. A representative ^1H NMR spectrum of DSHzC-3 is reproduced in **Figure 3.51**. The methyl group of methyl ester was completely disappeared and two new singlets appeared at $9.71\text{ }\delta$ ppm and $4.47\text{ }\delta$ ppm which correspond to $-\text{NH}$ and $-\text{NH}_2$ protons, respectively. The aromatic protons exhibited a singlet at $7.15\text{ }\delta$ ppm. The methylene protons attached to ether linkage showed a triplet at $4.09\text{ }\delta$ ppm and methoxy protons attached to aromatic ring appeared as a singlet at $3.76\text{ }\delta$ ppm. The remaining methylene protons showed a multiplet in the range $1.87\text{--}2.0\text{ }\delta$ ppm. ^{13}C NMR (**Figure 3.52**) and HRMS spectral data of diacylhydrazide were in good agreement with the proposed structure.

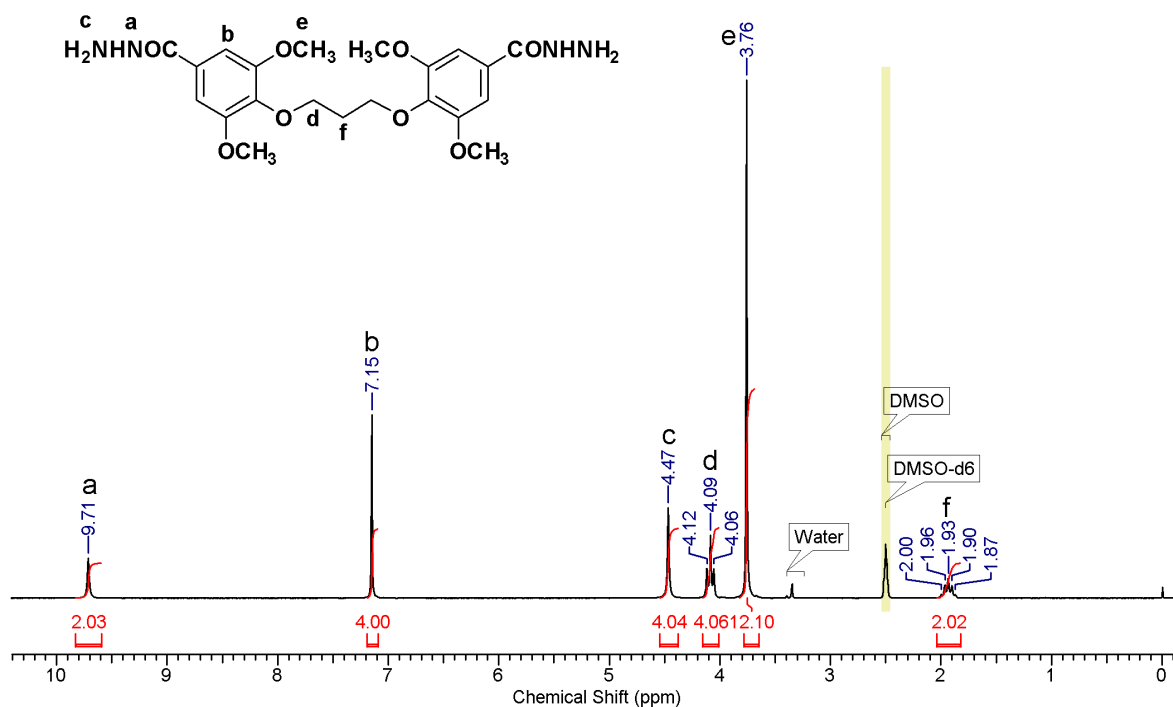


Figure 3.51 ^1H NMR spectrum of 4,4'-(propane-1,3-diylbis(oxy))bis(3,5-dimethoxybenzohydrazide) in DMSO-d_6

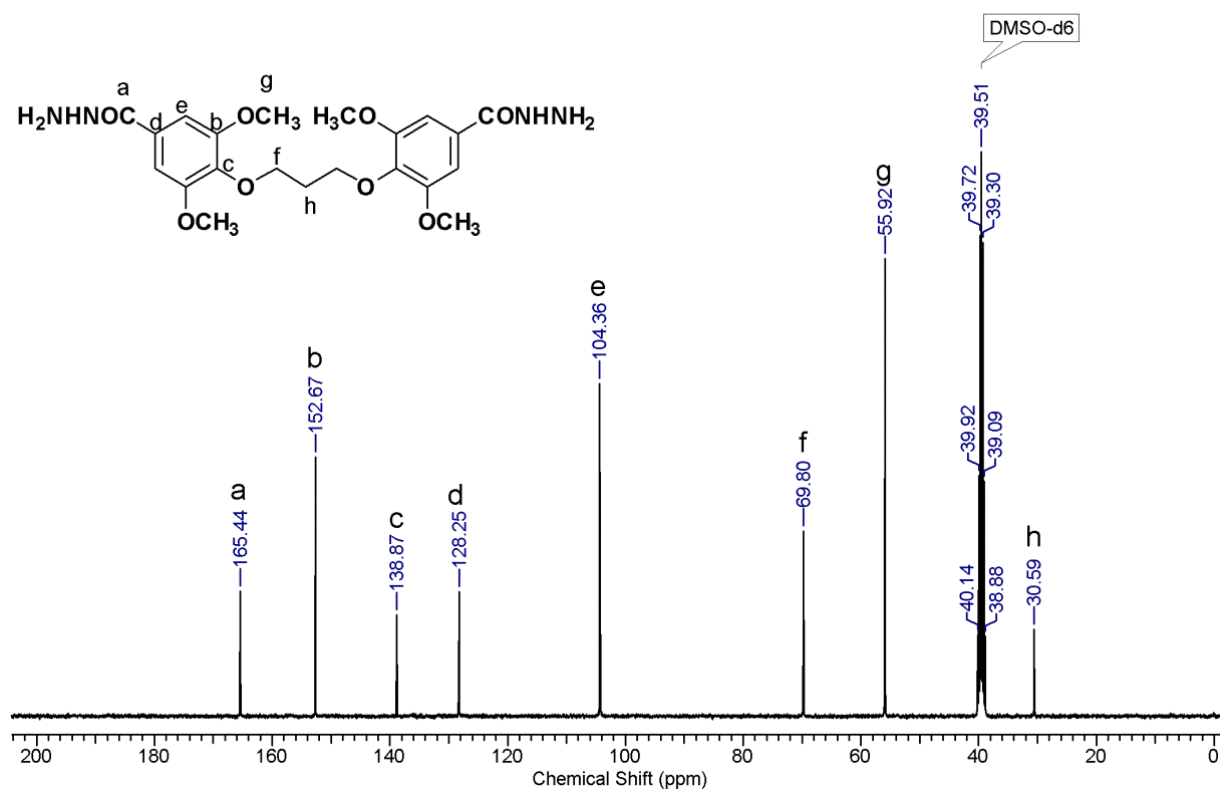


Figure 3.52 ^{13}C NMR spectrum of 4,4'-(propane-1,3-diylbis(oxy))bis(3,5-dimethoxybenzohydrazide) in DMSO-d_6

The structure of DVHzC-3 was also determined using single crystal X-ray diffraction analysis. Good quality single crystals of DVHzC-3 were obtained by slow evaporation from ethanol. The crystals were of the body centered orthorhombic type having *Iba2* space group containing half (1/2) molecule in the asymmetric unit and the other half is generated by twofold rotation operation. The ORTEP of DVHzC-3 drawn at the 50% ellipsoid probability level is shown in **Figure 3.53**. The H-atoms are drawn with an arbitrary radii. The crystallographic data is summarized in **Table 3.2**. The close inspection of molecular packing revealed that the self-assembly of the molecules is driven by strong hydrogen bonding interaction (N-H...O) between hydrazine H-atom and carbonyl oxygen to generate the wavy structure along the *a*-axis. The association is further supplemented by N-H... π contacts between NH₂ H-atom π -cloud of the phenyl ring. The neighboring parallel waves along the *c*-axis are linked weakly via C-H...O contacts to generate the 2D packing (**Figure 3.54**).

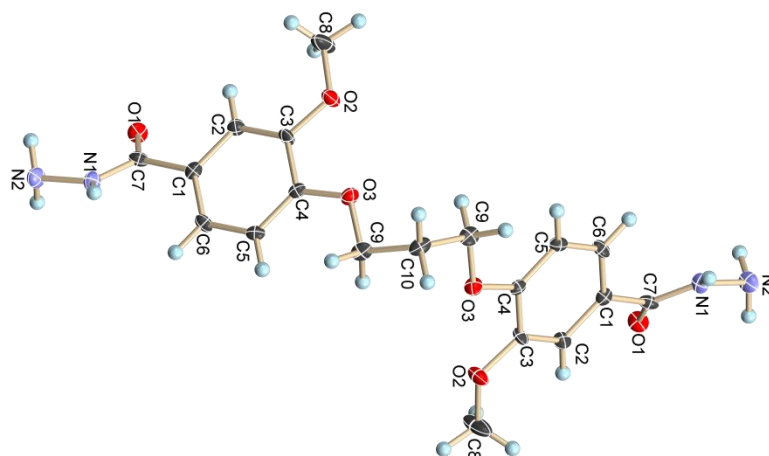


Figure 3.53 ORTEP diagram for 4,4'-(propane-1,3-diylbis(oxy))bis(3-methoxybenzohydrazide).

Table 3.2 X-Ray crystal data for 4,4'-(propane-1,3-diylbis(oxy))bis(3-methoxybenzohydrazide).

Empirical formula	C ₁₉ H ₂₄ N ₄ O ₆
Formula weight	404.42
Temperature	150(2) K
Wavelength	0.71073 Å
Crystal System	Orthorhombic
Space group	<i>Iba</i> 2
Unit cell dimensions	$a = 27.210(4)$ Å $\alpha = 90^\circ$
	$b = 7.8861(11)$ Å $\beta = 90^\circ$
	$c = 9.0700(15)$ Å $\gamma = 90^\circ$
Volume	1946.3(5) Å ³
Z	4
Density (calculated)	1.380 Mg/m ³
Absorption coefficient	0.104 mm ⁻¹
<i>F</i> (000)	856
Crystal size	0.43×0.31×0.25 mm ³
Theta range for data collection	2.69-24.98°
Absorption correction	Semi-empirical from equivalent
Max. and min. transmittance	0.9744 and 0.9566
Refinement method	Full-matrix least-squares on <i>F</i> ²
Data/restrains/parameters	1378/1/141
Goodness-of-fit on <i>F</i> ²	1.086
Final <i>R</i> indices [<i>I</i> >2σ(<i>I</i>)]	<i>RI</i> = 0.0599, <i>wRI</i> = 0.1032
<i>R</i> indices (all data)	<i>RI</i> = 0.0761, <i>wRI</i> = 0.1090
Largest diff. peak and hole	0.207 and -0.246 e. Å ⁻³

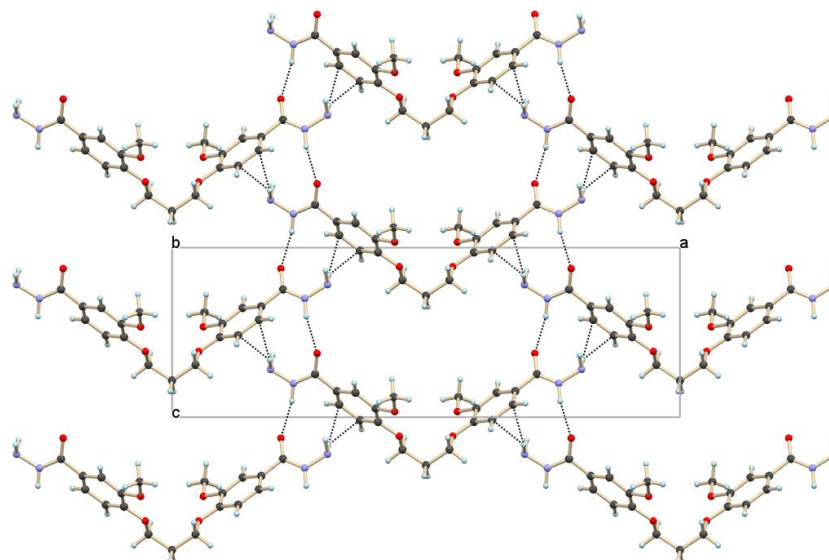
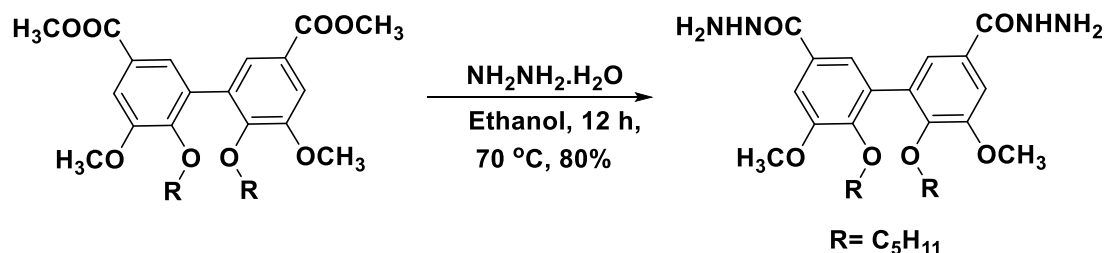


Figure 3.54 Molecular packing viewed down b-axis showing association of adjoining molecules through N-H \cdots O, N-H \cdots π and C-H \cdots O interactions.

3.4.4.2 Synthesis of diacyl hydrazide containing biphenylene linkage

Scheme 3.7 depicts synthesis of diacyl hydrazide containing biphenylene linkage.



Scheme 3.7 Synthesis of diacyl hydrazide containing biphenylene linkage

Dimethyl 5,5'-dimethoxy-6,6'-bis(pentyloxy)-[1,1'-biphenyl]-3,3'-dicarboxylate was reacted with hydrazine hydrate in ethanol at 70 °C. After completion of reaction, ethanol was evaporated under reduced pressure to afford biphenylene containing diacyl hydrazide, *viz.* 5,5'-dimethoxy-6,6'-bis(pentyloxy)-[1,1'-biphenyl]-3,3'-dicarbohydrazide. The monomer was purified by recrystallization from ethanol and was characterized by FT-IR, ^1H NMR, ^{13}C NMR spectroscopy and HRMS.

FT-IR spectrum of 5,5'-dimethoxy-6,6'-bis(pentyloxy)-[1,1'-biphenyl]-3,3'-dicarbohydrazide is shown in **Figure 3.55**. The absorption band at 3300 cm^{-1} is assigned to the -NH and -NH $_2$ group. The absorption band at 1630 cm^{-1} corresponds to carbonyl of the acid hydrazide group and disappearance of band for carbonyl of ester group confirmed the formation of diacyl hydrazide.

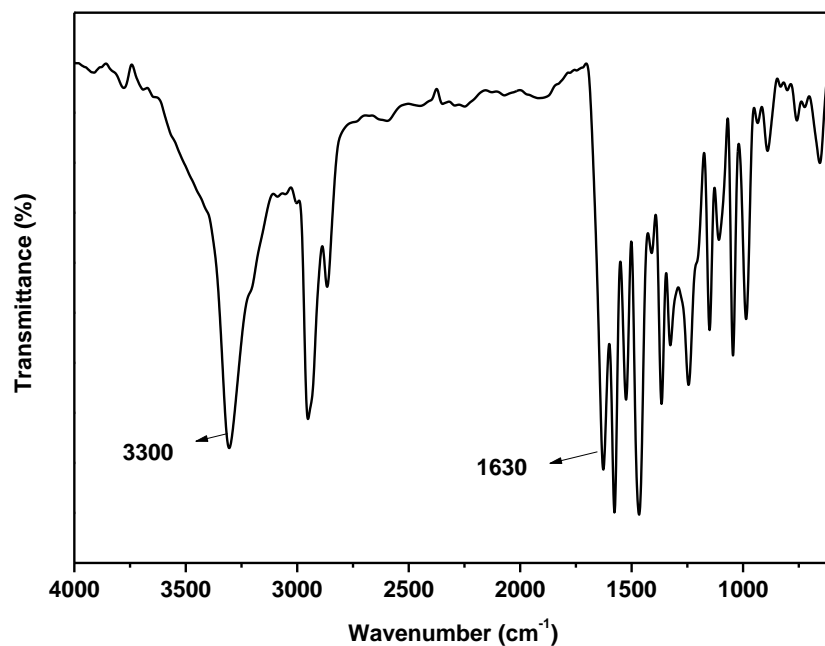


Figure 3.55 FT-IR spectrum of 5,5'-dimethoxy-6,6'-bis(pentyloxy)-[1,1'-biphenyl]-3,3'-dicarbohydrazide

^1H NMR spectrum of 5,5'-dimethoxy-6,6'-bis(pentyloxy)-[1,1'-biphenyl]-3,3'-dicarbohydrazide is reproduced in **Figure 3.56**.

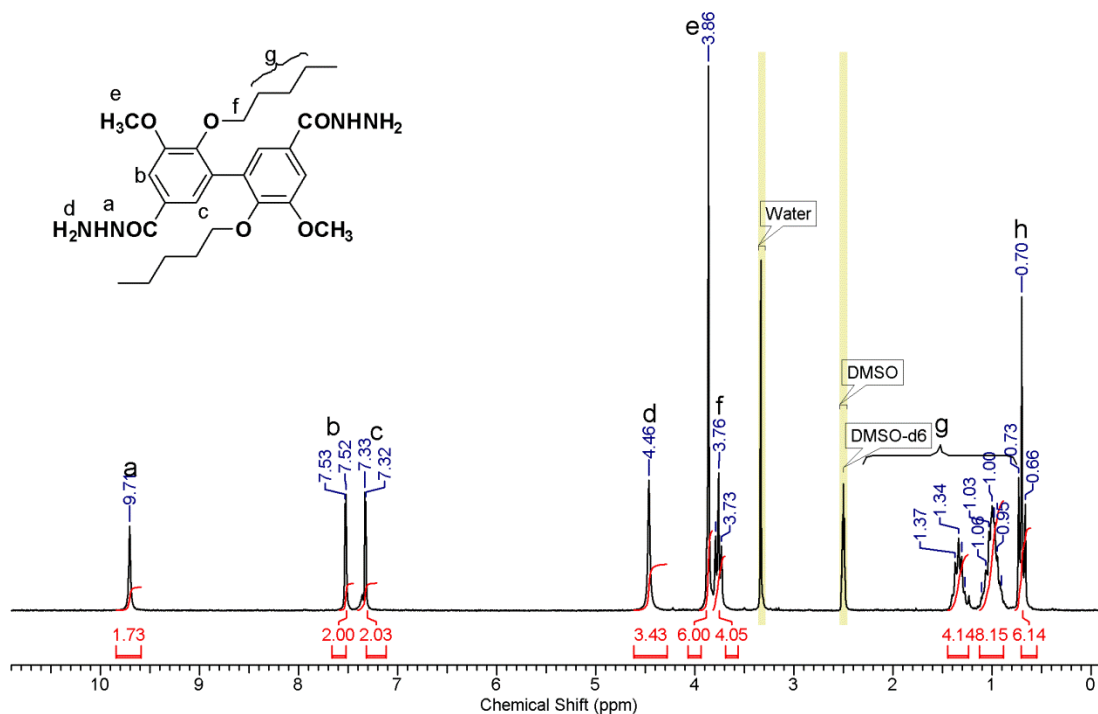
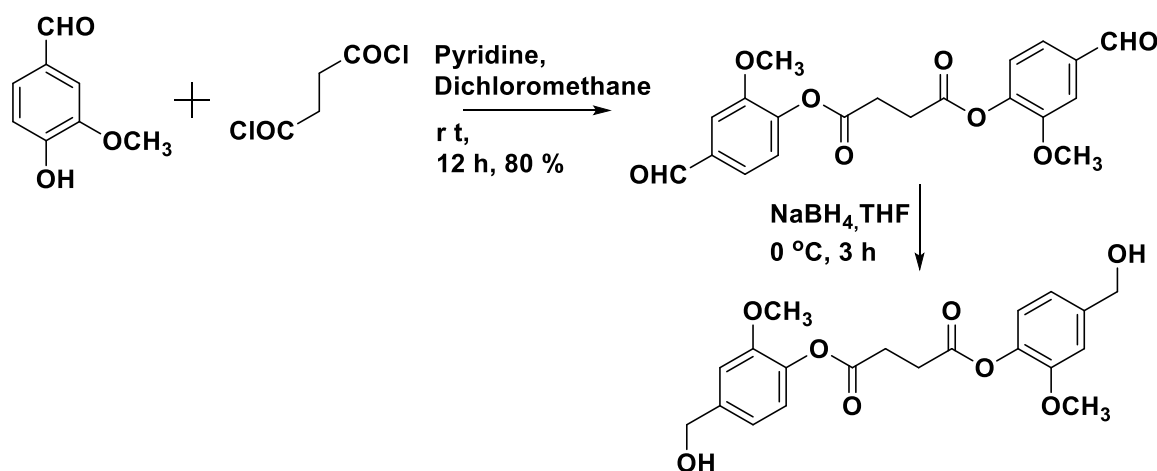


Figure 3.56 ^1H NMR spectrum of 5,5'-dimethoxy-6,6'-bis(pentyloxy)-[1,1'-biphenyl]-3,3'-dicarbohydrazide in DMSO-d_6

A singlet was observed at 9.71 δ ppm corresponding to the -NH- of acyl hydrazide group. The aromatic protons exhibited two doublets at 7.32 δ ppm and 7.52 δ ppm. A singlet at 4.46 δ ppm was observed due to -NH₂ protons of acid hydrazide group whereas methoxy proton exhibited a singlet at 3.86 δ ppm. The methylene protons of alkyl chain attached directly to oxygen atom appeared as a triplet at 3.76 δ ppm and methylene protons β to the oxygen atom appeared as a multiplet in the range 1.28-1.40 δ ppm. The remaining methylene protons of the alkyl chain exhibited a multiplet in the range 0.91-1.08 δ ppm and the terminal methyl group protons exhibited a triplet at 0.70 δ ppm.

3.4.5 Synthesis of dialdehyde containing ester linkages

Scheme 3.8 depicts route for the synthesis of dialdehyde containing ester linkage. Fully bio-based aromatic dialdehyde containing ester linkage was synthesized by condensation of vanillin with succinyl chloride in the presence of pyridine in dichloromethane at room temperature. After completion of reaction, reaction mixture was washed with water in order to remove pyridine hydrochloride. Dichloromethane was removed by distillation and product was purified by column chromatography.



Scheme 3.8 Synthesis of dialdehyde/diol containing ester linkages starting from vanillin

The synthesized ester containing dialdehyde was characterized by FT-IR, ¹H NMR, ¹³C NMR and HRMS.

FT-IR spectrum of bis(4-formyl-2-methoxyphenyl) succinate is shown in **Figure 3.57**. The characteristic absorption was observed at 2723 cm⁻¹ due to C-H

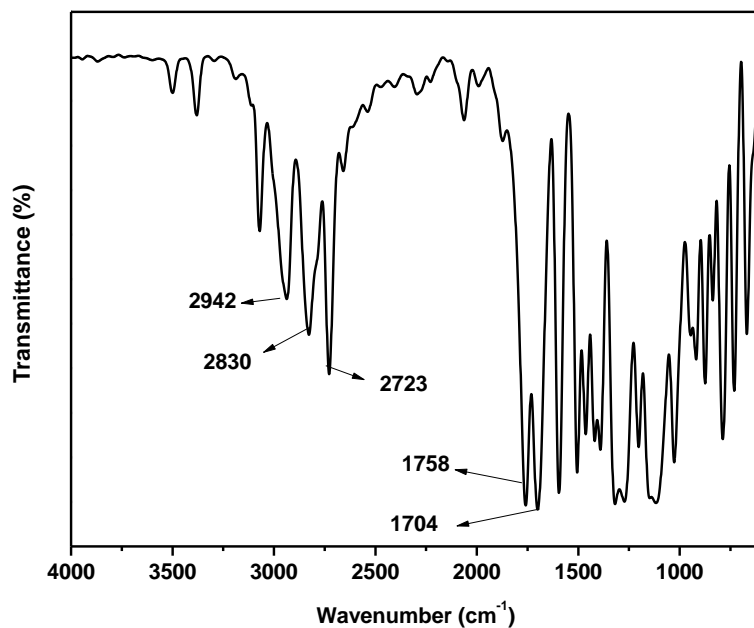


Figure 3.57 FT-IR spectrum of bis(4-formyl-2-methoxyphenyl) succinate

stretching of aldehyde group. The strong absorption band at 1758 cm^{-1} could be assigned to carbonyl of ester group while the absorption for carbonyl of aldehyde group appeared at 1704 cm^{-1} . ^1H NMR spectrum of bis(4-formyl-2-methoxyphenyl) succinate is reproduced in **Figure 3.58**.

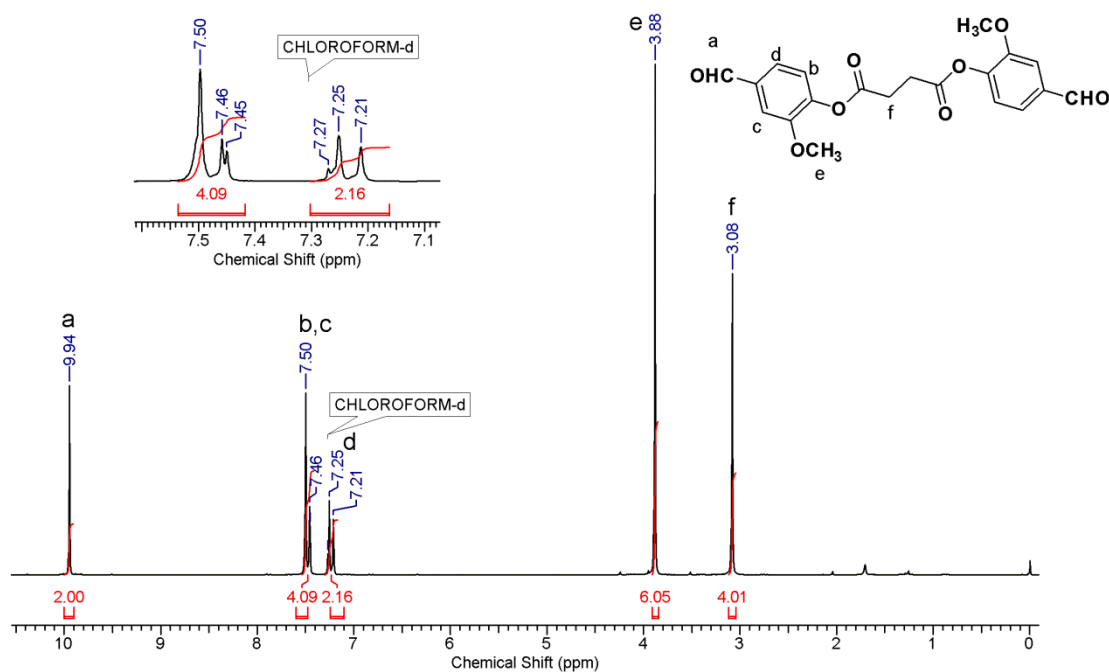


Figure 3.58 ^1H NMR spectrum of bis(4-formyl-2-methoxyphenyl) succinate in CDCl_3

A singlet was observed at 9.94 δ ppm which corresponds to aldehyde proton. The aromatic proton 'c' and 'b' appeared as a broad peak and a doublet at 7.50 δ and 7.46 δ ppm, respectively, whereas aromatic proton 'd' exhibited doublet at 7.23 δ ppm. The signal of methoxy protons was observed a singlet at 3.88 δ ppm and a singlet was observed at 3.08 δ ppm corresponds to the methylene protons. ^{13}C NMR spectrum of (bis(4-formyl-2-methoxyphenyl) succinate with individual carbon assignments is reproduced in **Figure 3.59**.

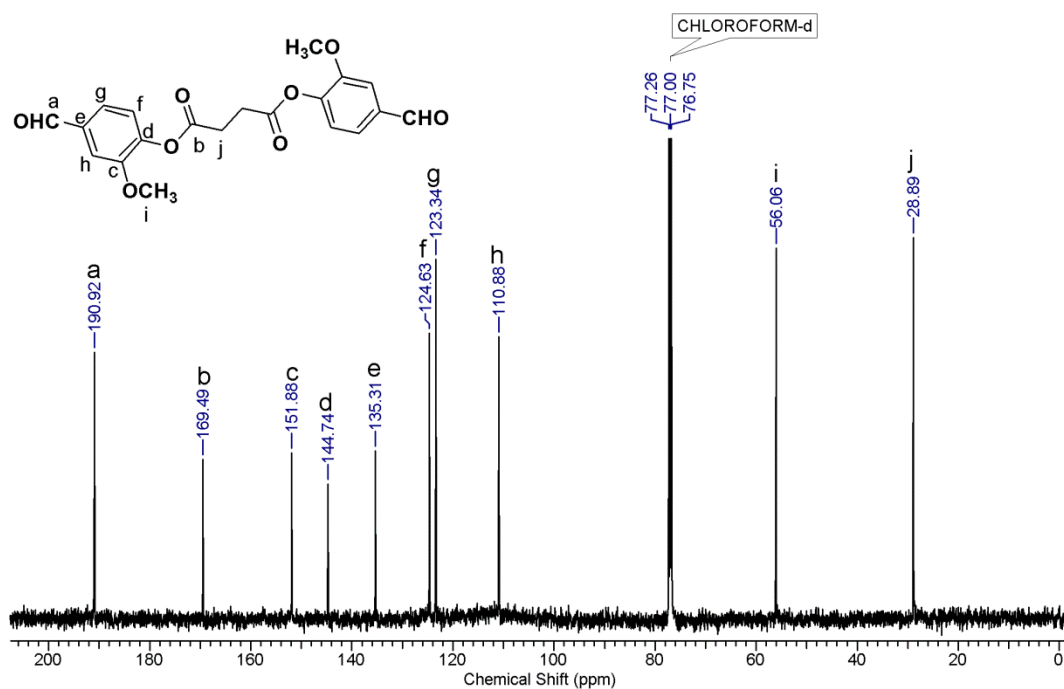


Figure 3.59 ^{13}C NMR spectrum of bis(4-formyl-2-methoxyphenyl) succinate in CHCl_3

3.4.6 Synthesis of diol containing ester linkages

Diol containing potentially 100 % renewable carbon, namely, bis(4-(hydroxymethyl)-3-methoxyphenyl) succinate was obtained by the reduction of bis(4-formyl-2-methoxyphenyl) succinate (Scheme 3.8). The reduction of bis(4-formyl-2-methoxyphenyl) succinate was carried out in tetrahydrofuran using sodium borohydride as the reducing agent. The structure of bis(4-(hydroxymethyl)-3-methoxyphenyl) succinate was confirmed by FT-IR, ^1H NMR and ^{13}C NMR spectroscopy.

FT-IR spectrum of (4-(hydroxymethyl)-3-methoxyphenyl) succinate is presented in **Figure 3.60**. The bands at 3533 and 1743 cm^{-1} correspond to hydroxyl group and ester carbonyl, respectively.

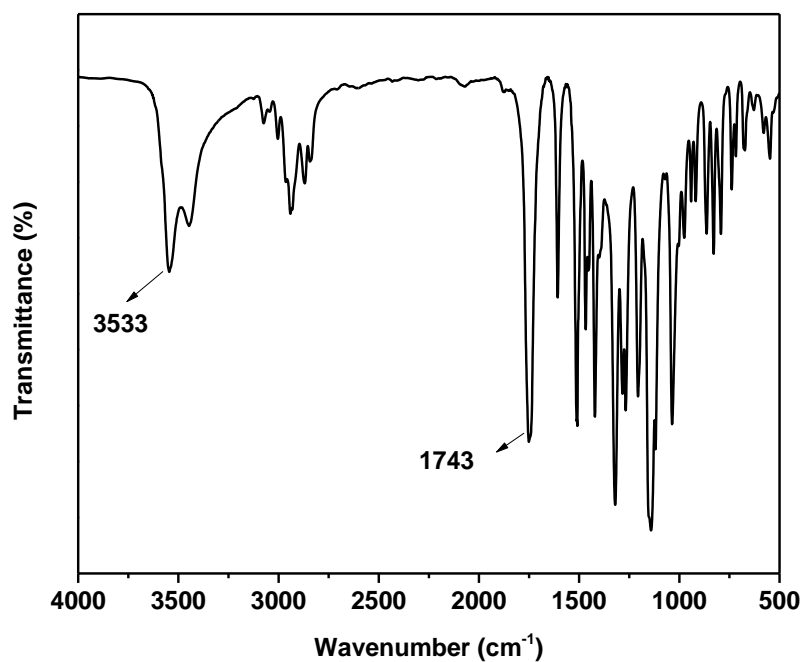


Figure 3.60 FT-IR spectrum of (4-(hydroxymethyl)-3-methoxyphenyl) succinate

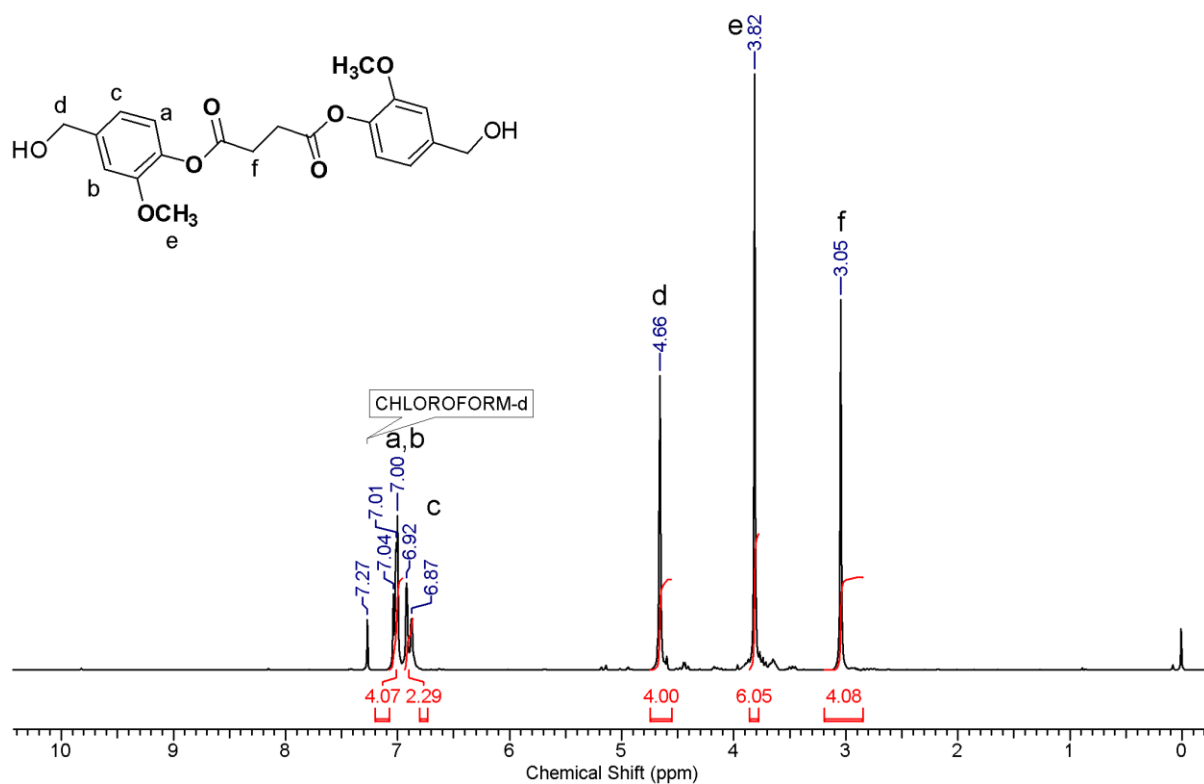
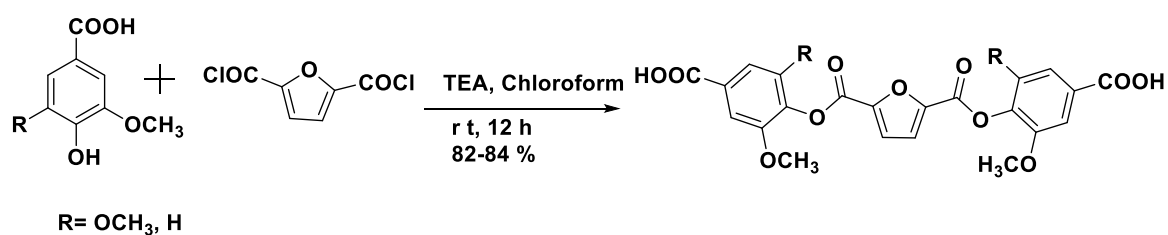


Figure 3.61 ¹H NMR spectrum of (4-(hydroxymethyl)-3-methoxyphenyl) succinate in CDCl₃

^1H NMR spectrum of (4-(hydroxymethyl)-3-methoxyphenyl) succinate is reproduced in **Figure 3.61**. ^1H NMR spectrum showed complete disappearance of aldehyde proton which was present in bis(4-formyl-2-methoxyphenyl) succinate (vide **Figure 3.58**). A new singlet was observed at 4.66 δ ppm due to the benzylic protons. Aromatic protons appeared in the range 6.87-7.04 δ ppm. The methoxy protons appeared as a singlet at 3.82 δ ppm whereas methylene protons exhibited a singlet at 3.05 δ ppm.

3.4.7 Synthesis of aromatic diacids containing ester linkage

Diacid monomers containing ester linkages namely, 4,4'-((furan-2,5-dicarbonyl)bis(oxy))bis(3-methoxybenzoic acid) and 4,4'-((furan-2,5-dicarbonyl)bis(oxy))bis(3,5-dimethoxybenzoic acid) were synthesized by condensation of vanillic/syringic acid with 2,5-furan dicarboxylic acid chloride (**Scheme 3.9**). The reaction was carried out in the presence of triethyl amine in chloroform at room temperature. The product was characterized by FT-IR, ^1H NMR, ^{13}C NMR spectroscopy and HRMS.



Scheme 3.9 Synthesis of diacids containing ester linkages starting from vanillic/syringic acid

FT-IR spectrum of 4,4'-((furan-2,5-dicarbonyl)bis(oxy))bis(3-methoxybenzoic acid) is shown in **Figure 3.62**. The broad absorption band was observed in the range 2500-3200 cm^{-1} due to the -COOH group. The absorption bands at 1780 cm^{-1} and 1706 cm^{-1} correspond to the carbonyl stretching of ester and acid group, respectively.

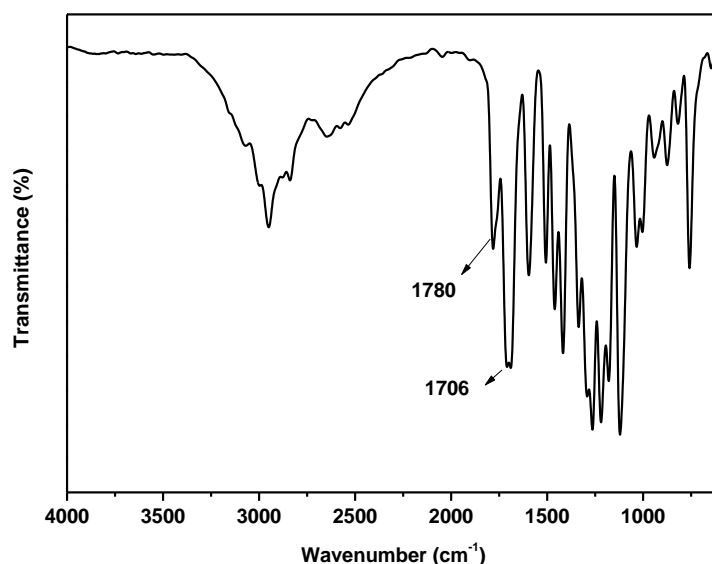


Figure 3.62 FT-IR spectrum of 4,4'-((furan-2,5-dicarbonyl)bis(oxy))bis(3-methoxybenzoic acid)

¹H NMR spectrum of 4,4'-((furan-2,5-dicarbonyl)bis(oxy))bis(3-methoxybenzoic acid) is displayed in **Figure 3.63**. A broad peak was observed at 13.18 δ ppm correspond to the acid protons. The furan protons 'b' exhibited a singlet at 7.81 δ ppm. The protons of aromatic ring *ortho* to acid group (proton 'c' and 'd') merged together and appeared in the range 7.67-7.69 δ ppm, while the protons of the aromatic ring *meta* to acid group exhibited a doublet at 7.44 δ ppm. The methoxy protons appeared as a singlet at 3.86 δ ppm. ¹³C NMR spectrum of 4,4'-((furan-2,5-dicarbonyl)bis(oxy))bis(3-methoxybenzoic acid) is shown in **Figure 3.64** along with the individual carbon assignments.

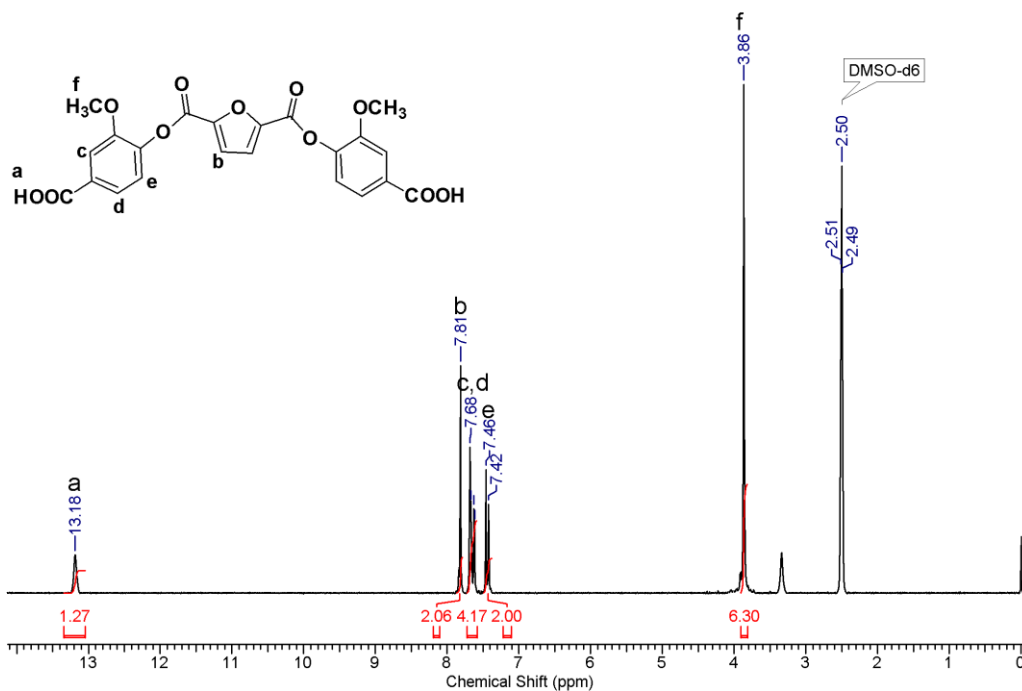


Figure 3.63 ^1H NMR spectrum of 4,4'-((furan-2,5-dicarbonyl)bis(oxy))bis(3-methoxybenzoic acid) in DMSO-d_6

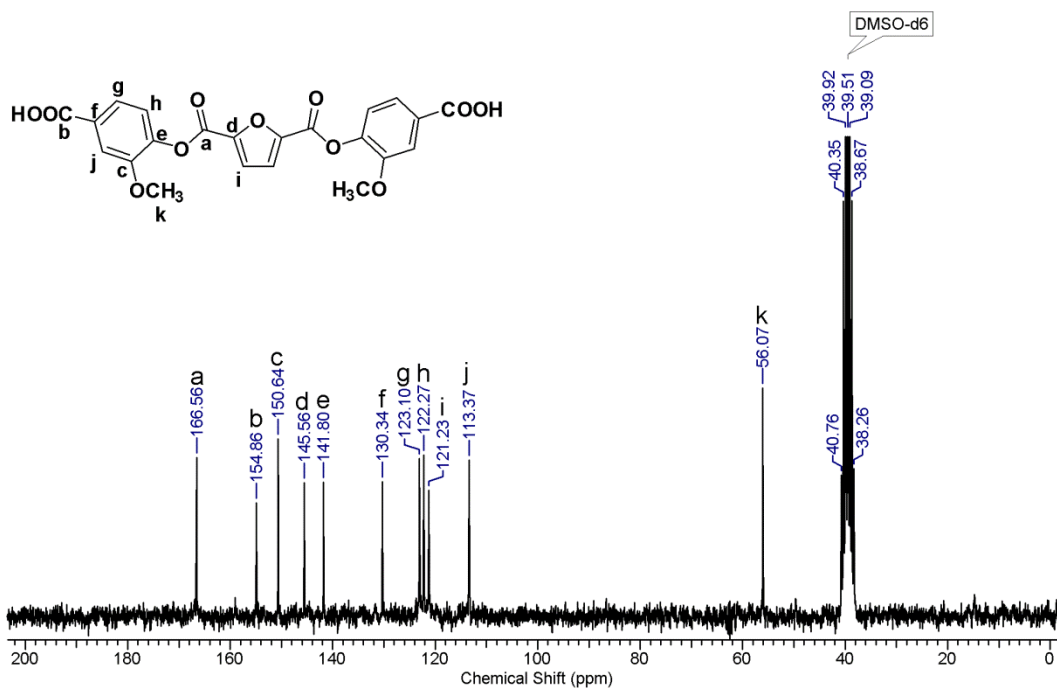


Figure 3.64 ^{13}C NMR spectrum of 4,4'-((furan-2,5-dicarbonyl)bis(oxy))bis(3-methoxybenzoic acid) in DMSO-d_6

3.5 Conclusions

- A series of new bio-based oxyalkylene linkage containing aromatic diisocyanates were synthesized from vanillic/syringic acids *via* the Curtius rearrangement.
- Two new biphenylene linkage containing aromatic diisocyanates namely, 5,5'-diisocyanato-2,2',3,3'-tetramethoxy-1,1'-biphenyl and 5,5'-diisocyanato-3,3'-dimethoxy-2,2'-bis(pentyloxy)-1,1'-biphenyl were synthesized from methyl vanillate.
- Four new A-B monomers namely, 4-((6-hydroxyhexyl)oxy)-3-methoxybenzoyl azide, 4-((6 hydroxyhexyl)oxy)-3,5-dimethoxybenzoyl azide, 4-((11-hydroxyundecyl)oxy)-3,5-dimethoxybenzoyl azide and 4-((11-hydroxyundecyl)oxy)-3-methoxy benzoyl azide were successfully synthesized starting from vanillic/syringic acid.
- Three new pendant furyl containing bisphenols were synthesized by condensation of guaiacol/syringol with furfural/methyl furfural.
- A new oxadiazole containing bisphenol *viz.* 4,4'-(1,3,4-oxadiazole-2,5-diyl)bis(2-methoxyphenol) was synthesized starting from vanillic acid.
- Two new oxyalkylene linkage containing aromatic diacyl hydrazide monomers namely, 4,4'-(propane-1,3-diylbis(oxy))bis(3-methoxybenzohydrazide) and 4,4'-(propane-1,3-diylbis(oxy))bis(3,5-dimethoxybenzohydrazide) were synthesized starting from methyl vanillate/methyl syringate.
- A new biphenylene linkages containing aromatic diacyl hydrazide monomer namely, 5,5'-dimethoxy-6,6'-bis(pentyloxy)-[1,1'-biphenyl]-3,3'-dicarbohydrazide was synthesized starting from methyl vanillate.
- New fully bio-based dialdehyde containing ester linkages *viz.* bis(4-formyl-2-methoxyphenyl) succinate was synthesized from vanillin and succinyl chloride.
- New diol containing ester linkage *viz.* bis(4-(hydroxymethyl)-3-methoxyphenyl) succinate was synthesized.
- Two new diacids containing ester linkages were synthesized from vanillic/syringic acid and 2,5-furan dicarboxylic acid chloride.

- All the monomers and intermediates were characterized by FT-IR and NMR spectroscopy and a few of them were further characterized by HRMS and single crystal X-ray diffraction analysis.
- Overall, the lignin-derived aromatics such as guaiacol, syringol, vanillic acid, syringic acid and vanillin, possess a great potential to serve as promising renewable resources for the synthesis of difunctional monomers *viz.* bisphenols, diols, dialdehyde, diacids, diacylhydrazide, and hydroxyl acyl azides.
- New difunctional monomers are potentially useful for the synthesis of step growth polymers.

References

- 1 A. David, D. J., Misra, *Relating materials properties to structure: Handbook and software for polymer calculations and materials properties*, Technomic Publishing Company, Inc., 1999.
- 2 J. Bicerano, *Prediction of Polymer Properties*, CRC Press, 2002.
- 3 C. W. Ulmer, D. A. Smith, B. G. Sumpter and D. I. Noid, *Comput. Theor. Polym. Sci.*, 1998, **8**, 311–321.
- 4 B. M. Pittman, Charles U, Culbertson, *New Monomers and Polymers*, Springer US, New York, 1st, 1984.
- 5 H. R. Kricheldorf, *Progress in Polyimide Chemistry I*, 1999.
- 6 M. Ghosh, *Polyimides: Fundamentals and Applications*, CRC Press, 1996.
- 7 A. Fuessl, M. Yamamoto and A. Schneller, in *Polymer Science: A Comprehensive Reference 2012*, **5**, 49–70.
- 8 R. Mülhaupt, *Macromol. Chem. Phys.*, 2013, **214**, 159–174.
- 9 R. Rajagopal, *Chem. Wkly.*, 2012, 195–200.
- 10 A. Llevot and M. A. R. Meier, *Green Chem.*, 2016, **18**, 4800–4803.
- 11 S. A. Madbouly, Z. Chaoqum and K. R. Michael, *Bio-Based Plant Oil Polymers and Composites*, Deans, M, Amstradam, 2016.
- 12 J. C. Philp, R. J. Ritchie and J. E. M. Allan, *Trends Biotechnol.*, 2004, **31**, 219–222.
- 13 L. Shen, E. Worrell and M. Patel, *Biofuels, Bioprod. Biorefining*, 2010, **4**, 25–

- 40.
- 14 P. F. H. Harmsen, M. M. Hackmann and H. L. Bos, *Biofuels, Bioprod. Biorefining*, 2014, **8**, 306–324.
- 15 M. N. Belgacem and A. Gandini, in *Monomers, Polymers and Composites from Renewable Resources*, eds. M. Belgacem and A. Gandini, Amstradam, Elsevier, 2008, pp. 39–66.
- 16 L. Montero De Espinosa and M. A. R. Meier, *Eur. Polym. J.*, 2011, **47**, 837–852.
- 17 <https://www.cardolite.com/>, .
- 18 <http://www.specificpolymers.fr/>, .
- 19 <https://www.avantium.com/yxy/products-applications/>, .
- 20 C. Voirin, S. Caillol, N. V. Sadavarte, B. V. Tawade, B. Boutevin and P. P. Wadgaonkar, *Polym. Chem.*, 2014, **5**, 3142–3162.
- 21 A. Llevot, E. Grau, S. Carlotti, S. Grelier and H. Cramail, *Macromol. Rapid Commun.*, 2016, **37**, 9–28.
- 22 M. Fache, E. Darroman, V. Besse, R. Auvergne, S. Caillol and B. Boutevin, *Green Chem.*, 2014, **16**, 1987.
- 23 A. Gandini and T. M. Lacerda, *Prog. Polym. Sci.*, 2015, **48**, 1–39.
- 24 A. Kumar, S. Tateyama, K. Yasaki, M. A. Ali, N. Takaya, R. Singh and T. Kaneko, *Polym. J.*, 2016, **83**, 182–189.
- 25 N. V. Sadavarte, C. V. Avadhani, P. V. Naik and P. P. Wadgaonkar, *Eur. Polym. J.*, 2010, **46**, 1307–1315.
- 26 D. Chatterjee, N. V. Sadavarte, R. D. Shingte, A. S. More, B. V. Tawade, A. D. Kulkarni, A. B. Ichake, C. V. Avadhani and P. P. Wadgaonkar, in *Cashew Nut Shell Liquid*, ed. Parambath Anilkumar, Springer International Publishing, Cham, 1st edn., 2017, pp. 163–214.
- 27 F. Pion, P.-H. Ducrot and F. Allais, *Macromol. Chem. Phys.*, 2014, **215**, 431–439.
- 28 I. A. Pearl and J. F. McCoy, *J. Am. Chem. Soc.*, 1947, **69**, 3071–3072.
- 29 T. Nakano, S. Terao and K. H. Lee, *J. Pharm. Sci.*, 1965, **54**, 1201–1203.
- 30 K. Kürschner and P. Stroehriegl, *Liq. Cryst.*, 2000, **27**, 1595–1611.
- 31 J. L. Cawse, J. L. Stanford and R. H. Still, *Die Makromol. Chemie*, 1984, **185**, 697–707.
- 32 C. N. D. Neumann, W. D. Bulach, M. Rehahn and R. Klein, *Macromol. Rapid*

- Commun.*, 2011, **32**, 1373–1378.
- 33 M. C. Davis, J. E. P. Dahl and R. M. K. Carlson, *Synth. Commun.*, 2008, **38**, 1153–1158.
- 34 Y. C. Charalambides and S. C. Moratti, *Synth. Commun.*, 2007, **37**, 1037–1044.
- 35 A. C. Chaskar, S. Yewale, R. Bhagat and B. P. Langi, *Synth. Commun.*, 2008, **38**, 1972–1975.
- 36 L. Maisonneuve, O. Lamarzelle, E. Rix, E. Grau and H. Cramail, *Chem. Rev.*, 2015, **115**, 12407–12439.
- 37 W. Lwowski, in *Azides and Nitrenes*, ed. E. Scriven, Elsevier B.V., 1984.
- 38 E. Laszlo, Pierre, Polla, *Tetrahedron Lett.*, 1984, **25**, 3701–3704.
- 39 J. M. Lago, A. Arrieta and C. Palomo, *Synth. Commun.* 1983, **13**, 289–296.
- 40 V. K. Gumaste, B. M. Bhawal and R. S. Deshmukh, *Tetrahedron Lett.*, 2002, **43**, 1345–1346.
- 41 R. H. Tale and K. M. Patil, *Tetrahedron Lett.*, 2002, **43**, 9715–9716.
- 42 R. Guo and J. E. McGrath, *Aromatic Polyethers, Polyetherketones, Polysulfides, and Polysulfones*, Elsevier B.V., 2012
- 43 A. Maiorana, A. F. Reano, R. Centore, M. Grimaldi, P. Balaguer, F. Allais and R. A. Gross, *Green Chem.*, 2016, **18**, 4961–4973.
- 44 S. F. Koelewijn, S. Van den Bosch, T. Renders, W. Schutyser, B. Lagrain, M. Smet, J. Thomas, W. Dehaen, P. Van Puyvelde, H. Witters and B. F. Sels, *Green Chem.*, 2017, **19**, 2561–2570.
- 45 A. V. Krishnan, P. Stathis, S. F. Permuth, L. Tokes and D. Feldman, *Endocrinology*, 1993, **132**, 2279.
- 46 J. A. Brotons, M. F. Olea-Serrano, M. Villalobos, V. Pedraza and N. Olea, *Environ. Health Perspect.*, 1995, **103**, 608.
- 47 H. A. Meylemans, B. G. Harvey, J. T. Reams, A. J. Guenther, L. R. Cambrea, T. J. Groshens, L. C. Baldwin, M. D. Garrison and J. M. Mabry, *Biomacromolecules*, 2013, **14**, 771–780.
- 48 H. A. Meylemans, T. J. Groshens and B. G. Harvey, *ChemSusChem*, 2012, **5**, 206–210.
- 49 B. G. Harvey, A. J. Guenther, H. A. Meylemans, S. R. L. Haines, K. R. Lamison, T. J. Groshens, L. R. Cambrea, M. C. Davis and W. W. Lai, *Green Chem.*, 2015, **17**, 1249–1258.
- 50 B. G. Harvey, A. J. Guenther, T. A. Koontz, P. J. Storch, J. T. Reams and T. J.

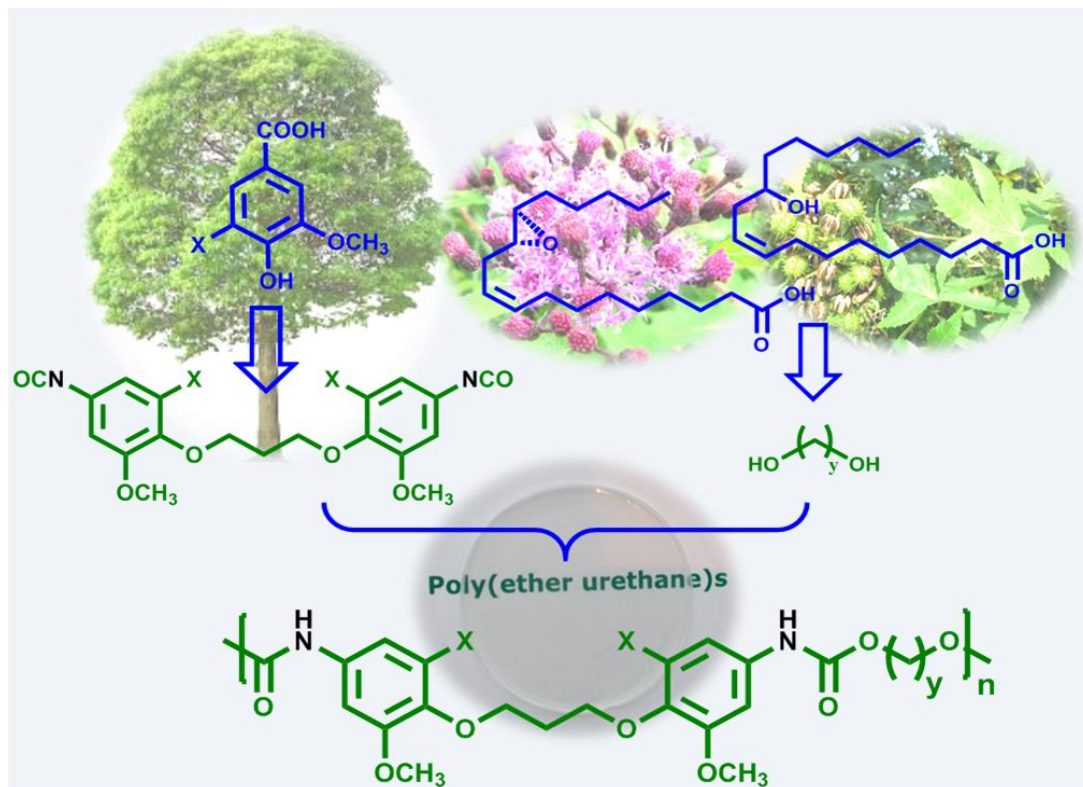
- Groshens, *Green Chem.*, 2016, **18**, 2416–2423.
- 51 G. D. Bittner, M. S. Denison, C. Z. Yang, M. A. Stoner and G. He, *Environ. Heal.*, 2014, **13**, 103.
- 52 S. G. Shetty, J. H. Kamps, G. Chandra, A. Tanwar, Methods for determining relative binding energy of monomers and methods of using the same, US2015338423A1, 2015.

Chapter - 4

Bio-Based Poly(ether urethane)s

Chapter - 4a

Poly(ether urethane)s from Aromatic Diisocyanates Based on Lignin-Derived Phenolic Acids



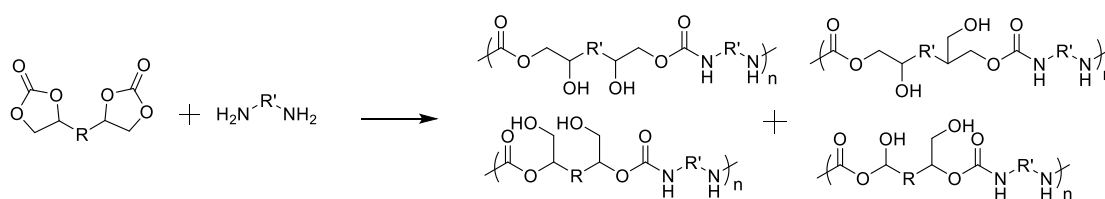
4a.1 Introduction

Polyurethanes are of great interest due to their multitude of industrial applications such as thermoplastic elastomers, foams, fibers, coatings, adhesives, sealants, etc¹⁻⁶(**Figure 4a.1**). The properties of polyurethanes could be tailored by appropriate choice of the starting materials *viz.* diols/polyols, di-/poly-isocyanates and chain extenders⁷⁻⁹. These starting materials are mostly derived from petroleum oil which is a non-renewable resource¹. It has been recognized that the long term dependence on petroleum oil as a source of monomers for polymer synthesis is at risk¹⁰⁻¹⁴.

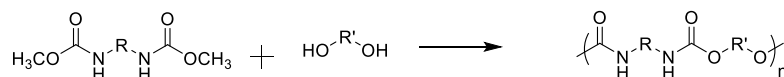


Figure 4a.1 Applications of polyurethanes

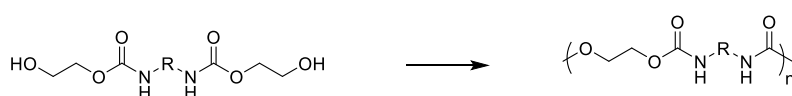
The current research efforts in the field of polyurethane preparation are focused on the following two themes: a) synthesis of key starting materials *viz* diols/polyols and diisocyanates starting from bio-based chemicals¹⁵⁻¹⁶ and b) development of non-isocyanate routes involving polymerization of bis-cyclic carbonates with diamines^{17,18} polycondensation of bis-carbamates with diols and self-condensation of bis-hydroxyalkylcarbamates^{19,20}(**Figure 4a.2**).



Synthesis of polyurethane from cyclic carbonate and diamine



Synthesis of polyurethane from bis-carbamate and diol



Synthesis of polyurethane by self-condensation of bis-hydroxyalkylcarbamate

Figure 4a.2 Reported synthetic strategies to polyurethanes *via* non-isocyanate routes.

A large number of bio-based polyols based on vegetable oils, sugars, etc.^{21–25} have already been developed as potential substitutes for their petroleum-based counterparts. Similarly, bio-derived diol chain extenders such as 1,3-propanediol, 1,6-hexanediol, isosorbide and so on have been made use of in synthesis of polyurethanes^{21,26,27}.

A range of aliphatic diisocyanates have been synthesized starting from renewable resource-based chemicals such as fatty acids²⁸, L-lysine^{29,30} furfural¹⁹, hydroxymethyl furfural³¹ and isosorbide³². However, the reports on synthesis of aromatic diisocyanates based on bio-derived chemicals are scanty expect for furan derivatives *viz.* 2,5-diisocyanatofuran, bis(5-isocyanatofurfuryl)ether and diisocyanates containing difurylalkane moieties^{31,33}.

We have reported in **Chapter 3** a general synthetic route to bio-based aromatic diisocyanates. It was considered of interest to study the utility of these diisocyanates for the synthesis of polyurethanes

In the present work, four new fully bio-based poly(ether urethane)s were synthesized by polymerization of newly synthesized aromatic diisocyanates namely 1,3-bis(4-isocyanato-2-methoxyphenoxy)propane and 1,3-bis(4-isocyanato-2,6-dimethoxyphenoxy)propane with potentially bio-based aliphatic diols, namely, 1, 10-decanediol and 1, 12-dodecanediol. Poly(ether urethane)s were characterized by inherent

viscosity measurements, solubility tests, FT-IR, ^1H NMR and ^{13}C NMR spectroscopy, X-ray diffraction, thermogravimetric analysis (TGA) and differential scanning calorimetric studies (DSC). The effects of number of methylene units in the backbone and methoxy substituents on aromatic rings on thermal properties of poly(ether urethane)s were investigated.

4a.2 Experimental

4a.2.1 Materials

Dibutyltin dilaurate (DBTDL) was purchased from Sigma–Aldrich and was used as received. Toluene, dichloromethane, chloroform, tetrahydrofuran (THF), *N,N*-dimethylformamide (DMF), *N,N*-dimethylacetamide (DMAc), *N*-methyl-2-pyrrolidone (NMP) and dimethyl sulfoxide (DMSO) were received from Thomas Baker Ltd, Mumbai. Toluene was dried over calcium hydride and distilled prior to use.

4a.2.2 Measurements

Inherent viscosity of poly(ether urethane)s was determined with 0.5 % (w/v) solution of polymer in chloroform at $30\pm 0.1^\circ\text{C}$ using Ubbelohde suspended level viscometer. Inherent viscosity was calculated using the equation

$$n_{inh} = \frac{2.303}{c} \times \log t/t_0$$

Where, t and t_0 are flow times of polymer solution and solvent, respectively and c is the concentration of polymer solution

Molecular weights and dispersity values of poly(ether urethane)s were determined on Thermo-Finnigan make gel-permeation chromatography (GPC) using chloroform as an eluent at a flow rate of 1 mL min^{-1} at 25°C . Sample concentration was 2 mg mL^{-1} and narrow dispersity polystyrenes were used as calibration standards.

FT-IR spectra were obtained on a Perkin–Elmer Spectrum GX spectrometer using polymer film.

NMR spectra were recorded on a Bruker 200, 400 or 500 MHz spectrometer at resonance frequencies of 200, 400 or 500 MHz for ^1H NMR and 50, 100 or 125 MHz for ^{13}C NMR measurements using CDCl_3 as a solvent.

Thermogravimetric analysis (TGA) was carried out on Perkin Elmer: STA 6000, at a heating rate of $10^\circ\text{C min}^{-1}$ under nitrogen atmosphere.

Differential scanning calorimetric (DSC) analysis was performed using DSC Q10 differential calorimeter from TA Instruments under nitrogen atmosphere (50 mL min^{-1}).

Analyses were carried out in a temperature range between 30 and 250 °C using a heating rate of 10 °C min⁻¹.

4a.2 .3 General procedure for synthesis of poly(ether urethane)s

Into a 100 mL two-necked round bottom flask equipped with a reflux condenser and a nitrogen inlet were charged, α,ω -diisocyanate (4.69 mmol), aliphatic diol (4.69 mmol), DBTDL (3×10^{-3} mmol) and dry toluene (25 mL). The reaction mixture was heated at 80 °C for 8 h. The toluene was removed under reduced pressure at 60 °C and solid polymer was obtained. The polymer was dissolved in chloroform, precipitated in methanol, filtered and dried in vacuum oven at 40 °C for 12 h.

Synthesis of poly(ether urethane) (PU-1) based on 1,3-bis(4-isocyanato-2-methoxyphenoxy)propane and 1,10-decanediol

IR (KBr): 3328, 1733, 1700 cm⁻¹; ¹H NMR (200 MHz, DMSO-*d*₆, δ /ppm): 1.18-1.30 (m, 12H), 1.52-1.62 (m, 4 H), 1.9-2.13 (m, 2H), 3.69 (s, 6H), 4.03 (t, 8H), 6.84-6.95 (m, 4H), 7.17 (d, 2H), 9.37 (s, 2H); ¹³C NMR (50 MHz, DMSO-*d*₆, δ /ppm): 25.3, 28.7, 28.9, 55.4, 64.0, 65.6, 103.9, 110.2, 114.2, 133.1, 143.3, 149.1, 153.6.

Synthesis of poly(ether urethane) (PU-2) based on 1,3-bis(4-isocyanato-2-methoxyphenoxy)propane and 1,12-dodecanediol

IR (KBr): 3331, 1732, 1709 cm⁻¹; ¹H NMR (200 MHz, DMSO-*d*₆, δ /ppm): 1.20-1.58 (m, 20H), 2.0-2.10 (m, 2H), 3.68 (s, 6H), 4.02 (t, 8H), 6.84-6.93 (m, 4H), 7.16 (d 2H), 9.37 (s, 2H); ¹³C NMR (100 MHz, DMSO-*d*₆, δ /ppm): 25.4, 28.7, 29.0, 55.4, 64.0, 65.6, 103.8, 110.1, 114.2, 133.1, 143.3, 149.1, 153.7.

Synthesis of poly(ether urethane) (PU-3) based on 1,3-bis(4-isocyanato-2,6-dimethoxyphenoxy)propane and 1,10-decanediol

IR (KBr): 3335, 1730, 1705 cm⁻¹; ¹H NMR (500 MHz, DMSO-*d*₆, δ /ppm): 1.25-1.33 (m, 12H), 1.56-1.61 (m, 4H), 1.86-1.91 (m, 2H), 3.67 (s, 12H), 3.93 (t, 4H), 4.04 (t, 4H), 6.82 (s, 4H), 9.45 (s, 2H); ¹³C NMR (125 MHz, DMSO-*d*₆, δ /ppm): 25.4, 28.5, 28.7, 28.9, 30.4, 55.6, 64.1, 69.9, 96.0, 131.8, 135.2, 152.9, 153.6.

Synthesis of poly(ether urethane) (PU-4) based on 1,3-bis(4-isocyanato-2,6-dimethoxyphenoxy)propane and 1,12-dodecanediol

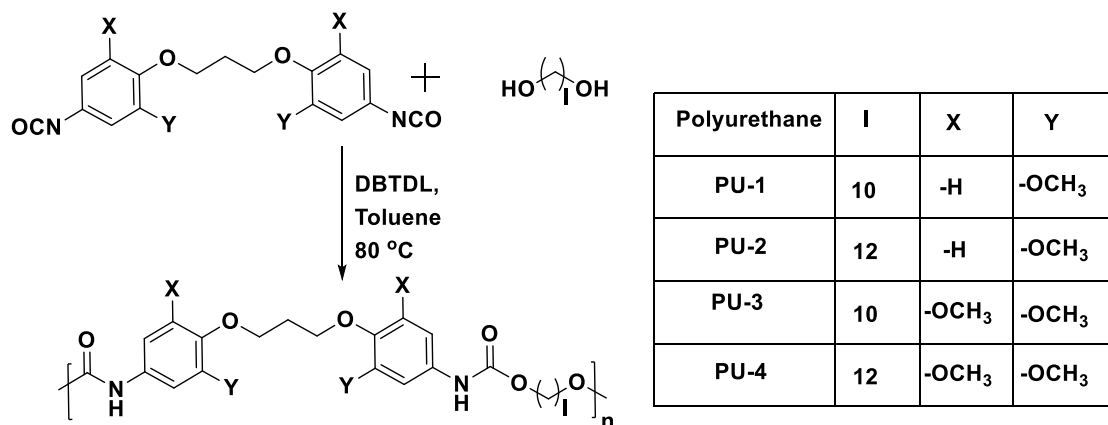
IR (KBr): 3332, 1731, 1705 cm⁻¹; ¹H NMR (400 MHz, DMSO-*d*₆, δ /ppm): 9.44 (s, 2H), 6.82 (s, 4H), 4.03 (t, 4H), 3.93 (t, 4H), 3.67 (s, 12H), 1.86-1.90 (m, 2H), 1.54-1.60 (m,

4H), 1.21-1.29 (m, 18H); ^{13}C NMR (100 MHz, $\text{DMSO-}d_6$, δ/ppm):25.4, 28.6, 28.7, 29.0, 30.4, 55.6, 64.1, 69.9, 96.0, 131.7, 135.2, 152.9, 153.6.

4a.3 Results and discussion

4a.3.1 Poly(ether urethane) synthesis

Four new poly(ether urethane)s were synthesized by polymerization of bio-based aromatic diisocyanates containing ether linkage viz. 1,3-bis(4-isocyanato-2-methoxyphenoxy)propane and 1,3-bis(4-isocyanato-2,6-dimethoxyphenoxy)propane with bio-based aliphatic diols viz. 1, 10-decanediol and 1, 12-dodecanediol. The polymerization reactions were carried out by using stoichiometric quantities of α,ω -diisocyanates and aliphatic diols in dry toluene at 80 °C in the presence of DBTDL as the catalyst (**Scheme 4a.1**).



Scheme 4a.1 Synthesis of poly(ether urethane)s based on 1,3-bis(4-isocyanato-2-methoxyphenoxy)propane/1,3-bis(4-isocyanato-2,6-dimethoxyphenoxy)propane and aliphatic diols.

The results of polymerization reactions are given in **Table 4a.1**. It is worth mentioning that the 100 % carbon content in poly(ether urethane)s comes from potentially bio-renewable resources. Poly(ether urethane)s exhibited inherent viscosities in the range 0.58–0.68 dLg^{-1} . Number average molecular weights (\overline{M}_n) and dispersity values of poly(ether urethane)s, determined by GPC, were in the range 32,100–58,500 g mol^{-1} and 1.6–1.9, respectively. These data indicated the formation of reasonably high molecular weight polymers. Transparent and flexible films could be cast from the chloroform solutions of poly(ether urethane)s.

Table 4a.1 Data on inherent viscosity, and molecular weight of poly(ether urethane)s.

Poly(ether urethane)	η_{inh} (dL/g) ^a	GPC ^b		
		\overline{M}_n	\overline{M}_w	Dispersity
PU-1	0.60	36,100	62,500	1.7
PU-2	0.65	45,500	88,200	1.9
PU-3	0.58	32,100	51,800	1.6
PU-4	0.68	58,500	1,00300	1.7

a; η_{inh} was measured with 0.5% (w/v) solution of poly(ether urethane) in chloroform at 30 ± 0.1 °C

b; measured by GPC in chloroform, polystyrene was used as the calibration standard

4a.3.2 Structural characterization

The chemical structures of poly(ether urethane)s were confirmed by FT-IR, ¹H NMR and ¹³C NMR spectroscopy. A representative FT-IR spectrum of PU-4 is given in **Figure 4a.3**, which showed complete disappearance of isocyanato band and a new absorbance band appeared at 3332 cm^{-1} corresponding to -NH- stretching indicating the formation of urethane linkages. The two resolved bands at 1705 cm^{-1} and 1731 cm^{-1} could be attributed to hydrogen bonded and non-hydrogen bonded carbonyl stretching of urethane group.

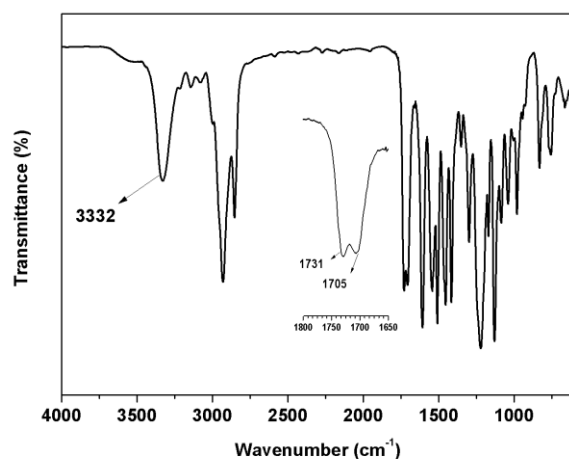


Figure 4a.3 FT-IR spectrum of poly(ether urethane) (PU-4) derived from 1,3-bis(4-isocyanato-2,6-dimethoxyphenoxy)propane and 1,12-dodecanediol.

¹H NMR spectrum of PU-4 is displayed in **Figure 4a.4**. A singlet was observed at $9.45\ \delta$ ppm for -NH- proton 'a' and aromatic proton 'b' exhibited a singlet at $6.82\ \delta$ ppm. The methylene protons 'c' attached to ether linkage appeared as a triplet at $4.04\ \delta$ ppm

and methylene protons 'd' attached to urethane linkage exhibited a triplet at 3.93 δ ppm. The methoxy group protons 'e' displayed a singlet at 3.67 δ ppm and remaining methylene protons appeared as a multiplet in the range 1.20-1.90 δ ppm. ^{13}C NMR spectrum of PU-4 along with assignments of carbon atoms is shown in **Figure 4a.5**. The spectral data indicated that aromatic diisocyanates successfully reacted with aliphatic diols and formed poly(ether urethane)s.

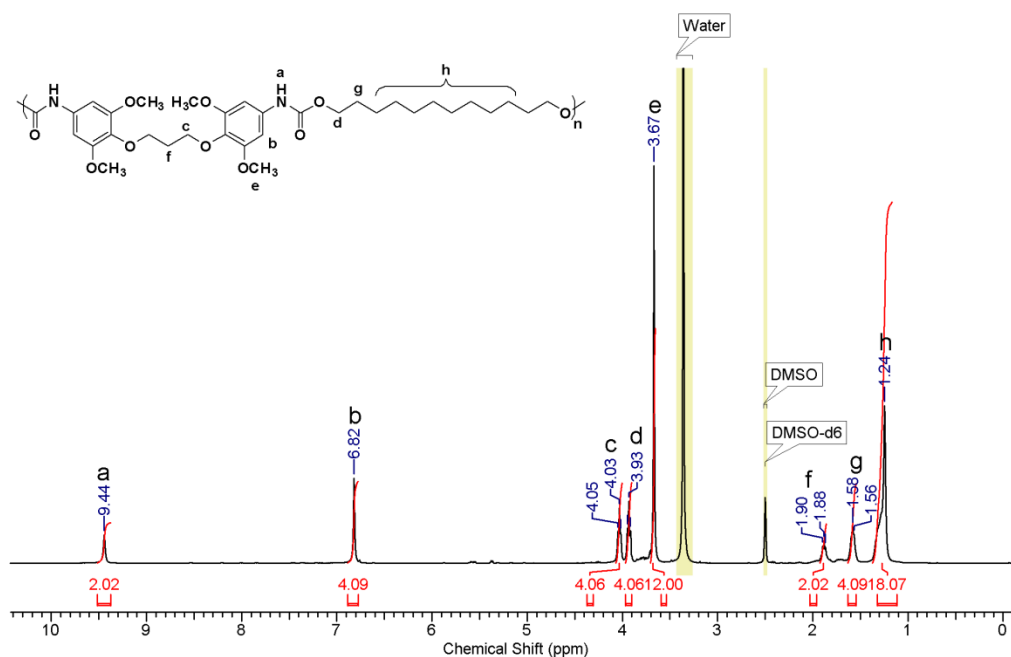


Figure 4a.4 ^1H NMR spectrum (in $\text{DMSO-}d_6$) of poly(ether urethane) (PU-4) derived from 1,3-bis(4-isocyanato-2,6-dimethoxyphenoxy)propane and 1,12-dodecanediol.

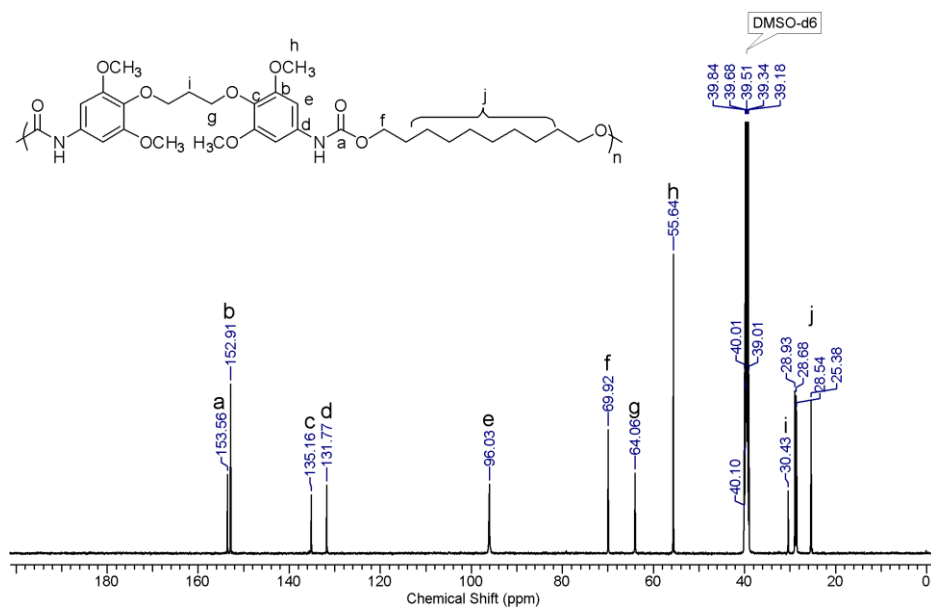


Figure 4a.5 ^{13}C NMR spectrum (in $\text{DMSO-}d_6$) of poly(ether urethane) (PU-4) derived from 1,3-bis(4-isocyanato-2,6-dimethoxyphenoxy)propane and 1,12-dodecanediol.

4a.3.3 Solubility

The solubility of poly(ether urethane)s was examined in various organic solvents at a concentration of 3 % (w/v). Poly(ether urethane)s dissolved readily at room temperature in solvents such as chloroform, dichloromethane, THF, DMAc, DMF, NMP and DMSO.

4a.3.4 Thermal properties

The thermal stability of poly(ether urethane)s was determined by thermogravimetric analysis (TGA). TG curves and 10 % decomposition temperature (T_{10}) are displayed in **Figure 4a.6** and **Table 4a.2**, respectively. T_{10} values of poly(ether urethane)s were observed in the narrow range 304 °C-308 °C. T_{10} values were not influenced by the structural changes in the studied diols and diisocyanates indicating that thermal stability was governed by stability of urethane linkages in poly(ether urethane)s.

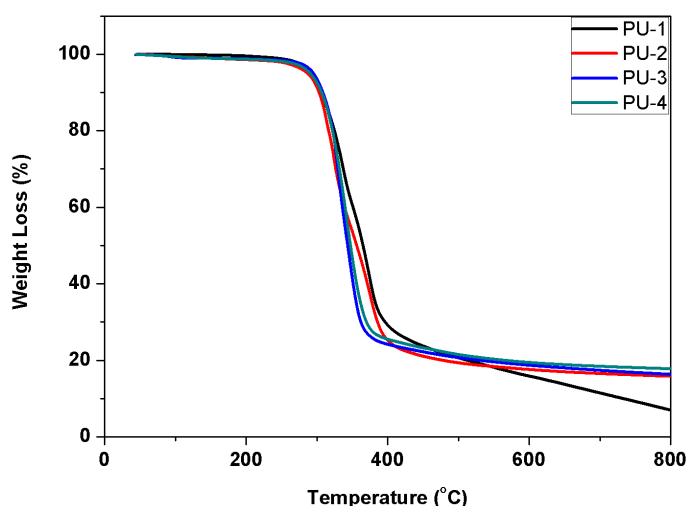


Figure 4a.6 TG curves of poly(ether urethane)s.

Table 4a.2 Thermal properties of poly(ether urethane)s.

Poly(ether urethane)	PU-1	PU-2	PU-3	PU-4
T_g (°C) ^c	55	49	74	66
T_{10} (°C) ^d	304	304	308	306

a; Measured by DSC on second heating scan with heating rate at 10 °C min⁻¹ under nitrogen atmosphere

b; Temperature at which 10% weight loss was observed in TGA under nitrogen atmosphere.

T_g of poly(ether urethane)s, determined by DSC (**Figure 4a.7**, **Table 4a.2**), were in the range 49-74 °C and the values were found to be dependent on the structure of diols

and diisocyanates. The higher T_g values were observed for poly(ether urethane)s PU-1 and PU-3 prepared from 1,10-decanediol than the corresponding poly(ether urethane)s PU-2 and PU-4 prepared from 1, 12-dodecanediol. This was attributed to the higher number of methylene units and reduction in the density of aromatic rings which results in increase in chain flexibility and consequently decrease in the value of T_g . The increased T_g values of poly(ether urethane)s PU-3 and PU-4 than the corresponding poly(ether urethane)s PU-1 and PU-2 could be explained on the basis of higher chain rigidity of the former due to the presence of higher number of methoxy groups which increase the conformational barrier to chain rotation.

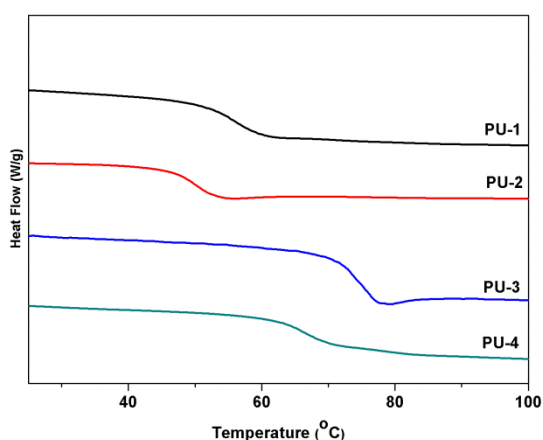


Figure 4a.7 DSC curves of poly(ether urethane)s.

Thus, the utility of newly synthesized bio-based aromatic diisocyanates in the synthesis of polyurethanes was successfully demonstrated. These diisocyanates could as well be used in the synthesis of thermoplastic polyurethanes by polymerization with commercially available polyols such as polyether polyols, polyester polyols, polycarbonate polyols, etc and appropriate chain extenders.

4a.4 Conclusions

1. Four new fully bio-based poly(ether urethane)s were synthesized from newly synthesized aromatic diisocyanates containing oxyalkylene linkage and commercially available bio-based aliphatic diols.
2. Inherent viscosities of poly(ether urethane)s were in the range of 0.58-0.68 dLg⁻¹ indicating formation of reasonably high molecular weight polymers.

3. Number average molecular weight of poly(ether urethane)s ranged from 32,100-58,500 g mol⁻¹ and could be cast to form tough, clear and flexible films from the solutions of poly(ether urethane)s in chloroform.
4. Poly(ether urethane)s were found to be soluble in organic solvents such as chloroform, dichloromethane, THF, DMAc, DMF, NMP and DMSO.
5. The T₁₀ values for all the poly(ether urethane)s were within a narrow range between 304- 308 °C.
6. T_g value of bio-based poly(ether urethane)s were observed in the range 49-74 °C and these values decreased with increase in the number of methylene units in diols and increased with increase in the number of methoxy substituents on aromatic rings of diisocyanates.

References

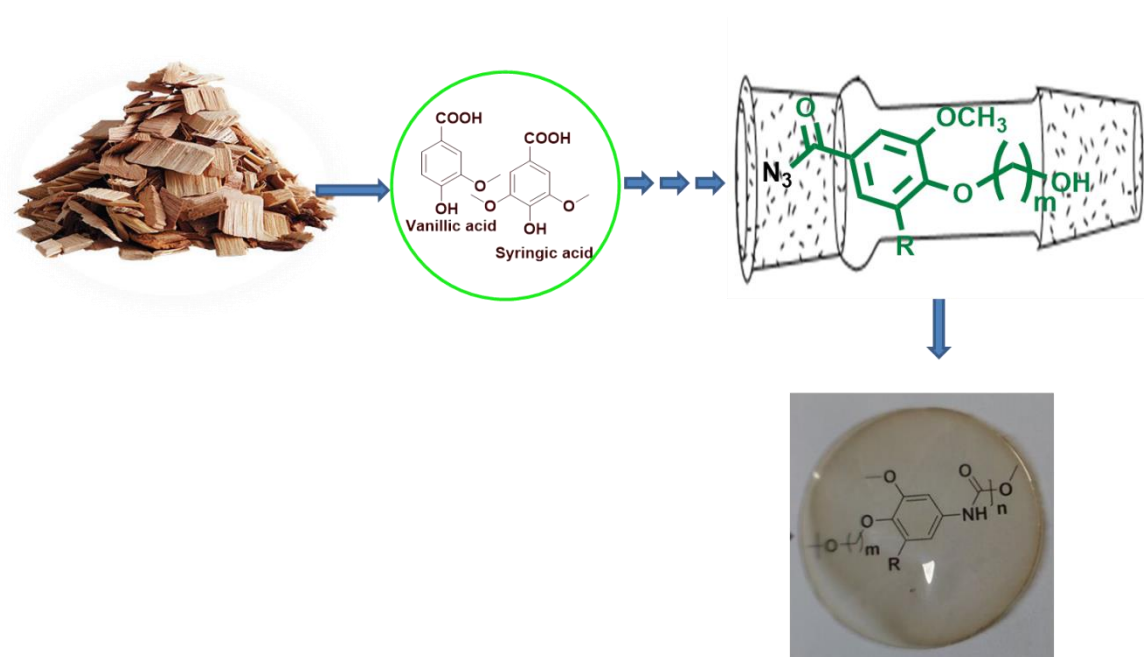
- 1 H. W. Engels, H. G. Pirkel, R. Albers, R. W. Albach, J. Krause, A. Hoffmann, H. Casselmann and J. Dormish, *Angew. Chem. Int. Ed.*, 2013, **52**, 9422–9441.
- 2 M. F. Sonnenschein, in *Polyurethanes*, John Wiley & Sons, Inc, Hoboken, NJ, 2014, pp. 336–374.
- 3 Huibo Zhang, Yadong Chen, Yongchun Zhang, Xiangdong Sun, Haiya Ye and Wen Li, *J. Elastomers Plast.*, 2008, **40**, 161–177.
- 4 M. F. Sonnenschein, in *Polyurethanes*, John Wiley & Sons, Inc, Hoboken, NJ, 2014, pp. 294–335.
- 5 M. F. Sonnenschein, in *Polyurethanes*, John Wiley & Sons, Inc, Hoboken, NJ, 2014, pp. 207–234.
- 6 D. M. Segura, A. D. Nurse, A. McCourt, R. Phelps and A. Segura, 2005, pp. 101–162.
- 7 Y. He, D. Xie and X. Zhang, *J. Mater. Sci.*, 2014, **49**, 7339–7352.
- 8 W. Panwiriyarat, V. Tanrattanakul, J. F. Pilard, P. Pasetto and C. Khaokong, *J. Appl. Polym. Sci.*, 2013, **130**, 453–462.
- 9 M. F. Sonnenschein, in *Polyurethanes*, John Wiley & Sons, Inc, Hoboken, NJ, 2014, pp. 10–104.
- 10 A. J. Ragauskas, *Science*, 2006, **311**, 484–489.
- 11 A. Fuessl, M. Yamamoto and A. Schneller *Polymer Science: A Comprehensive Reference*, 2012, **5**, 49–70.
- 12 X. S. Wool, Richard P., Sun, *Bio-Based Polymers and Composites*, Elsevier Inc.,

- Amstradam, 2005.
- 13 F. H. Isikgor and C. R. Becer, *Polym. Chem.*, 2015, **6**, 4497–4559.
 - 14 S. A. Madbouly, Z. Chaoqum and K. R. Michael, *Bio-Based Plant Oil Polymers and Composites*, Deans, M, Amstradam, 2016.
 - 15 A. S. More, T. Lebarbé, L. Maisonneuve, B. Gadenne, C. Alfos and H. Cramail, *Eur. Polym. J.*, 2013, **49**, 823–833.
 - 16 L. Hojabri, X. Kong and S. S. Narine, *Biomacromolecules*, 2009, **10**, 884–891.
 - 17 M. Firdaus and M. A. R. Meier, *Green Chem.*, 2013, **15**, 370–380.
 - 18 C. Carré, H. Zoccheddu, S. Delalande, P. Pichon and L. Averous, *Eur. Polym. J.*, 2016, **84**, 759–769.
 - 19 L. Maisonneuve, O. Lamarzelle, E. Rix, E. Grau and H. Cramail, *Chem. Rev.*, 2015, **115**, 12407–12439.
 - 20 G. Rokicki, P. G. Parzuchowski and M. Mazurek, *Polym. Adv. Technol.*, 2015, **26**, 707–761.
 - 21 P. F. H. Harmsen, M. M. Hackmann and H. L. Bos, *Biofuels, Bioprod. Biorefining*, 2014, **8**, 306–324.
 - 22 S. N. Goyanes and N. B. D’Accorso, *Industrial Applications of Renewable Biomass Products*, Springer International Publishing, Cham, 2017.
 - 23 D. A. Babb, in *Synthetic Biodegradable Polymers*, eds. B. Rieger, A. Künkel, G. W. Coates, R. Reichardt, E. Dinjus and T. A. Zevaco, Springer Berlin Heidelberg, 2011, vol. 245, pp. 315–360.
 - 24 D. P. Pfister, Y. Xia and R. C. Larock, *ChemSusChem*, 2011, **4**, 703–717.
 - 25 P. Rojek and A. Prociak, *J. Appl. Polym. Sci.*, 2012, **125**, 2936–2945.
 - 26 J. A. Galbis and M. G. García-Martín, in *Monomers, Polymers and Composites from Renewable Resources*, eds. M. Belgacem and A. Gandini, Amstradam, Elsevier, 2008, pp. 89–114.
 - 27 A. J. D. Silvestre, in *Monomers, Polymers and Composites from Renewable Resources*, eds. M. Belgacem and A. Gandini, Amstradam, Elsevier, 2008, pp. 67–88.
 - 28 R. J. González-Paz, C. Lluch, G. Lligadas, J. C. Ronda, M. Galià and V. Cádiz, *J. Polym. Sci. Part A Polym. Chem.*, 2011, **49**, 2407–2416.
 - 29 M. K. Hassan, K. A. Mauritz, R. F. Storey and J. S. Wiggins, *J. Polym. Sci. Part A Polym. Chem.*, 2006, **44**, 2990–3000.
 - 30 T. Calvo-Correas, A. Santamaria-Echart, A. Saralegi, L. Martin, Á. Valea, M. A.

- Corcuera and A. Eceiza, *Eur. Polym. J.*, 2015, **70**, 173–185.
- 31 J. L. Cawse, J. L. Stanford and R. H. Still, *Die Makromol. Chemie*, 1984, **185**, 697–707.
- 32 M. D. Zenner, Y. Xia, J. S. Chen and M. R. Kessler, *ChemSusChem*, 2013, **6**, 1182–1185.
- 33 C. N. D. Neumann, W. D. Bulach, M. Rehahn and R. Klein, *Macromol. Rapid Commun.*, 2011, **32**, 1373–1378.

Chapter - 4b

New Poly(ether urethane)s Based on Lignin Derived Aromatic Chemicals *via* A-B Monomer Approach: Synthesis and Characterization



4b.1 Introduction

Polyurethanes, prepared generally by the step-growth polymerization of di- or poly- functional hydroxyl compounds (polyols) and di- or poly- functional isocyanates, are versatile polymers whose properties could be tailored to afford elastomers, foams, fibers, coatings, adhesives, sealants, biomaterials and so on¹⁻⁸. Most commonly used diisocyanates are toluene diisocyanate (TDI), and methylene diphenyl diisocyanate (MDI) with demand of 34.1% and, 61.3%, respectively and are obtained from petroleum resources⁹. However, di-/poly-isocyanate monomers are reported to be toxic and are generally synthesized by phosgenation of diamines using phosgene which is even more toxic. The prolonged exposure of isocyanate vapours can result in some health hazards. It can be entered in the body by inhalation, skin contact, etc^{6,10}.

In this context, sustainable, isocyanate- and phosgene-free synthetic routes to polyurethanes have attracted considerable academic and industrial attention during the last decades^{1,9,11-14}. Many recent efforts have been focused on the preparation of non-isocyanate based-polyurethanes^{9,13,14}. Polyaddition of bis-cyclic carbonates with diamines and transurethanization of biscarbamates with diols are the most studied routes for polyurethane synthesis^{15-17,14}. Along these methods, polymerization of aziridines with carbon dioxide¹⁸⁻²⁰ and self-condensation of AB type monomers^{15,21,22} have been reported in the literature. Recently, Meier et al¹². and Cramail et al¹³ have independently reviewed sustainable and isocyanate free routes for polyurethane synthesis. Bio-based A-B monomers containing hydroxyl and acyl azide or hydroxyl and methyl urethane groups have also been prepared starting from vegetable oils^{21,22} and sorbitol²³ and polymerised to form thermoplastic polyurethanes.

We wish report herein synthesis and characterization of fully bio-based poly(ether urethane)s starting from non-edible renewable resources *via* A-B monomer approach. ω -Hydroxyalkyleneoxy benzoyl azides namely, 4-((6-hydroxyhexyl)oxy)-3-methoxybenzoyl azide, 4-((11-hydroxyundecyl)oxy)-3-methoxybenzoyl azide, 4-((6-hydroxyhexyl)oxy)-3,5-dimethoxybenzoyl azide, and 4-((11-hydroxyundecyl)oxy)-3,5-dimethoxybenzoyl azide were self-polycondensed at 80 °C in dry toluene in the presence of catalytic amount of dibutyltin dilaurate (DBTDL) to afford poly(ether urethane)s. Poly(ether urethane)s were characterized by inherent viscosity measurements, solubility tests, FT-IR, ¹H NMR and ¹³C NMR spectroscopy, UV-visible spectroscopy, X-ray diffraction, thermogravimetric analysis (TGA) and differential scanning calorimetric

studies (DSC). The effect of the chemical structure of poly(ether urethane)s on solubility and thermal properties was investigated.

4b.2 Experimental

4b.2.1 Materials

Dibutyltin dilaurate (DBTDL) was purchased from Sigma–Aldrich and was used as received. Toluene, dichloromethane, chloroform, tetrahydrofuran (THF), *N,N*-dimethylformamide (DMF), *N,N*-dimethylacetamide (DMAc), *N*-methyl-2-pyrrolidone (NMP) and dimethyl sulfoxide (DMSO) were received from Thomas Baker Ltd., Mumbai. Toluene was dried over calcium hydride and distilled prior to use.

4b.2.2 Measurements

Inherent viscosity of poly(ether urethane)s was determined with 0.5 % (w/v) solution of polymer in chloroform or DMAc at $30 \pm 0.1^\circ\text{C}$ using Ubbelohde suspended level viscometer. Inherent viscosity was calculated using the equation

$$n_{inh} = \frac{2.303}{c} \times \log t/t_0$$

Where, t and t_0 are flow times of polymer solution and solvent, respectively and c is the concentration of polymer solution

Molecular weights and dispersity of poly(ether urethane)s were determined from gel-permeation chromatography (GPC) equipped with spectra series UV 100 and spectra system RI 150 detectors using chloroform (Thermo Separation Products) or DMAc (Thermo-Finnigan) as an eluent at a flow rate of 1 mL min^{-1} at 25°C . Sample concentration was 2 mg mL^{-1} and narrow dispersity polystyrenes were used as calibration standards.

FT-IR spectra were obtained on a Perkin–Elmer Spectrum GX spectrometer using polymer film.

NMR spectra were recorded on a Bruker 200, 400 or 500 MHz spectrometer at resonance frequencies of 200, 400 or 500 MHz for ^1H NMR and 50, 100 or 125 MHz for ^{13}C NMR measurements using CDCl_3 as a solvent.

The % transmittance of poly(ether urethane) films ($\sim 1 \text{ mm}$ thickness) was measured at 800 nm on UV-Visible spectrophotometer (Perkin Elmer Lambda 35).

Thermogravimetric analysis (TGA) was carried out on Perkin Elmer: STA 6000, at a heating rate of $10^\circ\text{C min}^{-1}$ under nitrogen atmosphere.

Differential scanning calorimetric (DSC) analysis was performed using a DSC Q10 differential calorimeter from TA Instruments under nitrogen atmosphere (50 mL min^{-1}). Analyses were carried out in a temperature range between 30 and 250 °C using a heating rate of 10 °C min^{-1} .

4b.2.3 General procedure for synthesis of poly(ether urethane)s

Into a 100 mL two-necked round bottom flask equipped with a reflux condenser and an argon inlet were charged, ω -hydroxyalkyleneoxy benzoyl azide (6.32 mmol), DBTDL (3×10^{-3} mmol) and dry toluene (25 mL). The reaction mixture was heated at 80 °C for 12 h. The toluene was removed under reduced pressure to afford solid polymer. The polymer was dissolved in hot DMAc, precipitated in cold methanol, filtered and dried in vacuum oven at 60 °C for 12 h.

Synthesis of poly(ether urethane) (PEU-1) by self-polycondensation of 4-((6-hydroxyhexyl)oxy)-3-methoxybenzoyl azide

IR (KBr): 3325, 1725, 1695 cm^{-1} ; $^1\text{H NMR}$ (200 MHz, $\text{DMSO-}d_6$, δ/ppm): 1.32-1.75 (m, 8H), 3.69 (s, 3H), 3.86 (t, 2H), 4.04 (t, 2H), 6.80-6.94 (m, 2H), 7.15 (s, 1H), 9.38 (br. s, 1H); $^{13}\text{C NMR}$ (100 MHz, $\text{DMSO-}d_6$, δ/ppm): 25.2, 25.2, 28.5, 28.8, 55.4, 63.9, 68.6, 103.9, 110.1, 113.9, 132.9, 143.5, 149.1, 153.7.

Synthesis of poly(ether urethane) (PEU-2) by self-polycondensation of 4-((11-hydroxyundecyl)oxy)-3-methoxybenzoyl azide

IR (KBr): 3330, 1730, 1695 cm^{-1} ; $^1\text{H NMR}$ (400 MHz, CDCl_3 , δ/ppm): 1.27-1.46 (m, 14H), 1.62-1.68 (m, 2H), 1.77-1.85 (m, 2H), 3.85 (s, 3H), 3.97 (t, 2H), 4.14 (t, 2H), 6.60 (br. s., 1H), 6.75 - 6.83 (m, 2H), 7.18 (br. s, 1H); $^{13}\text{C NMR}$ (125 MHz, CDCl_3 , δ/ppm): 25.8, 25.9, 28.9, 29.2, 29.3, 29.4, 29.5, 55.9, 65.3, 69.6, 104.2, 110.7, 113.7, 131.7, 144.7, 149.8, 154.0.

Synthesis of poly(ether urethane) (PEU-3) by self-polycondensation of 4-((6-hydroxyhexyl)oxy)-3,5-dimethoxybenzoyl azide

IR (KBr): 3330, 1730, 1700 cm^{-1} ; $^1\text{H NMR}$ (400 MHz, $\text{DMSO-}d_6$, δ/ppm): 1.33-1.69 (m, 8H), 3.69 (s, 6H), 3.76 (t, 2H), 4.06 (t, 2H), 6.83 (s, 2H), 9.45 (br. s, 1H); $^{13}\text{C NMR}$ (100 MHz, $\text{DMSO-}d_6$, δ/ppm): 25.1, 28.5, 29.5, 55.7, 64.0, 72.3, 96.2, 131.9, 135.1, 152.9, 153.5.

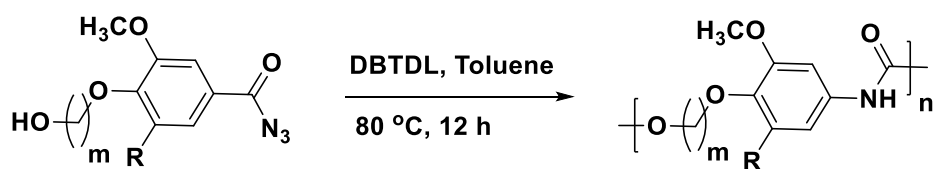
Synthesis of poly(ether urethane) (PEU-4) by self-polycondensation of 4-((11-hydroxyundecyl)oxy)-3,5-dimethoxybenzoyl azide

IR (KBr): 3330, 1730, 1700 cm^{-1} ; ^1H NMR (200 MHz, CDCl_3 , δ/ppm): 1.27-1.77 (m, 18H), 3.80 (s, 6H), 3.91 (t, 2H), 4.14 (t, 2H), 6.68 (s, 2H); ^{13}C NMR (100 MHz, CDCl_3 , δ/ppm): 25.8, 28.9, 29.2, 29.4, 29.4, 29.5, 29.5, 23.0, 56.0, 65.4, 73.6, 96.5, 133.2, 133.9, 153.6, 153.8.

4b.3 Results and discussion

4b.3.1 Synthesis of poly (ether urethane)s

In this study, four new fully bio-based poly(ether urethane)s were synthesized by self-polycondensation of ω -hydroxyalkyleneoxy benzoyl azides. ω -Hydroxyalkyleneoxy benzoyl azides and catalytic amount of DBTDL were dissolved in dry toluene and the solution was heated slowly up to 80 $^\circ\text{C}$. The evolution of nitrogen gas indicated the decomposition of aromatic carbonyl azide group. The heating was continued for 12 h to ensure the completion of polymerization reaction. During heat treatment, acyl azide groups undergo thermal Curtius rearrangement to form isocyanate groups which in situ react with the hydroxyl groups present in A-B monomers to afford poly(ether urethane)s (Scheme 4b.1). The results of polymerization reactions are summarized in Table 4b.1.



Scheme 4b.1 Synthesis of poly(ether urethane)s starting from ω -hydroxyalkyleneoxy benzoyl azides.

Inherent viscosities of poly(ether urethane)s were in the range 0.41-0.69 dLg^{-1} indicating formation of reasonably high molecular weight polymers. Number average molecular weights (\overline{M}_n), obtained from gel permeation chromatography (GPC), were in the range 20,000-40,400 g mol^{-1} and dispersity values were in the range 1.4-1.9. Tough, transparent and flexible films of poly(ether urethane)s could be cast either from chloroform or DMAc solution. The % transmittance data at 800 nm measured by UV-Visible spectrophotometer on poly(ether urethane) films (~1 mm thickness) is given in Table 4b.1. Poly(ether urethane) films exhibited good optical properties and possessed light transmittance in the range 80.2 -87.6 %.

Table 4b.1 Inherent viscosity, molecular weight and % transmittance of poly(ether urethane)s

Sr no	Poly(ether urethane)	R	m	η_{inh} (dLg ⁻¹)	\overline{M}_n	\overline{M}_w	Dispersity	Transmittance (%) ^e
1	PEU-1	H	6	0.69 ^a	40,400 ^c	56,900 ^c	1.4	87.6
2	PEU-2	H	11	0.54 ^b	29,800 ^d	57,900 ^d	1.9	84.0
3	PEU-3	OCH ₃	6	0.41 ^a	20,000 ^c	30,600 ^c	1.5	83.1
4	PEU-4	OCH ₃	11	0.53 ^b	28,200 ^d	48,800 ^d	1.7	80.2

a; η_{inh} was measured with 0.5% (w/v) solution of poly(ether urethane) in DMF at 30 ± 0.1 °C

b; η_{inh} was measured with 0.5% (w/v) solution of poly(ether urethane) in chloroform at 30 ± 0.1 °C

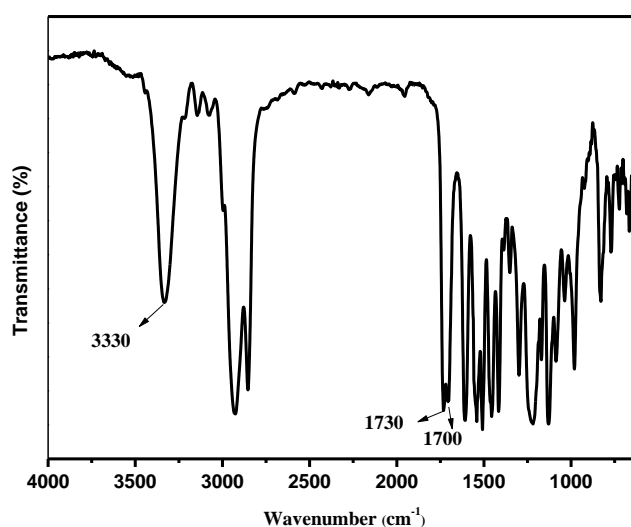
c; measured by GPC in DMF, polystyrene was used as the calibration standard

d; measured by GPC in chloroform, polystyrene was used as the calibration standard

e; % transmittance was measured at wavelength of 800 nm

4b.3.2 Structural characterization

The chemical structures of poly(ether urethane)s were confirmed by FT-IR, ¹H NMR and ¹³C NMR spectroscopy. A representative FT-IR spectrum of PEU-3 is shown in **Figure 4b.1**, which indicated complete disappearance of azido and isocyanate absorption bands (2155 and 2270 cm⁻¹) and an absorbance band appeared at 3330 cm⁻¹ attributable to –NH stretching indicating the formation of urethane linkages. Carbonyl stretching band was observed at 1730 and 1700 cm⁻¹ due to non-hydrogen bonded and hydrogen bonded carbonyl group, respectively.

**Figure 4b.1** FT-IR spectrum of poly(ether urethane) (PEU 3).

A representative ^1H NMR spectrum of PEU-3 is shown in **Figure 4b.2**. A singlet was observed at 9.45 δ ppm for -NH group and aromatic protons showed a singlet at 6.83 δ ppm. Methylene protons attached to ether linkage appeared as a triplet at 4.06 δ ppm, and methylene protons attached to urethane linkage showed a triplet at 3.76 δ ppm. Methoxy group attached to aromatic ring displayed a singlet at 3.69 δ ppm. The protons attached to carbon β to the ether and urethane linkages displayed a multiplet in the range 1.57-1.65 δ ppm and remaining methylene protons appeared as a multiplet in the region 1.35-1.47 δ ppm.

^{13}C NMR spectrum of PEU-3, along with assignments of the carbon atoms is shown in **Figure 4b.3**. In ^{13}C NMR spectrum, a peak was observed at 153.5 δ ppm corresponding to the carbon of urethane carbonyl group.

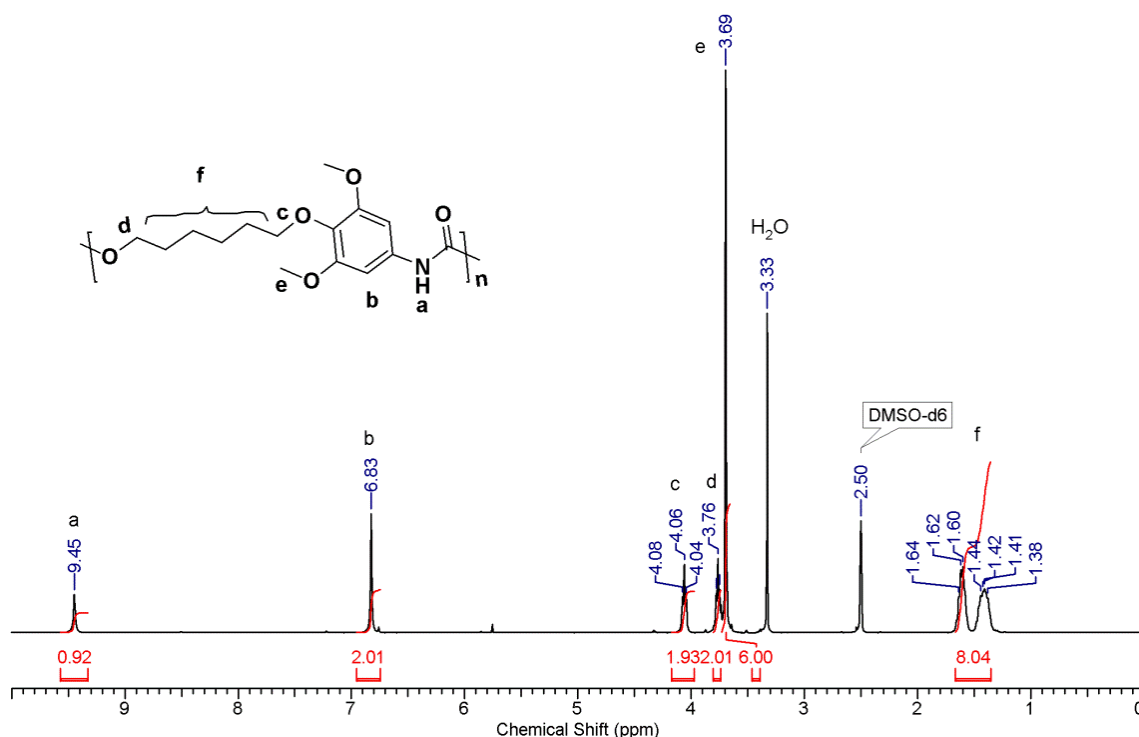


Figure 4b.2 ^1H NMR spectrum of PEU-3 in DMSO- d_6 .

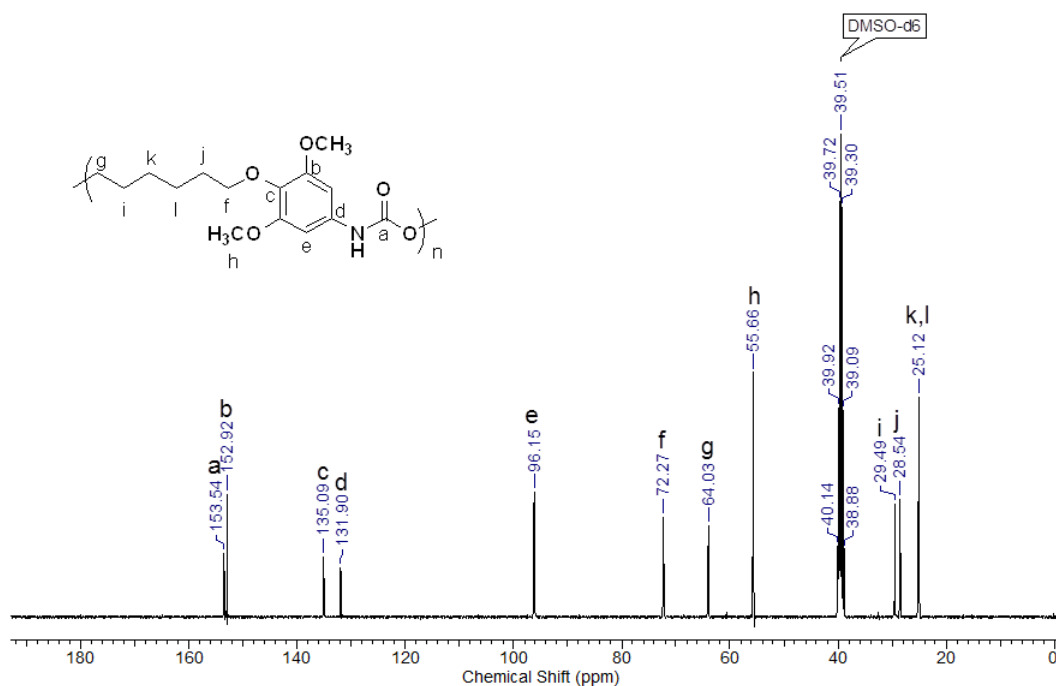


Figure 4b.3 ¹³C NMR spectrum of PEU-3 in DMSO-d₆.

4b.3.3 Solubility

The solubility of poly(ether urethane)s was examined at room temperature (at 3 wt % concentration) in various organic solvents. PEU-1, PEU-3 and PEU-4 were soluble at room temperature in dipolar aprotic solvents such as DMAc, DMF, NMP and DMSO. Additionally, PEU-4 was also soluble in dichloromethane and chloroform. PEU-2 was not soluble in above mentioned dipolar aprotic solvents at room temperature while it dissolved in these solvents at ~ 80 °C. Interestingly, the cooling of DMF solution of PEU-2 to room temperature showed spontaneous gelation thus indicating formation of an organogel. The formation of organogel in case of PEU-2 and its characterization is discussed in **Chapter 4c**.

4b.3.4 Thermal properties

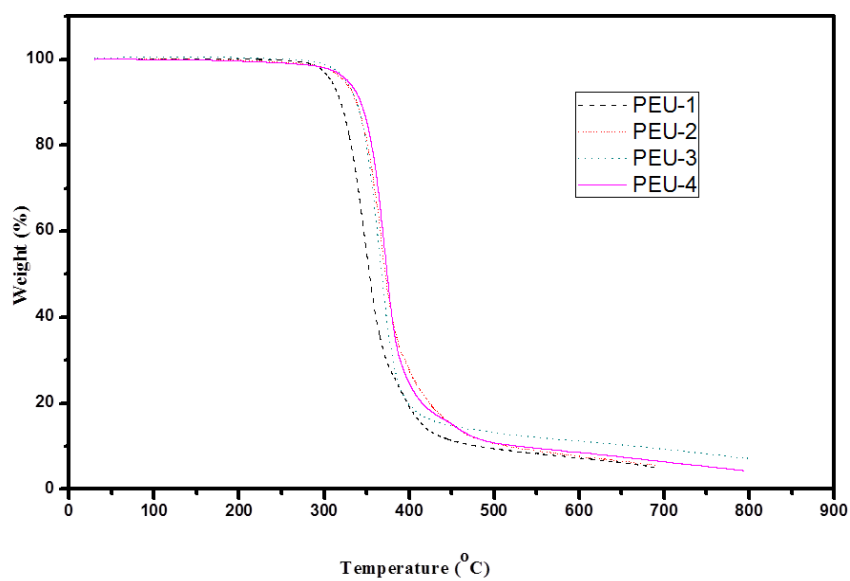
Thermal properties of poly(ether urethane)s were determined by thermogravimetric analysis (TGA) and differential scanning calorimetry (DSC) at a heating rate of 10 °C min⁻¹ under nitrogen atmosphere. TG and DSC curves are shown in **Figure 4b.4** and **Figure 4b.5**, respectively and data is included in **Table 4b.2**.

Table 4b.2 Thermal properties of poly(ether urethane)s

Sr no	Poly(ether urethane)s	R	m	T _g (°C) ^a	T ₁₀ (°C) ^b
1	PEU-1	H	6	65	320
2	PEU-2	H	11	40	340
3	PEU-3	OCH ₃	6	70	340
4	PEU-4	OCH ₃	11	50	340

a; measured by DSC on second heating scan with heating rate at 10 °C min⁻¹ under nitrogen atmosphere

b; temperature at which 10% weight loss was observed under nitrogen atmospheres

**Figure 4b.4** TG curves of poly(ether urethane)s

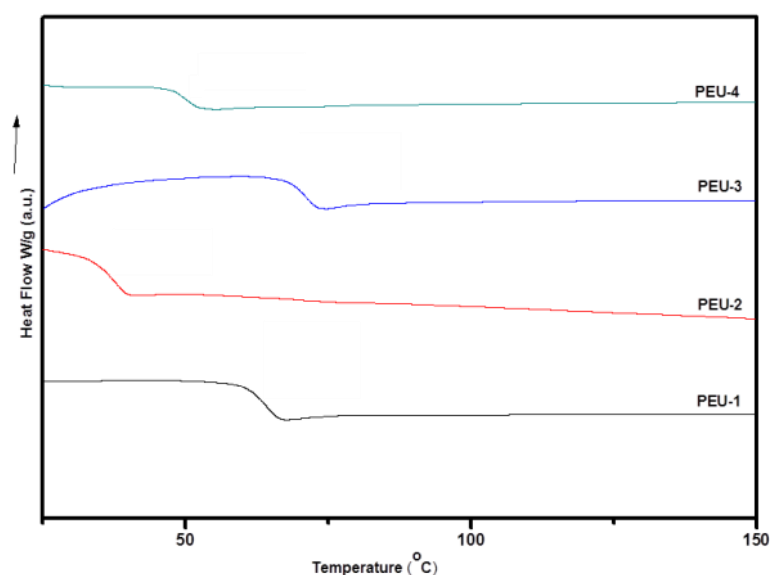


Figure 4b.5 DSC curves of poly(ether urethane)s

Poly(ether urethane)s showed temperature for 10 % weight loss in the range 320-340 °C. T_g of poly(ether urethane)s were observed in the range 40-70 °C. As expected, poly(ether urethane)s PEU-2 and PEU-4 containing 11-carbon alkylene spacer showed lower T_g values than corresponding poly(ether urethane)s PEU-1 and PEU-3 possessing 6-carbon alkylene spacer. The higher number of methylene units in oxyalkylene segment reduce the density of aromatic segment and consequently enhance flexibility of polymer chains. The number of methoxy substituents on aromatic ring also contributes to T_g of poly(ether urethane)s. Syringic acid-based poly(ether urethane)s (PEU-3 and PEU-4) containing two methoxy substituents on aromatic ring exhibited higher T_g values than corresponding vanillic acid-based poly(ether urethane)s (PEU-1 and PEU-2) containing one methoxy substituent. The presence of two methoxy substituents in case of poly(ether urethane)s, in which hydrogen bonds already exist, increases conformational barriers and consequently increase in T_g was observed. A similar trend was reported by Miller and co-workers for polyacetal ethers based on lignin-derived aromatics²⁴.

4b.4 Conclusions

1. Four new fully bio-based poly(ether urethane)s were synthesized by self-polycondensation of A-B monomers namely, 4-((6-hydroxyhexyl)oxy)-3-methoxybenzoyl azide, 4-((6-hydroxyhexyl)oxy)-3,5-dimethoxybenzoyl azide, 4-

- ((11-hydroxyundecyl)oxy)-3,5-dimethoxybenzoyl azide and 4-((11-hydroxyundecyl)oxy)-3-methoxybenzoyl azide *via* Curtius rearrangement.
2. Inherent viscosities of poly(ether urethane)s were in the range of 0.41-69 dLg⁻¹ indicating formation of reasonably high molecular weight polymers.
 3. Number average molecular weight of poly(ether urethane)s ranged from 20,000-40,400 g mol⁻¹ and could be cast into transparent and flexible films from the solution of poly(ether urethane)s in chloroform or DMAc.
 4. Poly(ether urethane) films exhibited good optical properties and possessed light transmittance at 800 nm in the range 80.2 -87.6 %.
 5. The T₁₀ values for all the poly(ether urethane)s were in the range of 320-340 °C.
 6. T_g value of bio-based poly(ether urethane)s were observed in the range 40-70 °C which were dictated by the length of oxyalkylene chain and number of methoxy substituents on aromatic ring.

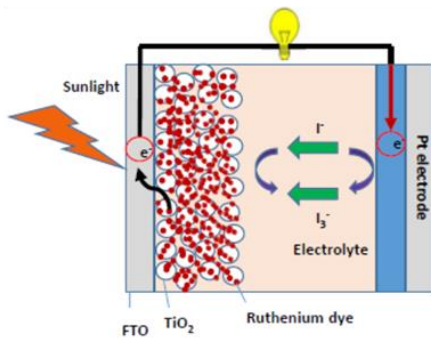
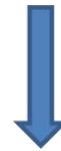
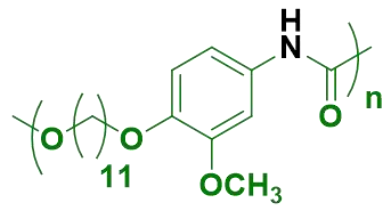
References

- 1 H.W. Engels, H.G. Pirkl, R. Albers, R. W. Albach, J. Krause, A. Hoffmann, H. Casselmann and J. Dormish, *Angew. Chem. Int. Ed.*, 2013, **52**, 9422–9441.
- 2 M. Desroches, M. Escouvois, R. Auvergne, S. Caillol and B. Boutevin, *Polym. Rev.*, 2012, **52**, 38–79.
- 3 M. F. Sonnenschein, in *Polyurethanes*, John Wiley & Sons, Inc, Hoboken, NJ, 2014, pp. 294–335.
- 4 M. F. Sonnenschein, in *Polyurethanes*, John Wiley & Sons, Inc, Hoboken, NJ, 2014, pp. 207–234.
- 5 M. F. Sonnenschein, in *Polyurethanes*, John Wiley & Sons, Inc, Hoboken, NJ, 2014, pp. 336–374.
- 6 C. A. Krone, J. T. A. Ely, T. Klingner and R. J. Rando, *Bull. Environ. Contam. Toxicol.*, 2003, **70**, 328–335.
- 7 N. Adam, G. Avar, H. Blankenheim, W. Friederichs, M. Giersig, E. Weigand, M. Halfmann, F. W. Wittbecker, D.-R. Larimer, U. Maier, S. Meyer-Ahrens, K.-L. Noble and H.-G. Wussow, in *Ullmann's Encyclopedia of Industrial Chemistry*, Wiley-VCH Verlag GmbH & Co. KGaA, Weinheim, Germany, 2005.
- 8 M. Zhang, S. M. June and T. E. Long, in *Polymer Science: A Comprehensive Reference*, 2012, **5**, 7–47.

- 9 O. Kreye, H. Mutlu and M. A. R. Meier, *Green Chem.*, 2013, **15**, 1431.
- 10 H. Cotarca, L Eckert, *Phosgenations - A Handbook*, Wiley, 2005.
- 11 M. Firdaus and M. A. R. Meier, *Green Chem.*, 2013, **15**, 370–380.
- 12 M. Meier, *Green Chem.*, 2014, **16**, 1672.
- 13 L. Maisonneuve, O. Lamarzelle, E. Rix, E. Grau and H. Cramail, *Chem. Rev.*, 2015, **115**, 12407–12439.
- 14 G. Rokicki, P. G. Parzuchowski and M. Mazurek, *Polym. Adv. Technol.*, 2015, **26**, 707–761.
- 15 D. C. Webster, *Prog. Org. Coat.*, 2003, **47**, 77–86.
- 16 B. Besse, V Camara, F Voirin, C Auvergne, R Caillol, S Boutevina, *Polym. Bull.*, 2013, **4**, 4545–4561.
- 17 O. Figovsky, L. Shapovalov, A. Leykin, O. Birukova and R. Potashnikova, *International Lett. Chem. Physics, Astron.*, 2012, **3**, 52–66.
- 18 R. D. Lundberg, S. Albans and Montgomery, Carbon dioxide polymers, US3523924, 1970
- 19 T. Ihata, O Kayaki, Y Ikariya and T. Ikariya, *Chem. Commun.*, 2005, 2268–2270.
- 20 T. Ihata, O Kayaki, Yoshihito, Y Ikariya, *Angew. Chemie Int. Ed.*, 2004, **42**, 717–719.
- 21 A. S. More, B. Gadenne, C. Alfos and H. Cramail, 2012, **3**, 1594–1605.
- 22 D. V. Palaskar, A. Boyer, E. Cloutet, C. Alfos and H. Cramail, *Biomacromolecules*, 2010, **11**, 1202–1211.
- 23 F. Bachmann, J. Reimer, M. Ruppenstein and J. Thiem, *Macromol. Rapid Commun.*, 1998, **19**, 21–26.
- 24 A. G. Pemba, M. Rostagno, T. A. Lee, S. A. Miller, S. Barazzouk, P. V. Kamat, J. Huuskonen, K. Rissanen, C. A. Schalley and K. H. Leong, *Polym. Chem.*, 2014, **5**, 3214–3221.

Chapter - 4c

Polyurethane-Based Organogels: Preparation, Characterization and Application as Electrolyte in Dye-Sensitized Solar Cell



4c.1 Introduction

Organogels are of interest as they find potential applications in drug delivery, cosmetics, cleaning agents, sensors, tissue engineering, enzyme immobilization matrices, phase selective gelation, water purification by dye absorption and as gel electrolyte for quasi-dye sensitized solar cells¹⁻⁶. A wide range of organic gelators are known in the literature⁶⁻⁹. The common forces which are responsible for supramolecular gel formations are some specific or non-covalent interactions, such as electrostatic, dipole-dipole, hydrogen bonding (H-bonding), π - π stacking, and van der Waals interactions¹⁰⁻¹⁴. In addition, hydrophobic or solvophobic effects, as well as the fine balance of the forces among gelator molecules and solvent molecules, often play an important role¹⁴.

A wide range of organic compounds were shown to form organo gelators *viz.* fatty acid derivatives, steroid derivatives, molecules containing steroidal, amino acid based gelator, n-alkanes, etc in organic solvents¹⁵⁻²⁴. To design a new gelator molecule; the understanding of molecular geometry as well as the various intermolecular forces is an essential requirement. However, precise structural requirements for organogelators are still poorly understood^{13,17,21,22,25-27}. Most organogelators have been discovered by serendipity rather than by design.

Majority of the reported organogels are based on the low molecular weight organogelators (LMWOGs)^{12-14,25}. However, gels composed of low-molecular-weight gelators are metastable and crystallize during prolonged storage. This crystallization process may occur within a few hours or within a few years, and the period until stabilization (that is, crystallization) occurs varies depending on the gel^{13,28}. In industrial applications for gelators, crystallization corresponds to a breakdown of gels and is a critical disadvantage. Unlike low-molecular-weight compounds, polymers and oligomers generally do not get separated out from a solution as crystals because of their molecular weight distributions and entanglement of their chains. Examples of polymeric gelators include polystyrene²⁹⁻³¹, poly(methyl methacrylate)^{32,33}, poly(3-hydroxybutyrate-co-3-hydroxyvalerate)³⁴, poly(γ -benzyl-L-glutamate)³⁵, polypeptide³⁶, poly(*N,N*-dimethylacrylamide)³⁷, poly(2,5-dinonyl-p-phenylene ethynylene)³⁸, poly(2-methoxy-5-(2-ethylhexyloxy)-1,4-phenylenevinylene)³⁹, poly(9,9-dioctylfluorene-2,7-diyl)⁴⁰, poly(pyridinium-1,4-diyliminocarbonyl-1,4-phenylene methylene)⁴¹ and polyurethanes⁴².

In the present study, gelation behaviour of a polyurethane obtained by self-polycondensation of 4-((11-hydroxyundecyl)oxy)-3-methoxybenzoyl azide was

investigated in various organic solvents. Microscopic property and sol-gel transition temperature (T_{gel}) of polyurethane organogel was characterized by FE-SEM and differential scanning calorimetry (DSC), respectively. Rheological studies were performed to study thermoreversibility of organogel, sol-gel transition and effect of gelator concentration on its strength. An application of prepared polyurethane organogel was demonstrated as a gel electrolyte in quasi-solid state dye-sensitized solar cells (DSSCs).

4c.2 Experimental

4c.2.1 Materials

Polyurethanes *viz.* PU-1, PU-2, PU-3 and PU-4 were synthesized as reported in **Chapter 4b**. Chloroform, dichloromethane, tetrahydrofuran (THF), *N,N*-dimethylformamide (DMF), *N,N*-dimethylacetamide (DMAc), *N*-methyl-2-pyrrolidone (NMP) and dimethyl sulfoxide (DMSO), were procured from Thomas Baker Ltd., Mumbai. Lithium chloride (LiCl), lithium iodide (LiI), and sulfolane were purchased from Sigma-Aldrich, USA. The organometallic dye **N-719** (di-tetrabutylammonium *cis*-bis(isothiocyanato)bis(2,2'-bipyridyl-4, 4'-dicarboxylato)ruthenium(II)) and 1-propyl-2, 3-dimethyl-imidazolium iodide were obtained from Solaronix, SA (Switzerland).

4c.2.2 Preparations and characterization

Gel preparation: A weighed amount of polyurethane was taken into a vial and dissolved in organic solvent by heating. The solution was cooled to room temperature and allowed to stand until gel formation which was confirmed by inversion of the vial.

DSC: The gel-sol transition temperature (T_{gel}) was analyzed by differential scanning calorimetry (TA Q-10 model). Typically, ~10 mg of a gel was massed and added to a sealed pan that passed through a heat-cool-heat cycle at 10 °C min⁻¹ under nitrogen atmosphere and temperature in the range of 25-80 °C.

Rheology: Rheological behavior of polyurethane-based organogels was studied using strain-controlled rheometer (MCR 301, Anton Paar, Austria). For rheological studies, polyurethane organogels with concentrations of 0.5, 1, 2 and 3 wt % were prepared in DMF. Cup and bob geometry was used for measuring dilute and moderately viscous solutions. Cone and plate geometry with 25 mm diameter was used for highly viscous solutions. Amplitude sweep measurements were performed to calculate the linear visco-elastic regime of the gels. Geometry was covered with in-house lids to prevent

evaporation of solvent during the measurements. Temperature ramp measurements with alternate heating and cooling cycles were performed to measure the thermo-reversible nature of the gels. Thermal cycles were performed at constant strain and frequency which was within the linear visco-elastic regime of the gel. Temperature was ramped from 25 °C to 80 °C at 0.25 °C min⁻¹. Shear modulus (G') and loss modulus (G'') was recorded as a function of temperature and time. Measurements were repeated thrice to ensure reproducibility.

FE-SEM: Field emission scanning electron microscopy images were taken under low vacuum condition on FEI QUANTA 200.

Fabrication of dye-sensitized solar cells: Fluorine doped tin oxide (FTO) coated glass substrates were cut into 2 cm x 2 cm dimension and cleaned by washing with soap solution, deionized water, and ethanol. A transparent layer of commercially available TiO₂ paste (18NRT, Dyesol) was coated onto cleaned FTO glass using doctor blade method. The FTO glass was heated at 450 °C for 45 min and then at 500 °C for 15 minutes in programmable furnace. After cooling to room temperature, a light harvesting layer of 18NR-AO paste (Dyesol) was coated by doctor blade method followed by the same heating protocol for transparent layer. The total thickness of 12-14 μm was maintained for TiO₂ layers. The films were then subjected to TiCl₄ treatment in which TiO₂ films were dipped in 20 mM solution of TiCl₄ at 70 °C for 30 minutes. The films were taken out from the solution, rinsed with deionized water followed by ethanol and then annealed at 450 °C for 30 min. TiO₂ films were dipped in 5 mM N-719 (di-tetrabutylammonium cis-bis(isothiocyanato)bis(2,2'-bipyridyl-4, 4'-dicarboxylato)ruthenium(II)) dye solution (1:1 v/v acetonitrile: t-butyl alcohol) at room temperature for 24 h. The dye loaded films were washed with ethanol to remove excess dye on the surface. Platinum (Pt) as counter electrode was prepared by drop casting 20 μL of 10 mM hexachloroplatinic acid (H₂PtCl₆) on clean FTO. It was allowed to dry at room temperature and then heated at 450 °C for 15 minutes.

Electrolyte preparation: The liquid electrolyte for DSSCs was composed of 0.6 M 1-propyl-2, 3-dimethyl-imidazolium iodide, 0.05M LiI, 0.05M I₂ and 0.5M 4-tertbutylpyridine in DMF. The gel electrolyte was prepared by addition of polyurethane based gelator into the liquid electrolyte and heating at 100 °C for 10 min.

4c.3 Results and discussion

The chemical structures of poly(ether urethane)s selected for the study are shown in **Figure 4c.1**. Initially, the solubility tests of polyurethanes were performed at 3 wt. % concentration in various organic solvents. The solubility data of polyurethanes is shown in **Table 4c.1**.

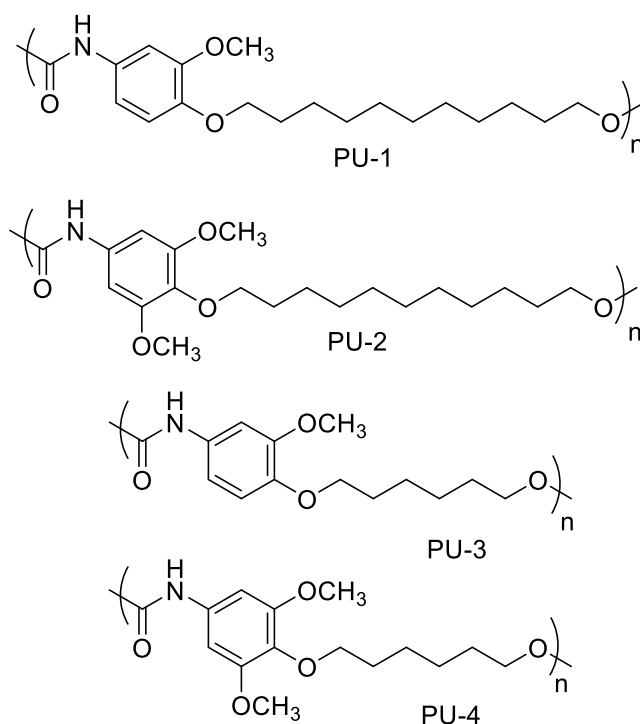


Figure 4c.1 Structures of polyurethanes for gel study

Table 4c.1 Gelation properties of 3% (w/v) solutions of PU-1, PU-2, PU-3 and PU-4 in various solvents

Polyurethane	DMAC	DMF	DMSO	NMP	THF	Dichloro methane	Chlorof orm	Toluene	Hexane	Chloro benzene
PU-1	*	*	*	*	*	+	+	-	-	-
PU-2	+	+	+	+	+	+	+	-	-	-
PU-3	+	+	+	+	+	-	-	-	-	-
PU-4	+	+	+	+	+	-	-	-	-	-

* gel formation at room temperature; + soluble at room temperature; - insoluble at room temperature

Some important conclusions were drawn from the results summarized in **Table 4c.1**. The increase in the number of methoxy substituents on aromatic ring of polyurethane backbone (two methoxy in case of PU-2 and PU-4) results in increase in solubility in polar organic solvents at room temperature due to the enhanced polarity of polymer. Furthermore, decrease in number of carbons in alkylene chain (6 in case of PU-2 and PU-4) also showed good solubility in polar organic solvents at room temperature because of less hydrophobic effect. Interestingly, polyurethane (PU-1) which contains one methoxy substituent on aromatic ring of polymer backbone and 11-carbon containing alkylene spacer was soluble in polar organic solvents only at elevated temperature (~ 60 °C), which upon reverting to room temperature exhibited spontaneous gelation. This could be due to the proper balance of hydrophobic effect and partial solubility in polar organic solvent.

In order to study gel formation in detail, a weighed amount (0.5-3 % w/v) of polyurethane was dissolved in organic solvents under heating conditions as per the need. The solution was cooled to room temperature and allowed to stand until gel formation which was confirmed by inversion of vial (**Figure 4c.2**). Using the same procedure, we also attempted to utilize various organic solvents such as chloroform, dichloromethane, THF, DMF, DMAc, DMSO, chlorobenzene and toluene for gel formation. It was found that only polar organic solvents could gelate polyurethane (**Table 4c.2**). Thus, the nature of solvent plays a key role in the gelation of polyurethane.

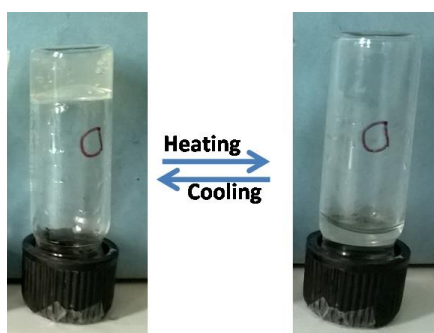


Figure 4c.2 Photograph of polyurethane gel

4c.3.1 Microstructural study

Xerogel of polyurethane organogel was obtained by drying gel at 30 °C for 24 h and then under vacuum. The morphology of xerogel was investigated by FE-SEM, SEM image showed uniform fibrous network, which can be seen in **Figure 4c.3**. It can be suggested that hydrogen bonding interactions are responsible for the gel formation, as the

polymer contains urethane linkages. Such type of hydrogen bonding interactions are reported in literature for polyurethane based organogel⁴².

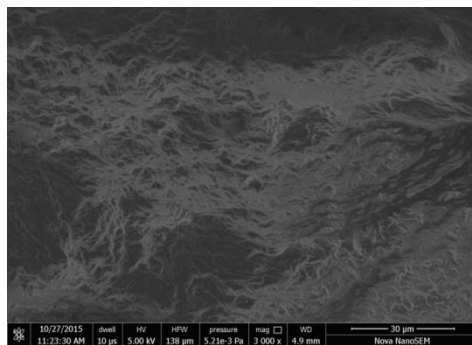


Figure 4c.3 SEM image of polyurethane-based xerogel gel.

4c.3.2 LiCl addition experiment

In general, hydrogen bonding is very common in most of the supramolecular organogels which can be denatured by addition of LiCl or urea due to their ability to vanish hydrogen bonding. When LiCl (10 mol. equivalent) was added to the polyurethane based organogel (DMF, 3 wt.%), the gel became weak instead of giving a clear solution (**Figure 4c.4**). This indicates that hydrogen bonding is one of the factors responsible for gelation, but hydrophobic interactions should also be taken into account.

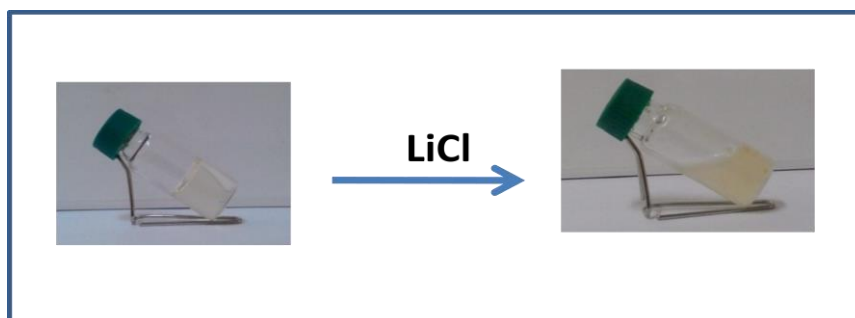


Figure 4c.4 LiCl mediated gel-sol transformation of polyurethane-based organogel in DMF

4c.3.3 Thermoreversibility of organogel

The thermoreversibility of polyurethane gel was examined by measuring gel-sol-gel transition temperature ($T_{\text{gel-sol-gel}}$), which was measured by DSC and rheology. Initially, thermoreversibility of polyurethane organogel was investigated by inverted vial method and further confirmed by rheology. **Figure 4c.5** shows DSC thermogram of polyurethane organogel with 3 wt. % concentration in DMF. In the first heating cycle, an

endothermic process took place in the range of 50-65 °C with sharp peak observed at 56 °C. However, neither endothermic nor exothermic peak was observed in cooling and second heating cycle, which indicated that sol cannot be reconstructed rapidly back in to the gel during timescale of DSC experiment.

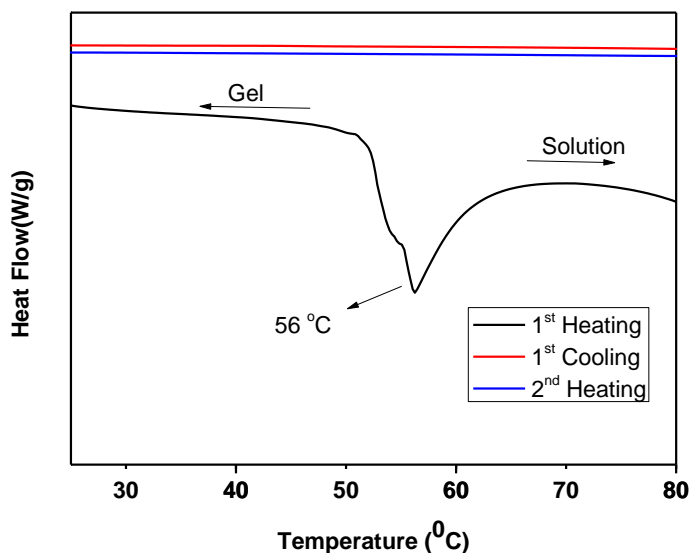


Figure 4c.5 DSC curves of polyurethane (PU-1) organogel.

In inverted vial method, thermoreversibility of polyurethane gel was determined by heating the gel in temperature controlled water bath at 60 °C until tube inversion showed that gel get converted into solution (~ 5 min) (**Figure 4c.2**). This solution was kept at room temperature for 5 h and the reformation of gel was observed..

4c.3.4 Rheological studies of polyurethane gel

4c.3.4.1 Viscoelastic property

The linear viscoelastic regime of the polyurethane organogel was determined by performing amplitude experiments sweep measurements at 25 °C (**Figure 4c.6a**). Results of the amplitude sweep showed that storage modulus (G') of the gel was independent of the applied strain over the range 10^{-5} to 0.1 %. At lower strain (from 10^{-5} to 10^{-3} %), G'' showed few scattered data points, which may be due to the detection limit of rheometer in this range. A frequency sweep measurement (**Figure 4c.6b**) at constant strain (0.05 %) and temperature (25 °C) showed that storage modulus (G') of polyurethane gel was independent of the frequency in the studied range. These results point towards a mechanically stable gel with elastic network⁴³.

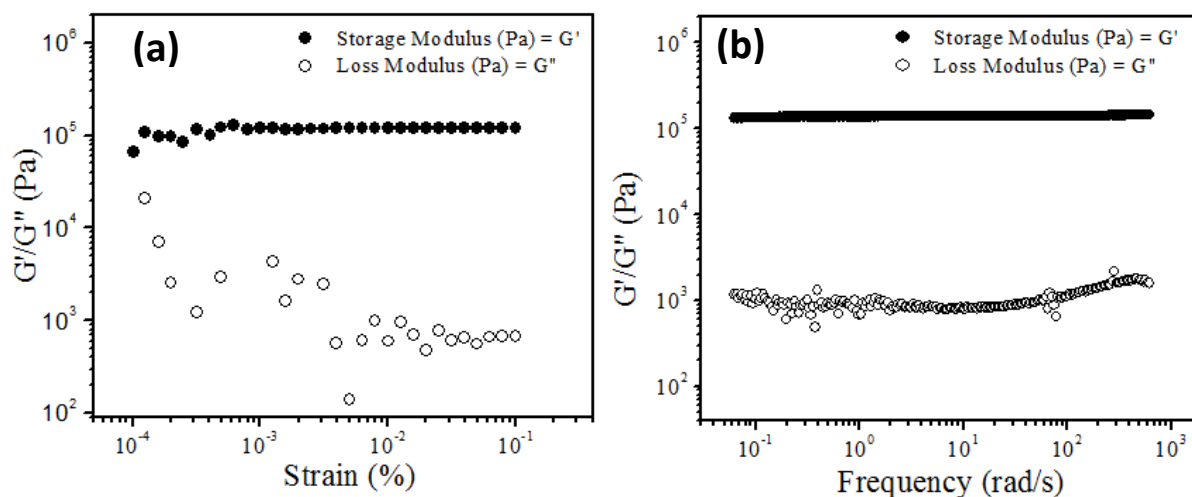


Figure 4c.6 (a) Amplitude and (b) frequency sweep measurements of polyurethane gel in DMF (3 wt. %)

4c.3.4.2 Effect of concentration

Storage modulus (G') of polyurethane gels in DMF was studied in the concentration range of 0.5-3.0 wt %. It is worth noting that even at 0.5 wt % concentration the formation of gel was observed. The storage modulus as a function of concentration is shown in **Figure 4c.7**. Polyurethane gel with 3.0 wt % concentration showed a modulus of the order of 10^5 Pa. These observations point towards the presence of intra-molecular interactions such as hydrogen bonding, hydrophobic interactions, etc and inter-molecular interactions between polyurethane chain and solvent molecules exist in the system.

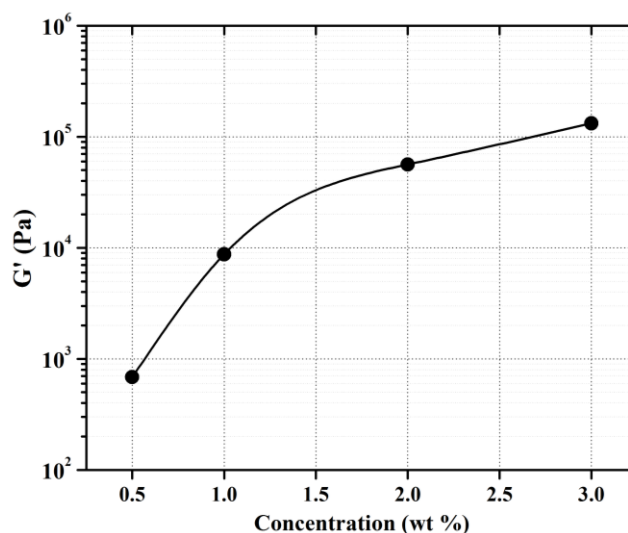


Figure 4c.7 Plot of the storage modulus (G') versus concentration of polyurethane gels prepared in DMF.

4c.3.4.3 Thermo-reversibility of gels

The flow behavior of polyurethane organogels as a function of temperature and time was studied by rheological measurements. **Figure 4c.8** shows histogram of the storage modulus (G') and loss modulus (G'') recorded during heating and cooling cycles (from 25 °C to 80 °C and back) as a function of time. During the heating cycle, the temperature was increased at the rate of 0.25 °C min⁻¹ from 25 to 80 °C.

Elastic nature of gel dominates when $G' > G''$, whereas the viscous nature is dominant in the sol state which is $G'' > G'$. Generally, gel-to-sol or sol-to-gel transition is depicted as $G' = G''$, where the transition from one domain to the other takes place⁴³.

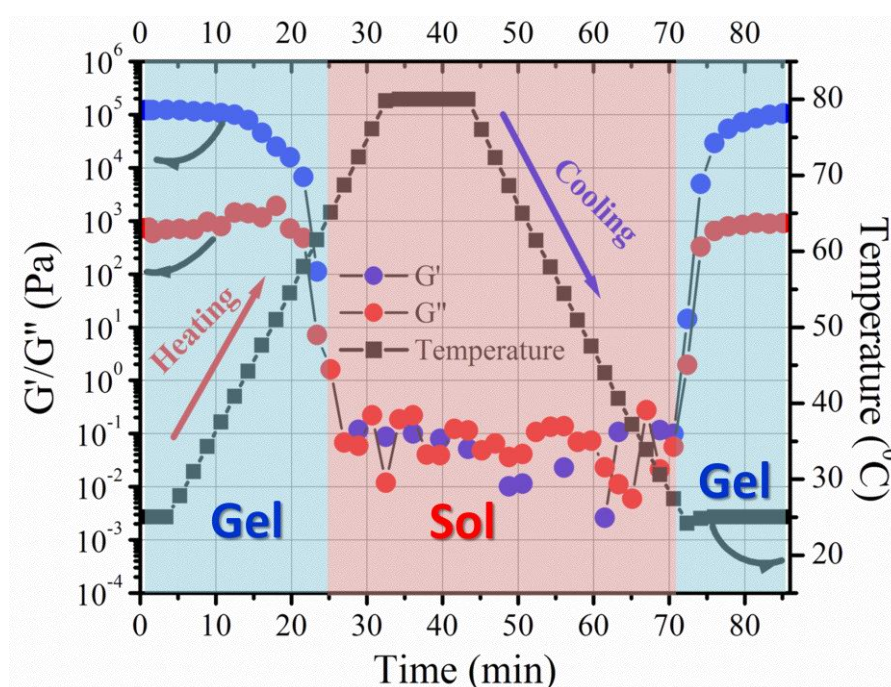


Figure 4c.8 Histogram of the gel-to-sol and sol-to-gel transition of polyurethane organogel in DMF (3 wt. %). Storage and loss modulus is plotted as a function of temperature and time.

Initially, before the heating cycle, polyurethane gel exhibited a modulus of the order of 10^5 Pa at 25 °C. During heating, storage modulus reduced gradually, and gel transitioned to the sol state. The transition from gel to sol occurred at 57 °C. This transition is calculated from the tangent of G' and G'' during the heating cycle. DSC results also supported this transition temperature (56 °C) (**Section 4c.3.3**). At the end of the heating cycle, the temperature was kept on hold at 80 °C for ten minutes. At this stage, the system remained in sol state. This hold time at 80 °C is required to ensure the complete transition from gel to sol state. At 80 °C, interactions between solvent and

polymer were minimized. In the cooling cycle, the temperature was reduced from 80 °C to 25 °C at the ramp rate of 0.25 °C min⁻¹. During the cooling, storage modulus increased and sol to gel transition was observed at 30.1 °C. Finally, at the end of the cooling cycle, the gel was kept on hold at 25 °C for ten minutes.

4c.3.5 Dye-sensitized solar cells (DSSC)

In the recent past, solar energy has emerged as the most practical and viable alternative to conventional fossil-based energy sources. To utilize solar energy for a variety of applications it is necessary to convert it into electricity using photovoltaic cells. The concept and architecture of dye sensitized solar cell (DSSC) is of significant interest and has captured tremendous attention ever since it was discovered by Grätzel *et al.* in 1991⁴⁴. DSSCs are considered as potential candidates to substitute the silicon based solar cells on account of their rationally facile processing methodology, amenable to scale-up, attractive performance to cost ratio, applicability under diffuse light and possibility of their effective functioning even on flexible substrates. The four major components present in DSSC include: semiconducting electrode, dye sensitizer, redox mediator and counter electrode^{45,46} (Figure 4c.9).

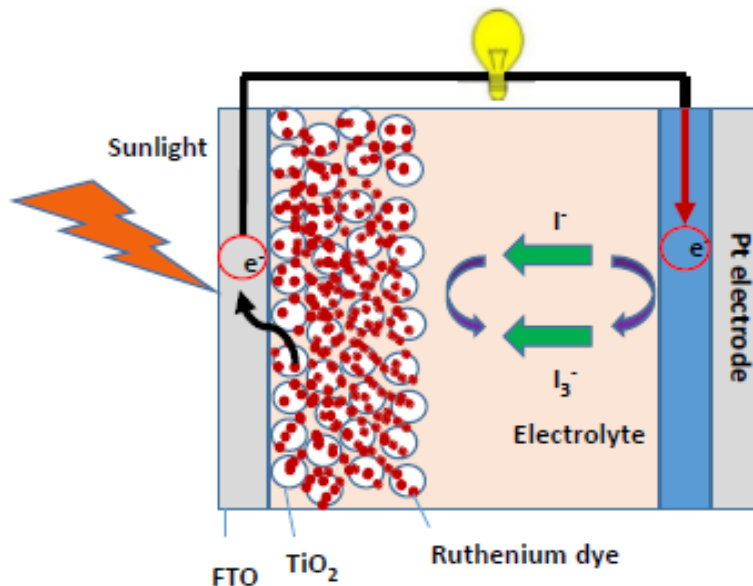
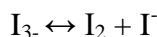
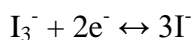


Figure 4c.9 Schematic representation of the components of DSSC

The redox electrolyte is one of the important components of DSSCs and is very crucial to the performance and long-term stability of DSSCs. The redox reactions involved for commonly used iodide/tri-iodide redox couple are:



This redox couple is generally prepared by dissolving iodine and lithium iodide in a suitable solvent. The liquid state of the redox electrolyte ensures intimate contact of TiO₂/dye and electrolyte forming a good interface which facilitates the dye regeneration process⁴⁷. Despite the fact that liquid electrolytes formed good interface, DSSCs are associated with drawbacks in terms of long term use and practicality. The fabrication and sealing procedure of DSSCs involves tedious task of injecting liquid redox electrolyte in DSSC assembly followed by sealing the hole from where the liquid electrolyte is injected. The liquid nature of redox electrolyte is disadvantageous because of its evaporation and leakage issues over the long period in DSSCs^{48,49}. To address these issues, efforts have been made towards replacing liquid electrolyte with solid state electrolytes such as p-type semiconductors⁵⁰, hole-conductors⁵¹, and polymeric materials incorporating the redox couple I₃⁻/I⁻⁵²⁻⁵⁵. However, the power conversion efficiencies for these types of electrolytes are still lower even if the long term stability is higher. These lower power conversion efficiencies can be primarily attributed to poor TiO₂/dye/electrolyte interface and lower ionic mobility in gel matrix.

To overcome the interface problems, the quasi-solid-state electrolytes based on organogels have attracted much attention in recent years⁵⁶⁻⁵⁸. These gel electrolytes have good ionic conductivity and pore-filling property, which are similar to the liquid electrolyte, and the network of the gel can reduce the leakage of the liquid electrolyte effectively to improve the long-term stability of DSSCs. A range of low molecular weight organogelators such as 12-hydroxystearic acid⁵⁹, cyclohexanecarboxylic acid-[4-(3-octadecylureido)phenyl]amide⁵⁷, 1-ethyl-3-methylimidazolium thiocyanate⁵⁸, and tetradodecylammonium bromide⁶⁰ were used for the fabrication of quasi-solid state dye sensitized solar cells. Polymeric gelators such as poly(ethylene oxide)-poly(vinylidene fluoride) (PEO-PVDF)⁶¹, poly(acrylonitrile) (PANI)⁶², poly(methyl acrylate) (PMA)⁶³, poly(methyl methacrylate) (PMMA)⁶⁴, and poly(vinylidene fluoride-co-hexafluoropropylene) (PVDF-HFP)⁵⁴ were also used for the fabrication of quasi-solid state DSSCs. Very recently, polyurethane-based organogel was used in DSSC and showed the power conversion efficiency 7.68 % with performance cut by only 15 % after 800 h⁶⁵. Inspired by this report, we undertook the studies dealing with evaluation of polyurethane organogelator in quasi-solid state DSSCs.

In the present work, polyurethane-based (PU-1) organogel was used as a gel electrolyte for DSSC. The thermoreversible nature of gel electrolyte offers an advantage in the fabrication and sealing procedure. Because of the reversibility, above T_{gel} the solution form of gel electrolyte can be easily injected in the DSSC forming a good $\text{TiO}_2/\text{dye}/\text{electrolyte}$ interface. When the gelation occurs in the gel electrolyte holds the redox couple efficiently, also maintaining the good interface.

The photovoltaic performance in terms of photocurrent density-voltage (J - V) curve of DSSC based on liquid and gel based electrolyte is shown **Figure 4c.10**.

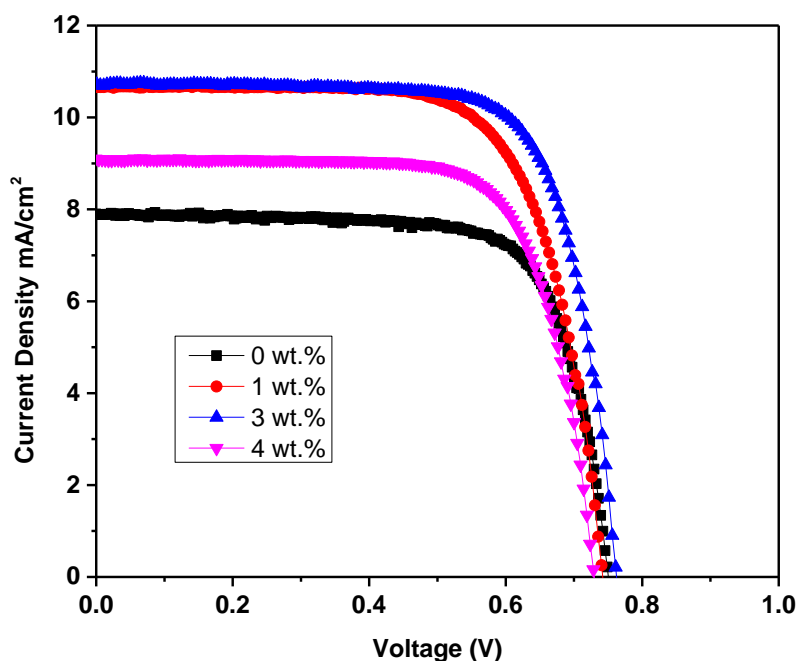


Figure 4c.10 Current–voltage characteristics of the DSSCs using liquid and polyurethane-based gel electrolytes.

The liquid electrolyte based controlled DSSC showed an efficiency of 4.5% whereas the polyurethane organogel-based electrolyte DSSC showed improved performance measured under an illumination of simulated AM 1.5 (100 mW cm^{-2}). When the concentration of polyurethane in DMF was varied, the efficiency was improved from 4.5% with 0 wt % of polyurethane to 6.2% with 3 wt % of polyurethane. When the polyurethane concentration was increased beyond 3 wt %, efficiency dropped down possibly due to hampered ionic mobility in a comparatively higher viscous gel matrix. The J - V parameters of DSSC are shown in **Table 4c.2**. The best performance DSSC

delivered efficiency of 6.2% with open circuit voltage (V_{oc}) of 0.76 V, short circuit current (J_{sc}) of 10.7 mA/cm² and fill factor (FF) of 74%.

Table 4c.2 Photovoltaic performance parameters of DSSC based on liquid electrolyte and polyurethane-based gel electrolyte with variable gelator concentration.

Gelator concentration (wt.%)	V_{oc} (V)	J_{sc} (mA/cm ²)	Fill Factor (FF)	Efficiency (%)
0	0.75	7.8	73	4.5
1	0.74	10.6	70	5.7
3	0.76	10.7	74	6.2
4	0.72	9.0	72	5.0

The stability performance of the optimized gelator concentration is shown in **Figure 4c.11**. After 12 days it showed efficiency of 6.1% indicating significant retention (98 %) in power conversion efficiency. The J - V parameters for stability data are shown in **Table 4c.3**.

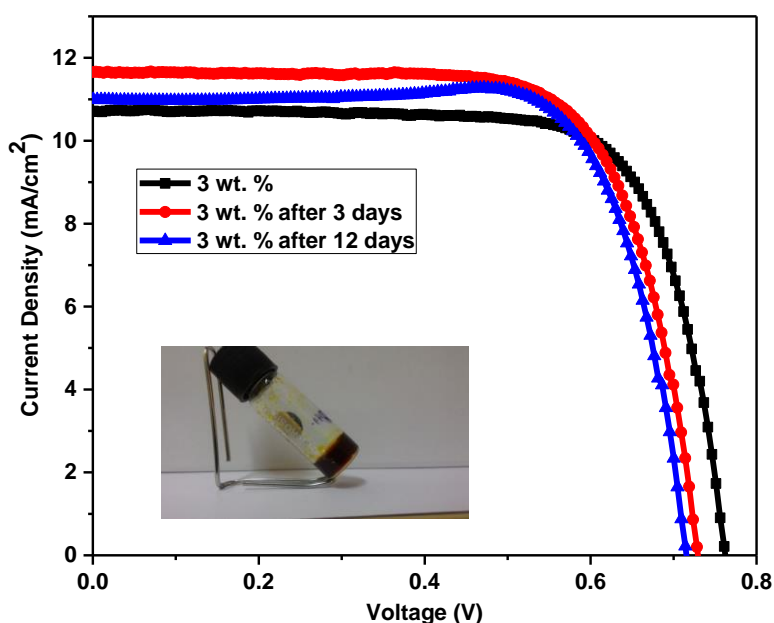


Figure 4c.11 Current–voltage characteristics of DSSCs using 3 wt. % polyurethane-based gel electrolytes.

Table 4c.3 Photovoltaic performance parameters of DSSC using 3 wt. % polyurethane-based gel electrolyte.

Day	V_{oc} (V)	J_{sc} (mA/cm ²)	Fill Factor (FF)	Efficiency (%)
0	0.76	10.7	74	6.2
3	0.73	11.5	72	6.3
12	0.71	11.0	75	6.1

In summary, polyurethane-based organogel was successfully demonstrated as a gel electrolyte for quasi-solid state dye-sensitized solar cells. The results indicated that, polyurethane-based gel electrolyte showed better efficiency (6.3 %) than the corresponding liquid electrolyte (4.5 %). The power conversion efficiency retained over 98 % of its initial power conversion efficiency after 12 days.

4c.4 Conclusions

- New polyurethane-based organogels were prepared in various polar organic solvents such as DMF, DMAc, DMSO, NMP and THF.
- Morphology of dry polyurethane-based organogel was studied by FE-SEM, which showed fibrous structure.
- The polyurethane-based organogel showed thermoreversibility and were confirmed by inverted vial method and rheology.
- Gel-sol-gel phase transition of 3 wt. % organogel in DMF was studied by rheology and DSC which showed gel-sol transition temperature of 57 °C and 56 °C, respectively.
- Utility of polyurethane-based organogel was demonstrated as a gel electrolyte for quasi-solid state dye-sensitized solar cells. The results indicated that, polyurethane-based gel electrolyte showed better efficiency (6.3 %) than the corresponding liquid electrolyte (4.5 %). The power conversion efficiency was retained over 98 % after 12 days.

References

- 1 S. Matsumoto, S. Yamaguchi, S. Ueno, H. Komatsu, M. Ikeda, K. Ishizuka, Y. Iko, K. V. Tabata, H. Aoki, S. Ito, H. Noji and I. Hamachi, *Chem. A Eur. J.*, 2008, **14**, 3977–3986.
- 2 S. I. Stupp, *Nano Lett.*, 2010, **10**, 4783–4786.
- 3 H. Maeda, *Chem. A Eur. J.*, 2008, **14**, 11274–11282.
- 4 S.-I. Kawano, N. Fujita and S. Seiji, *J. Am. Chem. Soc.*, 2004, **126**, 8592–8593.
- 5 P. Mukhopadhyay, Y. Iwashita, M. Shirakawa, S. Kawano, N. Fujita and S. Shinkai, *Angew. Chem. Int. Ed.*, 2006, **45**, 1592–1595.
- 6 T. Kato, Y. Hirai, S. Nakaso, M. Moriyama, N. Fujita, S. Shinkai, D. B. Amabilino, A. E. Rowan and R. J. M. Nolte, *Chem. Soc. Rev.*, 2007, **36**, 1857.
- 7 S. S. Babu, V. K. Praveen and A. Ajayaghosh, *Chem. Rev.*, 2014, **114**, 1973–2129.
- 8 M. O. M. Piepenbrock, G. O. Lloyd, N. Clarke and J. W. Steed, *Chem. Rev.*, 2010, **110**, 1960–2004.
- 9 J. H. Jung, M. Park, S. Shinkai, X. D. Uan, C. Li, Y. C. Wu, C. R. Martin, P. O. Brown, S. R. Paik and T. Hyeon, *Chem. Soc. Rev.*, 2010, **39**, 4286.
- 10 M. Moniruzzaman, A. Sahin and K. I. Winey, *Carbon*, 2009, **47**, 645–650.
- 11 M. D. Segarra-Maset, V. J. Nebot, J. F. Miravet and B. Escuder, *Chem. Soc. Rev.*, 2013, **42**, 7086–7098.
- 12 J. H. Jung, J. H. Lee, J. R. Silverman, G. John, J. A. K. Howard, J. W. Steed, J. H. Jung, S. Shinkai, K. A. Jolliffe, L. F. Lindoy and G. V. Meehan, *Chem. Soc. Rev.*, 2013, **42**, 924–936.
- 13 P. Terech and R. G. Weiss, *Chem. Rev.*, 1997, **97**, 3133–3160.
- 14 X. Yu, L. Chen, M. Zhang and T. Yi, *Chem. Soc. Rev.*, 2014, **43**, 5346.
- 15 N. Pilpel, *Chem. Rev.*, 1963, **63**, 221–234.
- 16 V. J. Bujanowski, D. E. Katsoulis and M. J. Ziemelis, *J. Mater. Chem.*, 1994, **4**, 1181.
- 17 T. Brotin, R. Utermöhlen, F. Fages, H. Bouas-Laurent and J. P. Desvergne, *J. Chem. Soc., Chem. Commun.*, 1991, 416–418.
- 18 A. Ajayaghosh and S. J. George, *J. Am. Chem. Soc.*, 2001, **123**, 5148–5149.
- 19 A. Ajayaghosh, S. J. George and V. K. Praveen, *Angew. Chem. Int. Ed.*, 2003, **42**, 332–335.
- 20 Y. C. Lin and R. G. Weiss, *Macromolecules*, 1987, **20**, 414–417.
- 21 K. Murata, M. Aoki, T. Suzuki, T. Harada, H. Kawabata, T. Komori, F. Ohseto, K.

- Ueda and S. Shinkai, *J. Am. Chem. Soc.*, 1994, **116**, 6664–6676.
- 22 J. Campbell, M. Kuzma and M. M. Labes, *Mol. Cryst. Liq. Cryst.*, 1983, **95**, 45–50.
- 23 K. Hanabusa, J. Tange, Y. Taguchi, T. Koyama and H. Shirai, *J. Chem. Soc. Chem. Commun.*, 1993, 390.
- 24 D. J. Abdallah and R. G. Weiss, *Langmuir*, 2000, **16**, 352–355.
- 25 D. J. Abdallah and R. G. Weiss, *Adv. Mater.*, 2000, **12**, 1237–1247.
- 26 R. Mukkamala and R. G. Weiss, *Langmuir*, 1996, **12**, 1474–1482.
- 27 L. Lu, T. M. Cocker, R. E. Bachman and R. G. Weiss, *Langmuir*, 2000, **16**, 20–34.
- 28 K. Hanabusa and M. Suzuki, *Polym. J.*, 2014, **46**, 776–782.
- 29 M. Kobayashi, T. Nakaoki and N. Ishihara, *Macromolecules*, 1990, **23**, 78–83.
- 30 C. Daniel, D. Alfano, G. Guerra and P. Musto, *Macromolecules*, 2003, **36**, 5742–5750.
- 31 C. Daniel, A. Avallone and G. Guerra, *Macromolecules*, 2006, **39**, 7578–7582.
- 32 A. Saiani and J.-M. Guenet, *Macromolecules*, 1997, **30**, 966–972.
- 33 A. Saiani, *Macromol. Symp.*, 2005, **222**, 37–48.
- 34 A. Pich, N. Schiemenz, V. Boyko and H.-J. P. Adler, *Polymer*, 2006, **47**, 553–560.
- 35 R. Tadmor, R. L. Khalfin and Y. Cohen, *Langmuir*, 2002, **18**, 7146–7150.
- 36 M. I. Gibson and N. R. Cameron, *Angew. Chem. Int. Ed.*, 2008, **47**, 5160–5162.
- 37 J. Da and T. E. Hogen-Esch, *Macromolecules*, 2003, **36**, 9559–9563.
- 38 D. Perahia, R. Traiphol and U. H. F. Bunz, *J. Chem. Phys.*, 2002, **117**, 1827–1832.
- 39 P. S. Wang, H. H. Lu, C. Y. Liu and S. A. Chen, *Macromolecules*, 2008, **41**, 6500–6504.
- 40 J. H. Chen, C. S. Chang, Y. X. Chang, C. Y. Chen, H. L. Chen and S. A. Chen, *Macromolecules*, 2009, **42**, 1306–1314.
- 41 M. Yoshida, N. Koumura, Y. Misawa, N. Tamaoki, H. Matsumoto, H. Kawanami, S. Kazaoui and N. Minami, *J. Am. Chem. Soc.*, 2007, **129**, 11039–11041.
- 42 T. Mondal and S. Ghosh, *J. Polym. Sci. Part A Polym. Chem.*, 2014, **52**, 2502–2508.
- 43 Y. Osada, in *Gels Handbook*, Elsevier, 2001, vol. 1, pp. 13–25.
- 44 B. O'Regan and M. Grätzel, *Nature*, 1991, **353**, 737–740.
- 45 A. Hagfeldt, G. Boschloo, L. Sun, L. Kloo and H. Pettersson, *Chem. Rev.*, 2010, **110**, 6595–6663.
- 46 J. Wang, K. Liu, L. Ma and X. Zhan, *Chem. Rev.*, 2016, **116**, 14675–14725.

- 47 J. Wu, Z. Lan, J. Lin, M. Huang, Y. Huang, L. Fan and G. Luo, *Chem. Rev.*, 2015, **115**, 2136–2173.
- 48 Z. Yu, N. Vlachopoulos, M. Gorlov, L. Kloo, W. Jaegermann, G. Tulloch, N. T. Oanh, T. Stergiopoulos, I. Arabatzis and M. Grätzel, *Dalt. Trans.*, 2011, **40**, 10289-10303.
- 49 M. Wang, C. Grätzel, S. M. Zakeeruddin, M. Grätzel, W. T. Huck, H. J. Snaith, R. H. Friend, M. Nazeeruddin, M. Grätzel, M. McGehee, E. H. Sargent and M. Grätzel, *Energy Environ. Sci.*, 2012, **5**, 9394-9405.
- 50 G. R. R. A. Kumara, A. Konno, G. K. R. Senadeera, P. V.V. Jayaweera, D. B. R. De Silva and K. Tennakone, *Sol. Energy Mater. Sol. Cells*, 2001, **69**, 195–199.
- 51 M. Grätzel, U. Bach, D. Lupo, P. Comte, J. E. Moser, F. Weissörtel, J. Salbeck and H. Spreitzer, *Nature*, 1998, **395**, 583–585.
- 52 M. A. K. L. Dissanayake, L. R. A. K. Bandara, R. S. P. Bokalawala, P. A. R. D. Jayathilaka, O. A. Ileperuma and S. Somasundaram, *Mater. Res. Bull.*, 2002, **37**, 867–874.
- 53 O. A. Ileperuma, M. A. K. L. Dissanayake and S. Somasundaram, *Electrochim. Acta*, 2002, **47**, 2801–2807.
- 54 P. Wang, S. M. Zakeeruddin, I. Exnar, M. Grätzel, P. Quagliotto, C. Barolo, G. Viscardi and M. Grätzel, *Chem. Commun.*, 2002, **18**, 2972–2973.
- 55 T. Asano, T. Kubo and Y. Nishikitani, *J. Photochem. Photobiol. A Chem.*, 2004, **164**, 111–115.
- 56 P. Wang, S. M. Zakeeruddin, J. E. Moser, M. K. Nazeeruddin, T. Sekiguchi and M. Grätzel, *Nat. Mater.*, 2003, **2**, 402–407.
- 57 Q. Yu, C. Yu, F. Guo, J. Wang, S. Jiao, S. Gao, H. Li, L. Zhao, S. M. Zakeeruddin and M. Grätzel, *Energy Environ. Sci.*, 2012, **5**, 6151.
- 58 N. Mohmeyer, D. Kuang, P. Wang, H. W. Schmidt, S. M. Zakeeruddin, M. Grätzel, S. J. Yanagida, M. Grätzel and A. Fujishima, *J. Mater. Chem.*, 2006, **16**, 2978–2983.
- 59 Z. Huo, S. Dai, C. Zhang, F. Kong, X. Fang, L. Guo, W. Liu, L. Hu, X. Pan and K. Wang, *J. Phys. Chem. B*, 2008, **112**, 12927–12933.
- 60 Z. Huo, C. Zhang, X. Fang, M. Cai, S. Dai and K. Wang, *J. Power Sources*, 2010, **195**, 4384–4390.
- 61 Y. Yang, C. Zhou, S. Xu, H. Hu, B. Chen, J. Zhang, S. Wu, W. Liu and X. Zhao, *J. Power Sources*, 2008, **185**, 1492–1498.

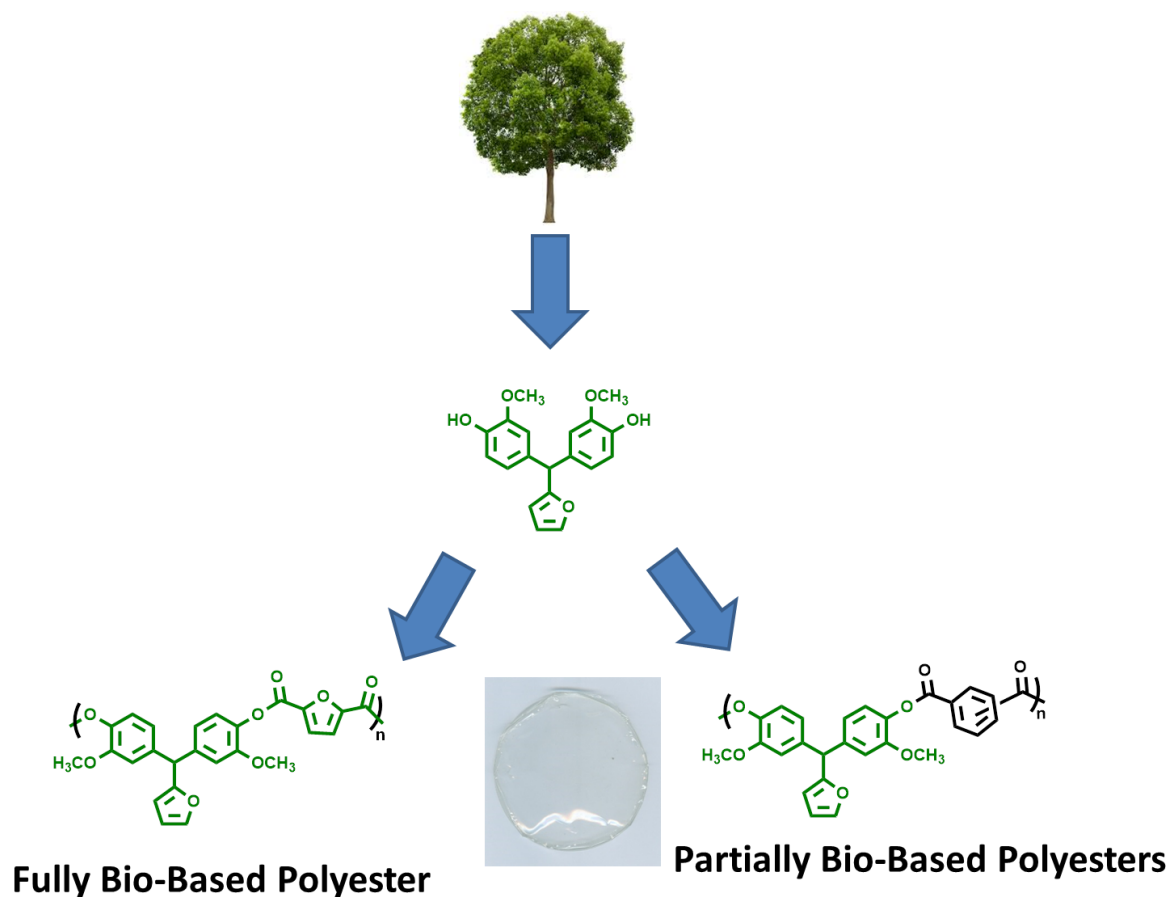
-
- 62 G. Wang, X. Zhou, M. Li, J. Zhang, J. Kang, Y. Lin, S. Fang and X. Xiao, *Mater. Res. Bull.*, 2004, **39**, 2113–2118.
- 63 C. W. Tu, K. Y. Liu, A. T. Chien, C. H. Lee, K. C. Ho and K. F. Lin, *Eur. Polym. J.*, 2008, **44**, 608–614.
- 64 H. Yang, M. Huang, J. Wu, Z. Lan, S. Hao and J. Lin, *Mater. Chem. Phys.*, 2008, **110**, 38–42.
- 65 P. Y. Chuang, L. Y. Chang, C. N. Chuang, S. H. Chen, J. J. Lin, K. C. Ho and K. H. Hsieh, *J. Polym. Res.*, 2016, **23**, 214.

Chapter - 5

Aromatic Polyesters and Polycarbonates Containing Pendant Furyl Groups

Chapter - 5a

Synthesis and Characterization of Aromatic Polyesters Containing Pendant Furyl Groups



5a.1 Introduction

Aromatic polyesters are the polymers containing ester linkages in the backbone. The first fully aromatic polyester was reported by Conix *et al*¹. in 1957 by the reaction of aromatic dicarboxylic acid with bisphenol A. One hundred and forty different types of polyarylates were reported before commencement of the commercial production by Unitica in 1974² of the first polyarylate (U-polymer), which is a polyester based on bisphenol-A and tere/isophthalates. Aromatic polyesters have wide applications in automotive, aviation and electrical industries due to their excellent thermal stability and mechanical properties.

The monomers *viz.* bisphenols and aromatic diacids used for the synthesis of aromatic polyesters are mostly obtained from petroleum resources^{3,4}. Due to the dwindling petroleum resources and escalation in their cost, development of monomers useful for preparation of aromatic polyesters from renewable resources is an active area of research⁵⁻⁷. A range of fully or partially bio-based diacid/bisphenol monomers for semi-aromatic/aromatic polyesters have been synthesized from hydroxymethylfurfural, vanillic acid, syringic acid, ferulic acid, limonene, CNSL, etc⁵⁻¹⁸.

Additionally, aromatic polyesters encounter processing difficulties due to their high glass transition temperatures and poor solubility in common organic solvents. There have been several attempts that have been reported to obtain processable aromatic polyesters *via* introduction flexibilizing linkages, bulky groups or crank shaft/bent units in polymer backbone^{7,18-27}.

Recently, much attention is being paid towards the synthesis of functional polymers which can be used for chemical modifications so as to tune polymer properties²⁸⁻³⁰. One of the functional groups of great interest is the furyl group which is known to undergo facile Diels-Alder reaction with maleimides^{30,31}. Aliphatic polyesters containing clickable furyl groups have been the subject of intensive research owing to their suitability for preparation of self-healable and thermo-reversibly crosslinked polyesters³¹⁻⁴¹. To the best of our knowledge, aromatic polyesters containing pendant clickable furyl groups have not been explored yet.

The objective of the present work was to synthesize fully aromatic polyesters containing pendant furyl groups based on bisphenols derived from lignocellulose-derived aromatics. A series of aromatic polyesters were synthesized by phase transfer-catalysed interfacial polycondensation of bisphenols containing pendant furyl group *viz* 4, 4'-(furan-2-ylmethylene)bis(2,6-dimethoxyphenol) (BPF-1) and 4,4'-(furan-2-

ylmethylene)bis(2-methoxyphenol) (BPF-2) with three aromatic diacid chlorides *viz* 2,5-furan dicarboxylic acid chloride, isophthaloyl chloride and terephthaloyl chloride. Polyesters were characterized by inherent viscosity measurements, solubility tests, FT-IR, ¹H NMR and ¹³C NMR spectroscopy, X-ray diffraction, thermogravimetric analysis (TGA), differential scanning calorimetric studies (DSC) and tensile testing. The effects of structure aromatic diacid chloride and methoxy substituent on aromatic ring of bisphenols on thermal and mechanical properties of polyesters were investigated.

5a.2 Experimental

5a.2.1 Materials

Bisphenols containing pendant furyl group, namely, 4, 4'-(furan-2-ylmethylene)bis(2,6-dimethoxyphenol) (BPF-1) and 4,4'-(furan-2-ylmethylene)bis(2-methoxyphenol) (BPF-2) were synthesized as described in **Chapter 3**. Terephthaloyl chloride (TPC) and isophthaloyl chloride (IPC) were received from Sigma Aldrich (USA) and were purified by distillation under reduced pressure. 2,5-Furandicarboxylic acid chloride (FDAC) was synthesized from 2,5-furandicarboxylic acid (Sigma Aldrich, USA) using excess thionyl chloride in the presence of *N,N*-dimethylformamide (DMF) as the catalyst and was purified by distillation under reduced pressure. Benzyltriethylammonium chloride (BTEAC) was purchased from Sigma Aldrich (USA) and was used as received. Thionyl chloride, sodium hydroxide, chloroform, dichloromethane, tetrahydrofuran (THF), DMF, *N,N*-dimethylacetamide (DMAc), *N*-methyl-2-pyrrolidone (NMP) and dimethyl sulfoxide (DMSO) were purchased from Thomas Baker Ltd., Mumbai and were purified as per literature procedures⁴².

5a.2.2 Measurements

Inherent viscosity of polyesters was determined with 0.5 % (w/v) solution of polymer in chloroform at 30±0.1°C using Ubbelohde suspended level viscometer. Inherent viscosity was calculated using the equation

$$n_{inh} = \frac{2.303}{c} \times \log t/t_0$$

where, *t* and *t*₀ are flow times of polymer solution and solvent, respectively and *c* is the concentration of polymer solution

Molecular weights and dispersity values of polyesters were determined on Thermo-Finnigan make gel-permeation chromatography (GPC) using chloroform as an eluent at a

flow rate of 1 mL min⁻¹ at 25 °C. Sample concentration was 2 mg mL⁻¹ and narrow dispersity polystyrenes were used as calibration standards.

FT-IR spectra were obtained on a Perkin–Elmer Spectrum GX spectrometer using polymer film.

NMR spectra were recorded on a Bruker 200, 400 or 500 MHz spectrometer at resonance frequencies of 200, 400 or 500 MHz for ¹H NMR and 50, 100 or 125 MHz for ¹³C NMR measurements using CDCl₃ as a solvent.

Thermogravimetric analysis (TGA) was carried out on Perkin Elmer: STA 6000, at a heating rate of 10 °C min⁻¹ under nitrogen atmosphere.

Differential scanning calorimetric (DSC) analysis was performed using a DSC Q10 differential calorimeter from TA Instruments under nitrogen atmosphere (50 mL min⁻¹). Analyses were carried out in a temperature range between 30 and 250 °C using a heating rate of 10 °C min⁻¹.

X-Ray diffraction patterns of polyesters were recorded using dried polymer film on a Rigaku Dmax 2500 X-ray diffractometer at a tilting rate of 2° min⁻¹.

The tensile properties of the polyester films were measured using Rheometrics Scientifics (Model Mark IV) (UK) instrument with a clamp length of 10 mm at room temperature at a crosshead speed of 1.5 mm min⁻¹.

5a.2.3 General procedure for the synthesis of polyesters

Polymerization reaction was carried out in a 100 mL two-necked round bottom flask equipped with a mechanical stirrer. BPF-1/BPF-2 (2.59 mmol) was dissolved in 5.5 mL of 1M aqueous solution of sodium hydroxide. The reaction mixture was stirred at 10 °C for 1 h. Next, BTEAC (30 mg) was added to the reaction mixture and stirring was continued. After 30 min, the solution of diacid chloride (2.59 mmol) in 15 mL of dichloromethane was added to the reaction mixture at 5 °C and the mixture was stirred vigorously at 2000 rpm for 1 h. The reaction mixture was poured into hot water; the precipitated polymer was filtered and washed several times with water. The polymer was dissolved in chloroform and precipitated into methanol. The polymer was filtered, washed with methanol, and dried under reduced pressure at 50 °C for 24 h.

Synthesis of PE-1 by polycondensation of 4, 4'-(furan-2-ylmethylene)bis(2,6-dimethoxyphenol) with isophthaloyl chloride

IR: 1739 cm⁻¹; ¹H NMR (500 MHz, CDCl₃, δ/ppm): 3.74 (s, 12H), 5.45 (s, 1H), 6.07 (s, 1H), 6.36 (s, 1H), 6.49 (s, 4H), 7.42 (s, 1H), 6.65 (t, 1H), 8.47 (d, 2H), 9.08 (br. s, 1H);

^{13}C NMR (100 MHz, CDCl_3 δ/ppm): 51.2, 56.2, 105.7, 108.6, 110.3, 127.5, 130.0, 132.3, 135.0, 139.8, 142.1, 152.2, 156.0, 163.7.

Synthesis of PE-2 by polycondensation of 4, 4'-(furan-2-ylmethylene)bis(2,6-dimethoxyphenol) with terephthaloyl chloride

IR: 1739 cm^{-1} ; ^1H NMR (200 MHz, CDCl_3 , δ/ppm): 3.76 (s, 12H) 5.47 (s, 1H) 6.08 (d, 1H) 6.38 (br.s, 1H) 6.51 (s, 4H) 7.44 (d, 1H) 8.36 (s, 4H); ^{13}C NMR (100 MHz, CDCl_3 δ/ppm): 51.2, 56.2, 105.7, 108.6, 110.3, 127.5, 130.4, 133.5, 139.9, 142.1, 152.1, 155.8, 163.7

Synthesis of PE-3 by polycondensation of 4, 4'-(furan-2-ylmethylene)bis(2,6-dimethoxyphenol) with 2,5-furandicarboxylic acid chloride

IR: 1741 cm^{-1} ; ^1H NMR (200 MHz, CDCl_3 , δ/ppm): 3.74 (s, 12H), 5.43 (s, 1H), 6.04 (d, 1H), 6.36 (t, 1H), 6.45 (s, 4H), 6.42 (d, 1H), 7.47 (s, 1H); ^{13}C NMR (100 MHz, CDCl_3 δ/ppm): 51.1, 56.1, 105.6, 108.7, 110.3, 119.9, 126.7, 140.1, 142.2, 146.5, 152.1, 155.5, 155.7

Synthesis of PE-4 by polycondensation of 4,4'-(furan-2-ylmethylene)bis(2-methoxyphenol) with isophthaloyl chloride

IR: 1738 cm^{-1} ; ^1H NMR (500 MHz, CDCl_3 , δ/ppm): 3.76 (s, 6H), 5.50 (s, 1H), 6.03 (d, 1H), 6.35 (d, 1H), 6.80 (dd, 2H), 6.87 (s, 2H), 7.12 (d, 2H), 7.42 (d, 1H), 7.66 (t, 1H), 8.46 (d, 2H), 9.04 (t, 1H); ^{13}C NMR (100 MHz, CDCl_3 δ/ppm): 50.4, 55.9, 108.6, 110.2, 113.1, 121.0, 122.6, 125.9, 130.0, 135.0, 138.6, 140.5, 142.1, 151.1, 156.0, 163.8

Synthesis of PE-5 by polycondensation of 4,4'-(furan-2-ylmethylene)bis(2-methoxyphenol) with terephthaloyl chloride

IR: 1738 cm^{-1} ; ^1H NMR (500 MHz, CDCl_3 , δ/ppm): 3.78 (s, 6H), 5.52 (s, 1H), 6.05 (d, 1H), 6.37 (t, 1H), 6.83 (dd, 2H), 6.87 (d, 2H), 7.15 (d, 2H), 7.43 (s, 1H), 9.04 (s, 4H); ^{13}C NMR (125 MHz, CDCl_3 , δ/ppm): 50.5, 55.9, 108.6, 110.2, 113.2, 121.0, 122.6, 130.3, 133.7, 138.6, 140.5, 142.2, 151.1, 155.9, 163.9.

Synthesis of PE-6 by polycondensation of 4,4'-(furan-2-ylmethylene)bis(2-methoxyphenol) with 2,5-furandicarboxylic acid chloride

IR: 1740 cm^{-1} ; ^1H NMR (500 MHz, CDCl_3 , δ/ppm): 3.76 (s, 6H), 5.48 (s, 1H), 6.01 (d, 1H), 6.35 (s, 1H), 6.78 (dd, 2H), 6.82 (d, 2H), 7.11 (d, 2H), 7.46 (s, 3H); ^{13}C NMR (125

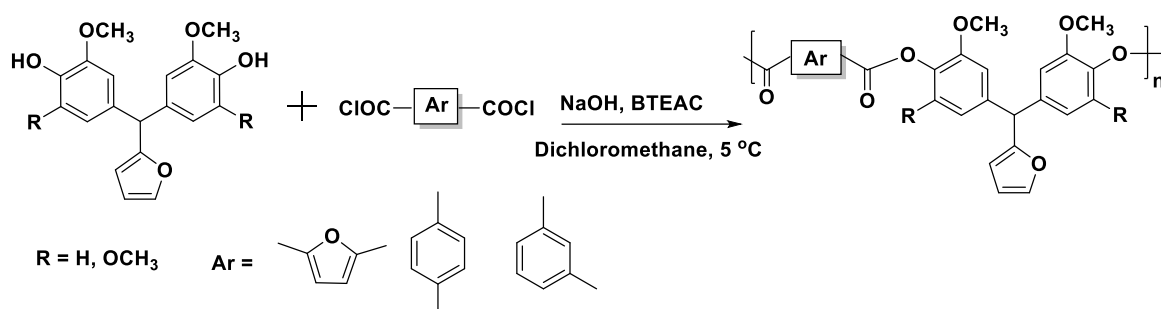
MHz, CDCl₃, δ/ppm): 50.3, 55.9, 108.6, 110.2, 113.2, 119.9, 121.0, 122.5, 137.7, 140.7, 142.1, 146.5, 150.9, 155.5, 155.7.

5a.3 Results and discussion

5a.3.1 Polyester synthesis

The two most widely studied routes for synthesis of aromatic polyesters are acid chloride and transesterification route. In the acid chloride route, diacids are converted into diacid chlorides followed by polycondensation with diphenols. Polymerization reactions can be performed by three methods 1) interfacial polymerization⁴³⁻⁴⁵ 2) low temperature solution polycondensation^{43,44} and 3) high temperature solution polycondensation⁴⁶. Transesterification reactions are carried out by three methods 1) reaction of diphenyl ester of aromatic dicarboxylic acid with diphenol^{47,48}, 2) reaction of aromatic dicarboxylic acid with diacetate derivative of diphenol^{49,50}, and 3) reaction of dialkylester of dicarboxylic acid with diacetate derivative of bisphenol⁵¹

In the present work, a series of aromatic polyesters were synthesized from bisphenols containing pendant furyl group and aromatic diacid chlorides *via* interfacial polycondensation route (**Scheme 5a.1**). Polymerization was carried out in a mixture of water and dichloromethane as the reaction medium and BTEAC as a phase transfer catalyst. 2,5-Furan dicarboxylic acid chloride was selected for the preparation of fully bio-based aromatic polyester while petroleum-derived IPC and TPC were used to study structure-property relationship. All the polyesters exhibited good solubility in organic solvents such as chloroform, dichloromethane, DMSO, DMAc and DMF.



Scheme 5a.1 Synthesis of aromatic polyesters from 4, 4'-(furan-2-ylmethylene)bis(2,6-dimethoxyphenol)/ 4,4'-(furan-2-ylmethylene)bis(2-methoxyphenol) and aromatic diacid chlorides

Inherent viscosities of polyesters were measured in chloroform and the values were found in the range 0.49-0.78 dLg⁻¹. GPC analysis indicated that number average

molecular weights (\overline{M}_n) and dispersities of polyesters were in the range 28,000-45,000 g mol⁻¹ and 1.9-2.8, respectively. GPC and inherent viscosity results showed the formation of reasonably high molecular weights of polyesters. Tough, transparent and flexible films could be cast from chloroform solutions of aromatic polyesters.

Table 5a .1 Synthesis of aromatic polyesters from 4, 4'-(furan-2-ylmethylene)bis(2,6-dimethoxyphenol)/4,4'-(furan-2-ylmethylene)bis(2-methoxyphenol) and aromatic diacid chlorides

Sr. No.	Polyester	Bisphenol	Diacid Chloride	η_{inh} (dLg ⁻¹) ^a	Molecular Weight ^b		
					\overline{M}_n	\overline{M}_w	Dispersity
1	PE-1	BPF-1	IPC	0.63	39,700	82,500	2.0
2	PE-2	BPF-1	TPC	0.49	28,000	77,700	2.7
3	PE-3	BPF-1	FDAC	0.65	45,000	86,700	1.9
4	PE-4	BPF-2	IPC	0.78	39,700	97,400	2.4
5	PE-5	BPF-2	TPC	0.60	30,000	82,300	2.7
6	PE-6	BPF-2	FDAC	0.62	34,800	97,440	2.8

a; η_{inh} was measured with 0.5 % (w/v) solution of polyester in chloroform at 30 ± 0.1 °C

b; measured by GPC in chloroform, polystyrene was used as calibration standard

5a.3.2 Structural characterization

The chemical structures of polyesters were confirmed by FT-IR and NMR spectroscopy. A representative FT-IR spectrum of polyester is reproduced in **Figure 5a.1**. Absorption bands appeared at 1734 cm⁻¹ and 1501 cm⁻¹ are assigned to carbonyl stretching of ester linkages and C=C stretching of furyl group, respectively. A representative ¹H NMR spectrum of polyester derived from BPF-1 and FDAC is shown in **Figure 5a.2**. A singlet at 7.47 δ ppm was assigned to protons of furan ring present in polymer backbone. The protons adjacent to the oxygen atom of furyl group exhibited a singlet at 7.42 δ ppm. The four aromatic protons 'c' appeared as a singlet at 6.45 δ ppm which indicates all protons are magnetically equivalent. A doublet at 6.04 δ ppm was assigned to proton 'e' of the pendant furyl group. Benzylic proton and methoxy group protons appeared as singlet at 5.43 δ ppm and 3.74 δ ppm, respectively.

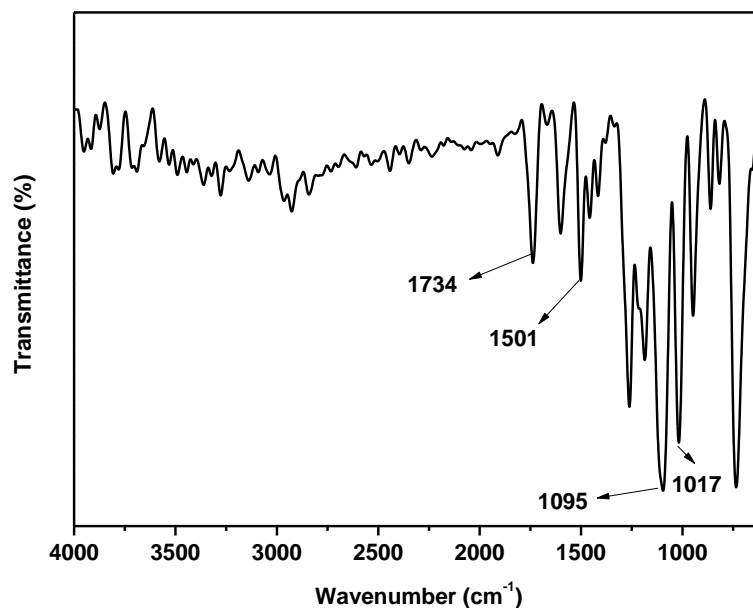


Figure 5a.1 FT-IR spectrum of polyester (PE-3) derived from 4,4'-(furan-2-ylmethylene)bis(2,6-dimethoxyphenol) and 2,5-furan dicarboxylic acid chloride

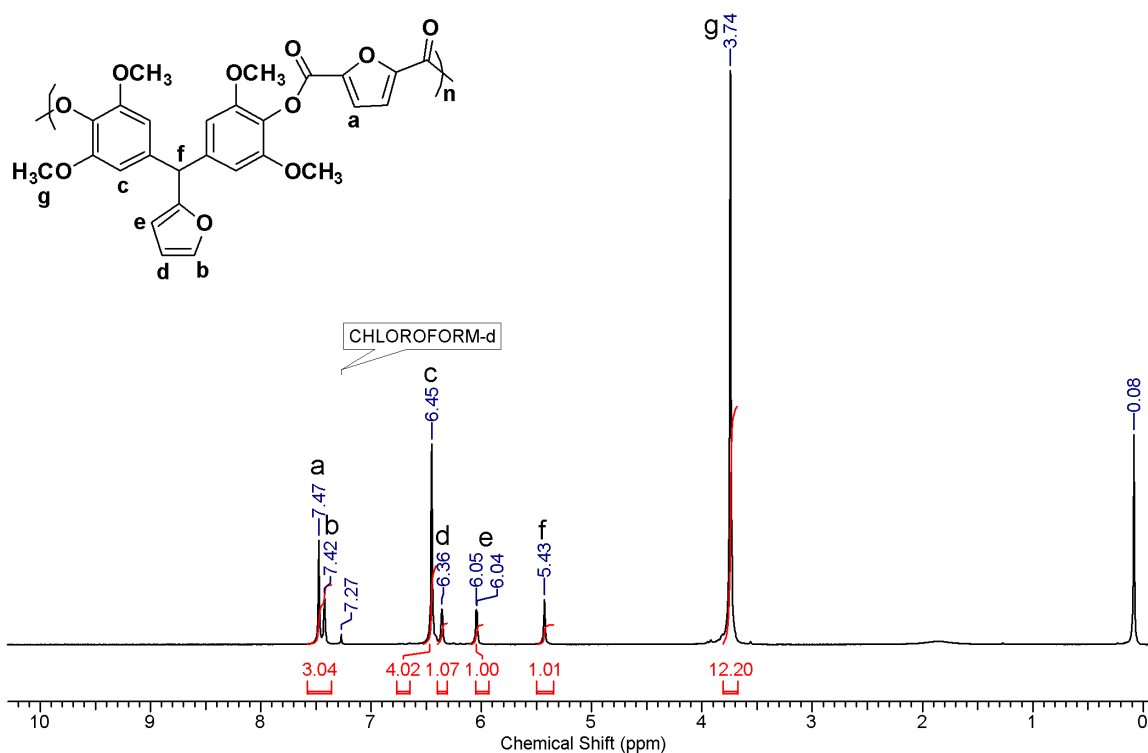


Figure 5a.2 ¹H NMR spectrum of polyester (PE-3) derived from 4,4'-(furan-2-ylmethylene)bis(2,6-dimethoxyphenol) and 2,5-furan dicarboxylic acid chloride in CDCl₃

^{13}C NMR spectrum of PE- 6 along with the peak assignments is shown in **Figure 5a.3**. The chemical shift of carbonyl carbon 'a' of ester group was observed at 155.7 δ ppm.

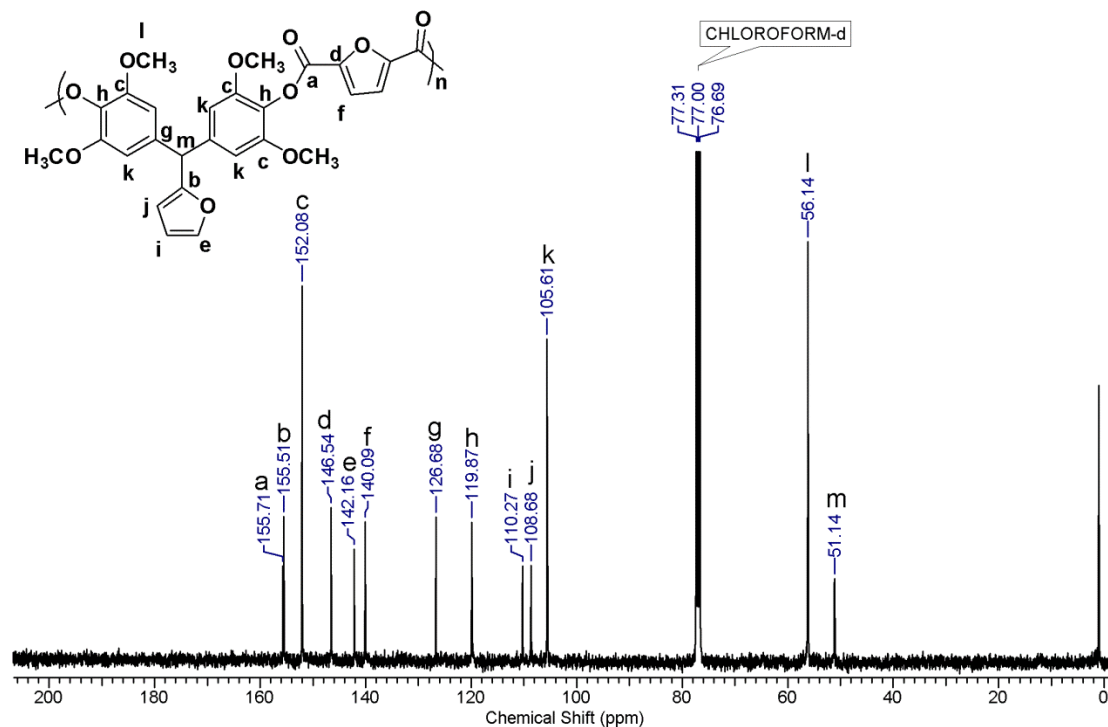


Figure 5a.3 ^{13}C NMR spectrum of polyester (PE-3) derived from 4,4'-(furan-2-ylmethylene)bis(2,6-dimethoxyphenol) and 2,5-furan dicarboxylic acid chloride in CDCl_3

5a.3.3 X-Ray diffraction studies

The crystallinity of polyesters results in their insolubility and is dependent on the structure of both the starting materials i.e. bisphenol and diacid chloride. It is reported that polymers possessing substituents on the backbone and/or pendant groups reduce the crystallinity and result into improvement in solubility characteristics^{19,55,56}. Wide-angle X-ray diffraction (WAXD) patterns of polyesters showed an amorphous halo over 2θ range $5\text{-}30^\circ$ (**Figure 5a.4**). The amorphous nature of polyesters could be attributed to the presence of methoxy substituents and pendant furyl groups which disturb the polymer chain packing.

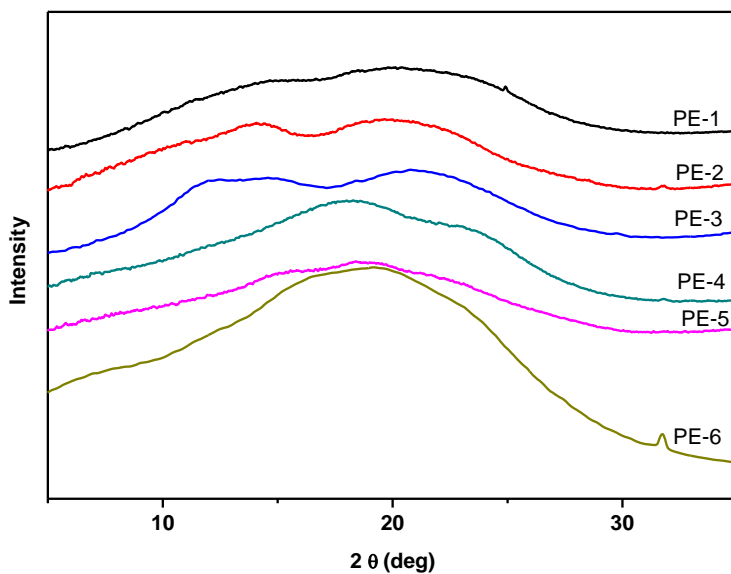


Figure 5a.4 X-Ray diffractograms of aromatic polyesters containing pendant furyl groups

5a.3.4 Thermal properties

Thermal stability of polyesters was analyzed by thermogravimetric analysis (TGA) under nitrogen atmosphere. TG curves of polyesters are shown in **Figure 5a.5** and data is listed in **Table 5a.2**. The 10 % weight loss of aromatic polyesters was found in the range 378-405 °C indicating their good thermal stability. A representative DTG curve of polyester PE-3 is reproduced in **Figure 5a.6**. Differential thermogravimetric analysis of polyesters showed a single stage degradation.

Table 5a.2 Thermal properties of polyesters derived from 4, 4'-(furan-2-ylmethylene)bis(2,6-dimethoxyphenol) and 4,4'-(furan-2-ylmethylene)bis(2-methoxyphenol) with aromatic diacid chlorides.

Sr. No.	Polyester	T ₁₀ (°C) ^a	Char yield (%) ^b	T _g (°C) ^c
1		398	40	204
2		390	33	214
3		386	38	190
4		401	42	164
5		405	45	178
6		378	35	160

a; temperature at which 10% weight loss was observed in TGA under nitrogen atmosphere;

b; weight residue at 800 °C;

c; measured by DSC on second heating scan with heating rate at 10 °C min⁻¹ under nitrogen atmosphere.

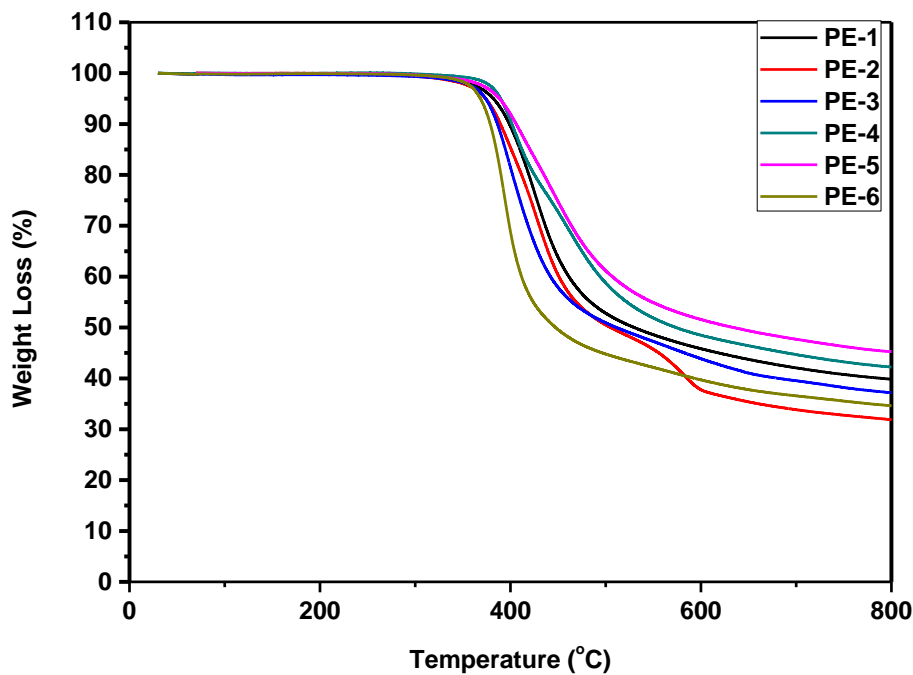


Figure 5a.5 TG curves of aromatic polyesters containing pendant furyl group

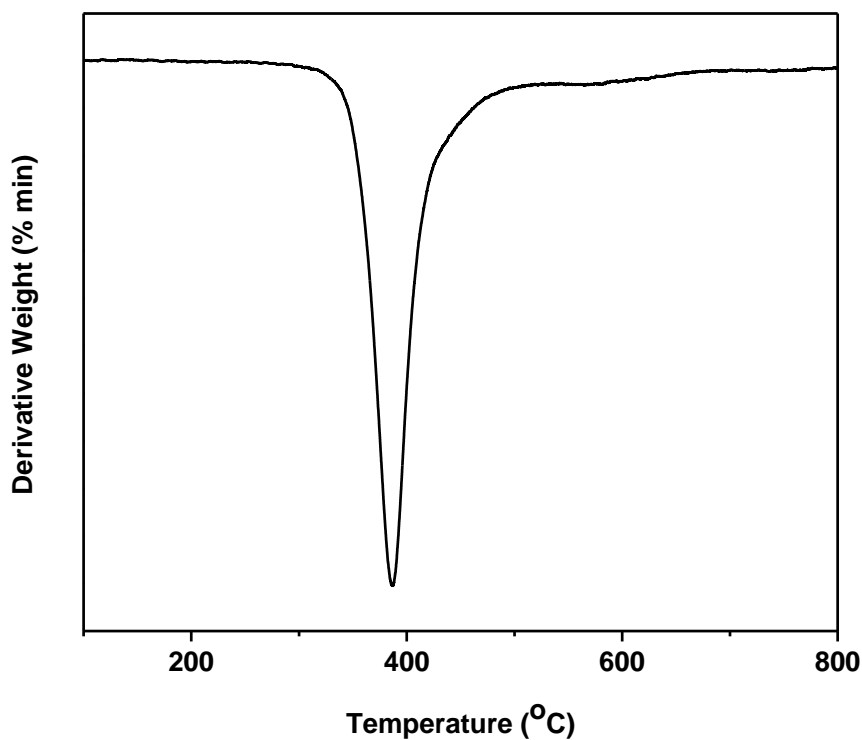


Figure 5a.6 DTG curve of aromatic polyester derived from 4, 4'-(furan-2-ylmethylene)bis(2,6-dimethoxyphenol) and 2, 5- furan dicarboxylic acid chloride

T_g values of polyesters were determined using differential scanning calorimetry (DSC) from 25-250 °C with heating rate 10 °C min⁻¹. The first heating cycle was employed to erase the thermal history and the second heating cycle was recorded for data analysis. DSC curves are reproduced in **Figure 5a.7** and results are included in **Table 5a.2**. It was observed that T_g values obtained for BPF-1 based polyesters with IPC, TPC and FDAC were higher than those of the corresponding polyesters based on BPF-2. This behavior is attributed to the presence of two methoxy substituents on aromatic ring in BPF-1 based polyesters which could increase the rotational barrier of the polymer chain leading to higher T_g values⁵². In both the series (BPF-1 and BPF-2 based), the T_g values decreased in the order TPC>IPC>FDAC. This trend clearly indicated that catenation in diacid chloride affects the T_g . The highest T_g values in both the series of TPC-based polyesters could be due to rigidity and linearity of the diacid chloride while the lowest T_g of FDAC-based polyesters could be attributed to non-linear character of FDAC. These structural features affect the packing of polymer chains and thus have an impact on T_g of polyesters. It is reported in the literature that FDAC-based aromatic-aliphatic polyesters exhibit higher T_g than corresponding IPC-based polymers^{53,54}. On the contrary, an opposite trend was observed in the case of aromatic polyesters synthesized in the present work. At this point of time, we do not have an explanation for this observation.

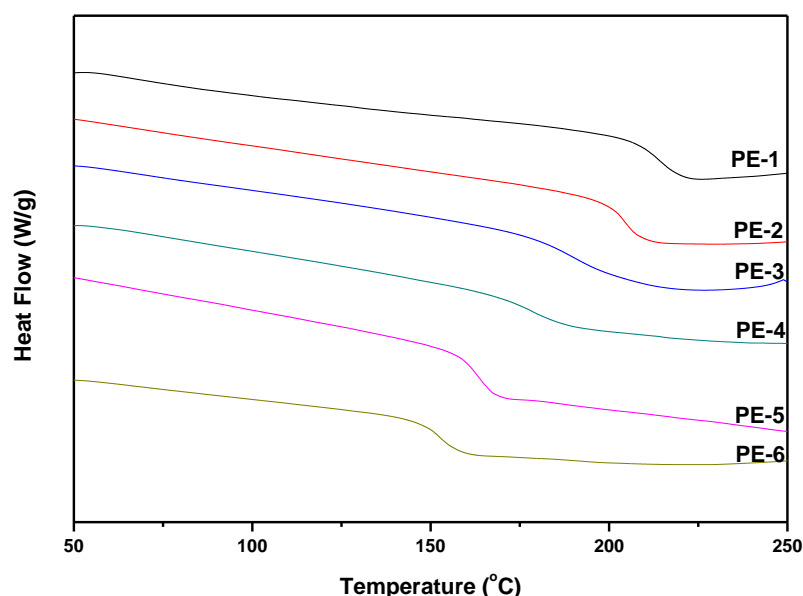
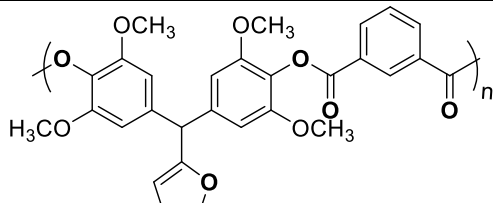
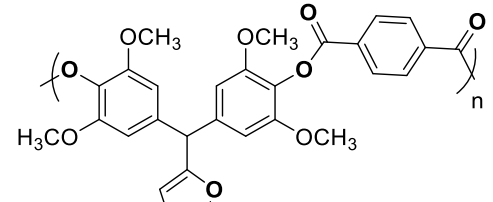
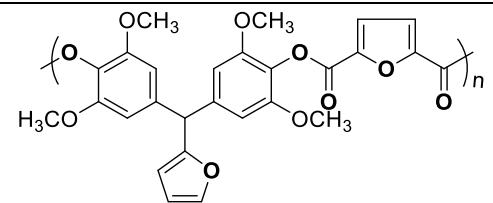
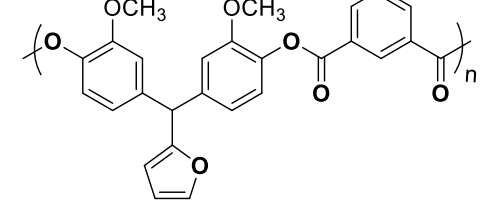


Figure 5a.7 DSC curves of aromatic polyesters containing pendant furyl groups

5a.3.5 Mechanical properties of polyesters

The mechanical properties of aromatic polyesters were evaluated using polyester films that were prepared by casting from their chloroform solutions. The strain-stress curves are shown in **Figure 5a.8**. The average values of three repeated measurements are collected in **Table 5a.3**. The nature of curves indicated the ductile nature of aromatic polyesters. Aromatic polyesters exhibited high tensile strength up to 70.8 MPa, Young's modulus up to 2.3 GPa and elongation at break up to 56.2 % which qualify them to be useful as structural materials in several applications. In both the series, IPC-derived polyesters exhibited higher elongation at break due to introduction of flexibility via *meta*-catenation

Table 5a.3 Mechanical properties of polyesters containing pendant furyl groups

Polyester Code	Polyester	Yield Point (MPa)	Young's Modulus (GPa)	Elongation at Break (%)
PE-1		64.6	2.11	34.1
PE-2		70.8	2.13	15.5
PE-3		63.3	1.91	19.9
PE-4		63.1	2.14	56.2

PE-5		68.3	2.38	29.8
PE-6		58.5	1.66	27.9

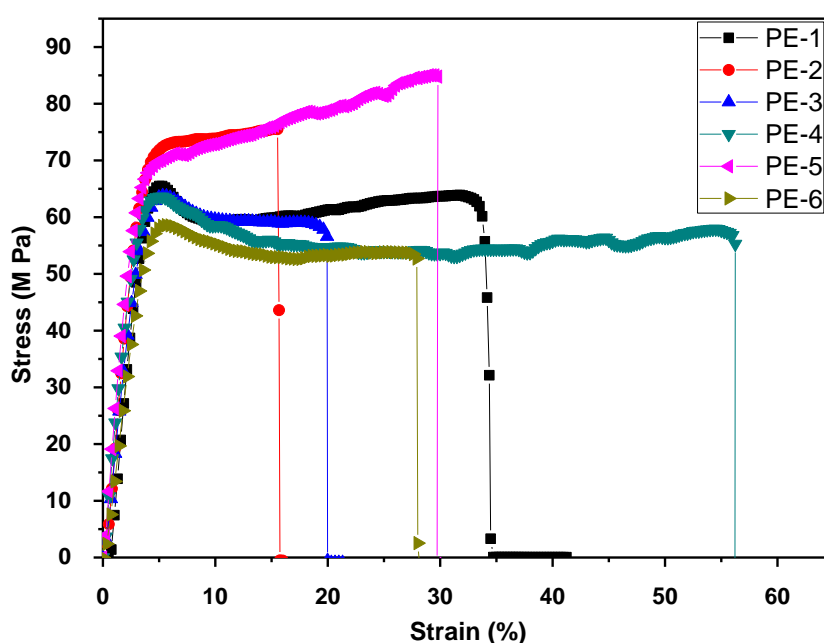


Figure 5a.8 Stress-strain curves of aromatic polyesters containing pendant furyl groups

The post modification studies of furyl containing polyesters are discussed in **Chapter 5c**.

5a.4 Conclusions

1. A series of aromatic polyesters containing pendant clickable furyl groups were synthesized from 4, 4'-(furan-2-ylmethylene)bis(2,6-dimethoxyphenol)/4,4'-(furan-2-ylmethylene)bis(2-methoxyphenol) and aromatic diacid chlorides *viz* 2,5-furan dicarboxylic acid chloride, isophthaloyl chloride and terephthaloyl chloride.
2. Inherent viscosities of aromatic polyesters were in the range of 0.49-0.78 dLg⁻¹ indicating formation of reasonably high molecular weight polymers.

3. Polyesters were found to be soluble in organic solvents such as chloroform, dichloromethane, DMSO, DMAc and DMF. This indicates that presence of methoxy substituents and pendant furyl groups played a significant role in the improvement in solubility of aromatic polyesters.
4. Tough, transparent and flexible films could be cast from the solutions of polyesters in chloroform.
5. Wide angle X-ray diffraction patterns showed that aromatic polyesters containing pendant furyl groups and methoxy substituents on aromatic rings were amorphous in nature.
6. T_{10} values of aromatic polyesters were in the range 378-405 °C indicating good thermal stability of polymers.
7. DSC analysis indicated that polyesters containing two methoxy substituents on aromatic ring showed higher T_g (190-214 °C) than the polymers containing one methoxy substituents on aromatic ring (160-178 °C).
8. Mechanical properties of aromatic polyesters were studied by tensile testing. Yield point and elongation at break were in the range 58.5-70.8 MPa and 15.5-56.2 % respectively, indicating their potential applications as structural materials.

References

- 1 A. J. Conix, *Ind. Chim. Belg.*, 1957, **22**, 1457–1462.
- 2 V. V. Korshak, in *Israel Program for Scientific Translations*, ed. Keter, London, 1971.
- 3 P. E. Cassidy, *Thermally stable polymers, synthesis and properties*, M. Dekker, New York, 1980.
- 4 M. Arroyo, in *Handbook of Thermoplastics*, ed. O. Olabisi, M. Dekker, New York, 2nd, 1997, pp. 417–449.
- 5 A. Gandini and T. M. Lacerda, *Prog. Polym. Sci.*, 2015, **48**, 1–39.
- 6 A. Llevot, E. Grau, S. Carlotti, S. Grelier and H. Cramail, *Macromol. Rapid Commun.*, 2016, **37**, 9–28.
- 7 C. Voirin, S. Caillol, N. V. Sadavarte, B. V. Tawade, B. Boutevin and P. P. Wadgaonkar, *Polym. Chem.*, 2014, **5**, 3142–3162.
- 8 A. Gandini, *Macromolecules*, 2008, **41**, 9491–9504.
- 9 F. Pion, P. H. Ducrot and F. Allais, *Macromol. Chem. Phys.*, 2014, **215**, 431–439.
- 10 L. Mialon, R. Vanderhenst, A. G. Pemba and S. A. Miller, *Macromol. Rapid*

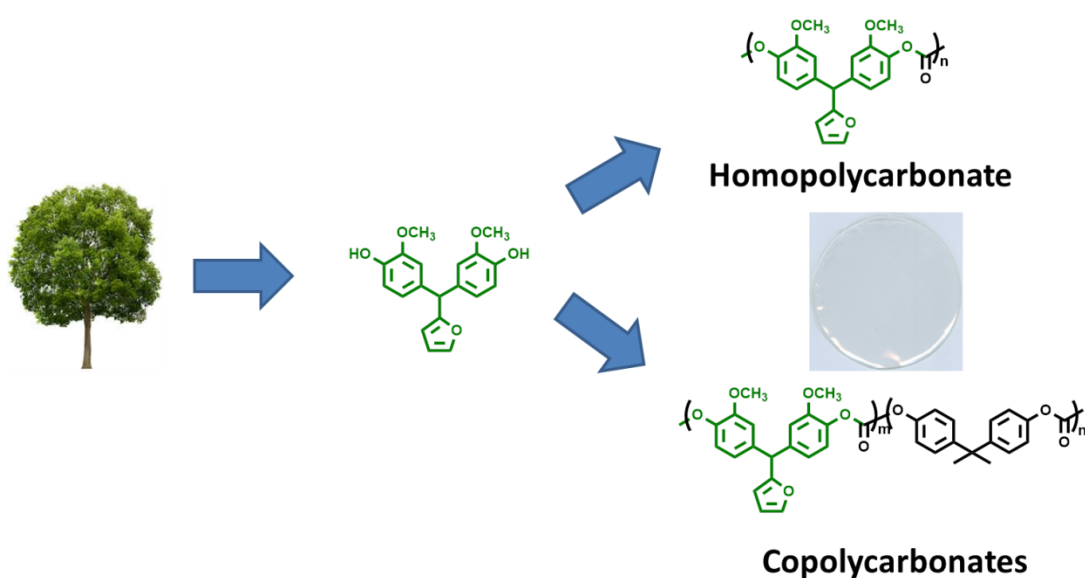
- Commun.*, 2011, **32**, 1386–1392.
- 11 L. Mialon, A. G. Pemba and S. A. Miller, *Green Chem.*, 2010, **12**, 1704.
 - 12 L. H. Bock and J. K. Anderson, *J. Polym. Sci.*, 1955, **17**, 553–558.
 - 13 H. R. Kricheldorf and G. Löhden, *Polymer*, 1995, **36**, 1697–1705.
 - 14 M. Nagata, *J. Appl. Polym. Sci.*, 2000, **78**, 2474–2481.
 - 15 Y. N. Sazanov, M. Y. Goykhman, I. V. Podeshvo, G. N. Fedorova, G. M. Mikhailov and V. V. Kudriavtsev, *J. Therm. Anal. Calorim.*, 1999, **55**, 721–726.
 - 16 M. Firdaus and M. A. R. Meier, *Eur. Polym. J.*, 2013, **49**, 156–166.
 - 17 B. V. Tawade, J. K. Salunke, P. S. Sane and P. P. Wadgaonkar, *J. Polym. Res.*, 2014, **21**, 617.
 - 18 D. Chatterjee, N. V. Sadavarte, R. D. Shingte, A. S. More, B. V. Tawade, A. D. Kulkarni, A. B. Ichake, C. V. Avadhani and P. P. Wadgaonkar, in *Cashew Nut Shell Liquid*, ed. P. Anilkumar, Springer International Publishing, Cham, 1st edn., 2017, pp. 163–214.
 - 19 S. H. Hsiao and H. W. Chiang, *Eur. Polym. J.*, 2004, **40**, 1691–1697.
 - 20 M. D. Joshi, A. Sarkar, O. S. Yemul, P. P. Wadgaonkar, S. V. Lonikar and N. N. Maldar, *J. Appl. Polym. Sci.*, 1997, **64**, 1329–1335.
 - 21 S. S. Vibhute, M. D. Joshi, P. P. Wadgaonkar, A. S. Patil and N. N. Maldar, *J. Polym. Sci. Part A Polym. Chem.*, 1997, **35**, 3227–3234.
 - 22 Y. T. Chern, *Macromolecules*, 1995, **28**, 5561–5566.
 - 23 Y. T. Chern and C. M. Huang, *Polymer*, 1998, **39**, 2325–2329.
 - 24 C. H. R. M. Wilsens, B. A. J. Noordover and S. Rastogi, *Polymer*, 2014.
 - 25 A. S. More, P. V. Naik, K. P. Kumbhar and P. P. Wadgaonkar, *Polym. Int.*, 2010, **59**, 1408–1414.
 - 26 A. S. More, S. K. Pasale, P. N. Honkhambe and P. P. Wadgaonkar, *J. Appl. Polym. Sci.*, 2011, **121**, 3689–3695.
 - 27 N. V. Sadavarte, M.R. Halhalli, C. V. Avadhani and P.P. Wadgaonkar, *Eur. Polym. J.*, 2009, **45**, 582–589.
 - 28 A. Qin, J. W. Y. Lam and B. Z. Tang, *Macromolecules*, 2010, **43**, 8693–8702.
 - 29 H. Nandivada, X. Jiang and J. Lahann, *Adv. Mater.*, 2007, **19**, 2197–2208.
 - 30 P. Theato and H. A. Klok, *Functional Polymers by Post-Polymerization Modification: Concepts, Guidelines, and Applications*, Wiley-VCH Verlag & Co. KGaA, Weinheim, Germany, 1st edn., 2013.
 - 31 A. Gandini, *Prog. Polym. Sci.*, 2013, **38**, 1–29.

- 32 C. Zeng, H. Seino, J. Ren, K. Hatanaka and N. Yoshie, *Polymer*, 2013, **54**, 5351–5357.
- 33 C. Zeng, H. Seino, J. Ren, K. Hatanaka and N. Yoshie, *Macromolecules*, 2013, **46**, 1794–1802.
- 34 A. Gandini and P. Hodge, *Macromolecules*, 1998, **1**, 314–321.
- 35 C. Varganici, O. Ursache, C. Gaina, V. Gaina, D. Rosu and B. C. Simionescu, *Ind. Eng. Chem. Res.*, 2013, **52**, 5287–5295.
- 36 A. Wang, H. Niu, Z. He and Y. Li, *Polym. Chem.*, 2017, **8**, 4494–4502.
- 37 F. Polgar, L. M. Duin, M. V Broekhuis, A. A. Picchioni, *Macromolecules*, 2015, **48**, 7096–7105.
- 38 Y. N. Yuksekdog, T. N. Gevrek and A. Sanyal, *ACS Macro Lett.*, 2017, **6**, 415–420.
- 39 Y. Zhang, A. A. Broekhuis and F. Picchioni, *Macromolecules*, 2009, **42**, 1906–1912.
- 40 D. Fournier and F. Du Prez, *Macromolecules*, 2008, **41**, 4622–4630.
- 41 M. Zhang, S. M. June and T. E. Long, *Polymer Science: A Comprehensive Reference* 2012, **5**, 7–47.
- 42 A. P. G. Kieboom, *Recl. des Trav. Chim. des Pays-Bas*, 1988, **107**, 685–685.
- 43 E. Bucio, J. W. Fitch, S. R. Venumbaka and P. E. Cassidy, *Polymer*, 2005, **46**, 3971–3974.
- 44 S. V. Vinogradova, V. A. Vasnev and P. M. Valetskii, *Russ. Chem. Rev.*, 1994, **63**, 833–851.
- 45 J. Preston, *Interfacial Synthesis. Volume 2: Polymer Applications and Technology*, California, 1977.
- 46 H. J. Jeong, K. Iwasaki, M. Kakimoto and Y. Imai, *Polym. J.*, 1994, **26**, 379–385.
- 47 F. Blaschike, W. Ludwing, Process for the preparation of linear thermoplastic mixed polyesters, US3395119 (A), 1968.
- 48 G. .M. Kosanovich, G. Salee, Semi or fully continuous process for polyester of bisphenol and dicarboxylic acid by transesterification polymerization and product thereof , US4465819 (A), 1984.
- 49 T. S. Chung, *Polym. Eng. Sci.*, 1986, **26**, 901–919.
- 50 E. E. Riecke and F. L. Hamb, *J. Polym. Sci. Polym. Chem. Ed.*, 1977, **15**, 593–609.
- 51 G. Bier, *Polymer*, 1974, **15**, 527–535.
- 52 A. G. Pemba, M. Rostagno, T. A. Lee and S. A. Miller, *Polym. Chem.*, 2014, **5**,

- 3214–3221.
- 53 F. Fenouillot, A. Rousseau, G. Colomines, R. Saint-Loup and J. P. Pascault, *Prog. Polym. Sci.*, 2010, **35**, 578–622.
- 54 S. K. Burgess, J. E. Leisen, B. E. Kraftschik, C. R. Mubarak, R. M. Kriegel and W. J. Koros, 2014.
- 55 D. J. Liaw, B. Y. Liaw, J. J. Hsu and Y. C. Cheng, *J. Polym. Sci. Part A Polym. Chem.*, 2000, **38**, 4451–4456.
- 56 Y. Chen, R. Wombacher, J. H. Wendorff and A. Greiner, *Polymer*, 2003, **44**, 5513–5520.

Chapter - 5b

Synthesis and Characterization of (Co)polycarbonates Containing Pendant Furyl Groups



5b.1 Introduction

Aromatic polycarbonates are polymers containing repeating carbonate groups (-O-CO-O-) in the polymer backbone. In 1953, Herman Schnell at Bayer, AG and Daniel Fox at GE independently reported aromatic polycarbonate based on bisphenol A¹. Polycarbonates exhibit high thermal stability, outstanding toughness, high flame retardancy, high dimensional stability, excellent optical properties, low water uptake and easy processability^{2,3}. The combination of these properties qualifies polycarbonates as suitable replacement for glass, wood, and other polymeric materials. Aromatic polycarbonates are useful in several applications such as electrical, optical, construction, household and consumer articles, medical devices, packaging, etc²⁻⁵.

Bisphenol-A (BPA) is the highest volume building block used for the synthesis of aromatic polycarbonates. Approximately, 5.4 million tonnes of BPA was produced worldwide in 2015⁶ and is extensively used for the synthesis of polycarbonates as well as polyesters, polyether sulfones, polyether ketones, cyanate esters, epoxy resins, etc^{7,8}. However, BPA is currently under scrutiny due to its potential health hazards and it has been banned for food packaging applications^{9,10}. Additionally, BPA is produced from petroleum-derived chemicals which are non-renewable. Because of the limited stocks, non-renewability and environmental issues associated with petroleum-derived chemicals, it has been recognized that sustainable and renewable resources should be used for polymer synthesis in the near future¹¹.

Over the past several years, researchers from academia and industries have been attempting to develop new sustainable bisphenols as a replacement for BPA. In this context, bio-based bisphenols starting from levulinic acid, limonene, cashew nut shell liquid (CNSL) and creosol have been reported¹²⁻¹⁹. However, it is unclear whether these bisphenols are endocrine disruptors or not. Trita et al. reported that CNSL-based bisphenol *viz.* 3,3'-dihydroxy-diphenylethane showed estrogenic activity in the same range as that of BPA¹⁸. In contrast, renewable bisphenols derived from eugenol, ferulic acid and guaiacol were found to be non-estrogenic¹⁸⁻²⁰. The non-estrogenic activity of these bisphenols was attributed to the presence of *ortho* methoxy group which might disrupt the hydrogen bonding interaction between the phenol and receptor site. Shetty et al. evaluated the effect of substituents on bisphenol on estrogenic activity and concluded that presence of *ortho* alkoxy substituents could reduce estrogenic activity of bisphenol²⁰.

The introduction of functional groups into polymers and subsequent post-modifications provides an efficient methodology to tailor the properties of polymers such as mechanical, thermal, crystallinity, hydrophilicity, etc²¹⁻²³. Such functionalized polymers broaden the application areas compared to the unfunctionalized precursor. A large number of reports are available on functional aliphatic polycarbonates^{24,25}. However, the reports on synthesis of functional aromatic polycarbonates are scanty except allyl^{26,27} and acid²⁸ functionalized aromatic polycarbonate

The present work deals with the synthesis of functional bio-based polycarbonates obtained by polycondensation of *ortho* methoxy substituted and pendant furyl containing bisphenol namely, 4,4'-(furan-2-ylmethylene)bis(2-methoxyphenol) (BPF-2) with triphosgene. Copolycarbonates were also prepared by polycondensation of varying compositions of BPF-2 and bisphenol-A with triphosgene. (Co)polycarbonates were characterized by inherent viscosity measurements, solubility tests, FT-IR, ¹H NMR and ¹³C NMR spectroscopy, X-ray diffraction, thermogravimetric analysis (TGA), differential scanning calorimetric studies (DSC) and tensile testing. The influence of BPF-2 monomer on the properties of copolycarbonates was investigated.

5b.2 Experimental

5b.2.1 Materials

Bisphenol containing pendant furyl group, namely, 4,4'-(furan-2-ylmethylene)bis(2-methoxyphenol) (BPF-2) was synthesized as described in **Chapter 3**. Triphosgene and bisphenol-A (BPA) were purchased from Sigma Aldrich (USA). Bisphenol A was sublimed before use. Triethyl amine, hydrochloric acid, chloroform, dichloromethane, tetrahydrofuran (THF), *N,N*-dimethylformamide (DMF), *N,N*-dimethylacetamide (DMAc), *N*-methyl-2-pyrrolidone (NMP) and dimethyl sulfoxide (DMSO) were procured from Thomas Baker Ltd., Mumbai. Triethyl amine and dichloromethane were dried over calcium hydride and distilled prior to use.

5b.2.2 Measurements

Inherent viscosity of polycarbonates was determined with 0.5 % (w/v) solution of polymer in chloroform at 30±0.1°C using Ubbelohde suspended level viscometer. Inherent viscosity was calculated using the equation

$$n_{inh} = \frac{2.303}{c} \times \log t/t_0$$

where, t and t_0 are flow times of polymer solution and solvent, respectively and c is the concentration of polymer solution

Molecular weights and dispersity values of polycarbonates were determined on Thermo-Finnigan make gel-permeation chromatography (GPC) using chloroform as an eluent at a flow rate of 1 mL min^{-1} at $25 \text{ }^\circ\text{C}$. Sample concentration was 2 mg mL^{-1} and narrow dispersity polystyrenes were used as calibration standards.

FT-IR spectra were obtained on a Perkin-Elmer Spectrum GX spectrometer using polymer film.

NMR spectra were recorded on a Bruker 200, 400 or 500 MHz spectrometer at resonance frequencies of 200, 400 or 500 MHz for ^1H NMR and 50, 100 or 125 MHz for ^{13}C NMR measurements using CDCl_3 as a solvent.

Thermogravimetric analysis (TGA) was carried out on Perkin Elmer: STA 6000, at a heating rate of $10 \text{ }^\circ\text{C min}^{-1}$ under nitrogen atmosphere.

Differential scanning calorimetric (DSC) analysis was performed using a DSC Q10 differential calorimeter from TA Instruments under nitrogen atmosphere (50 mL min^{-1}). Analyses were carried out in a temperature range between 30 and $250 \text{ }^\circ\text{C}$ using a heating rate of $10 \text{ }^\circ\text{C min}^{-1}$.

X-Ray diffraction patterns of polycarbonates were recorded using dried polymer films on a Rigaku Dmax 2500 X-ray diffractometer at a tilting rate of 2° min^{-1} .

The tensile properties of the polycarbonate films were measured using an Rheometrics Scientifics (Model Mark IV) (UK) instrument with a clamp length of 10 mm at room temperature at a crosshead speed of 1.5 mm min^{-1} .

5b.2.3 General procedure for the synthesis of (co)polycarbonates

Into a 100 mL three necked round bottom flask equipped with a nitrogen balloon, an addition funnel, and a magnetic stirrer were charged BPF-2/BPA (3 mmol) and dry dichloromethane (6 mL). The reaction mixture was cooled to $0 \text{ }^\circ\text{C}$ and the solution of triethyl amine (1.25 mL , 9 mmol) in dry dichloromethane (3 mL) was added dropwise over a period of 10 min . To the reaction mixture, the solution of triphosgene (373.9 mg , 1.26 mmol) in dichloromethane (3 mL) was added dropwise and stirred for at $0 \text{ }^\circ\text{C}$ 15 min . The reaction mixture was allowed to warm to $25 \text{ }^\circ\text{C}$ and stirring continued at that temperature for 4 h . The reaction mixture was neutralized with aqueous hydrochloric acid (2 M) and was extracted with dichloromethane ($2 \times 100 \text{ mL}$). The dichloromethane solution was washed with water ($2 \times 100 \text{ mL}$), dried over sodium sulfate, filtered and

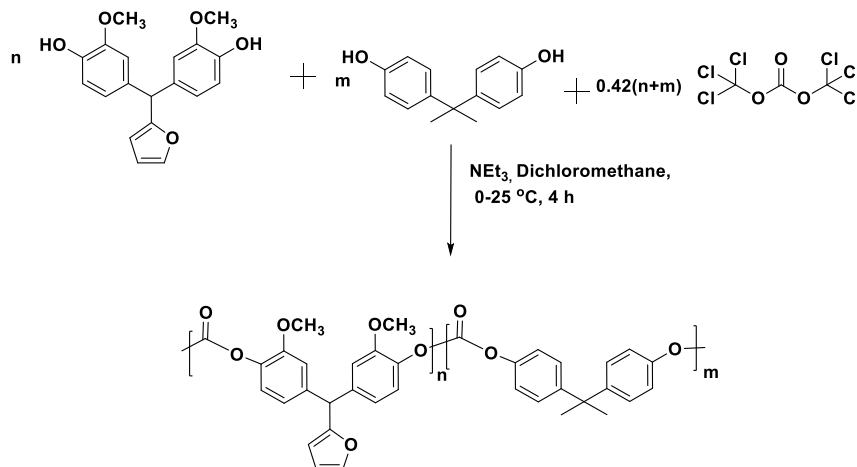
concentrated under reduced pressure at 30 °C. The concentrated polymer solution was poured into methanol (1000 mL) and the precipitated polymer was filtered and washed with methanol. The polymer was dissolved in dichloromethane (10 mL) and reprecipitated into methanol (1000 mL), filtered and dried at 100 °C under reduced pressure for 12 h.

5b.3 Results and discussion

5b.3.1 Synthesis of (co)polycarbonates

Aromatic polycarbonates are generally synthesized by two methods 1) reaction of bisphenol with phosgene by interfacial or solution polymerization and 2) reaction of bisphenol with diphenyl/dimethyl carbonate by melt polymerization. Phosgene is difficult to handle on the laboratory scale due to its high toxicity and gaseous nature. Triphosgene is a less hazardous substitute for phosgene with relatively equivalent reactivity and solid crystalline nature. Triphosgene is, therefore, preferred as a source of carbonate for the laboratory scale synthesis of polycarbonates^{29,30}.

In this study, aromatic (co)polycarbonates were synthesized by polycondensation of BPF-2 or a mixture of BPF-2 and BPA with triphosgene (**Scheme 5b.1**).



Scheme 5b.1 Synthesis of (co)polycarbonates from 4,4'-(furan-2-ylmethylene)bis(2-methoxyphenol) and/or bisphenol A with triphosgene.

Polymerization reactions were carried out in dichloromethane as a solvent (7-11, wt. % solid content) in the presence of triethyl amine as described in the experimental section (0 °C/15 min, 25 °C/4 h). No end capping agent was used in the polycarbonate synthesis. The molar stoichiometry of bisphenol:triphosgene employed was 1:0.42 which was based on the work of Boyles et al. who demonstrated the formation of high molecular

weight polycarbonates under such stoichiometric conditions³⁰. At the end of polymerization reactions, polycarbonates were isolated by precipitation in methanol and were purified by re-precipitation into excess methanol from chloroform solution. As a reference material, BPA-based polycarbonate *viz.* PC-5 was prepared using same reaction conditions. Results of synthesis of (co)polycarbonates are summarized in **Table 5b.1**

Table 5b.1 Synthesis of (co)polycarbonates from 4,4'-(furan-2-ylmethylene)bis(2-methoxyphenol) and/or bisphenol A with triphosgene.

Polycarbonate	BPF-2 (mol%)	BPA (mol%)	η_{inh} (dL/g) ^a	Molecular Weight ^b		Dispersity
				\overline{M}_n	\overline{M}_w	
PC-1	100	00	0.50	29,800	59,700	2.0
PC-2	50	50	0.72	43,800	93,700	2.1
PC-3	30	70	0.69	34,300	81,300	2.3
PC-4	10	90	0.59	32,400	84,200	2.6
PC-5	00	100	0.61	33,700	73,800	2.2

a; η_{inh} was measured with 0.5 % (w/v) solution of (co)polycarbonates in chloroform at 30 °C±1 °C

b; measured by GPC in chloroform, using polystyrenes as calibration standard

Inherent viscosity and number average molecular weights (\overline{M}_n) of (co)polycarbonates were in the range 0.50-0.72 dLg⁻¹ and 29,800-43,800 g mol⁻¹, respectively. The dispersity values for (co)polycarbonates were in the range 2.0-2.6 as can be expected for step growth polymerizations, The formation of reasonably high molecular weight polymers indicated that the presence of *ortho*-methoxy substituent does not impede the reactivity of BPF-2 in polycarbonate synthesis. All the (co)polycarbonates were readily soluble in organic solvents such as chloroform, dichloromethane, THF, DMSO, and DMAc and could be cast into transparent, tough and flexible films from their chloroform solutions. It is worth mentioning that polycarbonate based on BPF-2 contains 95 % renewable carbon as estimated from the theoretical amount of bio-based carbon in the polymer.

A representative GPC trace chromatogram of PC-2 is reproduced in **Figure 5b.1**. GPC chromatogram showed a Gaussian peak with a unimodal distribution and did not indicate the presence of any low molecular weight species.

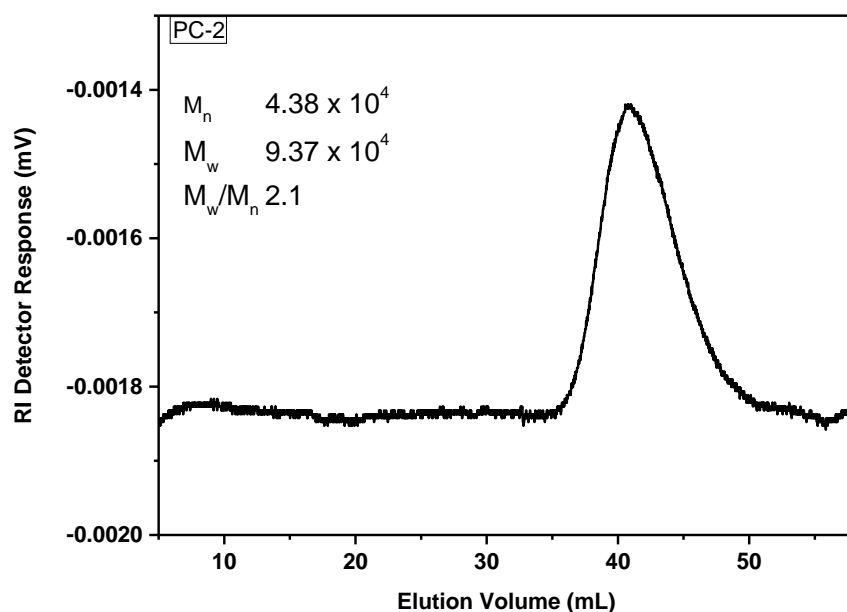


Figure 5b.1 GPC trace of polycarbonate (PC-2) derived from 4,4'-(furan-2-ylmethylene)bis(2-methoxyphenol): bisphenol A (50:50 mol. %) with triphosgene

5b.3.2 Structural characterization

The molecular structure determination of (co)polycarbonates was performed by FT-IR, ^1H NMR and ^{13}C NMR spectroscopy.

FT-IR spectrum of PC-1 is presented in **Figure 5b.2**, which showed characteristic absorption band at 1773 cm^{-1} corresponding to carbonyl of carbonate group. The furan ring (C=C) band was observed at 1500 cm^{-1} whereas furan ring breathing band was observed at 1013 cm^{-1} ³¹.

A representative ^1H NMR spectrum of PC-1 along with assignments is depicted in **Figure 5b.3**. The proton adjacent to oxygen atom of furyl group appeared as a singlet at $7.39\text{ }\delta$ ppm. The aromatic protons *meta* and *ortho* to the methoxy group appeared as doublet at 7.16 and $6.80\text{ }\delta$ ppm, respectively whereas the proton *para* to the methoxy group exhibited a doublet of doublet at $6.73\text{ }\delta$ ppm. The furyl protons 'e' and 'f' appeared as a singlet at $6.32\text{ }\delta$ ppm and a doublet at $5.97\text{ }\delta$ ppm, respectively. A singlet at $5.44\text{ }\delta$ ppm was assigned to benzylic proton and methoxy group proton exhibited a singlet at $3.79\text{ }\delta$ ppm.

^{13}C NMR of PC-1 along with assignments is shown in **Figure 5b.4**. The carbonyl carbon of carbonate linkage appeared at $151.3\text{ }\delta$ ppm.

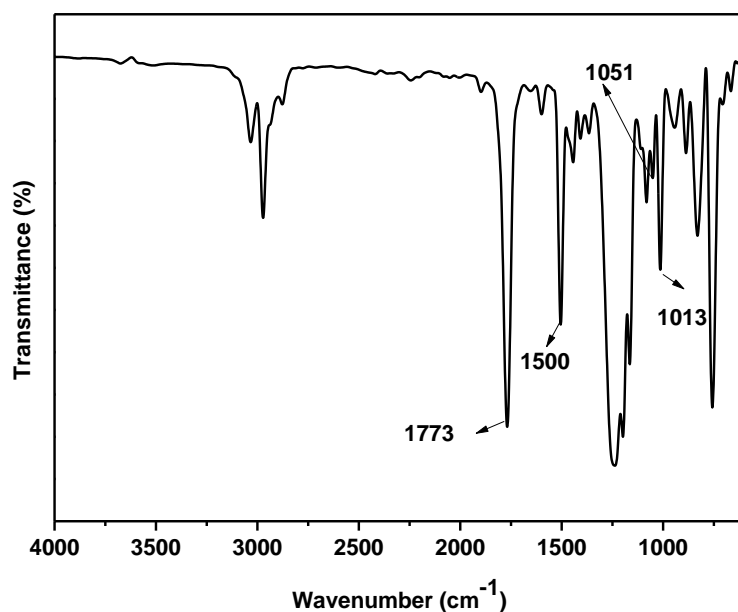


Figure 5b.2 FT-IR spectrum of polycarbonate (PC-1) derived from 4,4'-(furan-2-ylmethylene)bis(2-methoxyphenol) and triphosgene

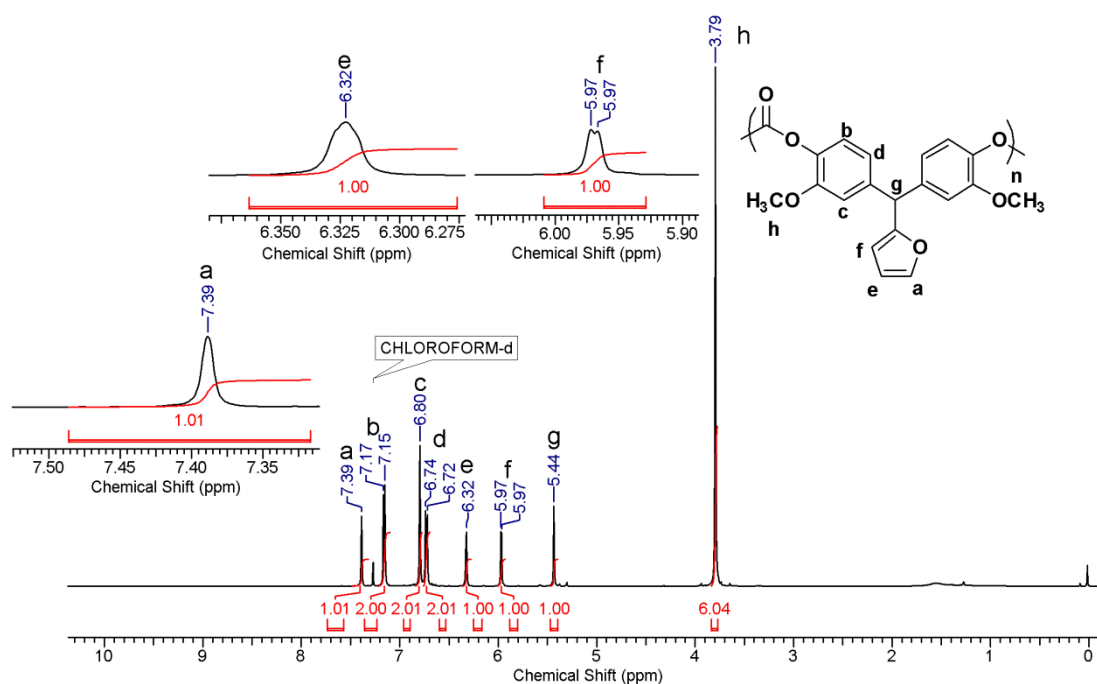


Figure 5b.3 ¹H NMR spectrum of polycarbonate (PC-1) derived from 4,4'-(furan-2-ylmethylene)bis(2-methoxyphenol) and triphosgene in CDCl₃

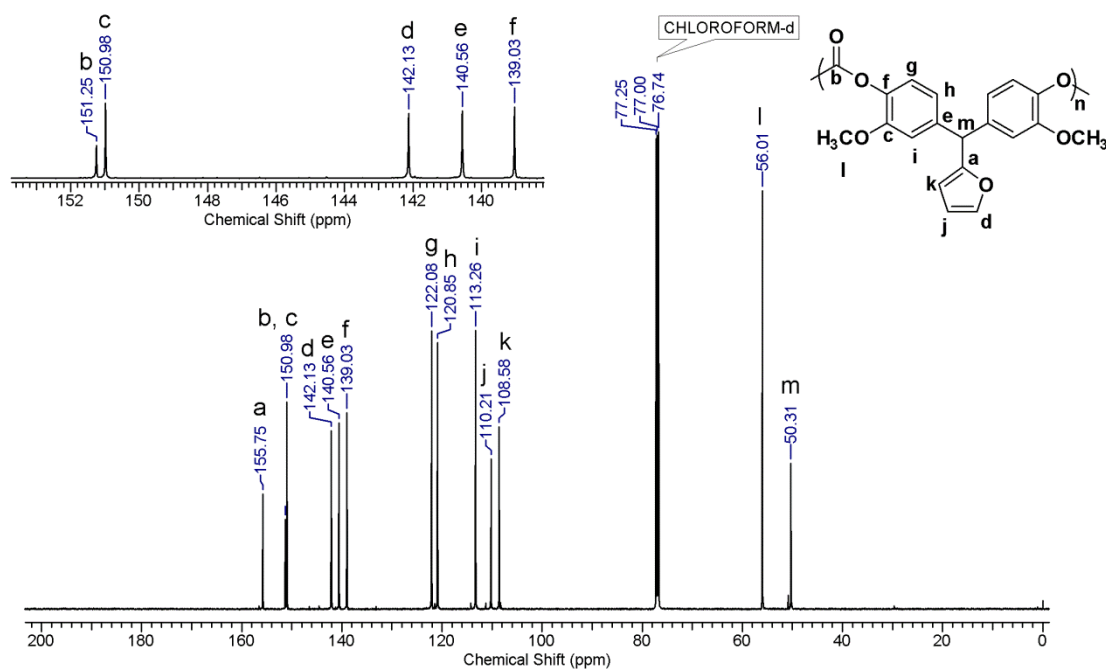


Figure 5b.4 ^{13}C NMR spectrum of polycarbonate (PC-1) derived from 4,4'-(furan-2-ylmethylene)bis(2-methoxyphenol) and triphosgene in CDCl_3

The compositions of co-polycarbonates were determined through ^1H NMR spectroscopy. ^1H NMR spectrum of co-polycarbonate (PC-2) obtained from a mixture of BPF-2 and BPA (50:50 mol.%) with triphosgene along with assignments is shown in **Figure 5b.5**. The integrated intensity of the methoxy protons ('j') of BPF-2 was compared with that of methyl group protons 'k' of BPA. The integrated intensity ratio of these peaks was used to determine molar percentage incorporation of BPF-2. The data in **Table 5b.2**, demonstrated that there was an excellent agreement between the observed incorporation and amount taken for polymerization.

Table 5b.2 Composition of copolycarbonates determined from ^1H NMR spectra

Copolycarbonate	Feed BPF-2, mol %	Observed BPF-2, mol %
PC-2	50	49.6
PC-3	30	29.3
PC-4	10	9.5

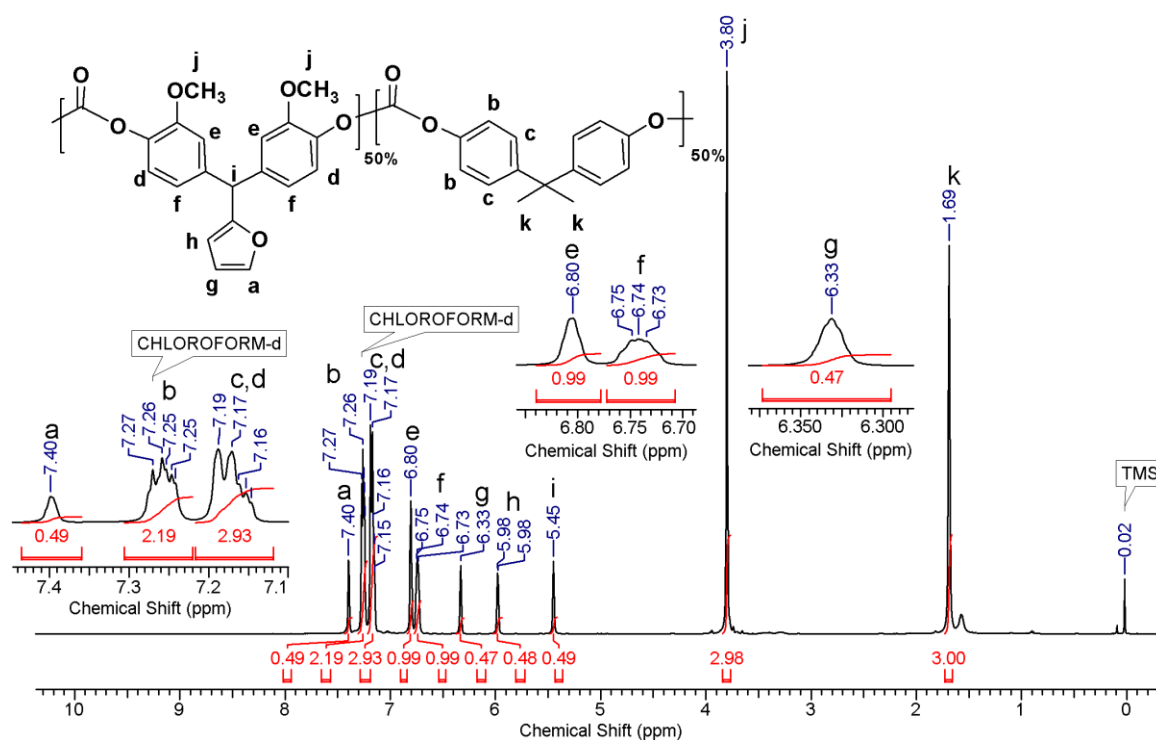


Figure 5b.5 ^1H -NMR spectrum of polycarbonate (PC-2) derived from 4,4'-(furan-2-ylmethylene)bis(2-methoxyphenol): bisphenol A (50:50 mol %) with triphosgene in CDCl_3

The microstructure of copolycarbonates derived from copolymerization of BPA and BPF-2 with triphosgene was studied by ^{13}C NMR spectroscopy. Under the employed experimental conditions the copolymerization of BPA and BPF-2 is expected to lead to formation of random copolymer with following possibilities of enchainment of the two bisphenol moieties wherein three adjacent monomer units are considered (**Figure 5b.6**). ^{13}C NMR spectra of copolycarbonates showed clear evidence not only for the random copolymer formation but also about the microstructural details as indicated by the multiplicity of the signals.

The assignments of carbon atoms in ^{13}C NMR spectrum of PC-2, as a representative example, were confirmed by heteronuclear multiple bond correlation spectroscopy (HMBC) and heteronuclear single quantum correlation spectroscopy (HSQC). The HMBC spectrum along with assignments is reproduced in **Figure 5b.7**.

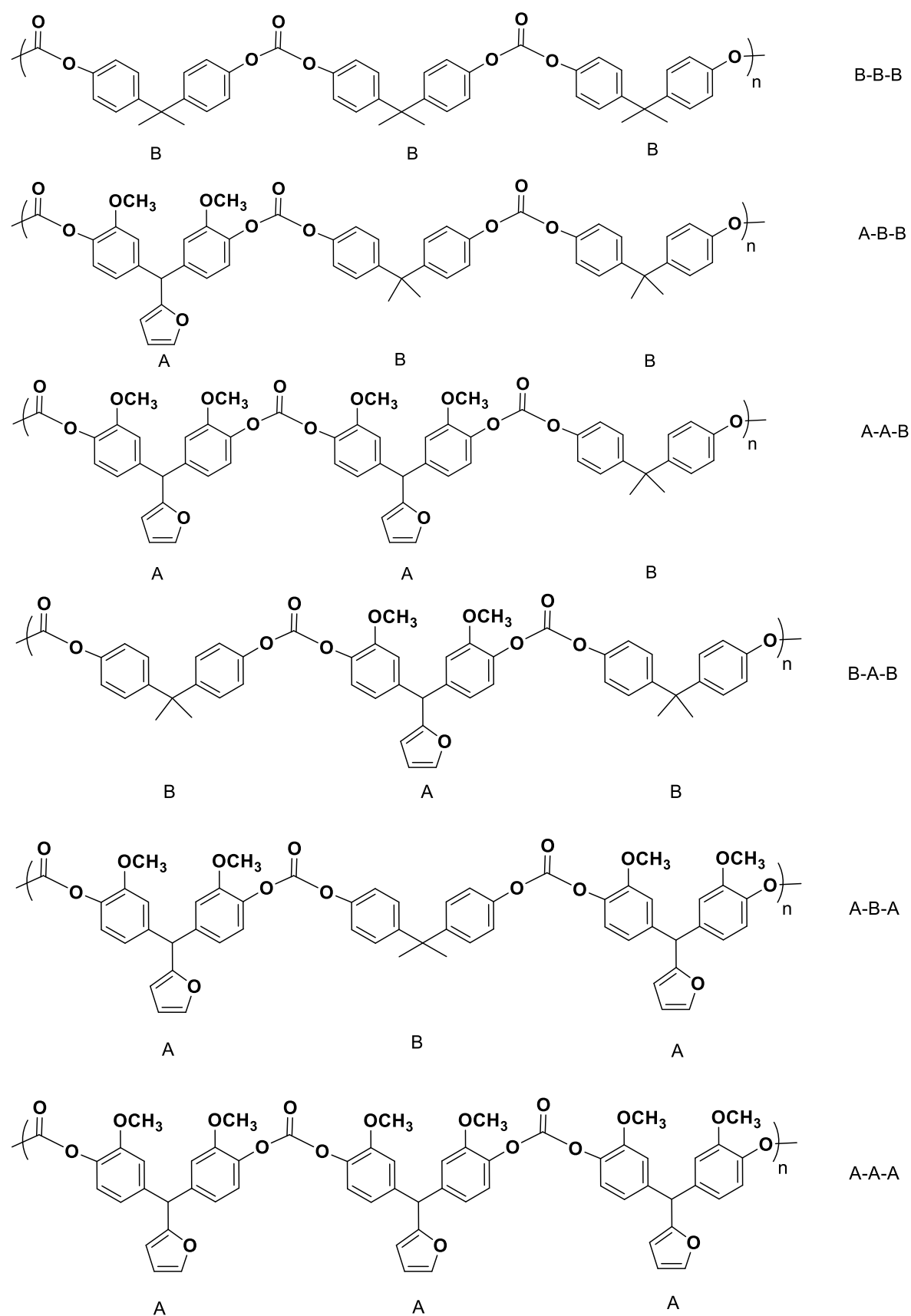


Figure 5b.6 Possible arrangements of BPF-2 and BPA units in copolycarbonates

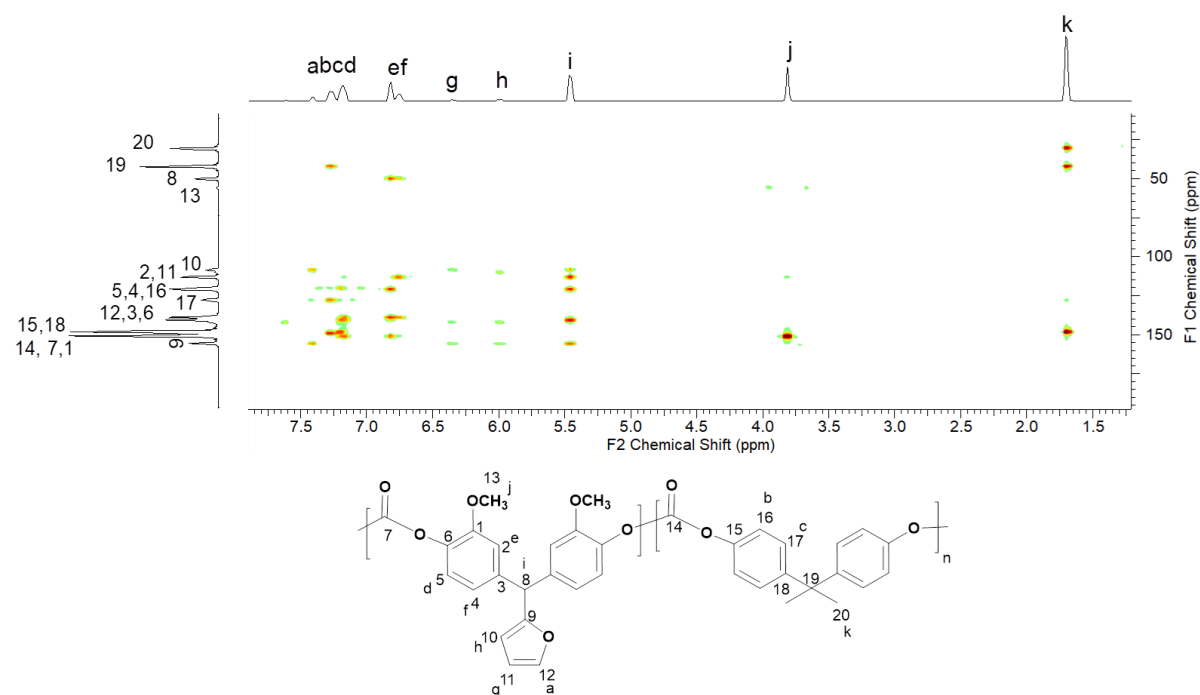


Figure 5b.7 HMBC spectrum of PC-2 in CDCl₃

¹³C NMR spectrum of PC-2 (50:50 mol % of BPF-2:BPA) along with assignments of carbon atoms is presented in **Figure 5b.8**. For easy comparison, ¹³C NMR spectra of homopolycarbonates of BPA (PC-5) and BPF-2 (PC-1) are also included in **Figure 5b.8**. It is interesting to note that the carbonyl carbon of carbonate linkage exhibited three distinct peaks at 151.3 δ ppm, 151.6 δ ppm and 152.1 δ ppm. A comparison of the spectrum of PC-2 with that of PC-1 and PC-5 inferred that carbonyl peaks appeared at 151.3 δ ppm and 152.1 δ ppm originated from AAA and BBB arrangement of co-monomer units, respectively in copolycarbonate sample while a peak at 151.6 δ ppm corresponds to BAB/ABA/BBA/AAB arrangement of co-monomer units.

Some of the other carbons in ¹³C NMR spectrum of PC-2 also exhibited similar features as indicated in **Figure 5b.8**. It is also interesting to note that some of the carbon atoms of aromatic ring also showed four signals in copolycarbonate which is likely to be due to the loss symmetry upon formation of copolymer comprising of comonomer units enchain in the manner as shown in **Figure 5b.6** (A-A-B and A-B-B). The exact peak assignments of multiple environments originating from arrangement of bisphenols units along the polycarbonate backbone needs further investigations using systematic variations in monomer compositions.

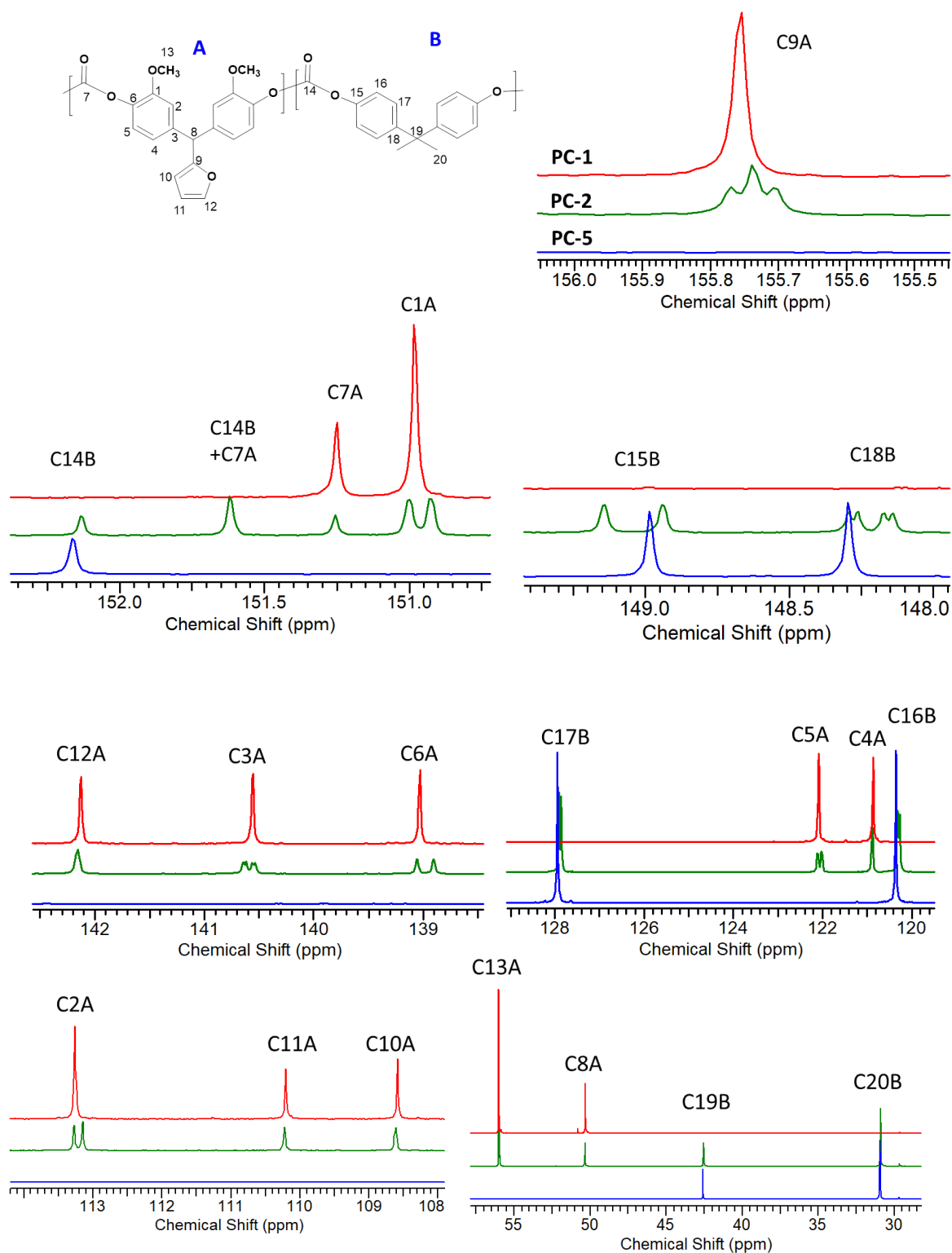


Figure 5b.8 ^{13}C NMR spectra of PC-1 (top), PC-2 (middle) and PC-5 (bottom) in CDCl_3

5b.3.3 X-Ray diffraction studies

The crystallinity of (co)polycarbonates was evaluated by wide angle X-ray diffraction (WAXD) and X-ray diffractograms are reproduced in **Figure 5b.9**. All the (co)polycarbonates showed broad halo at around $2\theta = 10\text{-}35^\circ$ which indicated that (co)polycarbonates are amorphous in nature.

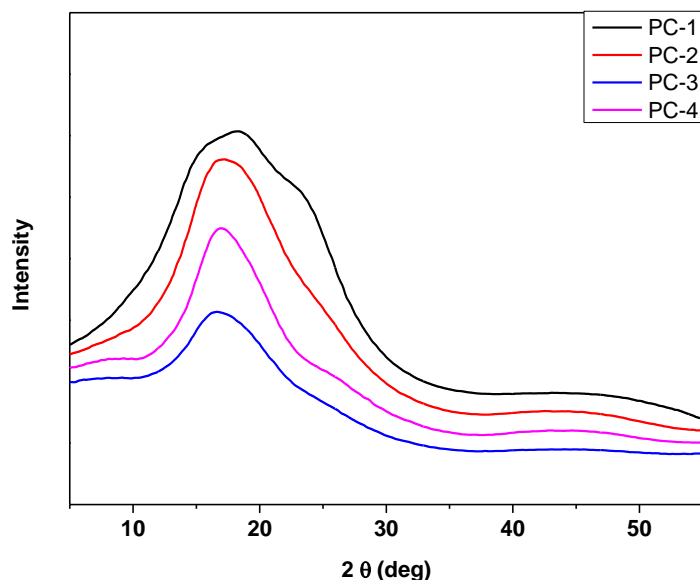


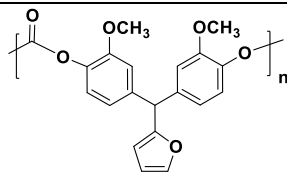
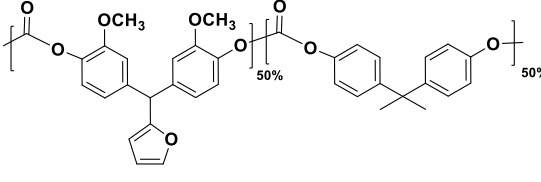
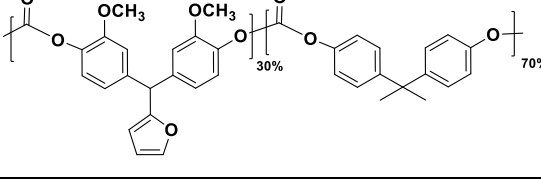
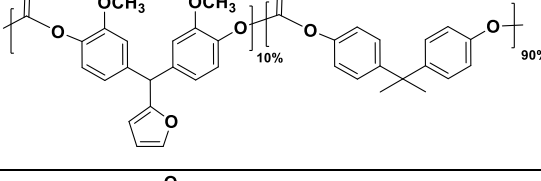
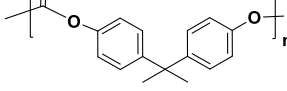
Figure 5b.9 X-Ray diffractograms of (co)polycarbonates

5b.3.4 Thermal properties

The thermal stability of (co)polycarbonates was determined by TGA at a heating rate at $10\% \text{ min}^{-1}$ under nitrogen. TG curves are shown in **Figure 5b.10**. The 10 % weight loss temperature and weight residue at 800°C are given in **Table 5b.3**. Differential thermogravimetric analysis (DTG) of (co)polycarbonates showed single stage degradation (**Figure 5b.11**). A comparison of T_{10} value (380°C) of BPF-2 based polycarbonate (PC-1, \overline{M}_n , 29,800) with that of T_{10} value (432°C) of BPA-based polycarbonate (PC-5, \overline{M}_n , 33,700) indicated that the former showed lower T_{10} value by 52°C . The lower T_{10} value of furyl containing polycarbonate could be ascribed to the presence of thermally labile methoxy groups and tertiary hydrogen. In any case, (co)polycarbonates containing pendant furyl groups exhibited 10 % weight loss in the range $380\text{-}423^\circ\text{C}$, which is well above the typical melt processing conditions of polycarbonates. In the series of copolycarbonates (PC-2, PC-3 and PC-4) the decrease in T_{10} values was observed with increase in the content of BPF-2.

The char yield of (co)polycarbonates at 800 °C was found in the range 16-32 %. Relatively higher char yield of furyl containing polycarbonate (PC-1) compared to reference BPA polycarbonate (PC-5) could be ascribed to the presence of furyl groups which possess aromatic character and thus contribute to formation of char residue³². The data clearly indicated that char yield of copolycarbonates increased with increase in BPF-2 content.

Table 5b.3 Thermal properties of (co)polycarbonates

Polycarbonate	Structure of (co)polycarbonate	T ₁₀ (°C) ^a	Char Yield (%) ^b	T _g (°C) ^c
PC-1		380	32	136
PC-2		386	25	142 (141.3) ^d
PC-3		398	23	144 (143.5) ^d
PC-4		423	18	146 (145.8) ^d
PC-5		432	16	147

a; 10 % weight loss on TGA thermograms at a heating rate of 10 °C min⁻¹ under nitrogen atmosphere

b; char yield was measured at 800 °C

c; measured by DSC on second heating scan with heating rate of 10 °C min⁻¹ under nitrogen atmosphere

d; T_g values calculated by Fox equation

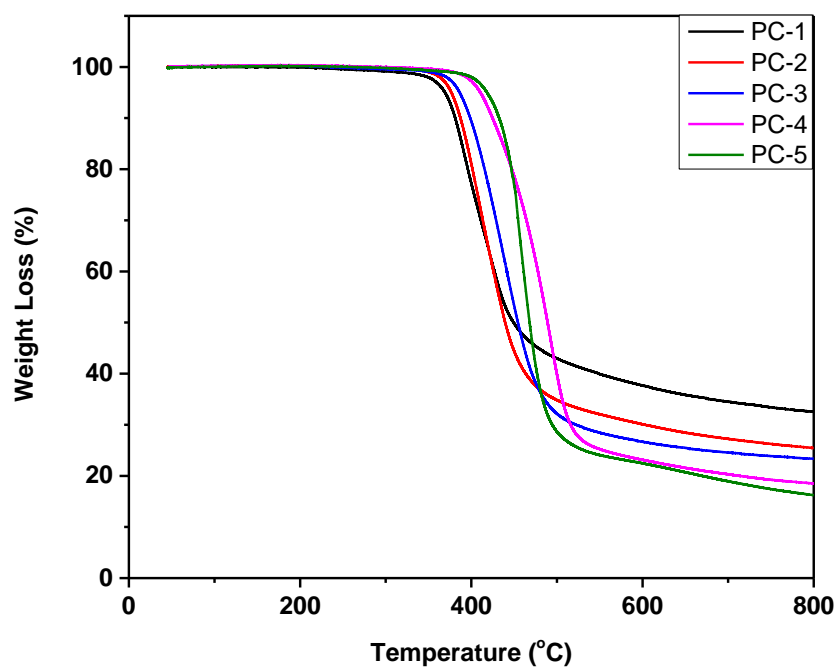


Figure 5b.10 TG curves of (co)polycarbonates

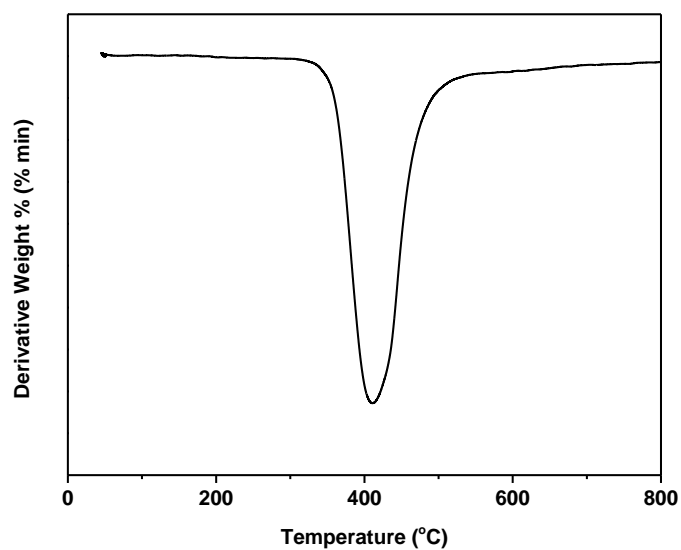


Figure 5b.11 DTG curve of PC-2 derived from 4,4'-(furan-2-ylmethylene)bis(2-methoxyphenol): bisphenol A (50:50 mol %) with triphosgene

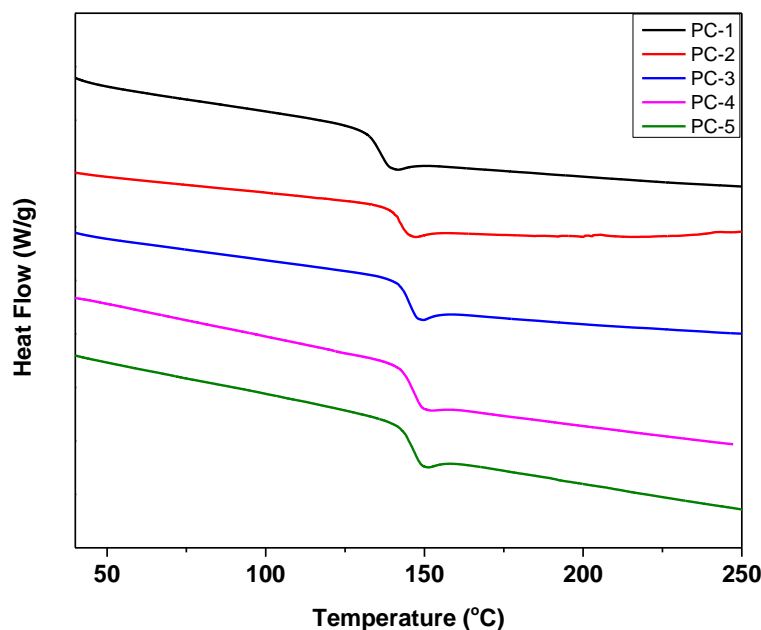


Figure 5b.12 DSC curves of (co)polycarbonates

Glass transition temperature (T_g) of (co)polycarbonates were determined by DSC under nitrogen atmosphere and data is presented in **Table 5b.3**. Thermal history of polymer was erased in first heating cycle and data was recorded in second heating cycle. T_g values of (co)polycarbonates containing pendant furyl groups were in the range from 136 °C-146 °C (**Figure 5b.12**). Bio-based homo polycarbonate (PC-1) showed lower T_g value (136 °C) compared to the BPA-based polycarbonate (147 °C) by 11 °C. In the series of copolycarbonates, T_g values decreased as the BPF-2 content was increased. It is difficult to identify a single factor affecting on T_g of polymer when comparing different chemical structures. Several factors are responsible for affecting T_g such as the intrinsic conformational flexibilities of polymer chains, sizes, steric hindrance, flexibility of pendant groups and non-covalent interactions between polymer chains (i.e. steric, dipolar, hydrogen-bonding, van der Waals, etc)³³⁻³⁵. The main probable reason for decreased T_g of polycarbonates containing pendant furyl groups compared to BPA based polycarbonate could be the presence of methoxy groups in the former. Methoxy substituent on BPF-2 results into an asymmetric segment, which can result in less efficient packing. The pendant furyl groups also results in disordering of the polymer chain packing.

The experimental T_g values of polycarbonates were compared to the theoretical T_g values calculated by Fox equation^{36,37}.

$$\frac{1}{T_{gc}} = \frac{W_1}{T_{g1}} + \frac{W_2}{T_{g2}}$$

where, T_{gc} is the T_g of the copolycarbonates and T_{g1} and T_{g2} are the T_g of homopolycarbonates derived from BPF-2 and BPA, respectively (i.e. $T_{g1} = 136$ °C, $T_{g2} = 147$ °C). W_1 and W_2 represent weight fractions of BPF-2 and BPA in the copolycarbonates. The T_g of (co)polycarbonates were plotted against mol % of BPF-2 and the plot is shown in **Figure 5b.13**. The T_g value obtained from the DSC exhibited a linear relationship with the mole % BPF-2. The calculated T_g are summarized in **Table 5b.3**.

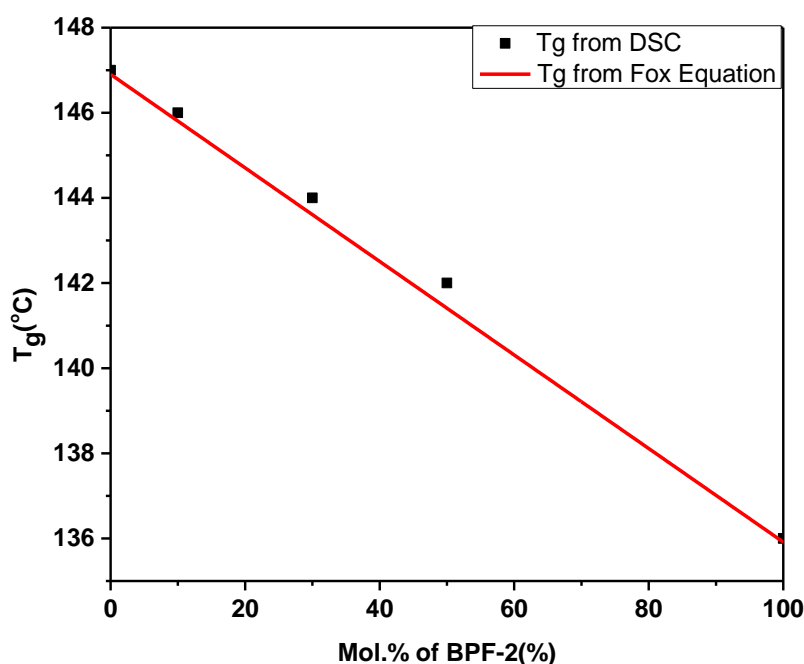


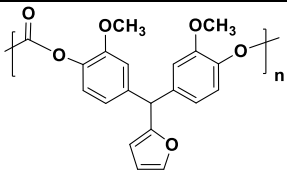
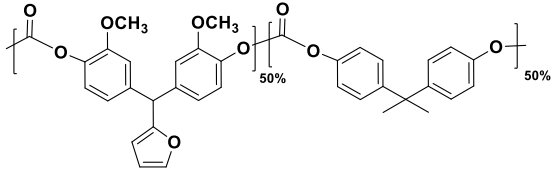
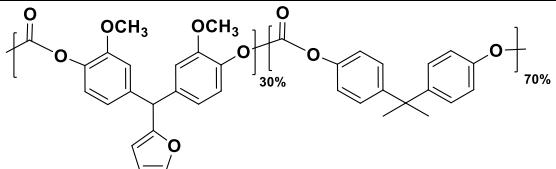
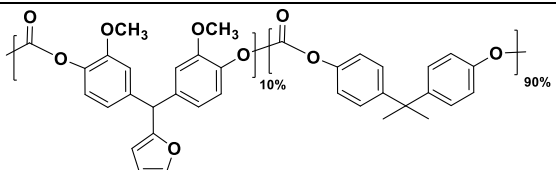
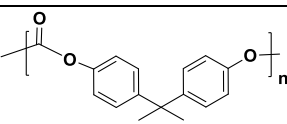
Figure 5b.13 T_g as a function of composition of BPF-2 in copolycarbonates derived from mixture of BPF-2 and BPA with triphosgene

5b.3.5 Mechanical properties of (co)polycarbonates

The mechanical properties of aromatic (co)polycarbonates were evaluated using polymer films that were prepared by casting from their chloroform solutions. Stress-strain curves are depicted in **Figure 5b.14**. The average values of yield point, Young's modulus and elongation at break based on three repeated measurements are collected in **Table 5b.4**. The stress-strain curves in uniaxial tension are typical of ductile nature of polycarbonates, having an initial Hookean region followed by shear induced yielding, necking and cold drawing before failure. (Co)polycarbonates showed high Young's modulus (1.49 to 1.54 GPa) and yield strength (56 to 57.7 MPa). The yield point and

Young's modulus of (co)polycarbonates revealed no significant variation across the compositional range studied. The elongation at break of homopolycarbonate of BPF-2 was 14.3 % which was significantly lower than that of BPA-based polycarbonate which exhibited elongation at break of 106.2 %. A decrease in % elongation at break in copolycarbonates was noticed with increase in the mol % of BPF-2. These data point out to the fact that ductility of (co)polycarbonates suffered upon incorporation of bisphenol containing pendant furyl group. Mechanical structure-property relationship requires further studies in order to probe the effect of incorporation of BPF-2 into copolycarbonates.

Table 5b.4 Mechanical properties of (co)polycarbonates

Polycarbonate	Structure of (co)polycarbonate	Yield Point (MPa)	Young's Modulus (GPa)	Elongation at Break (%)
PC-1		53.9	1.13	14.3
PC-2		56.0	1.54	28.3
PC-3		55.4	1.54	64.3
PC-4		57.7	1.49	100.5
PC-5		59.7 (65) ^{a,38}	1.50 (2.3) ³⁸	106.2 (110) ³⁸

a: the values of yield strength, Young's modulus and % elongation at break for BPA polycarbonate were taken from reference 38

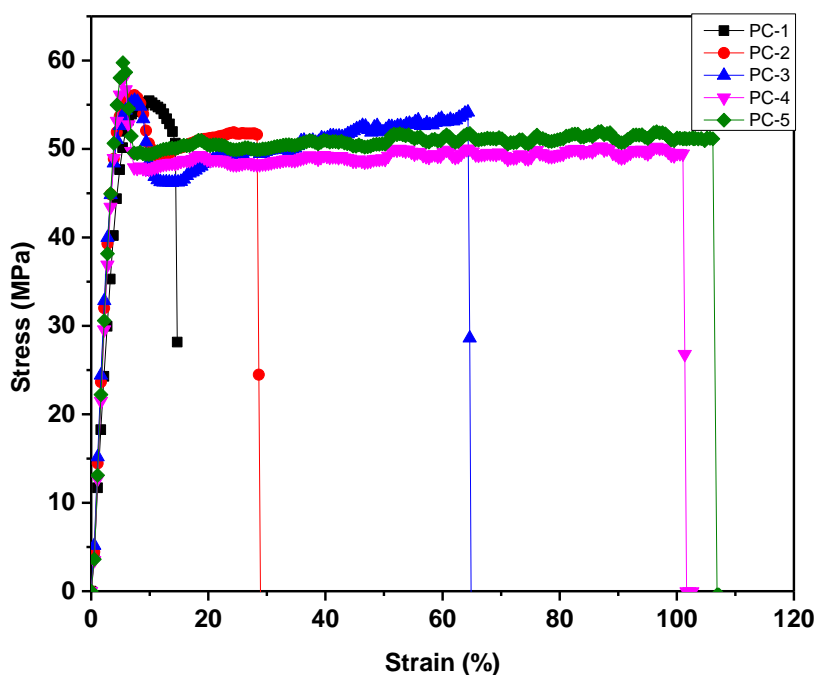


Figure 5b.14 Stress-strain curves of (co)polycarbonates

Overall, on the basis of polymerization process, molecular weights and thermal properties of resulting polymers, bisphenols containing pendant furyl groups are highly promising bio-based building blocks for the synthesis of high performance polymers. The distinct advantage is the ability to synthesize high performance polymers containing pendant furyl groups which are known to undergo Diels-Alder reactions with maleimides.

5b.4 Conclusions

1. A series of (co)polycarbonates containing pendant clickable furyl groups were synthesized from 4,4'-(furan-2-ylmethylene)bis(2-methoxyphenol) (BPF-2) and/or bisphenol A with triphosgene as carbonyl source *via* solution polymerization.
2. Inherent viscosities and number average molecular weights of (co)polycarbonates were in the range 0.50-0.72 dLg⁻¹ and 29,800-43,800 gmol⁻¹, respectively indicating formation of reasonably high molecular weight polymers.
3. (Co)polycarbonates were found to be soluble in organic solvents such as chloroform, dichloromethane, DMSO, DMAc and DMF. Tough and transparent films of (co)polycarbonates containing pendant clickable furyl groups could be cast from chloroform solutions.
4. By analysing triad sequence distribution using expanded ¹³C NMR spectra, it was found that the microstructure for all the copolycarbonates were random.

5. The T_{10} and T_g values of (co)polycarbonates containing pendant furyl groups were lower than that of reference polycarbonate based on BPA
6. Mechanical properties of (co)polycarbonates were studied by tensile testing. (Co)polycarbonates showed high Young's modulus (1.49 to 1.54 GPa) and yield strength (56 to 57.7 MPa), indicating good mechanical behaviour of bio-based (co)polycarbonates. A significant drop in % elongation at break was observed upon incorporation of bisphenol containing furyl group in (co)polycarbonates, indicating compromise on the ductility characteristics.

References

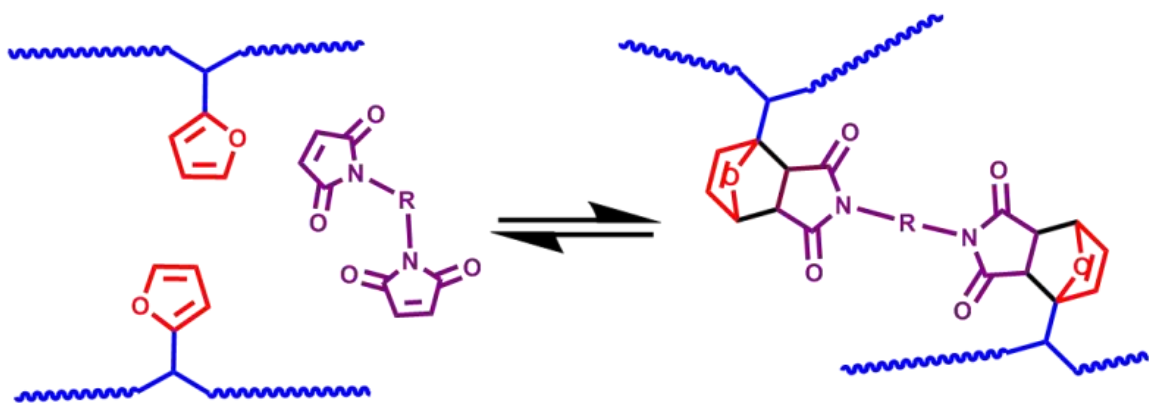
- 1 D. W. Fox, in *High Performance Polymers: Their Origin and Development*, Springer Netherlands, Dordrecht, 1986, pp. 67–70.
- 2 K. Takeuchi, *Polymer Science: A Comprehensive Reference*, 2012, **5**, 363–376.
- 3 T. Thompson, P. P. Klemchuk, A. Division and C. Corporation, In *Polymer Durability*; Clough, Roger L., *Advances in Chemistry*; American Chemical Society: Washington, DC, 1996, pp. 303–317.
- 4 D. Brunelle and M. Korn, Brunelle and Korn; in *Advances in Polycarbonates ACS Symposium Series*; American Chemical Society: Washington, DC, 2005 pp.1-5.
- 5 E. J. Pressman, B. F. Johnson and S. J. Shafer, in *Advances in Polycarbonates*; Brunelle, D., et al.; ACS Symposium Series; American Chemical Society: Washington, DC, 2005, pp. 22–38.
- 6 A. Llevot, E. Grau, S. Carlotti, S. Grelier and H. Cramail, *Macromol. Rapid Commun.*, 2016, **37**, 9–28.
- 7 R. Guo and J. E. McGrath, *Aromatic Polyethers, Polyetherketones, Polysulfides, and Polysulfones*, Elsevier B.V., 2012.
- 8 A. Maiorana, A. F. Reano, R. Centore, M. Grimaldi, P. Balaguer, F. Allais and R. A. Gross, *Green Chem.*, 2016, **18**, 4961–4973.
- 9 A. V. Krishnan, P. Stathis, S. F. Permeth, L. Tokes and D. Feldman, *Endocrinology*, 1993, **132**, 2279.
- 10 V. P. and N. O. José Antonio Brotons, María Fátima Olea-Serrano, Mercedes Villalobos, *Environ. Health Perspect.*, 1995, **103**, 608.
- 11 L. Shen, E. Worrell and M. Patel, *Biofuels, Bioprod. Biorefining*, 2010, **4**, 25–40.
- 12 D. Chatterjee, N. V. Sadavarte, R. D. Shingte, A. S. More, B. V. Tawade, A. D. Kulkarni, A. B. Ichake, C. V. Avadhani and P. P. Wadgaonkar, in *Cashew Nut*

- Shell Liquid*, ed. P. Anilkumar, Springer International Publishing, Cham, 1st edn., 2017, pp. 163–214.
- 13 C. Voirin, S. Caillol, N. V. Sadavarte, B. V. Tawade, B. Boutevin and P. P. Wadgaonkar, *Polym. Chem.*, 2014, **5**, 3142–3162.
- 14 H. A. Meylemans, B. G. Harvey, J. T. Reams, A. J. Guenther, L. R. Cambrea, T. J. Groshens, L. C. Baldwin, M. D. Garrison and J. M. Mabry, *Biomacromolecules*, 2013, **14**, 771–780.
- 15 H. A. Meylemans, T. J. Groshens and B. G. Harvey, *ChemSusChem*, 2012, **5**, 206–210.
- 16 B. G. Harvey, A. J. Guenther, H. A. Meylemans, S. R. L. Haines, K. R. Lamison, T. J. Groshens, L. R. Cambrea, M. C. Davis and W. W. Lai, *Green Chem.*, 2015, **17**, 1249–1258.
- 17 B. G. Harvey, A. J. Guenther, T. A. Koontz, P. J. Storch, J. T. Reams and T. J. Groshens, *Green Chem.*, 2016, **18**, 2416–2423.
- 18 G. D. Bittner, M. S. Denison, C. Z. Yang, M. A. Stoner and G. He, *Environ. Heal.*, 2014, **13**, 103.
- 19 S. F. Koelewijn, S. Van den Bosch, T. Renders, W. Schutyser, B. Lagrain, M. Smet, J. Thomas, W. Dehaen, P. Van Puyvelde, H. Witters and B. F. Sels, *Green Chem.*, 2017, **19**, 2561–2570.
- 20 S. G. Shetty, J. H. Kamps, G. Chandra, A. Tanwar, Methods for determining relative binding energy of monomers and methods of using the same US2015338423A1, 2015.
- 21 D. Fournier and F. Du Prez, *Macromolecules*, 2008, **41**, 4622–4630.
- 22 H. Nandivada, X. Jiang and J. Lahann, *Adv. Mater.*, 2007, **19**, 2197–2208.
- 23 A. Gandini, A. J. D. Silvestre, D. Coelho, B. Reis, A. J. D. Silvestre and P. J. Costanzo, *Polym. Chem.*, 2011, **2**, 1713–1719.
- 24 Y. Dai, X. Zhang and F. Xia, *Macromol. Rapid Commun.*, 2017, **38**, 1700357.
- 25 J. Feng, R. X. Zhuo and X. Z. Zhang, *Prog. Polym. Sci.*, 2012, **37**, 211–236.
- 26 M. S. I. Mollah, D. W. Seo, M. M. Islam, Y. D. Lim, S. H. Cho, K. M. Shin, J. H. Kim and W. G. Kim, *J. Macromol. Sci. Part A*, 2011, **48**, 400–408.
- 27 Y. Xin, J. Sakamoto, A. J. van der Vlies, U. Hasegawa and H. Uyama, *Polymer*, 2015, **66**, 52–57.
- 28 R. Zhang and J. A. Moore, *Macromol. Symp.*, 2003, **199**, 375–390.
- 29 H. R. Kricheldorf, S. Böhme, G. Schwarz and C. L. Schultz, *Macromolecules*,

- 2004, **37**, 1742–1748.
- 30 S. J. Sun, K. Y. Hsu and T. C. Chang, *Polym. J.*, 1997, **29**, 25–32.
- 31 C. Tarducci, J. P. S. Badyal, S. A. Brewer and C. Willis, *Chem. Commun.*, 2005, 406–408.
- 32 H. M. Wang and S. H. Hsiao, *Polymer*, 2009, **50**, 1692–1699.
- 33 J. E. Mark, *Physical Properties of Polymers Handbook*, Springer, New York, 2007.
- 34 A. J. Hill and M. R. Tant in ACS Symposium Series; American Chemical Society: Washington, DC, 1999, pp.1–20.
- 35 J. Shen, Y. Caydamli, A. Gurarslan, S. Li and A. E. Tonelli, *Polymer*, 2017, **124**, 235–245.
- 36 T. G. Fox, *Bull. Am. Phys. Soc.*, 1956, **1**, 123.
- 37 K. Cheah and W. D. Cook, *Polym. Eng. Sci.*, 2003, **43**, 1727–1739.
- 38 J. E. Mark, *Polymer Data Handbook*, Oxford University Press, New York, 1st edn., 1999.

Chapter - 5c

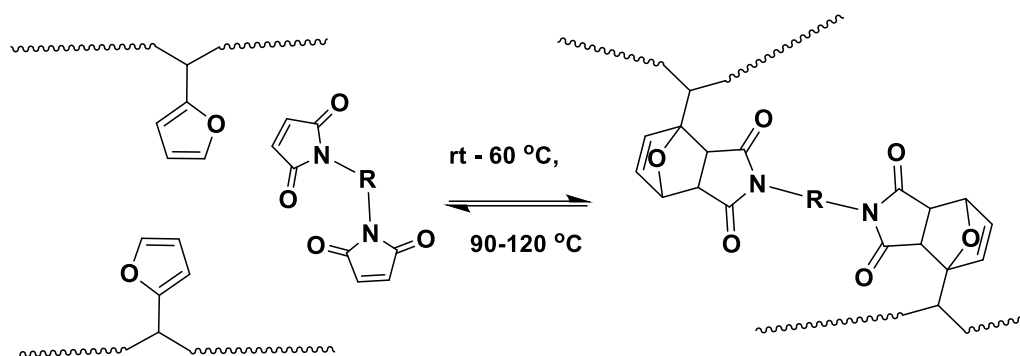
Thermally Reversible Crosslinked Polymers *via* Diels-Alder Click Chemistry



5c.1 Introduction

Crosslinked aromatic polymers such as epoxies, cyanate esters, bismaleimides, and polybenzoxazines are useful class of polymeric materials because of their attractive properties such as high modulus, high fracture strength, and excellent solvent resistance. These crosslinked polymers are useful in a number of applications such as coatings, adhesives, electrical insulations, printed circuit boards, etc¹⁻⁷. However, a major drawback of these systems is the lack of recyclability. After their intended use is over, these “difficult-to-recycle” crosslinked materials create an environmental issue^{8,9}. Thus, it is highly desirable to design reversibly crosslinked polymers that maintain their crosslinked structure under service conditions and undergo disconnection of crosslinking at high temperature to fulfil the processability and complete recyclability.

In general, reversibly crosslinked polymeric networks are obtained from non-covalent linkages such as hydrogen bonding, ionic bonding, Van der Waals forces, π - π interactions, etc¹⁰. However, such non-covalent linkages, being weak in nature, cannot hold up high strain/temperature- the property which is crucial for crosslinked polymers. On the other hand, reversibly crosslinked polymeric materials based on covalent linkages are strong with good mechanical performance. Several strategies have been demonstrated for covalently bonded reversibly crosslinked polymers which include: a) incorporation of cleavable linkages into monomers¹¹⁻¹⁵ b) utilization of monomers containing functional groups such as paraformaldehyde-diamine¹⁶, cyclopentadiene¹⁷, anthracene¹⁸, fulvenes¹⁹ or furan-maleimide, which can be broken by applying external stimuli. Of these, furan and maleimide functional groups have been widely applied to a broader range of polymers. Furan-maleimide reaction is an excellent choice for thermally reversible crosslinked polymers as it involves coupling of maleimide with furan at ambient temperature to form cyclic adduct and decoupling back to maleimide and furan in the temperature range 90-150 °C²⁰⁻²²(**Scheme 5c.1**). This reaction is clean, catalyst-free and can be repeated several times²³. In the literature, there are number of reports on recyclable crosslinked polymeric systems such as polyurethanes²⁴, polyamides²⁵, polyesters²⁶⁻²⁸, epoxy resins^{29,30}, etc wherein furan-maleimide Diels-Alder reactions was exploited.



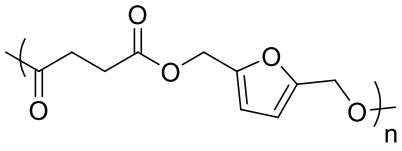
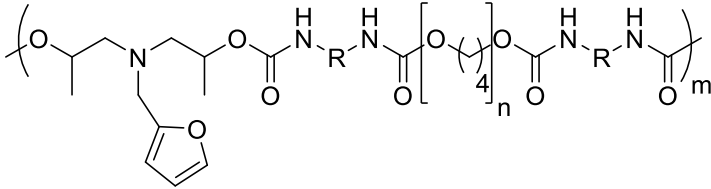
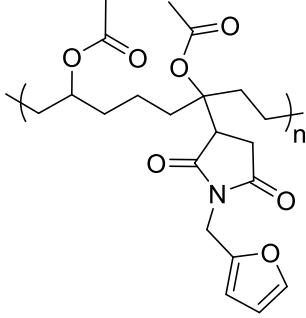
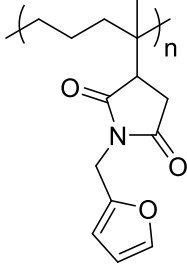
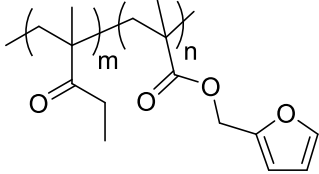
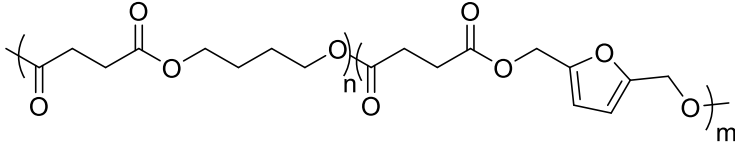
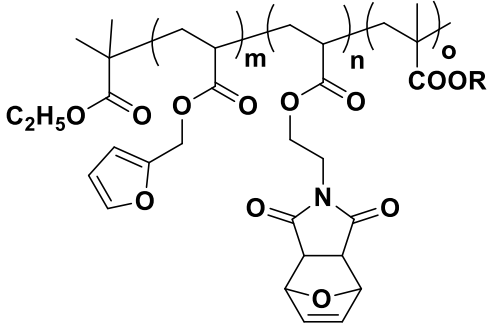
Scheme 5c.1 Furan-maleimide Diels-Alder/retro Diels-Alder reaction

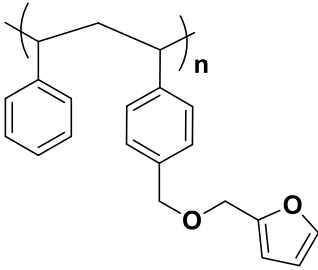
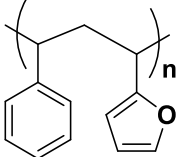
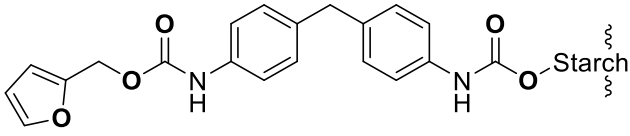
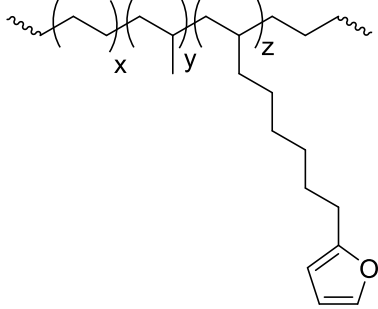
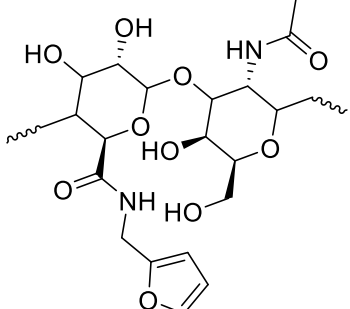
To the best of our knowledge, reports on recyclable fully aromatic step-growth polymers based on Diels-Alder reaction are scanty except for aromatic polyamides^{25,31}.

Table 5c.1 lists the reported examples of selected crosslinkable polymers containing furyl as functional groups.

Table 5c.1 List of the selected crosslinkable polymers containing furyl as a pendant clickable group

Sr. No.	Polymer	Ref.
1	<p>R= H or CH₃</p>	23
2		25,32
3	<p>R= H or CH₃</p>	33

4		26,27
5		24
6		23
7		34
8		35,36
9		37
10		38,39

11		40
12		41
13		42
14		9
15		23

In the present work, preliminary investigations were carried out on recyclable crosslinked aromatic polyester and aromatic polycarbonate. Polyester and polycarbonate containing pendant furyl groups were crosslinked with bismaleimides namely, 1,1'-(methylenedi-1,4-phenylene)bismaleimides (BMI) and 1,8-bis(maleimido)-triethylene glycol (TEG) and their thermo-mechanical properties were evaluated. Furthermore, polyester/polycarbonate-based gels were also prepared and their thermoreversibility was studied.

5c.2 Experimental

5c.2.1 Materials

Polyester and polycarbonate containing pendant furyl groups were prepared as described in **Chapter 5a** and **5b**, respectively. 1,1'-(Methylenedi-1,4-phenylene)bismaleimide (BMI) (95%) (Melting point-156 °C), 2,2'-(ethylenedioxy)bis(ethylamine) (98%) and maleic anhydride (99%) were purchased from Sigma Aldrich. 1,8-Bis(maleimido)-triethylene glycol (TEG) was prepared as per reported procedure⁴³ (Melting point-93 °C). *N,N*-Dimethylformamide (DMF), *N,N*-dimethylacetamide (DMAc), dimethyl sulfoxide (DMSO), chloroform, dichloromethane, acetone, triethylamine and acetic anhydride were purchased from Thomas Baker, Mumbai.

5c.2.2 Measurements

Differential scanning calorimetric (DSC) analysis was performed using DSC Q10 differential calorimeter from TA Instruments under nitrogen atmosphere (50 mL min⁻¹). Analyses were carried out in the temperature range between 30 and 200 °C using the heating and cooling rate of 10 °C min⁻¹.

The tensile properties of the polymer films were measured using Rheometrics Scientifics (Model Mark IV) (UK) instrument with a clamp length of 10 mm at room temperature at a crosshead speed of 1.5 mm min⁻¹.

The viscoelastic behavior of crosslinked gel was studied on MCR-301 (Anton Paar) Rheometer using 25 mm parallel plate geometry.

5c.2.3 Preparations

Preparation of cross-linked polymer films

To a solution of polyester or polycarbonate (200 mg) in chloroform (10 ml), a stoichiometric amount of bismaleimide (BMI or TEG) (furan/maleimide mol ratio = 1) was added. The mixture was stirred at 30 °C for 1 h and then the solution was poured into glass petri-dish and solvent was allowed to evaporate off. After complete evaporation of solvent, film was kept at 60 °C in an oven for 36 h. The obtained crosslinked polymer film was used for further characterization.

Recyclability of crosslinked polymer films

The crosslinked polymer films were heated in chloroform at 120 °C for 10 min in a pressure tube. The solution of polymer was poured into glass petri-dish and solvent was allowed to evaporate off. After complete evaporation of solvent, film was kept at 60 °C in

an oven for 36 h. Mechanical properties of crosslinked polymers were characterized by tensile testing. The same procedure was repeated twice and tensile data were recorded.

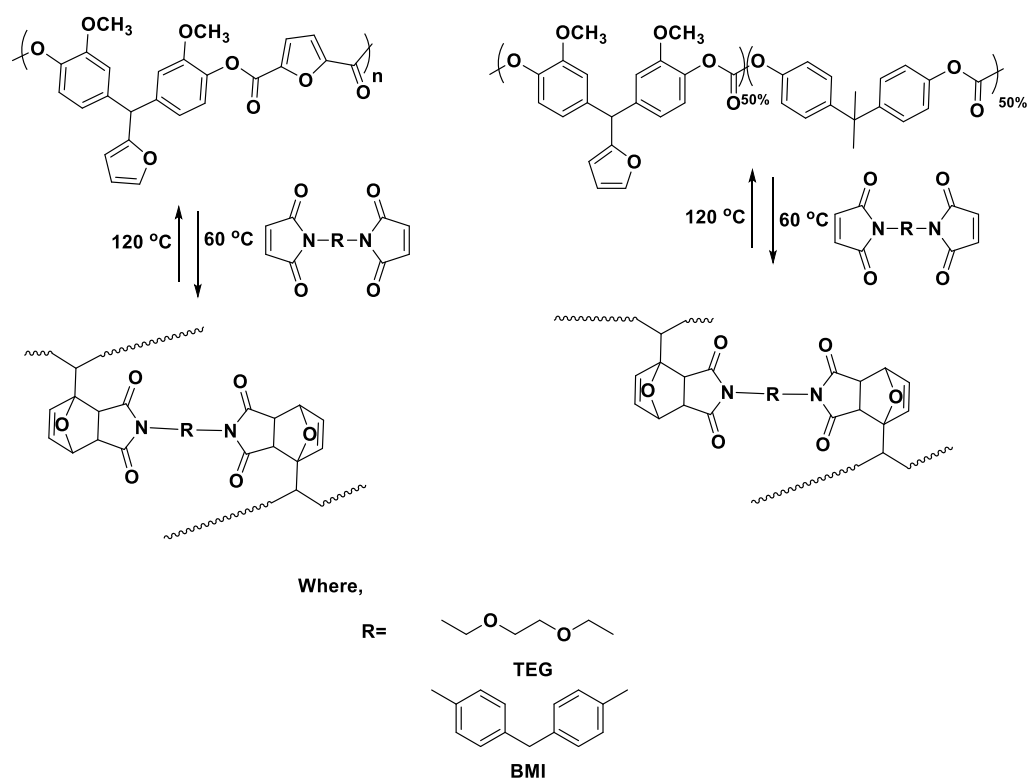
Preparation of thermoreversible cross-linked polymer gel

Polyester or polycarbonate (100 mg) and a stoichiometric amount of bismaleimide (BMI or TEG) (furan/maleimide mol ratio = 1) were dissolved in *N,N*-dimethylacetamide or sulfolane (1 mL) in a vial with a magnetic bar. After complete dissolution, solution was stirred at 60 °C. The gel point was determined when the magnetic stirring bar stopped rotating. The polymeric gel was heated to 120 °C for 5 min to effect retro Diels-Alder reaction and polymer solution was obtained. The thermal cycle was repeated thrice.

5c.3 Results and discussion

5c.3.1 Preparation of crosslinked polymers

The synthesis of polyesters and polycarbonates containing pendant furyl groups has been described in **Chapter 5a** and **5b**, respectively. Of these, homopolyester (PE-6) derived from 4,4'-(furan-2-ylmethylene)bis(2-methoxyphenol) (BPF-2) and 2,5-furan dicarboxylic acid chloride and co-polycarbonate (PC-2) derived from a mixture (50:50 mol %) of BPF-2 and BPA were selected for crosslinking studies. Both PE-6 and PC-2 were crosslinked with BMI and TEG (with furan/maleimide mol ratio =1) *via* Diels-Alder reaction (**Scheme 5c.1**). Hereafter, crosslinked polyester and polycarbonate sample with BMI is referred as PE6-BMI and PC2-BMI, whereas polyester and polycarbonate crosslinked with TEG is referred as PE6-TEG and PC2-TEG, respectively. A cast film of crosslinked polymer was prepared by dissolution of polymer (PE-6 or PC-2) and crosslinker (BMI or PEG) in chloroform. After complete evaporation of solvent, films were kept at 60 °C for 36 h. Thereafter, crosslinked polymer films were completely insoluble in chloroform which indicated that polymers were crosslinked successfully. In polyester (PE-6) the backbone furan functionality does not take part in Diels-Alder reaction due to the electron-withdrawing effect of the carbonyl groups directly connected to the furan group^{26,27}.



Scheme 5c.2 Preparation of thermally reversible crosslinked polyester and polycarbonate from corresponding linear polymers containing pendant furyl groups and bismaleimides

5c.3.2 Thermal studies of crosslinked polymers

Retro Diels-Alder reaction of PE6-BMI and PC2-BMI was investigated by DSC at a heating and cooling rate of $10\text{ }^{\circ}\text{C min}^{-1}$. DSC curves and data are presented in **Figure 5c.1** and **Table 5c.2**, respectively.

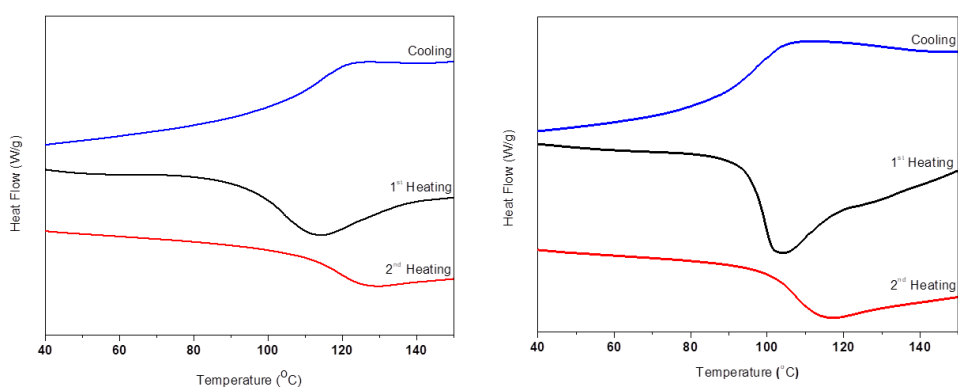


Figure 5c.1 DSC curves of first and second heating cycles of crosslinked polyester (PE6-BMI) (A) and polycarbonate (PC2-BMI) (B)

Table 5c.2 De-crosslinking temperature and absorbed energy for retro Diels-Alder reactions

Polymer	1 st Heating cycle		2 nd Heating cycle	
	ΔH (J/g) ^a	T _{rDA} (°C) ^b	ΔH (J/g) ^a	T _{rDA} (°C) ^b
PE6-BMI	24	112	6	123
PC2-BMI	24	101	7	110

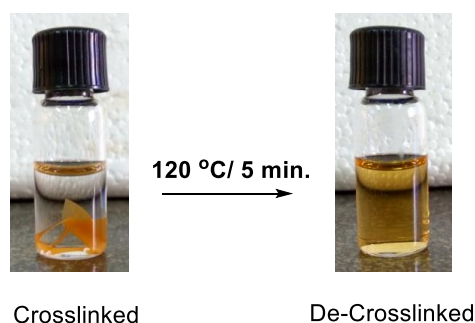
a; absorbed energy for retro Diels-Alder reaction

b; temperature corresponding to retro Diels-Alder reaction

PE6-BMI and PC2-BMI showed broad endothermic transition with maxima at 112 °C and 101 °C, respectively in the first heating cycle. The second heating cycle also showed endothermic transition at 123 °C for polyester and 110 °C for polycarbonate. Due to the fast heating rate (10 °C min⁻¹), complete de-crosslinking did not occur in the time scale of first heating cycle and hence the endothermic transition was observed in the second heating cycle too. Decrosslinking at slightly higher temperature in case of second heating cycle compared to the first cycle could presumably be attributed to retro Diels-Alder reaction of *exo* adduct. In general, *exo* adduct reverts at slightly higher temperature compared to *endo* adduct⁴⁴. In the first cooling cycle no transition was observed corresponding to Diels-Alder adduct formation because of its slow rate of formation²³.

5c.3.3 Solubility tests of crosslinked polymers

Solubility tests were performed to study the effect of crosslinking and de-crosslinking on the solubility properties. After crosslinking with both the bismaleimides *viz.* BMI and TEG, polymers were found to be insoluble in DMAc while their linear counterparts as well as de-crosslinked polymers were soluble in DMAc (**Figure 5c.2**).

**Figure 5c.2** Solubility test of crosslinked and de-crosslinked polymers

5c.3.4 Mechanical properties of crosslinked polymers

Tensile tests were performed on linear polyester (PE-6) and polycarbonate (PC-2) and the corresponding crosslinked materials. Tensile strength, Young's modulus and elongation at break were analyzed from tensile measurements. Stress-strain curves are presented in **Figure 5c.3** and stress-strain data is given in **Table 5c.3** and **Table 5c.4**.

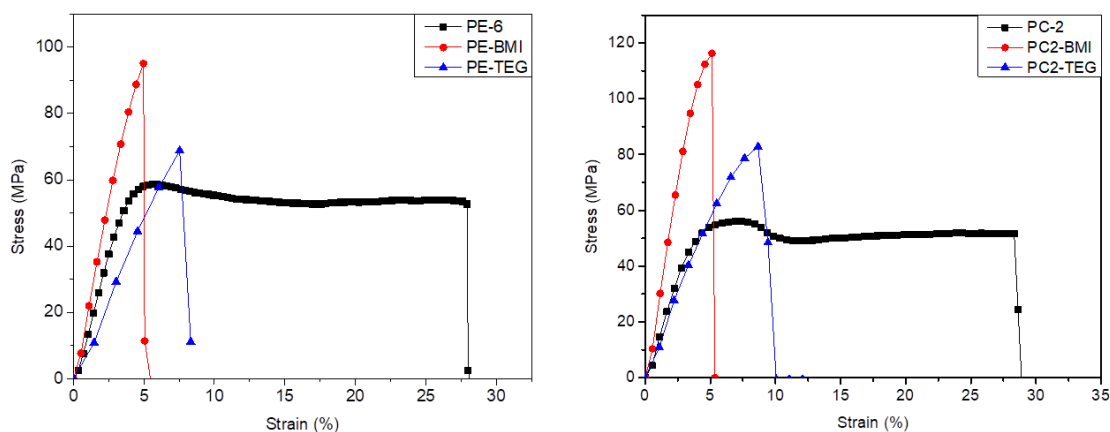


Figure 5c.3 Stress-strain curves of polyester/polycarbonate and the corresponding crosslinked materials.

Table 5c.3 Mechanical properties of polyester and the corresponding crosslinked materials

Polyester	Tensile strength (MPa)	Young's modulus (GPa)	Elongation at break (%)
PE-6	58.5	1.66	28
PE6-BMI	94.8	2.16	5
PE6-TEG	68.8	0.95	7

Table 5c.4 Mechanical properties of polycarbonate and the corresponding crosslinked materials

Polycarbonate	Tensile strength (MPa)	Young's modulus (GPa)	Elongation at break (%)
PC-2	56.0	1.54	28
PC2-BMI	116.3	2.60	5
PC2-TEG	82.0	1.09	9

In general, crosslinked polymeric materials exhibit higher tensile strength and lower elongation at break compared to their parent linear polymers⁹. Tensile strength and Young's modulus of PE-6 is 58.5 MPa and 1.66 GPa, respectively and it elongates up to 28 %. After crosslinking with BMI, tensile strength and Young's modulus increased to 94.8 MPa and 2.16 GPa whereas elongation at break decreased to the value of 5 %. Polycarbonate crosslinked with BMI also showed similar trend. As expected, PE6-TEG showed increased tensile strength to 68.8 MPa and decreased elongation to the value of 7 % compared to PE-6. Conversely, Young's modulus decreased to 0.95 GPa for PE6-TEG and similar trend was observed in case of polycarbonate (1.09 GPa). The possible explanation for decreased Young's modulus of polymers crosslinked with TEG is the presence of flexibilizing oxyalkylene segment²⁶.

5c.3.5 Mechanical properties of recycled polymers

Recyclability of cross-linked polyester and polycarbonate was evaluated by stress-strain studies conducted on representative cross-linked polymers (PE6-BMI and PC2-BMI), first recycled (PE6-BMIR1 and PC2-BMIR1) and second recycled (PE6-BMIR2 and PC2-BMIR2) polyester and polycarbonate. The mechanical properties data of polyester and polycarbonate are presented in **Table 5c.5** and **Table 5c.6**, respectively. The stress-strain curves are presented in **Figure 5c.5**.

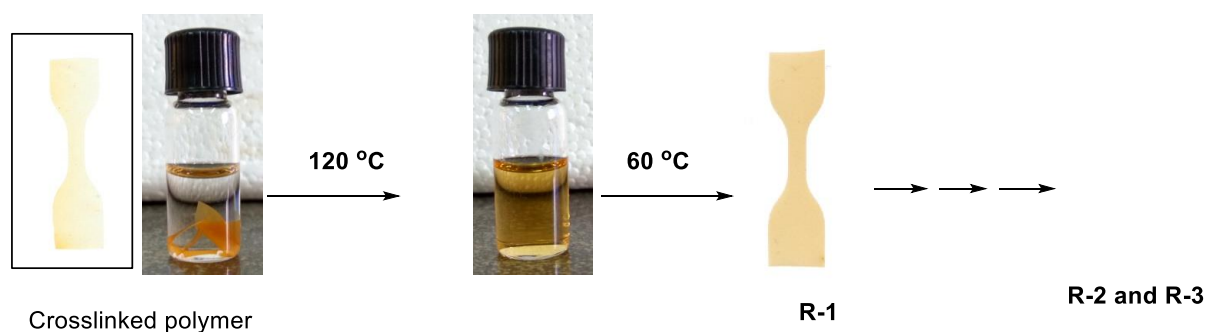


Figure 5c.4 Thermoreversibility of crosslinked polymers

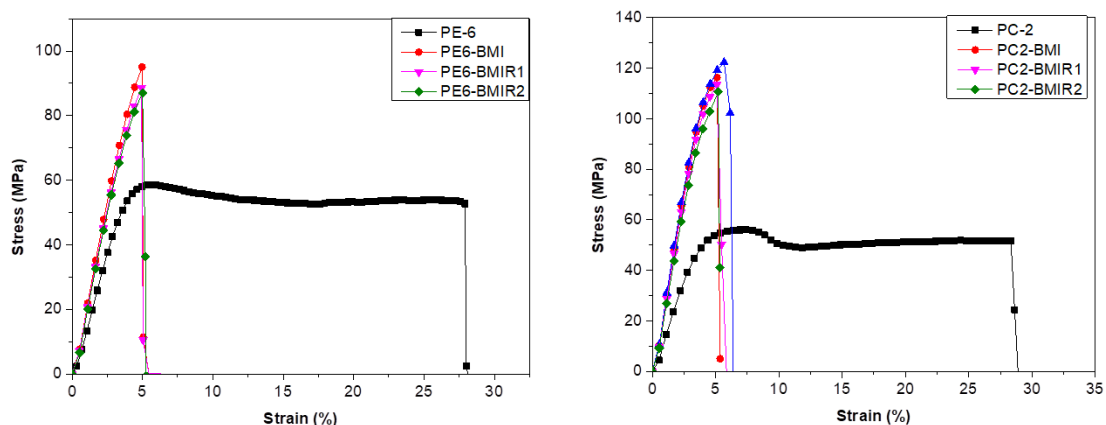


Figure 5c.5 Stress-strain curves of recycled crosslinked polyester /polycarbonate.

Table 5c.5 Mechanical properties of recycled polyester

Polyester	Tensile strength (MPa)	Young's modulus (GPa)	Elongation at break (%)
PE-6	58.5	1.66	28
PE6-BMI	94.8	2.16	5
PE6-BMI-R1	89.2	2.10	5
PE6-BMI-R2	87.0	1.98	5

Table 5c.6 Mechanical properties of recycled polycarbonate

Polycarbonate	Tensile strength (MPa)	Young's modulus (GPa)	Elongation at break (%)
PC-2	56.0	1.54	28
PC2-BMI	116.3	2.60	5
PC2-BMI-R1	114.6	2.51	5
PC2-BMI-R2	110.6	2.40	5

The results indicated that the mechanical properties of recycled polymers were closer to that of original crosslinked polymers. These data confirmed thermal reversibility of the Diels-Alder cross-linked polymers.

5c.3.6 Thermoreversible gels via Diels-Alder reaction

Polymer (PE-6 or PC-2) was dissolved in DMAc and treated with stoichiometric quantity of bismaleimide as described in experimental section. The solution was heated at 60 °C. A drastic increase in solution viscosity was observed by visual observation (**Figure 5c.6**). After 10 h, solution viscosity was so high that the gel did not flow even after inversion of vial. This gel was heated at 120 °C for 5 min when the gel was transformed back into solution due to the de-crosslinking *via* retro Diels-Alder reaction. In order to check reversibility, the experiment was repeated thrice and each time observation was the same.

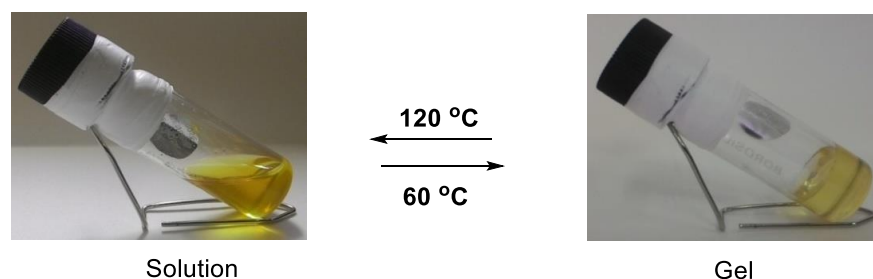


Figure 5c.6 Sol-gel transition of polymeric organogel

5c.3.7 Rheological behaviour of polyester gel

Preliminary rheological studies on PE6-BMI-based gel as a function of temperature were performed to investigate its thermo-reversible characteristics. Rheology can be used to study the visco-elastic characteristics and flow behavior of polymers, either in the form of solutions or in their solid-state. Adzima *et al* have reported the rheological analysis of reverse gelation in covalently cross-linked Diels-Alder polymer networks⁴⁵. Methodology employed in the present rheological studies was based on a previous report on healable network polymers prepared using Diels-Alder reaction⁴⁶. PE6-BMI gel was prepared by dissolving 100 mg polyester (PE-6) and 35 mg BMI (furan:maleimide mol ratio 1:1) in sulfolane and the solution was kept at 60 °C for 10 h. To minimize solvent evaporation during rheological experiments at high temperature (120 °C), sulfolane (boiling point-185 °C) was selected as the solvent. Gels with 25 mm diameter and 0.5 mm thickness were prepared for the study. A strain-controlled rheometer (Model MCR 301, Anton Paar, Austria) with cone and plate geometry was used for the study. Amplitude sweep measurements were performed to measure the linear visco-elastic regime of the gels at 60 °C. Since the Diels-Alder reaction carried out at 60 °C^{24,47}, this temperature is good enough for the initial starting temperature of the heating cycle in

the rheological measurements. Log-log plot of modulus versus strain is given in **Figure 5c.7**. The oscillatory shear measurements were performed at constant angular frequency (10 rad s^{-1}) with increasing strain from 0.01 to 5 %.

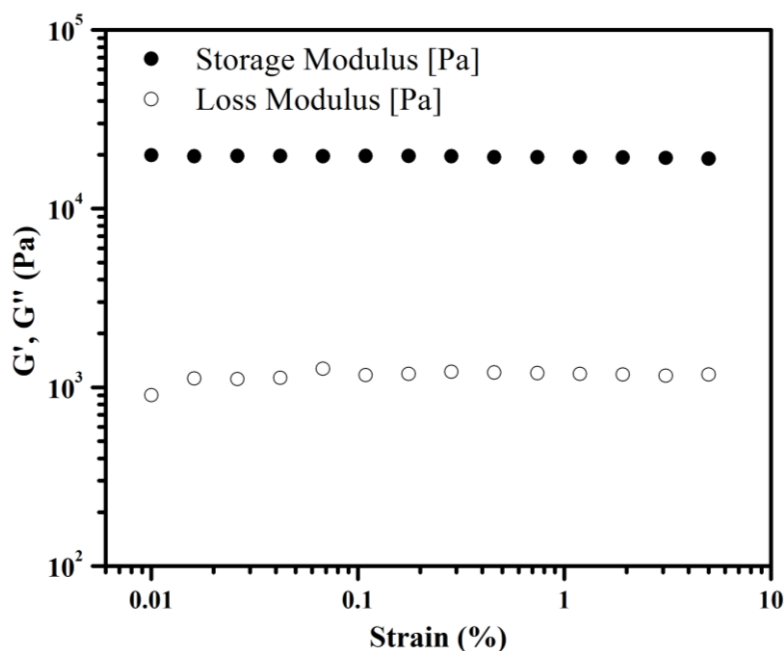


Figure 5c.7: Log-log plot of strain dependence versus storage and loss modulus of PE6-BMI-based gel.

It was observed that storage and loss modulus was almost constant over the entire range of applied strain and hence the values were independent of the applied strain. Gel showed a storage modulus (G') of $1.9 \times 10^4 \text{ Pa}$ at 60°C which is characteristic of soft gels with the elastic network⁴⁸.

The angular frequency dependence of storage and loss modulus were also studied by performing the frequency sweep experiment, within the detection limit of the rheometer and at constant strain (0.1 %) (**Figure 5c.8**). The steady increase in G' was observed with increase in frequency; hence it is dependent on frequency in the applied range.

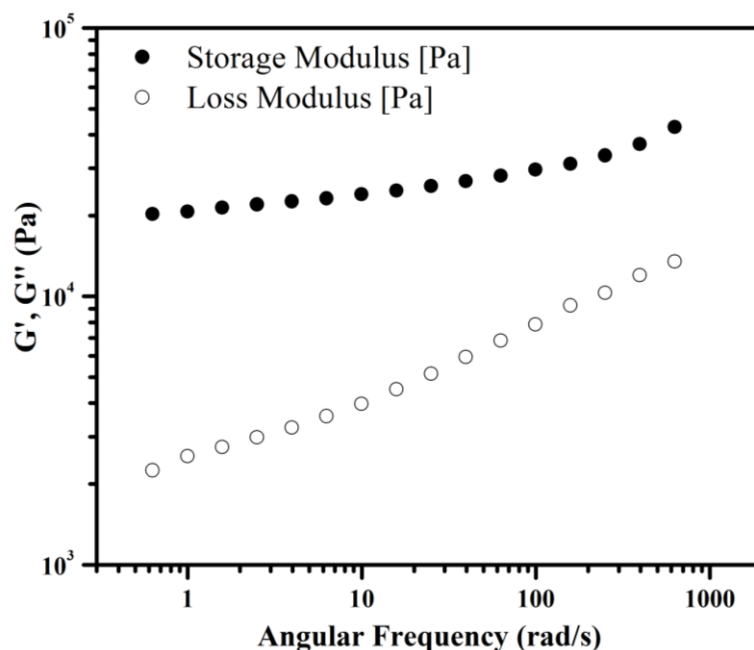


Figure 5c.8: The angular frequency dependence of storage and loss modulus of PE6-BMI-based gel.

The thermo-reversible characteristics of the gel were studied by temperature sweep experiments. Elastic nature of gel dominates when $G' > G''$, whereas the viscous nature is dominant in the sol state when $G'' > G'$. Generally, gel-to-sol or sol-to-gel transition is depicted as $G' = G''$, where the transition from one domain to the other takes place⁴⁸. The temperature sweep experiment was performed with varying temperature from 40-120 °C (heating cycle) and 120- 40 °C (cooling cycle). In between the heating and cooling cycles, the system was kept on hold at 120 °C for 15 min to ensure de-crosslinking of the gels by retro-Diels Alder reaction which was evident from sudden drop in the values of G' and G'' . However, the extent of de-crosslinking at this stage was not calculated.

The three cycles of repeated heating and cooling were performed on the gel. In these repeated cycles, the regular reversal of storage (G') and loss modulus (G'') were observed with varying temperature from 40-120 °C and 120-40 °C at constant angular frequency and strain (**Figure 5c.9**). The initial values of storage (G') and loss modulus (G'') were regained after the completion of each cycle which revealed the thermo-reversibility of network polymers. The thermo-reversibility of the PE6-BMI-based gel was demonstrated up to three repeated cycles which confirmed its thermal-reversibility.

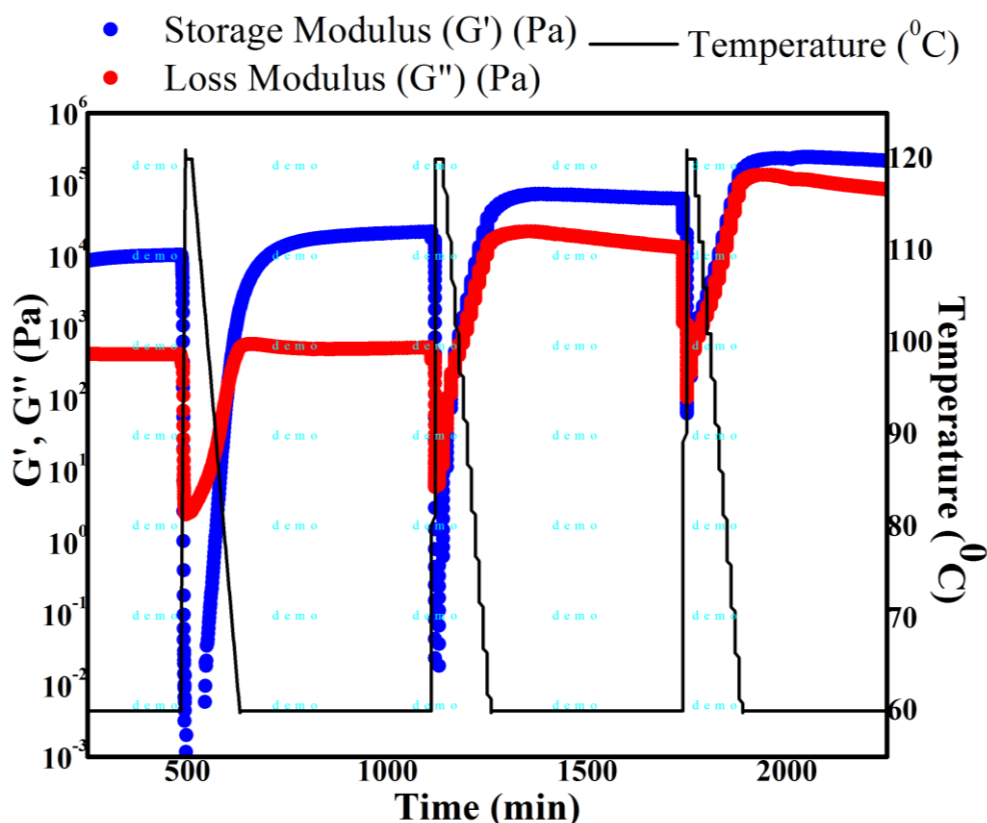


Figure 5c.9: Thermo-reversibility of gel with repeated heating and cooling cycles from 40-120 °C and 120-40 °C.

Even though appropriate over-head oven was used during the measurements, solvent evaporation during the measurement was evident from the gradual increase in G' and G'' values in every cycle. Condensation of solvent vapour was observed in the interior walls of the over-head oven after the measurement, which confirmed the evaporation of solvent during the measurement.

Temperature dependent reversibility of these gel networks may be attributed to the constant breaking and reforming of cross-link points across the network. These results further illustrate the potential of thermally reversible furan-maleimide Diels-Alder reaction for the creation of novel materials based on high performance polymers such as aromatic polyesters and polycarbonates.

5c.4 Conclusions

- Thermally reversible crosslinked polyester and polycarbonate were prepared from the corresponding linear polymers containing pendant furyl groups by reactions with bismaleimides *via* Diels-Alder reaction.

- The crosslinked polyester and polycarbonate showed improved mechanical properties and were recycled two times without significant loss of mechanical properties.
- Additionally, polymeric organogel was prepared from polyester containing pendant furyl groups by reaction with bismaleimide *via* Diels-Alder reaction. Thermoreversibility of crosslinked polyester gel was demonstrated by rheological experiments up to three repeated cycles

References

- 1 J. D. McCoy, W. B. Ancipink, C. M. Clarkson, J. M. Kropka, M. C. Celina, N. H. Giron, L. Hailesilassie and N. Fredj, *Polymer*, 2016, **105**, 243–254.
- 2 C. Mantzaridis, A. L. Brocas, A. Llevot, G. Cendejas, R. Auvergne, S. Caillol, S. Carlotti and H. Cramail, *Green Chem.*, 2013, **15**, 3091.
- 3 F. Pion, P. H. Ducrot and F. Allais, *Macromol. Chem. Phys.*, 2014, **215**, 431–439.
- 4 R. Auvergne, S. Caillol, G. David, B. Boutevin and J. P. Pascault, *Chem. Rev.*, 2014, **114**, 1082–1115.
- 5 D. Stenzengerger, H. Hergenrother and P. Wilson, *Polyimide*, Blackie & Son Ltd, Glasgow and London, 1990.
- 6 J. V. Crivello, *J. Polym. Sci. Polym. Chem. Ed.*, 1973, **11**, 1185–1200.
- 7 I. Hamerton, Ed., *Chemistry and Technology of Cyanate Ester Resins*, Springer Netherlands, Dordrecht, 1994.
- 8 F. Polgar, L. M. Duin, V. M. Broekhuis, A. A. Picchioni, *Macromolecules*, 2015, **48**, 7096–7105.
- 9 A. Wang, H. Niu, Z. He and Y. Li, *Polym. Chem.*, 2017, **8**, 4494–4502.
- 10 M. Suzuki, K. Hanabusa, C. Setoguchi, H. Shirai, K. Hanabusa, T. Shirosaki, H. Hachisako and N. Minami, *Chem. Soc. Rev.*, 2010, **39**, 455–463.
- 11 L. Wang, H. Li and C. P. Wong, *J. Polym. Sci. Part A Polym. Chem.*, 2000, **38**, 3771–3782.
- 12 V. R. Sastri and G. C. Tesoro, *J. Appl. Polym. Sci.*, 1990, **39**, 1439–1457.
- 13 K. Ogino, J. S. Chen and C. K. Ober, *Chem. Mater.*, 1998, **10**, 3833–3838.
- 14 P. I. Engelberg and G. C. Tesoro, *Polym. Eng. Sci.*, 1990, **30**, 303–307.
- 15 S. L. Buchwalter and L. L. Kosbar, *J. Polym. Sci. Part A Polym. Chem.*, 1996, **34**, 249–260.

- 16 J. M. Garcia, G. O. Jones, K. Virwani, B. D. McCloskey, D. J. Boday, G. M. ter Huurne, H. W. Horn, D. J. Coady, A. M. Bintaleb, A. M. S. Alabdulrahman, F. Alsewailam, H. A. A. Almegren and J. L. Hedrick, *Science*, 2014, **344**, 732–735.
- 17 J. P. Kennedy and K. F. Castner, *J. Polym. Sci. Polym. Chem. Ed.*, 1979, **17**, 2055–2070.
- 18 J. R. Jones, C. L. Liotta, D. M. Collard and D. A. Schiraldi, *Macromolecules*, 1999, **32**, 5786–5792.
- 19 P. J. Boul, P. Reutenauer and J. M. Lehn, *Org. Lett.*, 2005, **7**, 15–18.
- 20 A. Gandini, A. J. D. Silvestre, D. Coelho, B. Reis, A. J. D. Silvestre and P. J. Costanzo, *Polym. Chem.*, 2011, **2**, 1713.
- 21 G. Franc and A. K. Kakkar, *Chem. A Eur. J.*, 2009, **15**, 5630–5639.
- 22 X. Chen, *Science* 2002, **295**, 1698–1702.
- 23 A. Gandini, *Prog. Polym. Sci.*, 2013, **38**, 1–29.
- 24 C. Gaina, O. Ursache, V. Gaina and C. D. Varganici, *Express Polym. Lett.*, 2013, **7**, 636–650.
- 25 Y. L. Liu and Y. W. Chen, *Macromol. Chem. Phys.*, 2007, **208**, 224–232.
- 26 C. Zeng, H. Seino, J. Ren, K. Hatanaka and N. Yoshie, *Polymer*, 2013, **54**, 5351–5357.
- 27 C. Zeng, H. Seino, J. Ren, K. Hatanaka and N. Yoshie, *Macromolecules*, 2013, **46**, 1794–1802.
- 28 A. Gandini, *polymers*, 2005, **15**, 95–101.
- 29 F. Hu, J. J. La Scala, J. M. Sadler and G. R. Palmese, *Macromolecules*, 2014, **47**, 3332–2242.
- 30 Y. Liu and C. Hsieh, *J. Polym. Sci. Part A Polym. Chem.*, 2005, **44**, 905–913.
- 31 Y. L. Liu, C. Y. Hsieh and Y. W. Chen, *Polymer*, 2006, **47**, 2581–2586.
- 32 Y. Liu, C. Hsieh and Y. Chen, *Polymer*, 2006, **47**, 2581–2586.
- 33 C. Toncelli, D. C. De Reus, F. Picchioni and A. A. Broekhuis, *Macromol. Chem. Phys.*, 2012, **213**, 157–165.
- 34 F. Polgar, L. M. Duin, M. V Broekhuis, A. A. Picchioni, *Macromolecules*, 2015, **48**, 7096–7105.
- 35 S. Barrau, D. Fournier, G. Stoclet, P. Woisel and J. Lefebvre, *Polymer*, 2017, **117**, 342–353.
- 36 L. M. Polgar, E. Hagting, W. Koek, F. Picchioni and M. Van Duin, *Polymers*, 2017, **81**, 1–13.

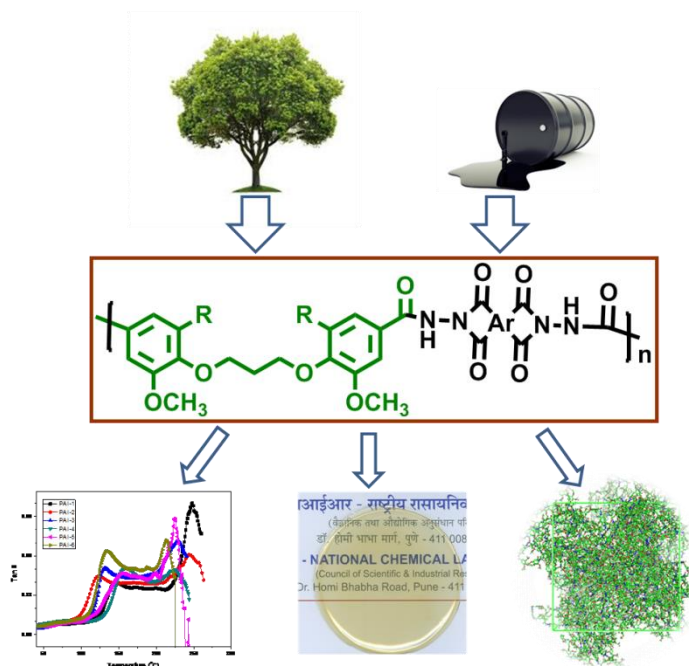
- 37 T. Ikezaki, R. Matsuoka, K. Hatanaka and N. Yoshie, *J. Polym. Sci. Part A Polym. Chem.*, 2014, **52**, 216–222.
- 38 J. Kötteritzsch, S. Stumpf, S. Hoepfner, J. Vitz, M. D. Hager and U. S. Schubert, *Macromol. Chem. Phys.*, 2013, **214**, 1636–1649.
- 39 S. J. Garcia, M. D. Hager, R. K. Bose, K. Julia, U. S. Schubert and S. Van Der Zwaag, *J. Polym. Sci. Part A Polym. Chem.*, 2014, **52**, 1669–1675.
- 40 C. Goussé, A. Gandini and P. Hodge, *Macromolecules*, 1998, **31**, 314–321.
- 41 S. Ortega Sánchez, F. Marra, A. Dibenedetto, M. Aresta and A. Grassi, *Macromolecules*, 2014, **47**, 7129–7137.
- 42 A. Gandini and T. M. Lacerda, *Prog. Polym. Sci.*, 2015, **48**, 1–39.
- 43 Y. H. Kim and W. E. Stites, *Biochemistry*, 2008, **47**, 8804–8814.
- 44 J. Canadell, H. Fischer, G. De With and R. A. T. M. van Benthem, *J. Polym. Sci. Part A Polym. Chem.*, 2010, **48**, 3456–3467.
- 45 B. J. Adzima, H. A. Aguirre, C. J. Kloxin, T. F. Scott and C. N. Bowman, *Macromolecules*, 2008, **41**, 9112–9117.
- 46 S. S. Patil, A. Torris and P. P. Wadgaonkar, *J. Polym. Sci. Part A Polym. Chem.*, 2017, **55**, 2700–2712.
- 47 L. Feng, Z. Yu, Y. Bian, J. Lu, X. Shi and C. Chai, *Polymer*, 2017, **124**, 48–59.
- 48 Y. Osada, in *Gels Handbook*, Elsevier, 2001, vol. 1, pp. 13–25.

Chapter - 6

Synthesis and Characterization of Poly(amide imide)s and Polyimides

Chapter - 6a

Synthesis and Characterization of Poly(amide imide)s Containing Oxyalkylene Linkages



6a.1 Introduction

Aromatic poly(amide imide)s represent an important class of high performance polymers due to their excellent thermal and mechanical properties¹⁻⁴. The excellent properties poly(amide imide)s are derived from their distinctive chemical structure, which combine both the amide and imide functional groups in the polymer backbone. Therefore, poly(amide imide)s find applications in several fields such as gas separation, nanofiltration, osmotic power generation and so on^{5,6}.

The widespread applications of poly(amide imide)s are somewhat limited due to the difficulties encountered in processing due to their high melting/softening temperatures and poor solubility in organic solvents⁷. To improve processability and solubility, several strategies have been adapted such as the incorporation of flexibilizing groups, bulky groups, *meta*-catenation and so on. All these structural modifications decrease rigidity and disturb interchain interactions and consequently improve processability of polymers⁸⁻¹¹.

The purpose of the present work was to synthesize partially bio-based aromatic poly(amide imide)s containing flexibilizing propylene linkages in the polymer backbone by polycondensation of bio-based diacylhydrazide monomers namely, 4,4'-(propane-1,3-diylbis(oxy))bis(3-methoxybenzohydrazide) (DSHzC-3) and 4,4'-(propane-1,3-diylbis(oxy))bis(3,5-dimethoxybenzohydrazide) (DVHzC-3) with commercially available aromatic dianhydrides *viz.* pyromellitic dianhydride (PMDA), 3,3',4,4'-biphenyltetracarboxylic dianhydride (BPDA) and 3,3',4,4'-oxydiphthalic anhydride (ODPA). Poly(amide imide)s were characterized by inherent viscosity measurements, solubility tests, FT-IR, ¹H NMR and ¹³C NMR spectroscopy, X-ray diffraction, thermogravimetric analysis (TGA), differential scanning calorimetric studies (DSC) and dynamic mechanical analysis (DMA). The effect of methoxy substituents on aromatic ring on T_g of poly(amide imide)s was investigated. Furthermore, to understand the molecular origin of the substituent effect on T_g, molecular dynamics (MD) simulation studies were performed.

6a.2 Experimental

6a.2.1 Materials

4,4'-(Propane-1,3-diylbis(oxy))bis(3-methoxybenzohydrazide) (DVHzC-3) and 4,4'-(propane-1,3-diylbis(oxy))bis(3,5-dimethoxybenzohydrazide) (DSHzC-3) were synthesized as described in **Chapter 3**. Pyromellitic dianhydride (PMDA), 3,3',4,4'-

biphenyltetracarboxylic dianhydride (BPDA) and 3,3',4,4'-oxydiphthalic anhydride (ODPA) were received from Sigma Aldrich, USA and sublimed before use. *N,N*-Dimethylformamide (DMF), *N,N*-dimethylacetamide (DMAc), dimethyl sulfoxide (DMSO), *N*-methyl-2-pyrrolidone (NMP), dichloromethane, chloroform and pyridine were received from Thomas Baker Ltd., Mumbai and were purified as per literature procedures¹².

6a.2.2 Measurements

Inherent viscosity of poly(amide imide)s was determined with 0.5 % (w/v) solution of polymer in DMAc at 30±0.1°C using Ubbelohde suspended level viscometer. Inherent viscosity was calculated using the equation

$$\eta_{inh} = \frac{2.303}{c} \times \log t/t_0$$

Where, t and t_0 are flow times of polymer solution and solvent, respectively and c is the concentration of polymer solution

Molecular weights and dispersity values of poly(amide imide)s were determined on Thermo-Finnigan make gel-permeation chromatography (GPC) using DMF as an eluent at a flow rate of 1 mL min⁻¹ at 25 °C. Sample concentration was 2 mg mL⁻¹ and narrow dispersity polystyrenes were used as calibration standards.

FT-IR spectra were recorded on a Perkin-Elmer Spectrum GX spectrometer using polymer film.

¹H and ¹³C NMR spectra were recorded on a Bruker-AV 200, 400 or 500 MHz spectrometer using DMSO-d₆ as solvent and TMS as an internal standard.

Thermogravimetric analysis was performed on Perkin Elmer: STA 6000 instrument at the heating rate of 10 °C min⁻¹ under nitrogen atmosphere.

Glass transition temperature (T_g) was determined on TA instruments DSC Q-10 with a heating rate of 10 °C min⁻¹ under nitrogen atmosphere. T_g of polymer was recorded on second heating cycles.

X-Ray diffraction patterns of poly(amide imide)s were recorded using dried polymer film on a Rigaku Dmax 2500 X-ray diffractometer at a tilting rate of 2° min⁻¹.

Dynamic mechanical analysis (DMA) of poly(amide imide)s as a function of temperature was carried out on films cast from DMAc solutions. The sample dimensions were 10 × 6 mm (length × width) and thickness was in the range 0.09-0.13 mm. The measurements were carried out on Rheometrics Scientifics (Model Mark IV) (UK), using the dynamic mode between 50-300 °C, at frequency of 1 Hz and heating rate of 5 °C min⁻¹.

Details of molecular dynamics simulation:

The initial configurations for MD simulations of poly(amide imide)s were obtained using geometry optimization of the structures of repeating units of poly(amide imide)s using Gaussian 09 code¹³. Sixteen of such repeating units were joined to form a polymer chain. 24 energy minimized chains for PAI-4 and 20 chains for PAI-1 were added randomly to a box to make the bulk polymer systems. A chain length of 16 mer was taken, since 8 mer of similar polyimides have been previously reported to reproduce various conformational and thermodynamic properties¹⁴.

All forcefield parameters were taken from OPLS-AA¹⁵ force field. All-atomistic model was employed except for the benzenoid and connecting carbons, which were treated as united atoms¹⁶. Simulations were performed in isothermal-isobaric ensemble (NPT). Berendsen¹⁷ barostat and V-rescale thermostat¹⁸ were used to keep the pressure and temperature fixed during simulations. Particle Mesh Ewald (PME) was used to calculate the long range electrostatics. A cut-off distance of 1.2 nm was given both for short range Coulomb and Lennard Jones interactions.

6a.2.3 Synthesis of poly(amide imide)s containing oxypropylene linkage.

General procedure for synthesis of poly(amide imide)s from 4,4'-(propane-1,3-diylbis(oxy))bis(3-methoxybenzohydrazide) / 4,4'-(propane-1,3-diylbis(oxy))bis(3,5-dimethoxybenzohydrazide) and aromatic dianhydrides

Into a 50 mL three necked round bottom flask equipped with a guard tube, a nitrogen inlet, and a magnetic stirring bar were charged DVHzC-3/DSHzC-3 (1.20 mmol) and DMAc (10 mL). After complete dissolution of diacylhydrazide, aromatic dianhydride (1.20 mmol) was added in one portion to the stirred solution of diacylhydrazide. The reaction was allowed to proceed for an additional 12 h under nitrogen atmosphere. At the end of the reaction time, the viscous solution of poly(hydrazide acid) was obtained. The solution of poly(hydrazide acid) was cast onto a glass plate and the solvent was evaporated by heating at 80 °C with continuous nitrogen flow for 1 h. The semi-dried film was heated at 230 °C/0.75 mm Hg for 12 h under reduced pressure to effect imidization.

Synthesis of PAI-1 from 4,4'-(propane-1,3-diylbis(oxy))bis(3,5-dimethoxybenzohydrazide) and PMDA

FT-IR (cm⁻¹): 3237, 1795, 1743, 1680, 1338, 730; ¹H NMR (500 MHz, DMSO-d₆, δ/ppm): 1.99-2.04 (m, 2H), 3.85 (s, 12H), 4.19 (t, 4H), 7.36 (s, 4H), 8.55 (s, 2H), 11.51 (s,

2H); ^{13}C NMR (125 MHz, DMSO- d_6 , δ/ppm): 30.6, 56.1, 69.9, 105.4, 119.2, 125.2, 135.4, 140.4, 153.0, 163.8, 164.7.

Synthesis of PAI-2 from 4,4'-(propane-1,3-diylbis(oxy))bis(3,5-dimethoxybenzohydrazide) and BPDA

FT-IR (cm^{-1}): 3236, 1790, 1742, 1680, 1340, 723; ^1H NMR (400 MHz, DMSO- d_6 , δ/ppm): 2.0-2.07 (m, 2H), 3.85 (s, 12H), 4.19 (t, 4H), 7.35 (s, 4H), 8.16 (dd, 2H), 8.44 (d, 2H), 8.52 (d, 2H), 11.36 (s, 2H); ^{13}C NMR (100 MHz, DMSO- d_6 , δ/ppm) 30.4, 55.9, 69.7, 105.1, 122.9, 124.4, 125.3, 129.2, 130.4, 134.3, 140.1, 144.7, 152.8, 164.5, 164.9.

Synthesis of PAI-3 from 4,4'-(propane-1,3-diylbis(oxy))bis(3,5-dimethoxybenzohydrazide) and ODPDA

FT-IR (cm^{-1}): 3240, 1789, 1742, 1680, 1346, 722; ^1H NMR (200 MHz, DMSO- d_6 , δ/ppm): 1.92-2.05 (m, 2H), 3.83 (s, 12H), 4.17 (t, 4H), 7.32 (s, 4H), 7.73 (dd, 2H), 7.79 (d, 2H), 8.10 (d, 2H), 11.31 (s, 2H); ^{13}C NMR (50 MHz, DMSO- d_6 , δ/ppm) 30.6, 56.1, 69.9, 105.3, 114.7, 125.2, 125.4, 126.6, 132.4, 140.3, 153.0, 161.1, 164.7, 164.8.

Synthesis of PAI-4 from 4,4'-(propane-1,3-diylbis(oxy))bis(3-methoxybenzohydrazide) and PMDA

FT-IR (cm^{-1}): 3240, 1790, 1741, 1677, 1339, 727; ^1H NMR (400 MHz, DMSO- d_6 , δ/ppm): 2.25-2.31 (m, 2H), 3.87 (s, 6H), 4.27 (t, 4H), 6.56 (d, 2H), 7.22 (d, 2H), 7.59 (s, 2H), 7.65 (d, 2H), 8.53 (s, 2H), 11.41 (s, 2H); ^{13}C NMR (100 MHz, DMSO- d_6 , δ/ppm): 28.5, 55.7, 65.1, 111.0, 112.3, 119.2, 121.7, 122.7, 135.4, 148.7, 151.8, 163.8, 163.9, 164.8.

Synthesis of PAI-5 from 4,4'-(propane-1,3-diylbis(oxy))bis(3-methoxybenzohydrazide) and BPDA

FT-IR (cm^{-1}): 3239, 1794, 1741, 1678, 1345, 720; ^1H NMR (400 MHz, DMSO- d_6 , δ/ppm): 2.20-2.30 (m, 2H), 3.85 (s, 6H), 4.25 (t, 4H), 7.20 (d, 2H), 7.56 (s, 2H), 7.63 (d, 2H), 7.70 (d, 2H), 7.78 (s, 2H), 8.90 (d, 2H), 11.21 (s, 2H); ^{13}C NMR (100 MHz, DMSO- d_6 , δ/ppm): 28.5, 55.7, 65.1, 111.0, 112.3, 114.6, 121.6, 122.9, 125.1, 125.5, 126.6, 132.4, 148.7, 151.7, 161.1, 164.8, 164.9.

Synthesis of PAI-6 from 4,4'-(propane-1,3-diylbis(oxy))bis(3-methoxybenzohydrazide) and ODPDA

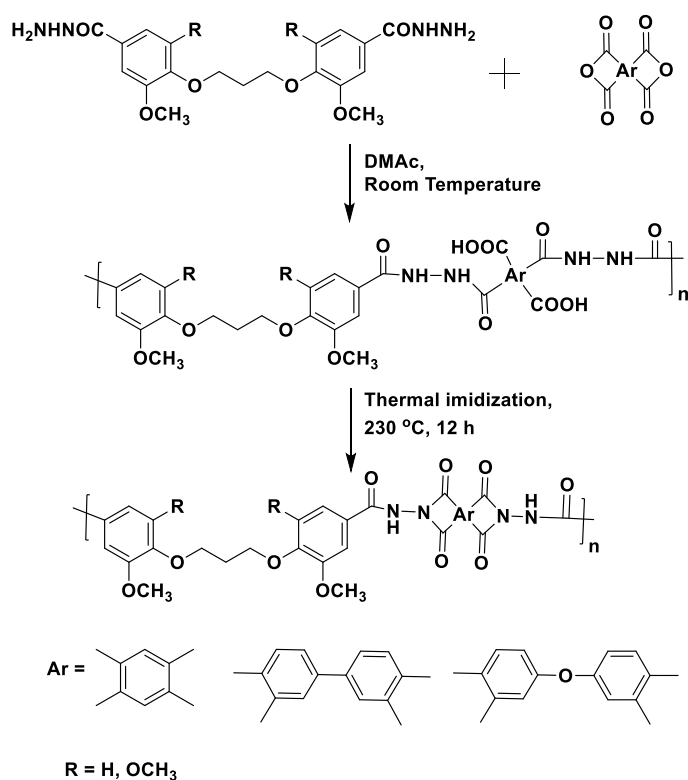
FT-IR (cm^{-1}): 3237, 1794, 1739, 1678, 1340, 734; ^1H NMR (400 MHz, DMSO-d_6 , δ/ppm): 2.27 (br. s, 2H), 3.85 (s, 6H), 4.25 (t, 4H), 7.19 (dd, 2H), 7.56 (dd, 2H), 7.60 (d, 2H), 7.66 (d, 2H), 7.78 (d, 2H), 8.09 (d, 2H), 11.21 (s, 2H); ^{13}C NMR (100 MHz, DMSO-d_6 , δ/ppm) 28.5, 55.7, 65.1, 111.0, 112.4, 114.7, 121.6, 122.8, 126.6, 132.4, 148.6, 151.7, 161.1, 164.8, 164.9.

6a.3 Results and discussion

6a.3.1 Synthesis of poly(amide imide)s

In the present work, a series of new partially bio-based poly(amide imide)s was synthesized by polycondensation of diacylhydrazide monomers *viz.* DVHzC-3 and DSHzC-3 with commercially available aromatic dianhydrides *viz.* PMDA, BPDA and ODPA by two-step polycondensation reaction (**Scheme 6a.1**).

In the first step, poly(hydrazide acid) was synthesized by the addition of stoichiometric quantity of aromatic dianhydride to the solution of diacylhydrazide in DMAc at room temperature. The polycondensation reactions proceeded in a homogenous solution throughout the course of reaction. In the second step, cyclization of poly(hydrazide acid) was carried out by thermal cyclo-imidization method. The poly(hydrazide acid) solution was poured into a glass petri dish and solvent was evaporated by heating at 80 °C with continuous nitrogen flow. The semi-dried poly(hydrazide acid) film was heated at 230 °C under reduced pressure for 12 h to form poly(amide imide)⁸.



Scheme 6a.1 Synthesis of poly(amide imide)s from 4,4'-(propane-1,3-diylbis(oxy))bis(3-methoxybenzohydrazide)/4,4'-(propane-1,3-diylbis(oxy))bis(3,5-dimethoxybenzohydrazide) and aromatic dianhydrides.

The results of polymerization reactions are summarized in **Table 6a.1**. Inherent viscosity values of poly(amide imide)s were in the range 0.44-0.56 dLg⁻¹. Poly(amide imide)s were soluble in DMF and their molecular weights were measured by GPC using polystyrenes as calibration standards. Number average molecular weights (\overline{M}_n) and dispersity values were in the range 25,500-40,800 g mol⁻¹ and 1.7-2.0, respectively. Inherent viscosity values and GPC molecular weight data indicated the formation of reasonably high molecular weight polymers. Poly(amide imide)s being semi-rigid in nature, the \overline{M}_n values reported with polystyrene standards are expected to be overestimated. Similar observations have been reported in the literature for measurements of molecular weight by GPC of polymers which adopt a rod-like conformation in solution^{19,20}. Poly(amide imide)s could be cast into transparent, flexible, and tough film from their DMAc solution.

Table 6a.1 Inherent viscosity and molecular weight data of poly(amide imide)s

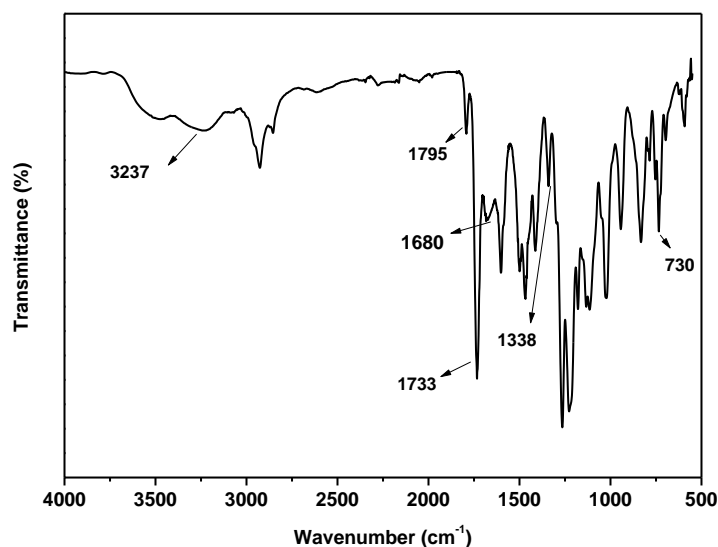
Poly(amide imide)s	Diacyl hydrazide	Dianhydride	η_{inh} (dLg ⁻¹) ^a	GPC ^b		Dispersity
				\overline{M}_n	\overline{M}_w	
PAI-1	DSHC-3	PMDA	0.53	38,400	67,800	1.7
PAI-2	DSHC-3	BPDA	0.56	40,800	72,600	1.7
PAI-3	DSHC-3	ODPA	0.47	36,600	63,000	1.7
PAI-4	DVHC-3	PMDA	0.44	25,500	53,500	2.0
PAI-5	DVHC-3	BPDA	0.51	37,000	66,600	1.8
PAI-6	DVHC-3	ODPA	0.45	29,400	56,000	1.9

a: η_{inh} was measured with 0.5% (w/v) solution of poly(amide imide) in DMAc at 30 ± 0.1 °C

b: measured by GPC in DMF, polystyrene was used as the calibration standard.

6a.3.2 Structural characterization

The chemical structures of poly(amide imide)s were confirmed by FT-IR, ¹H and ¹³C NMR spectroscopy. FT-IR spectrum of PAI-1 is reproduced in **Figure 6a.1**. The absorption band at 3237 cm⁻¹ corresponds to -NH- of amide linkage. The absorption band of the five membered imide carbonyl appeared at 1795 cm⁻¹ and 1733 cm⁻¹ corresponding to asymmetric and symmetric stretching vibration, respectively. A band at 1680 cm⁻¹ appeared due to carbonyl group of amide. The absorption bands at 1338 cm⁻¹ and 730 cm⁻¹ were assigned to stretching and bending vibrations, respectively of C-N-C linkage of imide ring⁸.

**Figure 6a.1** FT-IR spectrum of PAI-1

^1H NMR spectrum of PAI-1 is reproduced in **Figure 6a.2**. A multiplet in the range 1.99-2.04 δ ppm was observed due to methylene protons β to oxygen atom. Methoxy protons exhibited a singlet at 3.85 δ ppm while methylene protons attached to oxygen atom appeared as a triplet at 4.19 δ ppm. Aromatic protons *ortho* to amide group displayed a singlet at 7.36 δ ppm. The aromatic protons of PMDA moiety appeared as a singlet at 8.55 δ ppm. Amide protons (-NH-) exhibited a broad singlet at 11.51 δ ppm. ^{13}C NMR spectrum of PAI-1 along with assignments of carbon atoms is reproduced in **Figure 6a.3**.

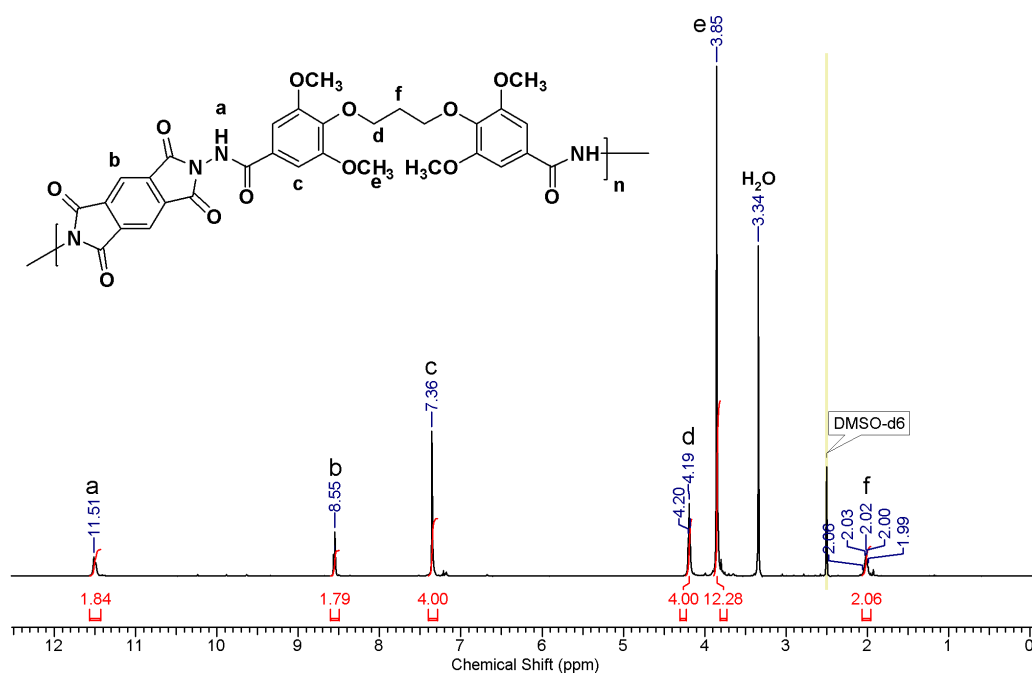


Figure 6a.2 ^1H NMR spectrum of PAI-1 in DMSO-d_6

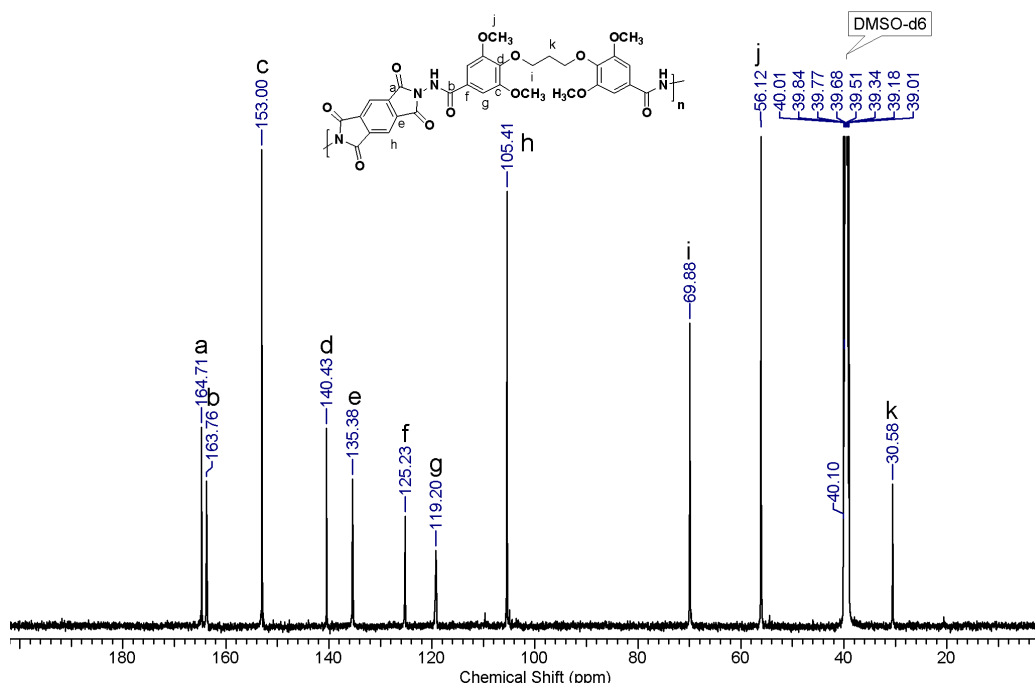


Figure 6a.3 ^{13}C NMR spectrum of PAI-1 in DMSO-d_6

6a.3.3 Solubility of poly(amide imide)s

The solubility of poly(amide imide)s was determined at 3 % concentration (w/v) in various organic solvents and data is summarized in **Table 6a.2**.

Table 6a.2 Solubility data of poly(amide imide)s

Poly(amide imide)	Chloroform	Dichloroform	DMF	DMAc	DMSO	NMP	Pyridine
PAI-1	--	--	++	++	++	++	++
PAI-2	--	--	++	++	++	++	++
PAI-3	--	--	++	++	++	++	++
PAI-4	--	--	++	++	++	++	++
PAI-5	--	--	++	++	++	++	++
PAI-6	--	--	++	++	++	++	++

--, insoluble; ++, soluble at room temperature; +-, soluble on heating

Poly(amide imide)s exhibited good solubility in organic solvents such as DMF, DMAc, DMSO, NMP and pyridine were insoluble in chloroform and dichloromethane. The improvement in solubility characteristics of poly(amide imide)s could be attributed to the combined effect of flexible oxypropylene linkages and polar methoxy substituents.

6a.3.4 X-Ray diffraction studies

X-Ray diffractograms of poly(amide imide)s are shown in **Figure 6a.4**. Poly(amide imide)s exhibited two broad halos in the range $2\theta = 20-30^\circ$ and $10-15^\circ$. The broad halos in XRD patterns indicated their amorphous nature, which could be mainly because of the presence of methoxy substituents which disrupt close packing of polymer chains.

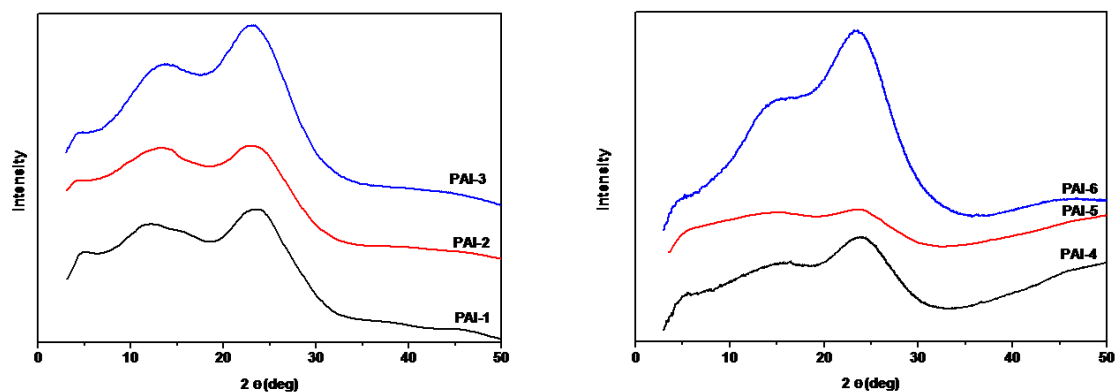


Figure 6a.4. X-Ray diffractograms of poly(amide imide)s

6a.3.5 Thermal properties of poly(amide imide)s

The thermal properties of poly(amide imide)s were determined by TGA and DSC at heating rate $10^\circ\text{C min}^{-1}$ under nitrogen atmosphere. TG and DSC curves are shown in **Figure 6a.5** and **6a.6**, respectively, and the data is summarized in **Table 6a.3**.

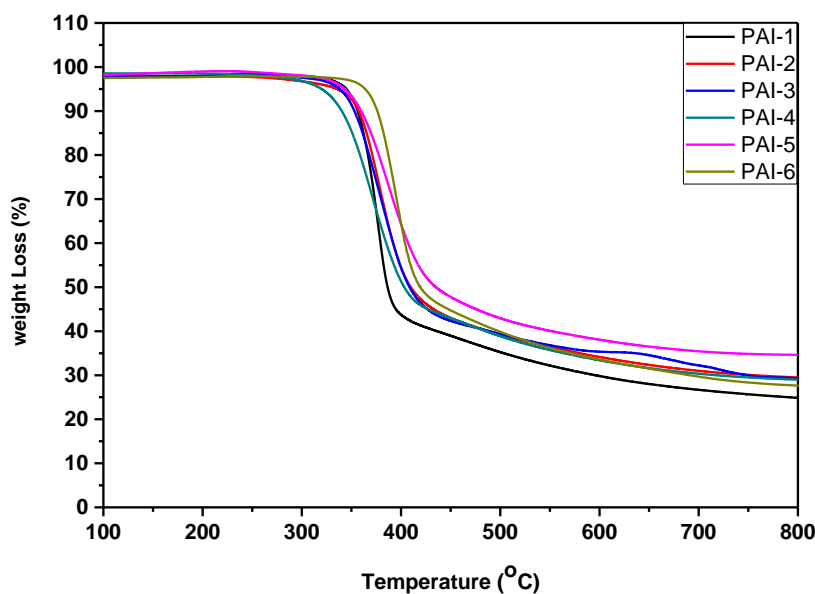


Figure 6a.5 TG curves of poly(amide imide)s

Table 6a.3 Thermo-mechanical properties of poly(amide imide)s

Polymer	Diacyl hydrazide	Dianhydride	T ₁₀ ^b (°C)	Char yield (%) ^c	T _g ^d (°C)	T _g ^e (°C)	E' (Pa)
PAI-1	DSHC-3	PMDA	355	25	ND	248	3.5 × 10 ⁹
PAI-2	DSHC-3	BPDA	356	29	223	246	2.2 × 10 ⁹
PAI-3	DSHC-3	ODPA	352	29	209	238	3.0 × 10 ⁹
PAI-4	DVHC-3	PMDA	340	31	218	226	1.6 × 10 ⁹
PAI-5	DVHC-3	BPDA	360	35	212	224	0.4 × 10 ⁹
PAI-6	DVHC-3	ODPA	364	28	201	214	1.1 × 10 ⁹

a: initial decomposition temperature;

b: temperature at which 10 % weight loss was observed

c: weight residue at 800 °C

d: measured by DSC on second heating scan with heating rate at 10 °C min⁻¹ under nitrogen atmospheres

e: T_g determined by DMA; ND = Not detected.

The 10 % weight loss temperature of poly(amide imide)s in nitrogen was in the range 340-364 °C. The thermal properties of present poly(amide imide)s are inferior compared to the conventional fully aromatic poly(amide imide)s⁵. The lowering of thermal stability of these poly(amide imide)s could be attributed to the presence of thermally labile oxypropylene linkages and methoxy groups. The weight residue of poly(amide imide)s at 800 °C were in the range 24-34%, which could be attributed to the formation of carbonaceous materials due to anaerobic heating of the polymers. T_g values of poly(amide imide)s were in the range 201-223 °C except for PAI-1 which did not show T_g in DSC analysis.

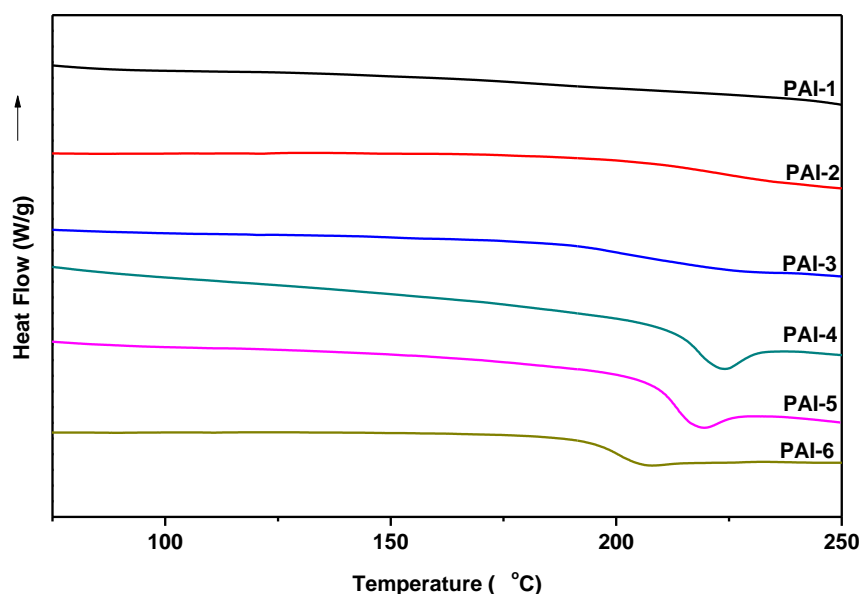


Figure 6a.6 DSC curves of poly(amide imide)s

6a.3.6 Dynamic mechanical analysis

The thermomechanical properties of poly(amide imide)s were determined by DMA. DMA curves of poly(amide imide)s are displayed in **Figure 6a.7** and data is included in **Table 6a.3**.

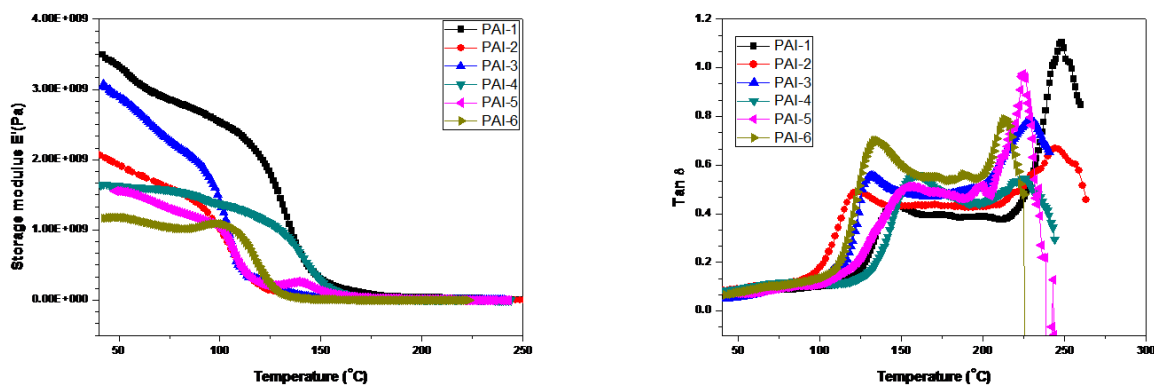


Figure 6a.7 Dynamic mechanical curves of poly(amide imide)s

The oxypropylene linkages are responsible for lowering the T_g of poly(amide imide)s due to increase in free volume. However, oxypropylene linkages apparently did not significantly decrease rigidity of the polymer chains and hence these poly(amide imide)s showed high storage moduli (0.4×10^9 - 3.5×10^9 Pa). The storage modulus of poly(amide imide)s based on DSHzC-3 and DVHzC-3 were in the range 3.0×10^9 - 3.5×10^9 and 0.4×10^9 - 1.6×10^9 Pa, respectively, indicating that poly(amide imide)s based on

DSHzC-3 exhibited higher storage modulus than corresponding poly(amide imide)s based on DVHzC-3. The storage modulus of poly(amide imide)s derived from PMDA (PAI-2 and PAI-5) showed lower than corresponding poly(amide imide)s derived from BPDA (PAI-3 and PAI-6). The storage modulus of a polymer is the measure of stiffness of chains and is dependent on several factors which include chain rigidity, chain order, molecular packing of chains, etc. One of the explanations for the higher storage modulus values of PAI-3 and PAI-6 compared to PAI-2 and PAI-5, respectively could be due to better molecular packing of the former on account of the presence of flexible ether linkage in the dianhydride component which allow better orientation of polymer chains. It has been reported in the literature that mean intermolecular distance, which is a parameter of molecular packing, is lower (4.6-4.7 Å) for polyimide derived from ODPA and para-phenylene diamine than that for polyimide derived from BPDA and para-phenylene diamine (4.7-4.8 Å)²¹. Further detailed investigations are needed to fully establish the influence of structure, chain orientation and molecular packing on storage modulus of these poly(amide imide)s differing in their chain rigidity. All the poly(amide imide)s showed two transitions above room temperature. The transition appearing at higher temperature i.e the α transition, corresponds to T_g . The transition that appeared in the temperature range 122-155 °C corresponds to the sub-glass transition or β transition²². The T_g values of poly(amide imide)s were in the range 214-248 °C and these values were slightly higher compared to corresponding T_g values measured by DSC. The difference in T_g values by DMA and DSC may be due to different principles of measurements; DMA measures the mechanical response while DSC records the changes in heat flow of polymer.

It was noticed that T_g values of poly(amide imide)s based on both diacylhydrazides followed the order: ODPA<BPDA<PMDA. The lowest T_g observed for ODPA-based poly(amide imide)s could be explained on the basis of introduction of additional ether linkages while the highest T_g values of PMDA-based poly(amide imide)s are attributed to rigidity imparted by the rigid dianhydride monomer. The similar trends in T_g values have been reported in the literature for polyimides and poly(amide imide)s¹¹.

The effects of methoxy substituents in diacylhydrazide monomers on T_g values of corresponding poly(amide imide)s were evaluated. Poly(amide imide)s derived from tetramethoxy substituted diacylhydrazide *viz.* DSHzC-3 showed higher T_g values than corresponding poly(amide imide)s based on dimethoxy substituted diacylhydrazide *viz.*

DVHzC-3. Molecular dynamics (MD) simulation studies were performed on representative poly(amide imide)s to analyze the molecular origin of the observed substituent effects on T_g .

6a.3.7 Molecular dynamics simulation studies of representative poly(amide imide)s (PAI-1 and PAI-4)

Two representative poly(amide imide)s, viz. PAI-1 and PAI-4 which differ in the number of methoxy substituents on aromatic rings were selected for MD simulation studies. All-atomistic models of the repeating units of poly(amide imide)s are shown in **Figure 6a.8**.

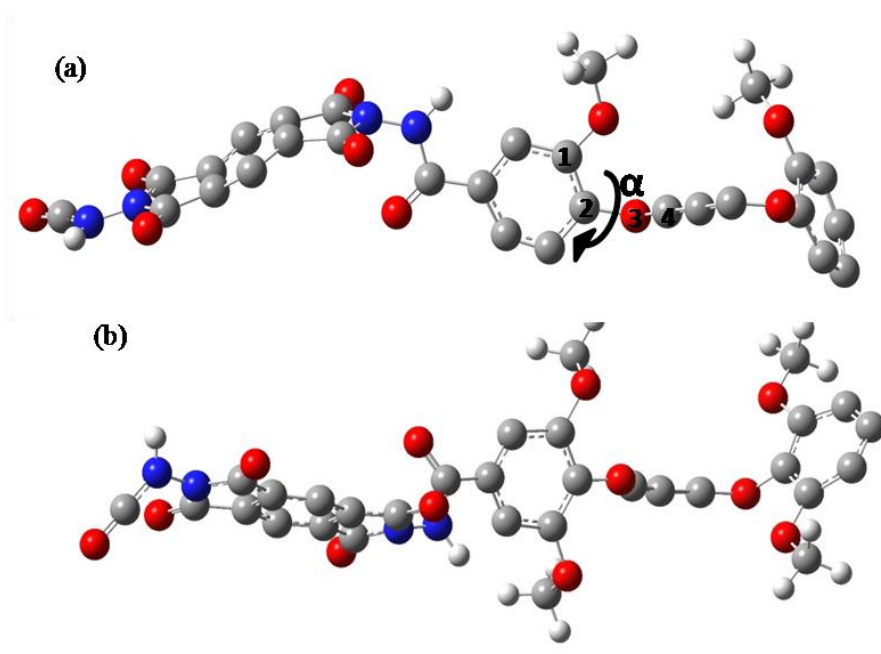


Figure 6a.8 Optimized geometries of (A) PAI-4 (B) PAI-1. The dihedral angle (α) between phenyl ring and oxypropylene linkage is marked.

The details of polymer melt preparation, equilibration and simulation procedure are given in experimental section. The simulation studies were carried out using Gromacs-5.0.5¹⁶ package and OPLA-AA¹⁵ force field. T_g values of PAI-1 and PAI-4 were calculated from temperature dependence of the density as shown in **Figure 6a.9**.

This approach of T_g calculation has been used previously for polyimides by Lyulin et al¹⁴. The calculated T_g values were higher compared to the corresponding experimental values obtained from DMA studies due to the higher cooling rates applied (10K ns⁻¹) in simulation studies. However, the shift in the experimental T_g value has been

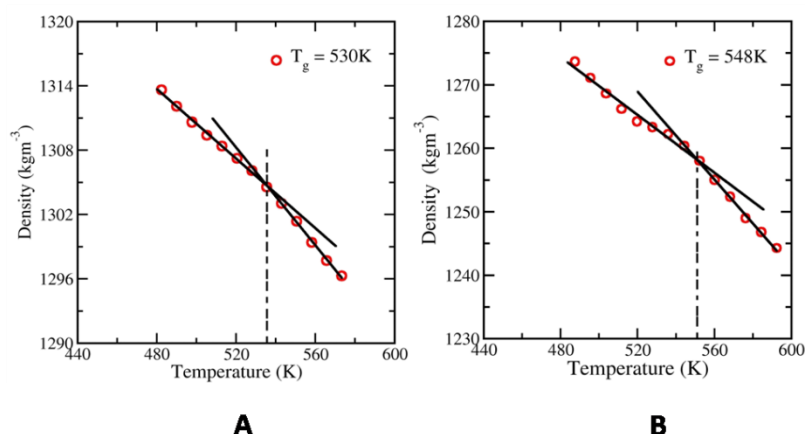


Figure 6a.9 T_g of poly(amide imide)s measured by MD simulation. **A.** Poly(amide imide) based on DVHzC-3 (PAI-4) **B.** Poly(amide imide) based on DSHzC-3 (PAI-1)

well reproduced. The calculated T_g of PAI-1 is 18K higher than PAI-4 as compared to an increase of 22K observed in DMA studies. It is generally accepted that T_g of an amorphous polymer is determined by α relaxation or segmental motion of the chains²³, which in turn is affected by the free volume²⁴ and/or rigidity²⁵ of the chains. The availability of more free volume and less chain rigidity leads to faster relaxation resulting in lower T_g and vice-versa. However, prior studies indicate that these two factors might work independently and either of them can be a controlling factor in affecting T_g ^{26,27}. The calculated free volume, densities along with other physical properties of PAI-1 and PAI-4 are shown in **Table 6a.4**.

Table 6a.4 System details and calculated properties for poly(amide imide)s PAI-4 and PAI-1.

Property	PAI-4	PAI-1
Number of chains	24	20
Total number of atoms	19584	19520
Density kg/m^3 (650K)	1354.41 ± 2.4	1337.19 ± 0.1
T_g	530 K	548 K
Free volume fraction (FVF)	0.473 ± 0.03	0.486 ± 0.007
Radius of gyration (nm)	1.44 ± 0.05	1.51 ± 0.05

Interestingly, despite having higher T_g , PAI-1 showed lower density and higher free volume as compared to PAI-4. The density of PAI-1 and PAI-4 would depend on the

intra- as well as inter-chain spacing/packing. The higher radius of gyration (**Table 6a.4**) of PAI-1 indicated a slightly expanded conformation that leads to the lower density. The radial distribution function (RDF) between the centers of mass of all the chains (**Figure 6a.10A**) showed the first peak at a larger distance for PAI-1 depicting higher inter-chain spacing. Similarly RDF between the centers of mass of the phenyl rings and all other atoms within single chains also showed peak at a larger distance for PAI-1 (**Figure 6a.10B**). This points out that the chains expand and span larger volume in the case of PAI-1.

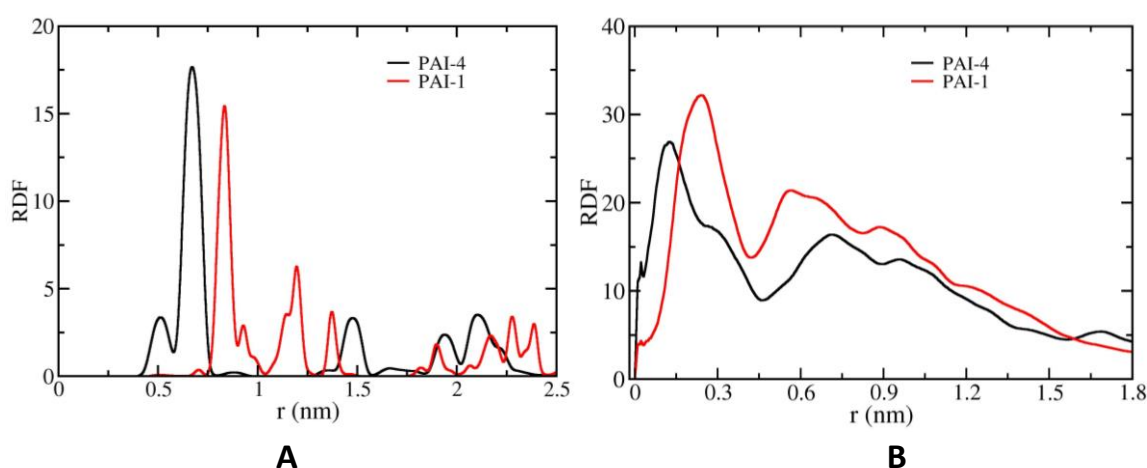


Figure 6a.10 (A) RDF between the centres of mass of chains (B) RDF between the centres of mass of phenyl rings with other atoms in single chains

Thus, more inter- and intra- chain spacing in PAI-1 leads to higher free volume and lesser density. Representative snapshots showing inter-chain spacing for PAI-1 and PAI-4 are shown in **Figure 6a.11**.

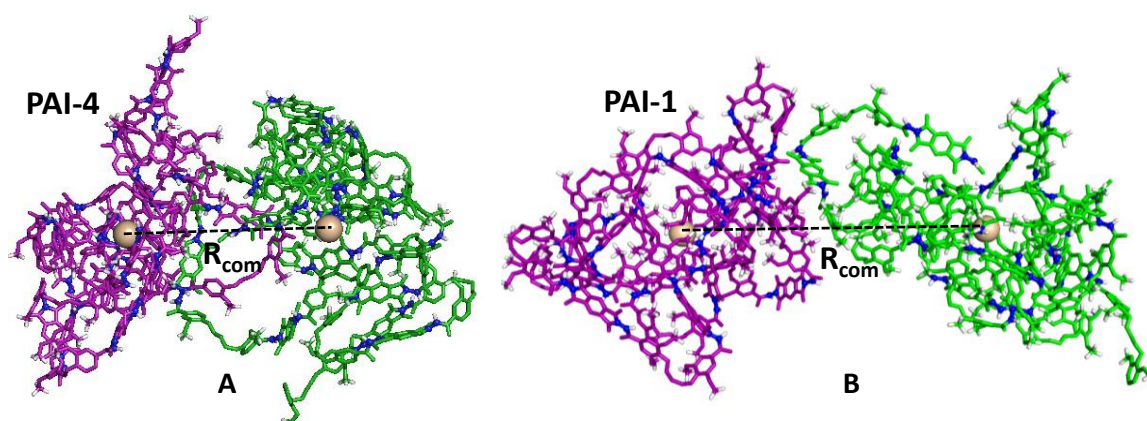


Figure 6a.11 Snapshots depicting distance between centre of mass of two chains: green and purple-carbon; blue-nitrogen; white-hydrogen; pink spheres: centre of mass of chains. R_{com} : distance between centre of mass of two chains

Similar counterintuitive observations of increased T_g accompanied with decreased density has been reported by Nair and Basu et al²⁸ for polyimide-HFPE-30 and Gu et al²⁹ for polyimide based on BPDA and 4,4'-oxydianiline. In both the studies, density of the higher T_g polymer was reported to be lesser than its counterpart. These reports attributed the observed increase in T_g with substitution and isomerization to the increased rigidity of polymer backbone. Both these studies have demonstrated higher rotational barrier associated with groups involving substitution or isomerization.

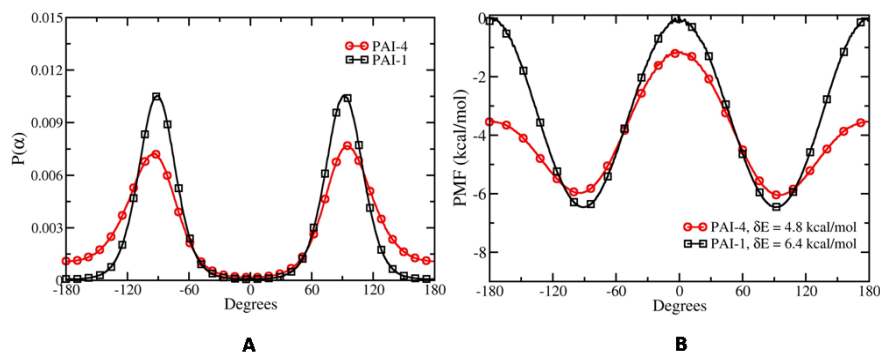


Figure 6a.12 (A) Torsional angle distributions of PAI-4 and PAI-1 (B) Rotational energy barrier from PMF for PAI-4 and PAI-1

Along the similar lines, effect of the chain rigidity, in particular the rotational barrier between the phenyl ring and the oxypropylene linkage on respective T_g values was explored. Torsional angle distribution of α (see **Figure 6a.8 A** for a structural representation) is shown in **Figure 6a.12**.

The dramatic increase in the peak intensities in PAI-1 indicated that the rotation around phenyl ring is more hindered due to the extra methoxy substituents. In order to quantify the increase in the rotational barrier with substitution, potential of mean force (PMF), $G(\alpha)$ was calculated from the torsional distributions using the Boltzmann inversion relation:

$$G(\alpha) = -k_B T \ln P_{(\alpha)}$$

The difference between the minima and maxima of PMF (**Figure 6a.12B**) corresponds to the free energy barrier for torsional rotation. PAI-1 exhibited 1.6 kcal mol⁻¹ higher rotational barrier than PAI-4. Thus, in PAI-1 rotation around phenyl ring is hindered, which restricts the segmental motion and thereby increases the relaxation time. To analyze the segmental relaxation, dihedral autocorrelation function²⁸ $C(t)$ was calculated as follows:

$$C(t) = \langle \cos[\alpha(t) - \alpha(t + \Delta t)] \rangle_t$$

where $\alpha(t)$ and $\alpha(t+\Delta t)$ denote the torsional angle at time t and time $t+\Delta t$, respectively. The time-scale of decay of $C(t)$ gives a measure of the rigidity of chains, where a longer time-scale would signify increased rigidity²⁴. The comparison of $C(t)$ for both PAI-4 and PAI-1 is shown in **Figure 6a.13**. It was observed that the decay in $C(t)$ for PAI-1 is substantially slower than PAI-4 indicating the higher rigidity due to hindered backbone rotation. Thus, the MD simulation data clearly established that molecular origin of the increased T_g in PAI-1 as compared to PAI-4 is the increase in the rotational barrier between the substituted aromatic rings. This leads to substantially slower segmental relaxation and increased rigidity in the polymer chain.

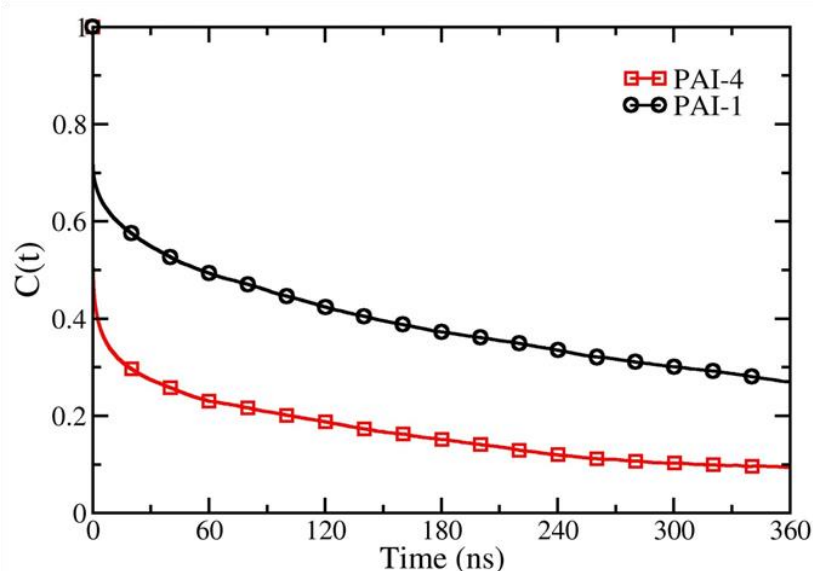


Figure 6a.13 Comparison of the decay of dihedral autocorrelation function ($C(t)$) for PAI-4 and PAI-1.

6a.4 Conclusions

- A new series of poly(amide imide)s containing oxypropylene linkages in backbone was synthesized from DSHC-3, DVHC-3 and aromatic dianhydrides using two-step polycondensation route.
- Inherent viscosities of poly(amide imide)s were in the range 0.44-0.56 dLg⁻¹, indicating formation of reasonably high molecular weights.

- Poly(amide imide)s bearing oxypropylene linkages showed good solubility in organic solvents such as DMAc, DMF, DMSO, NMP and pyridine. Tough, transparent and flexible film could be cast from their solution in DMAc.
- Wide angle X-ray diffraction patterns showed that poly(amide imide)s containing oxypropylene linkages were amorphous in nature.
- T_{10} values of poly(amide imide)s were in the range of 340-364 °C, indicating satisfactory thermal stability of polymers.
- Thermo-mechanical analysis showed that with increasing number of methoxy substituents, T_g and their mechanical strength also increased.
- MD simulation studies on representative poly(amide imide)s indicated chain rigidity as the molecular origin for the observed increase in the T_g of DSHC-3-based poly(amide imide)s.

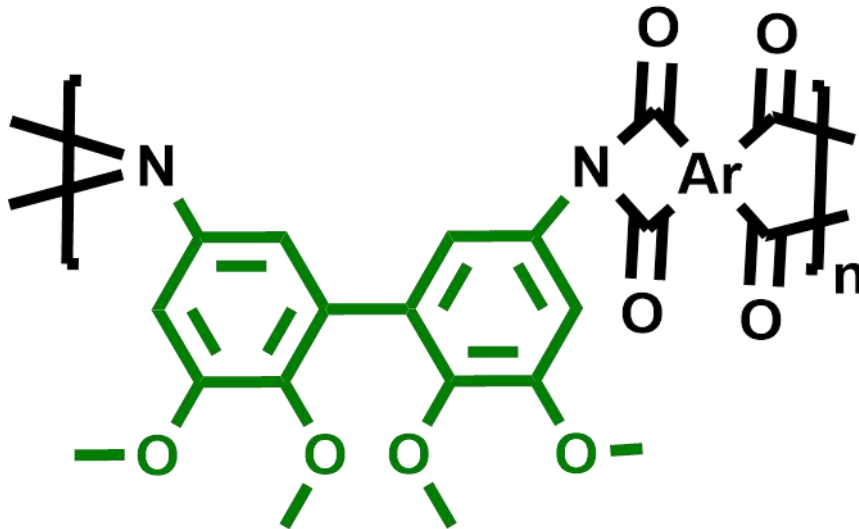
References

- 1 M. Ding, *Prog. Polym. Sci.*, 2007, **32**, 623–668.
- 2 D.-J. Liaw, K.-L. Wang, Y.-C. Huang, K.-R. Lee, J.-Y. Lai and C.-S. Ha, *Prog. Polym. Sci.*, 2012, **37**, 907–974.
- 3 D. M. Stoakley, A. K. St. Clair and C. I. Croall, *J. Appl. Polym. Sci.*, 1994, **51**, 1479–1483.
- 4 M. Ghosh, *Polyimides: Fundamentals and Applications*, CRC Press, 1996.
- 5 J. M. Dodda and P. Bělský, *Eur. Polym. J.*, 2016, **84**, 514–537.
- 6 X. M. Zhang, J. G. Liu and S. Y. Yang, *Rev. Adv. Mater. Sci.*, 2016, **46**, 22–38.
- 7 W. Wrasidlo and J. Augl, *J. Polym. Sci. Part A Polym. Chem.*, 1969, **7**, 321–332.
- 8 A. S. More, A. S. Patil and P. P. Wadgaonkar, *Polym. Degrad. Stab.*, 2010, **95**, 837–844.
- 9 C. V. Avadhani, P. P. Wadgaonkar and S. P. Vernekar, *J. Appl. Polym. Sci.*, 1990, **40**, 1325–1335.
- 10 C. Yang, G. Liou, C. Yang, S. Chen and T. Hsiang, *Polym. Bull.*, 1999, **28**, 21–28.
- 11 N. V. Sadavarte, C. V. Avadhani, P. V. Naik and P. P. Wadgaonkar, *Eur. Polym. J.*, 2010, **46**, 1307–1315.
- 12 A. P. G. Kieboom, *Recl. des Trav. Chim. des Pays-Bas*, 1988, **107**, 685–685.
- 13 H. A. Meylemans, T. J. Groshens and B. G. Harvey, *ChemSusChem*, 2012, **5**, 206–210.

- 14 S. V. Lyulin, S. V. Larin, A. A. Gurtovenko, V. M. Nazarychev, S. G. Falkovich, V. E. Yudin, V. M. Svetlichnyi, I. V. Gofman and A. V. Lyulin, *Soft Matter*, 2014, **10**, 1224–32.
- 15 W. L. Jorgensen, D. S. Maxwell and J. Tirado-Rives, *J. Am. Chem. Soc.*, 1996, **118**, 11225–11236.
- 16 B. Hess, C. Kutzner, D. van der Spoel and E. Lindahl, *J. Chem. Theory Comput.*, 2008, **4**, 435–447.
- 17 P. P. Van Uytvanck, G. Haire, P. J. Marshall and J. S. Dennis, *ACS Sustain. Chem. Eng.*, 2017, **5**, 4119–4126.
- 18 G. Bussi, D. Donadio and M. Parrinello, *J. Chem. Phys.*, 2007, **126**, 155101.
- 19 J. Liu, R. S. Loewe and R. D. McCullough, *Macromolecules*, 1999, **32**, 5777–5785.
- 20 J. M. Lupton, K. Becker, G. Gaefke, J. Rolffs and S. Ho, *Chem. Commun.*, 2010, **46**, 4686–4688.
- 21 M. Ree, K. Kim, S. H. Woo, H. Chang, M. Ree, K. Kim, S. H. Woo and H. Chang, *J. Appl. Phys.*, 1997, **81**, 698–708.
- 22 F. E. Arnold, K. R. Bruno, D. Shen, M. Eashoo, C. J. Lee, F. W. Harris and S. Z. D. Cheng, *Polym. Eng. Sci.*, 1993, **33**, 1373–1380.
- 23 A. Arbe, F. Alvarez and J. Colmenero, *Soft Matter*, 2012, **8**, 8257.
- 24 R. P. White and J. E. G. Lipson, *Macromolecules*, 2016, **49**, 3987–4007.
- 25 X. Li and A. F. Yee, *Macromolecules*, 2003, **36**, 9411–9420.
- 26 L. Y. S. Privalko V P, *J. Macromol. Sci. Part B - Phys.*, 1974, **9**, 551–564.
- 27 T.-T. Hsieh, C. Tiu and G. P. Simon, *J. Appl. Polym. Sci.*, 2001, **82**, 2252–2267.
- 28 S. Pandiyan, P. V. Parandekar, O. Prakash, T. K. Tsotsis, N. N. Nair and S. Basu, *Chem. Phys. Lett.*, 2014, **593**, 24–27.
- 29 M. Li, X. Y. Liu, J. Q. Qin and Y. Gu, *Express Polym. Lett.*, 2009, **3**, 665–675.

Chapter - 6b

Synthesis and Characterization of Polyimides Containing Biphenylene Linkages



6b.1 Introduction

Aromatic polyimides represent an important class of high performance/high temperature polymers due to their excellent thermal, mechanical and chemical resistance^{1,2}. Polyimides often replace glass and metal and are mainly used in automotive, aerospace, gas separation membranes, electronic packaging, adhesives, etc²⁻⁸. The various companies have commercialized polyimides with the trade names such as Kapton (DuPont), Apical (Kaneka), UPILEX (UBE), Kaptrex (Professional Plastics) Vespel (DuPont), Skybond (Monsanto), Pyre-ML (DuPont), VTEC PI (RBI), and Norton TH (Saint-Gobain)⁹.

Aromatic polyimides possess rigid chains and strong inter-chain interactions originating from their intra-/inter-chain charge transfer complex (CTC) formation and electronic polarization, which results in their poor solubility in organic solvents, and consequently poses difficulties in their processability^{6,10-12}. Therefore, significant efforts have been made to improve solubility and melt processability of aromatic polyimides by structural modifications which include i) incorporation of hinge atoms, alkylene or kinked structure in polymer backbone¹³⁻¹⁸ and ii) incorporation of pendant bulky substituents or flexible groups¹⁹⁻²⁹. The incorporation of 'kinked' units in polyimide backbone is of great interest because it results in solubility enhancement without much compromise on thermal characteristics^{30,31}.

The key starting monomers used for the synthesis of aromatic polyimides are diamines/diisocyanates and dianhydrides. Most of these monomers are derived from petroleum-derived chemicals^{5,32}. However, the use of petroleum resources for the synthesis of polymers is insecure because of finite stocks, non-renewability and environmental issues³³⁻³⁶. Lignin-derived aromatics and CNSL are promising precursors for the synthesis of aromatic difunctional monomers and polymers because of their abundant availability and non-edible nature. In the last few years, CNSL has been utilized for the synthesis of aromatic diamines/diisocyanates and their utility for the preparation of aromatic polyimides was demonstrated^{13,19-21,37,38}. A range of aromatic difunctional monomers suitable for the preparation of high performance polymers such as aromatic polycarbonates, semi-aromatic polyesters, aromatic polyesters, polyamides and polyacetals have been synthesized starting from lignin-derived aromatics³⁹. To the best of our knowledge, no mention was found in the literature of step-growth monomers based on lignin-derived aromatics suitable for synthesis of aromatic polyimides.

The synthesis of 5,5'-diisocyanato-2,2',3,3'-tetramethoxy-1,1'-biphenyl starting from lignin-derived aromatic *viz.* vanillic acid has been described in **Chapter 3**. It was considered of interest to synthesize new aromatic polyimides containing biphenylene linkages by one step polycondensation of 5,5'-diisocyanato-2,2',3,3'-tetramethoxy-1,1'-biphenyl with aromatic dianhydrides *viz.* 4,4'-oxydiphthalic anhydride (ODPA) 3,3',4,4'-benzophenonetetracarboxylic dianhydride (BTDA), 4,4'-(hexafluoroisopropylidene)diphthalic anhydride (6-FDA) 4,4'-biphenyltetracarboxylic dianhydride (BPDA) and pyromellitic dianhydride (PMDA). The synthesized polyimides were characterized by FT-IR, ¹H NMR, ¹³C NMR spectroscopy, X-ray diffraction studies, thermogravimetric analysis (TGA), and differential scanning calorimetry (DSC).

6b. 2 Experimental

6b.2.1 Materials

5,5'-Diisocyanato-2,2',3,3'-tetramethoxy-1,1'-biphenyl (BDI) was synthesized as described in **Chapter 3**. 4,4'-Oxydiphthalic anhydride (ODPA), 3,3',4,4'-benzophenonetetracarboxylic dianhydride (BTDA), 4,4'-(hexafluoroisopropylidene)diphthalic anhydride (6-FDA), 4,4'-biphenyltetracarboxylic dianhydride (BPDA) and pyromellitic dianhydride (PMDA) were received from Sigma Aldrich, USA and were sublimed before use. 1,4-Diazabicyclo[2.2.2]octane (DABCO) was recrystallized from n-hexane. Benzonitrile, *N,N*-Dimethylformamide (DMF), *N,N*-dimethylacetamide (DMAc), dimethyl sulfoxide (DMSO), *N*-methyl-2-pyrrolidone (NMP), dichloromethane, chloroform, n-hexane and pyridine were received from Thomas Baker Ltd., Mumbai and were purified as per literature procedures⁴⁰.

6b.2.2 Measurements

Inherent viscosity of polyimides was determined with 0.5 % (w/v) solution of polymer in DMAc at 30±0.1°C using Ubbelohde suspended level viscometer. Inherent viscosity was calculated using the equation

$$n_{inh} = \frac{2.303}{c} \times \log t/t_0$$

where, t and t_0 are flow times of polymer solution and solvent, respectively and c is the concentration of polymer solution.

Molecular weight and dispersity values of polyimides were determined on Thermo-Finnigan make gel-permeation chromatography (GPC) using *N,N*-dimethylformamide as

an eluent at a flow rate of 1 mL min⁻¹ at 25 °C. Sample concentration was 2 mg mL⁻¹ and narrow dispersity polystyrenes were used as calibration standards.

FT-IR spectra were obtained on a Perkin–Elmer Spectrum GX spectrometer using polymer films.

NMR spectra were recorded on a Bruker 200, 400 or 500 MHz spectrometer at resonance frequencies of 200, 400 or 500 MHz for ¹H NMR and 50, 100, 125 MHz for ¹³C NMR measurements using DMSO-d₆ as a solvent.

Thermogravimetric properties such as temperature at 10 % weight loss and char yield of polyimides were measured using Perkin Elmer: STA 6000. Approximately 7-10 mg of polymer sample was placed in platinum pan heated up to 800 °C at the rate of 10 °C min⁻¹ under nitrogen atmosphere with gas flow rate of 10 mL min⁻¹ and sample gas flow rate of 25 mL min⁻¹.

Differential scanning calorimetry (DSC) was performed using DSC Q100 differential calorimeter from TA Instruments under nitrogen atmospheres (50 mL min⁻¹). Analysis was carried out in a temperature range between 30 and 250 °C using heating rate of 10 °C min⁻¹.

X-Ray diffraction patterns of polyimides were recorded using dried polymer film on a Rigaku Dmax 2500 X-ray diffractometer at a tilting rate of 2° min⁻¹.

6b.2.3 Synthesis of polyimides

A representative procedure for synthesis of polyimides is described below:

Into a 50 mL two necked round bottom flask equipped with a magnetic stirrer bar, a nitrogen inlet and a reflux condenser were taken BDI (1 g, 2.8 mmol), aromatic dianhydride (2.8 mmol), DABCO (94 mg, 0.84 mmol) and benzonitrile (10 mL). The reaction mixture was heated at 140 °C for 10 h under nitrogen atmosphere. The reaction mixture was cooled to room temperature and poured into excess methanol and the precipitated polymer was filtered, washed with hot methanol and dried at 100 °C for 10 h under reduced pressure.

Synthesis of PI-1 starting from 5,5'-diisocyanato-2,2',3,3'-tetramethoxy-1,1'-biphenyl and ODP

FT-IR (cm⁻¹): 739, 1375, 1720, 1777; ¹H NMR (500 MHz, DMSO-d₆, δ/ppm): 3.75 (s, 6H), 3.92 (s, 6H), 7.00 (s, 4H), 7.45 (d, 2H), 7.97 (d, 2H); ¹³C NMR (125 MHz, DMSO-

d₆, δ/ppm): 55.9, 60.3, 112.0, 113.6, 121.5, 124.9, 126.1, 127.2, 131.5, 134.5, 145.9, 152.5, 160.8, 166.1, 166.3.

Synthesis of PI-2 starting from 5,5'-diisocyanato-2,2',3,3'-tetramethoxy-1,1'-biphenyl and 6-FDA

FT-IR (cm⁻¹): 725, 1378, 1727, 1784; ¹H NMR (500 MHz, DMSO-d₆, δ/ppm): 3.65 (s, 6H), 3.82 (s, 6H), 6.92 (s, 2H), 7.21 (s, 2H), 7.73 (s, 2H), 7.95 (d, 2H), 8.16 (d, 2H); ¹³C NMR (125 MHz, DMSO-d₆, δ/ppm): 55.9, 60.3, 112.1, 121.6, 123.6, 124.4, 126.8, 131.5, 132.6, 133.0, 135.8, 137.3, 146.1, 152.5, 166.0, 166.2.

Synthesis of PI-3 starting from 5,5'-diisocyanato-2,2',3,3'-tetramethoxy-1,1'-biphenyl and BTDA

FT-IR (cm⁻¹): 723, 1378, 1725, 1780; ¹H NMR (400 MHz, DMSO-d₆, δ/ppm): 3.67 (s, 6H), 3.84 (s, 6H), 6.95 (s, 2H), 7.24 (s, 2H), 8.13 (s, 2H), 8.22 (br. d, 4H); ¹³C NMR (125 MHz, DMSO-d₆, δ/ppm): 56.1, 60.3, 112.0, 121.5, 123.8, 129.5, 131.5, 132.2, 134.8, 141.6, 146.0, 152.5, 166.3, 193.4

Synthesis of PI-4 starting from 5,5'-diisocyanato-2,2',3,3'-tetramethoxy-1,1'-biphenyl and BPDA

FT-IR (cm⁻¹): 739, 1378, 1721, 1775; ¹H NMR (400 MHz, DMSO-d₆, δ/ppm): 3.70 (s, 6H), 3.87 (s, 6H), 6.97 (s, 2H), 7.23 (s, 2H), 8.03 (s, 2H), 8.3 (br. s, 4H); ¹³C NMR (125 MHz, DMSO-d₆, δ/ppm): 55.1, 59.9, 111.8, 113.3, 121.1, 124.5, 125.9, 127.0, 131.1, 134.6, 145.8, 152.3, 160.2, 166.0, 165.5

Synthesis of PI-5 starting from 5,5'-diisocyanato-2,2',3,3'-tetramethoxy-1,1'-biphenyl and PMDA

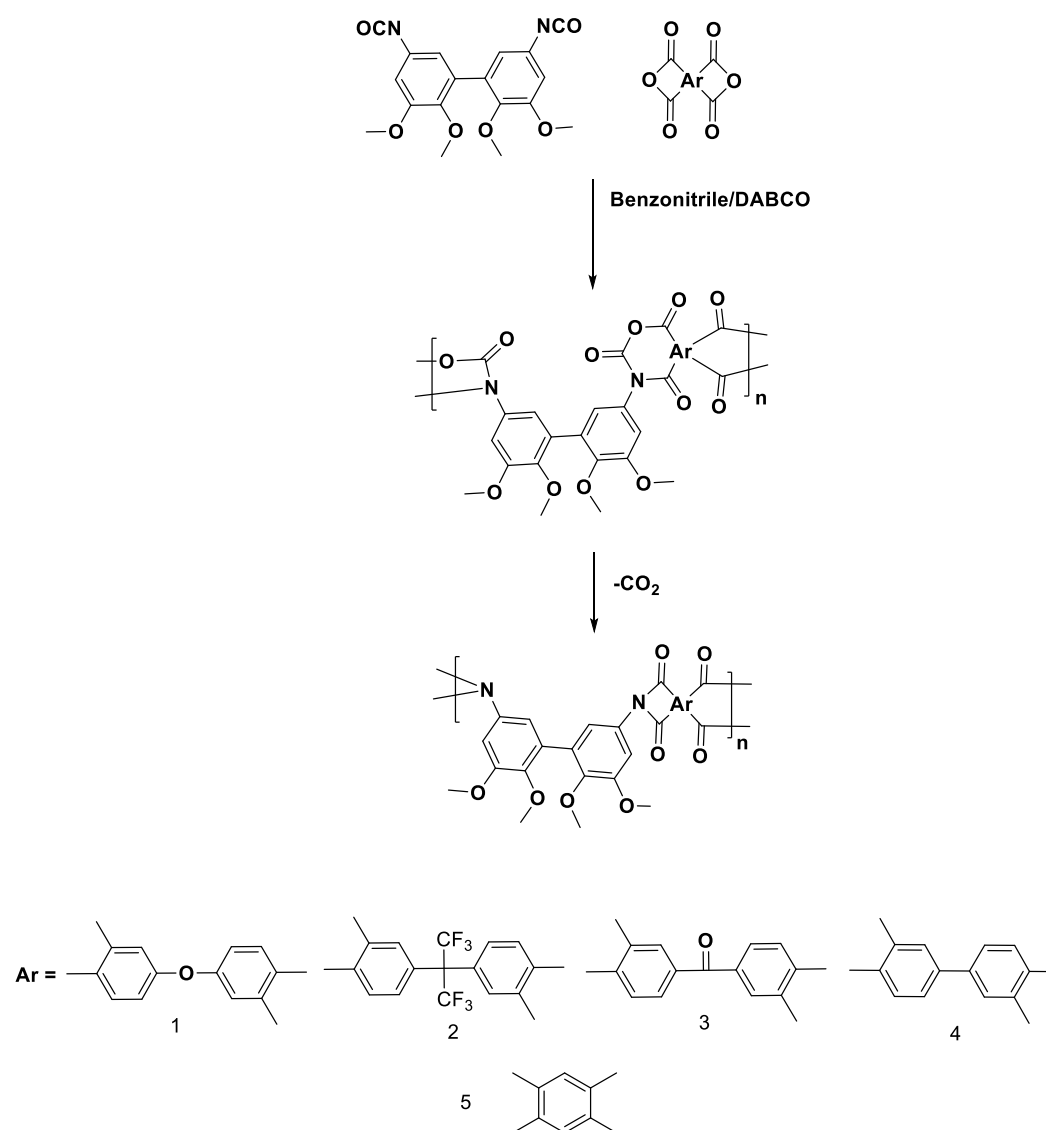
FT-IR (cm⁻¹): 736, 1375, 1731, 1771; ¹H NMR (400 MHz, DMSO-d₆, δ/ppm): 3.68 (s, 6H), 3.85 (s, 6H), 7.0 (s, 2H), 7.27 (s, 2H), 8.35 (s, 2H); ¹³C NMR (125 MHz, DMSO-d₆, δ/ppm): 56.0, 60.3, 112.0, 117.8, 121.5, 126.7, 131.5, 137.1, 146.1, 152.5, 165.5.

6b.3 Results and discussion

6b.3.1 Polyimide synthesis

New partially bio-based polyimides containing 'twisted' structure were synthesized by the polycondensation of bio-based aromatic diisocyanate *viz.* BDI with aromatic dianhydrides *viz.* 4,4'-oxydiphthalic anhydride (ODPA), 3,3',4,4'-benzophenonetetracarboxylic dianhydride (BTDA),

4,4'-(hexafluoroisopropylidene)diphthalic anhydride (6FDA), 4,4'-biphenyltetracarboxylic dianhydride (BPDA) and pyromellitic dianhydride (PMDA) using DABCO as the catalyst in benzonitrile at 140 °C (**Scheme 6b.1**). In this reaction, BDI and dianhydride react together to form seven-membered cyclic intermediate, which thermally decomposed to form polyimide with evolution of carbon dioxide. The reaction mixture was homogenous throughout the course of polymerization. The results of polymerization reactions are summarized in **Table 6b.1**. Inherent viscosity of polyimides was in the range of 0.30-0.40 dLg⁻¹. Molecular weights of polyimides were measured by GPC using DMF as a solvent and polystyrenes as the calibration standards. Number average molecular weights of polyimides were in the range 25,100-32,200 gmol⁻¹.



Scheme 6b.1 Synthesis of polyimides based on biphenylene containing diisocyanate and dianhydrides

Molecular weight of polyimide derived from BPDA and BDI could not be measured due its partial solubility in DMF. GPC molecular weight and inherent viscosity values indicated formation of reasonably high molecular weight of polymers. Tough, transparent and flexible films of polyimides could be cast from their solution in DMAc.

Table 6b.1 Synthesis of aromatic polyimides derived from 5,5'-diisocyanato-2,2',3,3'-tetramethoxy-1,1'-biphenyl and aromatic dianhydrides

Polyimide	Dianhydride	η_{inh} (dLg ⁻¹) ^a	GPC ^b		Dispersity
			\overline{M}_n	\overline{M}_w	
PI-1	ODPA	0.35	25,100	49,500	2.0
PI-2	6FDA	0.30	27,700	59,800	2.2
PI-3	BTDA	0.35	27,400	69,200	2.5
PI-4	BPDA	0.39	ND		
PI-5	PMDA	0.40	32,200	75,800	2.3

a: η_{inh} was measured with 0.5 % (w/v) solution of polyimide in DMAc at 30 °C \pm 0.1 °C

b: Measured by GPC in DMF, polystyrenes were used as the calibration standard.

ND Not characterized due to partial solubility in DMF at room temperature

6b.3.2 Structural characterization

The chemical structure of polyimides was confirmed by FT-IR, ¹H NMR and ¹³C NMR spectroscopy. A representative FT-IR spectrum of PI-5 is presented in **Figure 6b.1**.

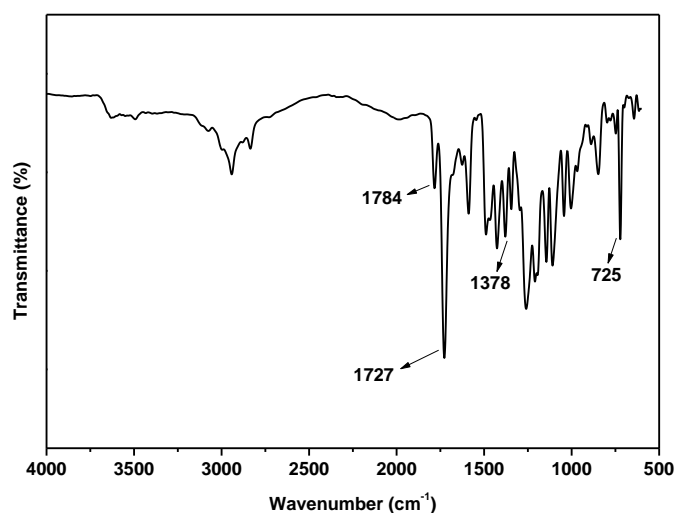


Figure 6b.1 FT-IR spectrum of polyimide (PI-5) derived from BDI and aromatic dianhydride

The characteristic absorption bands for imide ring were observed at 1784 cm^{-1} and 1727 cm^{-1} which correspond to asymmetric and symmetric carbonyl stretching, respectively. Absorption band at 1378 cm^{-1} corresponds to C-N stretching and absorption band at 725 cm^{-1} was ascribed to the imide ring deformation.

A representative ^1H NMR spectrum of polyimide derived from BDI and PMDA is shown in **Figure 6b.2**. The aromatic protons of dianhydride moiety showed a singlet at $8.35\text{ }\delta$ ppm. A singlet exhibited at $7.27\text{ }\delta$ ppm corresponds to the proton flanked by imide nitrogen and biphenylene linkage whereas proton flanked by imide group and methoxy group appeared as a singlet at $7.0\text{ }\delta$ ppm. Methoxy protons *meta* and *para* to imide nitrogen showed singlet at $3.85\text{ }\delta$ ppm and $3.68\text{ }\delta$ ppm, respectively.

^{13}C NMR spectrum of polyimide (PI-5) derived from BDI and PMDA shown in **Figure 6b.3** along with the assignments of carbon atoms.

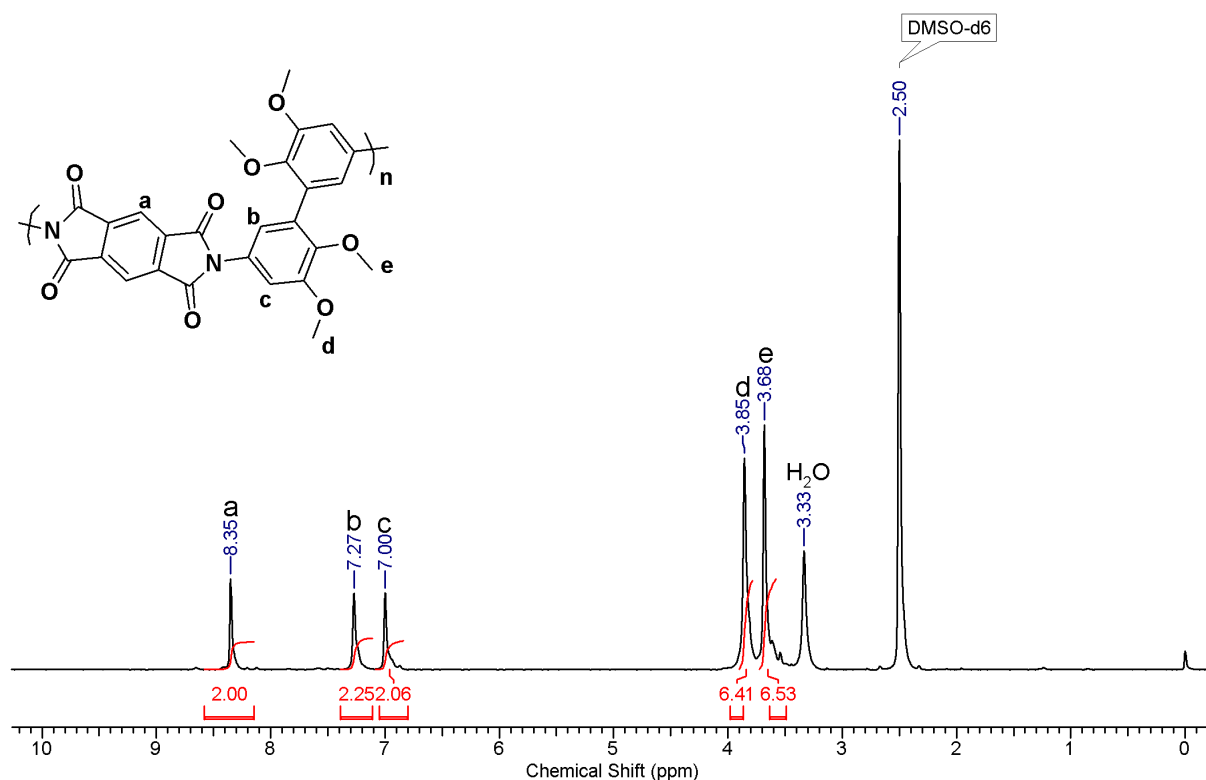


Figure 6b.2 ^1H NMR spectrum of polyimide derived from BDI and PMDA in DMSO-d_6

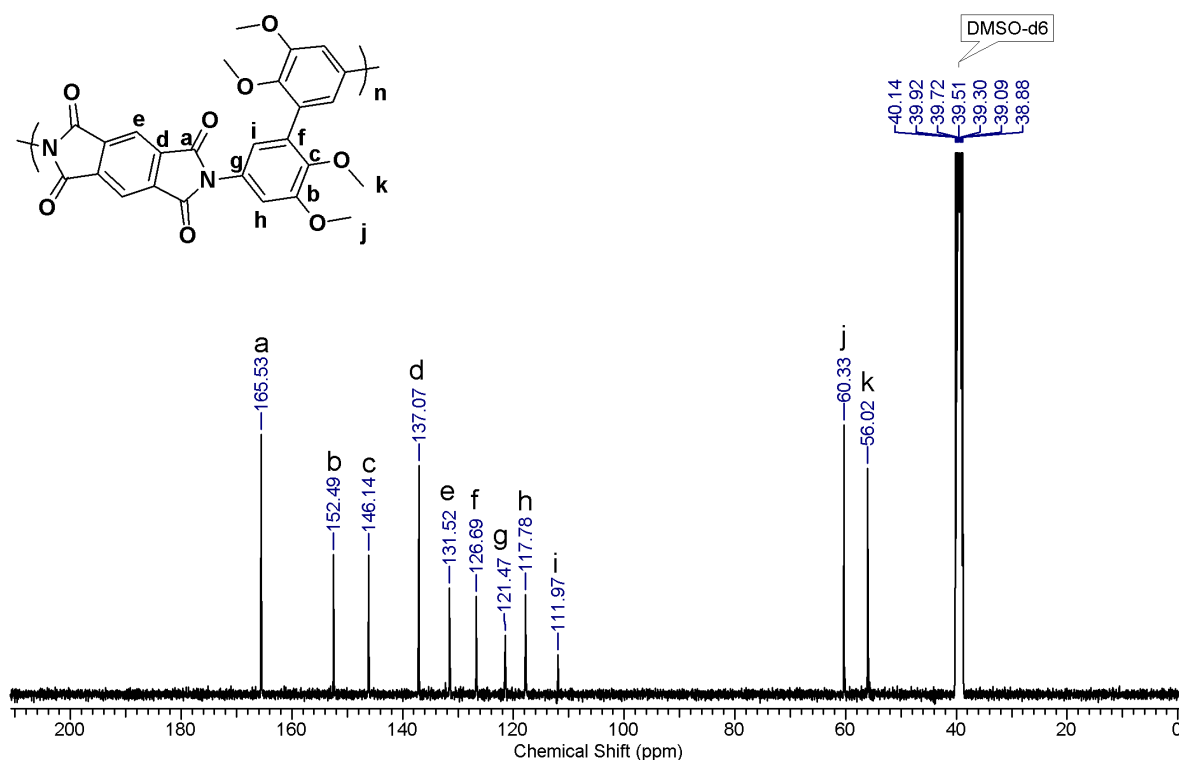


Figure 6b.3 ^{13}C NMR spectrum of polyimide derived from BDI and PMDA in DMSO-d_6 .

6b.3.3 Solubility of polyimides

The solubility of polyimides was tested at 3 wt % (w/v) concentration in various organic solvents and data is summarized in **Table 2**.

Table 6b.2 Solubility data of polyimides derived from 5,5'-diisocyanato-2,2',3,3'-tetramethoxy-1,1'-biphenyl and aromatic dianhydrides.

Polyimide	Dianhydride	Dichloromethane	Chloroform	DMAC	NMP	DMSO	DMF	Pyridine
PI-1	ODPA	++	++	++	++	++	++	++
PI-2	6FDA	++	++	++	++	++	++	++
PI-3	BTDA	--	--	++	++	++	++	++
PI-4	BPDA	--	--	++	++	++	+-	++
PI-5	PMDA	--	--	++	++	++	++	++

++ : soluble at room temperature; +- : insoluble at room temperature; --: insoluble at high temperature..

All the polyimides were soluble in polar organic solvents such as DMSO, DMAc, NMP and pyridine at room temperature. The solubility of biphenylene-containing polyimides could be ascribed to the kinked structure and the presence of methoxy groups which bring about disordering in the packing of the polymer chains. In addition, polyimides derived from 6FDA and ODPA were also soluble in halogenated solvents such as chloroform and dichloromethane. In case of 6FDA based polyimide (PI-2), the presence of bulky CF_3 substituents, which increased the disorder in the chains and hindered close packing, thereby decreasing the intermolecular interactions is the cause of further enhancement in solubility characteristics⁴¹. ODPA-derived polyimide showed excellent solubility due to the presence of flexible ether linkages in the polymer backbone.

6b.3.4 X-Ray diffraction studies

X-Ray diffractograms of polyimide films based on BDI and aromatic dianhydrides are reproduced in **Figure 6b.4** X-Ray diffractograms of polyimides showed a broad halo at around $2\theta = 10\text{-}30^\circ$ suggesting that all the polymers were amorphous. The amorphous nature of polyimides could be attributed to the presence of methoxy substituents situated at the *meta* and *para* position to the nitrogen of imide group and the 'kinked' structure. These structural features decrease interchain interactions thus disturbing the chain packing

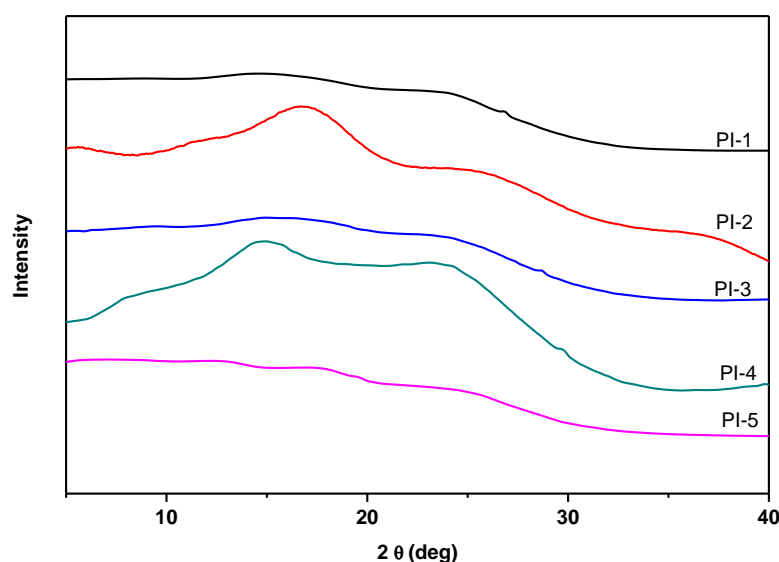


Figure 6b.4 X-Ray diffractograms of polyimides

6.3.5 Thermal properties of polyimides

Thermal characterization of polyimides were determined by TGA and DSC at heating rate of $10\text{ }^{\circ}\text{C min}^{-1}$ under nitrogen atmospheres. TG and DSC curves are showed in **Figure 6b.5** and **Figure 6b.6**, respectively and results are summarized in **Table 6b.3**.

Polyimides showed 10 % wt. loss and char yield at $800\text{ }^{\circ}\text{C}$ in the range $459\text{--}473\text{ }^{\circ}\text{C}$ and 45–55 %, respectively. Differential thermogravimetric analysis (**Figure 6b.5**) of polyimides displayed two-stage degradation: the first stage degradation was presumably due to the decomposition of pendant methoxy groups whereas the second stage degradation was observed due to decomposition of polyimide backbone.

It is interesting to compare the char yields of polyimides. In the series of polyimides, polyimide based on 6FDA (PI-2) showed the lowest char yield (45%). This could be due to the less thermally stable $-\text{C}(\text{CF}_3)_2-$ group, which gets lost in the form of $\cdot\text{CF}_3$ radicals^{42,43}. Polyimide based on BPDA (PI-4) showed highest char yield (55%) which is in line with the highest aromatic character.

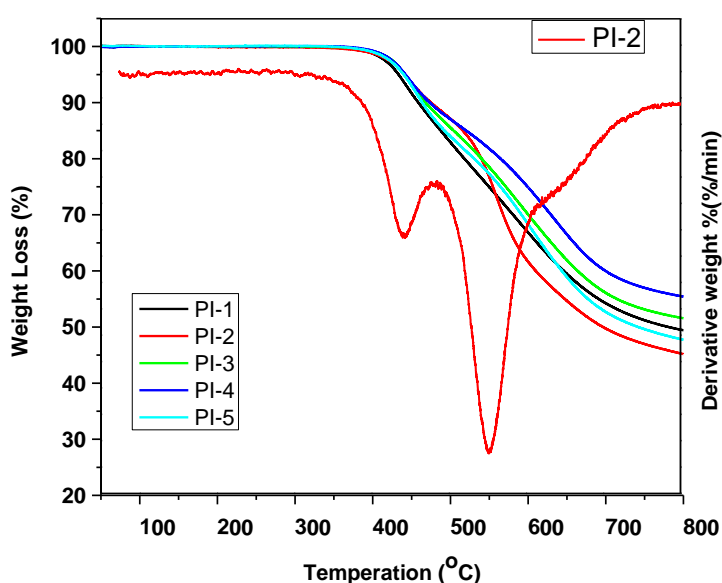


Figure 6b.5 TG curves of polyimides and DTG curve of PI-2.

T_g values of polyimides were in the range $262\text{--}329\text{ }^{\circ}\text{C}$ and the order is $\text{ODPA} < 6\text{FDA} < \text{BTDA} < \text{BPDA} < \text{PMDA}$. Generally, the T_g value increases with increasing chain rigidity of the polymer⁴⁴. Therefore, highest T_g value ($329\text{ }^{\circ}\text{C}$) was observed for polyimide based on PMDA due to highly rigid backbone. On the other hand, lowest T_g

value (262 °C) was observed for polyimide based on ODPA (PI-1) due to the presence of flexibilizing ether linkages⁴¹.

Table 6b.3 Thermal properties of polyimides derived from 5,5'-diisocyanato-2,2',3,3'-tetramethoxy-1,1'-biphenyl and aromatic dianhydrides

Polymer	Polyimide	T ₁₀ ^a (°C)	Char yield (%) ^b	T _g ^c (°C)
PI-1		459	50	262
PI-2		472	45	278
PI-3		466	52	277
PI-4		472	55	300
PI-5		462	47	329

a: temperature at which 10 % weight loss was observed in TGA under nitrogen atmospheres

b: weight residue at 800 °C

c: measured by DSC on second heating scan with heating rate at 10 °C min⁻¹ under nitrogen atmospheres

The results of polyimide synthesis and their properties indicated that bio-based diisocyanate *viz.* BDI is an interesting monomer for synthesis of organo-soluble aromatic polyimides with satisfactory thermal properties.

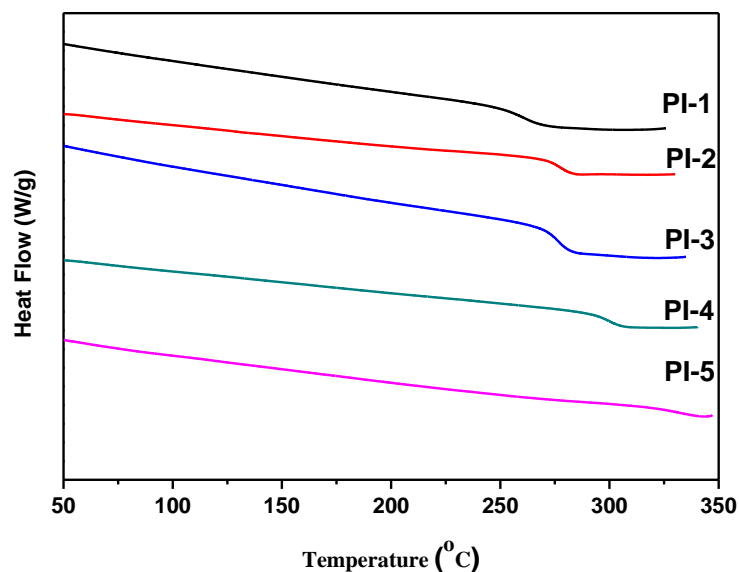


Figure 6b.6 DSC curves of polyimides

6b.4 Conclusions

- A series of new partially bio-based polyimides was synthesized by polycondensation of 5,5'-diisocyanato-2,2',3,3'-tetramethoxy-1,1'-biphenyl and aromatic dianhydrides.
- Inherent viscosity of polyimides was in the range 0.30-0.40 dLg⁻¹ indicating formation of reasonably high molecular weight polymers.
- Polyimides were found to be soluble in DMAc, DMSO, NMP, and pyridine.
- Wide-angle X-ray diffraction pattern showed that polyimides containing biphenylene linkages and methoxy groups were amorphous in nature.
- T₁₀ values of polyimides were in the range 459-472 °C indicating their satisfactory thermal stability.
- T_g values of polyimides were in the range 262-329 °C and order was ODPA<6FDA<BTDA<BPDA<PMDA.

References

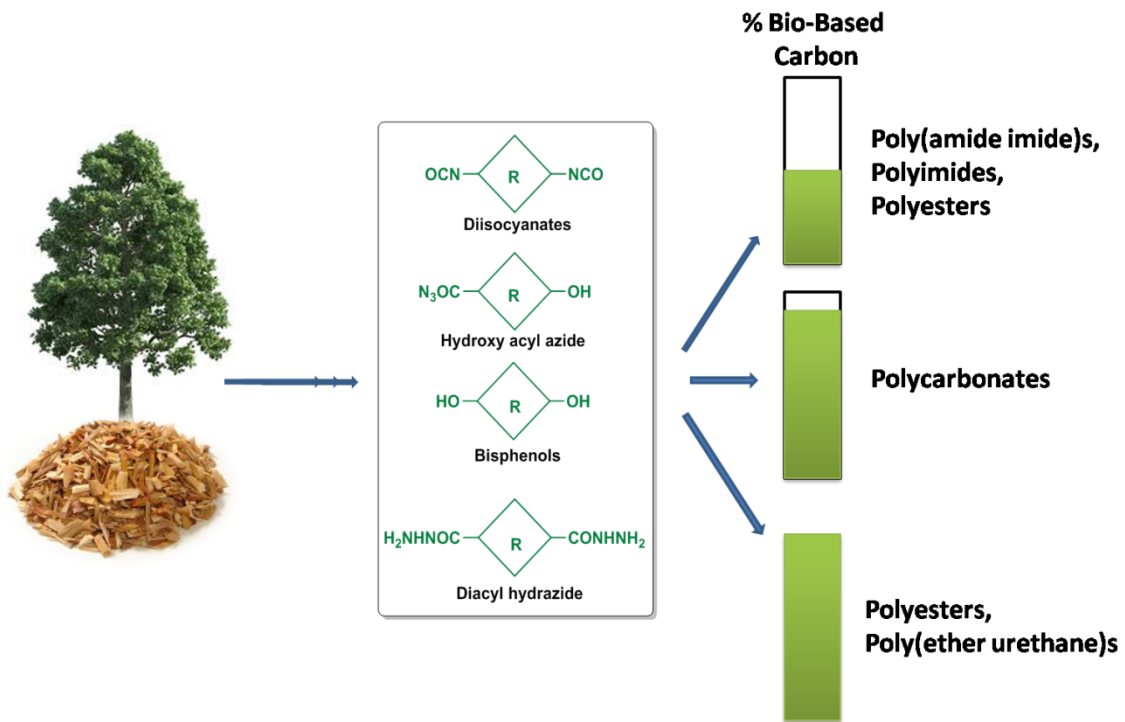
- 1 D. J. Liaw, K. L. Wang, Y. C. Huang, K. R. Lee, J. Y. Lai and C. S. Ha, *Prog. Polym. Sci.*, 2012, **37**, 907–974.
- 2 K. S. Y. Lau, *High-Performance Polyimides and High Temperature Resistant Polymers*, Elsevier Inc., 3rd ed., 2013.
- 3 D. J. Liaw, K. L. Wang, Y. C. Huang, K. R. Lee, J. Y. Lai and C. S. Ha, *Prog.*

- Polym. Sci.*, 2012, **37**, 907–974.
- 4 M. Ding, *Prog. Polym. Sci.*, 2007, **32**, 623–668.
- 5 H. R. Kricheldorf, *Progress in Polyimide Chemistry I*, 1999.
- 6 D. Stenzengerger, H. Hergenrother and P. Wilson, *Polyimide*, Blackie & Son Ltd, Glasgow and London, 1990.
- 7 K. L. Mittal, *Polyimides and Other High Temperature Polymers: Synthesis, Characterization and Applications*, CRC Press, 2005, vol. 2.
- 8 D. M. Stoakley, A. K. St. Clair and C. I. Croall, *J. Appl. Polym. Sci.*, 1994, **51**, 1479–1483.
- 9 P. M. Hergenrother, *High Perform. Polym.*, 2003, **15**, 3–45.
- 10 M. D. Kwan and M. T. Longaker, *Advances in Science and Technology*, 2008, **19**, 1136–1139.
- 11 T. L. St. Clair, in *Polyimides*, Springer Netherlands, Dordrecht, 1990, pp. 58–78.
- 12 Y. Imai, *React. Funct. Polym.*, 1996, **30**, 3–15.
- 13 N. V. Sadavarte, M. R. Halhalli, C. V. Avadhani and P. P. Wadgaonkar, *Eur. Polym. J.*, 2009, **45**, 582–589.
- 14 K. T. Hamcius Elena, Bruma Maria, Schulz Burkhard, *High Perform. Polym.*, 2003, **15**, 347.
- 15 C. Hamciuc, E. Hamciuc, I. Sava, I. Diaconu and M. Bruma, *High Perform. Polym.*, 2000, **12**, 265–276.
- 16 I. Sava, S. Chisca, M. Bruma and G. Lisa, *Polym. Bull.*, 2010, **65**, 363–375.
- 17 D. H. Wang, Z. Shen, M. Guo, S. Z. D. Cheng and F. W. Harris, *Macromolecules*, 2007, **40**, 889–900.
- 18 C. S. Wang and T. S. Leu, *Polymer*, 2000, **41**, 3581–3591.
- 19 R. D. Shingte, B. V. Tawade and P. P. Wadgaonkar, *Green Mater.*, 2017, **5**, 1–11.
- 20 C. Voirin, S. Caillol, N. V. Sadavarte, B. V. Tawade, B. Boutevin and P. P. Wadgaonkar, *Polym. Chem.*, 2014, **5**, 3142–3162.
- 21 D. Chatterjee, N. V. Sadavarte, R. D. Shingte, A. S. More, B. V. Tawade, A. D. Kulkarni, A. B. Ichake, C. V. Avadhani and P. P. Wadgaonkar, in *Cashew Nut Shell Liquid*, ed. P. Anilkumar, Springer International Publishing, Cham, 1st edn., 2017, pp. 163–214.
- 22 A. S. More, A. S. Patil and P. P. Wadgaonkar, *Polym. Degrad. Stab.*, 2010, **95**, 837–844.
- 23 N. V. Sadavarte, C. V. Avadhani, P. V. Naik and P. P. Wadgaonkar, *Eur. Polym.*

- J., 2010, **46**, 1307–1315.
- 24 B. V. Tawade, S. V. Shaligram, N. G. Valsange, U. K. Kharul and P. P. Wadgaonkar, *Polym. Int.*, 2016, **65**, 567–576.
- 25 A. Ghosh and S. Banerjee, *High Perform. Polym.*, 2009, **21**, 173–186.
- 26 E. M. Maya, A. E. Lozano, J. de Abajo and J. G. de la Campa, *Polym. Degrad. Stab.*, 2007, **92**, 2294–2299.
- 27 S. Mehdipour-Ataei and Y. Nazari, *J. Appl. Polym. Sci.*, 2012, **124**, 2891–2901.
- 28 M. Ghaemy and M. Barghamadi, *J. Appl. Polym. Sci.*, 2009, **112**, 815–821.
- 29 C. Wang, X. Zhao, G. Li and J. Jiang, *Polym. Degrad. Stab.*, 2009, **94**, 1746–1753.
- 30 G. S. Liou, Y. L. Yang and Y. O. Su, *J. Polym. Sci. Part A Polym. Chem.*, 2006, **44**, 2587–2603.
- 31 M. D. Damaceanu, C. P. Constantin, A. Nicolescu, M. Bruma, N. Belomoina and R. S. Begunov, *Eur. Polym. J.*, 2014, **50**, 200–213.
- 32 M. Ghosh, *Polyimides: Fundamentals and Applications*, CRC Press, 1996.
- 33 G. W. Huber, S. Iborra and A. Corma, *Chem. Rev.*, 2006, **106**, 4044–4098.
- 34 Y. Zhu, C. Romain and C. K. Williams, *Nature*, 2016, **540**, 354–362.
- 35 P. F. H. Harmsen, M. M. Hackmann and H. L. Bos, *Biofuels, Bioprod. Biorefining*, 2014, **8**, 306–324.
- 36 M. Bocqué, C. Voirin, V. Lapinte, S. Caillol and J. J. Robin, *J. Polym. Sci. Part A Polym. Chem.*, 2016, **54**, 11–33.
- 37 N. V. Sadavarte, S. S. Patil, C. V. Avadhani and P. P. Wadgaonkar, *High Perform. Polym.*, 2013, **25**, 735–743.
- 38 B. V. Tawade, A. D. Kulkarni and P. P. Wadgaonkar, *Polym. Int.*, 2015, **64**, 1770–1778.
- 39 A. Llevot, E. Grau, S. Carlotti, S. Grelier and H. Cramail, *Macromol. Rapid Commun.*, 2016, **37**, 9–28.
- 40 A. P. G. Kieboom, *Recl. des Trav. Chim. des Pays-Bas*, 1988, **107**, 685–685.
- 41 S. H. Hsiao, C. P. Yang and S. C. Huang, *J. Polym. Sci. Part A Polym. Chem.*, 2004, **42**, 2377–2394.
- 42 S.-J. Yang, C. Lee, W. Jang, J. Kwon, S. Sundar and H. Han, *J. Polym. Sci. Part B Polym. Phys.*, 2004, **42**, 4293–4302.
- 43 C. W. Lee, S. M. Kwak and T. H. Yoon, *Polymer*, 2006, **47**, 4140–4147.
- 44 I. A. Ronova and M. Bruma, *Struct. Chem.*, 2010, **21**, 1013–1020.

Chapter - 7

Summary and Conclusions



Step-growth polymerization processes are of significant interest for the preparation of polymeric materials useful in a vast array of applications. Currently, the monomers used for the synthesis of aromatic step-growth polymers are mostly derived from fossil resources, which are finite. Along with increasing industrialization, the rate of fossil fuel consumption is accelerated in order to meet the increased demands of energy, chemicals, polymeric materials, etc. Polymer industry utilizes around 7 % of petroleum resources. Keeping in mind their limited stocks, the complete dependence on fossil resources for polymer synthesis is insecure. In the recent years, replacing petroleum-derived materials by renewable materials has gained importance in both industrial and academic laboratories. An ample amount of literature is already available on the synthesis of bio-based polymers of aliphatic nature from vegetable oils, cellulose or starch. Such polymeric materials possess certain limitations such as poor mechanical properties, low T_g and poor flame retardancy. Additionally, in certain cases the resources used for synthesis of these polymers are edible, which may have adverse impact on food supply chain. Therefore, non-edible bio-based resources *viz.* lignin, hemicelluloses and CNSL are preferred options for replacement of petroleum-derived aromatic step-growth polymers.

The present thesis work is centered on four research themes: 1) utilization of lignin-derived phenolic derivatives *viz.* vanillin, vanillic acid, syringic acid, guaiacol and syringol for the synthesis of new difunctional monomers, 2) synthesis of fully/partially bio-based step-growth polymers such as poly(ether urethane)s, aromatic polyesters, aromatic polycarbonates, aromatic poly(amideimide)s and aromatic polyimides, 3) study of effect of methoxy substituents on thermal and mechanical properties of polymers and 4) preparation of recyclable crosslinked aromatic polyesters and aromatic polycarbonates using furan-maleimide Diels-Alder chemistry.

A total of 23 new difunctional monomers belonging to the following categories were synthesized:

- 1) Four new A-B monomers *viz.* ω -hydroxyalkyleneoxy benzoyl azides
- 2) A series of new aromatic diisocyanates containing oxyalkylene linkage
- 3) Two new aromatic diisocyanates containing biphenylene linkage
- 4) Two new bisphenols containing pendant furyl group
- 5) A new bisphenol containing oxadiazole ring
- 6) Two new α , ω -diacyl hydrazides containing oxyalkylene linkage

- 7) A new 3,3'-diacyl hydrazide containing biphenylene linkage
- 8) A new dialdehyde containing ester linkage
- 9) A new diols containing ester linkage
- 10) Two new aromatic diacids containing ester linkage

All these difunctional monomers and intermediates involved in their synthesis were characterized by FT-IR, ^1H NMR, and ^{13}C NMR spectroscopy. Some of the monomers and intermediates were also characterized by HRMS and single crystal X-ray diffraction analysis.

A series of new poly(ether urethane)s containing potentially 100% renewable carbon content were prepared by polymerization of aromatic diisocyanates containing oxyalkylene linkage with aliphatic diols *viz.* 1, 10-decanediol and 1, 12-dodecanediol. The chemical structures of poly(ether urethane)s were confirmed by FT-IR, ^1H NMR and ^{13}C NMR spectroscopy. The synthesized poly(ether urethane)s were of reasonably high molecular weights and could be cast into transparent and flexible films. Poly(ether urethane)s exhibited 10% weight loss in the temperature range 304-308 °C. Glass transition temperature (T_g) values of poly(ether urethane)s were observed in the range 49-74 °C and T_g values decreased with increasing number of methylene units in diols and increased with increasing number of methoxy substituents on aromatic rings of diisocyanates.

A series of new poly(ether urethane)s were synthesized by self-polycondensation of bio-derived A-B monomers, namely, 4-((6-hydroxyhexyl)oxy)-3-methoxybenzoyl azide, 4-((6-hydroxyhexyl)oxy)-3,5-dimethoxybenzoyl azide, 4-((11-hydroxyundecyl)oxy)-3,5-dimethoxybenzoyl azide and 4-((11-hydroxyundecyl)oxy)-3-methoxy benzoyl azide. Reasonably high molecular weight poly(ether urethane)s were formed as indicated by their inherent viscosities which were in the range 0.41–0.69 dL g⁻¹. Poly(ether urethane)s were soluble in various organic solvents and could be cast into tough, transparent and flexible films from their chloroform or *N,N*-dimethylacetamide (DMAc) solution. Poly(ether urethane) films exhibited good optical properties and possessed light transmittance at 800 nm in the range 80.2-87.6%. Poly(ether urethane)s showed 10% weight loss in the temperature range 320-340 °C. T_g values of poly(ether urethane)s were in the range 40-70 °C which were dictated by the length of oxyalkylene chain and number of methoxy substituents on aromatic ring.

Thermoreversible organogel was prepared from polyurethane based on 4-((11-hydroxyundecyl)oxy)-3-methoxy benzoyl azide. The gelation was possible only in polar

solvents such as tetrahydrofuran (THF), *N,N*-dimethylformamide (DMF), DMAc, *N*-methyl-2-pyrrolidone (NMP) and dimethyl sulfoxide (DMSO). A fibrous morphology of xerogel was observed by FESEM. The gelation behaviour of polyurethane in these solvents could be attributed to the combined effect of hydrophobic interactions and N-H...O hydrogen bonding. Thermoreversibility of organogel was studied by inverted vial method and rheological measurements. Gel-sol-gel phase transitions of organogel (3 wt. % in DMF), studied by rheology ($T_{\text{gel-sol}} = 57\text{ }^{\circ}\text{C}$) and DSC ($T_{\text{gel-sol}} = 56\text{ }^{\circ}\text{C}$) were correlated. The utility of polyurethane-based organogel as a gel electrolyte was demonstrated for quasi-solid state dye-sensitized solar cells. The result indicated that the polyurethane-based gel electrolyte showed better efficiency (6.3 %) than the corresponding liquid electrolyte (DMF, 4.5 %) and it could retain over 98 % of its initial photoelectric conversion efficiency after 12 days.

A series of aromatic polyesters were synthesized by interfacial polycondensation of bisphenols containing pendant furyl group *viz.* 4, 4'-(furan-2-ylmethylene)bis(2,6-dimethoxyphenol) (BPF-1) and 4,4'-(furan-2-ylmethylene)bis(2-methoxyphenol) with aromatic dicarboxylic acid chlorides *viz.* isophthaloyl chloride, terephthaloyl chloride and 2,5-furan dicarboxylic acid chloride. The chemical structures of polyesters were ascertained by FT-IR, ^1H NMR and ^{13}C NMR spectroscopy which confirmed that furyl group was preserved under the applied reaction condition. Reasonably high molecular weight polyesters were formed as indicated by their inherent viscosities (η_{inh} 0.49-0.78 dLg $^{-1}$) and GPC molecular weights (\overline{M}_n , 28,000-45,000 g mol $^{-1}$). T_g values of polyesters were in the range 160-214 $^{\circ}\text{C}$. The 10 % weight loss temperature of polyesters was found in the range 378-405 $^{\circ}\text{C}$, indicating their good thermal stability. Mechanical properties of aromatic polyesters were studied by tensile testing. Yield point and elongation at break were in the range 58.5-70.8 MPa and 15.5-56.2 % respectively, indicating their potential applications as structural materials.

A series of aromatic (co) polycarbonates were prepared by polycondensation of bisphenol containing pendant furyl group *viz.* 4,4'-(furan-2-ylmethylene)bis(2-methoxyphenol) (BPF-1) or a mixture of BPF-1 and bisphenol-A with triphosgene. (Co) polycarbonates showed inherent viscosity in the range 0.50-0.72 dLg $^{-1}$ and \overline{M}_n values obtained from GPC, were in the range 29,800-44,800 g mol $^{-1}$. By analysing triad sequence distribution using expanded ^{13}C NMR spectra, it was found that the microstructure for all the copolycarbonates were random. (Co) polycarbonates showed T_g

values in the range 136-147 °C. (Co) polycarbonates exhibited 10 % weight loss in the temperature range 380-432 °C which indicated that polymers are capable of sustaining typical melt processing conditions of aromatic polycarbonates. Tensile strength, Young's modulus and elongation at break, obtained from tensile testing of (co)polycarbonates containing pendant furyl groups, were in the range 53.9-57.7 MPa, 1.13-1.54 GPa and 14.3-100.5%, respectively. A significant drop in % elongation at break was observed upon incorporation of bisphenol containing furyl group in (co)polycarbonates, indicating compromise on the ductility characteristics.

Recyclable crosslinked aromatic polyesters and aromatic polycarbonates were prepared by Diels-Alder reaction of furan functionalized polycarbonate/polyester with bismaleimides namely, 1,1'-(methylenedi-1,4-phenylene)bismaleimides (BMI) and 1,8-bis(maleimido)-triethylene glycol (TEG). The resulting crosslinked polymers were characterized by solubility test experiments and tensile testing. The crosslinked polyesters and polycarbonates showed improved mechanical properties. Tensile strength of BMI-based crosslinked polymers increased by 62-107 % compared to parent linear polymers. The crosslinked polymers were recycled twice without observing any significant deterioration in their mechanical properties.

A series of new partially bio-based poly(amide imide)s were synthesized by polycondensation of bio-based diacylhydrazides *viz.* 4,4'-(propane-1,3-diylbis(oxy))bis(3-methoxybenzohydrazide) (DVHzC-3) and 4,4'-(propane-1,3-diylbis(oxy))bis(3,5-dimethoxybenzohydrazide) (DSHzC-3) with commercially available aromatic dianhydrides. Poly(amide imide)s exhibited amorphous nature and good solubility in polar organic solvents. Poly(amide imide)s could be cast into transparent, flexible and tough films from their DMAc solutions. Poly(amide imide)s showed inherent viscosity and \overline{M}_n values in the range 0.44-0.56 dLg⁻¹ and 25,500-40,800 g mol⁻¹ respectively. Poly(amide imide)s showed 10 % weight loss in the temperature range 340- 364 °C indicating their satisfactory thermal stability. Thermomechanical properties of poly(amide imide)s were studied by DMA which indicated that poly(amide imide)s based on DSHzC-3 exhibited higher storage modulus than corresponding poly(amide imide)s based on DVHzC-3. Both DMA and DSC analysis showed higher T_g values for poly(amide imide)s based on DSHzC-3 compared to the corresponding poly(amide imide)s based on DVHzC-3. Molecular dynamics simulation studies on representative poly(amide imide)s indicated that chain rigidity, imposed by additional methoxy substituents on aromatic ring, as the

molecular origin for the observed increase in T_g of poly(amide imide)s based on DSHzC-3.

A series of partially biobased aromatic polyimides were synthesized by polycondensation of 5,5'-diisocyanato-2,2',3,3'-tetramethoxy-1,1'-biphenyl with commercially available aromatic dianhydrides *viz.* 4,4'-biphenyltetracarboxylic dianhydride (BPDA), 3,3',4,4'-benzophenonetetracarboxylic dianhydride (BTDA), 4,4'-oxydiphthalic anhydride (ODPA) and 4,4'-(hexafluoroisopropylidene) diphthalic anhydride (6-FDA). Polyimides exhibited reasonably high molecular weight (\overline{M}_n , 25,100-32,200 g mol⁻¹) with good solubility in organic solvents such as DMAc, NMP and DMSO. The T_{10} values of biphenylene containing polyimides were observed in the range 459-462 °C, indicating their good thermal stability. Polyimides exhibited T_g values in the range 262-329 °C.

In summary, lignin-derived phenolic derivatives *viz.* vanillin, vanillic acid, syringic acid, guaiacol and syringol were successfully utilized for the synthesis of new difunctional monomers using simple organic transformations. Thus, a total of 23 new difunctional monomers were synthesized. These monomers are “drop-in” substitutes for currently used petroleum-based difunctional monomers in polymer industries. Six series of fully or partially bio-based step-growth polymers were synthesized using newly synthesized monomers which include: poly(ether urethane)s, aromatic polyesters, aromatic polycarbonates, aromatic poly(amideimide)s, and aromatic polyimides. Overall, the results demonstrated that lignin-derived phenolic derivatives serve as promising renewable feed stocks for synthesis of step-growth monomers and polymers with attractive properties.

Future Perspectives

Results and conclusions of the present research work related to design and synthesis of new difunctional monomers starting from lignin-derived aromatics, step-growth polymers, and furyl functionalized polymers have opened up various new prospects in terms of future research.

- Fully bio-based bisphenols containing pendant furyl group or oxadiazole ring are versatile monomers for the synthesis of aromatic step-growth polymers. Aromatic polyesters and polycarbonates were synthesized in the present work based on bisphenol containing pendant furyl group demonstrating their general usefulness.

Further studies need to address extensive characterization in terms of their thermo-mechanical properties and other material properties.

- The estrogenicity assay of the synthesized bisphenols needs to be studied.
- Bisphenols containing pendant furyl group are interesting starting materials for the synthesis of functional thermoplastic polymers such as polyethersulfones and polyetherketones and thermosets such as epoxy resins and cyanate ester resins.
- Oxadiazole containing bisphenol is a rigid bisphenol, which can enhance thermomechanical properties of step-growth polymers such as polycarbonates, polyesters, polyethersulfones and polyetherketones.
- Diisocyanates containing biphenylene linkage represent excellent bio-based aromatic diisocyanates for the synthesis of polyurethanes.
- Fully bio-based diols and dialdehyde containing ester linkage are interesting precursors for the synthesis of bio-based poly(ester urethane)s and poly(ester azomethine)s, respectively.
- Diacylhydrazides containing biphenylene linkage could be used for the synthesis of high performance polymers *viz.* poly(amide imide)s, poly(1,3,4-oxadiazole)s, etc.

List of Publications

1. New poly(ether urethane)s based on lignin derived aromatic chemicals *via* A-B monomer approach: Synthesis and characterization
Sachin S. Kuhire, C.V. Avadhani, Prakash P. Wadgaonkar
Eur. Polym. J. 71 (2015) 547–557.
2. Poly(ether urethane)s from aromatic diisocyanates based on lignin-derived phenolic acids
Sachin S. Kuhire, Samadhan S. Nagane, Prakash P. Wadgaonkar
Polym Int 66 (2017) 892–899.
3. Partially bio-based poly(amide imide)s by polycondensation of aromatic diacylhydrazides based on lignin-derived phenolic acids and aromatic dianhydrides: synthesis, characterization, and computational studies
Sachin S. Kuhire, Pragati Sharma, Suman Chakrabarty, Prakash P. Wadgaonkar
J. Polym. Sci. Part A: Polym. Chem. 55 (2017) 3636-3645.
4. Synthesis and Characterization of Partially Bio-Based Polyimides Based on Biphenylene-Containing Diisocyanate Derived from Vanillic Acid.
Sachin S. Kuhire, Etienne Grau, Henri Cramail, Prakash P. Wadgaonkar
(Manuscript under preparation)
5. New (co)polycarbonates from bisphenol containing pendant furyl groups: Synthesis, characterization and thermoreversible crosslinking studies
Sachin S. Kuhire, Prakash P. Wadgaonkar
(Manuscript under preparation)

List of Patents

1. **Sachin S. Kuhire**, Samadhan S. Nagane, Prakash P. Wadgaonkar
Pendant furyl containing bisphenols, polymers therefrom and a process for the preparation thereof
WO 2015140818 A1
2. **Sachin S.Kuhire**, Prakash P. Wadgaonkar
Bio-based aromatic diisocyanates for preparation of polyurethanes
WO2016103283 A1
3. Samadhan S. Nagane, **Sachin S.Kuhire**, Prakash P. Wadgaonkar
Bisphenols containing pendant clickable maleimide group and polymers therefrom
WO2016113760 A1